Investigation into the role of the SMC5/6 Complex in human cells.

A thesis submitted to the University of Sussex for the degree of Doctor of Philosophy

By

Grant Alexander McGregor.

Declaration

I hereby declare that this thesis has not been and will not be, submitted in whole or in part to another University for the award of any other degree

Signed……

Acknowledgements

Firstly, I would like to express my utmost gratitude to Dr Jo Murray for the opportunity to undertake a PhD and for her continued guidance and support through it all. A great deal of thanks must also go to all the members of the Murray and Carr labs past and present with special thanks to Owen Wells and Hung Quang Dang for all their assistance. I would also like to thank all the members of the GDSC including the Caldecott lab, especially Stuart, and the Sweet lab for sharing many reagents and an office with me, the O'Driscoll lab, the Downs lab and the Hochegger lab for their hints, tips and tricks and not to forget reagents. It's also important to thank the prep room and tissue culture staff without whom research would grind to a halt. I'd also like to give thanks to Velibor Savic for his many discussions and help in processing data and of course to Antony Oliver for his help, discussion and the sharing of an occasional gin.

The thanks I owe to my mother is without limit, I am extremely grateful to her for all her love and help, without her I would not have made it this far. Together with my Nana and Di, she raised me to try hard, enjoy myself but also to remain upbeat when things got tough. My family have always been a large part of my life and the support and perspective provided by my Auntie Norma, Uncle Johnny, Uncle Keith, Auntie Julie, Cousins John, Jillian, Greig, Keith and Molly have helped me immeasurably. I also have to thank my friends, without whom I'd never had made it this far, Kevin, Abu, Tomisin, Ross, Rachel, Owen, Matt and Sam, you all played your part. If I haven't mentioned you by name please note it's not because I've forgotten you, you all know who you are.

Thank you to everyone who has helped and supported me over these last 4 years, without you, I'd never have made it.

University of Sussex

Grant Alexander McGregor

Doctor of Philosophy Biochemistry

Investigation into the role of the SMC5/6 Complex in human cells.

Summary

The Structural Maintenance of Chromosome (SMC) family of proteins are required to regulate almost all aspects of chromosome biology and are critical for genomic stability. The SMC5/6 complex, a member of this family, is composed of two SMC heterodimers and six additional Non-SMC Elements 1-6. The components of SMC5/6 possess activities including ATPases, ubiquitin and SUMO ligases. SMC5/6 is required in homologous recombination and for accurate chromosome segregation. Loss of SMC5/6 is lethal in yeasts, embryonic lethal in mice and mutations in NSMCE2 leads to primordial dwarfism and insulin resistance.

This thesis focuses on a mutation in NSMCE3, found in American and Dutch families, that results in a novel chromosomal breakage syndrome characterized by fatal pulmonary disease. Another focus is the development, execution and validation of a microscopy based synthetic sick/lethal screen using cells with knockdown of NSMCE4a. Studies of SMC5/6 in yeasts predict that compromising SMC5/6 function would lead to a dependence on other DNA repair pathways. The results combined with patient data confirm that SMC5/6 is important in the absence of repair by non-homologous end joining and is particularly important under conditions of replication stress.

List of Abbreviations.

ALT	Alternate Lengthening of Telomeres
Alt-NHEJ	Alternate-NHEJ
AT	Ataxia-telangiectasia
ATM	Ataxia-telangiectasia mutated
ATP	Adenosine Triphosphate
ATR	Ataxia-telangiectasia mutated and Rad3-related
ATRIP	ATR interacting protein
BER	Base excision repair
BrdU	5'-bromo-2'-deoxyuridine
BSA	Bovine Serum Albumin
CDK	Cyclin-dependent kinase
CPD	Cyclobutane pyrminidine dimer
CPT	Camptothecin
(k)Da	(kilo)Dalton
DAPI	4' 6-diamino-2-phenylindole
DNA	Deoxyribonucleic acid
DSB	Double strand break
dsDNA	Double-strand DNA
EdU	5'-ethynyl-2'-deoxyuridine
FA	Fanconi Anaemia
FACS	Fluorescence Activated Cell Sorting
FCS	Foetal calf serum
GFP	Green Fluorescent Protein
HR	Homologous Recombination
hrs	Hours
HU	Hydroxyurea
IF	Immunofluorescence
IR	Ionizing Radiation
LB	Lysogeny Broth
mDNA	Mitochondrial DNA
MMC	Mitomycin C
MMR	Mismatch Repair
MMS	Methyl Methanesulphonate

MRN	MRE11-RAD50-NBS1
nDNA	Nuclear DNA
NEBD	Nuclear Envelope Breakdown
NER	Nucleotide Excision Repair
NHEJ	Non-Homologous End-Joining
NSE	Non-Smc Element
NSMCE	Non-SMC Element
OD	Optical density
PARP	Poly (ADP-Ribose) Polymerase
PBS	Phosphate Buffered Saline
PCR	Polymerase Chain Reaction
rDNA	ribosomal DNA
RFP	Red Fluorescent Protein
RISC	RNA-Induced Silencing Complex
RNA	Ribonucleic Ccid
RNAi	RNA interference
ROS	Reactive Oxygen Species
RPA	Replication Protein A
SAM	S Adenosyl Methionine
SC	Synaptonemal Complex
SCE	Sister Chromatid Exchange
SD	Standard Deviation
SEM	Standard Error of the Mean
shRNA	short hairpin RNA
siRNA	small interfering RNA
SMC	Structural Maintenance of Chromosome
SSB	Single-Strand Break
ssDNA	single-strand DNA
SUMO	Small Ubiquitin-like Modifier
TERT	Telomerase Reverse Transcriptase
TLS	Translesion Synthesis
UV	Ultra-Violet
WT	Wild-type
XP	Xeroderma Pigmentosum

Contents

Table of Contents

1.0 - Introduction

1.1 – Introduction to DNA repair

The genetic code of an organism encodes the information for its development, function, reproduction and metabolism. It must be faithfully copied from generation to generation. The genetic code is made up of deoxyribonucleic acid (DNA) and is wrapped around histones that form nucleosomes(Fernandez-Capetillo, Lee, Nussenzweig, *et al.*, 2004). The DNA must be unwound then replicated to duplicate its content before creating a new cell, or transcribed by the appropriate polymerases to create new proteins. Damage to the genetic material and/or failure to faithfully segregate the genetic code has been implicated in a large number of diseases and cancer(Macheret & Halazonetis, 2015)

The risk of developing cancer at some point in our lifetime is 1 in 2 (Ahmad, Ormiston-Smith & Sasieni, 2015). The identification of new targets for cancer therapy is at the forefront of research. There are many ways to identify potential therapeutic targets and this thesis will focus on the identification of synthetic sick/lethal interaction screen and the characterization of patient cells with a mutation in a subunit of a key DNA repair complex known as SMC5/6.

1.1.1 – Sources of DNA damage.

The requirement for accurate and efficient maintenance of DNA is absolute, however, the inherent structure of DNA and the modifications needed to allow normal cellular activities, including transcription and replication, make it liable to chemical attack from both endogenous and exogenous sources(Gupta & Lutz, 1999; Lindahl, 1993; Marnett, Riggins & West, 2003).

1.1.1.1 – Endogenous sources of DNA damage.

1.1.1.1.1 – DNA replication.

Replication of the genome occurs once in every cell cycle during S phase (Macheret & Halazonetis, 2015). Once origins of replication have been licensed replication can begin(Nasheuer, Smith & Bauerschmidt, 2002). Three polymerases are specifically required for replication; DNA polymerase α, DNA

polymerase δ, and DNA polymerase ε. DNA pol α is required to start DNA synthesis and synthesizes short RNA primers for both leading and lagging strands. Once DNA synthesis is primed Pol α is replaced by Pol ε or Pol δ for leading or lagging strand synthesis, respectively. These polymerases have proofreading capabilities and are used for bulk DNA synthesis (Kawasaki & Sugino, 2001; Fragkos, Ganier, Coulombe, *et al.*, 2015). Whilst polymerases have a high fidelity they can incorporate the incorrect base during DNA synthesis. DNA polymerases make errors once every 10^4-10^5 nucleotides polymerised. These mismatches if unrepaired can lead to permanent mutations in the genome. It is therefore not surprising that mutations in polymerases have been associated with disorders such as Alpers disease, neurodegenerative diseases such as Alzheimer's or Parkinson's and of course cancer (Loeb & Monnat, 2008))

1.1.1.1.2 – Reactive oxygen species

Reactive oxygen species (ROS) are a source of DNA damage. Twenty one percent O_2 has been known to cause deleterious effects in primary cells (Floyd, West & Hensley, 2001; Chance, Sies & Boveris, 1979; Jackson & Loeb, 2001; Calcerrada, Peluffo & Radi, 2011; Marnett, Riggins & West, 2003; Lee, Niles, Wishnok, *et al.*, 2002). Oxidative stress results in the formation of highly reactive free radicals that can cause damage to biomolecules within the cell, including, DNA, proteins, lipids and sugars (Lee, Niles, Wishnok, *et al.*, 2002; Chance, Sies & Boveris, 1979) (Calcerrada, Peluffo & Radi, 2011). Reactive oxygen species have been implicated in over 200 clinical disorders, including heart failure, endothelial dysfunction and atherosclerosis as well as many cardiovascular disorders(Tariq, 2009). Reactive oxygen species are developed under normal physiological conditions and play a role in cellular metabolic processes including various enzymatic cascades and transcriptional factors (Marnett, Riggins & West, 2003).

Through its definition, oxidative distress is an imbalance that favours the productions of ROS over the host organisms own antioxidant defence. There are

a number of ROS, such as the superoxide anion ($\bullet O_2^-$), hydrogen peroxide (H_2O_2) and the hydroxyl radical (•OH), these are generated by number of conditions *in vivo* and by several exogenous means (Floyd, West & Hensley, 2001; Jackson & Loeb, 2001). Inside the cell the main producer of ROS are the mitochondria, even under non-pathological conditions. ROS are formed through the course of normal cellular metabolism through leakage of electrons from the electron transport chain(Marnett, Riggins & West, 2003). The resulting moderate level of ROS plays a role in several physiological functions within the cells including gene expression and signal transduction. Oxidative stress can damage nucleic acids, deoxyribose residues or the phosphodiester backbone of DNA. If unrepaired, these lesions can lead to DNA base transitions and transcription stalling, causing both single and double-stranded breaks which can lead to cell death and disease(Lee, Niles, Wishnok, *et al.*, 2002; Chance, Sies & Boveris, 1979; Jackson & Loeb, 2001; Marnett, Riggins & West, 2003).

1.1.1.1.3 – DNA Methylation.

Whilst it is known that reactive oxygen species and nitrogen species are the main cause of endogenous DNA damage within the cell, they are not the only threat that the cell has to face(Holliday & Ho, 1998a; 1998b). Many cellular enzymes within metabolic pathways can also impact upon the fragile state of the DNA. S Adenosyl methionine (SAM) is a small molecular co-substrate consisting of ATP and methionine and is most commonly used in the methylation reactions of DNA, an epigenetic mechanism used in the control of gene expression(Rydberg & Lindahl, 1982). However, SAM can cause the non-enzymatic methylation of DNA, which can in turn become mutagenic, leading to cytotoxic lesions blocking replication(Tudek, Bioteux & Laval, 1992).

1.1.1.1.4 – Hydrolysis of DNA.

Given the chemical make-up of DNA, the N-glycosidic bond linking the base to the sugar phosphate backbone is labile under conditions including heating, alkylation of bases or cleavage by enzymes known as glycosylases (Lindahl, 1993). Whilst glycosylases are required for base excision repair, cleavage of the

glycosidic bond can be deleterious (Jacobs & Schär, 2011). Cleavage of the bond leads to generation of an abasic side (AP). Lindahl in 1993 estimated that approximately 10,000 lesions per human cell per day occur and AP sites are one of the most frequently found lesion with depurination of base occurring approximately 20 times more frequently than depyrimidination (Lindahl & Karlström, 1973) (Lindahl, 1993). If left unrepaired, AP sites can induce substitutions or frame-shift mutations leading to perturbed DNA synthesis and mutagenesis(Jackson & Loeb, 2001; Jackson, Chen & Loeb, 1998). This is due to preferential incorporation of adenine by polymerases next to an AP site during replication(Lawrence, Borden, Banerjee, *et al.*, 1990).

1.1.1.2 – Exogenous sources of DNA Damage.

1.1.1.2.1 – UV light damage.

Damage induced by UV light can be split into two types, UV-A and UV-B. UV-A damage is caused indirectly by producing reactive oxygen species within the cell. UV-B causes direct damage by inducing a variety of mutagenic and cytotoxic DNA lesions, such as cyclobutane pyrimidine dimers (CPDs) and 6-4, photoproducts (6-4PPs). These can interfere with base pairing during replication (Otoshi, Yagi, Mori, *et al.*, 2000). Translesion synthesis polymerases possess the ability to by-pass this damage during replication, however these polymerases are known to exhibit low fidelity and are prone to inserting adenine, thus causing a G:C-A:T transitions during replication (Sale, 2013).

1.1.1.2.2 – Ionizing radiation.

DNA damage from ionizing radiation comes from charged particles which may be an electron or ion that can pass through and ionize the DNA directly, known as direct action, or it can ionize water molecules in the vicinity of the DNA producing highly reactive •OH radicals that react with DNA through an indirect action (Santivasi & Xia, 2014). Sources of ionizing radiation can come from man made or natural sources. Types of ionizing radiation can be categorised into two groups: High linear energy transfer (HLET) such as alpha particles and low LET

(LLET) particles that arise from gamma (γ) or X-rays (Santivasi & Xia, 2014; Maier, Hartmann, Wenz, *et al.*, 2016).

Approximately 3000 damaged bases, 1000 single-strand breaks and 40 double strand breaks occur per 1 Gray (Gy) of X-ray damage. Base damage and single-strand breaks are of minor relevance for cell survival since these types of breaks are repaired by highly efficient base excision repair (BER) steps (Caldecott, 2014).The vast majority of double strand breaks induced by low-LET radiation are also repaired, however a small fraction (of approximately <5%) induced by low-LET radiation cannot be repaired due to their complexity, this can lead to cell death, senescence, mutation or genomic instability. Double strand breaks produced by high-LET radiation form most of the complex breaks and cells struggle to repair this type of damage(Maier, Hartmann, Wenz, *et al.*, 2016).

1.1.1.3 – Chemical sources of DNA damage.

1.1.1.3.1 – Methylmethane sulphonate (MMS).

MMS in an alkylating agent and carcinogen, despite this it has been used in cancer treatment (Lundin, 2005). Its method of action has been debated however it is known that HR deficient cells are sensitive to MMS. One of the proposed methods of action is that MMS methylates DNA predominantly on N7-deoxyguanosine and N3-deoxyadenosine (Lundin, 2005). Originally this action was imagined to directly lead to DNA double strand breaks, however it is now believed that HR deficient cells are particularly sensitive to MMS because it leads to stalled replication forks and cells with deficient homologous recombination have issues repairing the damaged forks(Lundin, 2005).

1.1.1.3.2 – Mitomycin C (MMC).

Mitomycin C (MMC) is administered as a prodrug and requires an enzymatic bioreduction to exert its effects. Following reduction, MMC is converted to a highly reactive bis-electrophilic intermediate that alkylates cellular nucleophiles(Paz, Zhang, Lu, *et al.*, 2012). Alkylation of DNA is known to be the most favoured mechanism of action for MMC. MMC has also been shown to

target thioredoxin reductase (TrxR), the mechanism of action has been proposed to be a stepwise process beginning with the reduction of the quinone ring of MMC by the selenothiol active site of TrxR and a subsequent alkylation of the active site by the now activated drug(Paz, Zhang, Lu, *et al.*, 2012).

1.1.1.3.3 – Camptothecin (CPT).

Camptothecin (CPT) is a cytotoxic quinolone alkaloid that binds and inhibits topoisomerase I (TOP1) (Liu, Desai, Li, *et al.*, 2000). CPT binds to TOP1 as its bound to DNA resulting in a ternary complex and stabilizes the interaction preventing the re-ligation of DNA after topo I cleavage. CPT primarily kills cells by causing S-phase specific damage (Liu, Desai, Li, *et al.*, 2000).

The reversible TOP1-CPT-DNA cleavable complexes are nonlethal by themselves, however their collision with advancing replication fork causes DNA damage, leading to cell death(Liu, Desai, Li, *et al.*, 2000). The collision is potentially lethal only if the cleavable complex is formed on the strand which is complementary to the leading strand of DNA synthesis. At high concentration, CPT causes damage to non-S phase cells, however S-phase specific cytotoxicity is unaffected by inhibition of DNA replication and involvement of transcription has been suggested (Liu, Desai, Li, *et al.*, 2000).

1.1.1.3.4 – Hydroxyurea (HU).

HU lowers the level of deoxyribonucleotides through inhibition of ribonucleotide reductase(Petermann, Orta, Issaeva, *et al.*, 2010a). During S phase, HU has been shown to inhibit the replication fork causing it to stall. Stalled replication forks eventually collapse leading to DSBs. Damage through hydroxyurea treatment is mostly conserved to S phase and results in synchronisation of the fraction of cells that survive(Petermann, Orta, Issaeva, *et al.*, 2010a; Fox, 2004).

Whilst there are a number of ways in which genomic integrity can be compromised, cells have developed intricate systems to identify and repair DNA damage in a timely and efficient manner (Iyama & Wilson, 2013; Bernstein, R,

Nfonsam, *et al.*, 2013). This process is termed the DNA damage response and consists of over 600 proteins (Bernstein, R, Nfonsam, *et al.*, 2013; Ghospurkar, Wilson, Severson, *et al.*, 2015).

1.1.2 – Mechanisms of DNA repair.

1.1.2.1 – DNA-damage signalling.

The most common chromatin modification associated with the DNA damage response is phosphorylation of the histone variant H2A.X (γH2A.X) (Fernandez-Capetillo, Lee, Nussenzweig, *et al.*, 2004). It is used to recruit various DDR factors to the vicinity of lesions to accelerate repair and also used to initiate and sustain a signalling network that activates cell cycle checkpoints preventing further genomic instability (Fernandez-Capetillo, Lee, Nussenzweig, *et al.*, 2004). ATM and ATR are serine, threonine kinases used in the DNA damage response(Jeggo & Downs, 2014). They exert cell cycle control in part through phosphorylating checkpoint kinases including Chk1, Chk2 and the transcription factor p53. ATR is activated following UV light induced damage, whereas ATM is activated in response to DSBs(Helt, Cliby, Keng, *et al.*, 2005). Both ATM and ATR can phosphorylate H2A.X to create γH2A.X. γH2A.X is used to recruit various DDR factors to the vicinity of lesions to accelerate the repair and to initiate and sustain a signalling network.

ATR-Interacting protein (ATRIP) binds to single-stranded DNA coated with RPA and interacts with ATR resulting in its accumulation at sites of DNA damage (Ball, Myers & Cortez, 2005). Binding of ATRIP to RPA-ssDNA is dependent on TOPBP1 and RAD17-dependent loading of the 9-1-1 complex (composed of Rad9, Rad1 and Hus1) which activates signalling at the site of damage (Burrows & Elledge, 2008).

1.1.2.2 – DNA Double Strand Breaks.

DNA DSBs are the most toxic type of lesion to the cells and have two main repair pathways, homologous recombination and non-homologous end-joining.

1.1.2.2.1 – Homologous recombination.

Homologous recombination uses a DNA template from a sister chromatid and as a results only occurs in replicating cells during S and G2 phases of the cell cycle(Krejci, Altmannova, Spirek, *et al.*, 2012).

Once the DSB has occurred, the MRN complex is recruited to sites of DNA damage where it binds to both sides of the break through MRE11 **(Figure 1.1)**. RAD50 then tethers the broken ends of DNA and NBS1 activates ATM through phosphorylation, which leads to ATM autophosphorylation (Marechal & Zou, 2013). ATM phosphorylates γH2A.X leading to signalling and recruitment and assembly of repair factors. Chromatin is relaxed and restructured, allowing repair proteins to access the damage. DNA is resected by MRE11, CtIP and EXO1 exposing single-stranded DNA(Krejci, Altmannova, Spirek, *et al.*, 2012; Panier & Boulton, 2013). RPA coats and protects the single-stranded DNA. RAD51 then binds and replaces the RPA, mediated by RAD52 and BRCA2(Krejci, Altmannova, Spirek, *et al.*, 2012). The RAD51-DNA nucleoprotein is made up of RAD51-DNA monomers and begins the process of strand invasion searching for sequences similar to that of the 3' overhang. Strand invasions mediated by BRCA1 leads to the formation of displacement loops (D-loop) (San Filippo, Sung & Klein, 2008). DNA synthesis occurs using the invaded strand as template and Ligase I seals the nicks creating a double Holliday junction. Holliday junctions are then resolved using MUS81/EME1 and SLX1/SLX4 or GEN1 resolvase, creating crossover products, or dissolved by TOPO3α, RMI1 and BLM RecQ helicase to generate non-crossover products.

Figure 1.1. The two main DNA double-strand break pathways NHEJ and HR. The process of NHEJ is initiated when KU70/80 binds to both ends of a DSB. This is followed by the recruitment of DNA-PK_{CS}. This functions to tether the ends and recruits other end processing factors such as Artemis. These enzymes prepare the DNA ends for re-ligation by the XRCC4-XLF-DNA LIG4 complex. NHEJ can function in all stages of the cell cycle. HR- directed DSB repair is restricted to late S and G2 stage of the cell cycle and is much more complex. DNA damage is detected by MRN (MRE11-RAD50-NBS1) complex and followed by end resection. The resection step is highly regulated and requires the activity of several nucleases including CtIP (CtBP-interacting protein). Resection generates long stretches of 3' single-stranded DNA which is coated by RPA before being replaced by RAD51 to create a RAD51-ssDNA nucleofilament. The nucleofilament searches for, finds and binds with a homologous sequence elsewhere in the genome to form a displacement D-loop, in which DNA synthesis is initiated to replace the DNA surrounding the break site. The D-loop is resolved either through dissociation of one of the invading strand, through synthesis-dependent single strand annealing (SDSA) or through migrating double Holliday junction intermediates that are cleaved through the use of resolvases or dissolved by the BLM-RMI-TOP3α complex. (Figure adapted from Panier et al., 2014)

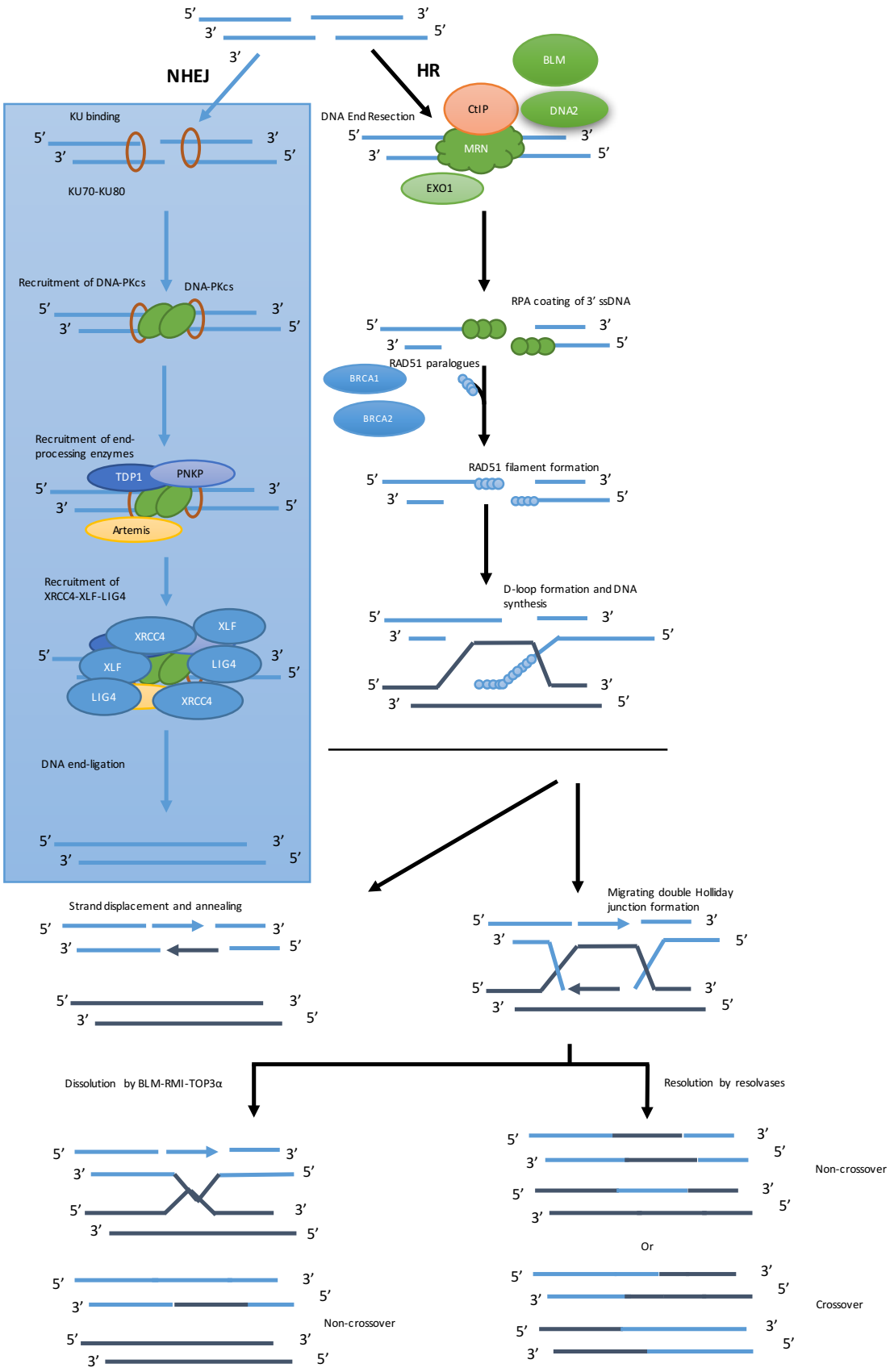
NHEJ
HR
KU binding
KU70-KU80
Recruitment of DNA-PKcs
DNA-PKcs
Recruitment of end-processing enzymes
TDP1
PNKP
Artemis
Recruitment of XRCC4-XLF-LIG4
XRCC4
XLF
LIG4
DNA end-ligation
DNA End Resection
BLM
CtIP
DNA2
MRN
EXO1
RPA coating of 3' ssDNA
RAD51 paralogues
BRCA1
BRCA2
RAD51 filament formation
D-loop formation and DNA synthesis
Strand displacement and annealing
Migrating double Holliday junction formation
Dissolution by BLM-RMI-TOP3α
Resolution by resolvases
Non-crossover
Or
Crossover
Non-crossover

1.1.2.2.2 – Non-homologous end-joining (NHEJ).

NHEJ occurs in both proliferating and in terminally differentiated cells and unlike HR, does not require a sister chromatid as a template. Instead NHEJ alters the two broken ends by various nucleases (Lees-Miller, 2003) (Lieber, Gu, Lu, *et al.*, 2009), so that they become compatible i.e. a 3'-hydroxyl and 5'-phosphate end is available for ligation. The ends are then re-ligated through the use of Ligase IV. The steps involved are outlined in **(Figure 1.1)**. It begins with the Ku70/Ku80 heterodimer binding to both ends of the break (Rivera-Calzada, Spagnolo, Pearl, *et al.*, 2006; Walker, Corpina & Goldberg, 2001). This aligns the ends of the DNA through binding of the sugar phosphate backbone. These proteins form a complex with DNA-PK and its catalytic subunit (DNA-PK_{CS}). The ends are processed by Artemis (Goodarzi, Yu, Riballo, *et al.*, 2006), XRCC4, DNA Ligase IV and XLF which facilitates the ligation of the DNA ends(Ahnesorg, Smith & Jackson, 2006a; Riballo, Woodbine, Stiff, *et al.*, 2008). There is a slight difference between classic and alternate NHEJ. Classical NHEJ involves the direct ligation of free DNA ends. However, alt-NHEJ may require end trimming that makes it less accurate. The choice between classic and the alternate pathway is regulated by 53BP1 and PARP1 (Moshous, Callebaut, de Chasseval, *et al.*, 2001). 53BP1 promotes classic NHEJ and PARP1 alternate NHEJ. Alt-NHEJ involves increased resection of the free ends to allow micro-homologies to be found, this makes alt-NHEJ less accurate and more likely to result in large deletions or translocations. Classic NHEJ is initiated by the binding of KU70/80 to protect the ends before recruiting DNA-PK_{CS}, Artemis and others to allow more efficient ligation. These factors limit resection and promote ligation of broken ends involving little or no micro-homology. Defects in classic NHEJ channels DSBs towards alt-NHEJ where PARP1 binds to the free ends instead of the KU complex. Alt-NHEJ requires resection by MRN and CtIP, this resection exposes micro-homologies to promote pairing of broken ends which are then ligated by Lig III/XRCC1. Suppression of Alt-NHEJ is achieved by 53BP1 which restricts end-processing by MRN/CtIP (Shaheen, Allen, Nickoloff, *et al.*, 2011).

Compared with HR, NHEJ is error-prone and though it is the main DNA repair pathway in human cells, it can lead to genomic rearrangements, deletions and mutations which can lead to cell death. Deficiencies in HR and NHEJ has been linked to various disorders (O'Driscoll & Jeggo, 2006).

1.1.2.3 – Repair of Altered Bases

Though double strand breaks are the most deleterious forms of DNA damage single strand breaks also occur. These are discontinuities in one strand of the DNA which if left unrepaired can turn into double strand breaks. There are many different pathways to repair single strand breaks (Caldecott, Abrahams & Geschwind, 2008).

1.1.2.3.1 – Nucleotide Excision Repair (NER).

NER deals with the major UV photoproducts in DNA as well as DNA adducts. NER works through a multi-step 'cut and patch' type reaction(Ogi, Limsirichaikul, Overmeer, *et al.*, 2010). There are two sub-pathways in NER, the first is the global genome NER (GG-NER) which prevents mutagenesis by probing the genome for helix distorting lesions and the other is transcriptional coupled NER (TC-NER) which removes transcription-blocking lesions to permit unperturbed gene expression (Marteijn, Lans, Vermeulen, *et al.*, 2014). Interestingly defects in GG-NER results in cancer predisposition and defects in TC-NER cause a variety of diseases such as Xeroderma pigmentosum and Cockayne syndrome (Rapin, Lindenbaum, Dickson, *et al.*, 2000). The difference between the two sub-pathways is at the point of damage recognition. In GG-NER XPC-RAD23B finds bulky distortions in the helix structures, whereas TC-NER involves the recruitment of CSB, CDSA and XAB2 to arrested RNA polymerases. Once the site of damage is identified the pathways come together to form a common repair process. TFIIH, a complex consisting of a 7 subunit core (XPD, XPB, P62, P52, P44, P34 and TTDA) and a 3 subunit (CDK7, Cyclin H and Mat1) cyclin activating kinase complex (CAK) is recruited to the site of damage(Dijk, Typas, Mullenders, *et al.*, 2014). XPB and XPD, 5'-3' and 3'-5' DNA helicases, found in the TFIIH complex unwind the helix in proximity to the lesion

located in the DNA(Rapin, Lindenbaum, Dickson, *et al.*, 2000). Following unwinding, recruitment of XPA and RPA results in the dissociation of the CAK complex and protection of the single stranded DNA. This allows the full opening of the DNA around the lesion to occur. This favours the recruitment of XPG and XPF endonucleases to incise and remove a short stretch of single-stranded DNA of about 25-30 nucleotides containing the lesion. Polymerases are then recruited through PCNA, RPA and the clamp loader RCF to fill in the excised fragment (Dijk, Typas, Mullenders, *et al.*, 2014; Rapin, Lindenbaum, Dickson, *et al.*, 2000). LigI-FEN1 in S phase, or Lig IIIα-XRCC1 throughout the remainder of the cell cycle are recruited to seal the phosphate backbone and restore the integrity of the DNA(Caldecott, 2014).

1.1.2.3.2 – Mismatch Repair (MMR).

Correct structure of the helical DNA and maintenance of genetic integrity is dependent on the fidelity of DNA replication and the need to follow the Watson-Crick base pairing sequence. This means that in the DNA sequence, Guanine must pair with Cytosine and Adenine must pair with Thymine. MMR is responsible for scanning and maintaining this sequence by correcting mismatch base substitutions and insertion-deletion mismatches. DNA replication must proceed with both efficiency and accuracy. To help ensure fidelity DNA polymerases have high nucleotide sensitivity and an ability to proof-read, a process that enables the polymerase to identify an incorrect base pair, reverse its direction by one base pair of DNA and excise and replace the mismatched base during DNA replication(Kunkel & Erie, 2005). Some polymerases, specifically translesion synthesis polymerases, increase the frequency of mismatch bases (Sale, Lehmann & Woodgate, 2012). Furthermore microsatellites can lead to polymerase slippage which can cause insertions and deletions (Goellner, Tester & Thibodeau, 1997; Kunkel, 2003; Lange, Takata & Wood, 2011).

Mismatched bases are identified by MutS, one of two major heterodimeric mismatch repair complexes. MutS consists of MutSα and MutSβ. The

identification and binding of MutS results in recruitment of multiple MutL complexes. MutL consists of MutLα, MutLβ and MutLγ (Kunkel & Erie, 2005). Once the mismatch repair pathway is activated PCNA binds and MutL's endonuclease activity creates a nick in the DNA backbone (Modrich, 1994; Kunkel & Erie, 2005). After the nick is created EXO1 can remove the stretch containing the mismatch leading to a region of ssDNA, which ends when EXO1 collides with an Okazaki fragment (Genschel, Bazemore & Modrich, 2002) or a second MutL created nick. RPA coats the newly exposed ssDNA until replicative polymerases and the relevant ligases repair the DNA.

1.1.2.3.3 – Base Excision Repair (BER)

Base excision repair removes small non-helix distorting base lesions which are often caused by deamination, oxidation and alkylation (Lindahl, 1999). The base damage is recognized and removed by glycosylases, either specific mono- or bi- functional proteins that results in a single-strand DNA break. The single-strand break is repaired by the single-strand break repair pathway(Dianov & Hübscher, 2013).

There are many different known DNA glycosylases that fall into one of six known super families (Brooks, Adhikary, Rubinson, *et al.*, 2013). They are divided into structural super families based upon their substrate action though their mode of action is shared throughout. The mode of action encompasses a flipping action of the damaged base, basically flipping the damaged base into the glycosylases active pocket(Jacobs & Schär, 2011). The cleavage mechanism is divided into mono- and bi-functional enzymes. Once the damaged base has been identified the N-glycosidic bond is cleaved through nucleophilic attack leaving an abasic site. This cleavage activity is found in both mono- and bi- functional enzymes. Unlike the mono-functional enzyme the bi-functional activity also has the capability to convert the base lesion into a DNA single strand break that does not require AP endonuclease activity (Dianov & Hübscher, 2013). Currently there are six mono-functional DNA glycosylases (UNG, SMUG1, MBD4, TDG, MYH

and MPG) and five bi-functional (OGG1, NTLH1, NEIL1, NEIL2 and NEIL3) (Jacobs & Schär, 2011).

1.1.2.3.4 – Single Strand Break Repair.

Whilst not as toxic as double-strand breaks, single-strand breaks are approximately one order of magnitude more frequent. Single strand breaks can occur as a result of direct damage caused by reactive oxygen species, collision with transcription machinery, due to stalled complexes of endogenous enzymes such as ligases and TOP1 or as mentioned previously as an intermediate of base excision repair (BÃ¼rkle & Virág, 2013). If single strand breaks are not repaired in a timely fashion this can impact the cell in multiple ways. In replicating cells, it can lead to replication fork collapse and double strand breaks. Collision with the RNA polymerase and the transcription complex can result in stalled transcription, premature termination of protein synthesis and incorporation of RNA loops(Dianov & Hübscher, 2013).

Single strand break repair is a multi-step process (Caldecott, Abrahams & Geschwind, 2008; Caldecott, 2014). Firstly, the single-stranded break is detected by poly-ADP ribose polymerase (PARP). Following this PARP becomes activated and synthesises chains of ADP-ribose(Caldecott, 2014). Activation of PARP allows for chromatin remodelling and sequestering of the XRCC1 chaperone protein.

XRCC1 interacts with several end-processing enzymes such as ligase III, PNKP, PARP and TDP1 and this allows the damaged termini to be processed.

Following detection, end-processing allows enzymes to modify the break termini to efficiently cleave the modification and restore the required 3'-OH and 5'-P for ligation (Caldecott, 2014). The next step involves gap filling, which can result in the divergence of this particular pathway. These are termed long patch or short patch repair. If only one nucleotide is required to fill the gap then this leads to short-gap repair where XRCC1 and LigIIIα are the main enzymes. However, long patch repair is involved for lesions between 2-12 nucleotides (Caldecott, 2014).

This results in the removal of the protrusion of single-strand DNA by FEN1, and gap filling by Polβ, Polδ or Polε before ligation. The final step in the repair pathway is the sealing of the phosphate backbone. This is done in an ATP dependent manner and varies depending on the repair pathways. If it involved short-patch repair then LigIIIα is used or LigI in long patch repair(Caldecott, 2014).

1.1.2.3.5 – Translesion synthesis.

Translesion synthesis (TLS) is a DNA damage tolerance process that allows the DNA replication machinery to replicate past DNA lesions such as thymine dimers or AP sites (Sale, 2013). This process involves switching out regular DNA polymerases for specialised translesion polymerases, such as DNA polymerase IV, or V from the Y polymerase family (Sale, 2013). The polymerase switching is thought to be mediated by, amongst other factors, the post-translational modification of PCNA(Bienko, Green, Sabbioneda, *et al.*, 2010). TLS polymerases often have low fidelity, that is they have a high propensity to insert wrong bases on undamaged templates relative to regular polymerases. From a cellular perspective, risking the introduction of point mutations during TLS may be preferable to resorting to more drastic mechanisms of DNA repair that could result in gross chromosomal aberrations or cell death(Kim & D'Andrea, 2012; Sale, 2013).

1.1.2.3.6 – The Global Response to DNA Damage.

The global response to DNA damage is the way cells act out of self-preservation. Cells can trigger multiple pathways of macromolecular repair, lesion bypass, tolerance or even apoptosis. Common features include checkpoint activation, transcription, cell cycle arrest and inhibition of cell division. Following DNA damage cell cycle checkpoints are activated, this pauses the cell cycle and allows repair of the damage. Checkpoint activation can arrest cells at the G1/S, and G2/M boundaries and coordinate events intra-S (Bartek, Lukas & Lukas, 2004; Chen, Szakal & Castellucci, 2013). Checkpoint activation is controlled by two master kinases, ATM and ATR (Marechal & Zou, 2013). Both ATM and ATR

kinases phosphorylate downstream targets in a signal transduction cascade leading to cell cycle arrest (Jazayeri, Falck, Lukas, *et al.*, 2006). An important downstream target of ATM/ATR is p53 and is required for inducing apoptosis following DNA damage (Bartkova, Horejsí, Koed, *et al.*, 2005). The cyclin-dependent kinase inhibitor p21 is induced by both p53-dependent and p53 independent mechanisms and can arrest the cell cycle at the G1/S and G2/M checkpoints by deactivating cyclin-dependent kinase complexes.

Pathological effects of poor DNA repair include genetic deficiencies, which, in animal models, often show decreased life span and increased cancer incidence. Mice deficient in telomere maintenance mechanisms or the NHEJ pathway develop lymphoma and infections more often resulting in shorter lifespans than wild-type mice. However not every DNA repair deficiency creates the predicted effects for example mice with deficiency in the NER pathway exhibit shortened lifespan without the higher rates of mutation(Harada, Shiomi, Koike, *et al.*, 1999).

Accurate DNA repair is critical to maintain genomic integrity, however accurate chromosome segregation during mitosis is also an important factor. To this end a family of macromolecular complex are employed for chromosome condensation, sister chromatid cohesion and accurate chromosomal segregation. These complexes are known as the SMC family of protein complexes and are made up of cohesin, condensin and the SMC5/6 complex.

1.2 – Structural Maintenance of Chromosomes Family of Complexes.

The Structural Maintenance of Chromosome (SMC) proteins regulate the structural and functional organization of chromosomes in organisms ranging from bacteria to humans (Hirano, 2006). SMC family complexes have a unique architecture so that they can act as dynamic linkers of the genome. A series of genetic screens revealed crucial roles in both mitosis and meiosis, chromosome-wide gene regulation and recombination repair (Hirano, 2006). The family currently consists of cohesin (SMC1/3), condensin (SMC2/4) and SMC5/6 (Uhlmann, 2016). Associated with the SMC heterodimers are a number of Non-

SMC subunits, Scc1 and Scc3 in the case of cohesin and CAP-H, CAP-D and CAP-G for condensin. Smc5/6 is associated with six Non-SMC Elements Nse1-6 in yeast and NSMCE1-4 in humans(Murray & Carr, 2008; Uhlmann, 2016). Structural analysis of SMC proteins shows they are similar in structure with two long coiled coil regions with a hinge region in the middle and globular amino and carboxyl groups at their terminal regions (Melby, Ciampaglio, Briscoe, *et al.*, 1998).

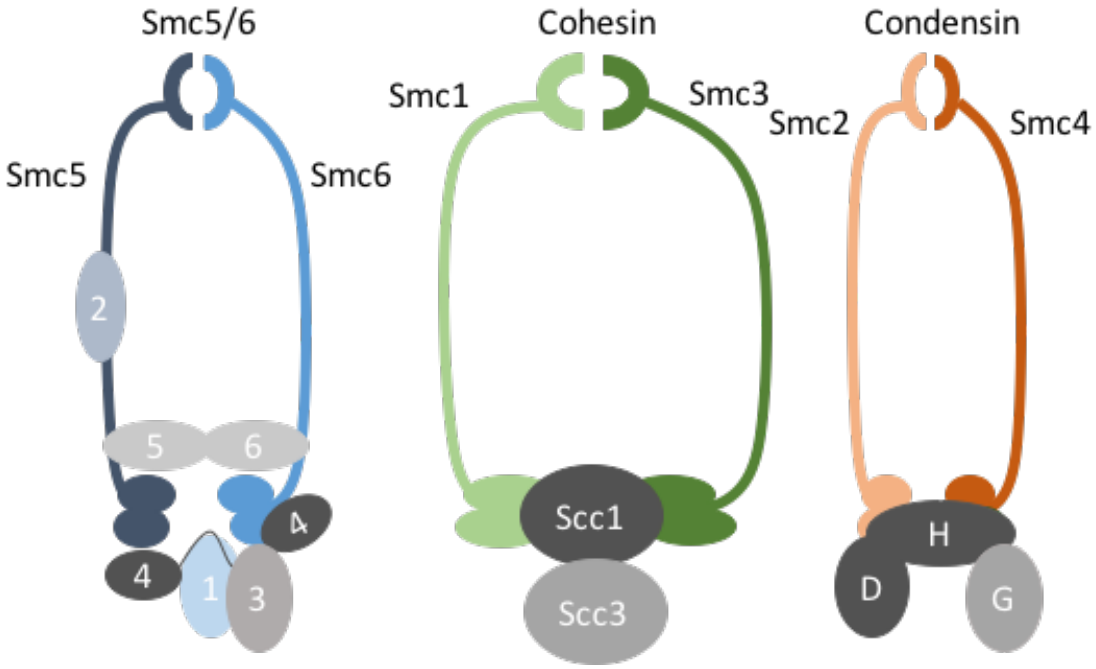

Figure 1.2. Representations of SMC family of complexes. Cohesin, condensin and Smc5/6. These complexes share a common architecture. Two SMC heterodimers, and a Kleisin subunit are common features shared by all three members of the SMC family. The Kleisin subunit bridges the heads of the SMC heterodimers and in the case of cohesin is cleaved to allow passage of DNA and is so named for the Greek word *kleisimo*. In the Smc5/6 image, 1, 2, 3, 4, 5 and 6 refer to Nse1-6 where Nse1 is a ubiquitin ligase, Nse2 is a SUMO ligase, Nse3 is a MAGE protein, Nse4 is the Kleisin subunit and Nse5/6 are HEAT repeat proteins. (Figure adapted from Murray and Carr 2008).

1.2.1 – Cohesin

The core cohesin complex contains two SMC proteins, SMC1 and SMC3 and two non-SMC proteins: Scc3 in yeast/ STAG1,2, 3 (SA1, 2, 3) in human cells and a Kleisin subunit (Scc1(yeast) /RAD21/RAD21L or REC8 in humans). The composition depends on where the complex is localised as SA1 is found mainly at telomeric regions and SA2 at centromeres. SA3 is found in meiosis(Brooker & Berkowitz, 2014; Nasmyth & Haering, 2009) where the kleisin is REC8. The SMC1/3 subunits are flexible coiled-coil proteins that link tail to tail at the hinge and head to head at their ATPase heads to form a heterodimer. The Scc1 protein bridges the SMC1 and SMC3 heads which stabilises their interaction and recruits the remaining Scc3 (SA1, 2, 3), Pds5 and Wapl subunits (Haering, Löwe, Hochwagen, *et al.*, 2002). Together these subunits form a ring-like complex that is proposed to physically interacts with the sister chromatids by topological

embrace from S phase of the cell cycle until the metaphase to anaphase transition(Nasmyth & Haering, 2009; Ocampo-Hafalla & Uhlmann, 2011).

Cohesin must bind to chromosomes before the onset of DNA replication as this allows cohesin to establish functional linkages and its loading is dependent on the Scc2/4 loader(Bermudez, Farina, Higashi, *et al.*, 2012). The mechanism in which cohesin binds to DNA has long been debated but it is thought to mediate sister chromatid cohesion by encircling the sister strands. Cleavage of the Scc1 subunit by the protease separase at the metaphase to anaphase transition opens the ring and releases the sister chromatids to allow segregation into daughter cells (Sun, Kucej, Fan, *et al.*, 2009).

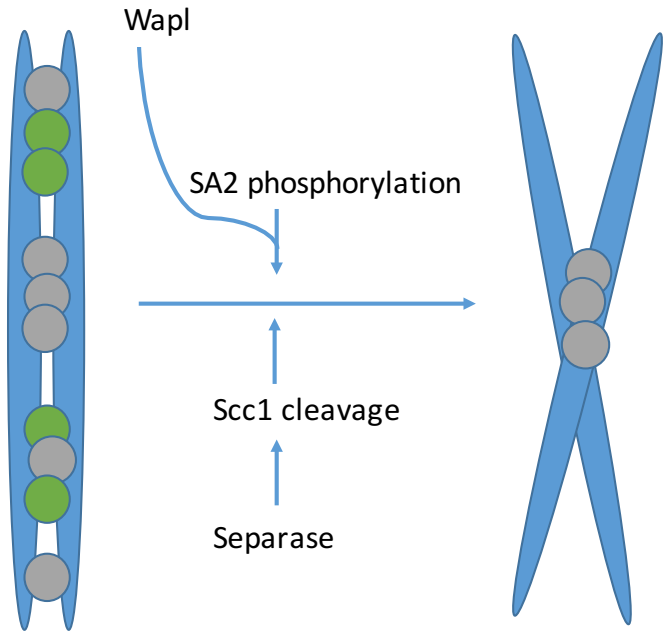

Figure 1.3. Cohesin is removed from DNA in two distinct mechanisms. Phosphorylation of STAG and the presence of Wapl degrades cohesion and cleavage of Scc1 by separase which initiates the final separation.

The cohesin complex has been shown to play a crucial role in chromosome condensation and during the repair of double-stranded DNA by HR between sister chromatids(Mizuguchi, Mizuguchi, Fudenberg, *et al.*, 2014; Wu & Yu,

2012). During S phase cohesion between sister chromatids is established and depends on Sororin, Esco1 and Esco2. Cohesin is removed from DNA in two distinct mechanisms, the first during prophase involves the phosphorylation of either STAG1 or STAG2 depending on the localisation of the cohesin. The second step involves the cleavage of Scc1 (RAD21) by separase (Sun, Kucej, Fan, *et al.*, 2009). This is restricted to the metaphase/anaphase transition, and is inhibited by the spindle assembly checkpoint until all the chromosomes are correctly aligned at the metaphase plate. Inhibition is achieved through phosphorylation of serine 1126 of separase, by securin binding to separase and lastly through the bulk of separase being excluded from the nucleus (Sun, Kucej, Fan, *et al.*, 2009).

1.2.1.1 – The Scc2-Scc4 Cohesin Loader Complex.

The Scc2/4 loader complex is conserved throughout many organisms (Bermudez, Farina, Higashi, *et al.*, 2012). The mechanism of loading is thought to be by opening the cohesin ring through regulation of the ATPase domains in the SMC1-3 heads. Bermudez et al, 2012 shows that cohesin and Scc2/4 are bound weakly to chromatin normally, however following replication cohesin stably interacted with DNA whereas Scc2/4 does not. Loss of Scc1 (Kleisin) stops Scc2/4 interacting with centromeres from anaphase until late G1. Cohesin appears to trigger its own loading by enabling Scc2/4 to connect with chromosomal landmarks marked by the Ctf19 kinetochore subcomplex in budding yeast and CENP-P in humans (Fernius, Nerusheva, Galander, *et al.*, 2013). In humans, mutation of the loader complex in one allele does not appear to affect levels of cohesin however it can lead to the severe developmental disorder Cornelia de Lange syndrome (CdLS) (Xu, Sowa, Cardenas, *et al.*, 2015; Kikuchi, Borek, Otwinowski, *et al.*, 2016; Gard, Light, Xiong, *et al.*, 2009).

1.2.1.2 – Cohesin complex and developmental disorders.

Disruption of normal cohesin activity during human development causes associated disorders known as Cohesinopathies. The most common of these is known as Cornelia de Lange Syndrome (CdLS), this affects between 1/10,000

and 1/30,000 live births(Xu, Sowa, Cardenas, *et al.*, 2015). CdLS patients show a large degree of phenotypic variation which can include craniofacial abnormalities, microcephaly, developmental delay, hirsutism and upper limb abnormalities. Heterozygous mutations in NIPBL are the most common cause of CdLS accounting for almost 65 % of cases. The remaining percentage of cases have been attributed to mutations in SMC1A, SMC3, HDAC8 and RAD21. Cell lines from CdLS patients shows a signature change in expression levels of Scc2/4 as well as reduced levels of cohesin association in the promoter region of many of the affected genes(Bermudez, Farina & Higashi, 2012; Ocampo-Hafalla & Uhlmann, 2011; Gard, Light, Xiong, *et al.*, 2009). Another similar, but extremely rare disorder termed Roberts syndrome (RBS) is caused by recessive mutation in ESCO2 which acetylates SMC3. Roberts syndrome patients exhibit many similar phenotypes as CdLS patients(Xu, Lu & Gerton, 2014).

1.2.1.3 – Cohesin complex and cancer.

Mutations in cohesin associated with cancer were first reported in 2008 when Barber et al, identified heterozygous somatic missense mutations in genes encoding SMC1A, SMC3, NIPBL and STAG3 (a component of meiotic cohesin) associated with colon cancers (Barber, McManus, Yuen, *et al.*, 2008; Hill, Kim & Waldman, 2016). Individual deletions of RAD21 and STAG2 were reported in 2010 to be found in chronic myelomonocytic (CML) and acute myeloid leukaemia (AML) amongst others(Xu, Balakrishnan, Malaterre, *et al.*, 2010; Deb, Xu, Tuynman, *et al.*, 2014). Since the initial discovery of cohesin mutations in colon cancer numerous studies have demonstrated that cohesin gene inactivation is a common and important event in the pathogenesis of diverse human cancers including bladder cancer, Ewing sarcoma and myeloid malignancies as well as glioblastoma multiforme, endometrial carcinoma and other tumour types(Hill, Kim & Waldman, 2016). The most commonly mutated of these is STAG2, with other cohesin genes including RAD21, SMC1A, SMC3 and NIPBL at a lower level suggesting STAG2 is a tumour suppressor (Hill, Kim & Waldman, 2016). It is likely that in the coming years a dramatic improvement in

the understanding of key cancer-relevant biochemical effects and phenotypes of cohesin inactivation in the pathogenesis of cancer will emerge.

1.2.2 – Condensin

Another member of the SMC superfamily is condensin and, as the name suggests, this plays a central role in chromosome condensation and segregation during both mitosis and meiosis(Piazza, Haering & Rutkowska, 2013). There are two forms of condensin in human cells, condensin I and condensin II. Both forms are comprised of five subunits, however they both have a pair of core subunits, SMC2 and SMC4 (Hirano, 2006). Each of the complexes contains a distinct set of Non-SMC regulatory subunits, a pair of HEAT-repeat subunits and a Kleisin subunit to bridge the SMC2/4 heads. Condensin I contains CAP-D2 and CAP-G as their HEAT repeats and CAP-H as the Kleisin. Condensin II contains CAP-D3 and CAP-G2 as its HEAT repeats and CAP-H2 as its Kleisin(Hirano, 2005). Condensin I is conserved from yeast to humans, but yeasts have no condensin II. Loss of members of the condensin complex leads to embryonic lethality, knockdown of SMC2 using siRNA show modest defects in condensation in metaphase but become severe in anaphase(Sutani, Sakata, Nakato, *et al.*, 2015).

In cells condensin I and condensin II have different activities depending on the stage of the cell cycle. In mammalian cells, condensin I is sequestered in the cytoplasm during interphase and only gains access to chromosomes after nuclear envelope breakdown (NEBD) in prometaphase(Hirano, 2012; Yokoyama, Zhu, Zhang, *et al.*, 2015). Condensin II on the other hand is localised to chromosomes from interphase through prophase and participates in the early stages of chromosome condensation within the prophase nucleus. After NEBD both condensin I and condensin II collaborate to support proper assembly of chromosomes in which sister chromatids are well resolved by metaphase.

Altering levels of condensin in various cells can have effects on the morphology of chromosomes, however this varies depending on the organism. In Xenopous extracts there is a 5:1 ratio of condensin I to condensin II, in HeLa cells there is

a 1:1 ratio. Altering levels of condensin I to 1:1 with condensin II in Xenopous extracts leads to shorter and thicker chromosomes (Green, Kalitsis, Chang, *et al.*, 2012). When condensin II was depleted to 1:0 the chromosomes appeared longer. This strongly suggested condensin II primarily contributes to axial shortening of chromatids, whereas condensin I supports their lateral compaction(Yokoyama, Zhu, Zhang, *et al.*, 2015).

1.2.2.1 – Cell cycle regulators of Condensins.

Attempting to understand the cell cycle regulation of condensin is very difficult given the multi-subunit architecture of both condensins and their diverse functionality in chromosome dynamics(Hirano, 2005). There are a wide range of regulatory signals imposed on condensin subunits that control their localization, loading/unloading, activation/inactivation and fine-tuning these events. The regulators of condensin are wide and varied, a multitude of mitotic kinases such as Ckd1, Aurora B and Polo-like kinases have been shown to phosphorylate and regulate condensins though their contribution is dependent on different organisms(Piazza, Haering & Rutkowska, 2013; Sutani, Sakata, Nakato, *et al.*, 2015).

1.2.3 – The SMC5/6 Complex.

1.2.3.1 – Discovery of SMC5/6

smc6 was first identified in 1975 as *rad18* in fission yeast in a screen for mutants sensitive to DNA damage (Nasim & Smith, 1975) and cloned and characterised in 1995 (Lehmann, Walicka, Griffiths, *et al.*, 1995). The *rad18-X* mutant was shown to have increased sensitivity to both UV and gamma irradiation (Lehmann, Walicka, Griffiths, *et al.*, 1995). The homologue in *Saccharomyces cerevisiae RHC18* was also identified. Both *rad18* and *RHC18* were found to be required for DNA repair and gene deletion showed both were essential for cell viability (Lehmann, Walicka, Griffiths, *et al.*, 1995). Five years later the *rad18* partner in *S. pombe*, *spr18*, was identified and also found to be essential (Fousteri & Lehmann, 2000). Sequence analysis revealed both Rad18 and Spr18

to be members of the SMC superfamily. To avoid confusion with the *S. cerevisiae* post replication repair protein Rad18 and to highlight the conservation with other SMC proteins, Rad18 and Spr18 were later named *smc6* and *smc5*, respectively, and this nomenclature is used across organisms in an effort to improve clarity.

1.2.3.2 – Composition of SMC5/6

Smc5 and Smc6, like other SMC proteins, have globular N- and C- terminal domains that are involved in ATP hydrolysis and Mg^{2+} binding(Lehmann, Walicka, Griffiths, *et al.*, 1995). They also contain two extended α-helical coiled coil domains separated by a hinge region that is essential for the interaction between Smc5 and Smc6. The coiled coils fold back at the hinge region creating two 50 nm structures. As with the other members of the SMC superfamily, cohesin and condensin, SMC5/6 was found to form a complex made of the core Smc5 and Smc6 proteins and Non-SMC-Elements. In yeasts these are referred to as NSE's whilst in humans they are referred to as NSMCE's (Sergeant, Taylor, Palecek, *et al.*, 2005). See **Table 1.1** for a list of genes and proteins that form the complex across various species. In 2001 human homologues of Smc5 and Smc6 were characterised(Taylor, Moghraby, Lees, *et al.*, 2001). In 2008 the other members of the SMC5/6 complex in humans were identified (Taylor, Copsey, Hudson, *et al.*, 2008a). Smc5/6 is associated with six Non-SMC Elements, Nse1-6 in yeast and NSMCE1-4 in humans(Murray & Carr, 2008; Uhlmann, 2016). Nse1 resembles a RING-finger ubiquitin E3 ligase, Nse2 functions as an E3 SUMO ligase, Nse3 forms a MAGE domain, Nse4 resembles a kleisin subunit to bridge the heads of Smc5 and Smc6 and Nse5 and Nse6 also associate with the head domains.

siRNA knockdown of members of the SMC5/6 complex showed that knockdown of any of the components drastically reduced the protein levels of other member of the complex, with the exception of NSMCE2. Similarly, knockdown of NSMCE2 resulted in reduced levels of NSMCE2 but not as significant a loss of the other components. These results suggest that all the components except for

NSMCE2 are necessary for the stability of the complex and in the absence of the complex the components are degraded (Taylor, Copsey, Hudson, *et al.*, 2008a).

SMC5/6 complex component.	S. cerevisae Gene/Protein	S. pombe Gene/Protein	H. sapien Gene/Protein	M. musculus Gene/Protein
SMC5	SMC5/Smc5	smc5/Smc5	SMC5/SMC5	Smc5/SMC5
SMC6	SMC6/Smc6	smc6/Smc6	SMC6/SMC6	Smc6/SMC6
NSE1	NSE1/Nse1	nse1/Nse1	NSMCE1/NSMCE1	Nsmce1/NSMCE1
NSE2	MMS21/Mms21	nse2/Nse2	NSMCE2/NSMCE2	Nsmce2/NSMCE2
NSE3	NSE3/Nse3	nse3/Nse3	NSMCE3/NSMCE3	Ndnl2/NSMCE3
NSE4	NSE4/Nse4	nse4/qri2/Nse4	NSMCE4a/NSMCE4A	Nsmce4a/NSMCE4A
NSE5	NSE5/Nse5	nse5/Nse5	SLF2/SLF2	Fam178a/FAM178A
NSE6	NSE6/Nse6	nse6/Nse6	SLF1/SLF1	Slf1/ SLF1

Table 1.1. SMC5/6 complex components across human, yeasts and mouse.

1.2.3.2.1 – SMC6

Mutations in Smc5/6 results in defects in growth and defective DNA repair. Deletion mutants of Smc6 are lethal and therefore hypomorphic mutations are most commonly used to explore phenotypes. The two first hypomorphic mutants to be identified in fission yeast, *smc6-74* and *smc6-X,* have been extensively characterised (Lehmann, Walicka, Griffiths, *et al.*, 1995; Verkade, Bugg, Lindsay, *et al.*, 1999; Irmisch, Ampatzidou, Mizuno, *et al.*, 2009; Ampatzidou, Irmisch, O'Connell, *et al.*, 2006). Both mutations are sensitive to DNA damage and have defects in homologous recombination (Verkade, Bugg, Lindsay, *et al.*, 1999; Ampatzidou, Irmisch, O'Connell, *et al.*, 2006; Irmisch, Ampatzidou, Mizuno, *et al.*, 2009). The *smc6-X* mutation (R706C) maps close to the hinge region. The *smc6-74* mutation (A151T) is within a highly conserved arginine finger in the ATP-binding pocket of the N-terminal globular domain. This suggests *smc6-74* might affect DNA-dependent ATP binding/hydrolysis as mutations which affect the ATP binding sites are lethal (Verkade, Bugg, Lindsay, *et al.*, 1999; Fousteri & Lehmann, 2000; Irmisch, Ampatzidou, Mizuno, *et al.*, 2009). Defects in *smc6-74* but not *smc6-X* can be suppressed through overexpression of a multi-BRCT domain protein Brc1 (Verkade, Bugg, Lindsay, *et al.*, 1999). Both mutants are defective in resolving HR-dependent intermediates that develop after collapsed replication forks (Ampatzidou, Irmisch, O'Connell, *et al.*, 2006). Therefore, the Smc5/6 complex has a function processing HR intermediates generated at collapsed replication forks.

1.2.3.2.2 – NSE2

Nse2 supports both functions of Smc5/6 in cell growth and DNA repair, through docking to the arm region of Smc5. There are two distinct regions of Nse2. The N-terminal which is dedicated to Smc5 binding through formation of a helix bundle with a coiled-coil region of Smc5. Its C-terminal half includes the SUMO ligase domain, which adopts a RING E3 structure. Structural and mutational analysis show the interaction of Nse2 and Smc5 are required for cell growth and resistance to DNA damage. However, the RING domain confers specificity to the unique SUMO E2-E3 interaction. The Nse2 subunit is essential, but its

activities can be separated out as mutations that ablate the SUMO ligase can grow at a reasonable rate (Zhao & Blobel, 2005; Andrews, Palecek, Sergeant, *et al.*, 2005; Sergeant, Taylor, Palecek, *et al.*, 2005). The fission yeast *nse2-SA* mutant, harbouring mutation in the SP-RING domain that ablates the SUMO ligase activity, causes sensitivity to HU and MMS, however no sensitivity to UV is observed(Andrews, Palecek, Sergeant, *et al.*, 2005). Mutations in Nse1 (C199S and C216S) can suppress the sensitivity of Nse2-SA (Tapia-Alveal & O'Connell, 2011a; Andrews, Palecek, Sergeant, *et al.*, 2005).

In mice the NSMCE2 subunit suppresses recombination and micronuclei formation and is critical to prevent the onset of cancer and aging in mice(Jacome, Gutierrez-Martinez, Schiavoni, *et al.*, 2015). Payne et al 2014 demonstrated an association between compound heterozygosity for rare frameshift mutations in *NSMCE2* in humans and primordial dwarfism, extreme insulin resistance and primary gonadal failure.

1.2.3.2.3 – NSE1

Nse1 contains a variant RING (Really Interesting New Gene) domain. Strains with cysteine to alanine mutations in the RING finger domain are viable but show DNA repair defects. Deletion of the RING finger domain is similarly defective in repair and inhibits the recruitment or retention of Smc5/6 to nuclear foci induced by DNA damage (Pebernard, McDonald, Pavlova, *et al.*, 2004). Nse1's RING finger domain has sequence similarity with an E3 ubiquitin ligase and has been demonstrated using recombinant proteins (McDonald, 2003; Pebernard, Perry, Tainer, *et al.*, 2008). The activity is stimulated through its interaction with Nse3 (Doyle, Gao, Wang, *et al.*, 2010; Pebernard, Perry, Tainer, *et al.*, 2008). Smc5/6 is unique in that it is the only member of the SMC superfamily whose subunits have their own enzymatic functions and whilst it is attractive to have both SUMO and E3 ubiquitin ligase functions in one complex it has also been shown that both the SUMO and E3 ubiquitin ligase is required for SMC5/6 function(Pebernard, McDonald, Pavlova, *et al.*, 2004; McDonald, 2003). Nse1 also has been shown to stabilize the interaction of Nse4 with Nse3 in the Nse1-3-4 subcomplex. Nse1-C216S also suppresses phenotypes associated with

smc6-X and *smc6-74* through post-replicative repair (PRR).(Tapia-Alveal & O'Connell, 2011b).

1.2.3.2.4 – NSE3

Nse3/NSMCE3 is related to the Melanoma Associated Antigen (MAGE) family of proteins. There are 55 MAGE genes in the human genome subdivided into different classes based on their protein structures. Many of them are expressed only in tumour cells or germ line cells. *NSMCE3* maps to chromosome 15q, close to the autistic susceptibility region but it not involved in these disorders. It is closely related to MAGEF1 and expressed in all tissues (Taylor, Copsey, Hudson, *et al.*, 2008a; Doyle, Gao, Wang, *et al.*, 2010)

1.2.3.2.5 – NSE4

In SMC5/6, the Kleisin subunit is Nse4/NSMCE4 and bridges the head between SMC5 and SMC6, it is structurally similar to that of other kleisins. Cohesin's kleisin, Scc1/RAD21 has an N-terminal helix-turn-helix which interacts with the SMC3 head whilst its C-terminal interacts with the two most C-terminal beta sheets of SMC1(Palecek, Vidot, Feng, *et al.*, 2006). Nse4 possesses conserved hydrophobic patterns similar to other Kleisins. Sequence threading algorithms revealed similar structural organisation compared to Scc1. Point mutations in Nse4 can disrupt interactions with Nse3 and Smc5 and some point mutations can disrupt the interaction with only Smc5 and still maintain an interaction with Nse3. Nse4's interaction with SMC5 can be abolished by deletion of the 55 aa sequence of the SMC5 C-terminal. In cohesin Scc1 is cleaved prior to anaphase by separase, however removal of Nse4 does not follow this method and levels of Nse4 does not change during the cell cycle (Palecek, Vidot, Feng, *et al.*, 2006). In humans there are two isoforms of NSMCE4, a and b, NSMCE4b is only found expressed in the male testis whereas NSMCE4a is expressed throughout the body(Bavner, 2005; Taylor, Copsey, Hudson, *et al.*, 2008b).

1.2.3.2.6 – NSE5 and NSE6

Finally, there are two additional components of Smc5/6 complex, Nse5 and Nse6. These are essential in budding yeast but non-essential in fission yeast (Pebernard, Wohlschlegel, McDonald, *et al.*, 2006; Stephan, Kliszczak & Morrison, 2011) and not part of the core SMC5/6 complex in human cells (Taylor, Copsey, Hudson, *et al.*, 2008a). Nse5 and Nse6 both interact with full length Smc5 and Smc6(Pebernard, Wohlschlegel, McDonald, *et al.*, 2006). The interaction of Nse5 with Smc5 and Smc6 can be ablated through deletion of the globular heads of both. Deletion of the 55 aa of Smc5 that ablates the Nse4-Smc5 interaction does not affect the interaction of Nse5-Smc5 showing that Nse5 binds Smc5 and Smc6 but at a site not shared by Nse4 (Palecek, Vidot, Feng, *et al.*, 2006).This is also observed in Nse6 though at slightly different sites (Palecek, Vidot, Feng, *et al.*, 2006).

The Nse5 subunit of Smc5/6 interacts with SUMO pathway components. Using temperature sensitive alleles in budding yeast, Bustard et al 2016 were able to show that Nse5 physically associates with Ubc9 through SUMO (Branzei, Sollier, Liberi, *et al.*, 2006; Bustard, Ball & Cobb, 2016). Cells carrying the Nse5-ts1 allele or lacking SIZ1 and SIZ2 results in a reduction of Smc5 SUMOylation after MMS treatment and a redundancy for SUMO mediated events in the presence of DNA damage. This suggests one new function of the Smc5/6 complex might be as a scaffold to allow SUMOylation events (Bustard, Ball & Cobb, 2016).

1.2.3.3 – SMC5/6 localization on Chromatin.

Smc5/6 has been found to be associated with chromatin in both budding and fission yeast, *Xenopus laevis* egg extracts and human cells (Zabrady, Adamus, Vondrova, *et al.*, 2016; Verver, Hwang, Jordan, *et al.*, 2015). Loading of Smc5/6 onto chromatin is likely to be coupled with replication (Gallego-Paez, Tanaka, Bando, *et al.*, 2014). ChIP analysis has shown some interesting overlap between localization between budding and fission yeast (Pebernard, Schaffer, Campbell, *et al.*, 2008). In fission yeast it appears to localize throughout chromosomes (Pebernard, Schaffer, Campbell, *et al.*, 2008), however in budding yeasts it is

enriched at intergenic regions and the relative abundance of Smc5/6 appears to increase as chromosome size increases (Potts, 2009). In both budding and fission yeast it is localized to centromeres and telomeres. The stage of the cell cycle affects the localization of Smc5/6 as *S. cerevisiae* shows maximal occupancy at centromeres during G2/M phase, where in *S. pombe* Smc5/6 maximal occupancy is during S phase. This may be due to the lack of centromeric heterochromatin in budding yeast compared to fission yeast. In fission yeast Smc5/6 localization to centromeres is abolished in the absence of silencing. It is enriched at rDNA repeats in both budding and fission yeast. Enrichment at rDNA in both *S. pombe* and *S. cerevisiae* is hypothesised to be due to the difficulty in replicating these regions. Treatment with HU which induces replication stress and S phase arrest results in increased localisation of Smc5/6 to rDNA in *S. pombe* (Pebernard, Schaffer, Campbell, *et al.*, 2008). In *S. cerevisiae* HU treatment diminishes the rDNA localisation. The reason for this is unclear but it is consistent with the fact that Smc5/6 shows maximal centromere localisation in G2/M rather than S phase (Pebernard, Schaffer, Campbell, *et al.*, 2008). In mouse and human cells SMC6 is translocated away from chromosomes during mitotic division, however, in budding yeast Smc6 is reported to be located at the centromeres (Gomez, Jordan, Viera, *et al.*, 2013; Betts Lindroos, Ström, Itoh, *et al.*, 2006; Yong-Gonzales, Hang, Castellucci, *et al.*, 2012). Smc5/6 has also been showed to be enriched at genomic loci which are prone to replication fork stalling and collapse (Pebernard, Schaffer, Campbell, *et al.*, 2008).

1.2.3.4 – SMC5/6 Complex Promotes DNA DSB Repair.

In both *S. cerevisiae* and *S. pombe* hypomorphic mutations in Smc5/6 results in sensitivity to a broad range of DNA damage agents. Inhibition of Smc5/6 in an HR-defective *rad51* mutant background does not result in increased sensitivity, showing Smc5/6 to function in HR repair in both yeasts. Hypomorphic mutations of Smc5/6 in *S. cerevisiae* have been shown to result in increased number of translocations, gross chromosomal rearrangements confirming the complex is

required for genome maintenance and stability (Hwang, Smith, Ceschia, *et al.*, 2008).

It was originally proposed that in humans the SMC5/6 complex promoted sister chromatid homologous recombination by recruiting the cohesin complex to double-strand breaks (Potts, Porteus & Yu, 2006a). Cohesin is thought to promote HR through maintaining the close proximity of sister chromatids to DSBs (Potts, Porteus & Yu, 2006b). However, this was subsequently shown to be the results of off target effects of the SMC5/6 complex siRNAs used by the group (Wu, Kong, Ji, *et al.*, 2012)

RNAi mediated knockdown of SMC5/6 complex components in DT40 cells increases the efficiency of gene targeting due to a specific requirement of SMC5/6 in sister chromatid HR (Stephan, Kliszczak, Dodson, *et al.*, 2011). Knockdown of SMC5/6 complex components decreases sister chromatid HR, but does not reduce NHEJ or intra-chromatid, homologue or extrachromosomal HR (Potts, Porteus & Yu, 2006b). SMC5/6 itself is recruited to nuclease induced DSBs. SUMOylation of cohesin SCC1 by NSMCE2 was shown to counteract the action of Wapl, a negative regulator of cohesin loading (Wu & Yu, 2012). ChIP analysis of mouse B cells showed SMC5 co-localizes with RPA and BRCA1 (Barlow, Faryabi, Callén, *et al.*, 2013). RPA is a single-strand binding protein required in DNA replication and repair (Liu, Doty, Gibson, *et al.*, 2010) whilst BRAC1 is a protein involved in DSB repair (Roy, Chun & Powell, 2012). This suggests SMC5/6 binds to ssDNA substrates created during HR and DNA replication (Barlow, Faryabi, Callén, *et al.*, 2013).

The SMC5/6 complex has been shown to be recruited to sites of DSBs following laser-induced DNA lesions. Räschle et al 2015 explored how SMC5/6 is physically recruited to DNA lesions. A RAD18-SLF1-SLF2 recruitment pathway for the SMC5/6 complex to RNF8/RNF168-generated ubiquitylation sites at damaged DNA sites was found. SLF2 appears to be a distant ortholog of yeast

NSE6. Depletion of SL1 or SLF2 led to a reduction in cell survival(Räschle, Smeenk, Hansen, *et al.*, 2015).

1.2.3.5 – SMC5/6 in Meiosis.

Meiosis is the process used in the production of egg and sperm cells for sexual reproduction(Youds & Boulton, 2011). The amount of DNA is halved and then restored when the sperm and egg unite to form a single cell in the offspring. It is a specialised cell division resulting in the generation of unique haploid cells. Similar to the mitotic cell cycle the steps involved include the normal G1, S and G2 stages. Meiosis differs from mitosis in that the cells undergo two cell divisions rather than the one observed in mitosis. Before the first division during S phase chromosomes are replicated and organised together as sister chromatids(Hirano, 2015). During mitosis identical sister chromatids undergo bi-orientation and are pulled to the opposite poles of the cell thereby separating two identical set of chromosomes and giving rise to daughter cells that are identical to the mother cell. In meiosis, however, sister chromatids are mono-orientated and separation of homologous chromosomes occurs instead in the first of two tandem division events (Argunhan, 2016). Before the first division event, homologous chromosomes pair and exchange genetic material. During the second division event, more like mitosis, sister chromatids undergo bi-orientation, at 90 degrees compared to the previous division, and are pulled to opposite poles of the cell. As a result of the exchange of genetic material and the variation in chromosome separation compared to mitosis, meiosis results in the production of four unique daughter cells each with one set of chromosomes.

Some specialized processes during meiosis I are used to facilitate the reduction in ploidy(Petronczki, Siomos & Nasmyth, 2003). Reciprocal recombination between nonsister chromatids of homologous chromosomes leads to the formation of chiasmata. The resulting exchange of genetic material can be advantageous for natural selection but also allows the homologous chromosome pairs to act as a single unit whilst aligning correctly on the metaphase plate during metaphase I(Petronczki, Siomos & Nasmyth, 2003). The

kinetochores of sister chromatids attach to spindles from the same pole through mono-orientation. Conversely, the kinetochores of homologues rather than sister chromatids attach to spindles from opposite poles of the cells, this is known as bi-orientation(Youds & Boulton, 2011). Therefore, homologous chromosomes as opposed to sister chromatids come under tension during meiosis I. Arm cohesion as opposed to centromeric cohesion is ablated at the onset of anaphase I. Loss of arm cohesion and resolution of chiasmata as crossover or noncrossover products liberates homologues from one another and leads to their separation in anaphase (Youds & Boulton, 2011). At this point centromeric cohesion is still maintained until the onset of anaphase II, where removal of cohesin allows for the separation of sister chromatids. Through this meiosis prevents the number of chromosome from doubling upon fertilisation and keeps the ploidy of a species with each successive generation.

HR is integral to meiosis. Meiotic HR differs slightly in comparison to the recombination that occurs in mitotic cells. Meiotic HR occurs in the context of the synaptonemal complex (SC). This complex adheres homologues along their length and components of the SC promote HR specifically between homologous chromosomes as opposed to sister chromatids (Lao and Hunter 2010). Meiotic HR is induced early on in prophase I by programmed DSBs which must be repaired before chromosomes migrate to the metaphase plate and segregate in anaphase I. The breaks have to be repaired before chromosomes segregate otherwise genetic material may be lost and result in meiotic catastrophe.

The Smc5/6 complex has been shown to be required to coordinate the formation and resolution of joint molecules to ensure meiotic divisions(Lilienthal, Kanno & SjÃ gren, 2013). During meiosis the SMC complex are required for two of the major functions of meiosis, recombination and chromosome segregation. Both cohesin and condensin’s function have been investigated; however, the role of SMC5/6 has remained ambiguous.

Copsey et al 2013 showed specific essential meiotic functions where Smc5/6 is required in the recombination step and for the regulation of cohesin(Copsey, Tang, Jordan, *et al.*, 2013). Data suggests Smc5/6 is required for specific recombination and chromosomal processes throughout meiosis and that in its absence attempts at cell division with unresolved joint molecule and residual cohesin leads to severe recombination induced meiotic catastrophe. *smc5* and *nse4* meiosis-specific shut off mutants in *S. cerevisiae* cells still try to undergo chromosome separation and this results in meiotic catastrophe. Smc5/6 mutants accumulate unresolved joint molecules and fail to stall meiosis in order to resolve these structures(Copsey, Tang, Jordan, *et al.*, 2013).

Pebernard et al 2004 showed *nse1*, *nse2* and *nse3* are essential for meiosis in fission yeast (Pebernard, McDonald, Pavlova, *et al.*, 2004). *nse1* mutants displays meiotic DNA segregation and HR defects and *nse2* and *nse3* mutants had issues with mutant spore viability being reduced. The frequency of meiotic crossovers is vastly reduced in *nse1* mutants whereas *nse2* and *nse3* mutants appear to be unaffected(Pebernard, McDonald, Pavlova, *et al.*, 2004). These meiotic studies using the *nse* mutants were performed using hypomorphic mutants rather than depletion suggesting that the differences observed in the *nse2* and *nse3* mutants may be due to residual function in the alleles. It is also possible the Nse- subunits play a role in both recombination dependent and independent pathways of meiosis. From the data it suggests Nse1 plays a role in both, whilst Nse2 and Nse3 play role only in the independent pathways(Pebernard, McDonald, Pavlova, *et al.*, 2004).

1.2.3.6 – SMC5/6 in ALT Pathway.

In comparison to many bacteria and archaea the eukaryotic nuclear genome is made up of linear chromosomes(Henson, Neumann & Yeager, 2002; Cesare & Reddel, 2010). Linear chromosomes pose a technical problem as their telomeres must be distinguished from chromosome breaks to avoid repair pathways being activated which may result in end-to-end fusions. Moreover, they have an issue

in that their ends cannot be completely replicated therefore the telomeres shorten following each round of DNA replication.

For a cell to live forever it must, amongst many other things counteract the telomere shortening that accompanies DNA replication. In human cancers this typically occurs through two mechanisms, either reactivation of telomerase activity or in approximately 15 % of cancers through the alternative lengthening of telomeres (ALT) pathway. This pathway is dependent on homologous recombination and is therefore important for targeting in cancer therapy(Henson, Neumann & Yeager, 2002).

Telomeres normally consist of a repetitive hexameric sequence (5'-TTAGGG-3') which are intertwined around the Shelterin complex. The telomeres form a protective cap at the end of each chromosome. As this sequence is highly repetitive, new telomeric DNA can be generated by copying another molecule that contains the same sequence through the use of HR(Brouwer, Schimmel, Wiegant, *et al.*, 2009). Interestingly, one of the main characteristics of ALT cancer cells is that the telomeric DNA is frequently dissociated from chromosomes. The extrachromosomal telomeric DNA can take many forms such as double-stranded telomeric circles (t-circles) or single-stranded C-circles if it's predominantly C rich or G-circles if it's predominantly G-rich(Cesare & Reddel, 2010). The extrachromosomal sequences appear to as serve as the template for ALT-mediated telomere elongation. The template can be taken from the end of a sister chromatid, the same telomere looping back on itself or even another telomere(Potts & Yu, 2007).

Cells can use the ALT pathway during the stages of embryonic development or in the reprogramming of murine somatic cells into induced pluripotent stem cells. Attempting to target the ALT pathway has been challenging. Unlike reactivation of telomerase, the ALT pathway has no known specific and unique enzymatic activity, the enzymes which could be targeted all have an essential role in normal cellular pathways(Henson, Neumann & Yeager, 2002). The

presence of ALT activity is characterised by presence of ALT-associated promyelocytic leukaemia (PML) nuclear bodies or APBs, which indicate the abnormal presence of telomeres inside a complex formed from normally distributed nuclear proteins. The levels of C,G or t-circles in cells have been shown to accurately reflect the level of ALT activity(Henson, Neumann & Yeager, 2002).

Recombination-dependent telomere elongation. It's generally agreed that telomere elongation in ALT cells require a DNA recombination step, the mechanism of which is uncertain(Draskovic, Arnoult, Steiner, *et al.*, 2009). Two suggested methods include the unequal T-SCE model or homologous recombination-dependent DNA replication model. In the HR-dependent DNA replication model, ALT can result from the recombination mediated synthesis of telomeric DNA using existing telomeric sequence(Henson, Neumann & Yeager, 2002; Cesare & Reddel, 2010).

SMC5, SMC6 and NSMCE2 have been found to be required for ALT. SMC5/6 is required for HR so it should come as no surprise that repeated transfection of SMC5 and NSMCE2 siRNA resulted in gradual telomere shortening consistent with inhibition of telomere lengthening(Potts & Yu, 2007). However, since the siRNAs used in this study have subsequently been shown to have off target effects (Wu, Kong, Ji, *et al.*, 2012) this study needs to be re-evaluated. Potts et al, 2006, showed, by overexpression of NSMCE2, NSMCE2-mediated SUMOylation of Shelterin complex components. NSMCE2 can SUMOylate TRF1, TRF2, TRF1-interacting nuclear protein and RAP1. The catalytic activity of NSMCE2 was necessary for the formation of APB. The exact mechanism of SMC5/6's requirement in ALT is unknown, however, given that APBs are structural centres for telomere extension in ALT cells, SMC5/6 may be required for telomere recruitment to APBs through SUMOylation of Shelterin complex components (Potts & Yu, 2007). SMC5/6 may also function up or downstream of MRN through recruiting telomeres to APBs in which MRN may initiate recombination or through promoting telomere extension in APBs following MRN-

dependent strand invasion respectively. SMC5/6 was observed to localise to PML bodies in ALT cells. 75 % of PML foci contained SMC5/6 complex and SMC5/6 colocalized with TRF2 in these PML bodies. This was observed in ALT positive cells, but not telomerase positive cells (Potts & Yu, 2007).

1.3 – RNA interference

The introduction of RNA into cells can be used to interfere with the function of endogenous gene expression. Andrew Fire and Craig Mello published that RNA interference (RNAi), as it would come to be known, exists in *Caenorhabditis elegans* to manipulate gene expression (Fire, Xu, Montgomery, *et al.*, 1998). Activation of the RNAi pathway is controlled by activation of the RISC complex and is initiated by dsRNA in cell cytoplasm when it interacts with Argonaute. RNA can be introduced through exogenous and endogenous means(Bagasra & Prilliman, 2004).

Endogenous RNAi is activated as dsRNA pre-mircoRNA which is expressed from RNA coding genes(Hamilton, Voinnet, Chappell, *et al.*, 2002). Primary RNA transcripts are first processed to create the characteristic stem-loop of the pre-mircoRNA in the nucleus which is then exported out of the nucleus and once it becomes part of the RISC complex is imported back into the nucleus. Exogenous RNAi can be delivered through naturally occurring viruses or experimentally in the lab using viruses or various transfection reagents before being processed by Dicer. Both exogenous and endogenous RNA pathways converge at the RISC step(MacRae, Zhou, Li, *et al.*, 2006; Ye, Chen, Lian, *et al.*, 2015) **(Figure 1.4)**.

Pre-miRNA is genomically encoded non-coding RNAs that help to regulate gene expression (Carthew & Sontheimer, 2009). Mature miRNAs are structurally similar to siRNA, however prior to becoming mature they must undergo extensive post-transcriptional modification(Carthew & Sontheimer, 2009). miRNA is expressed from a much longer RNA-coding gene as a primary transcript known as a pre-miRNA which is processed in the cell nucleus to a 70-

nucleotide stem-loop by the microprocessor complex(Moffat & Sabatini, 2006). This complex consists of RNase III enzyme called Drosha and a dsRNA binding protein DGCR8(Moffat & Sabatini, 2006). Typically, miRNAs have incomplete base pairing to a target and inhibits the translation of many different mRNAs with similar sequences. In contrast, siRNAs typically base-pair perfectly and induce mRNA cleavage in only a single, specific target. In different organisms, such as *Drosophila* and *C. elegans*, miRNA and siRNA are processed by different and distinct argonaute and dicer enzymes. The dsRNA protein is cleaved by Dicer to produce the mature miRNA that is then integrated into the RISC complex, thus siRNA and miRNA share the same downstream cellular machinery(MacRae, Zhou, Li, *et al.*, 2006; Ye, Chen, Lian, *et al.*, 2015).

Once the dsRNA has been created it needs to be unwound and only one strand can be bound by Argonaute and direct gene silencing(Ye, Chen, Lian, *et al.*, 2015). As the dsRNA forms two strands, one is known as the guide strand and the other the anti-guide or passenger strand(Kacsinta & Dowdy, 2015). The anti-strand is often degraded. It is not known how the activated RISC complex locates complementary mRNAs within the cell, however, it is believed this is related to translation(Kacsinta & Dowdy, 2015; Echeverri & Perrimon, 2006).

Exogenous activation of RNAi occurs when dsRNA is detected and bound to an effector protein, which in *C. elegans* is known as RDE-4 and in *Drosophila* R2D2, and this stimulates Dicer activity. TRBP (TAR RNA binding protein), which recruits Dicer to Ago2 for microRNA processing and facilitates the transfer of cleaved siRNAs into the RISC complex (Chendrimada, Gregory, Kumaraswamy, *et al.*, 2005).

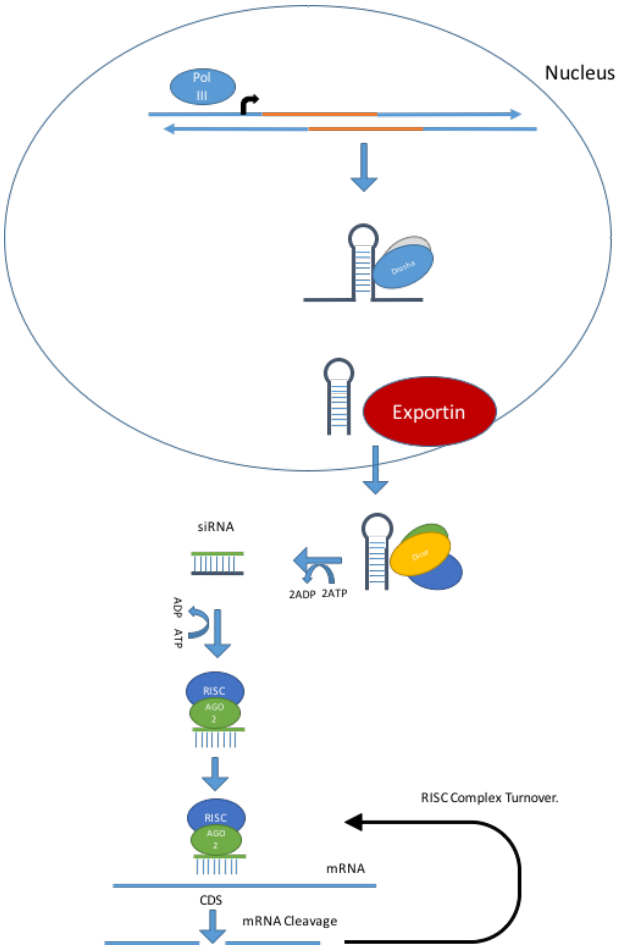

Figure 1.4. Schematic showing how RNA interference is carried out. In the case of shRNA RNA PolIII is used to create dsRNA with a hairpin loop. The hairpin is then isolated by Drosha and exported from the nucleus using Exportin 5. Following this the pathway is very similar between shRNA and siRNA, the RNAi pathway is initiated by the enzyme DICER, which cleaves long dsRNA molecules into short double stranded fragments. Each siRNA is then unwound into two single stranded (ssRNAs) known as the passenger and guide strand. Unless it can be used the passenger strand is degraded and the guide strand incorporated into the RISC complex. RNAi is used for is gene silencing. This is achieved when the guide RNA molecule pairs with a complimentary sequence in a mRNA molecule and through this induces cleavage by Argonaute, the catalytic component of the RISC complex, highlighted here by AGO2. After this is achieved the process begins again with RISC complex turnover resulting in efficient knockdown despite the relatively low molar volume of RNA used.

1.3.1 – Regulation of genes using RNAi

RNAi has many applications, the main one being gene regulation. Endogenously expressed miRNA are most important in translational repression and in the regulation of development especially on the timing of morphogenesis and maintenance of undifferentiated or incompletely differentiated cell types such as stem cells(Ye, Chen, Lian, *et al.*, 2015; Carthew & Sontheimer, 2009). Use of RNAi in downregulation of genes was first described in 1993 in *C. elegans* using miRNA. This was also observed in plants when a specific miRNA in *A. thaliana* was shown to be involved in the regulation of several genes that control plant shape. In many organisms, including humans, miRNA expression is linked to the formation of tumours and dysregulation of the cell cycle. miRNAs, by that logic, can function as both oncogenes and tumour suppressors(Luo, Emanuele, Li, *et al.*, 2009).

In addition to downregulation, RNAi can be used to upregulate genes (Luo, Emanuele, Li, *et al.*, 2009). The precise mechanism is unknown, however, Dicer and Argonaute are involved, possibly through histone demethylation(Wang, Lu, Wientjes, *et al.*, 2010). siRNA and miRNA complementary to parts of the promoter region can increase gene transcription, dubbed RNA inactivation(Carthew & Sontheimer, 2009). miRNA have been proposed to upregulate their target genes upon cell cycle arrest, however, the mechanisms are unknown.

1.3.2 – Use of RNAi in research

In experimental biology, RNAi is most often exploited to study the function of genes in cell culture and model organisms(Mohr, Smith, Shamu, *et al.*, 2014). dsRNA is synthesised with a sequence complementary to part of a gene of interest and then introduced into a cell or organisms whereupon it is recognised as exogenous genetic material and activates the RNAi pathway **(Figure 1.4).** Frequently, RNAi may not totally abolish expression of the gene, this technique is referred to as ‘knockdown’ rather than ‘knockout’ where expression of the gene is entirely eliminated. Exogenous RNAi can have off target effects so

extensive efforts have been directed toward the design of successful dsRNA reagents that maximise knockdown of the target whilst minimising the off-target effect. Off-target effects occur most frequently when the dsRNA contain repetitive sequence(Moffat & Sabatini, 2006; Luo, Emanuele, Li, *et al.*, 2009).

Knockdown of proteins can be achieved in a number of ways. Normally protein levels are affected through delivery of siRNA (a 21-27 double stranded oligonucleotide with a two nucleotide 3' overhang). Experimentally, RNAi can be delivered to cells in a number of ways(Mohr, Smith, Shamu, *et al.*, 2014). Transfection of siRNA into cells can be used to cause transient knockdown in the short term. Long term RNAi can be achieved through the expression of shRNA which is delivered through ectopic expression as stem-loop, hairpin structures that resemble pre-microRNA, the endogenous substrate of DICER.

Introduction of RNAi into cells and whole organisms can be achieved in a number of ways. In whole organisms such as *C. elegans* RNAi delivery can be achieved by feeding bacteria, such as *E. coli* that carry the dsRNA, to worms and the RNA payload is transferred via the intestinal tract (Sharma & Rao, 2009; Liu, Long, Xiong, *et al.*, 2014). This is just as effective at inducing gene silencing as other mechanisms such as soaking the worms in dsRNA solution or injecting dsRNA into the worms gonads(Liu, Long, Xiong, *et al.*, 2014).

Delivery of RNAi into cell culture models depends on the purpose of the experiment. The site of siRNA therapeutic effect is in the cytosol(Wang, Lu, Wientjes, *et al.*, 2010). Transfection of DNA or RNA molecules into mammalian cells in culture can be accomplished using various different protocols and reagents(Wang, Lu, Wientjes, *et al.*, 2010). Chemical methods include liposome-mediated, non-liposomal lipids, polyamines and dendrimers. Physical methods include electroporation or even microinjection. Viral-based systems can include retrovirus, adenovirus or lentivirus(Garvey, Spiller, Lindsay, *et al.*, 2016; Wang, Lu, Wientjes, *et al.*, 2010).

Lipid-based carriers use the formation of liposomes, micelles, microemulsions and solid lipid nanoparticles(Wang, Lu, Wientjes, *et al.*, 2010). These liposomes are globular vesicles with an aqueous core and phospholipid bilayer which is comprised of lipids or sterols. Due to their relative simplicity and well understood pharmaceutical properties liposomes are commonly used as siRNA carriers(Wang, Lu, Wientjes, *et al.*, 2010). They are synthetic analogues to mimic the phospholipid bilayer(Wang, Lu, Wientjes, *et al.*, 2010). Transfection compounds share a number of characteristics with their natural counterparts including the presence of both a hydrophobic and hydrophilic region. This allows the formation of spheroid molecules with the presence of free DNA or RNA. The DNA or RNA is sequestered into the middle of the liposome with the hydrophobic region coating the outside. The complex passes through the cell membrane and allows the nucleic acids to be released into the cytoplasm. Electroporation is one of the fastest and potentially most efficient technique for delivering exogenous nucleic acids to suspension or non-adherent cells(Moffat & Sabatini, 2006). It uses a pulse of electricity to create transient pores in the cellular membrane to enable to uptake of charged nucleic acid molecules. These are normally transient transfection methods; however, they can be used to establish stable cell lines also. Other common transfection methods from stable integration can include microinjection and virus-mediated gene delivery (transduction) (Liu, Long, Xiong, *et al.*, 2014). Microinjection requires targeting specific cells within a population for gene delivery through microinjecting specific DNA sequences into the nuclei of target cells. A limitation however is that the number of cells that can be transfected is limited by the skill and time of the person performing the microinjection. Viruses can be used to deliver RNAi. Exogenous genes or probes can be introduced through viral transduction techniques such as using viruses as carriers. Viral delivery is most useful for stably transfecting primary cell culture. Once the genetic material is integrated into the host genome, transcription is dependent on the host cell for expression(Perrimon & Mathey-Prevot, 2006).

RNAi's use in biotechnology is widespread from food, other crops, insecticides and transgenic plants. One of the biggest roles in biotechnology is genome scale RNAi using high-throughput screening technology (HTS). This allows the creation of genome-wide loss-of-function screening and broadly used in the identification of genes associated with specific phenotypes. RNAi HTS has the ability to interrogate thousands of genes with the capability to generate thousands of data points per experiment.

1.4 – Screening

By definition cellular phenotypes are observable characteristics of cells that arise as a result of interactions caused by intrinsic and extrinsic chemical or biochemical factors. Genetic screens have long been used to classify mutations on the basis of their visual phenotypes. One of the first screens was carried out in 1910 by Thomas Hunt Morgan who identified spontaneous mutations in *Drosophila melanogaster* that resulted in white eyes instead of red eyes (Kohler, 1994). Morgan et al, followed this up by not only mapping the mutation to a chromosome but also by using X-ray radiation to induce mutations and then analysing the phenotypic consequences and inheritance patterns(Kohler, 1994). Laying the foundation of modern genetics and genetic screening.

Image-based screens can explore a large number of basal or perturbed conditions that can be used to study the influences of these factors on cellular phenotypes (Zhang, 2011). Huge amounts of images can be taken of cells and these can be used to study hundreds of thousands of phenotypic descriptors in a vast array of experimental conditions. The use of normal phenotypic screening normally gives an arbitrary read out of cell viability(Bougen-Zhukov, Loh, Lee, *et al.*, 2016). A 50 % reduction in cell viability after exposure to condition 'x' can be interpreted as either 1) the cell doubling time was twice as long compared to control population or 2) twice as many cells died compared to the control population(Bougen-Zhukov, Loh, Lee, *et al.*, 2016).

1.4.1 – Synthetic lethality screens

Synthetic lethality was first described almost 100 years ago in 1922 and named approximately 20 years later by Calvin Bridges and his colleague Theodore Dobzhansky. This was following the observation of a combination of mutations in *Drosophila melanogaster* which lead to death(Bridges, 1922; Dobzhansky, 1946). Synthetic lethality arises when the combination of genetic perturbations leads to an increase in cell death, whilst the individual perturbations do not. To break it down further there are a range of outcomes following mutation or loss/knockdown of a gene. As shown in **(Figure 1.5)** synthetic lethality is the effect of mutating or knocking down/out both Gene A and Gene B resulting in cell death **(Figure 1.5.E)**, whereas loss of one of these genes does not affect cell viability **(Figure 1.5.B/D)**. If Gene A and B are both affected and viability is improved, then this is termed synthetic viable **(Figure 1.5.F)**. However, if loss of both genes does not affect cell viability or exacerbate a phenotype then they can be said to be neutral (**Figure 1.5.C).**

Synthetic lethal genetic interactions exist due to the way in which cells and organisms maintain their internal homeostasis (Kacsinta & Dowdy, 2015; Hopkins, McGregor, Murray, *et al.*, 2016). Cells or organisms with strong internal homeostasis have strong genetic robustness. This is achieved through the establishment of several buffering mechanisms such as proteins with functional redundancy known as capacitors (Fece de la Cruz, Gapp & Nijman, 2015). Functional redundancy is defined as the situation where a given biochemical function is redundantly encoded by two or more genes and this means that if one gene is affected then the other takes over to ensure no loss in viability.

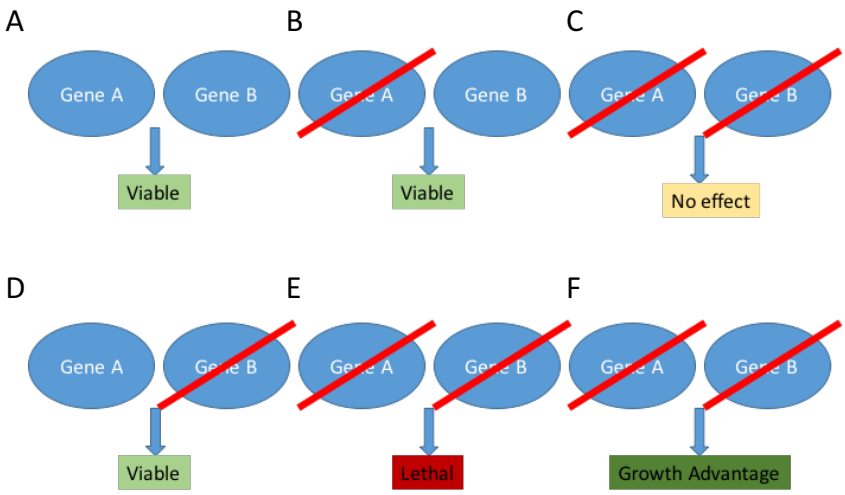

Figure 1.5. Schematic outlining the concept of synthetic lethality. A is a normal situation where the presence of Gene A and Gene B is unchanged and the cells are viable. **B** shows when Gene A is affected but Gene B still in effect within the pathway the cell is able to compensate and remain viable. **C** shows a neutral outcome when both Gene A and Gene B are affected but there is no effect on the cells indicating there is no crossover in function between the two. **D** shows a similar effect to A where Gene B is affected but Gene A, still being present, is able to overcome the stress and continue. **E** shows a synthetic lethality/sick outcome where the knockout/knockdown or mutation in Gene A and Gene B show lethality, indicating there is an overlap in function in these genes and loss of both is lethal to the cell. **F** shows an opposite outcome. When both Gene A and Gene B are affected, this confers a growth advantage to the cell, this is termed synthetic viability.

Much of the knowledge gained from exploring synthetic lethality has been acquired from experiments carried out in yeast(Forsburg, 2001). In yeasts, the large scale quantitative mapping of potential interaction has reached genome wide scales. The resulting information provides genetic interaction networks and are an invaluable source of knowledge about the function of genes (Dixon, Costanzo, Baryshnikova, *et al.*, 2009). Drug-gene synthetic lethality has been employed extensively to characterise the mechanism of action of drugs and also their interactions (Barbour & Xiao, 2006). This can facilitate the development of new treatments using existing drugs. Clinical drugs with relatively unknown mechanisms of action include paracetamol and derivatives of thalidomide including thalidomide itself. Thalidomide, traditionally used to treat morning sickness but with catastrophic side effects and has been rebranded to treat cancer(Rajkumar & Kyle, 2005) but yet, their mechanisms remains elusive.

Synthetic sick/lethal interaction screens can be used to design combination therapies and predict potential drug combinations that sensitize cells to other treatments or drugs with synergistic relationships. Identifying these situations can be particularly important in cases of cancer or infectious diseases which can quickly become resistant to conventional therapies.

Using synthetic sick/lethal interactions to design anti-cancer treatments and chemotherapeutics provides the framework to fully understand the genetic background required for long standing chemotherapeutics (Kim, Kim, Miyata, *et al.*, 2016; Turner, Lord, Iorns, *et al.*, 2008). Conventionally drugs were designed to target fast dividing cells and kill them. However, the mechanism through which this was achieved was not always obvious and some cells respond in a different way to others. Understanding the interactions that would enable the specific toxicity in cancer cells is imperative.

One of the biggest landmarks in synthetic lethality-based cancer therapy was the publication of papers describing the tumour suppressor and DNA repair genes BRCA1 and BRCA2 and their synthetic lethality with PARP inhibitors(Bryant, Schultz, Thomas, *et al.*, 2005; Farmer, McCabe, Lord, *et al.*, 2005; Aly & Ganesan, 2011). Patients with mutated BRCA1/BRCA2 display synthetic lethality with another DNA repair enzyme, Poly ADP-Ribose Polymerase (PARP) (Bryant, Schultz, Thomas, *et al.*, 2005; Farmer, McCabe, Lord, *et al.*, 2005; Aly & Ganesan, 2011). The mechanism by which DNA is repaired is dependent upon the stage of cell cycle, the damage that is encountered and the type of damage caused. BRCA1, BRCA2 and PALB2 are involved in homologous recombination which is essential during S and G2 phase of the cell cycle(Roy, Chun & Powell, 2012; Krejci, Altmannova, Spirek, *et al.*, 2012). When these genes are mutated, cells can accumulate errors in DNA repair pathways. This can lead to chromosomal rearrangements and transclocations, known hallmarks of cancer(O'Neil, van Pel & Hieter, 2013). PARP is required to repair DNA single strand breaks through the single strand break repair pathway(Krishnakumar & Kraus, 2010). If repair is inhibited, then in S phase

passage of the replication fork converts the single strand breaks to double strand breaks. Drugs that inhibit PARP work by binding PARP to DNA. As the DNA is being replicated the replication fork collides with the PARP-DNA complex inducing one-ended double strand breaks(Krishnakumar & Kraus, 2010; Aly & Ganesan, 2011), which must be repaired through HR. Cells deficient in BRCA1, BRCA2 or PALB2 cannot repair DSBs through HR. This leads to increased cell death (Bryant, Schultz, Thomas, *et al.*, 2005; Farmer, McCabe, Lord, *et al.*, 2005; Aly & Ganesan, 2011; Lord, Tutt & Ashworth, 2015).

Most synthetic lethality screens have been carried out in yeasts where gene knockout collections have driven this approach (Giaever & Nislow, 2014). Whilst understanding gene-gene interaction is easier in the relatively small genome size of yeasts screens in human cells have been limited by the fact that RNAi has until recently been prohibitively expensive. Screens were restricted to using chemical compounds as a scalable approach to identify gene-gene interactions was not unfeasible due to cost (Luo, Emanuele, Li, *et al.*, 2009). Recent reduction in cost of RNAi has made it possible to systematically identify synthetic lethal interactions in human cells and a variety of screening strategies have been developed. The development of screens involves many steps: 1) determining the target or marker, 2) creating a suitable cellular model, 3) finding and establishing the most relevant screening method, 4) determining assay kinetics and 5) optimisation.

1.4.2 – High-throughput and high content screens

High-throughput screens are cells based screens and measure a signal averaged over all cells within a microplate well then measuring the differences from the average(Zhang, 2011). A multitude of signals can be analysed including levels of a small molecule such as ATP and commonly cells can be assayed following perturbation of protein expression by RNAi or response after treatment with small molecules. Given the data is collected over the whole well it disregards information that may exist from individual cells(Zhang, 2011;

Echeverri & Perrimon, 2006). Homogenous cell-based assays are normally limited to one or two measures in parallel.

In contrast, microscopy-based, high-content assays allow for collection of data showing multiple several cell phenotypes. Cells can be modified to express fluorescently labelled proteins or stained with fluorescent markers that allow the visualisation of proteins and cellular phenotypes(Conrad & Gerlich, 2010; Garvey, Spiller, Lindsay, *et al.*, 2016). One of the major breakthroughs in this type of screen involved the technological advances made in the field of microscopy such as more stable light sources, faster autofocus and most importantly automation. Other advances in general biology such as new fluorescent probes and fluorescent protein variants for use as reporters and fusion proteins. Whilst these advances allow the generation of large number of data the biggest bottle-neck has been in the field of image analysis and the availability of standardised software(Boutros, Heigwer & Laufer, 2015).

Intrinsic-phenotype screens can be used to study phenotypes by monitoring different intrinsic factors while keeping cells under the same extrinsic factors or environmental conditions. Alternatively, extrinsic-phenotype screening can be used to monitor phenotypes by subjecting cells to different extrinsic factors or environmental conditions whilst keeping the same intrinsic biomolecular species. Although the purpose of the screen types may be different they often use similar experimental and computational methods. Intrinsic factors include biomolecules such as DNA, RNA, proteins or metabolites produced within the cells. Extrinsic factors include biomolecules or chemicals that originate from outside the cell such as the varying the environment or introducing radiation or drugs(Bougen-Zhukov, Loh, Lee, *et al.*, 2016).

If the molecular target of the extrinsic perturbation is known and specific, extrinsic screens can be used to infer the biomolecules that are involved in generating a specific phenotype such as apoptosis, cellular senescence or autophagy. This type of screen is referred to as reverse genetic or chemical

genetic screening(Turner, Lord, Iorns, *et al.*, 2008). RNAi and the CRISPR Cas9 system are two genetic perturbation techniques used routinely. RNAi is a form of post-transcriptional modification used to silence or reduce the levels of gene transcription. This involves long double-stranded RNA molecules, introduced as either siRNA or shRNA that are cleaved into siRNA and mediate sequence-specific degradation of mRNA molecules. Image based screens involving siRNA knockdown of specific genes have been used to identify targets involved in cell division, cell migration and chromosome segregation amongst many others(Turner, Lord, Iorns, *et al.*, 2008).

This is a procedure to construct quantitative representations (or profiles) of cellular phenotypes based on the images collected in large-scale phenotypic screens. The profiles are used to build models or templates which can be used to automatically screen groups of intrinsic or extrinsic factors in the screens(Bougen-Zhukov, Loh, Lee, *et al.*, 2016). Constructing a phenotypic profile involves identifying a subset of features that could be used to classify proteins localised in subcellular compartments, identify the effects of small molecules, determine new biomolecules that mediate biological process, identify protein localisation patterns amongst many others.

When designing an experiment and establishing conditions for subsequent high-throughput screens often require multiple rounds of protocol optimisations. Many factors must be considered before moving forward(Zhang, 2011). For example, what type of cells should be used, what is the intended size of the screen and what is the suitable scope of the experiment? Other considerations need to be taken too, for example what needs to be experimentally evaluated by examining a specific range of features. In setting up an assay the overall scientific question addressed by the experiment often dictates the parameters needing to be considered such as cell type used and phenotype screened. Many parameters are predetermined for example the cell type often controls the transfection protocol and timescale. An imaging assay often requires cell fixation

and staining. Image-analysis steps should be implemented in parallel as this provides direct feedback on the suitability of the assay.

The collection of data is often one of the quickest steps, however understanding the data takes the longest. Once the images have been obtained as a raw image it needs to go through a few processing steps. Firstly, the image has to go through noise filtering and illumination correction, secondly it must go through histogram based or adaptive thresholding to ensure the area of interest can be included whilst the remainder is excluded, finally the image then undergoes object identification. These steps are of massive importance and ensures a strict quality control over all screens. It is important to ensure that image artefacts can be excluded from analysis, for example difficult cell shapes, under-segmentation where cells are clustered together and difficult to resolve this can be overcome where only the cell nucleus is required to be imaged however this poses a major issue when imaging the cytoplasm. The opposite condition of over-segregation might also pose an issue as there maybe not be enough cells to screen. Heterogeneous illumination may also pose a problem as it means there isn't an even coverage of illumination throughout the field of view. Finally, general artefacts such as air bubbles or dirt may also pose an issue for screening a population of cells(Michael, Auld, Klumpp, *et al.*, 2008). It has been suggested that over 200 features can be extracted from each single cell in a high-content screen. The data available from each screen is vast and depending on the parameters and gating it can allow for many different conclusions from a single assay(Zhang, 2011; Conrad & Gerlich, 2010).

1.5 – Aims and Objectives.

The main aim of this thesis was to explore the SMC5/6 complex in human cells. The initial focus was the development, execution and validation of a synthetic sick/lethal screen using knockdown of NSMCE4a and consequently SMC5 and SMC6. However, during the course of this project a collaboration was set up to explore the effects of a homozygous point mutation in NSMCE3, one of the components of the SMC5/6 complex, which resulted in a novel human

chromosome breakage syndrome. My final chapter is therefore a characterisation of the cellular phenotypes resulting from this mutation in patient fibroblasts.

2.0 – Materials and Methods

2.1 – Human cells

Cell Line	Cell Type	Disease/Mutant
MG63	Fibroblast	Osteosarcoma
U2OS	Epithelial	Osteosarcoma
A549	Epithelial	Carcinoma
DLD1	Epithelial	Colorectal adenocarcinoma
411BR	Fibroblast	Ligase IV mutant
AT1BR	Fibroblast	$ATM^{-/-}$ mutant
1BR	Fibroblast	Wild-type primary
1BR hTert	Fibroblast	Wild-type immortalised
48BR	Fibroblast	Wild-type primary
GHV02	Fibroblast	NSMCE3-L264F mutant primary
GHV02 hTert	Fibroblast	NSMCE3-L264F mutant immortalised
HSC62	Fibroblast	BRCA2-deficient primary
HSC62 hTert	Fibroblast	BRCA2-deficient immortalised
CJ179	Fibroblast	$Artemis^{-/-}$ primary
CJ176 hTert	Fibroblast	$Artemis^{-/-}$ immortalised
P2	Fibroblast	XLF-defective primary

2.2 – *E.coli* Strains

DH5α – used for isolation of DNA

Genotype: dlacZ Delta M15 Delta(lacZYA-argF) U169 recA1 endA1 hsdR17(rK-mK+) supE44 thi-1 gyrA96 relA1

2.3 – *S. pombe* strains and plasmids

Strain number	genotype	notes
AMC501	h- ade6-704 ura4-d18 leu1-32	Wild type (WT)
JMM6	h- ade6-704 ura4-d18 leu1-32 smc6-X	smc6-X {Lehmann:1995vz}
JMM956	h- ade6-704 ura4-d18 leu1-32 smc6-74	smc6-74 {Verkade:1999vo}
Sp. 1123	h- ade6-704 ura4-d18 leu1-32 nse2-SA	nse2-SA {Andrews:2005bq}
JMM 2258	h- ade6-704 ura4-d18 leu1-32 nse3::loxP:nse3+:ura4+:loxM	nse3 base strain (Alan Lehmann)
GM01 (JMM 2539)	h- ade6-704 ura4-d18 leu1-32 nse3::loxP:nse3-L293F:loxM	nse3-L293F isolate 1, this study
GM02	h- ade6-704 ura4-d18 leu1-32 nse3::loxP:nse3-L293F:loxM	nse3-L293F isolate 2, this study
GM03	h- ade6-704 ura4-d18 leu1-32 nse3::loxP:nse3-L293F:loxM	nse3-L293F isolate 3, this study

2.4 – Materials.

Solutions were made up with distilled water unless otherwise stated. Material and solutions were autoclaved at 125 °C for 15 minutes for sterilisation where possible. Filter sterilisation was carried out through a 0.2 μm filter (Nalgene). Storage was at room temperature unless stated.

LB Broth (Autoclaved)

Adjusted to pH 7.5 and made to 1 L with dH_2O

10 g tryptone

5 g yeast extract

10 g NaCl

LB Agar (Autoclaved)

To 500 mL of the prepared LB broth

7.5 g Agar

TBE (5X) – to make 1 L of 5X stock

54 g Tris Base

27.5 g Boric Acid

20 mL 0.5 M EDTA pH 8.0

Transfer buffer (10X) – for 1 L of 10X stock

31 g Tris base

144 g glycine

Made to 1 L using dH_2O

Transfer buffer (1X)

100 mL 10X transfer buffer

100 mL MeOH

800 mL dH_2O

Tris-Glycine Electrophoresis buffer (running buffer)

31 g Tris base

144 g glycine

100 mL 10 % SDS

Made to 1 L using dH_2O

Protein loading buffer

40 % glycerol

240 mM Tris-HCl pH 6.8

8 % SDS

0.04 % bromophenol blue

5 % beta-mercaptoethanol – added just before use.

DNA loading dye

10 mM Tris-HCl (pH 7.6)

0.03 % (w/v) bromophenol blue

0.03 % (w/v) xylene cyanol FF

60 % glycerol

Phosphate buffered saline (PBS) – (Autoclaved)

One tablet in 200 mL dH_2O yields (pH 7.4)

10 mM Phosphate buffer

2.7 mM KCl

137 mM NaCl

siRNA buffer – 5X buffer

300 mM KCl

30 mM HEPES pH 7.5

1.0 mM $MgCl_2$

Kits

QIAprep Spin Miniprep Kit (Qiagen – 27104)

QIAGEN Plasmid Midi Kit (Qiagen – 12145)

Endofree Plasmid Maxi Kit (Qiagen – 12362)

QIAquick Gel Extraction Kit (Qiagen – 28704)

Buffer I – for competent DH5α cells

10 mM RbCl

50 mM $MnCl_2.4H_2O$

30 mM KOAc

10 mM $CaCl_2$

15 % v/v Glycerol

Buffer II – for competent DH5α cells

10 mM RbCl

10 mM MOPS

75 mM $CaCl_2$

15 % v/v Glycerol

Antibiotic selection – Bacterial and Human cells

G418 2 µg/mL - human

Puromycin 2.5 µg/mL - human

Ampicillin 100 µg/mL - bacteria

Kanamycin 50 µg/mL – bacteria

Methylene blue.

1 % (w/v) Methylene blue mixed with PBS. Used at 0.1 % final concentration.

2.5 – Cloning and molecular methods

2.5.1 – PCR, Restriction digests and ligations.

Polymerase chain reaction experiments (PCR) were carried out using KOD Hot Start DNA Polymerase (Merck Millipore) according to manufacturer's guidelines. Amplified products were run on 1 % agarose gels using EtBr and UV light to illuminate the bands and purified using Qiagen Gel Purification kit.

Restriction endonuclease digests were set up according to the conditions recommended by the manufacturer. Typically, New England Biolabs (NEB). Digests were allowed to incubate at 37 °C in a water bath for approximately 2 hours before purification on a 1 % gel as described previously. Ligations were carried out using T4 DNA ligase (NEB) and samples were left at 16 °C overnight. The ligated products were then transformed into *E. coli* DH5α cells before carrying out colony PCR to check integration.

2.5.2 – Site-directed mutagenesis and fusion PCR.

Site-directed mutagenesis (SDM) reactions were carried out using a PCR based method. Using a template from a gene of interest, primers were designed to allow a mutagenic overhang which was complemented by the homologous primer. Restriction digests were carried out to give ligatable ends, these were then ligated into a destination plasmid.

2.5.3 – DNA plasmids created or used

Name	Backbone	Resistance	Promoter	Source	Comment
pGIPZ2859	GIPZ	Amp/Puro	CMV	ThermoScientific	shRNA expressing plasmid to target NSMCE4a with sequence TGATTTCTAACTTGTGTGT
pGIPZ860	GIPZ	Amp/Puro	CMV	ThermoScientific	TCTTGATGAGATTCTTCCA
pGIPZ861	GIPZ	Amp/Puro	CMV	ThermoScientific	ATCTTAACATGTCAAAGGA
pGIPZNonS	GIPZ	Amp/Puro	CMV	ThermoScientific	Negative control for pGIPZ system
pGIPZEG5	GIPZ	Amp/Puro	CMV	ThermoScientific	Positive control for pGIPZ system
pGIPZGAPDH	GIPZ	Amp/Puro	CMV	ThermoScientific	Positive control for pGIPZ system
pGIPZ859-NLS-GFP	GIPZ	Amp/Puro	CMV	Adapted from ThermoScientific	As above with nuclear localised GFP
pGIPZ860-NLS-GFP	GIPZ	Amp/Puro	CMV	Adapted from ThermoScientific	As above with nuclear localised GFP
pGIPZ861-NLS-GFP	GIPZ	Amp/Puro	CMV	Adapted from ThermoScientific	As above with nuclear localised GFP
pGIPZNonS-NLS-GFP	GIPZ	Amp/Puro	CMV	Adapted from ThermoScientific	As above with nuclear localised GFP
pGIPZEG5-NLS-GFP	GIPZ	Amp/Puro	CMV	Adapted from ThermoScientific	As above with nuclear localised GFP
pGIPZGAPDH-NLS-GFP	GIPZ	Amp/Puro	CMV	Adapted from ThermoScientific	As above with nuclear localised GFP
pGIPZ859-NLS-mCherry	GIPZ	Amp/Puro	CMV	Adapted from ThermoScientific	As above with nuclear localised mCherry
pGIPZ861-NLS-mCherry	GIPZ	Amp/Puro	CMV	Adapted from ThermoScientific	As above with nuclear localised mCherry
pGIPZNonS-NLS-mCherry	GIPZ	Amp/Puro	CMV	Adapted from ThermoScientific	As above with nuclear localised mCherry
pAcGFP	pAcGFP-C1	Kan/Neo	CMV	Courtesy of Dr Velibor Savic	Used as a PCR template to create nuclear AcGFP
pFA6-4mCherryKanMC4	pFA6a-link	Amp/Genta	n/a	Courtesy of Dr Hung Quang Dang	Used as a PCR template to create nuclear mCherry
pCR2.1-TOPO-CMV-GFP	pCR2.1-TOPO	Amp	Plac	Courtesy of Dr Hung Quang Dang	Destination vector for CMV promoter, enhancer and AcGFP-NLS.
pCI-NSMCE3-WT	pCI-puro	Amp/Puro	CMV	Courtesy of Stuart Rulten/Keith Caldecott	Used to express NSMCE3 in primary cells.
pCI-NSMCE3-L264F	pCI-puro	Amp/Puro	CMV	Courtesy of Stuart Rulten/Keith Caldecott	Used to express NSMCE3 in primary cells.
pCI-EGFP	pCI-puro	Amp/Puro	CMV	Courtesy of Stuart Rulten/Keith Caldecott	Used to express EGFP in primary cells.
pAW8	pAW8	Amp/Ura	nmt	Courtesy of Adam Watson	Used as a destination to express mutant nse3 in S. pombe.
pAW8-Nse3	pAW8	Amp/Ura	nmt	Courtesy of Adam Watson	Expresses nse3 in S. pombe with Ura4+ selectable marker and Cre-Lox flanking sites either side of nse3
pAW8-Nse3-L293F	pAW8	Amp/Ura	nmt	Courtesy of Adam Watson	Expresses mutant nse3 in S. pombe with Ura4+ selectable marker and Cre-Lox flanking sites either side of nse3

Table 2.2. DNA plasmids created or used.

2.5.4 – List of oligonucleotides used

Oligonucleotides	Sequence
Nse3_5'UTR-Fseq	AGAGCGTGTTTATGCCGCTCG
Nse3_SalI-F	AATTAGAACTAATTCAATGTCGACATGAGCCAACTCAGTTTCACTGG
Nse3_NotI-R	CTAAAACAGATGGGCAAGCGCGGCCGCCTAGTGGTGGTGGTGGTGGTGGTGAGGACCTTGA AACAAAACTTCCAATGCTGCACTTGAGGAAGATTG
Nse3_F	CAAGGAGAAAAAACCTGCAGGAATTCTCTAGAATGAGCCAACTCAGTTTCAC
Nse3_R	GAAAAGGGGCCTGGCCATATGGGCCCTAGTGGTGGTGGTGGTGGTGGTGG
Nse3_f1	GTATACGCTAGCATGTTGCAAAAACCGAGGAAC
Nse3gfp_f2	GCCCAGCTCCATCCTCTGGGGGCGGAGGTGGGGGTGTGAGCAAGGGCGAGGAG
Nse3gfp_r2	CTCCTCGCCCTTGCTCACACCCCCACCTCCGCCCCCAGAGGATGGAGCTGGGC
Nse3_Gfp_r1	GTCCATCTCGAGTCACTTGTACAGCTCGTCCA
HsNse3_NdeI-F	GTATACCATATGATGTTGCAAAAACCGAGGAAC
HsNse3_BamHI-R	GTCCATGGATCCTCACTTGTACAGCTCGTCCA
pGIPZseq	TGCTGGGATTACTTCTTCAGG
SpNse3-SphI-F	TTATGCATGCGTGAATACGGTAGATACTTTAC
Nse3-L293F-R	ACGAATGATTTAAAGCCTTCAATAG
Nse3-L293F-F	CTATTGAAGGCTTTAAATCATTCGT
Nse3-SalI-R	GTTCGTCGACGGAACTTAAATAATATTACG
pGIPZ-CMV-XbaI-F	ACGTGCTGCAGGTCCGAGGTTCTAGACGTATTACC
pGIPZ-CMV-AcGFP-SpeI-R	GGTGGCAGAACTAGTTCCTCTAGTAGAGTCGGT
pGIPZ-CMV-AcGFP-SpeI-F	ACCGACTCTACTAGAGGAACTAGTTCTGCCACCATGGTGAGCAAGGGCG
pGIPZ-AcGFP-NotI-R	GGGGCGGAATTTGCGGCCGCTTATCTAGATCCGGTGGATCC
pGIPZ-mCherry-R1	CTTCTTTTTTGGATCAGCTCGAGATCTGAGTCCGGACTTGTACAGCTCGTCCATGCC
pGIPZ-mCherry-R2	GGGCGGAATTTGCGGCCGCTTATACCTTTCTCTTCTTTTTTGGATCTACCTTTCTCTTCTTTTTTGGAT CTACCTTTCTCTTCTTTTTTGGATCAGCTCG

Table 2.2. Table of Oligonucleotides.

2.5.5 – Competent Cells and Transformations.

2.5.5.1 – Creating Competent cells - *E.coli* DH5α cells.

A streak of DH5α cells were used to inoculate 5 mL LB and sample left to incubate overnight at 37 °C with shaking, 225 rpm. 1 mL of this overnight culture was diluted into 200 mL LB at 37 °C with shaking for approx. 2.5 hours until OD_{600} is no greater than 0.5. Cells were chilled on ice for 10 minutes before being transferred to 4x cold sterile 50 mL falcon tubes. Cells were centrifuged at 3500 rpm, 4 °C, for 15 minutes. The supernatant was discarded and pellet resuspended in 66 mL Buffer I and left on ice for 45 minutes. Cells were centrifuged at 3500 rpm, 4 °C, for 15 minutes and resuspended in 8 mL of Buffer II. This was incubated on ice for 15 minutes. Cells were aliquoted in 50 μL in cold sterile eppendorfs. These were snap frozen in liquid nitrogen and stored at -80 °C.

2.5.5.2 – Transformations.

DNA was transformed into DH5α cells for cloning. 50 μL of cells were transformed with either 1-2 μL of prepared miniprep plasmid DNA or entirety of ligation product. The DNA/*E.coli* mixture was incubated on ice for 10 minutes before being heat shocked at 42 °C for 45- 60 seconds. Then placed back on ice for 10 minutes. 1 mL of LB broth was then added to cells and left to incubate at 37 °C for approximately 1 hour to allow clonal expansion. Cells were pelleted and 1 mL of supernatant was removed leaving approximately 50 μL of supernatant plus cell pellet. This was resuspended in remaining volume and spread onto LB agar (LB solidified with 1.5 % agar) plates containing the appropriate antibiotic, and left overnight at 37 °C. Ampicillin or Kanamycin was added to the LB agar plates at a final concentration of 100 μg/ mL.

2.5.6 – Electrophoresis of DNA and Western blot analysis

2.5.6.1 – Electrophoresis of DNA.

DNA was resolved on a 1 % agarose gel (1 % agarose w/v dissolved in TBE) and stained with ethidium bromide (1/100 from stock solution). The gel was run at 100 V for 37 minutes in 0.5 X TBE. Samples were loaded in 1X loading buffer

and run alongside GeneRuler DNA ladder. DNA was visualized by UV illumination using a Syngene InGenius Bioimaging system. For gel extractions gels were placed over a UV box and band excised with a clean scalpel. Depending on size of DNA band required the percentage of gel was altered.

2.5.6.2 – Western blotting.

Whole cell extracts, prepared as described in the lysis method, were resolved via Sodium Dodecyl Sulphate Polyacrylamide Gel Electrophoresis (SDS-PAGE), alongside PageRuler protein marker (10 kDa – 250 kDa). Samples were resolved through a 5 % acrylamide stacking gel from a 30 % acrylamide stock (National Diagnostics), 0.125 M Tris pH 6.8, 0.1 % (w/v) SDS, 0.1 % (w/v) ammonium persulphate and 0.1 % (v/v) TEMED (N,N,N',N' – Tetramethylethylenediamine). The resolving gels were made up with 6 or 10 % acrylamide from a 30 % acrylamide stock (National Diagnostics). The resolving gel was made with 0.375 M Tris pH 8.8, 0.1 % (w/v) SDS, 0.1 % (w/v) ammonium persulphate and 0.04 % (v/v) TEMED. The ammonium persulphate and TEMED were added to mixtures last to allow polymerisation of the gel. Samples were denatured in a final concentration of 1X protein loading buffer and incubated at 99 °C for 10 minutes before loading. Gels were run at 150 V for 110 minutes before being transferred to a nitrocellulose membrane. Transfers were carried out using nitrocellulose membranes (0.2 μM pore size) at 30 V for 3 hours in 1X transfer buffer. Membranes were then stained with Ponceau S to ensure accurate transfer. Membranes were blocked using 3 % (w/v) non-fat dried milk (Marvel) dissolved in PBS and 0.1 % (v/v) Tween20 (PBST) for 30 minutes. This was followed by incubation with the primary antibody in 3 % non-fat milk PBST at 4 °C overnight. Membranes were washed 3X in 3 % non-fat milk PBST for 10 minutes. The appropriate horseradish peroxidase (HRP)-conjugated secondary antibody diluted in 3 % milk PBST was added to the membranes and allowed to incubate for 1 hour at room temperature. Again membranes were washed 3X for 10 minutes with 3 % milk PBST before detection of bands with addition of ECL chemiluminescent reagents as per manufacturers guidelines. Emission was captured using autoradiograph film and developed.

Table 2.4 – Antibodies

Name	Source Species	WB/IF Dilution	MW (kDa)	Source
Tubulin	Rabbit	1:1000	55	2133 Cell Signaling lot 4
Actin	Mouse	1:1000	42	Ab8229 – Cell Signaling
SMC5	Rabbit	1:100	130	In house – self purified
SMC6	Rabbit	1:100	130	In house – self purified
BRCA1	Mouse	1:500	220	9010 Cell Signaling
BRCA2	Rabbit	1:500	390	H300 Santa Cruz
EdU	Click-It Alkyl group	As per manufacturers guide	n/a	C10337 ThermoFisher
ɣH2AX	Mouse	1:800	n/a – IF – recognises phosph Ser139	05-636-1 Merck Millipore
CENPF	Rabbit	1:1000	n/a – IF	Ab5 - Abcam
FITC	Mouse	1:200	n/a – IF	F0257 – Sigma Aldrich
Cy3	Rabbit	1:200	n/a – IF	C2306 – Sigma Aldrich
HRP-Linked	Pig	1:2000	n/a	P0217 – Dako lot 0086784

Table 2.3. List of antibodies used.

2.6 – *S. pombe* methods

2.6.1 – *S. pombe* growth media

Media was used either in liquid or solid state. Indicated supplements were added to the media as required at 100 mg/L.

YE media

0.5 % w/v yeast extract

3.0 % w/v glucose

YES media

0.5 % w/v yeast extract

3.0 % w/v glucose

2.5 g/L Difco Bacto Agar

Phloxin containing plates using solid YES media.

20 mg/L Phloxin B (Sigma)

Edinburgh Minimal Media (EMM2) – 1L

50 mL 20x EMM2 salts

25 mL 20 % NH_4Cl

25 mL 0.4 M Na_2HPO_4

12.5 mL 40 % Glucose

1 mL 1000x Vitamins

0.1 mL 10000x Trace elements

20x EMM2 salts – 1L

61.2 g Potassium hydrogen phthalate

20.0 g Potassium chloride

21.4 g $MgCl_2.\ 6H_2O$

0.2 g Na_2SO_4

0.26 g $CaCl_2.\ 2H_2O$

1000x Vitamins

1.0 g/L Pantothenic acid

10.0 g/L Nicotinic acid

10.0 g/L Inositol

0.01 g/L d-Biotin

10000x Trace elements

5.0 g/L H_3BO_3

4.0 g/L $MnSO_4$

4.0 g/L $ZnSO_4.7H_2O$

2.0 g/L $FeCl_3.6H_2O$

1.5 g/L Na_2 MoO_4

1.0g/L KI

0.4 g/L $CuSO_4.5H_2O$

10.0 g/L Citric acid

Where necessarily supplemented with: adenine, histidine, leucine, thiamine, uracil at final concentration of 100 mg/L. The medium was filter sterilized after making.

2.6.2 – Yeast transformation

Cells were grown in YE overnight to a density of approximately 10^7 cells per mL and washed using dH_2O. Cells were then washed in 5 mL of LiAc-TE (0.1 M lithium acetate, pH 7.5, 10 mM Tris-HCl, pH 7.5, 1 mM EDTA). Cells were then resuspended in LiAc-TE to a density of 2 x 10^9 cells per mL. 1 µL of plasmid DNA and 2 µL of salmon sperm DNA was added to 100 µL of cell suspension. To this 260 µL of 40 % PEG/LiAc-TE was added. Cells were then incubated for 60 minutes at 30 ºC. 43 µL of DMSO was added and cells were heat-shocked at 42 ºC for 5 minutes before being washed in 1 mL of sterile water. Samples were then resuspended in 50 µL of sterile water and plated into relevant selection plates.

2.6.3 – Recombination mediated cassette exchange (RMCE)

pAW8 plasmids were transformed into the appropriate *S. pombe* base strain as described in Watson et al, 2008 (Watson, Garcia, Bone, *et al.*, 2008) and leu+ transformants selected. Transformants were then grown in media containing leucine to allow loss of the plasmid and Cre expression induced. The product of cassette exchange was selected for using 5' FOA plates. Cells which still expressed uracil gene were killed by 5' FOA selection. Cells which stably integrated the desired construct were picked, checked for lack of growth on plates lacking leucine or uracil, before colony PCR and sequencing was carried out to confirm targeted integration of alleles.

2.6.4 – Colony PCR

Colony PCR was performed to check for successful transformation of DNA. Samples of *E. coli* and *S. pombe* were mixed in PCR mixture and in the case of *S. pombe* boiled before PCR reaction was carried out as per manufacturer's instructions.

2.6.5 – Spot tests

S. pombe strains were grown overnight in YE and harvested the following day. Cells were counted in a hemocytometer and diluted to 10^7 cells per mL with sterile water. Serial dilutions were created to allow plating of $17.5x10^5$, $8.75x10^4$, $4.3x10^3$, $2.1x10^2$ and $1x10^1$ cells in 5 µL. Cells were spotted onto plates containing drugs or exposed to radiation prior to plating and incubated for 96 hours.

2.6.6 – Colony survival assays

Loops of logarithmically growing cells were inoculated in 1 mL of growth medium and counted using a hemocytometer before being diluted to a concentration of $1x10^4$ cells per mL. Equal numbers of cells were plated onto triplicate plates and incubated for 3-4 days at 25, 30 and 37 ºC until colonies formed. The number of colonies per plate was counted using a colony counter.

2.7 – Mammalian Cell Culture.

2.7.1 – Maintenance of Cell Lines.

Primary human cell lines: 1BR, 48BR, GVH02, HSC62, CJ179, AT1BR and 411BR, were cultured at 37 °C with 5 % CO_2 in Gibco Minimal Essential Media (MEM) supplemented with 15 % foetal calf serum (FCS), 2 mM L-glutamine, 100 U/mL Penicillin and 100 μg/mL streptomycin. Immortalised versions of these cell lines were cultured in Dulbecco's Modified Eagle Medium (DMEM) supplemented with 10 % FCS, 2 mM L-glutamine, 100 U/mL Penicillin and 100 μg/mL streptomycin. Similarly, cancerous cell lines: U2OS, MG63, A549 and DLD1 cells, were cultured in Dulbecco's Modified Eagle Medium (DMEM) supplemented with 10 % FCS, 2 mM L-glutamine, 100 U/mL Penicillin and 100 μg/mL streptomycin. Tetracycline inducible U2OS cells were also cultured in Dulbecco's Modified Eagle Medium (DMEM) supplemented with 10 % tetracycline free FCS, 2 mM L-glutamine, 100 U/mL Penicillin and 100 μg/mL streptomycin.

2.7.2 – Transfection

2.7.2.1 – Transfection of siRNA using HiperFect

2.7.2.1.1 – Topdown method for siRNA transfection

siRNA was used to transiently knock down proteins of interest by inhibition of mRNA. To do this cells were seeded in 6 well plates and allowed to adhere for 24 hours. After 24 hours' cells were washed with PBS and 2 mL fresh media applied. Transfection mixture was prepared typically using 10 μL Hiperfect transfection reagent, 2 μL siRNA and made to a final volume of 100 μL made up with Optimem. Optimem and Hiperfect were added together first and allowed to incubate at room temperature for 10 minutes before addition of siRNA. Samples allowed to incubate for a further 10 minutes before being added to relevant 6 well plate. 100 μL was prepared per required well.

2.7.2.1.2 – Reverse transfection.

Reverse transfection allows cells be to plated and transfected in one day. Transfection mixture was made up to 100 μL as before and added to plates before cells being added.

2.7.2.2 – Transfection of plasmids using GeneJuice (Merck Millipore).

To create stable cell lines or express proteins of interest, plasmids were transfected in using GeneJuice. As previously, cells were seeded in 6 well plates and allowed to adhere for 24 hours before transfection. A final volume of 100 μL was used as with the siRNA transfection. 1 μg of DNA per well of a 6 well dish was used and 3 μL of GeneJuice per 1 μg of DNA. Final volume was made up to 100 μL using Optimem and transfection mixtures were allowed to incubate for 15 minutes before adding to cells. If plasmid had a selection marker, selective antibiotic was applied after 24 hours.

2.7.2.3 – Transfection of plasmids using Calcium Phosphate.

U2OS cells from a 90% confluent T75 flask were trypsinized and diluted 1 in 10 in fresh media and made up to 10 mL per 10 cm plate. Dishes were allowed to incubate overnight at 37 °C with 5 % CO_2. Transfection solutions were prepared, 2X HBS was thawed at room temperature and 500 μL aliquots were made per transfection. Into a separate Eppendorf 10 μg DNA, 61 μL of $CaCl_2$ (2 mM stock) was added and made up to 500 μL with distilled water. Using a plugged aspirator to bubble the 2X HBS mixture, the DNA mixture was added dropwise. The final 1 mL preparation was then added dropwise to the 10 cm plate and cells were placed back in the incubator and left for 24 hours. The DNA precipitate is visible through a light microscope and potentially looks like infection, however this is not the case. After cells were left for 24 hours they were washed using PBS and fresh 10 mL of media applied.

2.7.3 – Flow cytometry.

T75 flasks were seeded with relevant cells and allowed to grow but not reach full confluency. If required samples were then exposed to 250 μM hydroxyurea

for either 2, 8 or 18 hours before being released into fresh media and prepared for flow cytometry. Cells were trypsinized and collected before being spun down at 2000 rpm for 2 minutes and washed using PBS, cells were then resuspended in 500 μL PBS before addition of 1 mL ice cold ethanol whilst gently vortexing and incubated for 30 minutes to fix. Cells were spun down and washed with PBS. Samples were spun down at 3500 rpm for 10 minutes and supernatant removed. Cells resuspended and incubated in 1 mL Triton X-100 (0.5 %) in PBS to permeabilise. Samples were then washed using PBS and spun down before being resuspended in 600 μL PBS/0.05 % Tween20 + 5 μg propidium iodide (PI) and 30 μL RNAse from stock solution.

2.7.3.1 – FACS Analysis

Samples were prepared as described in flow cytometry section. However, after fixing using 100 % ice cold EtOH the steps in the protocol varied. Once the cells were fixed they were prepared for BrdU labelling. Samples spun at 3500 rpm for 10 minutes at 10 °C, supernatant was removed carefully to avoid losing the pellet. Samples were vortexed slowly to loosen the pellet. Whilst vortexing 1 mL of 2 M HCl/PBS/Triton X-100 (0.5 %) was added drop-wise. Samples were incubated at room temperature for 30 minutes to denature DNA and produce single stranded DNA. Samples were then spun at 3500 rpm for 10 minutes at 10 °C. Supernatant was discarded and cells resuspended in 1 mL of 0.1 M Borax pH 8.5 to neutralise the acid. Samples were again spun as before, supernatant removed and pellet resuspended in 500 μL 1 % BSA/ 0.5 % Tween20/ PBS. 10 μL of anti-BrdU-FITC antibody was added to each sample and incubated at room temperature for 30 minutes whilst shielding from light. Samples were again spun down and washed with 1 % BSA/ 0.5 % Tween20/ in PBS. Samples we centrifuged for a final time and resuspended in 600 μL PBS/ 0.05 % Tween20 containing 5 μg propidium iodide (PI) + 30 μL RNAse from stock solution. Samples were then stored at 4 °C until required for FACs analysis.

2.7.4 – Colony formation assay.

These were used to analyse cellular response after treatment with specific agents. Assays were set up which determined how many colonies were formed depending on how many cells were seeded. Initially cells were plated in 6 cm dishes for 24 hours prior to treatment and allowed to grow for 7-10 days' post treatment before being fixed using methylene blue. The number of colonies counted. To analyse the data, the number of colonies formed were divided by the number of cells plated and multiplied by 100 to give the plating efficiency. The plating efficiency of the untreated control was then used as a baseline and the other plates compared against this.

2.7.5 – Clonogenic assay using primary cell lines.

Another assay used to determine cellular response to DNA damaging agent. 10 cm dishes were initially seeded with primary fibroblasts that had been exposed to 35 Gy ionizing radiation. Primary cells were exposed to either Camptothecin (CPT 1, 2, 5 or 10 μM), methylmethane sulphonate (MMS 50, 100, 150, 200, 250 mg/mL) , mitomycin c (MMC 1, 2, 5, 10 μM), hydroxyurea (HU 0.25, 1, 5, 10 μM), ultraviolet radiation (UV 2, 5, 7, 10 J/m^2) or ionizing radiation (IR 1, 3, 5, 7 Gy). Data was processed as with the colony formation assays.

2.7.6 – Hydroxyurea block and restart assay.

Primary cells were plated onto square glass coverslips in a well of a 6-well plate. They were allowed to adhere for 24 hours before carrying out the assay. Media was removed and washed using PBS before addition of 2 mL of fresh media with 250 μM hydroxyurea. Cells left to incubate at 37 °C for 0, 2, 8 or 18 hours in the presence of hydroxyurea. Media was discarded and cells washed using PBS. Cells were then incubated with 10 μM 5-Ethynyl-2'-deoxyuridine (EdU) with fresh media for 30 minutes.

2.7.6.1 – EdU Labelling.

After incubating the cells were labelled with EdU, following manufacturers guidelines (C10337 Life Technologies). Cells were removed from incubator,

media removed and washed using PBS, they were then fixed using 4 % paraformaldehyde (PFA) for 10 minutes at room temperature. Cells were washed once with PBS and permeabilised using 0.1 % Triton X-100 in PBS for 2 minutes. Cells were washed again using PBS and detection mixture added (50 μL per coverslip) and allowed to incubate for 30 minutes whilst protected from light. Cells were washed using PBS and coverslips mounted onto slides using Prolong Gold Antifade with DAPI (Thermo Fisher P36931).

2.7.7 – γH2AX Assay.

Cells were plated onto glass coverslips in a well of a 6-well plate. Cells were allowed to adhere and grow for approximately 24-48 hours before being exposed to 3 Gy ionizing radiation using a ^{137}Cs γ-ray source. The cells were allowed to recover at 37 °C for either 2, 8 or 14 hours. The cells were harvested altogether and the media removed. Cells were washed using PBS and fixed using 4 % PFA. They were then permeabilised using 0.1 % Triton X-100 in PBS for 2 minutes. Cells were washed with PBS and primary antibody added, anti-γH2AX antibody was used to detect phosphorylated Ser139 and anti-CENPF antibody used to allow detection of G2 cells. Cells were incubated with primary antibody for 35-60 minutes at room temperature protected from light, before being washed 3X with PBS. Cells were left to incubate with relevant secondary antibody, after incubation for 45-60 minutes in the dark. Coverslips were mounted onto slides using Prolong Gold Antifade with DAPI (Thermo Fisher P36931) as before. Cells were imaged using an Olympus IX73 microscope using an Lumencor LED light source, a 60x 1.4NA PlanApo lens (Olympus) and Orca Flash CMOS camera (Hamamatsu). Images were analysed using Micro-manager and ImageJ (NIH) software.

2.7.8 – High-throughput siRNA screen.

2.7.8.1 – Initial test screens.

2.7.8.1.1 – Plating efficiency.

Different ratios of either mCherry-NLS (non-silencing) or AcGFP-NLS (NSMCE4a shRNA) cells were plated in clear bottom 96-well plates. Between 72-120 hours later they were harvested, fixed using 4 % PFA, permeabilised using 0.1 % Triton X-100 in PBS and nuclear staining was carried out using DAPI in PBS. Cells incubated for 10 minutes before being washed off and the cells left under 200 μL PBS. The cells were then scanned using Olympus IX83 ScanR microscope to determine resultant ratios.

2.7.8.1.2 – siRNA test screen.

Cells were plated in varying ratios of red/green and in various densities. 10 μL final volume of transfection mixture (0.5 μL siRNA, 2.5 μL HiperFect and 7 μL Optimem) per well was plated into the bottom of each well and cells added on top of this in relevant ratios. Cells were harvested at various time points after incubation at 37 °C. Cells were washed using PBS, fixed using 4 % PFA for 10 minutes, washed with PBS and permeabilised using 0.1 % Triton X-100 for 5 minutes. Samples were washed using PBS, incubated with 1:10,000 DAPI for 10 minutes, washed and stored with 200 μL PBS at 4 °C until required.

2.7.8.2. – Screen protocol.

Using 6 black, clear bottom 96 well plates, 2 x 10^3 cells were plated in a 1:1 ratio and allowed to adhere for 24 hours. Cells then had media removed and washed using PBS. 190 μL media was then added. 10 μL transfection mixture was added (as described previously), mixed thoroughly and incubated for 72 hours, preferably over the weekend to minimise traffic and edge effect. After 72 hours plates were removed from the incubator and washed using 200 μL PBS, fixed using 200 μL 4 % PFA for 10 minutes at room temperature, washed using 200 μL PBS, permeabilised using 100 μL 0.1 % Triton X-100 in PBS, washed using 200 μL PBS, treated with 100 μL DAPI (as described previously), washed using 200 μL PBS and kept under 200 μL PBS. Plates were scanned and analysed

using Olympus IX83 ScanR microscopy platform. Cells were imaged using 10 x magnification in 16 frames per well. Images underwent background reduction analysis using Olympus ScanR Analysis software. Images were adjusted for fluorescence intensities and separate GFP-positive and mCherry-positive cells. Results were exported and further analysed in Microsoft Excel via binning and correlation.

2.7.9 – Micronuclei protocol

Patient fibroblasts were grown to approximately 70 % confluency, trypsinized, resuspended, counted and seeded onto glass coverslips. Twenty-four hours later cells were fixed using 4 % paraformaldehyde (PFA) for 10 minutes at room temperature, washed and permeabilised with 0.1 % Triton X-100 for 1 minute before being mounted onto glass slides using ProLong Gold Antifade Mountant with DAPI (Thermo Fisher P36931). Approximately 10^3 cells were analysed over three independent experiments.

Chapter 3 – Development of a high-throughput high-content synthetic sick/lethal screen to investigate knockdown of NSMCE4a in osteosarcoma cells.

3.1 – Introduction – Synthetic Lethality Screen

In this chapter the development of a synthetic sick/lethal interaction screen to investigate the SMC5/6 complex in human cells will be described. The aim was to set up a high-throughput microscopy screen that could be used as a pipeline for the development of translational links between the Genome Damage and Stability Centre and oncologists at the Brighton and Sussex Medical School and the Drug Discovery Group at Sussex. The screen would be set up with the SMC5/6 complex as the initial target but the protocol developed could then be applied to other complexes.

The development of screens involves many steps: 1) determining the target or marker, 2) creating a suitable cellular model, 3) finding and establishing the most relevant screening method, 4) determining assay kinetics and 5) optimisation. The steps involved in setting up a screen to investigate the requirement of SMC5/6 will be described here. Briefly, the determination of the target within the complex, the choice of cellular model, screening method, assay kinetics and optimisation. The cellular model initially chosen was U2OS cells, an immortalised osteosarcoma cell line, which is a suitable transfection host and amenable to imaging. A microscopy-based method was then developed to directly compare the relative viability of two cell lines with different knockdowns grown in the same well. This is outlined in **Figure 3.1.** Cells containing the target knockdown co-expressed with nuclear GFP were plated in equal ratio with control knockdown cells co-expressing nuclear RFP and after incubation with a DNA damage response siRNA library the relative numbers of red and green cells scanned and analysed using the ScanR imaging platform.

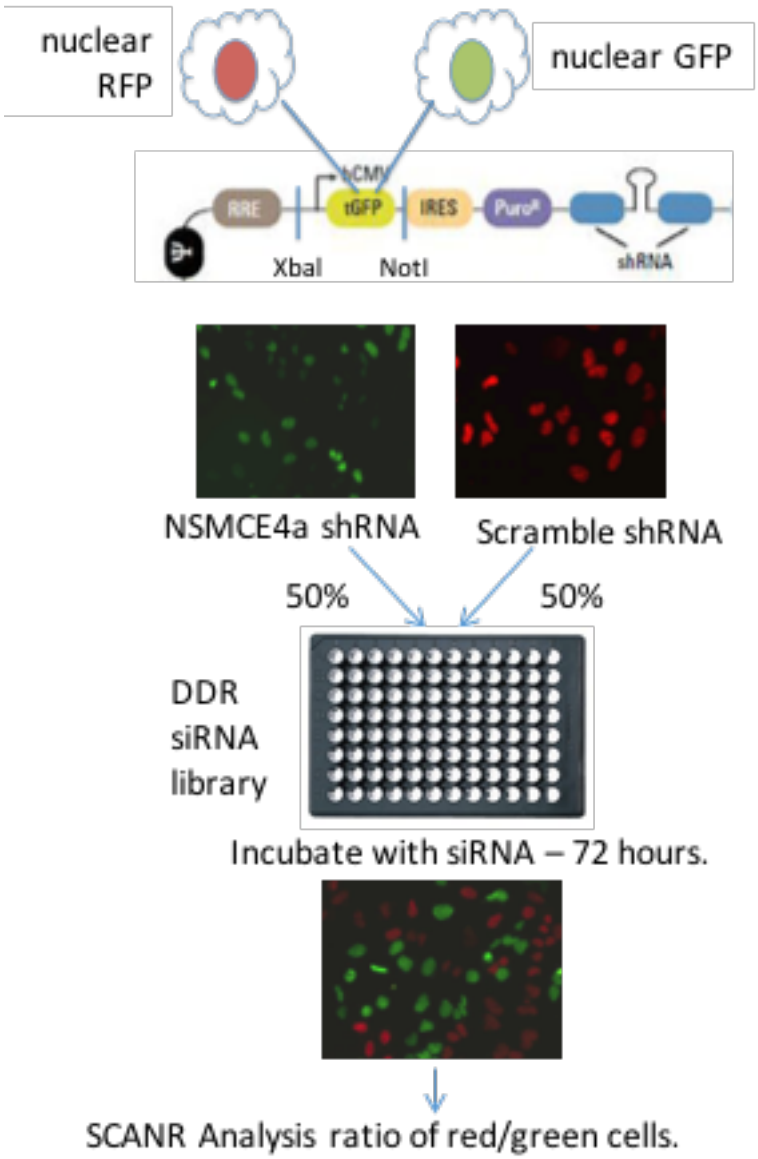

Figure 3.1. Schematic showing desired methodology of screening. Initially plasmids were designed to express shRNA of choice to knockdown target of interest or necessary controls, fluorophore and antibiotic selection. Cells with contrasting fluorophores would be mixed in a desired ratio, incubated with siRNA specific to DNA Damage response for a period of time and analysis of the resulting ratio carried out using Olympus ScanR microscope.

Experimentally, RNAi can be delivered to cells in a number of ways. Transfection of siRNA into cells can be used to cause transient knockdown in the short term. Long term RNAi can be achieved through the expression of shRNA which is delivered through ectopic expression as stem-loop, hairpin structures that resemble pre-microRNA, the endogenous substrate of DICER. As long term

knockdown was required shRNA would provide the most appropriate method for this screen.

3.2 – Results

3.2.1 – Choice of SMC5/6 subunit to knockdown

To determine the target of the screen to test the synthetic lethality of loss of the SMC5/6 complex with other genes the first requirement was to determine which subunit to target. Previously it was reported that targeting of SMC5 using siRNA was difficult as once the protein has been translated it is stable and resistant to degradation (Stephan, Kliszczak, Dodson, *et al.*, 2011). This is consistent with meiotic shutoff experiments in budding yeast, where the SMC5 shutoff had a less severe phenotype than the NSE4 shutoff (Copsey, Tang, Jordan, *et al.*, 2013). In addition, studies using recombinant SMC5 and SMC6 showed SMC6 to be much less stable than SMC5 (Alt, Dang, Wells, *et al.*, 2016). Therefore, the two candidates for targeting were shortlisted: SMC6 and NSMCE4a.

To initially determine which of these components of the SMC5/6 complex would be best suited to stably knockdown, transient knockdown using Smartpool (Dharmacon) siRNA was tested. Smartpool siRNA consists of a mixture of siRNA containing four different sequences targeting different regions of the gene. The siRNAs were tested in 1BR hTERT, a wild-type fibroblast and MG63, an immortalized osteosarcoma cell line. 5.0^4 – 10.0^4 1BR hTERT or MG63 cells was transfected with 20 pmol of Smartpool siRNA to SMC6, NSMCE4a or an siRNA control. After 24-96 hours' cells were harvested and immunoblots analysed. As predicted from previous studies, which showed that loss of any subunit resulted in destabilisation of the complex (Taylor, Copsey, Hudson, *et al.*, 2008a), successful knockdown of SMC6 **(Figure 3.2.A)** and NSMCE4a **(Figure 3.2.B)** resulted in a loss of other members of the SMC5/6 complex. Loss of SMC5 was observed following knockdown of NSMCE4a and SMC6 but was not observed in controls. Equal loading was confirmed using an anti-tubulin antibody, quantification of knockdown is seen in **(Table A.4.1.A/B)**.

Since loss of NSMCE4a resulted in loss of SMC5 and SMC6, NSMCE4a was chosen as the target to proceed with the screen, NSMCE4a was chosen as it bridges the heads between SMC5 and SMC6 and also forms interactions with NSMCE1 and NSMCE3. Whilst the lack of reliable antibody to NSMCE4a was a concern loss of SMC5 or SMC6 could be used as a measure of knockdown efficiency.

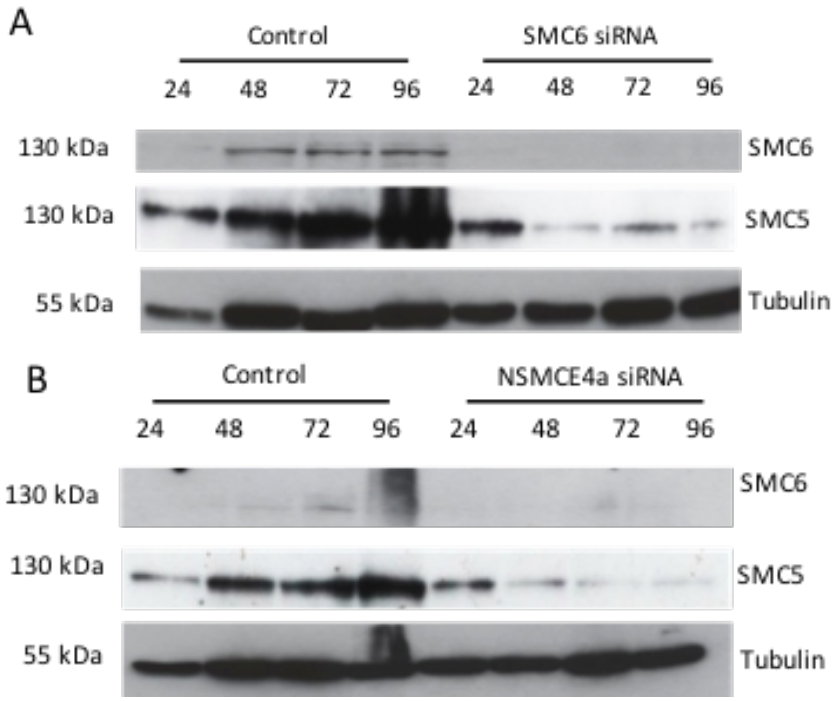

Figure 3.2. **A**. Western blot analysis using cell extracts from MG63 cells treated with siRNA to NSMCE4a over a period of 24 to 96 hours. Cells were transfected and harvest before being lysed using RIPA buffer. Supernatant extracts were loaded on SDS-PAGE gel and transferred to nitrocellulose membrane. Antibodies were used specific to SMC5 and SMC6 which showed reduction in protein levels in cells treated with NSMCE4a siRNA. Anti-tubulin was used as a loading control. **B**. As in A, Western blot analysis of cell extracts from MG63 cells treated with siRNA to SMC6. Supernatant extracts were loaded onto SDS-PAGE gel and transferred to nitrocellulose membrane. Antibodies specific to SMC5 and SMC6 show reduction in protein levels. Anti-tubulin was used as a loading control.

3.2.2 – Establishing stable cell lines expressing NSMCE4a shRNA.

To establish the synthetic sick/lethality screen an shRNA that could be constitutively expressed in the cells at all times was chosen. The pGIPZ plasmid (Thermoscientific) contains a number of features that make it ideal for this. It has puromycin selection, turboGFP and shRNA of choice and all under the co-cistronic expression of a single CMV promoter and enhancer **(Figure 3.3.A)**. This system means the expression of fluorophore and puromycin selection should be directly linked with the expression of the shRNA. The short hairpin RNA used to target NSMCE4a is expressed on the same mRNA as the fluorophore. Therefore, the overall expression of fluorophore can be used as an indicator of shRNA expression. High level of fluorophore expression would predict high levels of NSMCE4a knockdown (Hopkins, McGregor, Murray, *et al.*, 2016) **(Figure 3.3.B**).

The next step was to create a cellular model using an immortalised osteosarcoma cell line, U2OS. This cell line was chosen as it is a suitable transfection host and amenable to imaging using microscopy. pGIPZ plasmids with shRNA specific to NSMCE4a, the positive controls GAPDH and EG5 and a non-silencing control were transfected into cells. To ensure cells stably integrated the plasmid, cells were cultured under puromycin selection (1.5 µg/ mL) for 14 days. Expression of turboGFP was checked through use of fluorescence microscopy **(Figure 3.3.B)**.

After 14 days Immunoblot analysis confirmed knockdown of NSMCE4a **(Figure 3.3.C)**. Cells expressing shRNA to NSMCE4a showed SMC5 and SMC6 levels were reduced in all constructs, this was confirmed using Ponceau staining as a loading control. Quantification of proteins levels is seen in **(Table A.4.1.C)**. Surprisingly, the EG5 positive control also showed reduction of SMC5 and SMC6 protein levels. However, EG5 is a kinase essential in mitosis (Wojcik, Buckley, Richard, *et al.*, 2013) and therefore it is likely that cells expressing EG5 shRNA are arrested at M phase and this may affect SMC5/6 levels **(Figure 3.3.C)**. For this reason, EG5 knockdown cells were not taken forward.

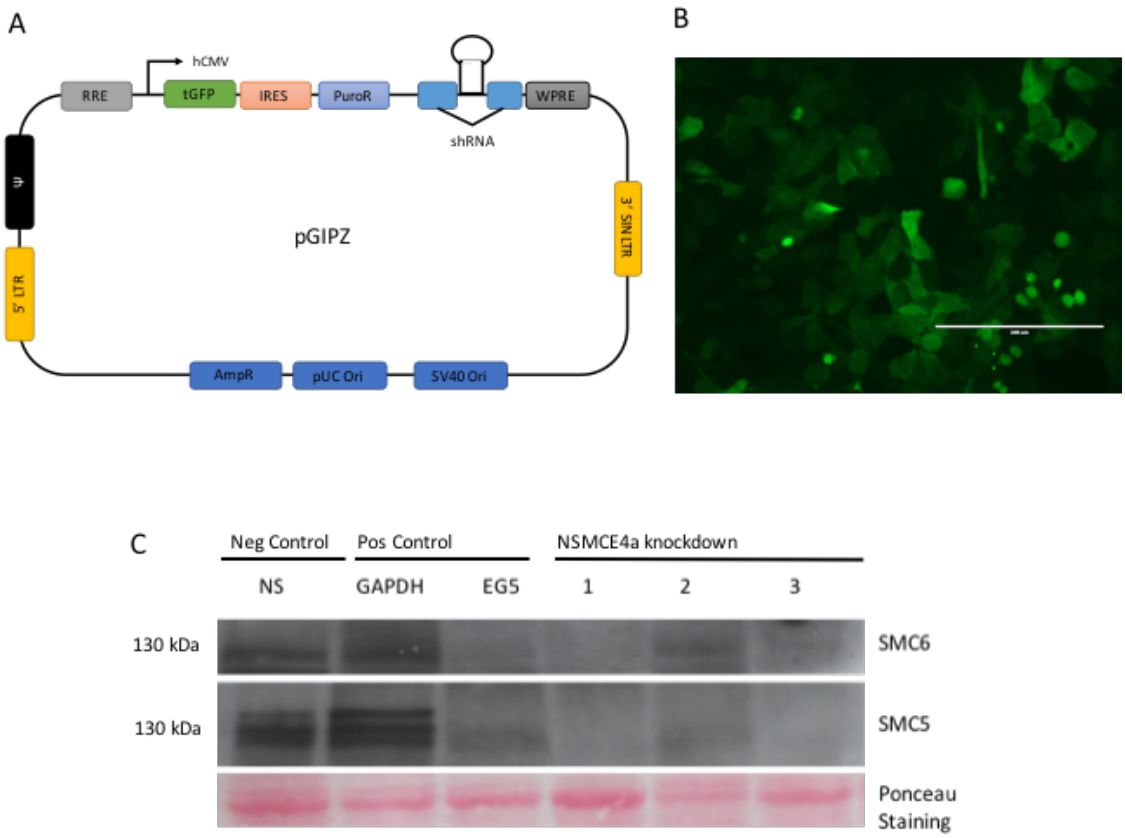

Figure 3.3. A. Schematic of pGIPZ plasmid used to create stably transfected cells with knockdown of NSMCE4a, EG5, GAPDH and non-silencing shRNA. Plasmid has co-cistronic expression of turboGFP, puromycin resistance and expression of shRNA. This plasmid allows for the selection of cells which express fluorophore and have puromycin resistance as shRNA should be expressed as well. **B**. Representative image showing expression of turboGFP fluorophore in U2OS cells. pGIPZ plasmid was transfected into the cells and expression checked after 24 hours. Cells were put under puromycin selection after 72 hours and maintained with passaging for at least 14 days to ensure stability. TurboGFP is expressed throughout the whole cell making it very difficult to distinguish individual cells. The cells show a range of GFP intensities and cells which have high expression of fluorophore have highest expression of shRNA. This allows the examination of phenotypes in a dose dependent manner. **C**. Western blot analysis on U2OS cells transfected with pGIPZ plasmid expressing non-silencing, GAPDH, EG5 shRNA controls and 3 NSMCE4a constructs. Cells were stably expressing the plasmids for 3 weeks before being harvest, lysed and ran on an SDS-PAGE gel, transferred to nitrocellulose and probed with anti SMC5 and SMC6 antibodies. All three NSMCE4a constructs showed reduction in both SMC5 and SMC6 levels consistent with what was observed previously using siRNA. Interestingly reduction in SMC5 and SMC6 levels was observed in EG5 positive control. This could be explained as EG5 is a mitotic kinase and loss of which stalls cells in the M phase. SMC5/6 is removed from chromosomes during M phase therefore would not be as detectable in cycling cells.

3.2.3 – Establishing stable cell lines expressing nuclear localised fluorophores.

The screening method was designed to distinguish knockdown and control cells cultured together on the basis of expression of different fluorophores (**Figure 3.1**). However, using the turboGFP fluorophore that was present in the pGIPZ plasmid proved not to be feasible. Imaging of the cells expressing turboGFP showed that cells above approximately 70 % confluent could not be resolved accurately. This was due to the overlapping of cells and the spread of fluorophore throughout the cell **(Figure 3.3.B)**. This was solved by the creation of nuclear localised fluorophores, which allowed the cells to be accurately resolved. To ensure that the fluorophore did not have an effect on cellular viability both AcGFP and mCherry variants of NSMCE4a and controls were created **(Figure 3.4.A)**. Construction of the nuclear localised fluorophores involved creating a CMV enhancer/promoter-AcGFP NLS construct by fusion PCR (see Methods table 2.2 for plasmids constructed) and cloning this into pCr2.1-Topo). The insert was then ligated using XbaI-NotI sites into the pGIPZ plasmids to replace the CMV enhancer/promoter-turboGFP. The mCherry variant was created through removal of the AcGFP and NLS using restriction enzymes SphI - NotI and ligation of the mCherry with NLS sequence in its place. A schematic of the cloning strategy is given in **Figure 3.4.A.**

Constructs were transfected into U2OS cells and a pool of stable integrants selected as before. Western blot analysis confirmed that knockdown of the SMC5/6 complex is not affected by the change in fluorophore **Figure 3.4.B**. In addition, it showed that shNSMCE4a construct 1 (861) had a greater level of knock down of Smc5 and Smc6 than construct 2 (859) and so construct 1 was taken forward to the screen. Quantification of proteins levels is seen in **(Table A.4.1.D**.

Comparison of cells expressing AcGFP and mCherry with nuclear localisation sequences **(Figure 3.4.C/D)** and cells with only turboGFP **(Figure 3.3.B)**

demonstrates that the NLS enables cells closer together to be differentiated due to the empty cytoplasmic space. It also facilitated a more accurate analysis of fluorophore intensity. Since expression of fluorophore and puromycin selection are still directly linked with the expression of the shRNA the overall expression of fluorophore can be used as an indicator of shRNA expression.

The ability to gate cells expressing the highest levels of fluorophore using the ScanR Analysis software had several advantages. Firstly, as shRNAs become silenced over time it was possible to check expression levels. Secondly, since knockout of NSMCE2 is cell lethal in mouse (Jacome, Gutierrez-Martinez, Schiavoni, *et al.*, 2015) it would be predicted that efficient knockdown would have a selective disadvantage. By screening a pool of integrants with a range of expression levels and gating for fluorophore intensity (rather than screening a clonal population) it is possible to set criteria to identify the top hits for a range of knockdown efficiencies.

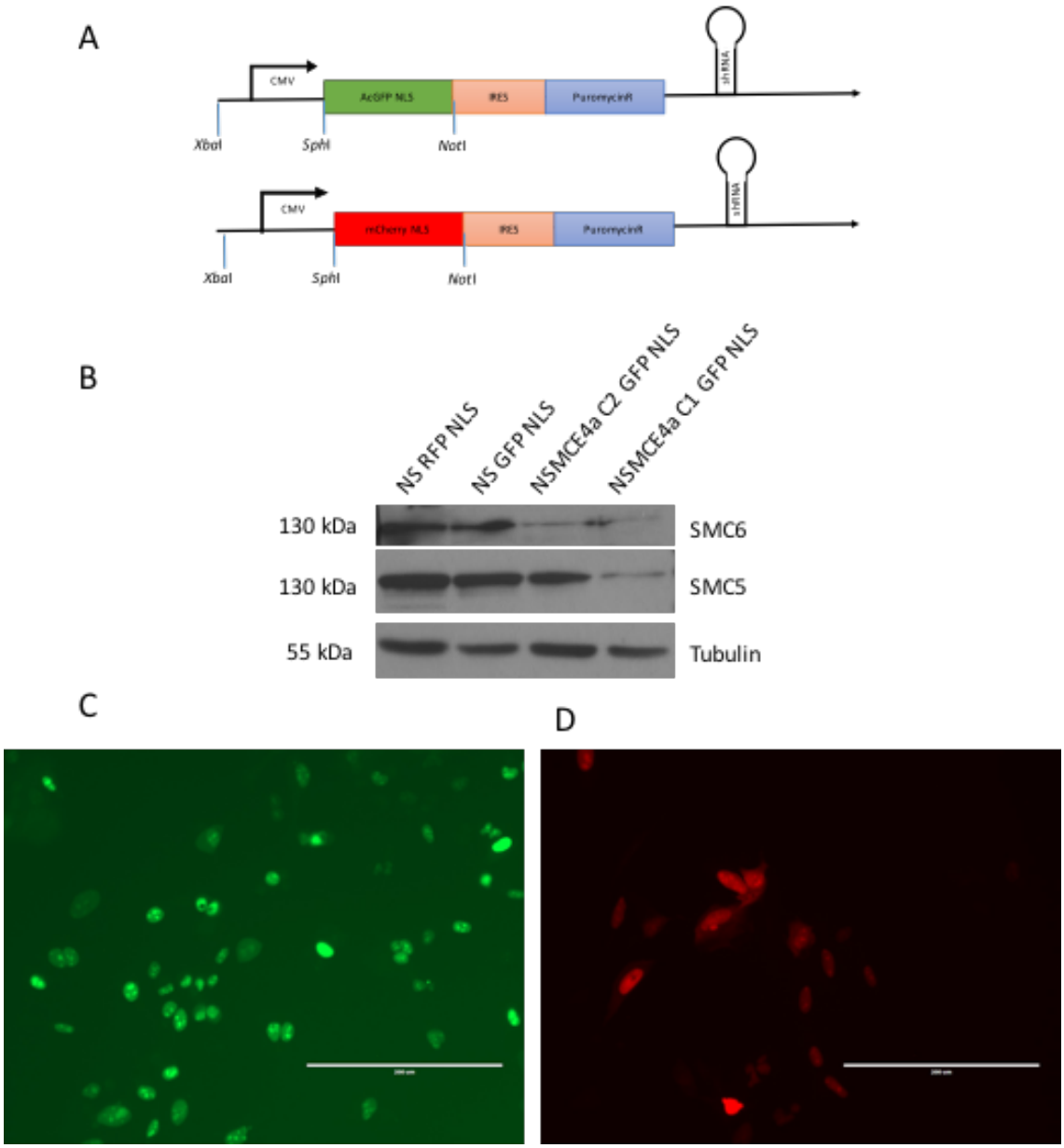

Figure 3.4. A. Schematic showing altered pGIPZ plasmid. turboGFP was replaced with AcGFP and mCherry tagged with a nuclear localization sequence. In order to do this, the CMV promoter and enhancer was also removed and replaced with a fragment created to contain CMV enhancer, promoter, fluorophore. Both GFP and mCherry plasmids were created for the Non-silencing control and for two NSMCE4a shRNA constructs. **B.** Western blot of SMC5 and SMC6 levels in stable integrants of Non-silencing with nuclear mCherry (NS RFP NLS), non-silencing with nuclear GFP (NS GFP-NLS), and two different shNSMCE4a constructs with nuclear GFP (NSMCE4a C1 and C2). Tubulin was used as a loading control. Both SMC5 and SMC6 levels were reduced in the shNSMCE4a cells but not in the controls. **C**. Representative images of U2OS cells containing altered pGIPZ plasmids. Left: AcGFP-NLS localized to the cell nucleus, right: Cherry-NLS is also localized to the nucleus.

3.2.4 – Expression of NSMCE4a shRNA does not negatively impact cell cycle progression.

The screen was designed to compare relative numbers of GFP and mCherry-expressing cells co-cultured in the same well. This would depend on the relative numbers of cells in the initial culture as well as the effects of the siRNA library and thus it was important to determine whether the relative plating efficiencies of the NSMCE4 knockdown cells compared to the scramble control. The effect of the different fluorophores was also checked to see whether they influenced plating efficiency. To determine the ratio at which the cells would be plated an experiment varying the ratio of cells was carried out. Cells were plated in 1:1, 1:2, or 2:1 ratios of shNon-silencing:GFP to shNon-silencing:mCherry as a control for the effects of the GFP and mCherry fluorophores. Two different shNSMCE4a:GFP constructs were compared to shNon-silencing:mCherry in similar ratios and cells cultured for a period of 72 hours **(Figure 3.5.A)**. The ratio of red to green cells was determined by counting the number of cells in each well and comparing to original plating ratio. Results comparing the initial and final ratios showed no significant effect of either the fluorophore or shNSMCE4a on the plating efficiency **(Figure 3.5.B)**. A ratio of 1:1 was therefore taken forward for the screen.

A

	1	2	3	4	5	6	7	8	9	10	11	12
A	1:1	1:2	2:1	1:1	1:2	2:1	1:1	1:2	2:1	NS R	NSMCE4a C1	NSMCE4a C2
B												
C										NS G		
D												

B

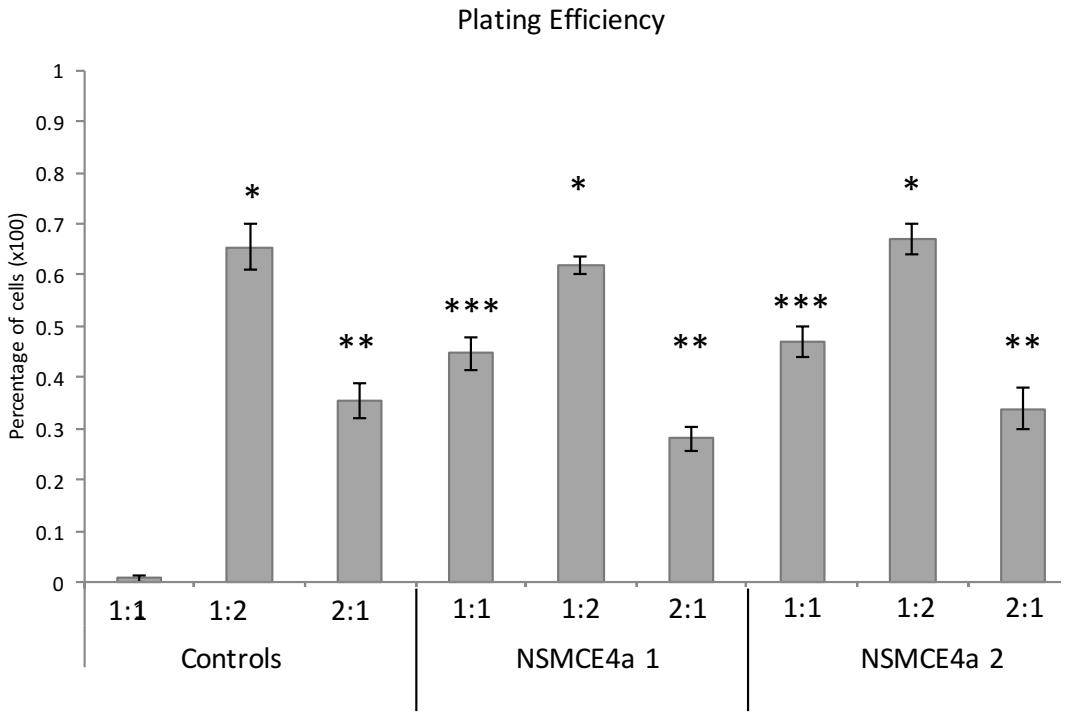

Figure 3.5. **A**. Plate map of an experiment to determine the appropriate plating efficiency and density required for the screen. Cells were plated in quadruplicate in varying ratios and repeated using varying cell number. In columns 1-3 non-silencing shRNA cells were analysed in either 1:1, 1:2, and 2:1 ratios. This was repeated in columns 4-6 contained NSMCE4a construct 1 and red non-silencing cells and again in columns 7-9 contained NSMCE4a construct 2 and red non-silencing cells. Column 10 rows A and B contained only non-silencing mCherry cells, row 10 C and D contained only non-silencing AcGFP cells. In columns 11 and 12 in all 4 well contained NSMCE4a construct 1 and construct 2. Columns 10-12 were used as controls to ensure the cells growing on their own maintained cell number. **B**. Graph showing result of plating efficiency experiments and percentage of cells that have AcGFP expression. Not shown on the graph is the three controls from columns 10-12 shows 100 % percentage. Column 1 showed no AcGFP expression, however this was due to experimental error. Experiment was still considered successful as other controls showed correct levels and no significant deviation from what was plated. A ratio of 1:1 was chosen to be taken forward for the full screen. (*, **, ***) denote non significance between same ratios.

Loss or reduction of SMC5/6 has been shown to result in delayed cell cycle progression and mitotic entry (Gallego-Paez, Tanaka, Bando, et al., 2014). Gallego Paez et al showed cell cycle progression in cells depleted of SMC5 or SMC6 had a significant delay, 2.5 fold, when compared with control cells (Gallego-Paez, Tanaka, Bando, et al., 2014). This is consistent with studies in yeast that showed SMC5/6 to be required for the stabilization of stalled replication forks and the restart of collapsed replication forks (Irmisch, Ampatzidou, Mizuno, et al., 2009; Ampatzidou, Irmisch, O'Connell, et al., 2006). Therefore, the cell cycle profiles of shNSMCE4 cells relative to the shNon-silencing control were examined. Cells were plated into 96 well plates at a 1:1 ratio of AcGFP:mCherry (NSMCE4a:Non-silencing) and analysed over a 72-120 hour period **(Figure 3.6.A)**. The cells were fixed at various time-points, permeabilised and DAPI stained before being analysed using the ScanR microscope. The resulting DAPI content was calculated and the number of cells binned based upon the amount of DAPI observed in each cell. Given the large number of cells screened, approximately 10,000 per well, an accurate profile of the cell cycle can be achieved. There did not appear to be an effect in cell cycle progression in shNSMCE4a cells compared to the non-silencing control cell line **(Figure 3.6.B).** The lack of cell cycle delay may be due to the fact that clonal populations were not selected but rather pools of puromycin resistant cells were analysed as these were what would be taken forward into the screen. The variable levels of knockdown, while an advantage for the screen as results could be gated against expression levels, would likely mask the slow growth of the more severe knockdowns.

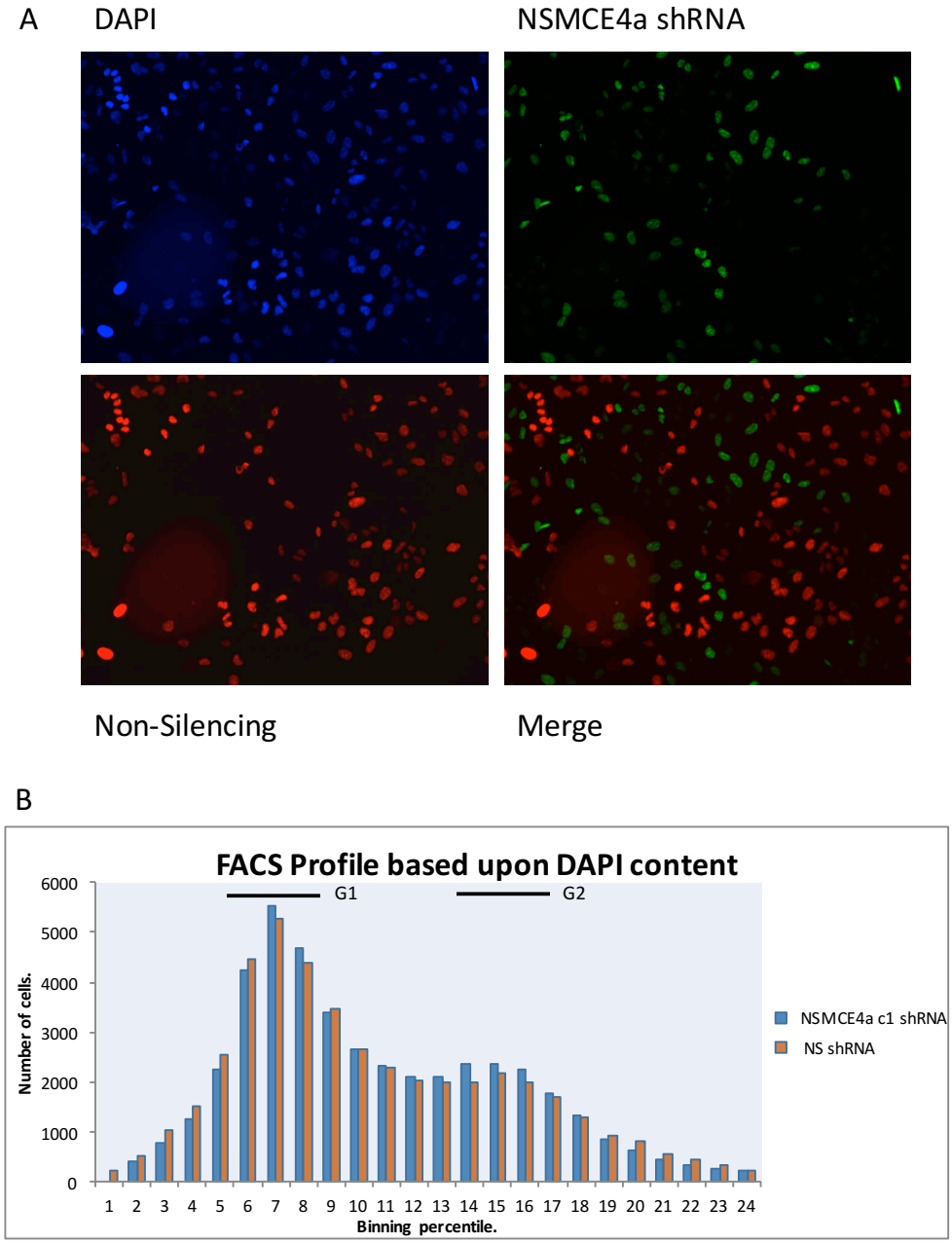

Figure 3.6. A. Representative images taken using Olympus ScanR microscope of shNSMCE4a:GFP and shNon-silencing:mCherry cells were co-cultured and analysed Cells were mixed together, plated into 96-well plates and allowed to incubate for between 72 and 120 hours. Cells were fixed, permeabilised and DAPI stained. Panels: top left DAPI, top right GFP, lower left mCherry, lower right merge. **B.** Graph showing cell cycle profile based upon DAPI content. Cells were scanned using Olympus ScanR microscope and the DAPI intensity calculated. Scores were binned into 24 percentiles of DAPI intensity and the number of cells in each bin plotted. The large number of cell scored allows for an accurate calculation of cell cycle profile. The peak at bin 7 represents G1 cells and the peak around bin 15 G2 cells and has twice the DAPI signal to the bin 7 peak. NSMCE4a (blue) and non-silencing (orange) showed no significant difference in cell cycle profile.

3.2.5 – Choice of controls for screen

Special consideration must be taken in a synthetic sick/lethal screen to ensure the plates are controlled both internally and throughout the screen. To this end the screen was designed with a number of controls in place. A mock siRNA needs to be used to check activation of the RISC pathway without targeting a protein sequence. Therefore, four scramble controls were used in each plate at different positions to ensure minimisation of edge effect and making sure position of the controls did not negatively impact the screen. Another negative control used in the screen was simply transfection reagent, whilst it doesn't activate the RISC pathway it carries out an important function by disrupting the plasma membrane and can reduce viability in cells **(Figure 3.7).**

Two positive controls were also used. The first was SMC3, a member of the related cohesin complex. Since cohesin and SMC5/6 hypomorphic mutants are synthetic lethal in yeasts it was expected this would be a positive hit in the screen and would be synthetic sick/lethal in combination with NSMCE4a knockdown (Tapia-Alveal, Lin & O'Connell, 2014). A Smartpool siRNA to GFP was also used to monitor transfection efficiency. siRNA to GFP was used as this allows the visualisation of transfection efficiency without negatively impacting the cells. In the screen it lowered expression of GFP to approximately 5-6 % of original levels and if this wasn't observed then screen results were not taken forward for further processing.

Throughout the screen, scramble siRNA was used as a negative control. It was important to ensure reproducibility throughout the screen and this was used during the processing of the data to make sure screens were controlled.

	1	2	3	4	5	6	7	8	9	10	11	12
A	Scramble											X
B	T. Reagent											Scramble
C	siGFP											T. Reagent
D	SMC3											Scramble
E	Scramble											siGFP
F	X											SMC3
G	X											X
H	X											X

Figure 3.7. Plate map that showing what was used in the screen. For negative controls, four scramble controls, two transfection reagent controls and six untreated controls to check plating efficiency accurately. Positive controls were siGFP and siSMC3. siGFP was used to ensure transfection efficiency. Controls were in different wells on column 1 and column 12 to ensure placement within the plate did not affect the results.

3.2.6 - Gathering data.

Once the screen had been carried out, the images collected and processed the resulting data was analysed. To do this the data was compared to the scramble siRNA to ensure there was a difference. Each well was then given a Z-score, calculated using the formula ($Z = ((X-\mu)/\sigma)$) in **(Figure 3.8)**. The Z-score is the distance between the raw score and the population mean in units of standard deviation, where σ is the standard deviation of the population, μ is the mean of the population and X is the individual score obtained from the well. At this point the scramble siRNA was not used in the calculation of the mean, which was instead calculated from the mean of the population. Z-score significance was assigned if the Z-score value is +/- 2 as this correlates to a p-value of 0.05. Screening is a hypothesis generating tool and whilst significance may not always be apparent compared with other targets in the screen it allows for the identification of hits that previously may not have been considered.

Calculating Z Score.

$$Z = \frac{X - \mu}{\sigma}$$

Z = Z-score
X = individual screen value
μ = mean of entire screen
σ = standard deviation of entire screen

Figure 3.8. Calculating Z-score.

3.3 – Discussion.

In order to establish a synthetic sick/lethality screen many different parameters had to be considered. Steps involved in establishing a screen began with determining the target of the screen, then establishing a cell line (firstly determining what system of gene editing needed to be used), ensuring availability of the reagents and treatment type, assay kinetics and finally optimisation. To optimise the screen, the necessary controls needed to be included on the plate, the number of cells plated optimised, and how the data was collected and analysed assessed.

In this chapter the establishment of a synthetic sick/lethality screen using U2OS osteosarcoma cells with a knockdown of the NSMCE4a subunit of the SMC5/6 complex is presented. The SMC5/6 complex is the target of the screen and whilst it is not possible to target all members of the complex with RNAi at once it is possible to reduce both the levels of the complex by targeting one component of the complex. To this end, siRNA to SMC6 and NSMCE4a were tested separately and both were found to reduce other members of the SMC5/6 complex. Following this, NSMCE4a shRNA was chosen to target the SMC5/6 complex. Due to the lack of a reliable NSMCE4a antibody, reduction in levels of SMC5 and SMC6 was used as a proxy for NSMCE4a knockdown.

Transfecting shRNA specific to NSMCE4a into U2OS was carried out with three separate targeting constructs and the supplied positive and negative controls.

The positive controls GAPDH and EG5 were tested and it was found that the EG5 shRNA resulted in reduction in levels of SMC5/6 complex members. This is likely due to the fact that EG5 is a mitotic kinase, lack of which arrests cells at G2/M of the cell cycle, the stage at which SMC5/6 is thought to be removed from the chromosomes. The other positive control GAPDH and negative scramble control did not result in reduced levels of SMC5/6 complex. All three constructs targeting NSMCE4a resulted in reduced level of both SMC5 and SMC6 but to different degrees. The best targeting construct (no. 1 (861)) was taken forward for the full screen.

Establishment of cell lines with shRNA knockdown of NSMCE4a and non-silencing controls didn't give a clear way to identify different cells above approximately 70 % confluency due to the fluorophore. The turboGFP in the pGIPZ plasmid spread throughout the cell and made it impossible to pick out individual cells. To overcome this problem turboGFP was replaced with nuclear AcGFP/mCherry (courtesy of Dr. Velibor Savic) with a nuclear localisation sequence. This allowed the individual cells to be clearly identified.

Co-culturing of mCherry and AcGFP cell lines allowed the cells to be analysed by measuring the variation in percentage in cell number from what was originally plated. To ensure there was no change in ratio resulting from a growth advantage or disadvantage conferred on either NSMCE4a and non-silencing constructs it was necessary to test the cells in varying cell numbers and ratios. Results showed knockdown of NSMCE4a did not confer either a growth defect or advantage over the non-silencing construct.

This screen can now be used to identify genes that are synthetically sick/lethal with reduction in SMC5/6 complex levels. Results will be analysed through comparing the numbers of red/green cells following siRNA knockdown of members of the DNA damage response library (Dharmacon). Once the data is collected the resulting ratio with be used to compare against the other members of the screen calculating the resultant Z-score.

Chapter 4.0 – Identification of genes required for survival following knockdown of NSMCE4a using synthetic sick/lethal screening.

4.1 – Introduction

In the previous chapter the development of a synthetic sick/lethal interaction screen in human cells was described. The SMC5/6 complex was chosen as the initial target for a number of reasons. Smc5/6 has been shown in multiple organisms to regulate HR, particularly in response to replication stress (Murray & Carr, 2008; Bustard, Menolfi, Jeppsson, *et al.*, 2012; Menolfi, Delamarre, Lengronne, *et al.*, 2015; Ampatzidou, Irmisch, O'Connell, *et al.*, 2006; Irmisch, Ampatzidou, Mizuno, *et al.*, 2009). Compromising HR is a potential route to therapy, as a sensitizer, in combination therapies with drugs that compromise parallel pathways and potentially in mono-therapy for HR-deficient tumours. Consistent with a defect in HR, in DT40 cells SMC5 or NSMCE2 null cells show chromosome segregation defects and are sensitive to PARP inhibitors (Stephan, Kliszczak, Dodson, *et al.*, 2011; Kliszczak, Stephan, Flanagan, *et al.*, 2012).

In addition to its role in HR a number of synthetic interactions identified in yeasts that suggested that targeting SMC5/6 would lead to lethality in a range of relevant tumour backgrounds. In budding yeast a genome-wide genetic interaction map has identified multiple synthetic interactions for the SMC5/6 complex (Costanzo, Baryshnikova, Bellay, *et al.*, 2010). In fission yeast Smc5/6 complex mutants are synthetically very sick with tdp1, encoding Tyrosyl-DNA phosphodiesterase 1, which removes DNA bound Top1 intermediates (Heideker, Prudden, Perry, *et al.*, 2011), cohesin and top2 mutants (Tapia-Alveal, Lin & O'Connell, 2014) and lethal with the ATR homologue but not CHK1 or CHK2 (Murray pers. Comm.).

Screens can also identify synthetic viability, where disrupting a second gene can result in an improved phenotype. For example, in budding yeast loss of the Mph1 helicase (FANCM) suppresses the sensitivity of Smc5/6 hypomorphic mutants to MMS, suggesting that SMC5/6 is required to process recombination structures generated by Mph1 (Chen, Choi, Szakal, *et al.*, 2009).

In this chapter the results of the screen to explore synthetic lethality/viability of known components of the DNA damage response library in conjunction with shRNA knockdown of NSMCE4a will be described.

4.2 – The identification of DNA damage response factors affecting cell viability in NSMCE4a deficient cells

446 different siRNAs specific to the DNA Damage Response (DDR) (Dharmacon DDR library and an additional custom library) were transfected into NSMCE4a deficient or Non-silencing control cells **(see Figure 4.1 and Appendix section A.1 and A.2 for full list of siRNA sequence and plate maps).** The screen was carried out according to the overview described in Chapter 3 **(Figure 3.1)**. Briefly, 2000 cells per well were co-cultured in a 1:1 ratio of AcGFP NSMCE4a and mCherry Non-silencing and transfected with siRNA 24 hours after seeding. Cells were left to incubate for 72 hours, at 37 ºC. Transfected cells were fixed using 4 % PFA, stained with DAPI and processed using an Olympus IX83 ScanR microscopy platform. 16 images per well in three separate channels were acquired. The resultant ratios were compared against the entire screen and Z scores calculated **(Figure 3.8)** The plate was set up as indicated in **(Figure 3.7)** with controls in columns 1 and 12. Two Non-silencing control siRNAs, transfection reagent, GFP and SMC3 were used as two negative and two positive controls respectively. Raw data is shown in **Appendix section A.3.**

Top down transfection was selected to minimise stress on cells as this works well for most adherent cells (Turner, Lord, Iorns, *et al.*, 2008). To minimise the effects of edge effect the timing of the screen was selected to coincide with least amount of traffic through the tissue culture suite. Edge effect is known to occur when the edge wells of a 96 and 384 well plates are exposed to variation in temperature, CO_2 and humidity (Lundholt, 2003). As such the middle of the plate will likely have been exposed to less conditional variability compared to the rest of the plate. Data showing volume of cells screened in all three screens is shown in **(Appendix Section A.3.5).**

DDR Plate 1	1	2	3	4	5	6	7	8	9	10	11	12
A	Scramble	RAD50	POLE2	RUVBL2	PRKCG	FANCC	FEN1	TCEA1	RTEL1	GCN5L2	APTX	X
B	T. Reagent	RAD18	TTRAP	GTF2H5	POLE	UBE2B	MDC1	IHPK3	SIRT1	TREX1	WRN	Scramble
C	siGFP	DDX11	APEX1	TDG	TOPBP1	RAD54L	RPA1	ATF2	VCP	ALKBH2	GTF2H4	T. Reagent
D	SMC3	PMS1	BRCA1	POLM	REV3L	HMGB2	GADD45A	IGHMBP2	PMS2	CSNK1E	BRIP1	Scramble
E	Scramble	CSPG6	RAD52	FANCL	FANCD2	TRIP13	TYMS	XPC	HUS1	RPS27L	DNA2L	siGFP
F	X	MAD2L2	KIAA1596	SETMAR	PRKDC	C11ORF13	PARP2	POLI	RAD17	TOP2A	PER1	SMC3
G	X	ADPRTL3	NEIL2	REV1L	SOD1	CSNK1D	MSH3	MSH4	XAB2	FANCG	ATR	X
H	X	HEL308	RAD51L3	UNG2	GTF2H2	YBX1	XRCC1	GTF2H1	ERCC5	MUS81	RAP80	X

DDR Plate 2	1	2	3	4	5	6	7	8	9	10	11	12
A	Scramble	FLJ13614	TRIM28	POLS	CXORF53	POLG2	DCLRE1A	UVRAG	TREX2	HTATIP	RECQL	X
B	T. Reagent	CHEK2	NUDT1	MBD4	RNF168	PRPF19	FRAP1	RAD23B	MJD	DCLRE1C	FANCB	Scramble
C	siGFP	CETN2	KUB3	TP73	OGG1	LIG3	MEN1	MLH1	MRE11A	RRM2B	FLJ40869	T. Reagent
D	SMC3	DCLRE1B	ERCC3	GIYD1	MUTYH	TDP1	POLH	GADD45G	EYA3	XPA	RAD23A	Scramble
E	Scramble	POLK	SHFM1	NEIL3	UBE2A	HRMT1L6	RNF8	TP53	RPA2	MMS19L	MGC2731	siGFP
F	X	POLN	MIZF	MSH6	FANCE	EME2	C2ORF13	TP53BP1	MNAT1	PMS2L5	SMC6L1	SMC3
G	X	CCNH	RBBP8	XRCC2	RECQL5	NEIL1	FLJ12610	XRCC4	DLG7	EXO1	ABL1	X
H	X	C7ORF11	HMGB1	RAD54B	ERCC6	LIG1	RPA3	CHAF1A	SPO11	DNMT1	USP1	X

DDR Plate 3	1	2	3	4	5	6	7	8	9	10	11	12
A	Scramble	EYA1	RECQL4	RAD52B	MLH3	CIB1	BTG2	MPG	TNP1	MSH2	RAD51	X
B	T. Reagent	RAD1	FLJ21816	KIAA1018	CNOT7	CDKN2D	DDB1	CKN1	PARP1	MGC32020	MGC4189	Scramble
C	siGFP	POLA	RAD9A	RENT1	NBS1	DMC1	PCNA	BAZ1B	ALKBH	POLB	NTHL1	T. Reagent
D	SMC3	DDB2	POLD1	MGMT	FANCF	PARG	ERCC2	TADA3L	ATRX	UBE2V1	POLL	Scramble
E	Scramble	GTF2H3	EME1	POLQ	RAD51C	MSH5	DEPC-1	LIG4	ATM	SMC1L1	CDK7	siGFP
F	X	FANCA	KIAA0625	FLJ10719	UBE2V2	SMUG1	RAD21	RAD51L1	UNG	CHEK1	ATRIP	SMC3
G	X	DUT	PNKP	BLM	APEX2	BRCA2	G22P1	CLK2	POLG	BRE	XRCC5	X
H	X	HSU24186	XRCC3	NPM1	ASF1A	H2AFX	FLJ22833	UBE2N	ERCC4	ERCC1	RRM2	X

Custom Plate1	1	2	3	4	5	6	7	8	9	10	11	12
A	Scramble	TELO2	RUVBL1	PPP6R1	COPS3	TIMELESS	INO80	PARP4	DAXX	COPS7A	UBA2	X
B	T. Reagent	TERF2IP	PPP4R2	GAR1	NSMCE4A	NHP2	ASF1B	POT1	SMC4	PDS5B	BAZ1A	Scramble
C	siGFP	CHRAC1	POLE3	POLE4	BRD7	NOP10	UBE2T	POLD4	CLSPN	COPS7B	ACTR5	T. Reagent
D	SMC3	ACTR8	OBFC1	PIF1	SMARCAD1	INO80B	TIPIN	WRAP53	COPS4	TINF2	MYBBP1A	Scramble
E	Scramble	HAUS7	TREX2	NCAPG	TEP1	BARD1	COPS8	CDC5L	NDNL2	NSMCE2	SMARCD1	siGFP
F	X	MCRS1	RMI2	PINX1	SMARCE1	CUL5	SMARCC1	COPS5	CCNB3	STAG1	NSMCE1	SMC3
G	X	PPP4R1	SMARCC2	WDR48	HUS1B	ARID1B	SMC1B	NFATC2IP	INO80E	ANKRD52	ANKRD44	X
H	X	CDKN2A	STAG2	CORT	EID3	SLX4	AMN1	SMC5	NCAPG2	TEN1	SMG6	X

Custom Plate 2	1	2	3	4	5	6	7	8	9	10	11	12
A	Scramble	PBRM1	COPS6	PAXIP1	RAD9B	INO80C	NFRKB	PPP4R4	NCAPH2	SUMO4	ARID2	X
B	T. Reagent	RIF1	SMEK2	UBE2NL	PPP6R3	INO80D	CRY2	UVSSA	CTC1	PDS5A	CRY1	Scramble
C	siGFP	TERF2	TCEB2	TCEB1	POLD3	NCAPD2	NCAPH	SHPRH	MVP	HLTF	HES1	T. Reagent
D	SMC3	TCEB3	CUL4A	CUL3	TOP3A	GPS1	SMARCB1	C17orf70	TOP2B	MDM2	CCNA1	Scramble
E	Scramble	RNF4	UBE2I	SUMO1	RBX1	POLR2L	POLR2G	POLR2F	COPS2	PPP4C	PER3	siGFP
F	X	SUMO3	SUMO2	TERF1	POLR2K	POLR2J	POLR2H	SMARCA4	SMARCA2	POLD2	CDKN2A	SMC3
G	X	NCAPD3	RFC3	RFC5	CDKN1A	POLR2I	RFC1	RFC2	RFC4	POLR2B	CDC25B	X
H	X	CDC25A	WEE1	CCND3	CCND2	CDK2	POLR2A	CCNE1	CCNC	CCND1	RRM1	X

Custom Plate 3	1	2	3	4	5	6	7	8	9	10	11	12
A	Scramble	UBA1	CCNA2	POLR2E	POLR2C	CCNB1	CDK4	TOP1	TFPT	DNTT	TOP3B	X
B	T. Reagent	SMC2	TNKS	CCNB2	BCAS2	PPP6R2	DKC1	SMARCA5	PLRG1	POLR2D	UBD	Scramble
C	siGFP	MDM4	ANKRD28	PER2	TERT	ARID1A	PPP6C	STRA13	HFM1	PIAS3	PARPBP	T. Reagent
D	SMC3	TONSL	FBXO18	PIAS4	SFR1	MMS22L	TTI2	SWI5	ZSWIM7	H2AFZ	PIAS1	Scramble
E	Scramble	PIAS2	TTI1	ACD	ACTL6A	UBB	UBC					siGFP
F	X											SMC3
G	X											X
H	X											X

Figure 4.1. Plate maps of siRNAs used in the screen. Dark blue headers indicate siRNA from the DDR library and light blue header indicates Custom library constructed from suggestions by members of the GDSC.

4.3 – Image acquisition and data analysis

Images were obtained using DAPI, TxRed and FITC channels using the system described previously. Images underwent spectral un-mixing and background correction to ensure accuracy. They were analysed for fluorescence intensity as per experimental parameters, cells were gated separately for AcGFP, mCherry and DAPI expression/incorporation. The data was collated and exported for further analysis in Microsoft Excel.

In this screen an average of 13,000 cells per siRNA were screened over three independent experiments. In each of the non-silencing control wells an average of 9,000 cells were screened over the three independent experiments. Calculation of the final ratio of AcGFP/mCherry cells highlighted the variation of ratio 72 hours after initial transfection. Calculating the Z-score gave the final data required from the screen. The Z-score is an absolute value that represents the distance between the raw score and the data population mean in units of standard deviation. The average Z-score over three independent experiments was calculated using the formulae ($Z = ((X-\mu)/\sigma)$). This was calculated using all the data points in screen minus the average of the scramble siRNA score. The data was processed and Z-score obtained; the results were then presented in a waterfall graph **(Figure 4.2.A)**. If the Z-score was less than -2 or greater than +2 it was deemed significant as this corresponds to – or + two standard deviations from the mean.

A

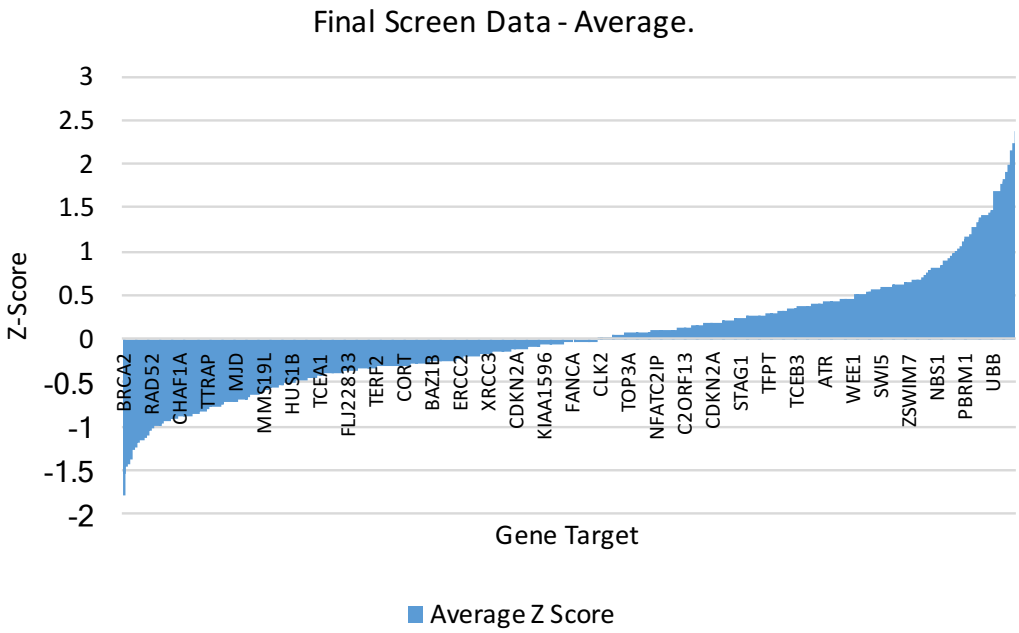
Final Screen Data - Average.
Z-Score
3
2.5
2
1.5
1
0.5
0
-0.5
-1
-1.5
-2
BRCA2
RAD52
CHAF1A
TTRAP
MJD
MMS19L
HUS1B
TCEA1
FLJ22833
TERF2
CORT
BAZ1B
ERCC2
XRCC3
CDKN2A
KIAA1596
FANCA
CLK2
TOP3A
NFATC2IP
C2ORF13
CDKN2A
STAG1
TFPT
TCEB3
ATR
WEE1
SWI5
ZSWIM7
NBS1
PBRM1
UBB
Gene Target
Average Z Score

B

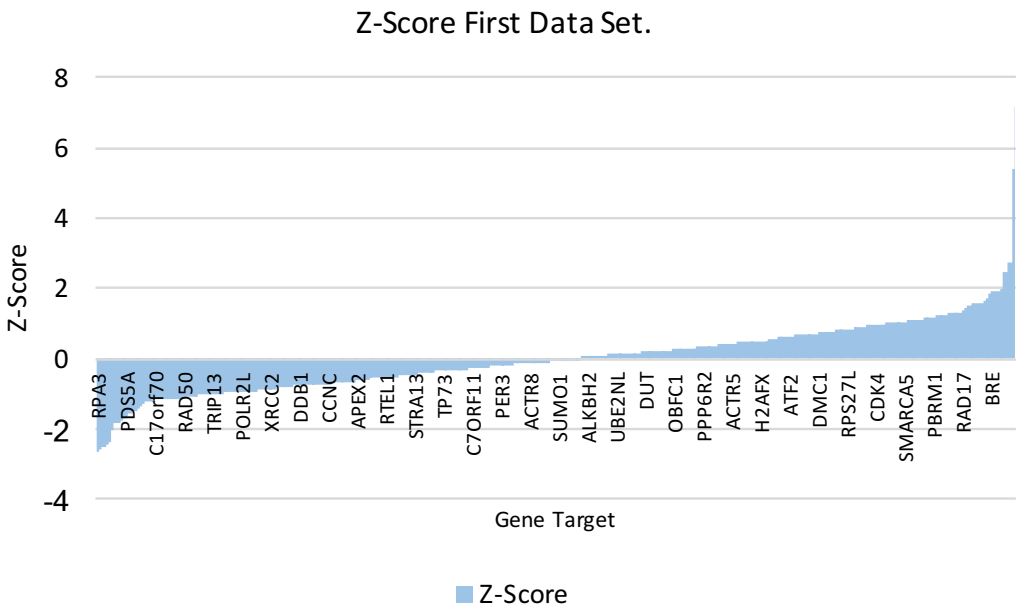
Z-Score First Data Set.
Z-Score
8
6
4
2
0
-2
-4
RPA3
PDS5A
C17orf70
RAD50
TRIP13
POLR2L
XRCC2
DDB1
CCNC
APEX2
RTEL1
STRA13
TP73
C7ORF11
PER3
ACTR8
SUMO1
ALKBH2
UBE2NL
DUT
OBFC1
PPP6R2
ACTR5
H2AFX
ATF2
DMC1
RPS27L
CDK4
SMARCA5
PBRM1
RAD17
BRE
Gene Target
Z-Score

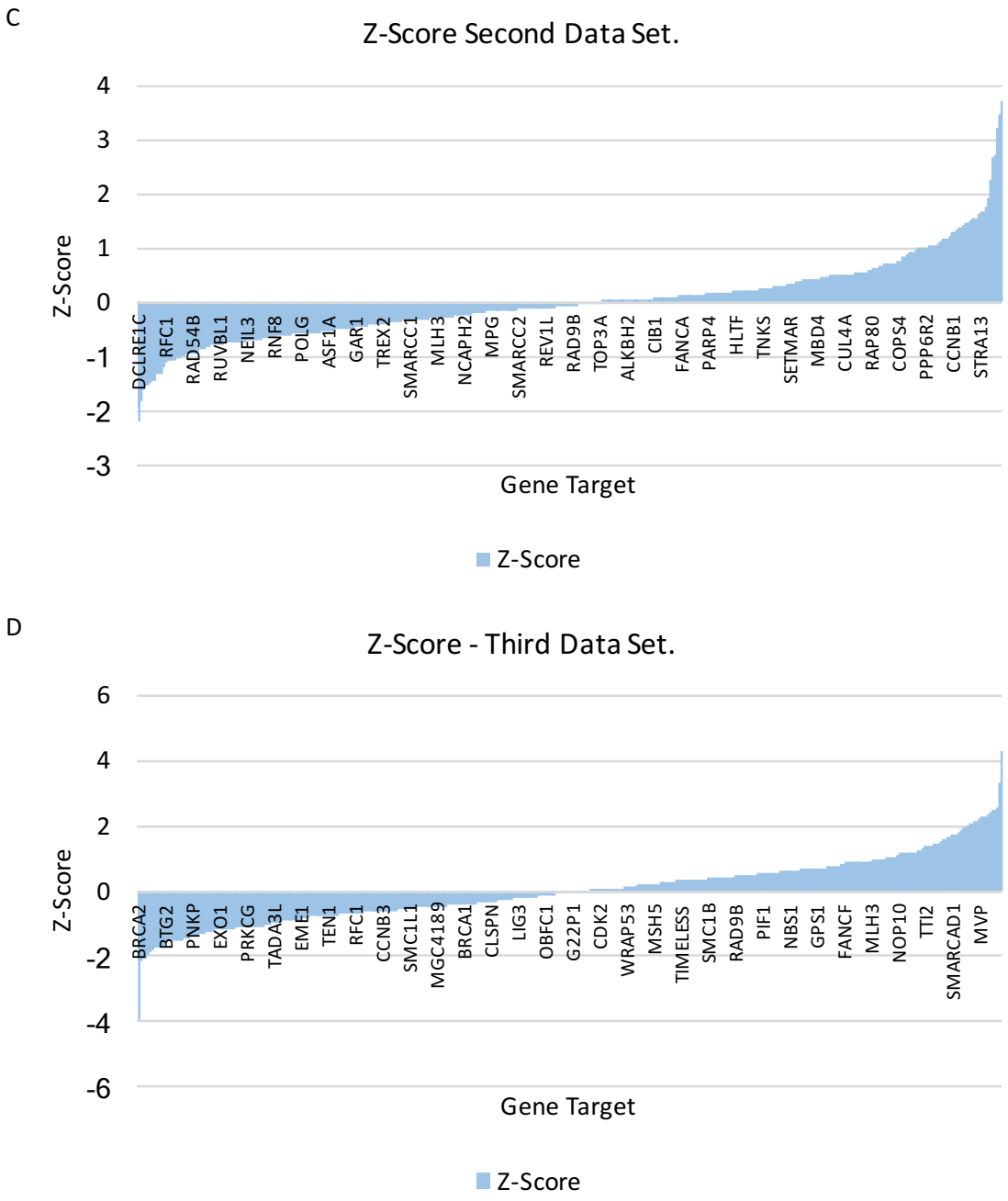

Figure 4.2. Graphs of the data sets calculated from three independent screens. **A.** Shows calculation of average Z-scores whilst **B/C/D** are the individual Z-scores from the three screens.

4.4 – Results of Screen

Given the list of genes that were probed, unsurprisingly the majority of hits had some role in the DNA damage response. The more relevant information is the categories the hits fall into. **Table 4.1** lists the top 60 hits in the combined screen

and **Table 4.2** shows a selection from the top 60 synthetic lethal hits grouped into pathways.

Rank	Gene	Z-Score	Rank	Gene	Z-Score	Rank	Gene	Z-Score
1	BRCA2	-1.780339492	26	COPS6	-0.914093232	51	LIG4	-0.751897775
2	DCLRE1C	-1.555161648	27	MEN1	-0.912936327	52	MRE11A	-0.734958265
3	XLF1	-1.4517663	28	DLGAP5	-0.912522944	53	DDB1	-0.72868854
4	RRM2	-1.446892156	29	CHAF1A	-0.892064554	54	TNP1	-0.726040509
5	VCP	-1.37465143	30	POLK	-0.891350814	55	SPO11	-0.724369656
6	PPP4R1	-1.273272453	31	NEIL3	-0.88907971	56	XRCC6BP1	-0.72332532
7	POLR2A	-1.252535464	32	POLE	-0.885481603	57	ATXN3	-0.71956649
8	RBBP8	-1.197857711	33	POLE4	-0.885008055	58	NEIL1	-0.715318031
9	USP1	-1.18618416	34	EXO1	-0.883702053	59	RAD51D	-0.705822766
10	MAD2L2	-1.152669525	35	NDNL2	-0.874906494	60	BRIP1	-0.696968517
11	NSMCE4A	-1.15027947	36	FANCC	-0.869918151			
12	RUVBL2	-1.136685293	37	PRKCG	-0.864968986			
13	FANCB	-1.095703236	38	XPA	-0.864101158			
14	IP6K3	-1.045933334	39	KAT5	-0.838304111			
15	RAD52	-1.042759303	40	RPA3	-0.83508408			
16	BTG2	-1.018032145	41	POLN	-0.831790396			
17	HELQ	-0.995063153	42	POLD4	-0.830259182			
18	UVRAG	-0.98849043	43	TDP2	-0.804780028			
19	RFC1	-0.985648871	44	RAD50	-0.773255795			
20	DNA2	-0.984074417	45	XRCC2	-0.770278736			
21	APTX	-0.967767083	46	UNG	-0.769842166			
22	APEX1	-0.95327886	47	TINF2	-0.767526242			
23	PMS1	-0.947580198	48	MTOR	-0.766517435			
24	PCNA	-0.936322645	49	UBE2B	-0.764092126			
25	RUVBL1	-0.925236346	50	MPLKIP	-0.762253096			

Table 4.1. Top 60 Synthetic Lethality Hits. Screening is a hypothesis generating tool, traditionally Z-scores of <2 or >2 are considered statistically significant as they correspond to P-values of 0.05 however top synthetic lethal hits can still be validated.

Hit.	Pathway	Appears in n of 3 screen with score over approximately -2
NSMCE4a, NSMCE3	Members of the SMC5/6 complex	NSMCE4a – 1, NSMCE3 – 2.
BRCA2, RBBP8, RAD52, EXO1, VCP	Involved in HR	BRCA2 – 2, RBBP8 – 2, RAD52 – 2, EXO1 – 0, VCP – 2.
Artemis, XLF	NHEJ and V(D)J recombination	Artemis – 2, XLF – 2.
RRM1, RRM2	Nucleotide synthesis.	RRM1 – 1, RRM2 – 2.
MRE11, RAD50	Initial response to DNA damage, activates ATM.	MRE11 – 0, RAD50 – 2.
MAD2L2	Controls DNA repair at telomeres and response to DNA breaks through inhibition of 5' end resection. Promotes NHEJ.	MAD2L2 – 1.
USP1, FANCB	Required for DSB repair and ubiquitination of FANCD2 or deubiquitinates of FANCD2. USP1 is involved in PCNA mediated TLS through removal of ubiquitin of PCNA. Promotion of HR.	USP1 – 2, FANCB – 1.
HEL308, DNA2L, RUVBL2, RUVBL1	Helicases and nucleases	HEL308 – 2, DNA2L – 1, RUVBL2 – 1, RUVBL1 – 1.
APTX	Resolves abortive DNA ligation during SSBR and DSBR	APTX – 1.
POLE, POLE4, POLN, POLD4, PCNA, RFC1	DNA replication	POLE – 2, POLE4 – 1, POLN – 1, POLD4 – 0, PCNA – 2, RFC1 – 1.
POLR2A	mRNA synthesis	POLR2A – 1.

Table 4.2. Grouping of selection from top 60 synthetic lethality hits into pathways.

The NSMCE4a shRNA resulted in knockdown but not complete ablation of NSMCE4a **(Figure 3.4.B).** Since loss of SMC5/6 is cell lethal in mouse (Jacome, Gutierrez-Martinez, Schiavoni, *et al.*, 2015), it would be predicted that further destabilisation of the complex by knockdown of additional subunits would lead to synthetic lethality and consistent with this both NSMCE4a and NSMCE3 appear as hits in the screen. The other components may not have been identified due to the efficiency of the siRNA knockdown.

Since SMC5/6 is required to regulate HR it would be predicted to be epistatic with HR factors and, indeed, RAD51 appears towards the middle of the waterfall plot (-0.481). However, BRCA2 came out as the top hit (-1.78). It acts through targeting RAD51 to ssDNA over dsDNA allowing RAD51 to replace RPA and stabilizing the RAD51-ssDNA complexes by blocking ATP hydrolysis. It also

forms a part of the PALB2-scaffolded HR complex containing RAD51C. Similarly, RAD52 also appeared high in the screen and is also involved in the same steps as BRCA2 through interacting with RAD51 and can mediate assembly of RAD51 in the absence of BRCA2 though with lower efficiency(Chun, Buechelmaier & Powell, 2012). It also promotes, in combination with ERCC1, single strand annealing. Whilst more error-prone, is required in the cases of some breaks which would not otherwise be repairable (Stark, Pierce, Oh, *et al.*, 2004).

SMC5/6 is required in response to replication stress. Loss of ribonucleotide reductase (RNR) or knockdown of replication factors induces replication stress and both RRM1 and RRM2 (RNR) and multiple replisome components (Polε, Polδ, RPA, Rfc1, PCNA) were identified.

Taking into account the known functions and pathways that SMC5/6 is involved in it is likely that knockdown of NSMCE4a would result in synthetic sick/lethal interactions with members of other DSB repair pathways such as the NHEJ pathway and two hits (Artemis and XLF) prominent in synthetic sickness were involved in NHEJ.

Overall, these results suggest that the screen has been successful and a number of interesting hits were identified.

4.5 Synthetic viability hits

A Z-score of approximately +2 or over indicates a preferential response in cells with NSMCE4a shRNA compared to Non-silencing shRNA. This may indicate that the combination of knockdowns results in either a growth advantage in the NSMCE4a cells or a loss of viability in the Non-silencing shRNA cells. Most screens focus on trying to kill cells however identifying situations for treatments which confer a growth advantage to cells is important for the treatment of cancer or other malignancies to be able to avoid unnecessarily promoting their growth (Aly & Ganesan, 2011).

Table 4.2 lists the top 50 hits in the combined screen and **Table 4.3** shows a selection from the top 50 synthetic viable hits grouped into pathways. Analysing the Z-score of each individual screen allows for the identification of potential false positive results. An example of a false positive is FANCD2, which presented with Z scores of 0.9, 6.4 and -0.27 indicating that there was a significant increase in NSMCE4a AcGFP cells only during screen 2 in this well. WRN is also likely to be a false positive with scores of 7.19, -0.27 and -1.23 in screens 1-3 respectively. This could be the result of a number of factors. For example, during plates of the cell it is possible that a single cell suspension was not achieved for a patch of Non-silencing shRNA cells. Another possibility is that the transfection efficiency in the other two screens was not optimal or that there was an abnormally high dosage of siRNA into the cells. However as FANCD2 loss has been shown to result in increased severe DNA defects and enhanced cell death (Kais, Rondinelli, Holmes, *et al.*, 2016) it is possible that this resulted in the death of the Non-silencing cells over the NSMCE4a shRNA cells.

Both MMS22L and TONSL came out as synthetic viable hits. The MMS22-TONSL complex stimulates recombination-dependent repair at stalled or collapsed replication forks. MMS22-TONSL also helps to promote HR and helps mediate the response of RAD51 filaments on ssDNA (Duro, Lundin, Ask, *et al.*, 2010). This suggests that the synthetic viability is due to repair no longer being channelled into HR-dependent pathways.

Other synthetically viable hits components of the ubiquitin and sumo modification systems. These include UBB/UBD and UBA1. UBD is a paralog of UBB and both play a major role in targeting cellular components for degradation (Fischer, De Vos, Van Dijk, *et al.*, 2003; Oh, Park, Lee, *et al.*, 2013). They are involved in the maintenance of chromatin structure, regulation of gene expression and stress response. UBA1 catalyses the first step in ubiquitin conjugation and has functions in DNA repair. It is essential for timely DNA repair

and in the response to replication stress. UBA1 also promotes the recruitment of TP53BP1 and BRCA1 to DNA damage site (Groen & Gillingwater, 2015).

Other synthetic viable hits include PIAS1, PIAS3, PIAS4 and SUMO2. PIAS proteins function as E3-type SUMO ligases (Mattoscio & Chiocca, 2015). PIAS1 stabilises the interaction between UBE2I and SUMO and the SUMOylation of PML bodies. Telomeric DNA is found in the nuclear PML bodies and SMC5/6 is found associated with PML bodies(Cesare & Reddel, 2010). Knockdown of SMC5 and NSMCE2 using siRNA results in gradual telomere shortening therefore it is possible that whilst there is a momentary increase in viability this may not last(Potts & Yu, 2007).

Three of the top synthetic viable hits are involved in telomere function. These are ACD, TERT and CCNA2. ACD forms one of the six core proteins in the Shelterin complex, which functions to maintain telomere length and protects telomere ends(de Lange, 2005). It promotes the binding of POT1 to telomeric ssDNA and modulates the inhibitory effects of POT1. Telomerase reverse transcriptase (TERT) maintains telomere length through addition of TTAGGG repeats (Ramlee, Wang, Toh, *et al.*, 2016). Given the requirement of SMC5/6 at telomeres and its involvement in the ALT pathway, it is interesting that combined knockdown of both results in a growth advantage instead of cell death(Henson, Neumann & Yeager, 2002). CCNA2 encodes for Cyclin A2. This is essential for the control of the cell cycle at the start of G1/S and the G2/M transition in mitosis. Also required for the packaging of telomere ends(Gong & Ferrell, 2010). Another potentially telomere interacting protein is TTI1, which interacts with TELO2. This is involved in the regulation of the DDR and involved in the resistance to DNA damage stress(Jiang, Benard, Kebir, *et al.*, 2003).

A H2A histone variant, H2AFZ was another synthetic viable hit. This is of particular interest given results published by Tapia-Alveal et al 2014 where they show that chromosome segregation defects observed in Smc5/6 null mutants or cells treated with siRNA is suppressed in cells lacking H2A.Z suggesting

together, H2A.Z and the cohesin or Smc5/6 complex ensure genome integrity (Tapia-Alveal, Lin, Yeoh, *et al.*, 2014).

Whilst the synthetic viable hits were interesting and worth further investigation, the remainder of this chapter will focus on the top synthetically lethal hits of the screen. In this case BRCA2, the NHEJ factors and replication stress factors were chosen for validation.

Hits.	Brief Summary.	Appears in n of 3 screen with score over approximately +2
ACD, TERT	Involved in telomere function and lengthening.	ACD – 2, TERT – 1.
PIAS1	E3-SUMO Ligase. Stabilizes interaction with UBE2I and SUMO. SUMOylates PML bodies to promote ubiquitin-mediated degradation.	PIAS – 1.
TOPBP1	Plays a role in stalled replication forks and checkpoint control. Binds to DSB breaks and nicks as well as ssDNA. Recruits SWI/SNF.	TOPBP1 – 1.
UBB, UBD, UBA1	Involved in ubiquitination to target for degradation. UBD is a paralog of UBB. UBA1 catalyzes the first step in ubiquitin conjugation. Promotes recruitment of TP53BP1 and BRCA1 to DNA damage sites.	UBB – 2, UBD - 1, UBA1 – 1.
STRA13	Binding component of Fanconi Anaemia complex involved in DNA damage repair and genome maintenance. Recruited to stalled forks by interstrand cross-link and required for resistance to lesions.	STRA13 – 2.
TTI1	Involved in regulation of the DDR. Part of the TTT complex required to stabilize proteins levels of the PIKK family kinases.	TTI2 – 2.
CCNA2	Essential for the control of the cell cycle at the start of G1/S and the G2/M transition in mitosis. Also required for the packaging of telomere ends.	CCNA2 – 2.
DDX11	Involved in cellular proliferation. Has ATPase and Helicase activities. Stimulates FEN1. Required for sister chromatid cohesion.	DDX11 – 1.
ACTL6A	Similar to Actin. Involved in vesicular transport, spindle orientation, nuclear migration and chromatin remodeling. Related to SWI/SNF in S. cerevisae and Drosophila.	ACTL6A – 2.
WRN	Part of the RecQ subfamily of DNA and RNA helicases. Involved in transcription, recombination and repair. Interacts with Ku70/80, involved in DSB repair.	WRN – 1.
MMS22L	Part of the TONSL protein complex. Recognizes and repairs DNA DSBs. Stimulates the recombination dependent repair of stalled or collapsed replication forks. Promotes HR.	MMS22L – 2.
ANKRD28	Involved in PP6-mediated dephosphorylation of NFKBIE opposing its degradation in response to TNF-α. Inhibits the phosphatase activity of PPP1C.	ANKRD28 – 2.
FANCD2	Part of the Fanconi Anaemia complex. Monoubiquitinated by FANCB. Localizes to nuclear foci with BRCA1 and BRCA2. Promotes BRCA2/FANCD1 loading on to damaged chromatin.	FANCD2 – 1.
H2AFZ	Variant of H2A that appears to alter nucleosome stability. It is partially redundant with nucleosome remodeling complexes and is involved in transcriptional control.	H2AFZ – 2.

Table 4.3 – Selection of top synthetically viable hits with details. Individual Z-scores were taken and the mean calculated, right hand column shows number of times each hit scored approximately +2.

4.6 Validation of synthetic lethality hits

The next step was to validate the hits. This is important to ensure the top hits are not false positives. Whilst siRNA libraries are a useful tool for high throughput screens, unless characterised further it is possible that the results could be due to off target effects of the siRNAs used or and lack of effect due to not lowering levels of the targeted protein.

4.6.1 Confirmation of NSMCE4a shRNA knockdown in later passage cells

After the screen was carried out it was important to check there was still a reduction in SMC5 and SMC6 levels in the NSMCE4a shRNA cells. Western blotting was carried out and showed a slight reduction in SMC5 and SMC6 levels. Loading was confirmed using anti-tubulin antibody **(Figure 4.3)**. Levels were not as reduced as what was initially observed in the previous chapter (compare **Figures 4.3** and **3.4**), quantification of these levels is seen in **(Table A.4.2.A)**. This is likely due to cells overcoming the knockdown with time, despite constant puromycin selection. Validation of hits was carried out in these cells but it is likely that a stronger phenotype would be observed in cells with stronger knockdown and this could have been achieved through use of the gating feature on the ScanR microscope.

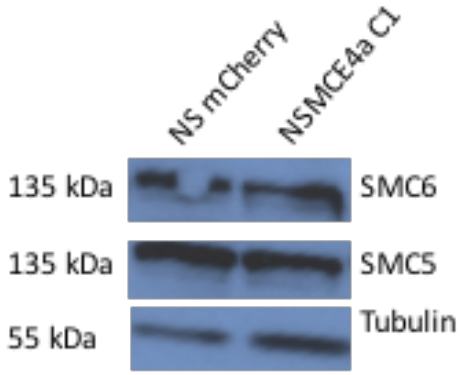

Figure 4.3. Western blot confirming knockdown of SMC5 and SMC6 in NSMCE4a shRNA cells after the screen had been carried out.

4.6.2 – BRCA2 is a top candidate in the synthetic sick/lethal screen

BRCA2 appears as a top hit in the screen whereas BRCA1 does not. Both are involved in homologous recombination. BRCA2-deficient cells exhibit increased

sensitivity to ionizing radiation, however cell cycle checkpoint and apoptotic responses to DNA damage remain intact. BRCA2 regulates the intracellular localisation and function of the recombinase RAD51(Tarsounas, Davies & West, 2003). Nuclear transport of RAD51 is impaired in BRCA2 deficient cells suggesting that once RPA has coated ssDNA following resection during cells deficient in BRCA2 cannot replace it with RAD51.

BRCA1 also functions in the HR pathway however in a different capacity to BRCA2 (Roy, Chun & Powell, 2012). In response to DNA damage BRCA1 is hyper-phosphorylated and localizes to sites of DNA damage. In response to ionizing radiation BRCA1 is bound and phosphorylated by ATM (Roy, Chun & Powell, 2012). Both BRCA1 and BRCA2 co-localize with RAD51 to form complexes and co-localize with MRN appearing to function as a regulator.

To validate that BRCA2 and not BRCA1 was synthetically sick with loss of NSMCE4a this was explored in two different approaches. Firstly, NSMCE4a shRNA and Non-silencing cells from the screen **(Figure 4.4.A)** were treated with siRNA Smartpools specific to BRCA1 and to BRCA2, quantification of BRCA1 levels is seen in **(Table A.4.2.D)**. These Smartpools are independent of the ones used in the screen, see Appendix section A.2 for details. The BRCA1 knockdowns led to loss of viability in both shNSMCE4a and non-silencing cells. However, no statistically significant difference in viability was seen between shNSMCE4a AcGFP cells (19.3%) and shNon-silencing mCherry cells (23.9 %). Reduction of BRCA1 was confirmed through western blotting shown in **(Figure 4.4.B)**, equal loading was confirmed using Ponceau staining.

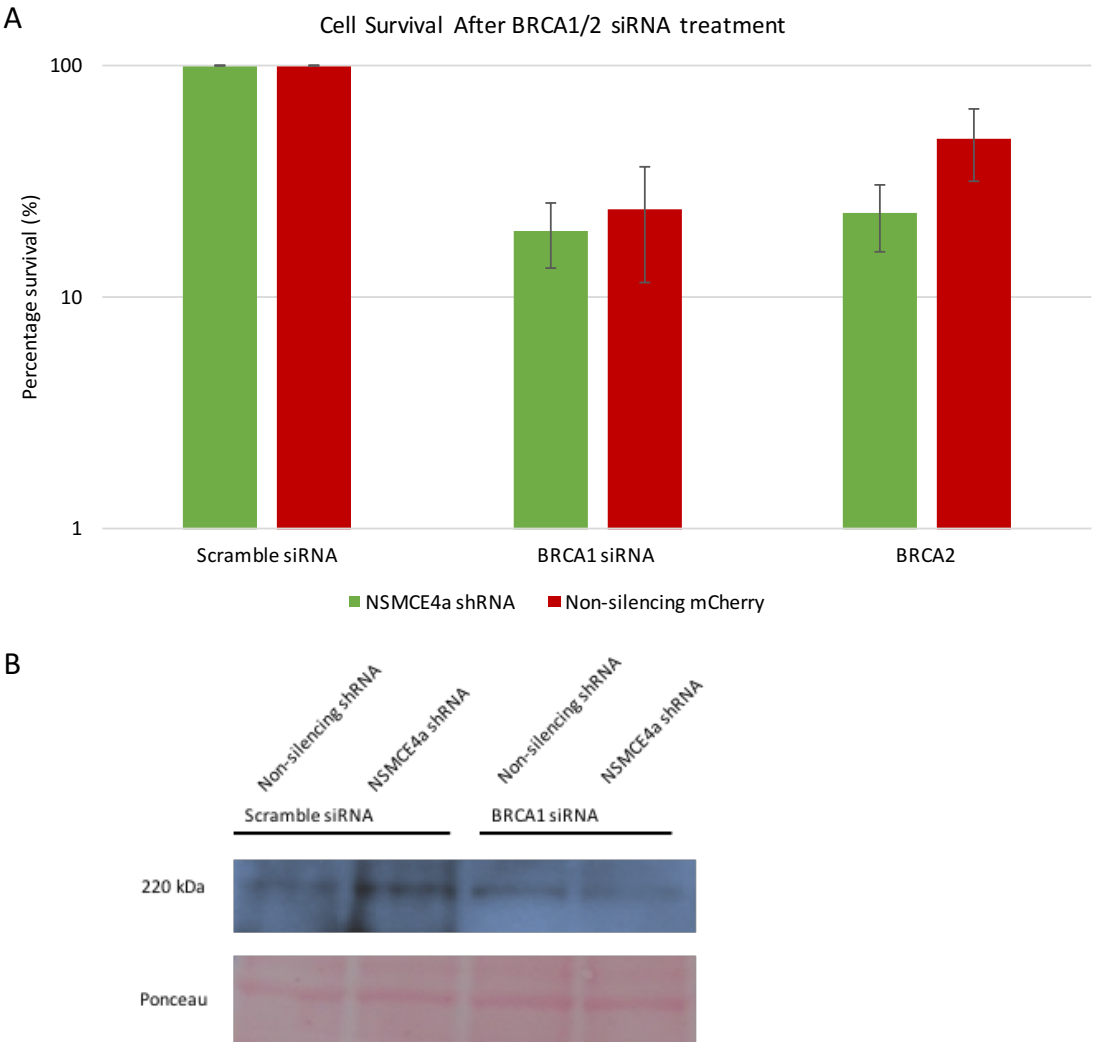

Figure 4.4. A. Results of colony formation assay showing treatment of NSMCE4a shRNA cells with BRCA1 siRNA (P-value 0.07) and BRCA2 siRNA (P-value 0.01). Assay was repeated 3 times in triplicate**B.** Western blot analysis showing knockdown of BRCA1 following siRNA treatment in Non-silencing mCherry and NSMCE4a AcGFP cells.

A marked reduction in viability was observed in cells with dual perturbation of SMC5/6 and BRCA2 as shown in **(Figure 4.4.A)**. Cell viability in the shNSMCE4a AcGFP cells was reduced to 23 % after exposure to BRCA2, in contrast to the shNon-silencing cells were viability was reduced to 48%. To confirm the synthetic sickness immortalised fibroblasts from wild-type (1BR hTERT), SMC5/6–deficient (NSMCE3-L264F, GVH02 hTERT (see **Chapter 5** for further details of this cell line)) and BRCA2-deficient (HSC62 hTERT) individuals were treated with siRNA specific to NSMCE4a **(Figure 4.5.A)**. Both WT and NSMCE3-L264F cells showed a slight reduction in viability but the BRCA2-deficient cells

showed significantly increased sensitivity. In the primary patient fibroblasts after NSMCE4a siRNA exposure cell viability was reduced to 80.9 %, 80.3 % and 60.9 % in WT1, NSMCE3-L264F and BRCA2 deficient cells respectively. SMC6, a marker of complex stability and NSMCE4a knockdown, was examined using western blotting **(Figure 4.5.B)**. Equal loading was confirmed using ponceau staining, quantification of protein levels can be seen in **(Table A.4.2.B)**. SMC6 is reduced in the untreated NSMCE3-L264F cells compared to WT (see **Chapter 5** for a full characterisation) and was also reduced in the BRCA2-deficient cell line. To confirm this the extract was rerun and **Figure 4.5.C** shows that SMC6 is present in the BRCA2 deficient cells and is reduced on siNSMCE4a treatment. After siNSMCE4a SMC6 levels reduced in WT but no changes were seen the other cell lines. Overall, this analysis supports results in the screen that BRCA2 but not BRCA1 was synthetically sick with loss of NSMCE4a. It is possible that this is due to BRCA1 being essential in both cell types, whereas BRCA2 is only essential in NSMCE4a knockdown cells. However this must be investigated further before any such conclusion can be made.

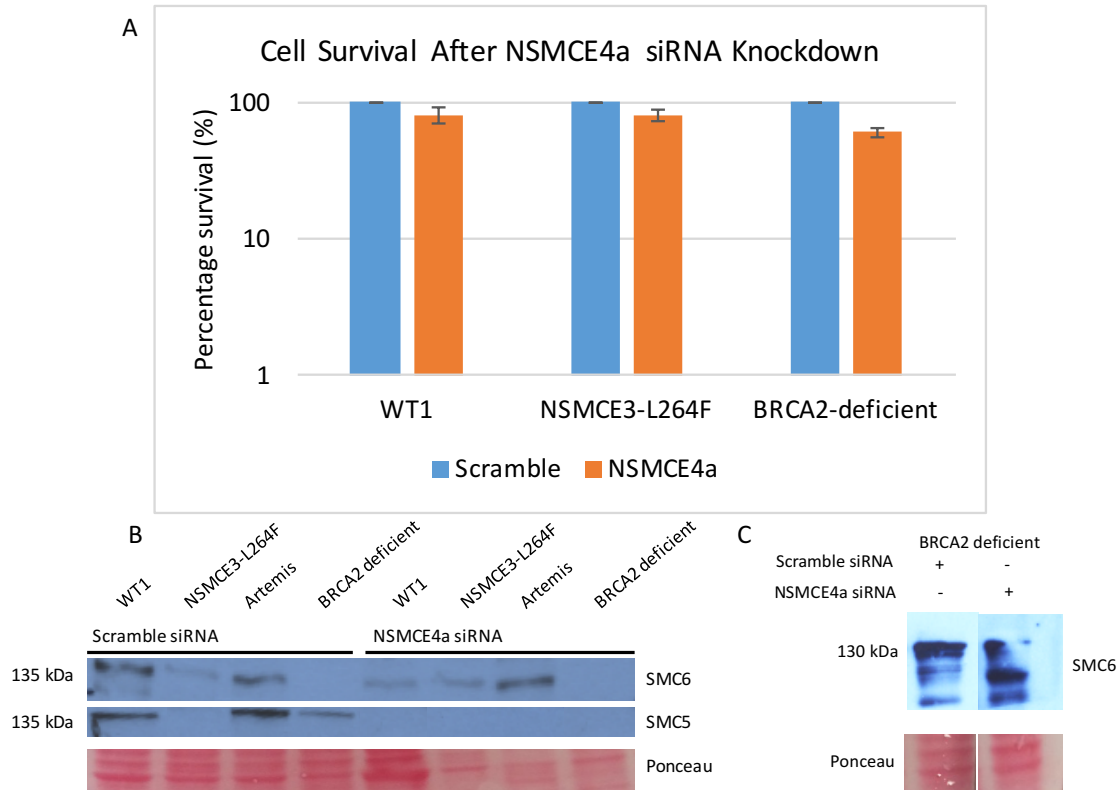

Figure 4.5. A. Colony formation in WT (1BR hTERT), NSMCE3-L264F (SMC5/6 deficient GVH02 hTERT), Artemis deficient (CJ176 hTERT), and BRCA2-deficient (HSC62 hTERT) cells following treatment with siRNA specific to NSMCE4a. Results indicate a statistically relevant reduction in cell viability of the BRCA2 deficient cells compared to WT or SMC5/6 deficient (p=0.005). **B.** Western blot showing knockdown of SMC6 in indicated cell lines. **C.** Initially SMC6 in BRCA2 cells were not knocked down, however upon repetition knockdown was observed.

4.6.3 – Knockdown of NSMCE4a leads to increased sensitivity to MRE11 inhibitor Mirin

MRE11 was also a candidate for synthetic lethality as it came up in the top 60 hits in the screen. MRE11 is part of the MRN complex, required for initiation of HRs and for ATM signalling (Álvarez-Quilón, Serrano-Benítez, Lieberman, *et al.*, 2014). To investigate this further clonogenic survival assays were carried out with wild-type (WT1, 1BR hTERT), NSMCE3-L264F (GVH02 hTERT), Artemis null (CJ176 hTERT) and BRCA2 deficient (HSC62 hTERT) mutant cells in the presence of 0, 5, 10, 25 and 50 μM of the MRE11 inhibitor, Mirin **(Figure 4.6.B)**. Mirin was identified as a small molecule that inhibits the MRN-dependent activation of ATM by perturbing the nuclease activity of MRE11, **(Figure 4.6.A)** shows the structure of Mirin (Dupré, Boyer-Chatenet, Sattler, *et al.*, 2008; Kuroda, Urata & Fujiwara, 2012). WT1 cells showed cell survival of 100, 39, 17, 6 and 2 % respectively. NSMCE3-L264F cells showed 100, 36, 11, 3 and 1 %. Artemis cells had 100, 47, 13, 3 and 1 % and finally BRCA2 showed 100, 58, 25, 6 and 2 % survival after 10 days. This showed that perturbation of SMC5/6 levels and inhibition of MRE11 results in increased sensitivity, consistent with the reduction in viability observed in the screen. The reduction in viability is similar to that seen in the NHEJ-defective Artemis cells where an inhibition of MRE11 results in sensitivity.

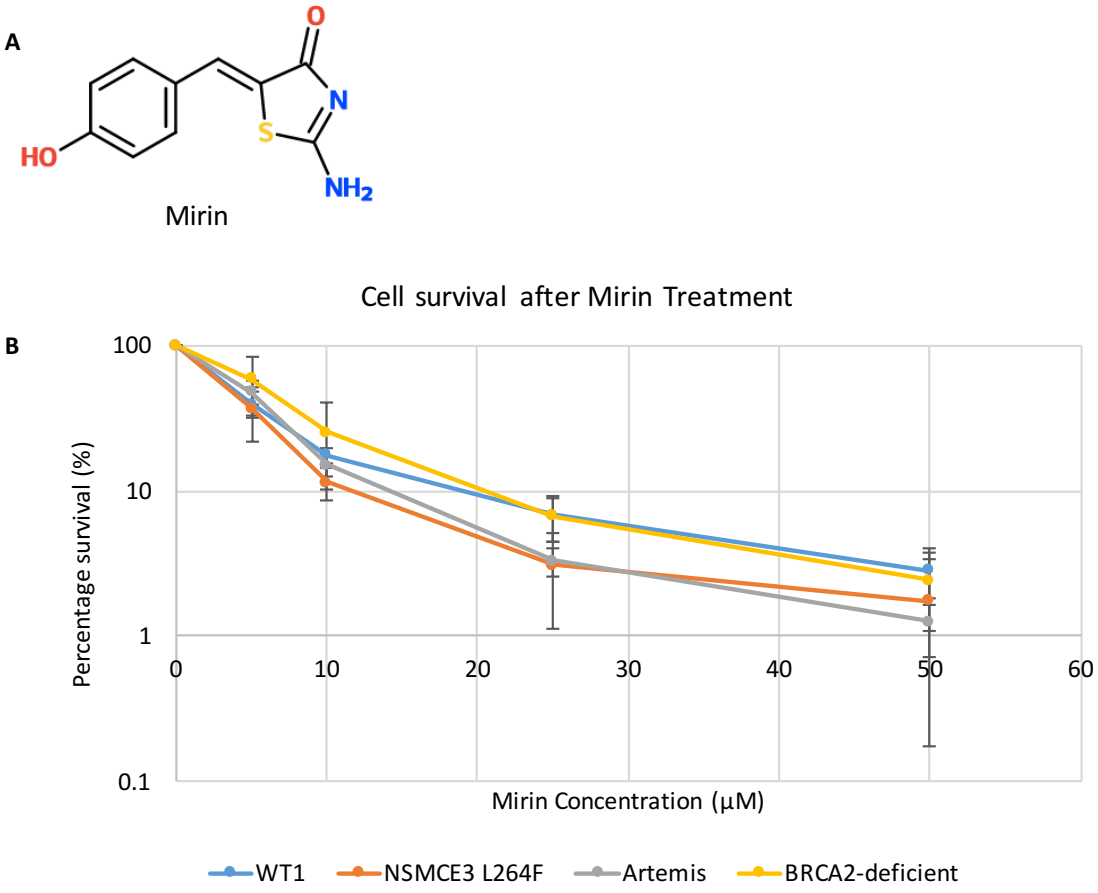

Figure 4.6. A. ChemSketch drawing of Mirin – MRE11 inhibitor. **B**. Graph showing response to Mirin exposure. Clonogenic survival assays were carried out with wild-type (WT1, 1BR hTERT), NSMCE3-L264F (GVH02 hTERT), Artemis null (CJ176 hTERT) and BRCA2 deficient (HSC62 hTERT) mutant cells in the presence of 0, 5, 10, 25 and 50 µM of the MRE11 inhibitor, Mirin. NSMCE3-L264F cells showed increased sensitivity, as observed in Artemis cells, this was not observed in BRCA2-deficient cells.

4.6.4 – Knockdown of NSMCE4a is synthetic lethal with loss of NHEJ factors.

NHEJ plays a major role in the DNA damage response and is the main pathway used in human cells (Lieber, Gu, Lu, *et al.*, 2009). Whist error prone in comparison to HR the cell can carry out NHEJ at all phases of the cell cycle. HR on the other hand can only occur in late S and G2 phases of the cell cycle (Kass & Jasin, 2010).

The identification of XLF and Artemis as two of the most lethal interactions and Ligase IV in the top 60 hits indicates that NHEJ is required when SMC5/6 is

compromised (Schematic of NHEJ repair showing where these proteins function is given in **Figure 1.1**). In order to show that proteins required for NHEJ are critical to cell survival when HR is compromised though loss of NSMCE4a, wild-type (1BR hTERT), NSMCE3-L264F (GVH02-hTERT), Artemis (CJ176 hTERT) and XLF (2BN hTERT) cells were transfected with NSMCE4a siRNA or a non-silencing control and colony formation assays were performed. While viability after knockdown of NSMCE4a in the Artemis cell line was not significantly different to WT, in the XLF cells there was significant loss of viability **(Figure 4.7.B)**. All data from colony formation assays was normalised to 100 % in the scramble. WT1 cells showed 80 % survival following NSMCE4a siRNA, NSMCE3-L264F cells similarly showed 80 % survival and Artemis cells showed 74 % survival. XLF treated cells dropped to a viability of 9 % compared to wild-type, this is statistically significant with a p-value of 0.002. The lack of decreased viability in the Artemis cell line may be due to lack of efficient knockdown as SMC6 levels did not decrease (**Figure 4.6.B**). Reduction of SMC5/6 levels in the other NSMCE4a siRNA treated cells was confirmed using western blotting with ponceau used to confirm equal loading **(Figure 4.7.C),** quantification of protein levels is shown in **(Table A.4.2.C).**

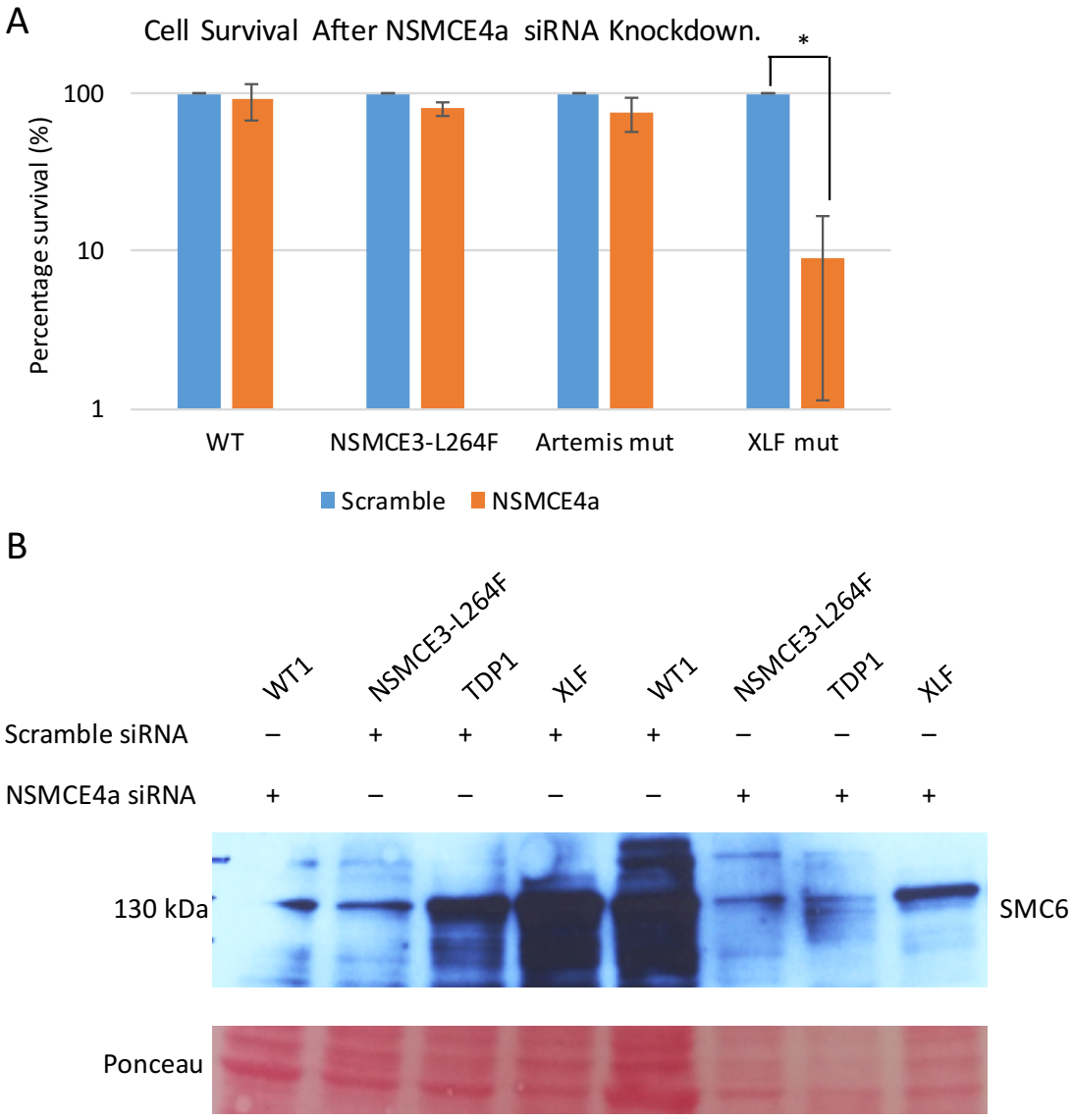

Figure 4.7. A. Graph showing percentage cell survival after exposure to NSMCE4a siRNA in wild-type (1BR hTERT), NSMCE3-L264F (GVH02-hTERT), Artemis (CJ176 hTERT) and XLF (2BN hTERT) cells. **B**. Western blot showing knockdown of SMC5 and SMC6 in WT, NSMCE3-L264F and XLF cells.

4.6.5 – NSMCE4a knockdown is synthetic lethal with knockdown of RRM1 and RRM2.

Replication stress is a hallmark of cancer (Macheret & Halazonetis, 2015). Several hits within the screen indicated factors that were synthetically sick/lethal with NSMCE4a shRNA knockdown were involved in DNA replication or

production of dNTPs, consistent with a requirement for SMC5/6 in response to replication stress.

In the screen siRNA specific to ribonucleotide reductase subunits (RNR) RRM1, RRM2 and RRM2B were assessed. Both RRM1 and RRM2 showed a synthetic lethal interaction with NSMCE4a shRNA however RRM2B did not. RMM2B is P53 inducible through DNA hypomethylation (Link, Baer, James, *et al.*, 2008) and, therefore, it is likely this is the reason a lethal interaction was not observed. Another possibility could be that transfection efficiency was lower and knockdown was not achieved.

Hydroxyurea (HU) is an inhibitor of RNR and arrests cells in S phase by depleting nucleotide pools. (A schematic of the RNR pathway is shown in **Figure 4.9.A**). To validate these hits cells were blocked in S phase by HU, released into fresh media in the presence of the nucleotide analogue EdU and the percentage of cells with EdU positive nuclei scored with and without the HU block.

Cells containing shRNA to NSMCE4a or Non-silencing shRNA cells were treated with 250 μM HU for up to 18 hours before being released into fresh media containing 10 μM EdU for 30 minutes. Plates were analysed using the Olympus ScanR microscopy platform. The percentages of cells that incorporated EdU was analysed both with and without HU block and release. Cells which expressed Non-silencing shRNA showed 63, 83.9 and 87 % incorporation at 0, 12 and 14 hours and NSMCE4a shRNA showed 50, 75 and 79 % respectively. The assay was carried out using four replicates and with three independent repeats. The differences at 12 and 14 hours between Non-silencing and NSMCE4a shRNA was statistically significant with p-values of 0.002 and 0.05 **(Figure 4.9.B)**. The apparent high level of incorporation could be false positive however due to bleed through into the TxRed channel from the FITC channel. To examine this further use of an siRNA to GFP or use of an inducible knock-out cell line would help confirm the result. Given the reduced number of cells in S phase in the –HU control does not suggest that the results +HU is not significant,

however when gating for high EdU incorporating cells at 14 hours shows reduction in NSMCE4a shRNA expressing cells numbers suggesting cells with NSMCE4a shRNA expression are less efficient to restart replication than Non-silencing shRNA cells **(Figure 4.9.C)**. These results suggest that SMC5/6 is required under conditions of replication stress and therefore may function as a tumour suppressor.

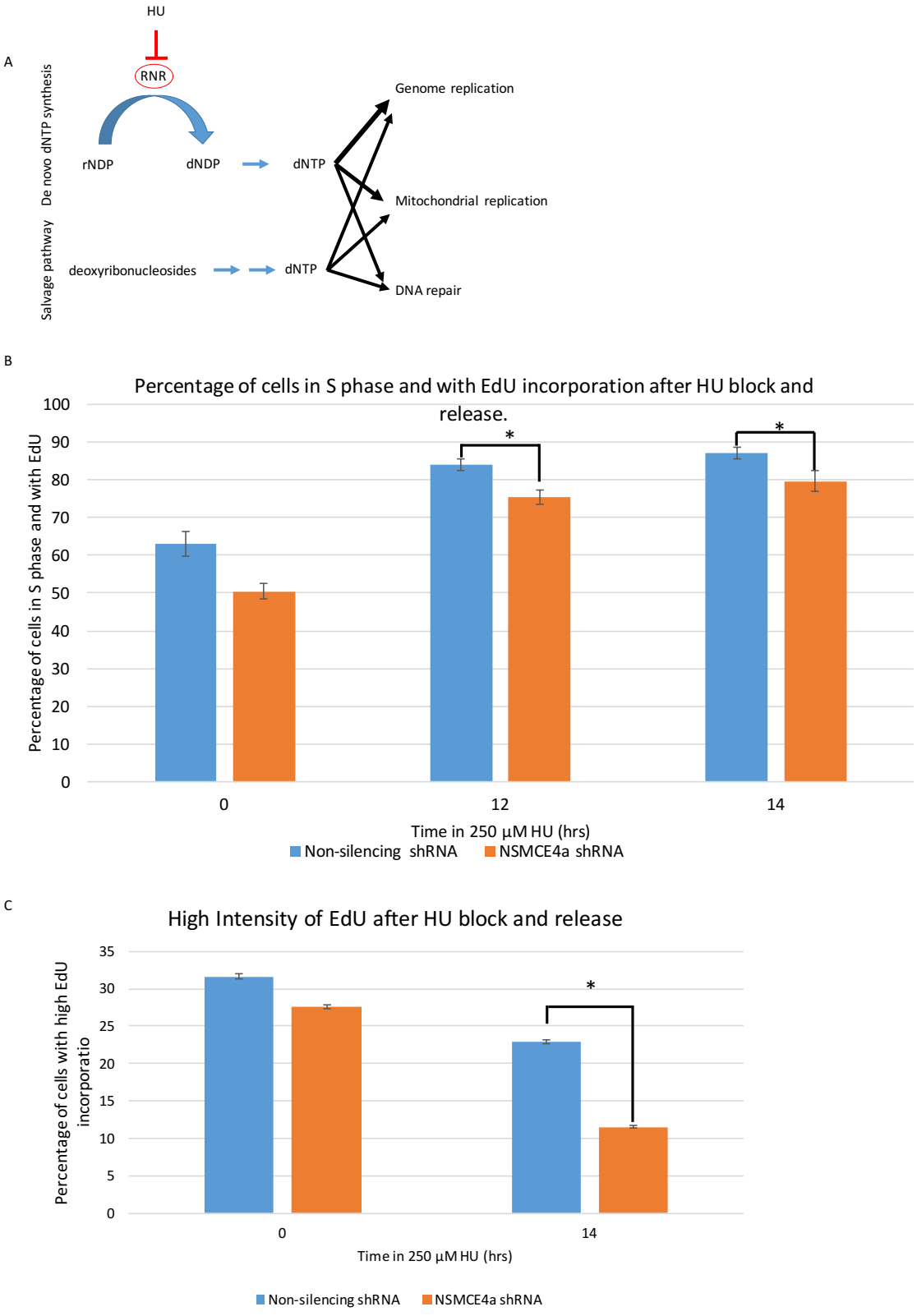

Figure 4.8. A. Schematic representation of RNR pathway. **B.** Graph of percentage cells with incorporation of EdU with and without 12 and 14 hour HU block and release. P-value = 0.002 and 0.05 respectively. **C.** Gating for the highest EdU incorporating cells shows reduction in number of NSMCE4a shRNA cells being able to incorporate EdU compared with Non-silencing control P-value 0.001.

4.7 – Discussion.

4.7.1 Synthetic lethality hits

In this chapter the results of a synthetic sick/lethal screen were presented. The high-throughput microscopy screen was carried out in triplicate and in each screen analysed large numbers of cells per well. For example, an average of 768 NSMCE4a AcGFP and 1023 Non-silencing mCherry cells were screened per experiment in the RRM1 well. In RRM2 an average of 965 NSMCE4a AcGFP cells and 1326 Non-silencing mCherry were screened.

A pool of shNSMCE4a GFP cells were used with a range of expression of the shRNA. This had the advantage that results could be gated for GFP intensity (increased GFP correlating with increased knockdown) but this was not carried out for this analysis. While useful for the initial screen, the mixed population was a disadvantage for the validation. Western blot analysis showed that SMC5/6 was still knocked down in later passage cells but not to the same degree as had been observed before **(Figure 4.3)**. This may be due to the age of the cells as shRNA knockdown can be overcome through incorporation of mutations in cells. This was observed is a parallel screen (Hopkins, McGregor, Murray, *et al.*, 2016) despite the presence of constant puromycin selection when the cells were not under screening.

The results indicated that loss of SMC5/6 results in a pronounced sensitivity under conditions of replication stress, loss of some HR factors and some NHEJ factors.

BRCA2 is the top hit in the screen and functions to replace RPA with RAD51. RAD52 has a similar role and also appears highly in the screen. MRE11 is within the top 60 hits. However, consistent with the epistasis seen in yeasts RAD51 is neutral in the screen and BRCA1 does not appear as a top hit. Therefore, within the HR pathway there appears to be a split in the response to NSMCE4a knockdown, with early steps showing synthetic lethality. In yeasts RAD52 and MRN genes are also synthetically sick with hypomorphic SMC5/6 mutants and

this has been suggested to be due to their role in single strand annealing which becomes essential when later stages of HR are disrupted. An important question to arise is why BRCA2 appears as the top hit whereas BRCA1 does not, when both are involved in HR and in similar steps. It is possible that loss of BRCA1 is equally deleterious for both the NSMCE4a and Non-silencing shRNA cells.

NHEJ factors also appeared as top hits within the screen but key NHEJ factors were not seen. Neither DNAPK-cs nor KU70 or KU80 were identified. This may be due to the efficiency of knockdown and consistent with this KU70 and KU80 are very abundant proteins which are difficult to knockdown (Jeggo lab pers. comm.). Alternatively, the synthetic lethality seen with Artemis and XLF points to a requirement for end processing when SMC5/6 function is compromised.

The requirement for the SMC5/6 complex in response to replication stress was highlighted in the screen. The RNR subunits, RRM1 and RRM2 were strong hits. This is consistent with the replication stress phenotype associated with the NSMCE3-L264F cells described in **CHAPTER 5.** NSMCE4a shRNA AcGFP cells showed a reduction in capability to restart replication in comparison with Non-silencing mCherry cells. In fission yeast an SMC5/6 mutant have been shown to have shorter replication tracts after exposure to replication stress (Jo Murray, pers. comm). A synthetic sick/lethal interaction was also observed with knockdown of NSMCE4a and DNA replication factors, POLE, POLE4, POLN, POLD4, RFC1 and PCNA, and depletion of these factors would also cause problems during replication.

In budding yeast the Smc5/6 complex is required to mediate replication of repetitive genomic regions such as rDNA and telomeres (Gallego-Paez, Tanaka, Bando, *et al.*, 2014). MAD2L2, another hit in the screen, has, among other functions, been found to control DNA repair at telomeres and also the response to DNA breaks through inhibition of 5’ end resection. Depletion of MAD2L2 results in elongated 3’ telomeric overhangs suggesting MAD2L2 inhibits 5’ end

resection. 5' end resection typically results in blockage of NHEJ whilst committing cells to homology driven repair (Boersma, Moatti, Segura-Bayona, *et al.*, 2015). MAD2L2 also promotes NHEJ-mediated repair, therefore depletion of MAD2L2 in NSMCE4a knockdown cells suggests breaks which would typically be committed to repair by NHEJ are repaired by HR during S and late G2 and this may prove deleterious. The associated activity of SMC5/6 and MAD2L2 at telomeres may also explain why SMC5/6 and MAD2L2 is synthetic sick/lethal (Boersma, Moatti, Segura-Bayona, *et al.*, 2015).

Another top hit is Valosin Containing Protein (VCP) (van den Boom, Wolf, Weimann, *et al.*, 2016). VCP is involved in the DNA damage response where it is recruited to DSBs in an RNF8- and RNF168 dependent manner and promotes recruitment of 53BP1 to damage sites. It is also recruited to stalled replication forks by SPTRN (Lessel, Vaz, Halder, *et al.*, 2014) therefore given the crossover in functions between VCP and SMC5/6 it is likely that affecting both results in cell death. Another DNA repair pathway is represented, ssDNA break repair, with Aprataxin, encoded by the APTX gene. This play a role through its nucleotide-binding activity. It is also involved in DSB repair and BER where it is used to resolve abortive DNA ligation intermediates at base excision sites. It is also required at sites where DNA ligases attempted to repair non-ligatable ends following damage caused by reactive oxygen species(Schellenberg, Tumbale & Williams, 2015).

Helicases are also well represented with HEL308, DNA2L, RUVBL1 and RUVBL2 in the top 24 hits. SMC5/6 has previously been shown to have interactions with helicases (Chen, Choi, Szakal, *et al.*, 2009; Xaver, Huang, Chen, *et al.*, 2013). HEL308 is encoded by the HELQ gene, as the name alludes it is a helicase with ATPase activity. Part of the superfamily 2 helicase it is thought to function in the early stage of recombination following replication fork arrest (Richards, Johnson, Liu, *et al.*, 2008). The principal role of HEL308 appears to be to assist in the repair of replication fork blocking lesions, such as interstrand DNA cross-links(Woodman & Bolt, 2011; Tafel, Wu & McHugh, 2011). DNA2L is a key

enzyme required for accurate DNA replication and DNA repair. It is involved in Okazaki fragment processing by cleaving long flaps that FEN1 cannot deal with. In *S. cerevisae* Dna2 is also required for its nuclease activity but also checkpoint activation(Wanrooij & Burgers, 2015). RUVBL1 and RUVBL2 encodes for the human homologue of bacterial RuvB gene. In humans RUVBL1 and RUVBL2 possesses ssDNA stimulated ATPase and an ATP-dependent DNA helicase (5' to 3' and 3' to 5') both interacts with the Fanconi Anaemia core complex and depletion leads to DNA damage sensitivity and elevated chromosomal instability (Rajendra, Garaycoechea, Patel, *et al.*, 2014). This suggests loss of helicases and as their associated defects accumulate in a synthetic sick/lethal manner with knockdown of NSMCE4a.

4.7.2 – Synthetic viability hits

A number of synthetic viable hits were also identified **(see Appendix section A.3.6 and A.3.6.1)**, the most interesting of which are the MMS22L-TONSL complex and H2A.Z. The MMS22-TONSL complex stimulates recombination dependent repair at stalled or collapsed replication forks (Duro, Lundin, Ask, *et al.*, 2010). Given the roles of SMC5/6 in HR and the requirement for SMC5/6 in response to replication stress (supported by the synthetic lethal hits in this study) this suggests that in the absence of the MMS22L-TONSL complex lesions are processed by HR-independent pathways and SMC5/6 is not required. The identification of H2A.Z as synthetic viable is supported by a study in fission yeast that identified H2A.Z as a suppressor of chromosome segregation defects in SMC5/6 hypomorphic mutants (Tapia-Alveal, Lin, Yeoh, *et al.*, 2014). It would be interesting to follow up these and other hits but this was not possible due to time constraints.

Chapter 5 – Characterisation of the cellular defects associated with mutation in NSMCE3, which leads to LICS syndrome.

5.1 – Introduction

In this chapter the characterisation of the cellular defects due to mutation in NSMCE3, a subunit of SMC5/6, is presented. The mutation in NSMCE3 was first identified in two Dutch sisters, daughters of distantly related parents **(Figure 5.1.A)**, who both presented at hospital at about 13 months with severe lung failure following pneumonia (van der Crabben, Hennus, McGregor, *et al.*, 2016). Karyotyping of the patients' cells showed high levels of chromosomal rearrangements **(Figure 5.1.C)**. Whole exome sequencing of the patients' DNA identified a homozygous missense mutation in NSMCE3 (c. 790G>T, pLeu164Phe). Another family with compound heterozygous mutations in NSMCE3 was also identified from America **(Figure 5.1.B)**, (c. 626C>T) p.Pro209Leu and (c. 790G>T) p.Leu264Phe **(Figure 5.1.D).** These patients presented with similar symptoms of lung disease, weight loss, eczema and food allergies. The first sibling died at a similar age to the Dutch sisters, of pulmonary failure following pneumonia, while the younger sibling underwent lung transplantation at 15 months old due to pulmonary damage but died at 31 months old following bone marrow failure and increased susceptibility to infection. The syndrome has been named LICS, as it is characterised by **l**ung disease, **i**mmunodeficiency and **c**hromosome instability.

NSMCE3 (also called NDNL2 or MAGEG1) is a 35 kDa protein which forms a subcomplex with NSMCE1 and NSMCE4a in the SMC5/6 complex in humans(Taylor, Copsey, Hudson, *et al.*, 2008a; Doyle, Gao, Wang, *et al.*, 2010). It is a member of the Melanoma Antigen (MAGE) protein family and has been shown to enhance the E3 ubiquitin ligase function of NSMCE1 *in vitro* (Doyle, Gao, Wang, *et al.*, 2010). Its yeast homologue, Nse3, forms a similar strong interaction with Nse1. It is the founder and only MAGE protein present in yeast and most eukaryotes but in mammals the MAGE family has diversified.

There are 55 MAGE genes in the human genome which have been subdivided into different classes based upon their protein structures(Doyle, Gao, Wang, *et al.*, 2010). MAGE proteins were first identified as cell surface markers on cancer

cells and the focus of studies has been to examine their potential as targets in cancer immunotherapy (Barker & Salehi, 2002). Individual members of the MAGE proteins have been reported as playing important roles in neuronal development, apoptosis and cell cycle control(Bush & Wevrick, 2008) but a biochemical function is yet to be identified for many of the MAGE proteins(Taylor, Copsey, Hudson, *et al.*, 2008a).

Nse3 is essential in yeasts, where most research into the roles of the Smc5/6 complex has been carried out. This chapter will focus on the characterisation of the cellular effects of the NSMCE3-L264F mutation in patient cells and of the analogous mutation in *S. pombe*.

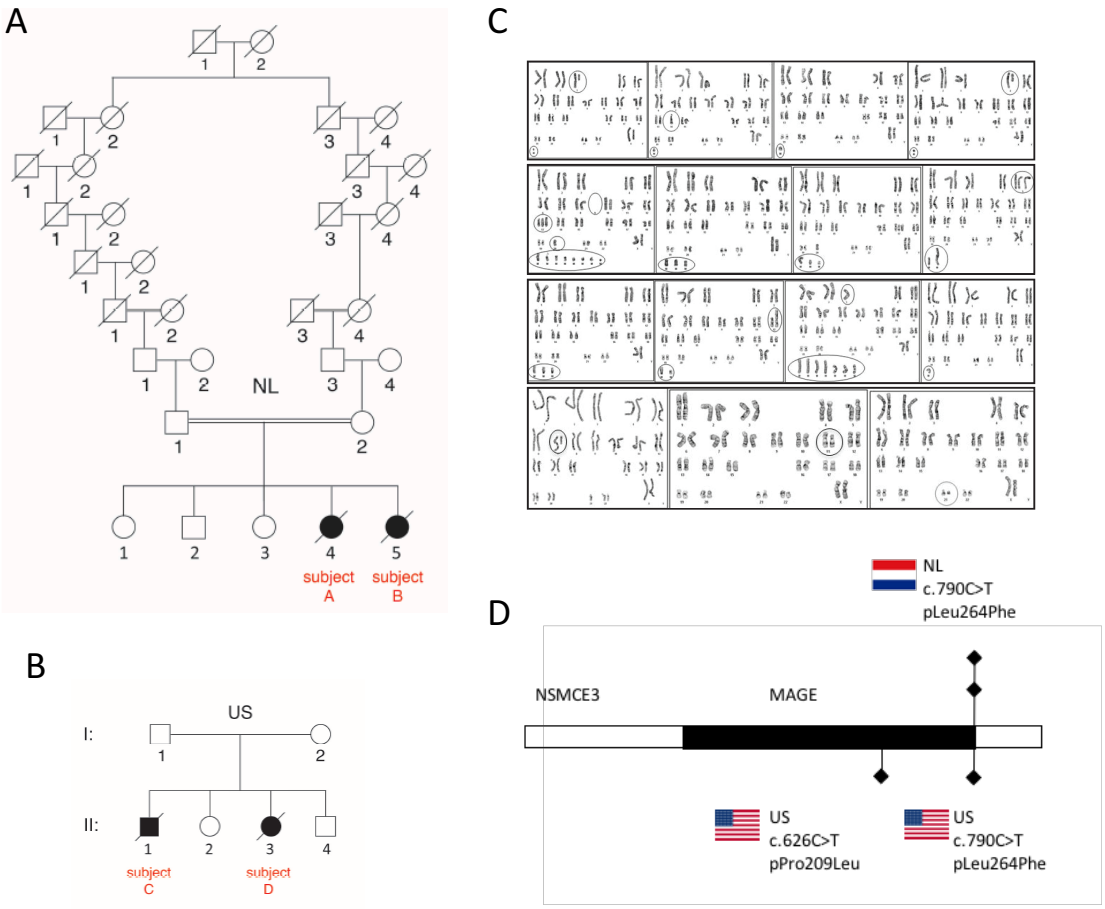

Figure 5.1. A., B. Family trees from both Dutch and US families. The Dutch family show consanguinity six generations previously. **C.** Karyotyping of lymphocytes from one of the Dutch patients, samples were obtained two weeks after admission to hospital and show large levels of genomic rearrangements and supernumerary markers. **D.** Schematic showing position of mutations in the NSMCE3 gene. Dutch patients show homozygous mutations c.790C>T p.L264F. American patients have heterozygous mutations c.626C>T p.P209L and c.790C>T p.L264F.

5.2 Results

5.2.1 – The equivalent mutation in *S. pombe, nse3*-L293F, does not lead to sensitivity to DNA damaging agents

To determine the effect of the NSMCE3-L264F mutation the comparative orthologous mutation was modelled in *S. pombe* and compared against well-characterised Smc5/6 complex mutants. Sequence alignment, using Jalview, of *H. sapien* NSMCE3*, S. pombe* Nse3 and *S. cerevisae* Nse3 proteins indicated the corresponding mutation was Leu293Phe **(Figure 5.2.A)**.

The sequence encoding Nse3-L293F was created by site-directed mutagenesis PCR **(Figure 5.2.B)**. The mutated *nse3* gene was ligated into the pAW8 plasmid (Watson, Garcia, Bone, *et al.*, 2008), between flanking LoxP and LoxM3 sites **(Figure 5.2.C)**. The mutated gene was integrated under the control of the endogenous *nse3* promoter in the host genome through Recombination Mediated Cassette Exchange (RMCE)(Watson, Garcia, Bone, *et al.*, 2008). The base strain for this integration, which consists of the *nse3* gene and *ura4* selectable marker flanked by loxP and loxM3 sites, was a gift from Prof Alan Lehmann. RMCE is an efficient method for gene tagging and gene replacement using Cre recombinase **(Figure 5.2.C)** (Watson, Garcia, Bone, *et al.*, 2008)**.** Following integration of the cassette, positive clones were selected for by replacement of the *ura4* marker using 5'-fluoroorotic acid (5'-FOA). Successful integration of the mutated gene was confirmed by colony PCR and sequencing **(Figure 5.2.D)**.

Creation of *nse3*-L293F in *S. pombe* showed the mutation was viable. To investigate the effect of the mutation, cells were compared to wild type (WT) cells and well characterised mutants under a range of conditions and DNA damaging agents.

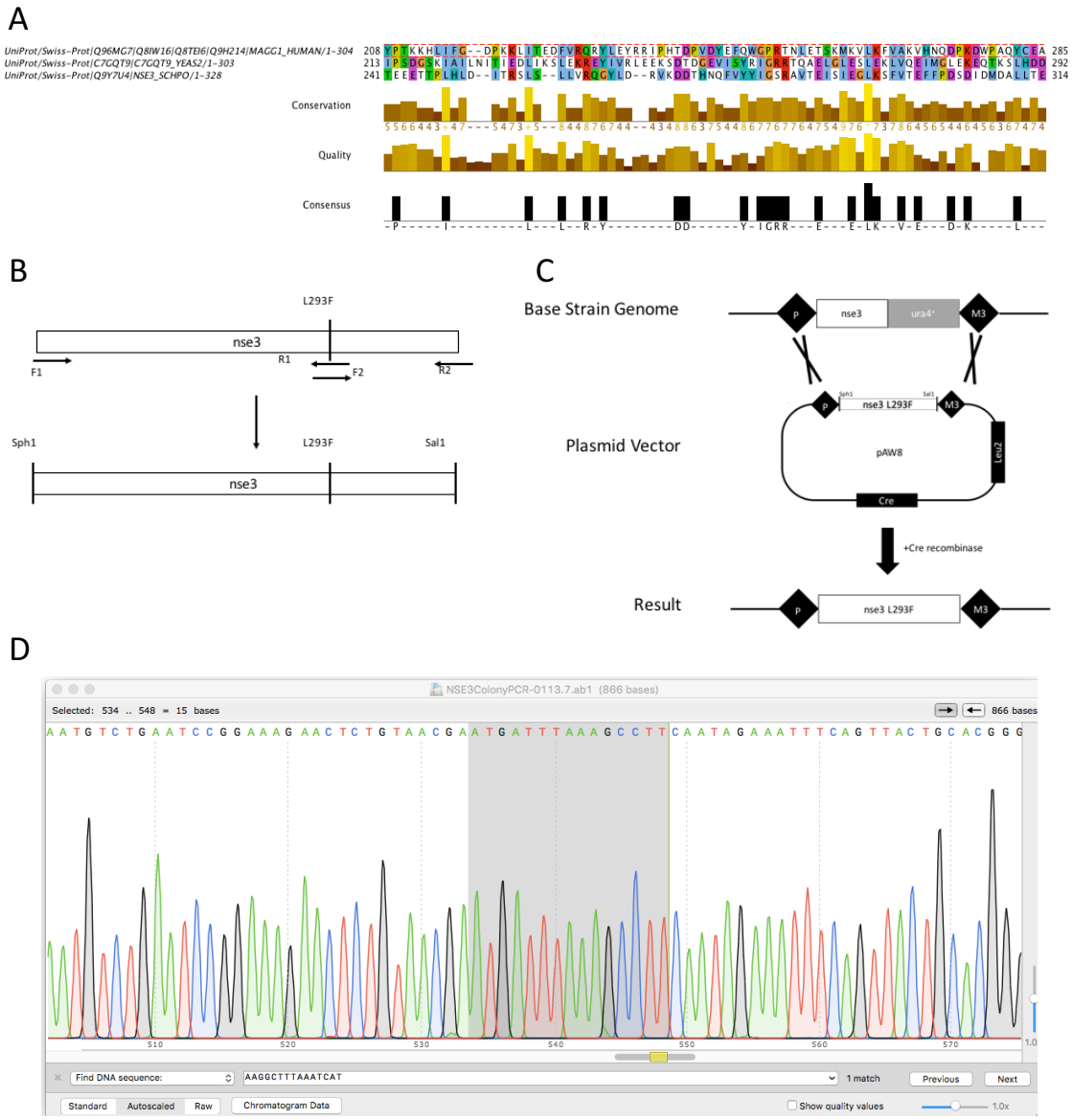

Figure 5.2.A. Sequence alignment of NSMCE3 genes from H. sapiens, S. pombe, S. cerevisiae. Sequences were obtained from Uniprot using accession numbers Q96MG7, Q9Y7UA and QO5541. Sequences were aligned using Jalview and coloured using ClustalX. **B.** Schematic of site-directed mutagenesis to create *nse3*-L293F mutation. Fusion PCR was used to create two separate fragments and fuse them together using the F1 and R2 primers whilst incorporating the L293F mutation that had been created in the previous PCR. Restriction sites were incorporated at the beginning and end of the gene fragment to allow it to be ligated into destination plasmid pAW8. **C.** Schematic representation of Recombination Mediated Cassette Exchange. The gene incorporating the *nse3*-L293F mutation in pAW8 plasmid was transformed into the *nse3* Base Strain which contains LoxP and LoxM3 sites flanking nse3-ura4+ gene. Induction of Cre recombinase expression led to recombination between wild-type nse3 in the genome and nse3-L293F on the pAW8 plasmid. Replacement of the ura4 marker was selected by growth on 5-FOA plates. **D.** Confirmation of successful mutagenesis of *nse3*-WT to *nse3*-L264F.

5.2.1.1 – Examining the effects of non-permissive temperatures on cells with mutated *nse3*

Smc5/6 is essential in fission yeast and mutants that destabilise the complex lead to loss of viability or slow growth defects (Lehmann, Walicka, Griffiths, *et al.*, 1995; Fousteri & Lehmann, 2000). In addition, conditionally lethal mutants have also been identified (Sergeant, Taylor, Palecek, *et al.*, 2005). To determine whether the *nse3*-L293F mutation confers a sensitivity to increased/decreased temperature and to ensure that these cells can grow at standard conditions (30 ºC) cells were grown at 25 ºC and 37 ºC as well as 30 ºC. Serial dilutions of cells ($17.5x10^5$ – $8.75x10^4$ – $4.3x10^3$ – $2.1x10^2$ – $1x10^1$) were plated onto YEA plates with Phloxin B, as a marker for cell viability, and grown for 4 days at the indicated temperatures. Wild-type cells (WT) and the *nse3* base strain (*nse3*-bs) were used as controls to show that the flanking *lox* sites did not contribute to the phenotype. Two well characterised mutants *smc6-X* (Lehmann, Walicka, Griffiths, *et al.*, 1995) and *smc6-74* (Verkade, Bugg, Lindsay, *et al.*, 1999) were plated for comparison. All three isolates of *nse3-L293F* strains grew similarly to wild-type at all temperatures **(Figure 5.3)**. In contrast and as expected, the most sensitive of the smc6 mutants, *smc6-X*, had a slight growth defect at all temperatures.

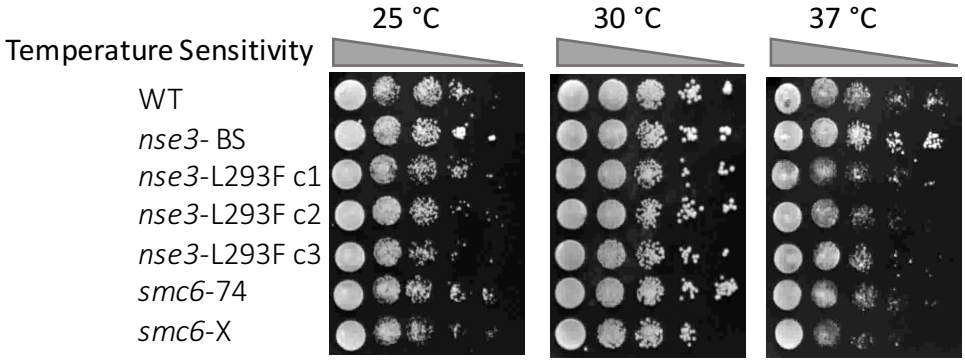

Figure 5.3. Spot test showing *nse3*-L293F lack of sensitivity to shifting temperatures. Wild-type (WT), *nse3* base-strain (bs), three isolates of *nse3*-L293F, *smc6*-74 and *smc6*-X cells were plated in varying dilutions and exposed to different temperatures. No sensitivity to different temperatures was observed except for *smc6*-X which had a slight defect at all temperatures.

5.2.1.2 – Exposure of *nse3-L293F* cells to UV radiation does not show increased sensitivity compared to wild-type and base strain controls.

Since Smc5/6 mutants in *S. pombe* exhibit sensitivity to DNA damaging agents and inhibition of replication the response of the *nse3*-L293F mutant was tested. Spot tests were carried out using the same strains as previously described (*nse3-L293F* with wild-type (WT), *nse3*-base strain, *smc6-X* and *smc6-74* as controls).

Five dilutions of cells ($17.5x10^5$ – $8.75x10^4$ – $4.3x10^3$ – $2.1x10^2$ – $1x10^1$) were plated onto YEA plates with Phloxin B, exposed to 50, 100, 150 or 200 J/m^2 of UV radiation and left to incubate for 4 days. Wild-type and base strain cells were not sensitive to low doses of UV. Whilst *smc6-74* and *smc6-X* showed high sensitivity, with *smc6-X* the more sensitive. This is consistent with previous reports (Ampatzidou, Irmisch, O'Connell, *et al.*, 2006). *nse3-L293F* cells were slightly more sensitive than base strain cells, but not as sensitive as the *smc6* mutants **(Figure 5.4.A)**.

To examine this potential defect further a more accurate and quantitative colony formation assay was carried out. The *nse3-L293F* strain was compared to wild-type (WT), *nse3*-base strain, and *smc6-74*. In addition, *nse2-SA* was included in the analysis. This mutation inactivates the Nse2 SUMO ligase activity and leads to sensitivity to DNA damage in S phase but not to UV sensitivity (Andrews, Palecek, Sergeant, *et al.*, 2005). Log phase cells were plated onto YEA plates, UV irradiated at doses ranging from 50-200 J/m^2 and the number of colonies formed counted.

Wild-type cells showed survival of 77, 66, 28 and 3 % at 50, 100, 150 and 200 J/m^2 respectively, whilst the *nse3*-base strain did not show a significant increase in sensitivity with survival rates of 76, 51, 48 and 4 % at respective dosages **(Figure 5.4.B)**. Interestingly, *nse3-L293F* showed no decrease in viability with 85, 77, 77 and 3 % survival. *nse2-SA* showed 69, 50, 34 and 20 % survival. Finally, the most sensitive strain *smc6-74* showed 6 % survival at the lowest

dose of irradiation (50 J/m^2) and only 1 % at 100 J/m^2. In conclusion, while *smc6*-74 cells show sensitivity at low doses, there was no increase in sensitivity in *nse3-L293F* cells when compared to the base strain. Thus, the slight UV sensitivity of *nse3*-L293F cells seen in spot tests was not reproduced in the more quantitative colony formation assay **(Figure 5.4.B)**.

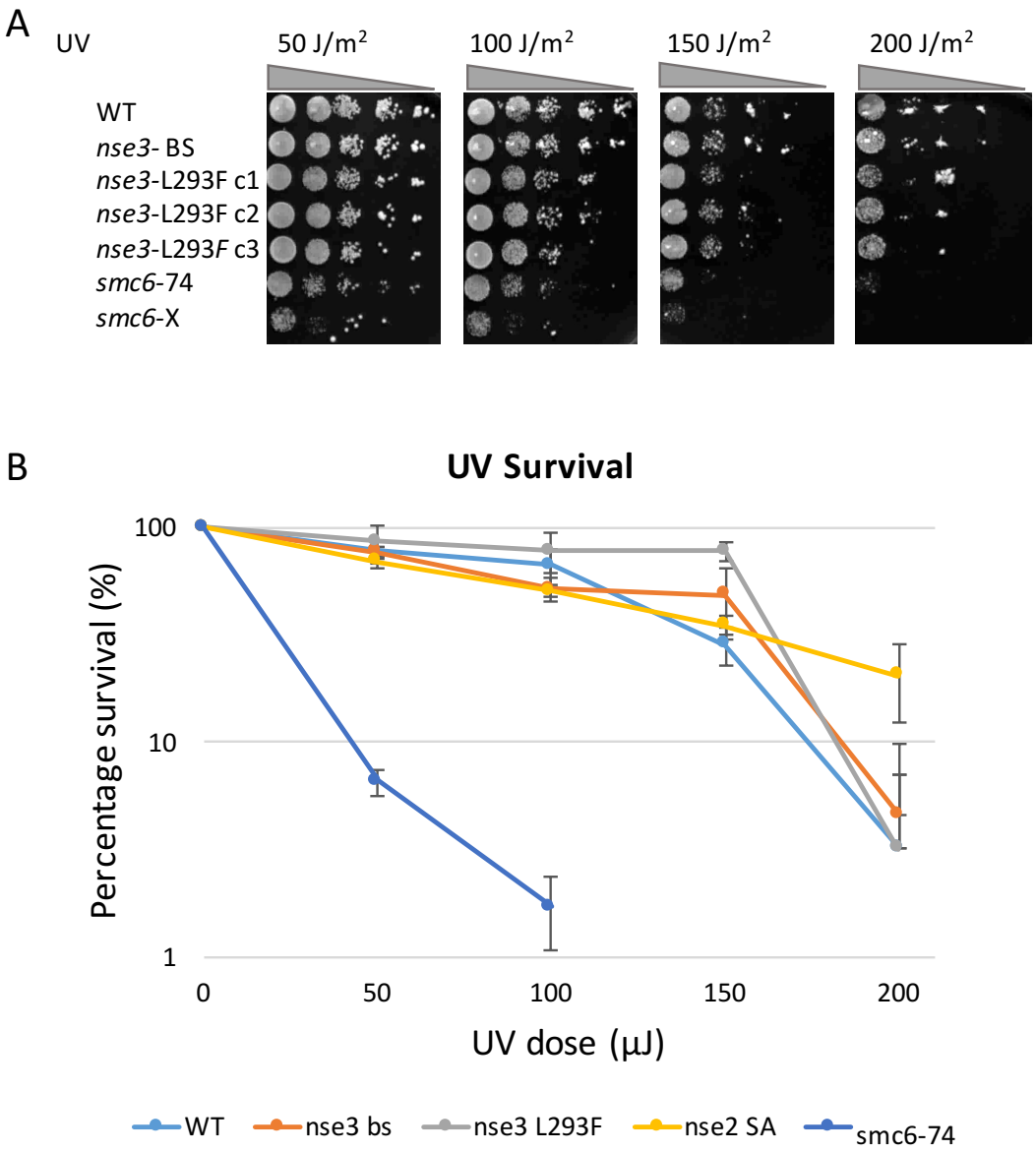

Figure 5.4. A. Spot test showing slight sensitivity to UV radiation. Wild-type (WT), *nse3*-base strain, three isolates of *nse3*-L293F, *smc6*-74 and *smc6*-X cells were plated in varying dilutions and exposed to doses of UV radiation ranging between 50 and 200 J/m^2. smc6-74 and *smc6*-X showed high levels of sensitivity to UV. *nse3*-L293F showed slight increase in sensitivity to UV at dosages of at 150 J/m^2. **B.** Colony formation assay after exposure to UV radiation. Wild-type (501), *nse3*-base strain, *nse3*-L293F, *nse2*-SA and *smc6*-74 cells were plated in triplicate and exposed to UV radiation. *Smc6*-74 cells were sensitive to UV at dosages of 50 J/m^2 and dropped to under 10 % viability whereas sensitivity was not observed in all other strains.

5.2.1.3 – *nse3*-L293F cells do not exhibit increased sensitivity to replication stress

Treatment using hydroxyurea (HU) results in depletion of the dNTP pool resulting in stalled replication forks (Petermann, Orta, Issaeva, *et al.*, 2010b). Prolonged replication fork stalling can lead to collapsed replication forks and DNA double strand breaks. Smc5/6 mutants, *smc6*-74 and *smc6*-X, have previously been shown to be very sensitive to HU (Ampatzidou, Irmisch, O'Connell, *et al.*, 2006). As before, wild-type (501), *nse3*-base strain, *nse3*-L293F, *smc6-74* and *smc6-X* cells were plated onto YEA with Phloxin B, containing 1-10 mM hydroxyurea and incubated for 4 days. Sensitivity to HU was seen in both *smc6-74* and *smc6-X* cells beginning at 2.5 mM HU, but no sensitivity was observed in *nse3*-L293F cells compared to wild-type and base-strain controls **(Figure 5.5.A).**

5.2.1.4 – *nse3*-L293F does not result in increased sensitivity to MMS

Methyl methanesulphonate (MMS) is an alkylating agent. Alkylated DNA is repaired by base excision repair but in S phase can lead to stalling of the replication fork(Lundin, 2005). *smc6-X* and *smc6-74* cells have been shown to be sensitive to MMS treatment as published previously (Sheedy, 2005). As before wild-type (WT), *nse3*-base strain, *nse3-L293F*, *smc6-X* and *smc6-74* cell were plated onto YEA with Phloxin B containing 0.0005, 0.001, 0.002, 0.005 and 0.01 % MMS and incubated for 4 days at 30 ºC. Strong sensitivity in *smc6-X* was observed even at low doses of 0.0005 % MMS and continues to 0.01 % MMS. *smc6-74* began to show sensitivity at 0.001 %. However, *nse3-L293F* did not show any sensitivity until 0.005 % MMS. However, this was comparable to the *nse3*-base strain suggesting any sensitivity seen was probably due to presence of the flanking LoxP and LoxM3 sites **(Figure 5.5.B).**

5.2.1.5 – *nse3*-L293F cells do not exhibit increased sensitivity to Camptothecin

The topoisomerase inhibitor Camptothecin (CPT) is a cytotoxic quinolone alkaloid. It acts through inhibition of topoisomerase I (topo1) through the formation of the reversible topo1-CPT-DNA covalent complex resulting in a protein linked DNA break (Liu, Desai, Li, *et al.*, 2000). Sensitivity to Camptothecin has been reported previously for *smc6-X* and *smc6-74* (Zabrady, Adamus, Vondrova, *et al.*, 2015). Wild-type (WT), *nse3*-base strain, *nse3-L293F*, *smc6-X* and *smc6-74* cells were plated on YEA plates with Phloxin B and exposed to 0.5, 5, 10, 15 and 20 μM CPT. Slight sensitivity was observed in *nse3*-L293F at 15 μM CPT compared with wild-type (WT). However, the *nse3*-base strain was also as sensitive, this again suggests the sensitivity is due to the LoxP and LoxM3 sites flanking the *nse3* gene rather than the mutation **(Figure 5.5.C).** Therefore, the *nse3* mutation does not sensitise cells to CPT. Given there was no observed increased in sensitivity to DNA damage, replication stress or growth defect in *nse3*-L293F cells we next tested the effect the analogous mutation may have in mammalian cells.

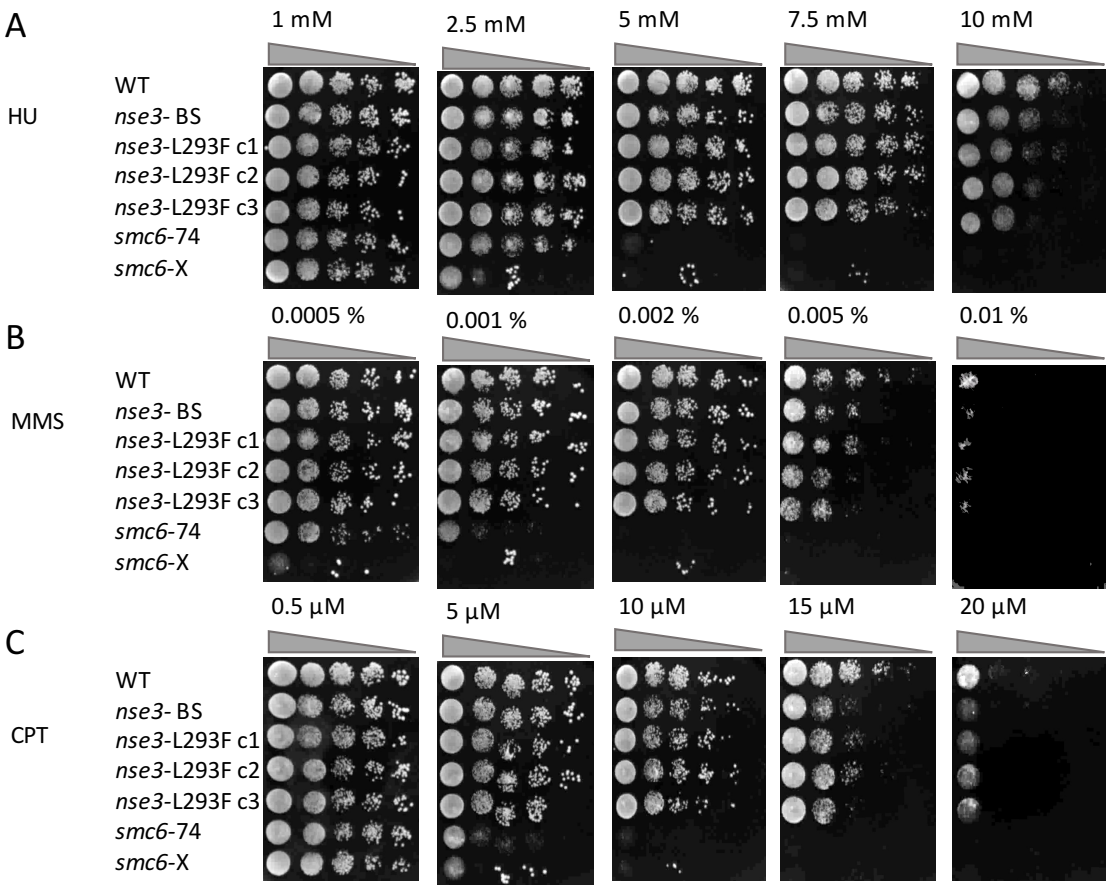

Figure 5.5. A. Spot test showing lack of sensitivity to replication stress. Wild-type (501), *nse3*-base strain, three isolates of *nse3*-L293F, *smc6*-74 and *smc6*-X cells were plated in varying dilutions and exposed to varying concentrations of hydroxyurea (HU). Sensitivity was observed in *smc6*-74 and *smc6*-X that was not observed in *nse3*-L293F. **B.** Sensitivity to MMS. Strains as in A, cells were exposed to MMS. smc6-X began to show sensitivity at 0.0005 % with *smc6*-74 showing sensitivity at 0.001 %. *nse3*-L293F and *nse3*-base stain showed slight sensitivity at 0.005 % MMS. All strains were sensitive at 0.01 % MMS. **C.** Sensitivity to Camptothecin. Strains as in A, cells were exposed to Camptothecin (CPT). Sensitivity to CPT was observed in *smc6*-74 and *smc6*-X. Slight sensitivity in nse3-L293F was observed at 15 µM CPT however this was also observed in *nse3*-base strain indicating sensitivity was due to the presence of the LoxP and LoxM3 sites flanking nse3.

5.2.2 – Analysis of primary patient fibroblasts isolated from a Dutch patient with mutated *NSMCE3*

5.2.2.1 – Mutation in *NSMCE3* results in increased levels of chromosome instability

The *NSMCE3* patients were categorised as having a chromosomal breakage syndrome due to the abnormal karyotypes seen in lymphocytes (van der Crabben, Hennus, McGregor, *et al.*, 2016). A known hallmark for chromosomal mis-segregation and instability is the presence of micronuclei. Micronuclei (MN) and other nuclear abnormalities such as nucleoplasmic bridges (NPBs) and nuclear buds (NBUDs) are biomarkers of genotoxic events and chromosomal instability **(Figure 5.1.C).** Given the high level of chromosomal instability observed in the NSMCE3-L264F lymphocytes and the fact that mutations in another subunit of SMC5/6 complex, NSMCE2, resulted in increased micronuclei and chromosomal bridges (Payne, Colnaghi, Rocha, *et al.*, 2014), we investigated micronuclei levels in primary patient fibroblasts, compared to fibroblasts isolated from patients with a well-defined chromosomal breakage syndrome, Ataxia telangiectasia (AT)(Vral, Thierens & De Ridder, 1996; Migliore, Coppede, Fenech, *et al.*, 2010; Wang, Su, Smilenov, *et al.*, 2011). Examples of micronuclei scored are shown in **(Figure 5.6.A)**.

The NSMCE3-L264F patient cells (primary fibroblasts) were compared with two wild-type cell lines (1BR and 48BR) and $ATM^{-/-}$ (AT1BR, an AT patient cell line). Approximately 1000 cells were scored for each cell line over three independent repeats. Micronuclei were observed in 3 % and 6% of 1BR and 48BR fibroblasts (Wild-type 1/2). Unsurprisingly, a 2-4 fold increase (13 %) of micronuclei were seen in $ATM^{-/-}$ fibroblasts. Furthermore, 21 % of NSMCE3-L264F fibroblasts contained micronuclei, which is a 4-7 fold increase when compared to control cells. This indicates large levels of chromosomal instability. The results were statistically significant according to Students T-Test (NSMCE3-L264F to wild-type 1 $p=7.59\times10^{-7}$, to wild-type 2 $p=1.325\times10^{-8}$) **(Figure 5.6.B).**

Due to the high levels of micronuclei observed the patient cells it was important to study the phenotypes associated with the NSMCE3-L264F mutation when exposed to various DNA damaging agents and also on the levels of the complex itself.

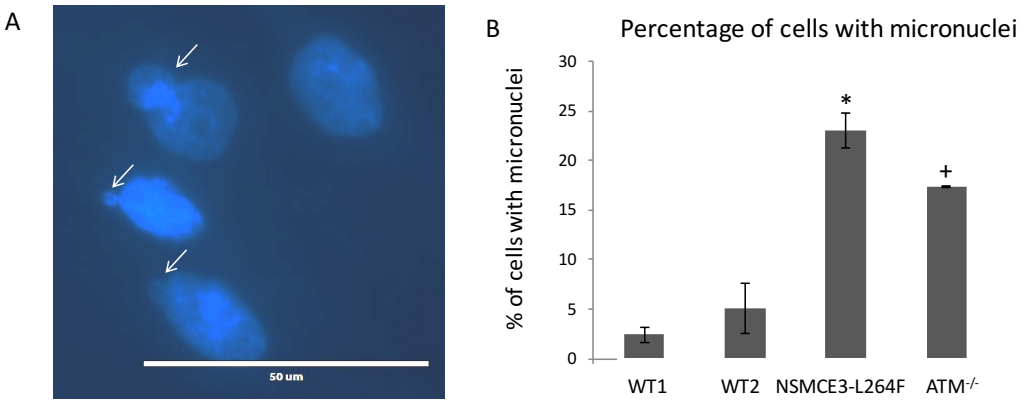

Figure 5.6. A. Examples of micronuclei scored for assay. Primary fibroblasts were plated into 10 cm dishes and allowed to seed and grow. Cells were then fixed in 4 % pfa, permeabilised and DAPI stained before scoring. Two wild-type cell lines, ATM-/- and NSMCE3-L264F cells were scored and approximately 1000 cells were counted for each cell line over three independent experiments. **B.** Graph showing percentage of cells with micronuclei abnormalities. Wild-type 1 (WT1, 1BR) and wild-type 2 (WT2, 48BR) cells were used as wild-type controls and showed low levels of micronuclei, 3 % and 6 % respectively. However, $ATM^{-/-}$ (AT1BR) exhibit 13 % abnormalities and NSMCE3-L264F (GVH02) show 21 % indicating a very high level of chromosomal instability in these cells. * denotes statistically significant difference according to Student's T-Test of NSMCE-L264F cells $p<0.005$. + denotes significance of ATM-/- cells compared with wild-types, p-value <0.05.

5.2.2.2 – NSMCE3 is required to maintain levels of SMC5/6

Modelling of the mutation *in silico* by Dr Tony Oliver suggested the NSMCE3-L264F mutation destabilised the interaction of NSMCE3 with NSMCE1 and NSMCE4. Computational analyses of models based on the crystal structure of the NSMCE1-NSMCE3 dimer (Protein Data Bank [PDB] ID 3NW0; http://www.rcsb.org) (Doyle, Gao, Wang, *et al.*, 2010) predicted destabilization

to disrupt the fold in NSMCE3 WH/B-e domain due to the presence of steric clashes with side chains of the adjacent helix. Purification of recombinant NSMCE1 and NSMCE3 proteins from *E. coli* resulted in an approximately 1:1 stoichiometric ratio of NSMCE1 and NSMCE3 in both wild-type and L264F mutation forms(van der Crabben, Hennus, McGregor, *et al.*, 2016). Wild-type NSMCE1 and NSMCE3 formed a stable dimer when analysed using size-exclusion chromatography. The L264F variant still interacted with NSMCE1 but eluted over a larger volume and with a non-uniform distribution suggesting a non-specific interaction with the chromatography resin and longer retention on the column(van der Crabben, Hennus, McGregor, *et al.*, 2016) indicating a slight unfolding of the complex. Yeast2Hybrid analysis confirmed this by showing loss of interaction between NSMCE3 and NSMCE4, whilst incorporation of the P209L mutation resulted in loss of interaction between NSMCE3 and NSMCE1 and NSMCE4.

Since structural modelling and biochemical assays indicated a destabilisation of NSMCE3 and loss of complex formation, levels of endogenous protein from patient fibroblasts were analysed to study what impact this might have. Western blot analysis of NSMCE3-L264F fibroblasts and two wild-type control cell lines (1BR and 48BR) showed low levels of SMC5 and SMC6 in the NSMCE3-L264F cells compared to controls **(Figure 5.7)**. Tubulin content was used as loading control to ensure this reduction was not due to difference in the amount of cell extract loaded.

These results were subsequently confirmed and, in addition, cells from an American patient who had heterozygous mutations in NSMCE3, p.Pro209Leu and p.Leu264Phe, were also shown to contain substantially reduced levels of NSMCE3, SMC5 and SMC6 (van der Crabben, Hennus, McGregor, *et al.*, 2016). The reduction in protein levels but not complete ablation is consistent with viability as knockout of SMC5/6 in mice shows embryonic lethality and knockout in yeasts is lethal. This results indicates the mutation in NSMCE3 results in a reduction of total protein levels of the whole complex, quantification of protein

levels can be seen in **(Table A.4.3.A)**. Such a destabilisation of the complex may affect the ability of the complex to carry out its cellular function at an optimal level.

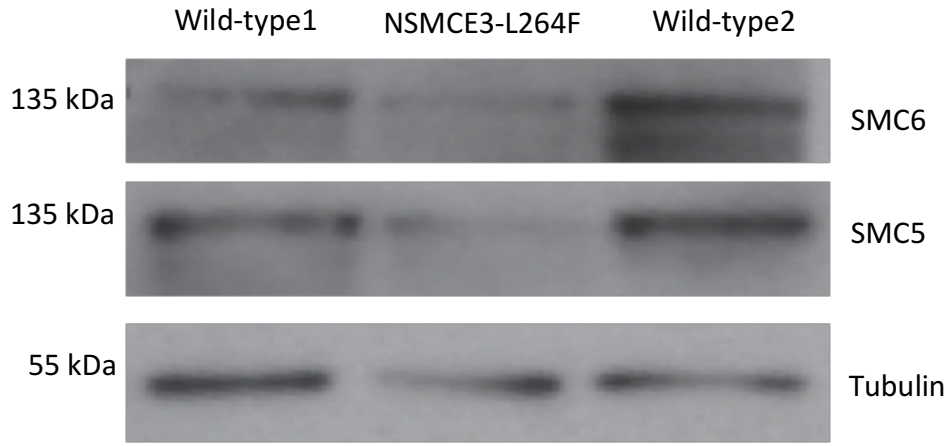

Figure 5.4. Western blot analysis comparing SMC5/6 complex members. NSMCE3-L264F cells show decreased levels of SMC5 and SMC6 compared with wild-type controls. This was also confirmed in patient cells taken from one of the American patients.

5.2.2.3 – Analysis of NSMCE3-L264F fibroblasts sensitivity to DNA damaging agents and replication stress

To determine whether the NSMCE3-L264F mutation results in increased sensitivity to DNA damaging agents, patient fibroblasts were exposed to a variety of these agents and clonogenic survival assays carried out. Sensitivity to DNA damaging agents has been reported for a number of SMC5/6 mutants in yeasts and slight sensitivity to MMS has been reported in chicken DT40 cells with a knock-out of SMC5 (Stephan, Kliszczak, Dodson, *et al.*, 2011).

Primary fibroblasts from patients with NSMCE3-L264F and a wild-type (48BR) cell line were cultured and exposed to varying doses of genotoxic agents, these include: IR, UV, MMC, CPT, HU and MMS. Cells were grown on 10 cm dishes with a feeder layer of wild-type cells irradiated with 35 Gy IR to ensure assay cells were able to adhere to bottom of the plate.

5.2.2.3.1 – NSMCE3-L264F fibroblasts have a slight slow growth phenotype

The growth rate of NSMCE3-L264F (GVH02) cells was examined **(Figure 5.8)** and compared to two wild-type cell lines (1BR and 48BR) and an $ATM^{-/-}$ cell line (AT1BR). It was found to be marginally slower compared with the wild-type controls but slightly faster than the $ATM^{-/-}$ cells.

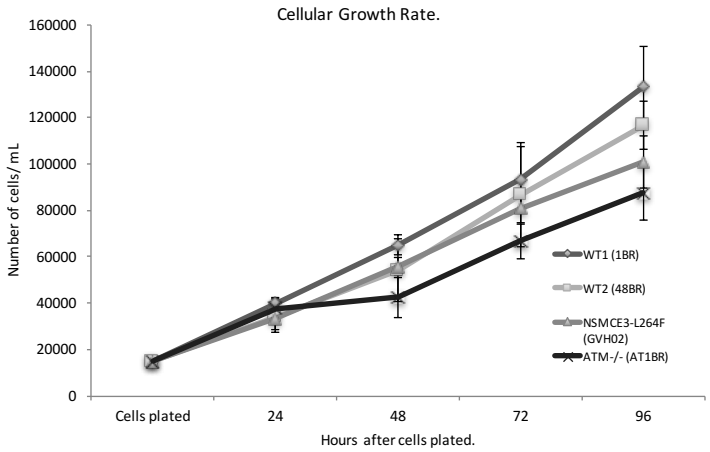

Figure 5.5. Growth rates of NSMCE3-L264F (GVH02) compared to two wild-type cell lines (1BR and 48BR) and an $ATM^{-/-}$ cell line (AT1BR) were calculated by plating 10^4 cells of each cell line into 3 cm dishes and incubated at 37 ºC for up to 96 hours before being trypsinised and resuspended. The number of cell per mL counted using a haemocytometer.

5.2.2.3.2 – NSMCE3-L264F cells show increased sensitivity to ionizing radiation

Ionizing radiation (IR) results in DNA single and double strand breaks (DSBs). DSBs generated by IR are the most lethal form of damage. To examine the ability of NSMCE3-L264F cells to repair double strand breaks patient cells were treated with increasing doses of IR.

Slight sensitivity was observed when NSMCE3-L264F cells were compared to wild-type cells after exposure to ionizing radiation **(Figure 5.9.A)**. Cell viability for wild-type cells was 53, 11, 2, and 0.2 % compared with NSMCE3-L264F 35,

4, 0.7 and 0.05 %. Statistical significance at 1 and 3 Gy IR according to Students T-Test, p-values were 0.05 and 0.03 respectively.

5.2.2.3.3 – NSMCE3-L264F cells show sensitivity to UV damage

Smc5/6 mutants have been shown to been sensitive to UV damage in yeasts but in *S. pombe* the equivalent mutant to NSMCE3-L264F*, nse3*-L293F, was not sensitive (see Figure 5.4). However, NSMCE3 is not well conserved in this c-terminal wing helix extension domain (see Figure 5.2) and so the mutations are not necessarily equivalent.

In human fibroblasts, the NSMCE3-L264F mutation resulted in a slight sensitivity to UV radiation when compared to wild-type cells. At doses of 2, 5, 7, 10 J/m^2 of UV survivals of wild-type cells were: 55 %, 19 %, 2.8 %, and 0.5 %. NSMCE3-L264F cells resulted in survivals of 49 %, 10 %, 1.75 %, and 0.5 %. However, this sensitivity is not significant at any point according to Student's T-test and this is consistent with what was observed in *S. pombe nse3*-L293F **(Figure 5.9.B).**

5.2.2.3.4 – Exposure of NSMCE3-L264F cells to Mitomycin C does not result in increased sensitivity

Mitomycin C (MMC) is used as a chemotherapeutic agent which crosslinks DNA. This results in blocked replication forks which causes replication arrest and cell death if the crosslink is not repaired(Paz, Zhang, Lu, *et al.*, 2012).

Cells were treated with doses of MMC at 2, 5 and 10 μM and results indicated a mild but not statistically significant sensitivity to MMC when comparing NSMCE3-L264F to wild-type cells. Cell viability at doses of MMC of 2, 5 and 10 μM were 54 %, 23 % and 10 % for wild-type and 45 %, 17 % and 5 % for NSMCE3-L264F cells respectively **(Figure 5.9.C).**

5.2.2.3.5 – Exposure of NSMCE3-L264F cells to Camptothecin results in slight sensitivity

Since only slight sensitivity was seen in IR and UV treated cells the next step was to test a more S phase specific damage. Exposing cells to Camptothecin will cause protein-DNA coupled induced breaks.

After exposure to Camptothecin, NSMCE3-L264F cells show slight increase in sensitivity over wild-type cells. At doses of 1, 2.5, 5 and 10 μM CPT, NSMCE3-L264F cells showed 33, 14, 2 and 2 % survival, whilst wild-type cells showed survival rates of 49, 30, 16 and 12 %. This was not statistically significant according to Student's T-Test **(Figure 5.9.D).**

5.2.2.3.6 – Clonogenic analysis of NSMCE3-L264F cells exposed to HU shows slightly increased sensitivity to replication stress

Since the SMC5/6 complex is well known to be required for stabilisation of replication forks and for fork restart, cells were treated with hydroxyurea to deplete the dNTP pool. Mutations in the Smc5/6 complex have been shown sensitise cells to HU (Ampatzidou, Irmisch, O'Connell, *et al.*, 2006).

Clonogenic analysis of cells with NSMCE3-L264F mutation compared with wild-type showed slight increase in sensitivity over dosages 0.25, 1 and 5 μM of HU. Wild-type cells showed survival of 63, 38 and 26 % compared to NSMCE3-L264F patient cells with 52, 27 and 16 %. The only statistically significant point was at 0.25 μM where wild-type showed 63 % survival compared to 52 %, p-value = 0.008. This suggests only a slight sensitivity to damage induced in S phase **(Figure 5.9.E).**

5.2.2.3.7 – Exposure of NSMCE3-L264F cells to MMS results in slight sensitivity

MMS damage can lead to collapsed replication forks and double strand breaks. Sensitivity of Smc5/6 mutants in yeast strains to MMS has previously been reported, as has slight sensitivity to MMS in DT40 SMC5 knock-out cells (Stephan, Kliszczak, Dodson, *et al.*, 2011).

Slight sensitivity was observed in NSMCE3-L264F cells compared to wild-type cells. Wild-type cells showed cell viability at doses of 65 %, 19 %, 5 %, 3 % and 2 % at MMS doses of 50, 100, 150, 200, 250 μg/mL. NSMCE3-L264F showed cell viability of 61 %, 13 %, 1.5 %, 0.7 % and 0.2 %. However, this was not statistically significant. **(Figure 5.9.F).**

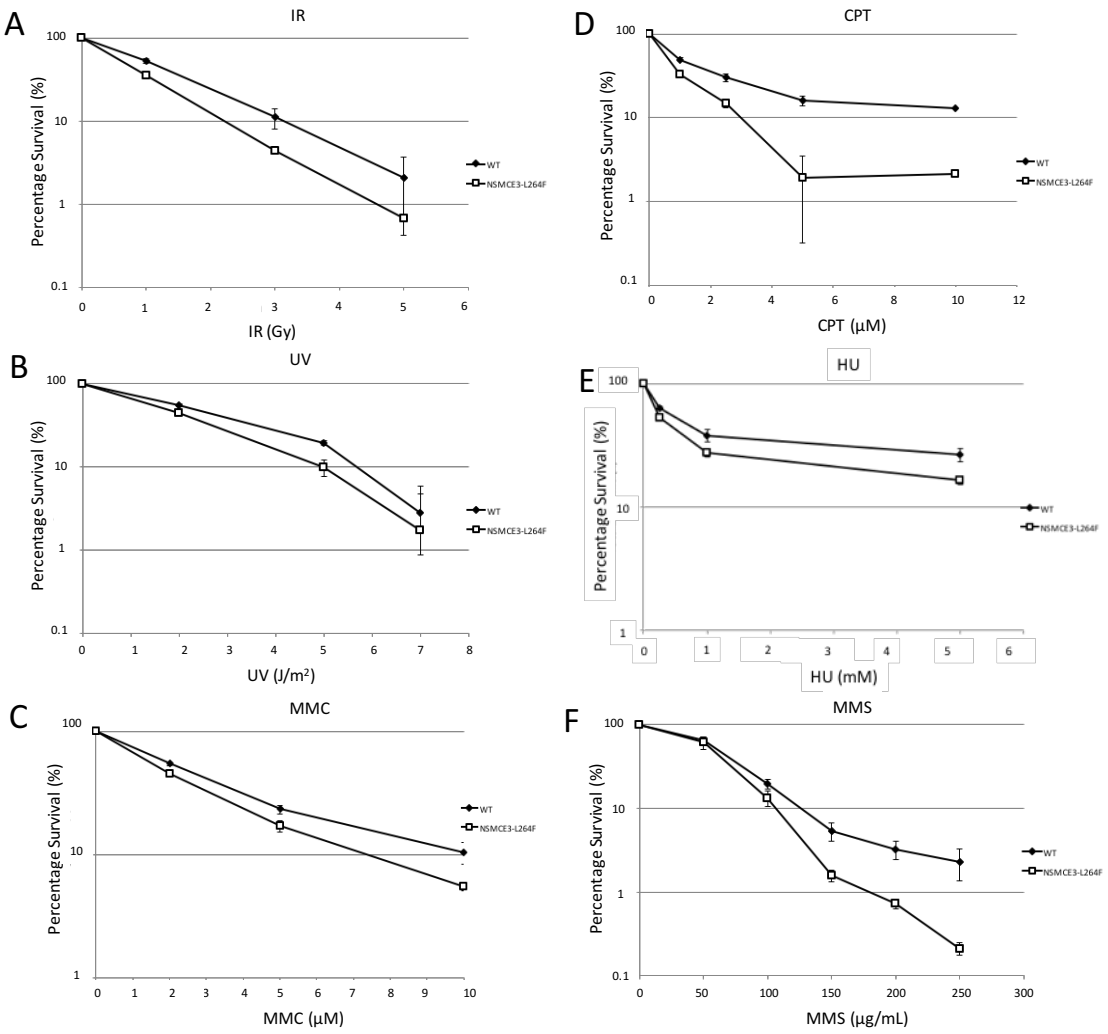

Figure 5.9. Clonogenic analysis of WT (48BR) and NSMCE3-L264F (GVH02) cells exposed to varying doses of DNA damaging agents, **(A)** IR, **(B)** UV, **(C)** MMC, **(D)** CPT, **(E)** HU and **(F)** MMS. Cells were plated in triplicate with an irradiated feeder layer to allow attachment and exposed to damage before being allowed to recover and grow for 21 days. Graphs represent the surviving percentage compared to untreated controls. NSMCE3-L264F cells showed modest sensitivity to IR, CPT and MMS. Results are the average of 3 independent experiments with triplicate plates. * denotes statistical significance with p-value <0.05 according to students T-Test, 2-tailed.

5.2.3 – The SMC5/6 complex is required for repair in G2 in mammalian cells

Sensitivity to DNA damaging agents indicates a defect in DNA repair. In order to determine which repair pathway was affected we induced DNA damage and determined how long it took to repair the damage by analyzing the rate of removal of DNA damage markers. Phosphorylated H2AX (γH2AX) foci were used as a surrogate marker of DNA damage and analyzed over time after exposure to

ionizing radiation(Löbrich, Shibata, Beucher, *et al.*, 2014; Ivashkevich, Redon, Nakamura, *et al.*, 2012). Non-homologous end-joining (NHEJ) is the major pathway for repair of DSBs in mammalian cells in both G1 and G2 cells but in G2 homologous recombination (HR) is required for repair of a subset of DSBs (O'Driscoll & Jeggo, 2006). Therefore, a defect in NHEJ results in a repair defect in both G1 and G2 but in HR a defect in recovery is only seen in the slow repair fraction in G2.

In yeasts SMC5/6 is required for HR, which is the main DSB repair pathway in yeasts (Haber, Ira, Malkova, *et al.*, 2004). Therefore, patient cells with mutations in SMC5/6 and/or reduced levels of SMC5/6 would be predicted to show a defect in repair in G2 compared to wild-type cells. Since the patient lymphocytes were proficient in V(D)J recombination it was hypothesised NHEJ that would be unaffected in the NSMCE3-L264F patient fibroblasts.

To determine if there was a defect in the NHEJ or HR repair pathway γH2AX foci were quantified over a time course following IR damage. Cells were subjected to 3 Gy IR and samples collected over a time course of 2, 8 and 14 hours. CENPF staining was used to identify G2 cells and pan-nuclear γH2AX staining was indicative of cells in S phase. HR is required in S phase but as the presence of γH2AX cannot be accurately quantified at this cell cycle stage, S phase cells were excluded from analysis. G1 and G2 cells were analysed of γH2AX levels **(Figure 5.10.A)**.

Patient cells were compared against wild-type (1BR), BRCA2 deficient (HSC62) (defective in HR), and $ATM^{-/-}$ (AT1BR) (defective NHEJ and HR) cells. Background levels of γH2AX were found to be an average of approximately 1 focus in all cells screened. Maximal γH2AX levels were seen at two hours after IR radiation and were found to range from 28-36 foci in all the cells tested.

In G1 cells, where NHEJ is essential for repair of DSBs, $ATM^{-/-}$ cells, which are defective in NHEJ, show slower repair kinetics compared to wild-type cells. In

ATM-/- cells there were 150 % more foci (Statistically significant with a p-value of 0.0002) at 8 hours and 300 % more foci (Statistically significant with a p-value of 0.002) at 14 hours compared with wild-type cells. BRCA2 deficient cells, that are defective in HR, show no statistically significant difference between the levels of foci at 8 and 14 hours compared with wild-type cells. This is consistent with HR not being required in the G1 phase of the cell cycle. Similarly, patient cells also showed no defect in repair kinetics in G1, thus confirming that SMC5/6 does not play a major role in NHEJ **(Figure 5.10.B)**.

To analyse repair kinetics in G2, only cells containing γH2AX and co-stained with CENPF were counted. CENPF is a component of the nuclear matrix during G2 and is therefore used as a marker of G2. At 0 hours wild-type, NSMCE3-L264F, $ATM^{-/-}$ and BRCA2 deficient cells showed on average 3, 5, 6 and 6 foci per cell respectively. At 2 hours post irradiation cells showed maximal levels of γH2AX with 61, 58, 56 and 52 foci per cell scored. At 8 and 14 hours post irradiation levels of γH2AX had dropped to an average of 17 and 11 foci per cell respectively in wild-type cells. In the HR defective cells (ATM-/- and BRCA2 deficient) the number of γH2AX foci at 8 and 14 hours post radiation dropped to 27, 18, and 29, 21 foci per cell respectively. Compared with wild-type this rate of removal was statistically significant with p-values of 0.02 for the 8-hour time point for the ATM-/- cells and p=0.01 and 0.02 for the BRCA2 deficient cells at 8 and 14 hours. In NSMCE3-L264F cells the level of γH2AX foci at later time points was also increased compared with wild-type cells. At 8 and 14 hours 24 and 18 foci were observed and was statistically significant with p-values of 0.01 and 0.02 compared to wild-type cells. This shows NSMCE3-L264F cells show similar repair kinetics to the HR deficient cells and, thus, is consistent with a requirement for SMC5/6 in HR repair in G2.

Figure 5.10. A. Image showing how the cells were stained and scored for ɣH2AX foci analysis. Cells were DAPI stained, CENPF was used to mark G2 stage of the cell cycle, ɣH2AX foci levels for scoring. **B.** Analysis of ɣH2AX foci in wild-type (1BR), NSMCE3-L264F (GVH02), $ATM^{-/-}$ (AT1BR) and BRCA2-deficient (HSC62) cells. Cells were irradiated with 3 Gy IR and allowed to recover for 2, 8 and 14 hours. NSMCE3-L264F cells shows no increase in foci levels compared with NHEJ proficient cells. CENPF staining was used to pick out S and G2 cells. Cells without CENPF staining were scored as G1/G0 cells. S phase cells with pan-cellular ɣH2AX were also excluded. $ATM^{-/-}$ cells show increased levels of foci in 8 and 14 hours statistically significant compared with wild-type controls suggesting deficiency in NHEJ. NSMCE3-L264F does not appear to have defect in this stage of the cell cycle. * denotes statistical significance according to Students T-Test. **C.** ɣH2AX assay of cells in G2 stage of the cell cycle. Cells were stained with CENPF to pick out G2 cells and these cells scored for their ɣH2AX foci levels. NSMCE3-L264F, $ATM^{-/-}$ and BRCA2-deficient cells showed higher levels of ɣH2AX foci compared with wild-type cells. At 8 and 14 hours the difference between NSMCE3-L264F and WT controls are statistically significant according to Students T-Test. * denotes statistical significance according to Students T-Test p-value <0.05.

A

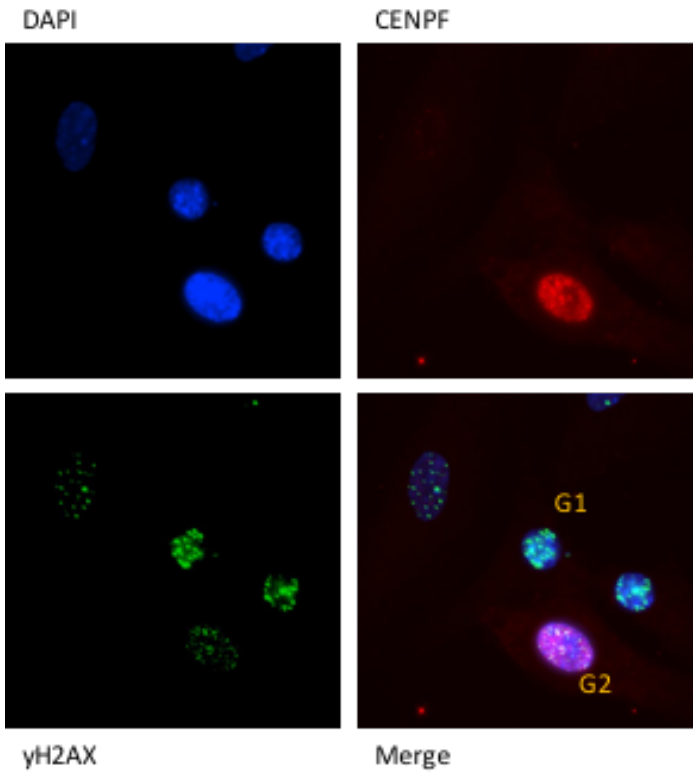
DAPI
CENPF
G1
G2
γH2AX
Merge

B

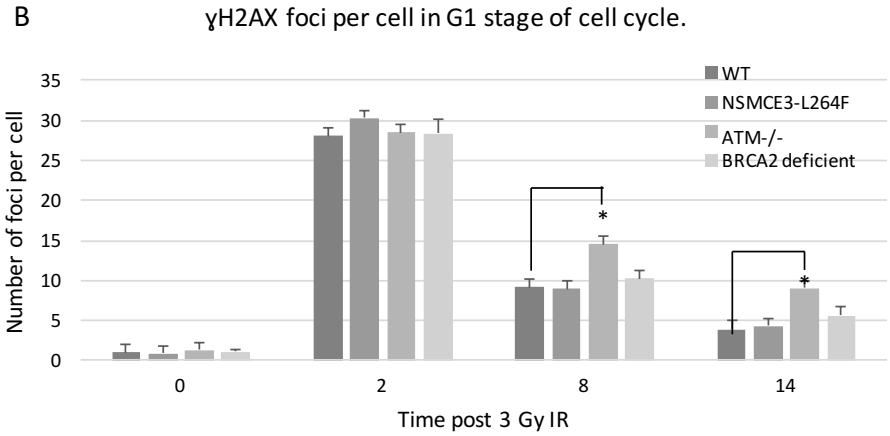
γH2AX foci per cell in G1 stage of cell cycle.
Number of foci per cell
35
30
25
20
15
10
5
0
0
2
8
14
Time post 3 Gy IR
WT
NSMCE3-L264F
ATM-/-
BRCA2 deficient
*
*

C

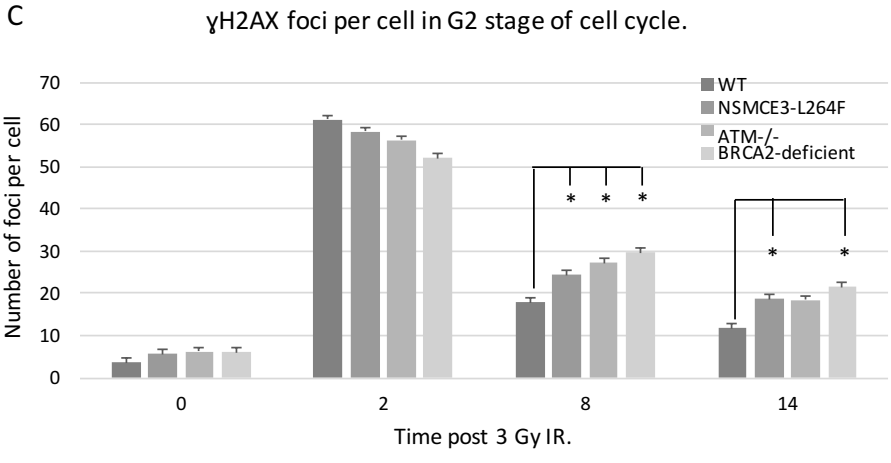
γH2AX foci per cell in G2 stage of cell cycle.
Number of foci per cell
70
60
50
40
30
20
10
0
0
2
8
14
Time post 3 Gy IR.
WT
NSMCE3-L264F
ATM-/-
BRCA2-deficient
*
*
*
*
*

5.2.4 – NSMCE3 is required for replication fork restart

SMC5/6 has previously been reported to be required for replication restart (Irmisch, Ampatzidou, Mizuno, *et al.*, 2009). Payne et al 2014 also showed that cells with a mutation in the NSMCE2 subunit of SMC5/6 showed a reduced recovery from replication stress. To test whether the NSMCE3-L264F cells also had a defect in recovery from replication stress the cells were exposed to low levels of HU, which depletes the dNTP pools leading to stalled replication, and released into media containing the thymidine analogue EdU.

EdU incorporation was chosen over BrdU as BrdU-labelled DNA is quantitated using a detection method which involves some very harsh treatments to expose the BrdU. This is a time consuming step and is difficult to perform consistently and can often affect sample integrity. The choice of EdU kit also allowed the potential for co-staining with BrdU. Cells were scored for EdU incorporation as seen in **(Figure 5.11.A)**. Wild-type (48BR) and NSMCE3-L264F (GVH02) cells were treated with/without 250 μM HU for 18 hours and allowed to recover for 30 min in media containing 10 μM EdU. It has previously been shown that most forks are able to restart replication after release from a 1-2 hour HU block, with nucleotide incorporation in most cells resuming within 12-18 hours. However, most forks remained stalled after 24 hours in HU block with induction of double strand breaks after 18 hours (Petermann, Orta, Issaeva, *et al.*, 2010b; Hanada, Budzowska, Davies, *et al.*, 2007).

Untreated wild-type cells showed 35 % of cells were currently in S phase as measured by their incorporation of EdU. When exposed to HU for 18 hours 42 % of cells were able to incorporate EdU suggesting they were able to restart replication. In NSMCE3-L264F cells, 41 % of cells without HU were in S phase, however after exposure to HU only 4 % of cells were EdU positive suggesting they had reduced capability to restart replication following stalled replication. According to Student's T-Test this was statistically significant ($p=0.005$) **(Figure 5.11.B).** To determine whether these results were due to a reduced number of

cells in S phase, FACS analysis was carried out. The FACs results from HU treated wild-type and NSMCE3-L264F cells confirm that similar numbers of cells accumulated in S phase during the HU block. After 18 hours in HU both wild-type and NSMCE3-L264F cells accumulated in S phase showing the cell cycle profile of both cell lines were similar **(Figure 5.12).** This confirms that NSMCE3-L264F cells were able to enter S phase but had issues restarting replication. Since the viability of cells of NSMCE3-L264F cells on chronic exposure to HU (Figure 5.9) is only slightly reduced it is likely that replication restart is delayed rather than abolished.

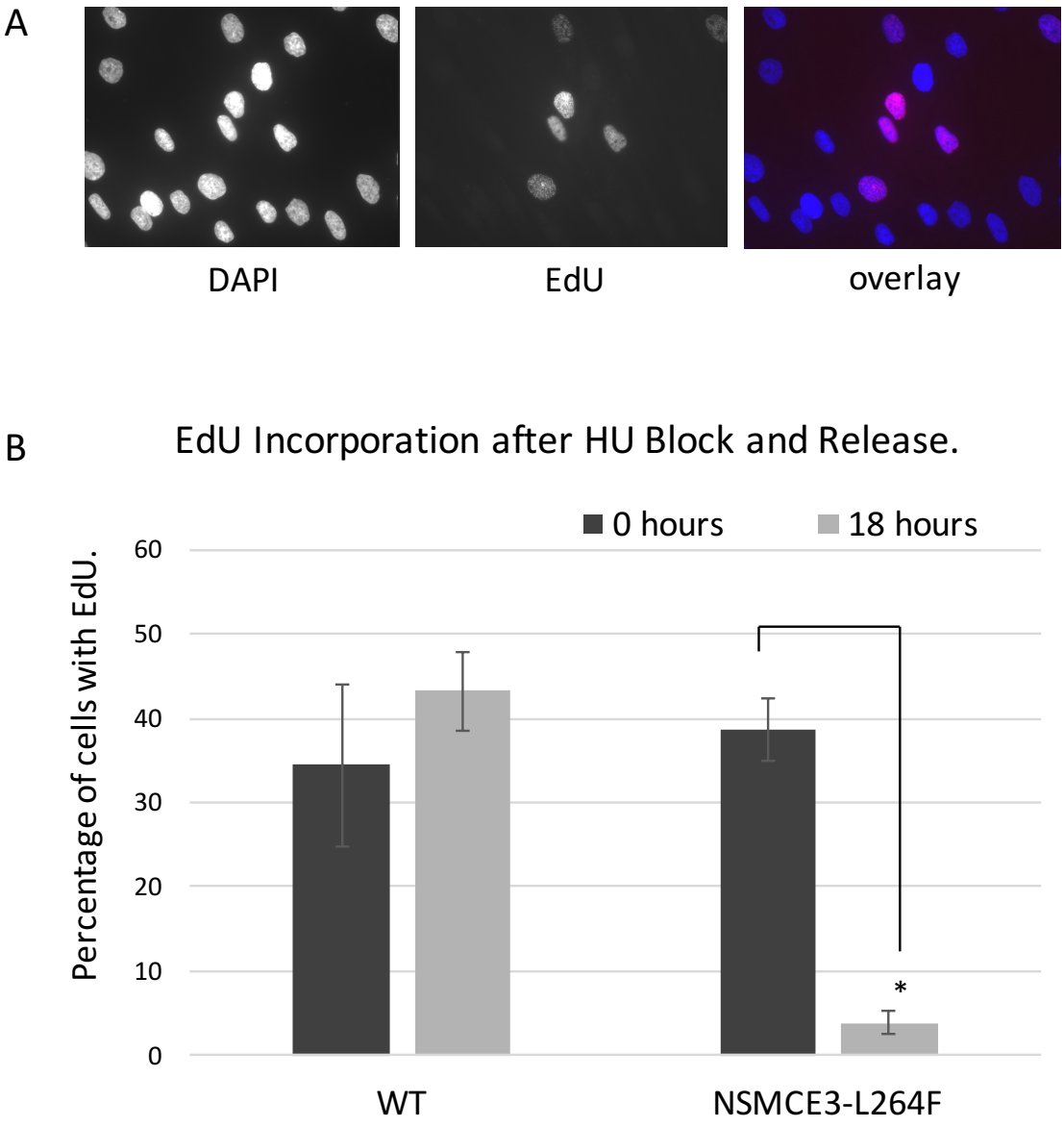

Figure 5.11. **A**. Representative images highlighting the scoring of EdU positive cells. Cells were plated onto glass coverslips and were treated with/without 250 µM HU for 18 hours before being released into fresh media containing 10 µM EdU. Cells were then either processed to label EdU according to manufacturer's instruction. Cells which incorporated EdU were scored. **B.** Graph showing percentage of cells which incorporated EdU compared with number of cells counted. NSMCE3-L264F cells showed comparable levels of EdU incorporation when compared with wild-type 0 hour HU treatment but vastly reduced levels after 18 hours in HU. Results at 18 hours are statistically significant according to Students T-Test, 2-tailed, p-value <0.05.

A

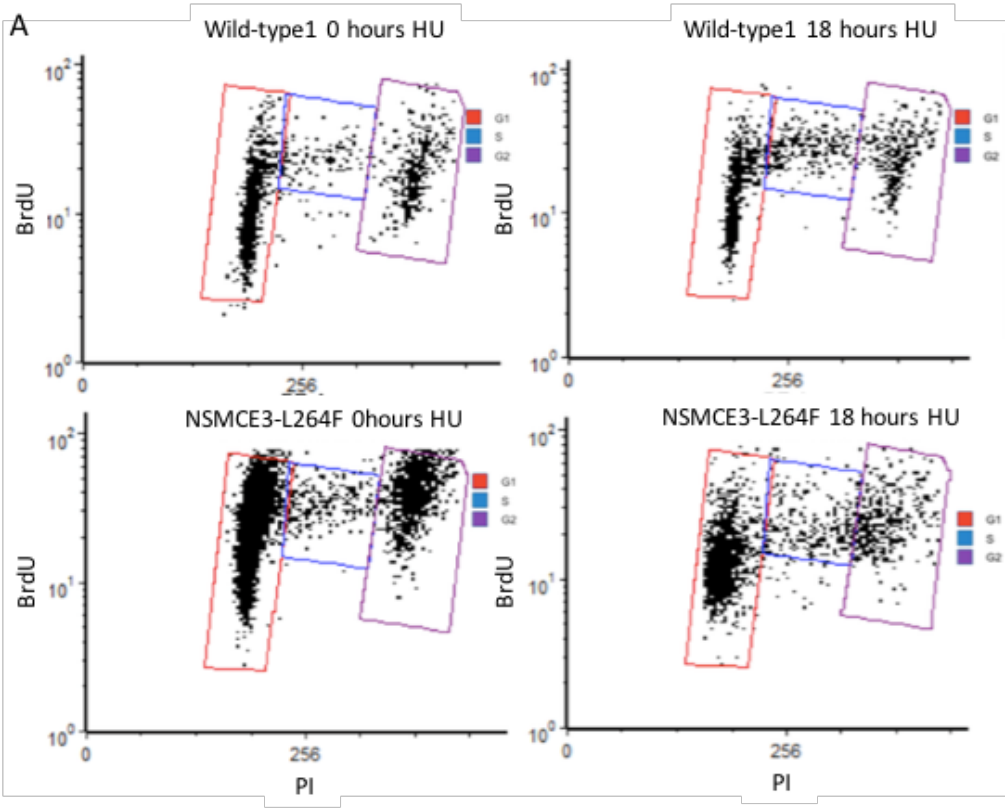

B

	G1 (%)	S (%)	G2 (%)
Wild-type 0 hour HU	69.7	7.2	22.55
Wild-type 18 hour HU	63.09	16.53	20.97
NSMCE3-L264F 0 hour HU	74.61	3.38	20.95
NSMCE3-L264F 18 hour HU	66.6	11.94	20.09

C

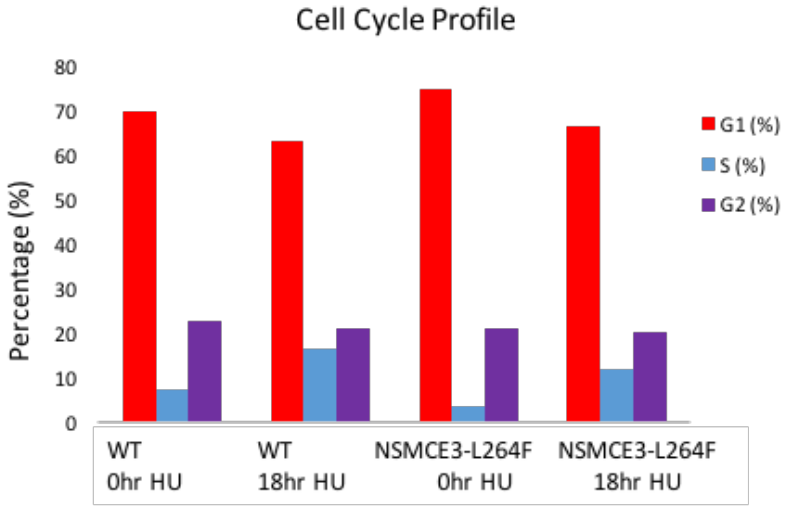

Figure 5.12. **A.** FACS profiles comparing wild-type and NSMCE3-L264F cells with and without exposure to 250 µM hydroxyurea for 18 hours. Results indicate cells are able to enter S phase whilst in HU block. **B.** Table showing percentage of cells in each respective gate. **C.** Graph of table in B, showing reduction of percentage of cells in G1 allowing passage into S phase.

5.2.5 – Complementation of patient fibroblasts with wild-type NSMCE3 rescues S phase replication restart phenotype

To determine whether the recovery defect observed in 5.2.4 was due to the NSMCE3-L264F mutation we examined whether the defect could be complemented by expression of the wild-type protein. eGFP tagged versions of wild-type NSMCE3, NSMCE3-L264F and eGFP vector controls were constructed. These constructs were transfected into hTERT immortalised primary NSMCE3-L264F fibroblasts and allowed to incubate for 48 hours. Cells were then analysed for their ability to restart replications as described previously.

Patient cells complemented with wild-type NSMCE3 were able to restart replication showing 32 % EdU incorporation at 0 hour and 28 % after 18 hours in HU. Cells expressing the NSMCE3-L264F mutation construct showed 29 and 7 % EdU incorporation and so failed to rescue the phenotype similarly to eGFP vector control, which had percentage EdU incorporation of 22 % and 10 % at 0 and 18 hours respectively **(Figure 5.13).** This shows that only the wild-type NSMCE3 was able to complement the HU recovery defect and demonstrates that the defect is due to the NSMCE3-L264F mutation. This confirms that the SMC5/6 complex that is required for replication restart.

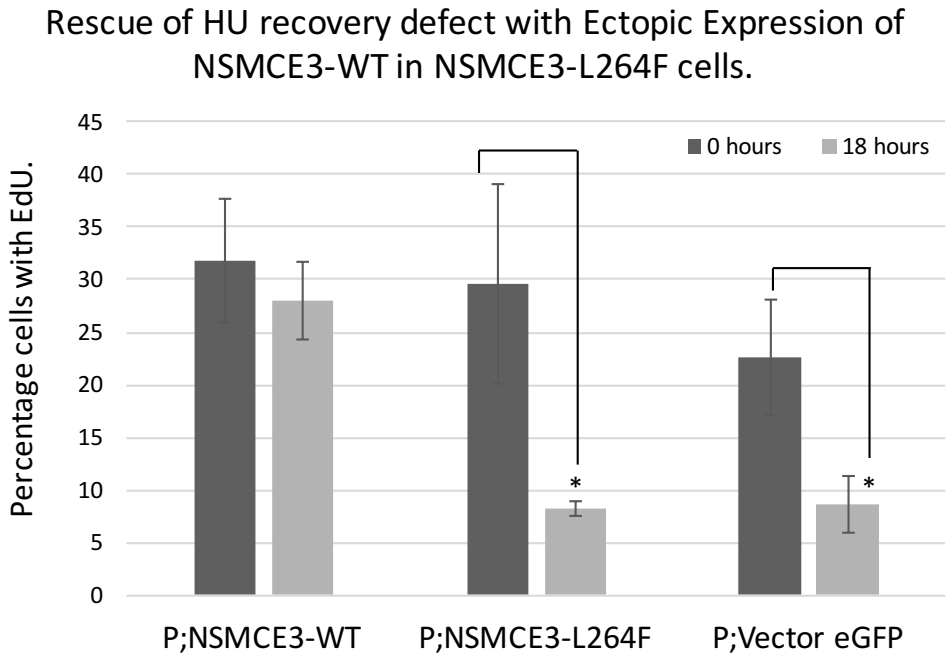

Figure 5.13. Ectopic expression wild-type NSMCE3 results in rescue of replication stress phenotype. NSMCE3-L264F cells were transfected with either wild-type NSMCE3-eGFP, NSMCE3-L264F-eGFP or eGFP control plasmid. 48 hours after transfection cells were treated with/without 250 µM HU and released into 10 µM EdU as before. Cells were fixed and processed as previously described and scored for their incorporation of EdU. Expression of wild-type NSMCE3 resulted in the rescue of the replication stress phenotype. Results were statistically significant according to 2-tailed Students T-Test p-value <0.05.

5.3 – Discussion

SMC5/6 is required for homologous recombination and accurate chromosome segregation. In humans homozygous and heterozygous mutations in *NSMCE3,* L264F and L264F/P209L, result in a new chromosomal breakage syndrome called LICS (**l**ung disease, **i**mmunodeficiency and **c**hromosome instability **s**yndrome). The associated destructive and fatal pulmonary damage has not been reported in other studies of patients with a mutation in another SMC5/6 subunit, NSMCE2. The O'Driscoll lab published a set of mutations in *NSMCE2* linked to primordial dwarfism and insulin resistance, something that is not observed in the NSMCE3 patients(Payne, Colnaghi, Rocha, *et al.*, 2014). In the NSMCE2 syndrome linear growth and weight were severely impaired whereas

in the NSMCE3 patient's linear growth and weight were only slightly affected. In mice NSMCE2 is required to prevent aging and cancer (Jacome, Gutierrez-Martinez, Schiavoni, *et al.*, 2015). No malignancies were observed in any of the four NSMCE3 patients in contrast to patients with AT or NBS chromosomal breakage syndromes, however this is likely to be due to the young age at which the patients died (van der Crabben, Hennus, McGregor, *et al.*, 2016).

Karyotyping of Dutch patient lymphocytes also revealed a high level of rearrangements and supernumerary markers and this correlated with high levels of micronuclei in fibroblasts **(Figure 5.6)** indicative of chromosomal instability. IgA and IgG levels were normal showing that patients did not have a defect in V(D)J) or class switch recombination, processes that requires NHEJ. However, T cell proliferation and antibody titres were reduced and there was no response to recall antigens indicative of primary immunodeficiency. Again this immunodeficiency was not seen in the NSMCE2 patients(Payne, Colnaghi, Rocha, *et al.*, 2014).

To examine the effects of the Dutch patient mutation, NSMCE3-L264F, in more detail it was initially modelled in yeast with the equivalent mutation *nse3*-L293F. Whilst a slight sensitivity was observed in spot tests this was attributed to the presence of LoxP and LoxM3 sites flanking the *nse3*, as it was also seen in the base strain. There was a slight sensitivity in spot tests when cells were exposed to UV radiation however this was not observed in cell survival assays. A lack of sensitivity to DNA damaging agents could also be explained by the low level of sequence similarity between human NSMCE3 and *S. pombe nse3* in the C-terminal domain. Alignment of the protein sequence using UniProt and the program ClustalX indicate only 19.034 % sequence similarity with only 67 identical and 97 similar positions when comparing *H. sapien* and *S. pombe NSMCE3/nse3.*

Analysis of primary fibroblasts isolated from one of the Dutch patients revealed the cellular phenotypes associated with the NSMCE3-L264F mutation. The

mutation destabilized NSMCE3 and reduced levels of SMC5 and SMC6 showing the SMC5/6 complex to be destabilised. Further analysis subsequently showed that the levels of NSMCE3 were below detection levels in a cell extract isolated from a compound heterozygote (NSMCE3-L264F, NSMCE3-P209L) individual from the American family (van der Crabben, Hennus, McGregor, *et al.*, 2016). This could be due to lack of expression of NSMCE3, however since loss of *SMC6* or *NSMCE2* is lethal in early embryonic mice it is more likely that NSMCE3 is present at low levels. SMC5 and SMC6 levels were dramatically reduced showing that a stable complex cannot be maintained. Purification of the recombinant NSMCE3-P209L mutant protein co-expressed with NSMCE1 in *E.coli* showed destabilisation of the complex, indicating an unfolding of NSMCE3 that destabilised the interaction. However, the interaction between NSMCE3-L264F and NSMCE1 was more stable. Yeast two hybrid analysis also indicated a destabilisation of the interaction between both NSMCE3 mutant proteins and NSMCE4 (van der Crabben, Hennus, McGregor, *et al.*, 2016).

A slight sensitivity to DNA damaging agents was observed in NSMCE3-L264F cells. Exposure to broad range damaging agents such as ionizing or UV radiation indicated a slight increase in sensitivity whilst exposure to a range of drugs such as MMC, CPT, HU and MMS indicated a slight increase in sensitivity, specifically to those which create damage in S phase. This would be consistent with a requirement for SMC5/6 in S phase and homologous recombination.

To further analyse the repair pathway affected in NSMCE3-L264F cells a ɣH2AX assay was used. Since SMC5/6 is required for homologous recombination in yeast and patients did not have a defect in V(D)J) or class switch recombination, processes that requires NHEJ, it was predicted that NSMCE3-L264F patient cells would be proficient in NHEJ repair. This was supported when analysis of repair kinetics after ionising radiation in G1 revealed no significant difference in the rate of decline of ɣH2AX foci levels in NSMCE3-L264F cells compared to wild-type.

In contrast, analysis of repair kinetics after ionising radiation in G2 revealed that NSMCE3-L264L cells maintained ɣH2AX foci levels for longer than wild-type cells. This is similar to the HR-defective BRCA2 deficient cell line and is consistent with a defect in HR.

Consistent with a defect in homologous recombination fibroblasts showed failure to recover from replication stress. Treatment of NSMCE3-L264F cells using hydroxyurea to stall replication resulted in cells not being able to restart replication. FACS analysis confirmed cells not in S phase were able to enter S phase during the HU block. This defect was complimented by ectopic expression of WT-NSMCE3 showing the defect to be a direct result of the mutation. The lack of recovery from replication stress is also seen in cells with mutated *NSMCE2* showing it to be a common consequence of misregulation of the SMC5/6 complex.

In summary, the work described in this chapter shows the first examples of a new autosomal recessive chromosomal breakage syndrome, LICS. This results from either homozygous or heterozygous mutations in *NSMCE3*. Patients with LICS present with destructive and fatal pulmonary disease whilst cells with the NSMCE3-L264F mutation have reduced stability of SMC5/6 complex and defective homologous recombination with increased levels of micronuclei and chromosomal instability.

Chapter 6.0 –Discussion.

This thesis explores the role of the SMC5/6 complex in human cells. It examines the execution and validation of a synthetic sick/lethal screen using RNAi of NSMCE4a and describes the effects of a novel homozygous mutation in NSMCE3, resulting in a new chromosomal breakage disorder, which leads to a fatal pulmonary disease.

One focus of this thesis involved the development of a synthetic sick/lethal screen using shRNA knockdown of NSMCE4a. As has been shown previously, loss or knockdown of one subunit of SMC5/6 leads to reduction in levels of other members of the SMC5/6 complex. In Chapter 3 data was presented that highlights the steps involved in setting up the screen. These steps involved identification of a target (NSMCE4A), choosing a cell line to knockdown the target (U2OS) and ensuring that cells with reduced levels of the chosen target were still viable. The cell line was then created and the screening protocol optimised.

Whilst Chapter 3 describes the set up of a high-throughput screen to further characterise the role of the SMC5/6 complex this protocol can now be used as a tool to investigate synthetic lethality for multiple genes of interest and is being used throughout the department (Hopkins, McGregor, Murray, *et al.*, 2016).

The results indicated that targeting the NSMCE4a subunit using siRNA did not negatively impact the unperturbed growth rate of U2OS cells. Once this was established cell lines using shRNA were created. Initially the system contained a tGFP sequence expressed pan-cellular and single cells could not accurately be resolved by the microscope. To overcome this tGFP was replaced with AcGFP or mCherry with nuclear localisation sequences. This allowed single cell resolution with the microscope.

Conclusions from the set up chapter laid the basis for the screen carried out in Chapter 4 and the main findings of this chapter were:

- Smartpool siRNA knockdown of NSMCE4a and SMC6 leads to loss of other members of the SMC5/6 complex.
- pGIPZ expression of NSMCE4a shRNA leads to knockdown of SMC5/6 complex members.
- AcGFP-NLS and mCherry-NLS replacement of native tGFP in pGIPZ allows cells to be resolved accurately whilst having internal controls in the well.
- Using a topdown transfection method allows for cells to recover from plating stress and 2000 cells per well in 1:1 relationship of AcGFP:mCherry allows a large number of cells to be counted without the cells becoming over confluent.
- Edge effect is real and requires timing and handling to minimise.

The second results chapter, Chapter 4, uses the technology developed from the previous chapter and allows us to analyse the effects of reduced levels of NSMCE4 when combined with siRNA knockdown of proteins found in the DNA damage response pathway. Unsurprisingly, many proteins involved in the homologous recombination repair pathway appeared as synthetically lethal with NSMCE4a shRNA knockdown, suggesting that consistent with the theory published by Heyer et al, flux through the pathway is important and loss of factors at different stages can lead to the accumulation of toxic intermediates (Heyer, 2015). One key member of HR - BRCA2 appeared as the top hit in the screen and RAD52, another protein involved in homologous recombination, was also synthetic sick/lethal with reduction of NSMCE4. This suggested that there is a crossover in the functions of BRCA2 and RAD52 as both are synthetically lethal following reduction of SMC5/6 levels. BRCA2 and RAD52 function to replace RPA with RAD51 during homologous recombination(Tarsounas, Davies & West, 2003; Roy, Chun & Powell, 2012; Sugiyama & Kantake, 2009). BRCA1 also interacts with RAD51 however this does not appear as a top hit in the screen. It is possible that the knockdown of BRCA1 is not efficient in either cell line types or that knockdown of NSMCE4a does not have an additive effect when BRCA1 is lost. RAD51 also does not appear as a top hit in the screen, consistent

with it being epistatic in yeasts (Gallego-Paez, Tanaka, Bando, *et al.*, 2014). RAD52 was often ignored in consideration of HR in mammalian calls as the mouse knockout showed largely no phenotype(Lok & Powell, 2012). However, synthetic lethal approaches have indicated RAD52 plays a key role in cells lacking the BRCA1-BRCA2 pathway and it is required for single strand annealing (Schlacher, Christ, Siaud, *et al.*, 2011). Following processing and end resection by CtIP, MRN and EXO1; BRCA1 and PALB2 facilitates the recruitment of BRCA2 to allow loading of RAD51 onto ssDNA.

Two of the strongest synthetic lethal hits are factors involved in NHEJ. Double strand breaks are mainly repaired through the use of HR or NHEJ with the major pathway being NHEJ. Therefore, if HR is compromised it is not surprising that NHEJ becomes essential. Two enzymes involved in NHEJ, Artemis and XLF, were synthetically sick/lethal with loss of NSMCE4a and this has been further validated through use of patient cells with mutation in Artemis and XLF. This shows that NHEJ is essential when HR is perturbed.

Artemis and XLF are both involved at different stages of NHEJ. Artemis deficient cells are more sensitive to X-rays and show larger numbers of breaks following irradiation(Beucher, undefined author, undefined author, *et al.*, 2009). Artemis is required in the slow repair fraction of DSB repair rather than the more immediate fast repair(Shibata, Conrad, Birraux, *et al.*, 2011). XLF works in the fast repair section and interacts with XRCC4-LigaseIV and shows a stronger lethal phenotype when exposed to NSMCE4a siRNA (Ahnesorg, Smith & Jackson, 2006b).

Previously it has been reported that SMC5/6 is required during S phase for repair of collapsed replication forks and stabilization of stalled replication forks (Irmisch, Ampatzidou, Mizuno, *et al.*, 2009; Ampatzidou, Irmisch, O'Connell, *et al.*, 2006). This thesis also shows that NSMCE3-L264F patient cells exposed to low levels of hydroxyurea show a reduced ability to restart replication (van der Crabben, Hennus, McGregor, *et al.*, 2016). Data from this screen also supports

this idea as knockdown of RRM1 or RRM2, components of the RNR complex that are required to catalyse the formation of dNTPs resulted in a synthetic lethal interaction with NSMCE4a shRNA. RRM2B was also in the screen but was not observed to be lethal. This can be explained, as RRM2B is P53 inducible therefore it is likely that RRM2B was not being expressed during the time of the screen.

In the screen the number of cell screened in both RRM1 and RRM2 wells appeared to be much lower than RRM2B, however, it is likely that this was due to the cells being unable to complete the cell cycle. This could be tested by with FACS analysis in the knockdown cell lines. The loss of viability of NSMCE4a shRNA cells appear to be more prominent compared with Non-silencing shRNA cells and supports the idea that SMC5/6 is required to restart replication and may function as a tumour suppressor.

Synthetic viability hits also play an important role in this screen and these hits need to be explored further. Many of these hits appear to be involved in telomere maintenance such as ACD and TERT. Three hits were involved in ubiquitylation of proteins to target substrates for degradation by the proteasome; these are UBB and UBD which are paralogs and UBA1 which catalyses the first step in ubiquitin conjugation. UBA1 is also involved in the recruitment of TP53BP1 and BRCA1 to sites of DNA damage. It is possible the loss of SMC5/6 and ubiquitylation factors leads to cells being unable to trigger an apoptotic response, however the reasons remain unclear and need further investigation.

MMS22L is another top hits in synthetic viability. This is part of the TONSL protein complex, TONSL also appear highly in the viable section, and is required to recognize and stimulates the recombination dependent repair of stalled or collapsed replication forks through promotion of HR(Duro, Lundin, Ask, *et al.*, 2010). This suggests that loss of proteins that promote HR bypasses the requirement for SMC5/6 to regulate the HR pathways.

One of the most interesting synthetic viable hits is that of H2AFZ. H2AFZ is a variant of H2A and has been shown to alter nucleosome stability(Tapia-Alveal, Lin, Yeoh, *et al.*, 2014). Tapia-Alveal 2014 show that in fission yeast H2A.Z and both Cohesin and Smc5/6 ensure genomic integrity through accurate chromosome segregation (Tapia-Alveal, Lin & O'Connell, 2014). H2A.Z appears to operate in opposition to Smc5/6 by promoting sister chromatid cohesion along chromosome arms but not centromeres. Cells lacking H2A.Z show chromosome defects thought to be in part likely due to disruption of the cohesin cycle and in cells lacking both, H2A.Z suppress the mitotic defects of Smc5/6 dysfunction. Therefore, the result that cells with knockdown of NSMCE4a and siRNA knockdown of H2AFZ appear to grow better than control cells shows that this function is conserved.

One of the issues with the screen that could be addressed further involves using a doxycycline inducible knockdown construct to ensure strongest possible knockdown of NSMCE4a. Another issue involves the transfection efficiency, given the large amount of siRNAs used it may be that not all the siRNAs were able to sufficiently knockdown their target. To further confirm the screen more experiments with knock-out cells or even more confirmation with patient cells. Interestingly, expected hits from synthetic lethality screens in yeasts did not come out in human cells, therefore more experiments are needed to identify the function of SMC5/6 in human cells.

Conclusions from the screen validation chapter:

- NSMCE4a knockdown leads to synthetic lethal interaction with a host of HR factors including RBBP8, VCP, EXO1, BRCA2 and RAD52.
- NHEJ is required to repair DNA damage following reduction in HR activity.
- SMC5/6 complex is required during replication and loss of replication factors is deleterious in cells lacking SMC5/6.

- SMC5/6 is required in response to replication stress pointing to a vital role for the SMC5/6 complex in coordinating the response to replication stress.
- Loss of NSMCE4a also leads to synthetic viability with knockdown of ANKRD28, MMS22L and UBB/UBD/UBA1 as well as factors required in the lengthening of telomeres. This needs to be investigated further to ensure that viability is not a short-term relief before leading to defects further on.
- Increased cell viability with knockdown of H2AFZ confirms previously published work by Tapia-Alveal 2014.

The last chapter describes novel homozygous and compound heterozygous missense mutations that have been identified in the *NSMCE3 gene* in Dutch and American families respectively. These mutations, homozygous p.Leu264Phe and compound heterozygous p.Leu264Phe and p.Pro209Leu, have been identified as the cause of a new autosomal recessive chromosome breakage syndrome, termed Lung Immunodeficiency and Chromosome breakage Syndrome (LICS). It is characterized by failure to thrive, immune deficiency leading to severe and eventually fatal pulmonary disease in early childhood (van der Crabben, Hennus, McGregor, *et al.*, 2016). Levels of NSMCE3 protein were below detection levels in patient fibroblasts and levels of SMC5 and SMC6 was also reduced. It is possible that this could be due to a lack of expression of NSMCE3 which stops the formation of the complete SMC5/6 complex, however as loss of *SMC6* or *NSMCE2* is lethal in early embryonic mice it is likely that NSMCE3 is present at low levels in the patient cells but is below the detection levels of the antibodies(van der Crabben, Hennus, McGregor, *et al.*, 2016).

In vitro analysis of the mutations suggested that the Leu264Phe variant was still able to form a complex with NSMCE1, but has a reduced capability to interact with NSMCE4 and SMC6. The Pro209Leu mutation on the other hand led to a C-terminal truncation and disruption of the interaction with NSMCE1 and NSMCE4. The destabilizing effect on the SMC5/6 complex of mutations in

NSMCE3 is much more pronounced than what was observed in cells isolated from patients with truncating mutations in *NSMCE2*, which encodes for the SUMO ligase activity of SMC5/6 (Payne, Colnaghi, Rocha, *et al.*, 2014). The NSMCE2 SUMO ligase is not required for all the functions of the SMC5/6 complex and this may explain the differences in clinical features. Both Leu264Phe and Pro209Leu mutations disrupt the interaction with NSMCE4 therefore it is possible that this is the root cause of the pulmonary failure phenotype.

In Chapter 5 a ɣH2AX assay showed that in cells isolated from one of the Dutch patients, destabilisation of the SMC5/6 complex resulted in defective repair in G2 but not in G1, consistent with a defect in HR but not NHEJ. This is consistent with previous findings of SMC5/6 being required for HR, however whether SMC5/6 was required for NHEJ had not been previously reported (Irmisch, Ampatzidou, Mizuno, *et al.*, 2009; Ampatzidou, Irmisch, O'Connell, *et al.*, 2006; Lehmann, Walicka, Griffiths, *et al.*, 1995; Potts, Porteus & Yu, 2006b). A secondary way to confirm SMC5/6 being required for HR would have involved the use of a HR reporter assay using GFP fragments and an I-SceI recognition site to examine levels of HR repair (Wang, Pan, Su, *et al.*, 2013). However, low transfection efficiency precluded this analysis in the primary fibroblasts.

Patient fibroblasts with the NSMCE3-L264F mutation had a defect in recovery from replication stress that could be complemented through expression of wild-type NSMCE3 protein but not NSMCE3-L264F. This shows the lack of recovery from replication stress to be a direct consequence of the mutation. The lack of recovery from replication stress was also observed in cells with mutated *NSMCE2* showing it to be a common consequence of misregulated SMC5/6 (Payne, Colnaghi, Rocha, *et al.*, 2014; van der Crabben, Hennus, McGregor, *et al.*, 2016). FACS analysis of NSMCE3-L264F patient cells compared with wild-type patient cells indicated no issue with entering S phase during induction of replication stress.

It is worth noting that the allele frequency of NSMCE3-L264F is low making LICS a rare syndrome. In both the American and Dutch families diagnosis and detection of the patients only occurred after the identification of a second patient. Since publication of the syndrome another Dutch family has been identified with similar disease progression. While not closely related to the first Dutch family they also come from the north of the country, suggesting that there is a hotspot for this allele in this region. There is therefore a possibility of further undiagnosed patients presenting with similar symptoms.

In summary, the phenotypes of LICS syndrome are:

- Affected individuals present with terminal lung damage following pneumonia and chromosome rearrangements in lymphocytes.
- Patients with NSMCE3-L264F mutation show normal antibody and V(D)J recombination but have a defect in B and T cell expansion which is consistent with an HR defect and no response to recall antibodies.
- Cells isolated from patients have increased levels of micronuclei consistent with chromosome missegregation.
- Patient cells show no repair defect in G1, however they do have a defect in G2 that is consistent with a defect in HR.
- Mutation in NSMCE3 destabilises SMC5/6 and a failure to recover from replication stress that can be complemented with ectopic expression of WT NSMCE3.

Additional work carried out during the past four years, which is not discussed throughout this thesis, focused on the SMC5 subunit of the SMC5/6 complex. A recent publication from the Murray/Oliver/Pearl lab describes the structure of the SMC5/6 hinge. The Oliver lab solved the structure of the hinge at 2.8A resolution. A structure function analysis using *S. pombe* by the Murray lab then defined key interfaces. The hinge, like that of cohesin and condensin, is toroidal but uniquely is stabilised by an essential ‘latch’ on SMC5, which contacts onto SMC6. Further work defined a region of the hinge from the latch round a positively charged channel to a further regulatory region that binds single strand DNA. Defined

mutations in these interfaces cause a severe loss of function with increased sensitivity to DNA damaging agents. Mutations in the latch led to loss of viability in S. pombe. To explore the requirements for this region in human cells I created doxycycline-inducible constructs and transfected these into U2OS cells. These constructs either expressed eGFP-tagged wild-type SMC5 or mutant SMC5-Y626G, the human equivalent to the *S. pombe* Y612G mutation. In the absence of doxycycline cells were viable, as judged by a trypan blue assay which measures inclusion of a dye by dead cells. When expression was induced through addition of doxycycline for 48 hours the cell viability dropped in the SMC5-Y626G expressing cells, showing this to be dominant negative. This suggests that the SMC5 'latch' is an essential feature of the SMC5/6 complex (Alt, Dang, Wells, *et al.*, 2016).

In summary, discussed in this thesis are several new observations for the SMC5/6 complex in human cells. The development, execution and validation of a synthetic sick/lethal screen is presented. Several interesting hits from this screen are described including several potential interactions that need further investigation. Lastly, a novel chromosome breakage syndrome caused by mutation in NSMCE3 is presented. Patients are shown to have higher levels of chromosomal instability, have a defect in HR and failure to recover from replication stress.

Publications.

Co-first author.

Van der Crabben, S.N., Hennus, M.P., McGregor, G.A., Ritter, D.I., Chinn, I.K., Alt, A., Vondrova, L., Hostenbach. R., van Montfrans, J.M., Terheggen-Lagro, S.W., van Lieshout, S., van Roosmalen, M.J., Renken, I., Duran, K., Nijman, I.J., Kloosterman, W.P., Hennekam, E., Orange, J.S., van Hasselt, P.M., Wheeler, D.A., Palecek, J.J., Lehmann, A.R., Oliver, A.W., Pearl, L.H., Plon, S.E., Murray, J.M., van Haaften, G., 2016. Destabilized smc5/6 complex leads to chromosome breakage syndrome with severe lung disease. *Journal of Clinical Investigation* 126(8):2881-2892.

Second author.

Hopkins, S.R., McGregor, G.A., Murray, J.M., Downs, J.A., 2016. Novel synthetic lethality screening method identifies TIP60-dependent radiation sensitivity in the absence of BAF180. *DNA Repair* 46(2016):47-54.

Contributing author.

Alt, A., Dang, H.Q., Wells, O.S., Polo, L, M., Smith, M.A., McGregor, G.A., Welte, T., Lehmann, A.R., Pearl, L.H., Murray, J.M., Oliver, A.W., 2016., Specialised Interfaces of Smc5/6 Control Hinge Stability and DNA-association. *Nature Communications*

A.0 – Appendix Section.

A.1 – List of siRNA sequences.

A.1.1 – SMC6 Smartpool siRNA

AGAAAUAGAUAAUGCGGUU

GGACAAAGAAAUUAAUCGA

CAGCAUAGAUGGAAGUCGA

CUUUAAAGCCAGUGUGUAU

A.1.2 – NSMCE4a Smartpool siRNA

AAUGAAGUGUCCCGAGCAA

GUGAAGUCCAAAACGGAAA

ACACAGAGCCGUCGGAUUC

GUGCCAAAGCCACGAGUUG

A.1.3 – BRCA1 siRNA

CAGCUACCCUUCCAUCAUA

A.1.X – BRCA2 siRNA

GUAAAGAAAUGCAGAAUUC

A.1.4 – GFP siRNA

GCAAGCUGACCCUGAAGUUC

A.1.5 – SMC3 Smartpool siRNA

CAACGUAGCUUACAGAGUU

GGUGUAAAGUUCAGAAAUA

GAGAGUAGAUGCACUGAAU

GCAGUGCAACACAGAAUUA

A.1.6 – Non-silencing siRNA

UGGUUUACAUGUCGACUAA

A.1.7 – pGIPZ 859 shRNA

UGAUUUCUAACUUGUGUGU

A.1.8 – pGIPZ 860 shRNA

UCUUGAUGAGAUUCUUCCA

A.1.9 – pGIPZ 861 shRNA

AUCUUAACAUGUCAAGGA

A.2. – siRNA Sequences used in screen.

A.2.1 – Screen – DDR Plates.

Dharmacon ON-TARGETplus® SMARTpool® siRNA Library - Human DNA Damage Response G-106005 Lot 11137

Plate	Well	Pool Catalog	Duplex Catalog	Gene	GENEI	Gene	GINumb	Sequence
Plate 1	A02	L-005232-00	J-005232-06	RAD50	10111	NM_133482	1992413	ACAAGGAUCUGGAUA
Plate 1	A02	L-005232-00	J-005232-07	RAD50	10111	NM_133482	1992413	UAACCUCACUGUUGG
Plate 1	A02	L-005232-00	J-005232-08	RAD50	10111	NM_133482	1992413	GAAUUGAAUCGUAAG
Plate 1	A02	L-005232-00	J-005232-09	RAD50	10111	NM_133482	1992413	GACACAAGGUCAGAA
Plate 1	A03	L-018612-02	J-018612-17	POLE2	5427	NM_002692	3218936	GCAUAAUGUUUGCUG
Plate 1	A03	L-018612-02	J-018612-18	POLE2	5427	NM_002692	3218936	CCGUGAAGACUUAGU
Plate 1	A03	L-018612-02	J-018612-19	POLE2	5427	NM_002692	3218936	AGAUGUUUCGUGAGC
Plate 1	A03	L-018612-02	J-018612-20	POLE2	5427	NM_002692	3218936	GAUCCUUUCACUACG
Plate 1	A04	L-012299-00	J-012299-05	RUVBL2	10856	NM_006666	5730022	UAACAAGGAUUGAGC
Plate 1	A04	L-012299-00	J-012299-06	RUVBL2	10856	NM_006666	5730022	CGCAGUACAUGAAGG
Plate 1	A04	L-012299-00	J-012299-07	RUVBL2	10856	NM_006666	5730022	GAAACGCAAGGGUAC
Plate 1	A04	L-012299-00	J-012299-08	RUVBL2	10856	NM_006666	5730022	GCGAGAAAGACACGA
Plate 1	A05	L-004654-00	J-004654-06	PRKCG	5582	NM_002739	4713262	GCCCGUAACCUAAUU
Plate 1	A05	L-004654-00	J-004654-07	PRKCG	5582	NM_002739	4713262	GGAGGGCGAGUAAUA
Plate 1	A05	L-004654-00	J-004654-08	PRKCG	5582	NM_002739	4713262	GGGAGCGGCUGGAA
Plate 1	A05	L-004654-00	J-004654-09	PRKCG	5582	NM_002739	4713262	CAGAAGACCCGAACG
Plate 1	A06	L-011033-00	J-011033-05	FANCC	2176	NM_000136	5611823	GGCAAAAGCUUGUUG
Plate 1	A06	L-011033-00	J-011033-06	FANCC	2176	NM_000136	5611823	GGAAUCGUCUUGGCA
Plate 1	A06	L-011033-00	J-011033-07	FANCC	2176	NM_000136	5611823	GAUGAGAUGUUCAGG
Plate 1	A06	L-011033-00	J-011033-08	FANCC	2176	NM_000136	5611823	GGUAUGCACCUAUAG
Plate 1	A07	L-010344-00	J-010344-06	FEN1	2237	NM_004111	1971877	GGUGAAGGCUGGCAA
Plate 1	A07	L-010344-00	J-010344-07	FEN1	2237	NM_004111	1971877	GGGUCAAGAGGCUGA
Plate 1	A07	L-010344-00	J-010344-08	FEN1	2237	NM_004111	1971877	CAAACUAAUUGCUGA
Plate 1	A07	L-010344-00	J-010344-09	FEN1	2237	NM_004111	1971877	CAAGUACCCUGUGCC
Plate 1	A08	L-010496-00	J-010496-05	TCEA1	6917	NM_201437	4543935	GACAAAUGCUCGAGA
Plate 1	A08	L-010496-00	J-010496-06	TCEA1	6917	NM_201437	4543935	AGACUGACUUGUUCA
Plate 1	A08	L-010496-00	J-010496-07	TCEA1	6917	NM_201437	4543935	GUACAAACCCGUAGU
Plate 1	A08	L-010496-00	J-010496-08	TCEA1	6917	NM_201437	4543935	GCAAUUACAUCGCAG
Plate 1	A09	L-013379-00	J-013379-05	RTEL1	51750	NM_016434	3008996	CCGCAGAGCACACAA
Plate 1	A09	L-013379-00	J-013379-06	RTEL1	51750	NM_016434	3008996	UAUUCAUGCCGUACA
Plate 1	A09	L-013379-00	J-013379-07	RTEL1	51750	NM_016434	3008996	GACAUUAUCCAGAUU
Plate 1	A09	L-013379-00	J-013379-08	RTEL1	51750	NM_016434	3008996	CCAAGGUCCUGGAAU
Plate 1	A10	L-009722-00	J-009722-05	GCN5L2	2648	NM_021078	1083510	AAUGGAACCUGUAAG
Plate 1	A10	L-009722-00	J-009722-06	GCN5L2	2648	NM_021078	1083510	GCGCAUGCCUAAGGA
Plate 1	A10	L-009722-00	J-009722-07	GCN5L2	2648	NM_021078	1083510	CGACGCUGAUGGAGU
Plate 1	A10	L-009722-00	J-009722-08	GCN5L2	2648	NM_021078	1083510	GAGCGUUCCUGGCAU
Plate 1	A11	L-013368-00	J-013368-05	APTX	54840	NM_175071	2832942	ACAAGAGGCUGGUAG
Plate 1	A11	L-013368-00	J-013368-06	APTX	54840	NM_175071	2832942	ACAGAAUACUUCCUA
Plate 1	A11	L-013368-00	J-013368-07	APTX	54840	NM_175071	2832942	CAAAGGCCCGUUACC
Plate 1	A11	L-013368-00	J-013368-08	APTX	54840	NM_175071	2832942	GAAAGAACAUCUCAG
Plate 1	B02	L-004591-00	J-004591-05	RAD18	56852	NM_020165	1455040	CCAAGAAACAAGCGU
Plate 1	B02	L-004591-00	J-004591-06	RAD18	56852	NM_020165	1455040	GGGAGCAGGUUAAUG
Plate 1	B02	L-004591-00	J-004591-07	RAD18	56852	NM_020165	1455040	GCUCUCUGAUCGUGA
Plate 1	B02	L-004591-00	J-004591-08	RAD18	56852	NM_020165	1455040	GAAAUGAGUGGUUCU
Plate 1	B03	L-017578-00	J-017578-05	TTRAP	51567	NM_016614	2351034	GUACAGCCCAGAUGU
Plate 1	B03	L-017578-00	J-017578-06	TTRAP	51567	NM_016614	2351034	GCAGAAGAGGGACAC
Plate 1	B03	L-017578-00	J-017578-07	TTRAP	51567	NM_016614	2351034	UCUAAGGGAUCGAGA
Plate 1	B03	L-017578-00	J-017578-08	TTRAP	51567	NM_016614	2351034	AAAGGGCUCUGAACU
Plate 1	B04	L-032021-01	J-032021-09	GTF2H5	4E+05	NM_207118	4635985	AGGAGCAUGCCACGG
Plate 1	B04	L-032021-01	J-032021-10	GTF2H5	4E+05	NM_207118	4635985	GGAGCGAGUGGGUG
Plate 1	B04	L-032021-01	J-032021-11	GTF2H5	4E+05	NM_207118	4635985	AGGUGACUGAUUAGA
Plate 1	B04	L-032021-01	J-032021-12	GTF2H5	4E+05	NM_207118	4635985	CGUCUUGAAAGGAGU
Plate 1	B05	L-020132-00	J-020132-05	POLE	5426	NM_006231	6219823	GCGAGGAACAGGCGA
Plate 1	B05	L-020132-00	J-020132-06	POLE	5426	NM_006231	6219823	GGAGGAGGGUGCUU
Plate 1	B05	L-020132-00	J-020132-07	POLE	5426	NM_006231	6219823	GGACAGGCGUUACGA
Plate 1	B05	L-020132-00	J-020132-08	POLE	5426	NM_006231	6219823	CUCGGAAGCUGGAAG
Plate 1	B06	L-009930-00	J-009930-05	UBE2B	7320	NM_003337	3296728	GGAAUGCAGUUAUAU
Plate 1	B06	L-009930-00	J-009930-06	UBE2B	7320	NM_003337	3296728	GAACCGAAUCCUAAC
Plate 1	B06	L-009930-00	J-009930-07	UBE2B	7320	NM_003337	3296728	GAGUUUCGGCCAUUG
Plate 1	B06	L-009930-00	J-009930-08	UBE2B	7320	NM_003337	3296728	UAGAUAUCCUUCAGA
Plate 1	B07	L-003506-00	J-003506-07	MDC1	9656	NM_014641	7661965	CAGAAGAGGUGCCAC
Plate 1	B07	L-003506-00	J-003506-08	MDC1	9656	NM_014641	7661965	UAACUGAAAUCCAGC
Plate 1	B07	L-003506-00	J-003506-09	MDC1	9656	NM_014641	7661965	GGUCAGCCAUUAUGC
Plate 1	B07	L-003506-00	J-003506-10	MDC1	9656	NM_014641	7661965	GAGCCCACAUCUCAG
Plate 1	B08	L-006739-00	J-006739-05	IHPK3	1E+05	NM_054111	7819179	GGAAUGAGCACACCA
Plate 1	B08	L-006739-00	J-006739-06	IHPK3	1E+05	NM_054111	7819179	ACAUGAGCGUGAUGA
Plate 1	B08	L-006739-00	J-006739-07	IHPK3	1E+05	NM_054111	7819179	UCUAUCAGUUCCUAC
Plate 1	B08	L-006739-00	J-006739-08	IHPK3	1E+05	NM_054111	7819179	GUUCAUACCGCUUCU
Plate 1	B09	L-003540-00	J-003540-09	SIRT1	23411	NM_012238	1377559	GCAAAGGAGCAGAUU
Plate 1	B09	L-003540-00	J-003540-10	SIRT1	23411	NM_012238	1377559	GCGAUUGGGUACCGA
Plate 1	B09	L-003540-00	J-003540-11	SIRT1	23411	NM_012238	1377559	GGAUAGGUCCAUAUA
Plate 1	B09	L-003540-00	J-003540-12	SIRT1	23411	NM_012238	1377559	CCACCUGAGUUGGAU
Plate 1	B10	L-013239-01	J-013239-20	TREX1	11277	NM_033629	1486138	GCCACAACCAGGAAC
Plate 1	B10	L-013239-01	J-013239-21	TREX1	11277	NM_033629	1486138	GCGCAUGGGCGUCAA
Plate 1	B10	L-013239-01	J-013239-22	TREX1	11277	NM_033629	1486138	CAGAACACGGCCCAA
Plate 1	B10	L-013239-01	J-013239-23	TREX1	11277	NM_033629	1486138	UGUCACAACCACUGC
Plate 1	B11	L-010378-00	J-010378-05	WRN	7486	NM_000553	1992417	GAUCCAUUGUGUAUA
Plate 1	B11	L-010378-00	J-010378-06	WRN	7486	NM_000553	1992417	GCACCAAAGAGCAUU
Plate 1	B11	L-010378-00	J-010378-07	WRN	7486	NM_000553	1992417	AUACGUAACUCCAGA
Plate 1	B11	L-010378-00	J-010378-08	WRN	7486	NM_000553	1992417	GAGGGUUUCUAUCUU

Plate 1	C02	L-011843-00	J-011843-05	DDX11	1663	NM_004399	4758135	CGGCAGAACCUUUGU
Plate 1	C02	L-011843-00	J-011843-06	DDX11	1663	NM_004399	4758135	GAACUGGCCCCUUAC
Plate 1	C02	L-011843-00	J-011843-07	DDX11	1663	NM_004399	4758135	GCAGAGCUGUACCGG
Plate 1	C02	L-011843-00	J-011843-08	DDX11	1663	NM_004399	4758135	GGGAUCAACUUCUCU
Plate 1	C03	L-010237-00	J-010237-06	APEX1	328	NM_080648	1837550	CAAAGUUUCUUACGG
Plate 1	C03	L-010237-00	J-010237-07	APEX1	328	NM_080648	1837550	GAGACCAAAUGUUCA
Plate 1	C03	L-010237-00	J-010237-08	APEX1	328	NM_080648	1837550	CUUCGAGCCUGGAUU
Plate 1	C03	L-010237-00	J-010237-09	APEX1	328	NM_080648	1837550	UAACAGCAUAUGUAC
Plate 1	C04	L-003780-01	J-003780-13	TDG	6996	NM_0010084	5654914	UCGUGAAGGAGGACG
Plate 1	C04	L-003780-01	J-003780-14	TDG	6996	NM_0010084	5654914	GUUGAAAGGCAUUGA
Plate 1	C04	L-003780-01	J-003780-15	TDG	6996	NM_0010084	5654914	CUUUAAAUUAUGACG
Plate 1	C04	L-003780-01	J-003780-16	TDG	6996	NM_0010084	5654914	GGAAGUAUGGUAUUG
Plate 1	C05	L-012358-00	J-012358-08	TOPBP1	11073	NM_007027	2014394	ACAAAUACAUGGCUG
Plate 1	C05	L-012358-00	J-012358-09	TOPBP1	11073	NM_007027	2014394	ACACUAAUCGGGAGU
Plate 1	C05	L-012358-00	J-012358-10	TOPBP1	11073	NM_007027	2014394	GAGCCGAACAUCCAG
Plate 1	C05	L-012358-00	J-012358-11	TOPBP1	11073	NM_007027	2014394	CCACAGUAGUUGAGG
Plate 1	C06	L-004592-00	J-004592-05	RAD54L	8438	NM_003579	1992413	AGAAUGAUCUGCUUG
Plate 1	C06	L-004592-00	J-004592-06	RAD54L	8438	NM_003579	1992413	CGAAUUACACCCAGA
Plate 1	C06	L-004592-00	J-004592-07	RAD54L	8438	NM_003579	1992413	GCACGAUGUCCAUUA
Plate 1	C06	L-004592-00	J-004592-08	RAD54L	8438	NM_003579	1992413	AUACGGAGGACUUCU
Plate 1	C07	L-015749-01	J-015749-09	RPA1	6117	NM_002945	2007017	CCCUAGAACUGGUUG
Plate 1	C07	L-015749-01	J-015749-10	RPA1	6117	NM_002945	2007017	AAGCAGGAAUUAUGU
Plate 1	C07	L-015749-01	J-015749-11	RPA1	6117	NM_002945	2007017	CCACUGUGAUGGACG
Plate 1	C07	L-015749-01	J-015749-12	RPA1	6117	NM_002945	2007017	CAGAAUGGAAGCUCG
Plate 1	C08	L-009871-00	J-009871-05	ATF2	1386	NM_001880	2253842	GAGAAGAGCAGCUAA
Plate 1	C08	L-009871-00	J-009871-06	ATF2	1386	NM_001880	2253842	CAUGGUAGCGGAUUG
Plate 1	C08	L-009871-00	J-009871-07	ATF2	1386	NM_001880	2253842	GGAAGUACCAUUGGC
Plate 1	C08	L-009871-00	J-009871-08	ATF2	1386	NM_001880	2253842	UGAGGAGCCUUCUGU
Plate 1	C09	L-008727-00	J-008727-09	VCP	7415	NM_007126	7669552	GCAUGUGGGUGCUG
Plate 1	C09	L-008727-00	J-008727-10	VCP	7415	NM_007126	7669552	CAAAUUGGCUGGUGA
Plate 1	C09	L-008727-00	J-008727-11	VCP	7415	NM_007126	7669552	CCUGAUUGCUCGAGC
Plate 1	C09	L-008727-00	J-008727-12	VCP	7415	NM_007126	7669552	GUAAUCUCUUCGAGG
Plate 1	C10	L-032261-00	J-032261-05	ALKBH2	1E+05	NM_0010016	4871722	GACUUUGUCUUCCGG
Plate 1	C10	L-032261-00	J-032261-06	ALKBH2	1E+05	NM_0010016	4871722	CACGGGAGCUUACUA
Plate 1	C10	L-032261-00	J-032261-07	ALKBH2	1E+05	NM_0010016	4871722	GCACCGAGAUGAUGA
Plate 1	C10	L-032261-00	J-032261-08	ALKBH2	1E+05	NM_0010016	4871722	CCAGGAAGCAGGCAA
Plate 1	C11	L-028674-00	J-028674-05	GTF2H4	2968	NM_001517	5414465	CUGAGGGUGUCCUG
Plate 1	C11	L-028674-00	J-028674-06	GTF2H4	2968	NM_001517	5414465	GAACCGAGUACACCU
Plate 1	C11	L-028674-00	J-028674-07	GTF2H4	2968	NM_001517	5414465	GAUGGGAGGUGGUC
Plate 1	C11	L-028674-00	J-028674-08	GTF2H4	2968	NM_001517	5414465	GGCCAUCAAUCUCUC
Plate 1	D02	L-009344-00	J-009344-05	PMS1	5378	NM_000534	5372934	GCGAAUGGUUUCAAG
Plate 1	D02	L-009344-00	J-009344-06	PMS1	5378	NM_000534	5372934	CAUAAACAGUCGACC
Plate 1	D02	L-009344-00	J-009344-07	PMS1	5378	NM_000534	5372934	CCACAAGCGUAGAUG
Plate 1	D02	L-009344-00	J-009344-08	PMS1	5378	NM_000534	5372934	GCAAUCGAGUAAUCA
Plate 1	D03	L-003461-00	J-003461-09	BRCA1	672	NM_007298	6325287	CAACAUGCCCACAGA
Plate 1	D03	L-003461-00	J-003461-10	BRCA1	672	NM_007298	6325287	CCAAAGCGAGCAAGA
Plate 1	D03	L-003461-00	J-003461-11	BRCA1	672	NM_007298	6325287	UGAUAAAGCUCCAGC
Plate 1	D03	L-003461-00	J-003461-12	BRCA1	672	NM_007298	6325287	GAAGGAGCUUUCAUC
Plate 1	D04	L-010035-01	J-010035-09	POLM	27434	NM_013284	7019492	GGAGAGAGUUCGGC
Plate 1	D04	L-010035-01	J-010035-10	POLM	27434	NM_013284	7019492	CGGGAAGGACUGCGA
Plate 1	D04	L-010035-01	J-010035-11	POLM	27434	NM_013284	7019492	CUGCAGCUCCGAAGC
Plate 1	D04	L-010035-01	J-010035-12	POLM	27434	NM_013284	7019492	CUGGACAUAAGCUGG
Plate 1	D05	L-006302-00	J-006302-05	REV3L	5980	NM_002912	4506482	GGAGUUCUCUGCUGA
Plate 1	D05	L-006302-00	J-006302-06	REV3L	5980	NM_002912	4506482	ACACAGAAGUUGAGU
Plate 1	D05	L-006302-00	J-006302-07	REV3L	5980	NM_002912	4506482	GGAUGUAAGUCCAUG
Plate 1	D05	L-006302-00	J-006302-08	REV3L	5980	NM_002912	4506482	GAUAUGAGAUUCAGA
Plate 1	D06	L-011689-00	J-011689-05	HMGB2	3148	NM_002129	1414117	GCAAAGAAAUUGGGU
Plate 1	D06	L-011689-00	J-011689-06	HMGB2	3148	NM_002129	1414117	GAACAUCGCCCAAAG
Plate 1	D06	L-011689-00	J-011689-07	HMGB2	3148	NM_002129	1414117	GAAUAAAUGGCUAUC
Plate 1	D06	L-011689-00	J-011689-08	HMGB2	3148	NM_002129	1414117	GAAGAAGAACGAACC
Plate 1	D07	L-003893-00	J-003893-07	GADD45A	1647	NM_001924	9790904	UCAAUGGGUUCCAGU
Plate 1	D07	L-003893-00	J-003893-08	GADD45A	1647	NM_001924	9790904	CCGAAAGGAUGGAUA
Plate 1	D07	L-003893-00	J-003893-09	GADD45A	1647	NM_001924	9790904	GAUCCUGCCUUAAGU
Plate 1	D07	L-003893-00	J-003893-10	GADD45A	1647	NM_001924	9790904	CCGAUAACGUGGUGU
Plate 1	D08	L-019657-00	J-019657-05	IGHMBP2	3508	NM_002180	4504622	GAAAUACACCCGCUG
Plate 1	D08	L-019657-00	J-019657-06	IGHMBP2	3508	NM_002180	4504622	GUACGAUGCUGCUAA
Plate 1	D08	L-019657-00	J-019657-07	IGHMBP2	3508	NM_002180	4504622	GAUACUGUCCUUCGU
Plate 1	D08	L-019657-00	J-019657-08	IGHMBP2	3508	NM_002180	4504622	CCGAGAGAAUUCCUA
Plate 1	D09	L-010032-00	J-010032-05	PMS2	5395	NM_0010180	6408507	UAAUGAAGCUGUUCU
Plate 1	D09	L-010032-00	J-010032-06	PMS2	5395	NM_0010180	6408507	UCUAUGAGUUCUUUA
Plate 1	D09	L-010032-00	J-010032-07	PMS2	5395	NM_0010180	6408507	GGAUGUUGAAGGUAA
Plate 1	D09	L-010032-00	J-010032-08	PMS2	5395	NM_0010180	6408507	GGAAUAUUAAGAAGG
Plate 1	D10	L-003479-00	J-003479-10	CSNK1E	1454	NM_001894	4054939	CCACCAAGCGCCAGA
Plate 1	D10	L-003479-00	J-003479-11	CSNK1E	1454	NM_001894	4054939	CCUCCGAAUUCUCAA
Plate 1	D10	L-003479-00	J-003479-12	CSNK1E	1454	NM_001894	4054939	CGACUACUCUUACCU
Plate 1	D10	L-003479-00	J-003479-13	CSNK1E	1454	NM_001894	4054939	GAUCAGCCGCAUCGA
Plate 1	D11	L-010587-00	J-010587-05	BRIP1	83990	NM_032043	1404297	AGUCAAGAGUCAUCG
Plate 1	D11	L-010587-00	J-010587-06	BRIP1	83990	NM_032043	1404297	GAUAGUAUGGUCAAC
Plate 1	D11	L-010587-00	J-010587-07	BRIP1	83990	NM_032043	1404297	UAACCCAAGUCGCUA
Plate 1	D11	L-010587-00	J-010587-08	BRIP1	83990	NM_032043	1404297	GUGCAAAGCCUGGGA

Plate 1	E02	L-006834-00	J-006834-05	CSPG6	9126	NM_005445	63054826	CAACGUAGCUUACAGAGUU
Plate 1	E02	L-006834-00	J-006834-06	CSPG6	9126	NM_005445	63054826	GGUGUAAAGUUCAGAAAUA
Plate 1	E02	L-006834-00	J-006834-07	CSPG6	9126	NM_005445	63054826	GAGAGUAGAUGCACUGAAU
Plate 1	E02	L-006834-00	J-006834-08	CSPG6	9126	NM_005445	63054826	GCAGUGCAACACAGAAUUA
Plate 1	E03	L-011760-00	J-011760-05	RAD52	5893	NM_002879	20143951	CAGAAGGUGUGCUACAUUG
Plate 1	E03	L-011760-00	J-011760-06	RAD52	5893	NM_002879	20143951	GGUCAUCGGGUAAUUAAUC
Plate 1	E03	L-011760-00	J-011760-07	RAD52	5893	NM_002879	20143951	GGCCCAGAAUACAUAAGUA
Plate 1	E03	L-011760-00	J-011760-08	RAD52	5893	NM_002879	20143951	GGAAGAGCCAGGACAUGAA
Plate 1	E04	L-021486-00	J-021486-05	FANCL	55120	NM_018062	49472818	GCGGAUACCUGCUUCAGUA
Plate 1	E04	L-021486-00	J-021486-06	FANCL	55120	NM_018062	49472818	CAGCUGAGAACAAUACUUA
Plate 1	E04	L-021486-00	J-021486-07	FANCL	55120	NM_018062	49472818	AGUGUUGCCUGAAGAUUUA
Plate 1	E04	L-021486-00	J-021486-08	FANCL	55120	NM_018062	49472818	GCAAUAGAAUCACUAAAGG
Plate 1	E05	L-016376-00	J-016376-05	FANCD2	2177	NM_001018115	66528887	UGGAUAAGUUGUCGUCUAU
Plate 1	E05	L-016376-00	J-016376-06	FANCD2	2177	NM_001018115	66528887	CAACAUACCUCGACUCAUU
Plate 1	E05	L-016376-00	J-016376-07	FANCD2	2177	NM_001018115	66528887	GGAUUUACCUGUGAUAAUA
Plate 1	E05	L-016376-00	J-016376-08	FANCD2	2177	NM_001018115	66528887	GGAGAUUGAUGGUCUACUA
Plate 1	E06	L-016262-00	J-016262-05	TRIP13	9319	NM_004237	20149561	GUACCGAUAUGGCCAAUUA
Plate 1	E06	L-016262-00	J-016262-06	TRIP13	9319	NM_004237	20149561	GCAAAUCACUGGGUUCUAC
Plate 1	E06	L-016262-00	J-016262-07	TRIP13	9319	NM_004237	20149561	ACAAUUAGACUUUCAAGCA
Plate 1	E06	L-016262-00	J-016262-08	TRIP13	9319	NM_004237	20149561	GACCAGAAAUGUGCAGUCU
Plate 1	E07	L-004717-00	J-004717-06	TYMS	7298	NM_001071	4507750	CCAAACGUGUGUUCUGGAA
Plate 1	E07	L-004717-00	J-004717-07	TYMS	7298	NM_001071	4507750	UGGGAGAUGCACAUAUUUA
Plate 1	E07	L-004717-00	J-004717-08	TYMS	7298	NM_001071	4507750	UCACAUCGAGCCACUGAAA
Plate 1	E07	L-004717-00	J-004717-09	TYMS	7298	NM_001071	4507750	GGGCAGAAUACAGAGAUAU
Plate 1	E08	L-016040-00	J-016040-05	XPC	7508	NM_004628	54607142	GCAAAUGGCUUCUAUCGAA
Plate 1	E08	L-016040-00	J-016040-06	XPC	7508	NM_004628	54607142	UGAAAUAUGAGGCCAUCUA
Plate 1	E08	L-016040-00	J-016040-07	XPC	7508	NM_004628	54607142	GAGAAGUACCCUACAAGAU
Plate 1	E08	L-016040-00	J-016040-08	XPC	7508	NM_004628	54607142	GGAGGGCGAUGAAACGUUU
Plate 1	E09	L-003267-00	J-003267-09	HUS1	3364	NM_004507	31077213	ACAAGUAAAUCCCACAAAG
Plate 1	E09	L-003267-00	J-003267-10	HUS1	3364	NM_004507	31077213	UGAAGUGCACAUAGAUAUU
Plate 1	E09	L-003267-00	J-003267-11	HUS1	3364	NM_004507	31077213	CCAUAAAGGUGAUUCCUAG
Plate 1	E09	L-003267-00	J-003267-12	HUS1	3364	NM_004507	31077213	UCAGUAACAUGAUAGCCAA
Plate 1	E10	L-013231-01	J-013231-09	RPS27L	51065	NM_015920	76563938	AGACAGUGGUUCUUUGUGU
Plate 1	E10	L-013231-01	J-013231-10	RPS27L	51065	NM_015920	76563938	GAAGGGUGUUCAUUUAGAA
Plate 1	E10	L-013231-01	J-013231-11	RPS27L	51065	NM_015920	76563938	GCAACACUAAUGAUUCAAA
Plate 1	E10	L-013231-01	J-013231-12	RPS27L	51065	NM_015920	76563938	CUGGCUAAUUUGUGUCUCA
Plate 1	E11	L-026431-01	J-026431-09	DNA2L	1763	XM_938629	89032012	AGACAAGGUUCCAGCGCCA
Plate 1	E11	L-026431-01	J-026431-10	DNA2L	1763	XM_938629	89032012	UAACAUUGAAGUCGUGAAA
Plate 1	E11	L-026431-01	J-026431-11	DNA2L	1763	XM_938629	89032012	AAGCACAGGUGUACCGAAA
Plate 1	E11	L-026431-01	J-026431-12	DNA2L	1763	XM_938629	89032012	GAGUCACAAUCGAAGGAUA
Plate 1	F02	L-003272-00	J-003272-14	MAD2L2	10459	NM_006341	6006019	GACAAGACCUCAACUUUGG
Plate 1	F02	L-003272-00	J-003272-15	MAD2L2	10459	NM_006341	6006019	GAAAUUCGUCUUUGAGAUC
Plate 1	F02	L-003272-00	J-003272-16	MAD2L2	10459	NM_006341	6006019	CAACGUGCCGGUCCAGAUG
Plate 1	F02	L-003272-00	J-003272-17	MAD2L2	10459	NM_006341	6006019	UCCAGAAACGCAAGAAGUA
Plate 1	F03	L-021955-00	J-021955-05	KIAA1596	57697	NM_020937	74959746	GGGUAGAACUGGCCGUAAA
Plate 1	F03	L-021955-00	J-021955-06	KIAA1596	57697	NM_020937	74959746	GAGAGGAACGUAUUUAUAA
Plate 1	F03	L-021955-00	J-021955-07	KIAA1596	57697	NM_020937	74959746	AAACAGACAUCGCUGAAUU
Plate 1	F03	L-021955-00	J-021955-08	KIAA1596	57697	NM_020937	74959746	GCAUGUAGCUAGGAAGUUU
Plate 1	F04	L-020013-00	J-020013-05	SETMAR	6419	NM_006515	5730038	GAUUGACCCUUGAGACUAU
Plate 1	F04	L-020013-00	J-020013-06	SETMAR	6419	NM_006515	5730038	CCAAAGAAAGGCUAGAUCA
Plate 1	F04	L-020013-00	J-020013-07	SETMAR	6419	NM_006515	5730038	CGACUCCAAUUACAUUAUA
Plate 1	F04	L-020013-00	J-020013-08	SETMAR	6419	NM_006515	5730038	GAAGGUUUGUCUGUGAAUA
Plate 1	F05	L-005030-00	J-005030-06	PRKDC	5591	NM_006904	31340617	GGAAGAAGCUCAUUUGAUU
Plate 1	F05	L-005030-00	J-005030-07	PRKDC	5591	NM_006904	31340617	GAGCAUCACUUGCCUUUAA
Plate 1	F05	L-005030-00	J-005030-08	PRKDC	5591	NM_006904	31340617	GCAGGACCGUGCAAGGUUA
Plate 1	F05	L-005030-00	J-005030-09	PRKDC	5591	NM_006904	31340617	AGAUAGAGCUGCUAAAUGU
Plate 1	F06	L-019554-00	J-019554-05	C11ORF13	8045	NM_003475	24475884	GAACGCUGCCUAAUUCGUG
Plate 1	F06	L-019554-00	J-019554-06	C11ORF13	8045	NM_003475	24475884	UGCCAGCGAUGUCCAGUUU
Plate 1	F06	L-019554-00	J-019554-07	C11ORF13	8045	NM_003475	24475884	GGUCAUCGCACUAGCCCAA
Plate 1	F06	L-019554-00	J-019554-08	C11ORF13	8045	NM_003475	24475884	CAGCAGAGCGAGCCUUGCA
Plate 1	F07	L-010127-00	J-010127-05	PARP2	10038	NM_005484	110825960	CAUCACAGGUUACAUGUUU
Plate 1	F07	L-010127-00	J-010127-06	PARP2	10038	NM_005484	110825960	AAGGAUUGCUUCAAGGUAA
Plate 1	F07	L-010127-00	J-010127-07	PARP2	10038	NM_005484	110825960	GCAAGUGACACAGGAAUUC
Plate 1	F07	L-010127-00	J-010127-08	PARP2	10038	NM_005484	110825960	CAGGUUACCAGUCUCUUAA
Plate 1	F08	L-019650-00	J-019650-05	POLI	11201	NM_007195	6005847	CCACAGUUGGUAUUAGUUA
Plate 1	F08	L-019650-00	J-019650-06	POLI	11201	NM_007195	6005847	GCACUAUGGUCGUGAGAGU
Plate 1	F08	L-019650-00	J-019650-07	POLI	11201	NM_007195	6005847	CGGGUCAUGUAUACAAUAA
Plate 1	F08	L-019650-00	J-019650-08	POLI	11201	NM_007195	6005847	GAACAUCAGGCUUUAAUAG
Plate 1	F09	L-003294-00	J-003294-09	RAD17	5884	NM_133341	19718789	AGAUUUACCUAACCAGUUU
Plate 1	F09	L-003294-00	J-003294-10	RAD17	5884	NM_133341	19718789	CAACUUACGGCCAAGGAAA
Plate 1	F09	L-003294-00	J-003294-11	RAD17	5884	NM_133341	19718789	GAGCGACAAAGUAUAACAA
Plate 1	F09	L-003294-00	J-003294-12	RAD17	5884	NM_133341	19718789	UCGAUGUCCUCUUAUAUUU
Plate 1	F10	L-004239-00	J-004239-06	TOP2A	7153	NM_001067	19913405	CGAAAGGAAUGGUUAACUA
Plate 1	F10	L-004239-00	J-004239-07	TOP2A	7153	NM_001067	19913405	GAUGAACUCUGCAGGCUAA
Plate 1	F10	L-004239-00	J-004239-08	TOP2A	7153	NM_001067	19913405	GGAGAAGAUUAUACAUGUA
Plate 1	F10	L-004239-00	J-004239-09	TOP2A	7153	NM_001067	19913405	GGUAACUCCUUGAAAGUAA
Plate 1	F11	L-011350-00	J-011350-05	PER1	5187	NM_002616	4505712	CCAAUAAGGCGGAGAGUGU
Plate 1	F11	L-011350-00	J-011350-06	PER1	5187	NM_002616	4505712	CCAGUGACCUGCUCGAACU
Plate 1	F11	L-011350-00	J-011350-07	PER1	5187	NM_002616	4505712	GGCCGAAUCGUCUACAUUU
Plate 1	F11	L-011350-00	J-011350-08	PER1	5187	NM_002616	4505712	CAACGGGCAUGAGUCUAGA

Plate 1	G02	L-009297-00	J-009297-06	ADPRTL3	10039	NM_0010039	5155872	GGUGAUACAGACCUA
Plate 1	G02	L-009297-00	J-009297-07	ADPRTL3	10039	NM_0010039	5155872	ACGCAGAAGCUCAUC
Plate 1	G02	L-009297-00	J-009297-08	ADPRTL3	10039	NM_0010039	5155872	GACCGAGACUACCAG
Plate 1	G02	L-009297-00	J-009297-09	ADPRTL3	10039	NM_0010039	5155872	GCAAGGAGAUGUUCA
Plate 1	G03	L-016345-01	J-016345-09	NEIL2	3E+05	NM_145043	2145079	GAAUGAACCUAGAGC
Plate 1	G03	L-016345-01	J-016345-10	NEIL2	3E+05	NM_145043	2145079	GGUCAUGAAGGAGGC
Plate 1	G03	L-016345-01	J-016345-11	NEIL2	3E+05	NM_145043	2145079	GGGCAGCAGUAAGAA
Plate 1	G03	L-016345-01	J-016345-12	NEIL2	3E+05	NM_145043	2145079	GCGAGGAUGAUUCUG
Plate 1	G04	L-008234-00	J-008234-05	REV1L	51455	NM_0010378	8404396	GAAGUUAAUUGAUGG
Plate 1	G04	L-008234-00	J-008234-06	REV1L	51455	NM_0010378	8404396	CAUAUCAGCUGUACA
Plate 1	G04	L-008234-00	J-008234-07	REV1L	51455	NM_0010378	8404396	GUGGAGACUUGCAGU
Plate 1	G04	L-008234-00	J-008234-08	REV1L	51455	NM_0010378	8404396	CAUCAGAGCUGUAUA
Plate 1	G05	L-008364-00	J-008364-09	SOD1	6647	NM_000454	4876294	GGAAGUCGUUUGGCU
Plate 1	G05	L-008364-00	J-008364-10	SOD1	6647	NM_000454	4876294	GCACACUGGUGGUCC
Plate 1	G05	L-008364-00	J-008364-11	SOD1	6647	NM_000454	4876294	GUGCAGGGCAUCAUC
Plate 1	G05	L-008364-00	J-008364-12	SOD1	6647	NM_000454	4876294	CAAUAAACAUUCCCU
Plate 1	G06	L-003478-01	J-003478-17	CSNK1D	1453	NM_001893	2054414	ACGAAAGGAUUAGCG
Plate 1	G06	L-003478-01	J-003478-18	CSNK1D	1453	NM_001893	2054414	CGACCUCACAGGCCG
Plate 1	G06	L-003478-01	J-003478-19	CSNK1D	1453	NM_001893	2054414	GCCAAGAAGUACCGG
Plate 1	G06	L-003478-01	J-003478-20	CSNK1D	1453	NM_001893	2054414	AGGCUACCCUUCCGA
Plate 1	G07	L-019665-00	J-019665-05	MSH3	4437	NM_002439	6830363	GCACAUAGCUACAGA
Plate 1	G07	L-019665-00	J-019665-06	MSH3	4437	NM_002439	6830363	CCCGAGAGCUCAAUA
Plate 1	G07	L-019665-00	J-019665-07	MSH3	4437	NM_002439	6830363	GGACAGGAGUUUAUG
Plate 1	G07	L-019665-00	J-019665-08	MSH3	4437	NM_002439	6830363	GAUUCGAAACGUCAA
Plate 1	G08	L-019116-00	J-019116-05	MSH4	4438	NM_002440	3694936	GAGAUUAGAUUGUGU
Plate 1	G08	L-019116-00	J-019116-06	MSH4	4438	NM_002440	3694936	CAAGAGGUUUGGAAU
Plate 1	G08	L-019116-00	J-019116-07	MSH4	4438	NM_002440	3694936	CGACUUCGUUCUAAU
Plate 1	G08	L-019116-00	J-019116-08	MSH4	4438	NM_002440	3694936	CGACCAGAAUUUACU
Plate 1	G09	L-004914-01	J-004914-09	XAB2	56949	NM_020196	5577090	ACGCAGCACUCUCGA
Plate 1	G09	L-004914-01	J-004914-10	XAB2	56949	NM_020196	5577090	CCAAAUUCAUUGCCC
Plate 1	G09	L-004914-01	J-004914-11	XAB2	56949	NM_020196	5577090	CCUUGCGGCUGCUG
Plate 1	G09	L-004914-01	J-004914-12	XAB2	56949	NM_020196	5577090	AGGAGAGCUUCAAGG
Plate 1	G10	L-011899-00	J-011899-05	FANCG	2189	NM_004629	4759335	CAGGUAAUCGAGACA
Plate 1	G10	L-011899-00	J-011899-06	FANCG	2189	NM_004629	4759335	GAGUGGAGCCUCUAA
Plate 1	G10	L-011899-00	J-011899-07	FANCG	2189	NM_004629	4759335	GGACCUGGCCUUGUU
Plate 1	G10	L-011899-00	J-011899-08	FANCG	2189	NM_004629	4759335	GCAGGGAUGUAAGUC
Plate 1	G11	L-003202-00	J-003202-19	ATR	545	NM_001184	2014397	GAGAAAGGAUUGUAG
Plate 1	G11	L-003202-00	J-003202-20	ATR	545	NM_001184	2014397	GCAACUCGCCUAACA
Plate 1	G11	L-003202-00	J-003202-21	ATR	545	NM_001184	2014397	CCACGAAUGUUAACU
Plate 1	G11	L-003202-00	J-003202-22	ATR	545	NM_001184	2014397	CCGCUAAUCUUCUAA
Plate 1	H02	L-015379-01	J-015379-09	HEL308	1E+05	NM_133636	1952573	CGACUCAAAUUAUCG
Plate 1	H02	L-015379-01	J-015379-10	HEL308	1E+05	NM_133636	1952573	GUUUGAAGAUUGCAA
Plate 1	H02	L-015379-01	J-015379-11	HEL308	1E+05	NM_133636	1952573	GCAUGAAGCUAUCUG
Plate 1	H02	L-015379-01	J-015379-12	HEL308	1E+05	NM_133636	1952573	CGUAAGGACAAUUGA
Plate 1	H03	L-017467-00	J-017467-05	RAD51L3	5892	NM_133629	1992412	CCACAUAACUCGAGA
Plate 1	H03	L-017467-00	J-017467-06	RAD51L3	5892	NM_133629	1992412	GAUCAGACAUGACCU
Plate 1	H03	L-017467-00	J-017467-07	RAD51L3	5892	NM_133629	1992412	GGCCAAAUCUUCCCG
Plate 1	H03	L-017467-00	J-017467-08	RAD51L3	5892	NM_133629	1992412	AGAAAUGUGGCUUGU
Plate 1	H04	L-008515-00	J-008515-06	UNG2	10309	NM_021147	6684138	GCUCAUCGCUUGCAA
Plate 1	H04	L-008515-00	J-008515-07	UNG2	10309	NM_021147	6684138	CUACAGACCUUCCGC
Plate 1	H04	L-008515-00	J-008515-08	UNG2	10309	NM_021147	6684138	CAUAAACAGUACUUC
Plate 1	H04	L-008515-00	J-008515-09	UNG2	10309	NM_021147	6684138	GAAUCCCGCUGUAAG
Plate 1	H05	L-011291-00	J-011291-05	GTF2H2	2966	NM_001515	3174757	GGUAGUAGAUGGAUC
Plate 1	H05	L-011291-00	J-011291-06	GTF2H2	2966	NM_001515	3174757	AGACUGACGUGUACU
Plate 1	H05	L-011291-00	J-011291-07	GTF2H2	2966	NM_001515	3174757	GAGAAGUACUAAUCA
Plate 1	H05	L-011291-00	J-011291-08	GTF2H2	2966	NM_001515	3174757	GAUUCCAGCAUGUAG
Plate 1	H06	L-010213-00	J-010213-06	YBX1	4904	NM_004559	3409894	CUGAGUAAAUGCCGG
Plate 1	H06	L-010213-00	J-010213-07	YBX1	4904	NM_004559	3409894	CGACGCAGACGCCCA
Plate 1	H06	L-010213-00	J-010213-08	YBX1	4904	NM_004559	3409894	GUAAGGAACGGAUAU
Plate 1	H06	L-010213-00	J-010213-09	YBX1	4904	NM_004559	3409894	GCGGAGGCAGCAAAU
Plate 1	H07	L-009394-00	J-009394-06	XRCC1	7515	NM_006297	5454171	CCGCAAGCCUGAAGU
Plate 1	H07	L-009394-00	J-009394-07	XRCC1	7515	NM_006297	5454171	GGAAUGAUGGCUCAG
Plate 1	H07	L-009394-00	J-009394-08	XRCC1	7515	NM_006297	5454171	AAACUCAUCCGAUAC
Plate 1	H07	L-009394-00	J-009394-09	XRCC1	7515	NM_006297	5454171	AGGCAGACACUUACC
Plate 1	H08	L-010924-00	J-010924-05	GTF2H1	2965	NM_005316	1992330	CAACAAGUCAGGACA
Plate 1	H08	L-010924-00	J-010924-06	GTF2H1	2965	NM_005316	1992330	UUACAAGAGUCCAUU
Plate 1	H08	L-010924-00	J-010924-07	GTF2H1	2965	NM_005316	1992330	GAAGUCAGAUAGGUA
Plate 1	H08	L-010924-00	J-010924-08	GTF2H1	2965	NM_005316	1992330	GUAACGGUCUAAGAU
Plate 1	H09	L-006626-00	J-006626-05	ERCC5	2073	NM_000123	5198889	GACUGAAGCCUUUCC
Plate 1	H09	L-006626-00	J-006626-06	ERCC5	2073	NM_000123	5198889	GAUCCUGGCUGUUGA
Plate 1	H09	L-006626-00	J-006626-07	ERCC5	2073	NM_000123	5198889	GCAAGAAACAAGUAG
Plate 1	H09	L-006626-00	J-006626-08	ERCC5	2073	NM_000123	5198889	CGAUAGAUAUUGAGU
Plate 1	H10	L-016143-01	J-016143-09	MUS81	80198	NM_025128	3414759	CAGCCCUGGUGGAUC
Plate 1	H10	L-016143-01	J-016143-10	MUS81	80198	NM_025128	3414759	CAUUAAGUGUGGGCG
Plate 1	H10	L-016143-01	J-016143-11	MUS81	80198	NM_025128	3414759	UGACCCACACGGUGC
Plate 1	H10	L-016143-01	J-016143-12	MUS81	80198	NM_025128	3414759	CUCAGGAGCCCGAGU
Plate 1	H11	L-006995-00	J-006995-06	RAP80	51720	NM_016290	4247612	AGAGGCAGCUCCUUA
Plate 1	H11	L-006995-00	J-006995-07	RAP80	51720	NM_016290	4247612	AGAGCAGGCUAGUGA
Plate 1	H11	L-006995-00	J-006995-08	RAP80	51720	NM_016290	4247612	AAAUGAAUCUCCCGU
Plate 1	H11	L-006995-00	J-006995-09	RAP80	51720	NM_016290	4247612	GUAAAUCCCUGGUCC

Plate 2	A02	L-016775-01	J-016775-09	FLJ13614	84142	NM_139076	2058996	UAUUAGUGGUAACGU
Plate 2	A02	L-016775-01	J-016775-10	FLJ13614	84142	NM_139076	2058996	ACACAAGACAAACGA
Plate 2	A02	L-016775-01	J-016775-11	FLJ13614	84142	NM_139076	2058996	GGUAGUAGUAACCAA
Plate 2	A02	L-016775-01	J-016775-12	FLJ13614	84142	NM_139076	2058996	CAGGGUACCUUUAGU
Plate 2	A03	L-005046-00	J-005046-07	TRIM28	10155	NM_005762	1497141	GAAAUGUGAGCGUGU
Plate 2	A03	L-005046-00	J-005046-08	TRIM28	10155	NM_005762	1497141	GCGAUCUGGUUAUGU
Plate 2	A03	L-005046-00	J-005046-09	TRIM28	10155	NM_005762	1497141	AGACAGCACUGGCGU
Plate 2	A03	L-005046-00	J-005046-10	TRIM28	10155	NM_005762	1497141	GAACGAGGCCUUCGG
Plate 2	A04	L-009807-00	J-009807-05	POLS	11044	NM_006999	6254886	GGAGUGACGUUGAUU
Plate 2	A04	L-009807-00	J-009807-06	POLS	11044	NM_006999	6254886	CGGAGUUCAUCAAGA
Plate 2	A04	L-009807-00	J-009807-07	POLS	11044	NM_006999	6254886	AAACAGAGACGCCGA
Plate 2	A04	L-009807-00	J-009807-08	POLS	11044	NM_006999	6254886	GCGAAUAGCCACAUG
Plate 2	A05	L-005798-00	J-005798-12	CXORF53	79184	NM_0010180	6476248	CAUAAUGGCUCAGUG
Plate 2	A05	L-005798-00	J-005798-13	CXORF53	79184	NM_0010180	6476248	CGUCAGAAUUGUUCA
Plate 2	A05	L-005798-00	J-005798-14	CXORF53	79184	NM_0010180	6476248	GAAGGACCGAGUAGA
Plate 2	A05	L-005798-00	J-005798-15	CXORF53	79184	NM_0010180	6476248	GCAUAUACUGGAACU
Plate 2	A06	L-019659-02	J-019659-17	POLG2	11232	NM_007215	7088778	CCGGAGCUGUUGACG
Plate 2	A06	L-019659-02	J-019659-18	POLG2	11232	NM_007215	7088778	GAACCUAGGAGAUCA
Plate 2	A06	L-019659-02	J-019659-19	POLG2	11232	NM_007215	7088778	GGCGUAGAGUUGCG
Plate 2	A06	L-019659-02	J-019659-20	POLG2	11232	NM_007215	7088778	GACACUAAGCAGAUA
Plate 2	A07	L-010790-00	J-010790-05	DCLRE1A	9937	NM_014881	4273431	GCAAGAGGUUAUCCG
Plate 2	A07	L-010790-00	J-010790-06	DCLRE1A	9937	NM_014881	4273431	GAUGAAGGAUUGUAU
Plate 2	A07	L-010790-00	J-010790-07	DCLRE1A	9937	NM_014881	4273431	GUAAUGAAGCAAAUG
Plate 2	A07	L-010790-00	J-010790-08	DCLRE1A	9937	NM_014881	4273431	GAAUUCAAGUUGUGG
Plate 2	A08	L-015465-00	J-015465-05	UVRAG	7405	NM_003369	2168721	CAUCUGGUCUCCAUG
Plate 2	A08	L-015465-00	J-015465-06	UVRAG	7405	NM_003369	2168721	GAGGUGGCAUUACUG
Plate 2	A08	L-015465-00	J-015465-07	UVRAG	7405	NM_003369	2168721	UGGAUGGGCUGAAAU
Plate 2	A08	L-015465-00	J-015465-08	UVRAG	7405	NM_003369	2168721	UCUACCAGCUGUUGA
Plate 2	A09	L-032280-00	J-032280-05	TREX2	11219	NM_080701	6307971	CCGGAAGGCUGGCUU
Plate 2	A09	L-032280-00	J-032280-06	TREX2	11219	NM_080701	6307971	CGACGAGUCUGGUGC
Plate 2	A09	L-032280-00	J-032280-07	TREX2	11219	NM_080701	6307971	ACAAUGGCUUUGAUU
Plate 2	A09	L-032280-00	J-032280-08	TREX2	11219	NM_080701	6307971	CCAUGUACUUGCCGC
Plate 2	A10	L-006301-00	J-006301-08	HTATIP	10524	NM_182709	3628705	CGUAAGAACAAGAGU
Plate 2	A10	L-006301-00	J-006301-09	HTATIP	10524	NM_182709	3628705	AUGAAUGGGUGACGC
Plate 2	A10	L-006301-00	J-006301-10	HTATIP	10524	NM_182709	3628705	GGACAGCUCUGAUGG
Plate 2	A10	L-006301-00	J-006301-11	HTATIP	10524	NM_182709	3628705	GACCAAGUGUGACCU
Plate 2	A11	L-013597-00	J-013597-05	RECQL	5965	NM_032941	1459190	GAGCUUAUGUUACCA
Plate 2	A11	L-013597-00	J-013597-06	RECQL	5965	NM_032941	1459190	CUACGGCUUUGGAGA
Plate 2	A11	L-013597-00	J-013597-07	RECQL	5965	NM_032941	1459190	GAUUAUAAGGCACUU
Plate 2	A11	L-013597-00	J-013597-08	RECQL	5965	NM_032941	1459190	GGGCAAGCAAUGAAU
Plate 2	B02	L-003256-00	J-003256-17	CHEK2	11200	NM_145862	5411240	GUAAGAAAGUAGCCA
Plate 2	B02	L-003256-00	J-003256-18	CHEK2	11200	NM_145862	5411240	GCAUAGGACUCAAGU
Plate 2	B02	L-003256-00	J-003256-19	CHEK2	11200	NM_145862	5411240	GUUGUGAACUCCGUG
Plate 2	B02	L-003256-00	J-003256-20	CHEK2	11200	NM_145862	5411240	CUCAGGAACUCUAUU
Plate 2	B03	L-005218-00	J-005218-09	NUDT1	4521	NM_002452	4028827	GGGCAAAGUGCAAGA
Plate 2	B03	L-005218-00	J-005218-10	NUDT1	4521	NM_002452	4028827	GGAGAGCGGUCUGAC
Plate 2	B03	L-005218-00	J-005218-11	NUDT1	4521	NM_002452	4028827	GAAAUUCCACGGGUA
Plate 2	B03	L-005218-00	J-005218-12	NUDT1	4521	NM_002452	4028827	UGUUUGAGUUCGUG
Plate 2	B04	L-011554-00	J-011554-06	MBD4	8930	NM_003925	4505120	GAAGAUUUGAUGUGU
Plate 2	B04	L-011554-00	J-011554-07	MBD4	8930	NM_003925	4505120	GGAACAGAAUGCCGU
Plate 2	B04	L-011554-00	J-011554-08	MBD4	8930	NM_003925	4505120	GAAGAUACCAUCCCA
Plate 2	B04	L-011554-00	J-011554-09	MBD4	8930	NM_003925	4505120	UAACUUUACUUCCAC
Plate 2	B05	L-007152-00	J-007152-05	RNF168	2E+05	NM_152617	3137756	GACACUUUCUCCACA
Plate 2	B05	L-007152-00	J-007152-06	RNF168	2E+05	NM_152617	3137756	CAAAGUAAGGCCUGG
Plate 2	B05	L-007152-00	J-007152-07	RNF168	2E+05	NM_152617	3137756	AGAAGAACAGGACAG
Plate 2	B05	L-007152-00	J-007152-08	RNF168	2E+05	NM_152617	3137756	GAAAUUCUCUCGUCA
Plate 2	B06	L-004668-00	J-004668-05	PRPF19	27339	NM_014502	3422231	GAUAACAACUUUGAG
Plate 2	B06	L-004668-00	J-004668-06	PRPF19	27339	NM_014502	3422231	GCACGGAUGUCCAGA
Plate 2	B06	L-004668-00	J-004668-07	PRPF19	27339	NM_014502	3422231	GUACUAAUGUGGCCA
Plate 2	B06	L-004668-00	J-004668-08	PRPF19	27339	NM_014502	3422231	GAUCUGCGCAAGCUU
Plate 2	B07	L-003008-00	J-003008-11	FRAP1	2475	NM_004958	1992429	GGCCAUAGCUAGCCU
Plate 2	B07	L-003008-00	J-003008-12	FRAP1	2475	NM_004958	1992429	CAAAGGACUUCGCCC
Plate 2	B07	L-003008-00	J-003008-13	FRAP1	2475	NM_004958	1992429	GCAGAAUUGUCAAGG
Plate 2	B07	L-003008-00	J-003008-14	FRAP1	2475	NM_004958	1992429	CCAAAGCACUACACU
Plate 2	B08	L-011759-00	J-011759-05	RAD23B	5887	NM_002874	5117373	GCAGAUAGGUCGAGA
Plate 2	B08	L-011759-00	J-011759-06	RAD23B	5887	NM_002874	5117373	GAACGAGAGCAAGUA
Plate 2	B08	L-011759-00	J-011759-07	RAD23B	5887	NM_002874	5117373	GAAGUGGUCAUAUGA
Plate 2	B08	L-011759-00	J-011759-08	RAD23B	5887	NM_002874	5117373	CAACAACCCUGACAG
Plate 2	B09	L-012013-00	J-012013-05	MJD	4287	NM_030660	6693288	ACAGGAAGGUUAUUC
Plate 2	B09	L-012013-00	J-012013-06	MJD	4287	NM_030660	6693288	GGACAGAGUUCACAU
Plate 2	B09	L-012013-00	J-012013-07	MJD	4287	NM_030660	6693288	GCACUAAGUCGCCAA
Plate 2	B09	L-012013-00	J-012013-08	MJD	4287	NM_030660	6693288	GCAGGGCUAUUCAGC
Plate 2	B10	L-004269-00	J-004269-09	DCLRE1C	64421	NM_022487	7649649	GUACGGAGCCAAAGU
Plate 2	B10	L-004269-00	J-004269-10	DCLRE1C	64421	NM_022487	7649649	GCACAACUAUGGAUA
Plate 2	B10	L-004269-00	J-004269-11	DCLRE1C	64421	NM_022487	7649649	UGAAUAAGCUAGACA
Plate 2	B10	L-004269-00	J-004269-12	DCLRE1C	64421	NM_022487	7649649	CACCAAAGCUUUUCA
Plate 2	B11	L-016941-00	J-016941-05	FANCB	2187	NM_152633	6652868	GAAAGAGUGUGUACA
Plate 2	B11	L-016941-00	J-016941-06	FANCB	2187	NM_152633	6652868	ACAAACAAGAGAAUC
Plate 2	B11	L-016941-00	J-016941-07	FANCB	2187	NM_152633	6652868	GGACUAAAGGAAUGU
Plate 2	B11	L-016941-00	J-016941-08	FANCB	2187	NM_152633	6652868	GGUCCUUAAUGGCCC

Plate 2	C02	L-011822-00	J-011822-05	CETN2	1069	NM_004344	4757901	GUGAGAACCUGACUG
Plate 2	C02	L-011822-00	J-011822-06	CETN2	1069	NM_004344	4757901	GAUGAAACUGGGAAG
Plate 2	C02	L-011822-00	J-011822-07	CETN2	1069	NM_004344	4757901	GCAUCAAGUUCUCAG
Plate 2	C02	L-011822-00	J-011822-08	CETN2	1069	NM_004344	4757901	CAAGAGUUCCUGCGC
Plate 2	C03	L-015098-02	J-015098-17	KUB3	91419	NM_033276	5479278	CAGACUUGUGUGCGA
Plate 2	C03	L-015098-02	J-015098-18	KUB3	91419	NM_033276	5479278	GCCAGAAUAAUAUCC
Plate 2	C03	L-015098-02	J-015098-19	KUB3	91419	NM_033276	5479278	ACAAGACUUAUGCAA
Plate 2	C03	L-015098-02	J-015098-20	KUB3	91419	NM_033276	5479278	UGAUCAUUGUCGUGC
Plate 2	C04	L-003331-00	J-003331-09	TP73	7161	NM_005427	4885644	GAGACGAGGACACGU
Plate 2	C04	L-003331-00	J-003331-10	TP73	7161	NM_005427	4885644	GCAAUAAUCUCUCGC
Plate 2	C04	L-003331-00	J-003331-11	TP73	7161	NM_005427	4885644	GAACUUUGAGAUCCU
Plate 2	C04	L-003331-00	J-003331-12	TP73	7161	NM_005427	4885644	CCACCAUCCUGUACA
Plate 2	C05	L-005147-00	J-005147-09	OGG1	4968	NM_016827	8670537	CGACAAGACCCCAUC
Plate 2	C05	L-005147-00	J-005147-10	OGG1	4968	NM_016827	8670537	GGACAAUCUUUCCGG
Plate 2	C05	L-005147-00	J-005147-11	OGG1	4968	NM_016827	8670537	GCUCAGAAAUUCCAA
Plate 2	C05	L-005147-00	J-005147-12	OGG1	4968	NM_016827	8670537	UACCCUGGCUCAACU
Plate 2	C06	L-009227-00	J-009227-06	LIG3	3980	NM_002311	7374784	GGACUUGGCUGACAU
Plate 2	C06	L-009227-00	J-009227-07	LIG3	3980	NM_002311	7374784	GACAUUGCCUCCAGG
Plate 2	C06	L-009227-00	J-009227-08	LIG3	3980	NM_002311	7374784	CAGAAGUGGUGCACA
Plate 2	C06	L-009227-00	J-009227-09	LIG3	3980	NM_002311	7374784	GAAGGGCGUAUGCCG
Plate 2	C07	L-011082-00	J-011082-05	MEN1	4221	NM_130801	1886085	CGCAAAGGCCUCUGA
Plate 2	C07	L-011082-00	J-011082-06	MEN1	4221	NM_130801	1886085	GAUCAUACAUGCGCU
Plate 2	C07	L-011082-00	J-011082-07	MEN1	4221	NM_130801	1886085	GAUCAUGCCUGGGUA
Plate 2	C07	L-011082-00	J-011082-08	MEN1	4221	NM_130801	1886085	GAACACAUCUACCCC
Plate 2	C08	L-003906-00	J-003906-09	MLH1	4292	NM_000249	2855908	GGAAGUUGUUGGCAG
Plate 2	C08	L-003906-00	J-003906-10	MLH1	4292	NM_000249	2855908	CCAGAUGGUUCGUAC
Plate 2	C08	L-003906-00	J-003906-11	MLH1	4292	NM_000249	2855908	GAAGUAGUGAUAAGG
Plate 2	C08	L-003906-00	J-003906-12	MLH1	4292	NM_000249	2855908	UAUCUUCAUUCUUCG
Plate 2	C09	L-009271-00	J-009271-05	MRE11A	4361	NM_005591	5655010	GGAGGUACGUCGUUU
Plate 2	C09	L-009271-00	J-009271-06	MRE11A	4361	NM_005591	5655010	GGAAAUGAUACGUUU
Plate 2	C09	L-009271-00	J-009271-07	MRE11A	4361	NM_005591	5655010	CGAAAUGUCACUACU
Plate 2	C09	L-009271-00	J-009271-08	MRE11A	4361	NM_005591	5655010	GAAAGGCUCUAUCGA
Plate 2	C10	L-010575-00	J-010575-05	RRM2B	50484	NM_015713	4254413	ACUCAGAGAUGUACA
Plate 2	C10	L-010575-00	J-010575-06	RRM2B	50484	NM_015713	4254413	CAGAAGAGGUCGACU
Plate 2	C10	L-010575-00	J-010575-07	RRM2B	50484	NM_015713	4254413	GCUAUAUUCUGGCUA
Plate 2	C10	L-010575-00	J-010575-08	RRM2B	50484	NM_015713	4254413	GAACUUGGAUUCUCA
Plate 2	C11	L-018757-01	J-018757-09	FLJ40869	3E+05	NM_182625	4727149	UAUGCAAACCACUCG
Plate 2	C11	L-018757-01	J-018757-10	FLJ40869	3E+05	NM_182625	4727149	GCGUAAUCUUGGUGG
Plate 2	C11	L-018757-01	J-018757-11	FLJ40869	3E+05	NM_182625	4727149	GCCCUAAGAUACAUA
Plate 2	C11	L-018757-01	J-018757-12	FLJ40869	3E+05	NM_182625	4727149	UCUAAGACCUUUGGC
Plate 2	D02	L-015780-00	J-015780-05	DCLRE1B	64858	NM_022836	2443199	GAUCCAUACUUUAUA
Plate 2	D02	L-015780-00	J-015780-06	DCLRE1B	64858	NM_022836	2443199	GCACGUCUCUUCUUC
Plate 2	D02	L-015780-00	J-015780-07	DCLRE1B	64858	NM_022836	2443199	UCAGUGCACUUAAGG
Plate 2	D02	L-015780-00	J-015780-08	DCLRE1B	64858	NM_022836	2443199	ACUCUGACCAUUCCU
Plate 2	D03	L-011028-00	J-011028-05	ERCC3	2071	NM_000122	4557562	GAUCAAGGUUAUAGC
Plate 2	D03	L-011028-00	J-011028-06	ERCC3	2071	NM_000122	4557562	CGAGAAUGCCGCUUA
Plate 2	D03	L-011028-00	J-011028-07	ERCC3	2071	NM_000122	4557562	CCCUAUGUCUCCUGA
Plate 2	D03	L-011028-00	J-011028-08	ERCC3	2071	NM_000122	4557562	CCGCGAAGAUGACAA
Plate 2	D04	L-034933-01	J-034933-05	GIYD1	5E+05	NM_0010150	6286820	GCUAAGGGCCCAUGU
Plate 2	D04	L-034933-01	J-034933-06	GIYD1	5E+05	NM_0010150	6286820	CAGAAUUAGAAGAGG
Plate 2	D04	L-034933-01	J-034933-07	GIYD1	5E+05	NM_0010150	6286820	GGACACUGAGAAAGA
Plate 2	D04	L-034933-01	J-034933-08	GIYD1	5E+05	NM_0010150	6286820	GCUGGAGACCUGAUC
Plate 2	D05	L-012806-00	J-012806-06	MUTYH	4595	NM_012222	6912519	CGGAAGAGGUGGUAU
Plate 2	D05	L-012806-00	J-012806-07	MUTYH	4595	NM_012222	6912519	UAUAUGGGCUGGCCU
Plate 2	D05	L-012806-00	J-012806-08	MUTYH	4595	NM_012222	6912519	CAUACCAUCUAUUCA
Plate 2	D05	L-012806-00	J-012806-09	MUTYH	4595	NM_012222	6912519	CCGGAUGGAUGCAGA
Plate 2	D06	L-016112-00	J-016112-05	TDP1	55775	NM_0010087	5724280	GGAGUUAAGCCAAAG
Plate 2	D06	L-016112-00	J-016112-06	TDP1	55775	NM_0010087	5724280	UCAGUUACUUGAUGG
Plate 2	D06	L-016112-00	J-016112-07	TDP1	55775	NM_0010087	5724280	GACCAUAUCUAGUAG
Plate 2	D06	L-016112-00	J-016112-08	TDP1	55775	NM_0010087	5724280	CUAGACAGUUUCAAA
Plate 2	D07	L-006454-00	J-006454-09	POLH	5429	NM_006502	5729981	GUCCAACUGUAAAGC
Plate 2	D07	L-006454-00	J-006454-10	POLH	5429	NM_006502	5729981	GAUUGAACGUGCCAG
Plate 2	D07	L-006454-00	J-006454-11	POLH	5429	NM_006502	5729981	GCCAAGCACUUACAU
Plate 2	D07	L-006454-00	J-006454-12	POLH	5429	NM_006502	5729981	GCCGAGGGAUUGAAC
Plate 2	D08	L-003895-00	J-003895-05	GADD45G	10912	NM_006705	9790905	GAGGAGAGCCGCAGC
Plate 2	D08	L-003895-00	J-003895-06	GADD45G	10912	NM_006705	9790905	GAACGACAUCGACAU
Plate 2	D08	L-003895-00	J-003895-07	GADD45G	10912	NM_006705	9790905	CGAGUCAGCCAAAGU
Plate 2	D08	L-003895-00	J-003895-08	GADD45G	10912	NM_006705	9790905	GGAAAGCGCUGCAUG
Plate 2	D09	L-011653-00	J-011653-05	EYA3	2140	NM_172098	2666724	GAUCCUAUGCCCAGA
Plate 2	D09	L-011653-00	J-011653-06	EYA3	2140	NM_172098	2666724	GAGAGCAAACUAUAA
Plate 2	D09	L-011653-00	J-011653-07	EYA3	2140	NM_172098	2666724	GUUCUUACCUGCACU
Plate 2	D09	L-011653-00	J-011653-08	EYA3	2140	NM_172098	2666724	UAUCCCACCUAUACU
Plate 2	D10	L-005067-00	J-005067-05	XPA	7507	NM_000380	3154396	CGUAAGACUUGUACU
Plate 2	D10	L-005067-00	J-005067-06	XPA	7507	NM_000380	3154396	GGAGACGAUUGUUCA
Plate 2	D10	L-005067-00	J-005067-07	XPA	7507	NM_000380	3154396	GAGCCACCUCUUAAA
Plate 2	D10	L-005067-00	J-005067-08	XPA	7507	NM_000380	3154396	GGAGGCAUGGCUAAU
Plate 2	D11	L-005231-00	J-005231-05	RAD23A	5886	NM_005053	1992413	GCUCUGAGUAUGAGA
Plate 2	D11	L-005231-00	J-005231-06	RAD23A	5886	NM_005053	1992413	GAAGAUAGAAGCUGA
Plate 2	D11	L-005231-00	J-005231-07	RAD23A	5886	NM_005053	1992413	GAUCUUGAGUGACGA
Plate 2	D11	L-005231-00	J-005231-08	RAD23A	5886	NM_005053	1992413	GAAGAACUUUGUGGU

Plate 2	E02	L-021038-00	J-021038-05	POLK	51426	NM_016218	7705343	GGAUGGGACUUAAUG
Plate 2	E02	L-021038-00	J-021038-06	POLK	51426	NM_016218	7705343	GAAGAGCAAUACAGC
Plate 2	E02	L-021038-00	J-021038-07	POLK	51426	NM_016218	7705343	CUACCAAAGUUAACA
Plate 2	E02	L-021038-00	J-021038-08	POLK	51426	NM_016218	7705343	CCAAGCAAGUCUUUU
Plate 2	E03	L-021353-00	J-021353-05	SHFM1	7979	NM_006304	5453639	GUUAUAAGAUGGAGA
Plate 2	E03	L-021353-00	J-021353-06	SHFM1	7979	NM_006304	5453639	AGACUGGGCUGGCUU
Plate 2	E03	L-021353-00	J-021353-07	SHFM1	7979	NM_006304	5453639	GUUACGAGCUGAACU
Plate 2	E03	L-021353-00	J-021353-08	SHFM1	7979	NM_006304	5453639	CAAUGUAGAGGAUGA
Plate 2	E04	L-020939-01	J-020939-09	NEIL3	55247	NM_018248	8922721	GCUAAUGGAUCAGAA
Plate 2	E04	L-020939-01	J-020939-10	NEIL3	55247	NM_018248	8922721	UAAUGAAGUACCCGU
Plate 2	E04	L-020939-01	J-020939-11	NEIL3	55247	NM_018248	8922721	CUAUGUAUUUCAUCG
Plate 2	E04	L-020939-01	J-020939-12	NEIL3	55247	NM_018248	8922721	AGAAGACAACAAACG
Plate 2	E05	L-009424-00	J-009424-05	UBE2A	7319	NM_181762	3296727	CUAUGCAGAUGGUAG
Plate 2	E05	L-009424-00	J-009424-06	UBE2A	7319	NM_181762	3296727	GCGUGUUUCUGCAAU
Plate 2	E05	L-009424-00	J-009424-07	UBE2A	7319	NM_181762	3296727	GGACAUACUUCAGAA
Plate 2	E05	L-009424-00	J-009424-08	UBE2A	7319	NM_181762	3296727	GAACAAACGGGAAUA
Plate 2	E06	L-007773-00	J-007773-05	HRMT1L6	55170	NM_018137	8922514	GAGCAAGACACGGAC
Plate 2	E06	L-007773-00	J-007773-06	HRMT1L6	55170	NM_018137	8922514	GCACCGGCAUUCUGA
Plate 2	E06	L-007773-00	J-007773-07	HRMT1L6	55170	NM_018137	8922514	GGAGAUCGUUGUGCA
Plate 2	E06	L-007773-00	J-007773-08	HRMT1L6	55170	NM_018137	8922514	GCAAGACGGUACUGG
Plate 2	E07	L-006900-00	J-006900-05	RNF8	9025	NM_183078	3430433	AGAAUGAGCUCCAAU
Plate 2	E07	L-006900-00	J-006900-06	RNF8	9025	NM_183078	3430433	GAGAUGGUCUGGAG
Plate 2	E07	L-006900-00	J-006900-07	RNF8	9025	NM_183078	3430433	CAACAAGAGUCUAAA
Plate 2	E07	L-006900-00	J-006900-08	RNF8	9025	NM_183078	3430433	GAGCGCGUCUGGAAC
Plate 2	E08	L-003329-00	J-003329-14	TP53	7157	NM_000546	8400737	GAAAUUUGCGUGUGG
Plate 2	E08	L-003329-00	J-003329-15	TP53	7157	NM_000546	8400737	GUGCAGCUGUGGGU
Plate 2	E08	L-003329-00	J-003329-16	TP53	7157	NM_000546	8400737	GCAGUCAGAUCCUAG
Plate 2	E08	L-003329-00	J-003329-17	TP53	7157	NM_000546	8400737	GGAGAAUAUUUCACC
Plate 2	E09	L-017058-01	J-017058-09	RPA2	6118	NM_002946	3414762	AACAUGAAGUUCUGC
Plate 2	E09	L-017058-01	J-017058-10	RPA2	6118	NM_002946	3414762	UGGAACAGUGGAUUC
Plate 2	E09	L-017058-01	J-017058-11	RPA2	6118	NM_002946	3414762	GAGCAGGACCAGGGC
Plate 2	E09	L-017058-01	J-017058-12	RPA2	6118	NM_002946	3414762	GGAAGUAGGUUUCAU
Plate 2	E10	L-017823-01	J-017823-09	MMS19L	64210	NM_022362	3154320	GCACAAUCCAGUGAC
Plate 2	E10	L-017823-01	J-017823-10	MMS19L	64210	NM_022362	3154320	AGAAGAGACUGGUGC
Plate 2	E10	L-017823-01	J-017823-11	MMS19L	64210	NM_022362	3154320	AAAUUUGACUAACGG
Plate 2	E10	L-017823-01	J-017823-12	MMS19L	64210	NM_022362	3154320	CGUACAAACCACAGG
Plate 2	E11	L-014288-01	J-014288-09	MGC2731	79035	NM_024068	3414735	CCACCCAGCACCCGA
Plate 2	E11	L-014288-01	J-014288-10	MGC2731	79035	NM_024068	3414735	CAAGACAAAGGACGG
Plate 2	E11	L-014288-01	J-014288-11	MGC2731	79035	NM_024068	3414735	AGGUUGAGGUGAGCC
Plate 2	E11	L-014288-01	J-014288-12	MGC2731	79035	NM_024068	3414735	CCAGCAACCCUGUUA
Plate 2	F02	L-021393-01	J-021393-09	POLN	4E+05	NM_181808	3269879	UGUUAAAUGCUCUGC
Plate 2	F02	L-021393-01	J-021393-10	POLN	4E+05	NM_181808	3269879	GGGCACAAGCAGAGC
Plate 2	F02	L-021393-01	J-021393-11	POLN	4E+05	NM_181808	3269879	GCAAUAACCAGCUUC
Plate 2	F02	L-021393-01	J-021393-12	POLN	4E+05	NM_181808	3269879	GGAUUAUGGUUUAUG
Plate 2	F03	L-013942-00	J-013942-05	MIZF	25988	NM_198971	3972594	CGACAAUCCUGAGUG
Plate 2	F03	L-013942-00	J-013942-06	MIZF	25988	NM_198971	3972594	CAAGUCCCAUUACCG
Plate 2	F03	L-013942-00	J-013942-07	MIZF	25988	NM_198971	3972594	GCAGGGCAUUAUUCU
Plate 2	F03	L-013942-00	J-013942-08	MIZF	25988	NM_198971	3972594	GAACGUCGCUGAACG
Plate 2	F04	L-019287-00	J-019287-05	MSH6	2956	NM_000179	4504190	CGAAGUAGCCGCCAA
Plate 2	F04	L-019287-00	J-019287-06	MSH6	2956	NM_000179	4504190	CCACAUGGAUGCUCU
Plate 2	F04	L-019287-00	J-019287-07	MSH6	2956	NM_000179	4504190	GCAGAAGGGCUAUAA
Plate 2	F04	L-019287-00	J-019287-08	MSH6	2956	NM_000179	4504190	GGGCCAAGAUGGAGG
Plate 2	F05	L-013991-00	J-013991-05	FANCE	2178	NM_021922	6687966	CCAAGUAUCAGGCUA
Plate 2	F05	L-013991-00	J-013991-06	FANCE	2178	NM_021922	6687966	GCCCAAAGCUAUCCA
Plate 2	F05	L-013991-00	J-013991-07	FANCE	2178	NM_021922	6687966	GAAUCUGGAUGAUGC
Plate 2	F05	L-013991-00	J-013991-08	FANCE	2178	NM_021922	6687966	CAACUGCCCUGACCU
Plate 2	F06	L-032783-01	J-032783-05	EME2	2E+05	NM_0010108	5819755	AGGCAGUUCAGUCGG
Plate 2	F06	L-032783-01	J-032783-06	EME2	2E+05	NM_0010108	5819755	GGGCAAACCUGGACG
Plate 2	F06	L-032783-01	J-032783-07	EME2	2E+05	NM_0010108	5819755	UCAAGGCAGUACCGG
Plate 2	F06	L-032783-01	J-032783-08	EME2	2E+05	NM_0010108	5819755	CUGCAGGUGAACAGG
Plate 2	F07	L-018493-02	J-018493-17	C2ORF13	2E+05	NM_173545	2773490	GCACAAGAUAGAAUA
Plate 2	F07	L-018493-02	J-018493-18	C2ORF13	2E+05	NM_173545	2773490	CUUCAUAUUACGUGA
Plate 2	F07	L-018493-02	J-018493-19	C2ORF13	2E+05	NM_173545	2773490	AGCAAUCAGUGGAGG
Plate 2	F07	L-018493-02	J-018493-20	C2ORF13	2E+05	NM_173545	2773490	UGAUUAUGGAGGUGU
Plate 2	F08	L-003548-00	J-003548-06	TP53BP1	7158	NM_005657	5032188	GAAGGACGGAGUACU
Plate 2	F08	L-003548-00	J-003548-07	TP53BP1	7158	NM_005657	5032188	GCUAUAUCCUUGAAG
Plate 2	F08	L-003548-00	J-003548-08	TP53BP1	7158	NM_005657	5032188	GAGCUGGGAAGUAUA
Plate 2	F08	L-003548-00	J-003548-09	TP53BP1	7158	NM_005657	5032188	GGACUCCAGUGUUGU
Plate 2	F09	L-003281-00	J-003281-17	MNAT1	4331	NM_002431	4957451	UAGAUGAGCUGGAGA
Plate 2	F09	L-003281-00	J-003281-18	MNAT1	4331	NM_002431	4957451	GUAUUUAAACCAUGU
Plate 2	F09	L-003281-00	J-003281-19	MNAT1	4331	NM_002431	4957451	CAGCCCAGUUAACCA
Plate 2	F09	L-003281-00	J-003281-20	MNAT1	4331	NM_002431	4957451	GGCUAUACUUCUUCU
Plate 2	F10	L-017846-00	J-017846-05	PMS2L5	5383	NM_174930	3134138	GGACAACGUGAUCAC
Plate 2	F10	L-017846-00	J-017846-06	PMS2L5	5383	NM_174930	3134138	UGUCAAGAAUGGUCC
Plate 2	F10	L-017846-00	J-017846-07	PMS2L5	5383	NM_174930	3134138	GCAAAACUGACUCCU
Plate 2	F10	L-017846-00	J-017846-08	PMS2L5	5383	NM_174930	3134138	GCCAUUAGCAUUGGA
Plate 2	F11	L-018408-01	J-018408-09	SMC6L1	79677	NM_024624	5269467	AGAAAUAGAUAAUGC
Plate 2	F11	L-018408-01	J-018408-10	SMC6L1	79677	NM_024624	5269467	GGACAAAGAAAUUAA
Plate 2	F11	L-018408-01	J-018408-11	SMC6L1	79677	NM_024624	5269467	CAGCAUAGAUGGAAG
Plate 2	F11	L-018408-01	J-018408-12	SMC6L1	79677	NM_024624	5269467	CUUUAAAGCCAGUGU

Plate 2	G02	L-003218-00	J-003218-09	CCNH	902	NM_001239	1773831	GGGUACGGCUUGUAU
Plate 2	G02	L-003218-00	J-003218-10	CCNH	902	NM_001239	1773831	GAGCUUGCACUUAAC
Plate 2	G02	L-003218-00	J-003218-11	CCNH	902	NM_001239	1773831	GCAAAGUAGAUGAAU
Plate 2	G02	L-003218-00	J-003218-12	CCNH	902	NM_001239	1773831	GACCCGCUAUCCCAU
Plate 2	G03	L-011376-00	J-011376-05	RBBP8	5932	NM_203292	4271801	GGAGCUACCUCUAGU
Plate 2	G03	L-011376-00	J-011376-06	RBBP8	5932	NM_203292	4271801	GAGGUUAUAUUAAGG
Plate 2	G03	L-011376-00	J-011376-07	RBBP8	5932	NM_203292	4271801	GAACAGAAUAGGACU
Plate 2	G03	L-011376-00	J-011376-08	RBBP8	5932	NM_203292	4271801	GCACGUUGCCCAAAG
Plate 2	G04	L-004361-00	J-004361-05	XRCC2	7516	NM_005431	4885656	GAGCACAGACUAUCC
Plate 2	G04	L-004361-00	J-004361-06	XRCC2	7516	NM_005431	4885656	ACACUUUACUCACUA
Plate 2	G04	L-004361-00	J-004361-07	XRCC2	7516	NM_005431	4885656	CCUAACAGCACGAUG
Plate 2	G04	L-004361-00	J-004361-08	XRCC2	7516	NM_005431	4885656	GAAAUGUUCUCAGUG
Plate 2	G05	L-019338-00	J-019338-05	RECQL5	9400	NM_0010037	5124294	GAACGCUGGUGCAGA
Plate 2	G05	L-019338-00	J-019338-06	RECQL5	9400	NM_0010037	5124294	GGACUAGAGAGGCUU
Plate 2	G05	L-019338-00	J-019338-07	RECQL5	9400	NM_0010037	5124294	CCUGGUGCCGUCUCU
Plate 2	G05	L-019338-00	J-019338-08	RECQL5	9400	NM_0010037	5124294	CUUGCUAACCCUAAA
Plate 2	G06	L-008327-00	J-008327-06	NEIL1	79661	NM_024608	1337581	UACGAAACCUAGCGG
Plate 2	G06	L-008327-00	J-008327-07	NEIL1	79661	NM_024608	1337581	GACCAGAGGUUCUUC
Plate 2	G06	L-008327-00	J-008327-08	NEIL1	79661	NM_024608	1337581	UGACAUCCCAUCCUU
Plate 2	G06	L-008327-00	J-008327-09	NEIL1	79661	NM_024608	1337581	GGACCAAGCUGCAGA
Plate 2	G07	L-014446-01	J-014446-09	FLJ12610	79840	NM_024782	1337614	GGGCUACGCUGAUUC
Plate 2	G07	L-014446-01	J-014446-10	FLJ12610	79840	NM_024782	1337614	GAGGGAGCUAGCAAC
Plate 2	G07	L-014446-01	J-014446-11	FLJ12610	79840	NM_024782	1337614	CCUUCAGAUUCUUCG
Plate 2	G07	L-014446-01	J-014446-12	FLJ12610	79840	NM_024782	1337614	AGAAAGAGUCCACGG
Plate 2	G08	L-004494-00	J-004494-07	XRCC4	7518	NM_003401	1240864	UGACCGAGAUCCAGU
Plate 2	G08	L-004494-00	J-004494-08	XRCC4	7518	NM_003401	1240864	GAACCCAGUAUAACU
Plate 2	G08	L-004494-00	J-004494-09	XRCC4	7518	NM_003401	1240864	CAGCUGAUGUAUACA
Plate 2	G08	L-004494-00	J-004494-10	XRCC4	7518	NM_003401	1240864	CCUCUUUGAUGAGAU
Plate 2	G09	L-016846-00	J-016846-05	DLG7	9787	NM_014750	2136164	AGACUAAGAUUGAUA
Plate 2	G09	L-016846-00	J-016846-06	DLG7	9787	NM_014750	2136164	GUACAGAUCUGGAUG
Plate 2	G09	L-016846-00	J-016846-07	DLG7	9787	NM_014750	2136164	GGUCUAAACUGCAGU
Plate 2	G09	L-016846-00	J-016846-08	DLG7	9787	NM_014750	2136164	UAAAGUGGGUCGUUA
Plate 2	G10	L-013120-00	J-013120-05	EXO1	9156	NM_003686	3999506	GCACGUAAUUCAAGU
Plate 2	G10	L-013120-00	J-013120-06	EXO1	9156	NM_003686	3999506	GUAAAUGGACCUACU
Plate 2	G10	L-013120-00	J-013120-07	EXO1	9156	NM_003686	3999506	CCACCUAGGACGAGA
Plate 2	G10	L-013120-00	J-013120-08	EXO1	9156	NM_003686	3999506	CGGAAGAGAAGUUUC
Plate 2	G11	L-003100-00	J-003100-09	ABL1	25	NM_005157	6236241	UCACUGAGUUCAUGA
Plate 2	G11	L-003100-00	J-003100-10	ABL1	25	NM_005157	6236241	AGAUAACACUCUAAG
Plate 2	G11	L-003100-00	J-003100-11	ABL1	25	NM_005157	6236241	AAGGGAGGGUGUACC
Plate 2	G11	L-003100-00	J-003100-12	ABL1	25	NM_005157	6236241	CAACAAGCCCACUGU
Plate 2	H02	L-016379-02	J-016379-17	C7ORF11	1E+05	NM_138701	1885957	GAUCAGGGCGUGUUA
Plate 2	H02	L-016379-02	J-016379-18	C7ORF11	1E+05	NM_138701	1885957	UGUAGUGGAUAUAAG
Plate 2	H02	L-016379-02	J-016379-19	C7ORF11	1E+05	NM_138701	1885957	GAUUUACCGUUUCCA
Plate 2	H02	L-016379-02	J-016379-20	C7ORF11	1E+05	NM_138701	1885957	GGAGGUUGGGGUAG
Plate 2	H03	L-018981-00	J-018981-05	HMGB1	3146	NM_002128	3198287	CAAACUCAUUCAUUA
Plate 2	H03	L-018981-00	J-018981-06	HMGB1	3146	NM_002128	3198287	CAAAGCAUGGGAUUA
Plate 2	H03	L-018981-00	J-018981-07	HMGB1	3146	NM_002128	3198287	CCACUUACAUUUACA
Plate 2	H03	L-018981-00	J-018981-08	HMGB1	3146	NM_002128	3198287	CGAAAUAAUUGUUGU
Plate 2	H04	L-010572-00	J-010572-05	RAD54B	25788	NM_134434	2014392	GUUUAAAUCUGCCUA
Plate 2	H04	L-010572-00	J-010572-06	RAD54B	25788	NM_134434	2014392	CACCUACACUGGCAA
Plate 2	H04	L-010572-00	J-010572-07	RAD54B	25788	NM_134434	2014392	UCAUUCGGCUCCUAA
Plate 2	H04	L-010572-00	J-010572-08	RAD54B	25788	NM_134434	2014392	AGAUUGAGCUUUAUC
Plate 2	H05	L-004888-00	J-004888-07	ERCC6	2074	NM_000124	4557564	GCAGUAACUUCUAAU
Plate 2	H05	L-004888-00	J-004888-08	ERCC6	2074	NM_000124	4557564	GAAGCAAGGUUGUAA
Plate 2	H05	L-004888-00	J-004888-09	ERCC6	2074	NM_000124	4557564	GCAUGUGUCUUACGA
Plate 2	H05	L-004888-00	J-004888-10	ERCC6	2074	NM_000124	4557564	CAAACAGAGUUGUCA
Plate 2	H06	L-011076-00	J-011076-05	LIG1	3978	NM_000234	4557718	GCAGCGAAGUAUCAU
Plate 2	H06	L-011076-00	J-011076-06	LIG1	3978	NM_000234	4557718	GAACAACUAUCAUCC
Plate 2	H06	L-011076-00	J-011076-07	LIG1	3978	NM_000234	4557718	GAAGCCCGGUUCAUC
Plate 2	H06	L-011076-00	J-011076-08	LIG1	3978	NM_000234	4557718	CGUCUGAGAUCCAGG
Plate 2	H07	L-003322-00	J-003322-09	RPA3	6119	NM_002947	5285143	CAUCUUAUGUCCAGU
Plate 2	H07	L-003322-00	J-003322-10	RPA3	6119	NM_002947	5285143	GCAACAUGAUUGAUC
Plate 2	H07	L-003322-00	J-003322-11	RPA3	6119	NM_002947	5285143	GAAGAUAGCCAUCCU
Plate 2	H07	L-003322-00	J-003322-12	RPA3	6119	NM_002947	5285143	UUACAAUGAAGCUGU
Plate 2	H08	L-019938-00	J-019938-07	CHAF1A	10036	NM_005483	5051324	CCACAGCCAUGGAUU
Plate 2	H08	L-019938-00	J-019938-08	CHAF1A	10036	NM_005483	5051324	GGGCAAGCAGCUCAA
Plate 2	H08	L-019938-00	J-019938-09	CHAF1A	10036	NM_005483	5051324	GACAUAGACUUUAGA
Plate 2	H08	L-019938-00	J-019938-10	CHAF1A	10036	NM_005483	5051324	AAACAACUGUCAUGU
Plate 2	H09	L-020043-00	J-020043-05	SPO11	23626	NM_198265	3820167	GCACCAAAGUGAAUU
Plate 2	H09	L-020043-00	J-020043-06	SPO11	23626	NM_198265	3820167	ACAGUCAACUCUUUG
Plate 2	H09	L-020043-00	J-020043-07	SPO11	23626	NM_198265	3820167	CCAAAAGGGACAUAU
Plate 2	H09	L-020043-00	J-020043-08	SPO11	23626	NM_198265	3820167	CUGAGGAGACCUUAU
Plate 2	H10	L-004605-00	J-004605-06	DNMT1	1786	NM_001379	4503350	GCACCUCAUUUGCCG
Plate 2	H10	L-004605-00	J-004605-07	DNMT1	1786	NM_001379	4503350	AUAAAUGAAUGGUGG
Plate 2	H10	L-004605-00	J-004605-08	DNMT1	1786	NM_001379	4503350	CCUGAGCCCUACCGA
Plate 2	H10	L-004605-00	J-004605-09	DNMT1	1786	NM_001379	4503350	GGACGACCCUGACCU
Plate 2	H11	L-006061-00	J-006061-07	USP1	7398	NM_0010174	6305352	GCACAAAGCCAACUA
Plate 2	H11	L-006061-00	J-006061-08	USP1	7398	NM_0010174	6305352	CAAAGCAGAUUAUGA
Plate 2	H11	L-006061-00	J-006061-09	USP1	7398	NM_0010174	6305352	CAUAGUGGCAUUACA
Plate 2	H11	L-006061-00	J-006061-10	USP1	7398	NM_0010174	6305352	GUUUGGAGUUUGAUU

Plate 3	A02	L-017392-00	J-017392-05	EYA1	2138	NM_172059	2666721	GCAACAAGCUACAGC
Plate 3	A02	L-017392-00	J-017392-06	EYA1	2138	NM_172059	2666721	CGACGGGUCUUUAAA
Plate 3	A02	L-017392-00	J-017392-07	EYA1	2138	NM_172059	2666721	CGGACAAACUGUGUG
Plate 3	A02	L-017392-00	J-017392-08	EYA1	2138	NM_172059	2666721	GGUCCUACGCCAACA
Plate 3	A03	L-010559-00	J-010559-05	RECQL4	9401	NM_004260	4759029	CCUAGAUCCUGGCUG
Plate 3	A03	L-010559-00	J-010559-06	RECQL4	9401	NM_004260	4759029	GCGACCACCUAUACC
Plate 3	A03	L-010559-00	J-010559-07	RECQL4	9401	NM_004260	4759029	GAAAAUACCUGCACC
Plate 3	A03	L-010559-00	J-010559-08	RECQL4	9401	NM_004260	4759029	CAAUACAGCUUACCG
Plate 3	A04	L-017410-01	J-017410-09	RAD52B	2E+05	NM_0010348	7787393	GCGAAUUACUACUUU
Plate 3	A04	L-017410-01	J-017410-10	RAD52B	2E+05	NM_0010348	7787393	ACUGUUGAUUGUUGU
Plate 3	A04	L-017410-01	J-017410-11	RAD52B	2E+05	NM_0010348	7787393	GCAUUGGCUUGGUG
Plate 3	A04	L-017410-01	J-017410-12	RAD52B	2E+05	NM_0010348	7787393	UGUCAGAUGCAUUCC
Plate 3	A05	L-009939-00	J-009939-05	MLH3	27030	NM_014381	7657336	CCAAACCAAUCGUCC
Plate 3	A05	L-009939-00	J-009939-06	MLH3	27030	NM_014381	7657336	GCUGAGAGCUUAGCA
Plate 3	A05	L-009939-00	J-009939-07	MLH3	27030	NM_014381	7657336	ACACAGAGUUCUAGG
Plate 3	A05	L-009939-00	J-009939-08	MLH3	27030	NM_014381	7657336	AGACACGUUUCCAAU
Plate 3	A06	L-012261-00	J-012261-05	CIB1	10519	NM_006384	9951921	CGGCUUAGUGCGUCU
Plate 3	A06	L-012261-00	J-012261-06	CIB1	10519	NM_006384	9951921	GAGCGAAUCUGCAGG
Plate 3	A06	L-012261-00	J-012261-07	CIB1	10519	NM_006384	9951921	CCAAAGACAGCCUUA
Plate 3	A06	L-012261-00	J-012261-08	CIB1	10519	NM_006384	9951921	UGAACUGCCUCACGG
Plate 3	A07	L-012308-00	J-012308-05	BTG2	7832	NM_006763	2887271	GAACCGACAUGCUCC
Plate 3	A07	L-012308-00	J-012308-06	BTG2	7832	NM_006763	2887271	GCAUUCGCAUCAACC
Plate 3	A07	L-012308-00	J-012308-07	BTG2	7832	NM_006763	2887271	GGUCAUAGAGCUACC
Plate 3	A07	L-012308-00	J-012308-08	BTG2	7832	NM_006763	2887271	AGACAAAGGUUACUA
Plate 3	A08	L-005146-00	J-005146-05	MPG	4350	NM_0010150	6263277	UCGUGGAGACCGAGG
Plate 3	A08	L-005146-00	J-005146-06	MPG	4350	NM_0010150	6263277	GGAUGAAGCUGUAUG
Plate 3	A08	L-005146-00	J-005146-07	MPG	4350	NM_0010150	6263277	GCGACUUCCUAAUGG
Plate 3	A08	L-005146-00	J-005146-08	MPG	4350	NM_0010150	6263277	CCACACAGCUCGUCC
Plate 3	A09	L-017809-01	J-017809-09	TNP1	7141	NM_003284	3485006	AGGAGGAGCAAGAGC
Plate 3	A09	L-017809-01	J-017809-10	TNP1	7141	NM_003284	3485006	GCAAAAGAAAAUACC
Plate 3	A09	L-017809-01	J-017809-11	TNP1	7141	NM_003284	3485006	GCCGCAAAUUAAAGA
Plate 3	A09	L-017809-01	J-017809-12	TNP1	7141	NM_003284	3485006	GCCUAUGGAAUGUGG
Plate 3	A10	L-003909-00	J-003909-07	MSH2	4436	NM_000251	4557760	GCAGAUGAAUAGUGC
Plate 3	A10	L-003909-00	J-003909-08	MSH2	4436	NM_000251	4557760	GAAGAGACCUUAACU
Plate 3	A10	L-003909-00	J-003909-09	MSH2	4436	NM_000251	4557760	CAACAUAUAUUCGAC
Plate 3	A10	L-003909-00	J-003909-10	MSH2	4436	NM_000251	4557760	GAGAAUGAUUGGUAU
Plate 3	A11	L-003530-00	J-003530-09	RAD51	5888	NM_133487	1992413	UAUCAUCGCCCAUGC
Plate 3	A11	L-003530-00	J-003530-10	RAD51	5888	NM_133487	1992413	CUAAUCAGGUGGUAG
Plate 3	A11	L-003530-00	J-003530-11	RAD51	5888	NM_133487	1992413	GCAGUGAUGUCCUGG
Plate 3	A11	L-003530-00	J-003530-12	RAD51	5888	NM_133487	1992413	CCAACGAUGUGAAGA
Plate 3	B02	L-003293-00	J-003293-09	RAD1	5810	NM_0010336	7688181	CCACGUGUUUCGCAA
Plate 3	B02	L-003293-00	J-003293-10	RAD1	5810	NM_0010336	7688181	CAAAGUGUGUGCAAG
Plate 3	B02	L-003293-00	J-003293-11	RAD1	5810	NM_0010336	7688181	GAUGAUCAGUACAGC
Plate 3	B02	L-003293-00	J-003293-12	RAD1	5810	NM_0010336	7688181	GUAUGACAAUUCACU
Plate 3	B03	L-012928-01	J-012928-09	FLJ21816	79728	NM_024675	2743690	GAGAGUGAGUCGUUG
Plate 3	B03	L-012928-01	J-012928-10	FLJ21816	79728	NM_024675	2743690	CAUAACUGCUUGCGA
Plate 3	B03	L-012928-01	J-012928-11	FLJ21816	79728	NM_024675	2743690	GUGAUUAACCCUAAG
Plate 3	B03	L-012928-01	J-012928-12	FLJ21816	79728	NM_024675	2743690	CCUGGAAGGUGACGU
Plate 3	B04	L-020327-00	J-020327-05	KIAA1018	22909	NM_014967	6219823	GAAGGGAAUUGUAAC
Plate 3	B04	L-020327-00	J-020327-06	KIAA1018	22909	NM_014967	6219823	CGUAGAAGCUUAUCA
Plate 3	B04	L-020327-00	J-020327-07	KIAA1018	22909	NM_014967	6219823	GUAAUGAUGUGGUGU
Plate 3	B04	L-020327-00	J-020327-08	KIAA1018	22909	NM_014967	6219823	AAACCGUACUUGAGA
Plate 3	B05	L-012897-00	J-012897-05	CNOT7	29883	NM_054026	1797849	CAGCUAGGACUGACA
Plate 3	B05	L-012897-00	J-012897-06	CNOT7	29883	NM_054026	1797849	GGAGAAUUCAGGAGC
Plate 3	B05	L-012897-00	J-012897-07	CNOT7	29883	NM_054026	1797849	UCAUAGCGGUUACGA
Plate 3	B05	L-012897-00	J-012897-08	CNOT7	29883	NM_054026	1797849	GUUAGAGCUGGAACG
Plate 3	B06	L-003247-00	J-003247-11	CDKN2D	1032	NM_079421	3999507	CAAUCCAUCUGGCAG
Plate 3	B06	L-003247-00	J-003247-12	CDKN2D	1032	NM_079421	3999507	AAUCUGAUCUCCAUC
Plate 3	B06	L-003247-00	J-003247-13	CDKN2D	1032	NM_079421	3999507	GUACCAGUCCAGUCC
Plate 3	B06	L-003247-00	J-003247-14	CDKN2D	1032	NM_079421	3999507	CUGCAGGUCAUGAUG
Plate 3	B07	L-012890-00	J-012890-06	DDB1	1642	NM_001923	1343535	CACUAGAUCGCGAUA
Plate 3	B07	L-012890-00	J-012890-07	DDB1	1642	NM_001923	1343535	GAAGGUUCUUUGCGG
Plate 3	B07	L-012890-00	J-012890-08	DDB1	1642	NM_001923	1343535	CAUCGACGGUGACUU
Plate 3	B07	L-012890-00	J-012890-09	DDB1	1642	NM_001923	1343535	CAUCUCGGCUCGUAU
Plate 3	B08	L-011008-00	J-011008-05	CKN1	1161	NM_0010072	5595677	GUAAAGCAGUGUGUU
Plate 3	B08	L-011008-00	J-011008-06	CKN1	1161	NM_0010072	5595677	CAGACAAUCUUAUUA
Plate 3	B08	L-011008-00	J-011008-07	CKN1	1161	NM_0010072	5595677	CAUCAUAUGUCUCCA
Plate 3	B08	L-011008-00	J-011008-08	CKN1	1161	NM_0010072	5595677	GAUUGUACUUUAUGA
Plate 3	B09	L-006656-00	J-006656-05	PARP1	142	NM_001618	1149698	GAUUUCAUCUGGUGU
Plate 3	B09	L-006656-00	J-006656-06	PARP1	142	NM_001618	1149698	GAAAACAGGUAUUGG
Plate 3	B09	L-006656-00	J-006656-07	PARP1	142	NM_001618	1149698	GUUCUUAGCGCACAU
Plate 3	B09	L-006656-00	J-006656-08	PARP1	142	NM_001618	1149698	CCAAUAGGCUUAAUC
Plate 3	B10	L-016958-00	J-016958-05	MGC3202	91442	NM_152266	2274862	GCAUCCAGCAACUGA
Plate 3	B10	L-016958-00	J-016958-06	MGC3202	91442	NM_152266	2274862	CGGGUUAGAAAUUCC
Plate 3	B10	L-016958-00	J-016958-07	MGC3202	91442	NM_152266	2274862	CCAAAGAGCCCAGUA
Plate 3	B10	L-016958-00	J-016958-08	MGC3202	91442	NM_152266	2274862	CCAGUUGGUUCAAGA
Plate 3	B11	L-014848-01	J-014848-09	MGC4189	84268	NM_032308	1414961	GUCCAUCAUCAGCGA
Plate 3	B11	L-014848-01	J-014848-10	MGC4189	84268	NM_032308	1414961	UCUAUGGGGUUGAAG
Plate 3	B11	L-014848-01	J-014848-11	MGC4189	84268	NM_032308	1414961	CUGAGGAGCCUUGUA
Plate 3	B11	L-014848-01	J-014848-12	MGC4189	84268	NM_032308	1414961	GAGCUUGCAGUUUGA

Plate 3	C02	L-020856-00	J-020856-05	POLA	5422	NM_016937	8393994	GAUGGUAAAGCACGC
Plate 3	C02	L-020856-00	J-020856-06	POLA	5422	NM_016937	8393994	GACAUUAGACGUUUC
Plate 3	C02	L-020856-00	J-020856-07	POLA	5422	NM_016937	8393994	CAUGUGAGCUGUUGU
Plate 3	C02	L-020856-00	J-020856-08	POLA	5422	NM_016937	8393994	GUACUACUGCAGAGA
Plate 3	C03	L-003295-00	J-003295-11	RAD9A	5883	NM_004584	1992411	GUAAGAUCCUGAUGA
Plate 3	C03	L-003295-00	J-003295-12	RAD9A	5883	NM_004584	1992411	AUGACGACAUUGACU
Plate 3	C03	L-003295-00	J-003295-13	RAD9A	5883	NM_004584	1992411	GCGGAAGACUCACAA
Plate 3	C03	L-003295-00	J-003295-14	RAD9A	5883	NM_004584	1992411	UCAGCAAACUUGAAU
Plate 3	C04	L-011763-00	J-011763-05	RENT1	5976	NM_002911	1837567	CAGCGGAUCGUGUGA
Plate 3	C04	L-011763-00	J-011763-06	RENT1	5976	NM_002911	1837567	CAAGGUCCCUGAUAA
Plate 3	C04	L-011763-00	J-011763-07	RENT1	5976	NM_002911	1837567	GCAGCCACAUUGUAA
Plate 3	C04	L-011763-00	J-011763-08	RENT1	5976	NM_002911	1837567	GCUCGCAGACUCUCA
Plate 3	C05	L-009641-00	J-009641-06	NBS1	4683	NM_002485	6718976	CCAACUAAAUUGCCA
Plate 3	C05	L-009641-00	J-009641-07	NBS1	4683	NM_002485	6718976	GCAGAUACAUGGGAU
Plate 3	C05	L-009641-00	J-009641-08	NBS1	4683	NM_002485	6718976	GAAUAGAAACGUCUU
Plate 3	C05	L-009641-00	J-009641-09	NBS1	4683	NM_002485	6718976	AACAAUAUGUGCACU
Plate 3	C06	L-009551-00	J-009551-05	DMC1	11144	NM_007068	2323821	GGACAUUGCUGAUCG
Plate 3	C06	L-009551-00	J-009551-06	DMC1	11144	NM_007068	2323821	CCAGGAAUUUGAUAA
Plate 3	C06	L-009551-00	J-009551-07	DMC1	11144	NM_007068	2323821	AGAAUAAGCUUGCGA
Plate 3	C06	L-009551-00	J-009551-08	DMC1	11144	NM_007068	2323821	GAACAAACUAAUUGA
Plate 3	C07	L-003289-00	J-003289-15	PCNA	5111	NM_182649	3323945	GCACGUAUAUGCCGA
Plate 3	C07	L-003289-00	J-003289-16	PCNA	5111	NM_182649	3323945	AACGAGGCCUGCUGG
Plate 3	C07	L-003289-00	J-003289-17	PCNA	5111	NM_182649	3323945	GCGGAUAUGGGACAC
Plate 3	C07	L-003289-00	J-003289-18	PCNA	5111	NM_182649	3323945	CACUAAGGGCCGAAG
Plate 3	C08	L-006901-00	J-006901-06	BAZ1B	9031	NM_032408	1467039	AUAAGGAGAUAGUUC
Plate 3	C08	L-006901-00	J-006901-07	BAZ1B	9031	NM_032408	1467039	CCAAUAAGCUGCACA
Plate 3	C08	L-006901-00	J-006901-08	BAZ1B	9031	NM_032408	1467039	GCACGUAGAUCGCCA
Plate 3	C08	L-006901-00	J-006901-09	BAZ1B	9031	NM_032408	1467039	GCAUUCAGAUUGGUG
Plate 3	C09	L-004283-00	J-004283-05	ALKBH	8846	NM_006020	5174384	GGUAUAAAGAAGCGA
Plate 3	C09	L-004283-00	J-004283-06	ALKBH	8846	NM_006020	5174384	UGACCAGAAUAGCGA
Plate 3	C09	L-004283-00	J-004283-07	ALKBH	8846	NM_006020	5174384	GUGGUGACAUCAUGA
Plate 3	C09	L-004283-00	J-004283-08	ALKBH	8846	NM_006020	5174384	GAAGACCGCUCGUGU
Plate 3	C10	L-005164-00	J-005164-06	POLB	5423	NM_002690	4505930	UCACAGAACUCGCAA
Plate 3	C10	L-005164-00	J-005164-07	POLB	5423	NM_002690	4505930	UAAGAAAUUGCCUGG
Plate 3	C10	L-005164-00	J-005164-08	POLB	5423	NM_002690	4505930	GAGCCAAGCUAUCCA
Plate 3	C10	L-005164-00	J-005164-09	POLB	5423	NM_002690	4505930	GAGCGAAUGAGGCCU
Plate 3	C11	L-009345-00	J-009345-05	NTHL1	4913	NM_002528	3845539	ACACGCAUGUGCACA
Plate 3	C11	L-009345-00	J-009345-06	NTHL1	4913	NM_002528	3845539	CGUGAAGCGUCCGCG
Plate 3	C11	L-009345-00	J-009345-07	NTHL1	4913	NM_002528	3845539	GGAGCAAGGUGAAAU
Plate 3	C11	L-009345-00	J-009345-08	NTHL1	4913	NM_002528	3845539	CGAGAUCAAUGGACU
Plate 3	D02	L-011022-00	J-011022-05	DDB2	1643	NM_000107	4557514	GAUAUCAUGCUCUGG
Plate 3	D02	L-011022-00	J-011022-06	DDB2	1643	NM_000107	4557514	GCCGAUACCCAGAUC
Plate 3	D02	L-011022-00	J-011022-07	DDB2	1643	NM_000107	4557514	GAAGACCUCCGAGAU
Plate 3	D02	L-011022-00	J-011022-08	DDB2	1643	NM_000107	4557514	GGCAUCAGUUCGCUU
Plate 3	D03	L-019687-00	J-019687-06	POLD1	5424	NM_002691	4505932	AGUUGGAGAUUGACC
Plate 3	D03	L-019687-00	J-019687-07	POLD1	5424	NM_002691	4505932	CGAGAGAGCAUGUUU
Plate 3	D03	L-019687-00	J-019687-08	POLD1	5424	NM_002691	4505932	GCAAAGGCAUCUUCC
Plate 3	D03	L-019687-00	J-019687-09	POLD1	5424	NM_002691	4505932	GCACAGAAACUGGGC
Plate 3	D04	L-008856-01	J-008856-09	MGMT	4255	NM_002412	4957451	GGUUGUGAAAUUCGG
Plate 3	D04	L-008856-01	J-008856-10	MGMT	4255	NM_002412	4957451	GAUGGAUGUUUGAGC
Plate 3	D04	L-008856-01	J-008856-11	MGMT	4255	NM_002412	4957451	AAAUAAAGCUCCUGG
Plate 3	D04	L-008856-01	J-008856-12	MGMT	4255	NM_002412	4957451	UGGCCGAAACUGAGU
Plate 3	D05	L-014206-00	J-014206-05	FANCF	2188	NM_022725	4271628	CUUAUUAGCUCUUCG
Plate 3	D05	L-014206-00	J-014206-06	FANCF	2188	NM_022725	4271628	GGUCAACGUUUGCAC
Plate 3	D05	L-014206-00	J-014206-07	FANCF	2188	NM_022725	4271628	GCGCUUCAAUGGCUA
Plate 3	D05	L-014206-00	J-014206-08	FANCF	2188	NM_022725	4271628	GAACCCGGCAUCCAC
Plate 3	D06	L-011488-00	J-011488-05	PARG	8505	NM_003631	7061013	CCAGUUGGAUGGACA
Plate 3	D06	L-011488-00	J-011488-06	PARG	8505	NM_003631	7061013	GAUGGUAGUUCCUCC
Plate 3	D06	L-011488-00	J-011488-07	PARG	8505	NM_003631	7061013	UACCAGAGCAGUUUA
Plate 3	D06	L-011488-00	J-011488-08	PARG	8505	NM_003631	7061013	GGAAACGGUACUCUA
Plate 3	D07	L-011027-00	J-011027-06	ERCC2	2068	NM_000400	4006851	CAUACUUCCUUGCUC
Plate 3	D07	L-011027-00	J-011027-07	ERCC2	2068	NM_000400	4006851	GCAAGGCCGUCGUG
Plate 3	D07	L-011027-00	J-011027-08	ERCC2	2068	NM_000400	4006851	AGGAACAAGCUGCUC
Plate 3	D07	L-011027-00	J-011027-09	ERCC2	2068	NM_000400	4006851	GGAAGGACGUCGAUG
Plate 3	D08	L-017508-00	J-017508-05	TADA3L	10474	NM_133481	1974389	CCGCACACUUGAGGA
Plate 3	D08	L-017508-00	J-017508-06	TADA3L	10474	NM_133481	1974389	CCGACUGGCAGGAUA
Plate 3	D08	L-017508-00	J-017508-07	TADA3L	10474	NM_133481	1974389	UGACCGAACUGGACA
Plate 3	D08	L-017508-00	J-017508-08	TADA3L	10474	NM_133481	1974389	GAACAAGCCCUUCAG
Plate 3	D09	L-006524-00	J-006524-05	ATRX	546	NM_138270	2033620	GAUGUUAGCUGGAUG
Plate 3	D09	L-006524-00	J-006524-06	ATRX	546	NM_138270	2033620	AGUCAUAGAUGCUAA
Plate 3	D09	L-006524-00	J-006524-07	ATRX	546	NM_138270	2033620	GCUUGAGGUUUCUGA
Plate 3	D09	L-006524-00	J-006524-08	ATRX	546	NM_138270	2033620	GUACAGGCGUUAGCA
Plate 3	D10	L-010064-00	J-010064-06	UBE2V1	7335	NM_0010322	7376554	UGAAUGGAGUAAAUA
Plate 3	D10	L-010064-00	J-010064-07	UBE2V1	7335	NM_0010322	7376554	GCCGAAGCAUAGAUU
Plate 3	D10	L-010064-00	J-010064-08	UBE2V1	7335	NM_0010322	7376554	CACAUGAUCCCUCUG
Plate 3	D10	L-010064-00	J-010064-09	UBE2V1	7335	NM_0010322	7376554	CAGGACCACUAAAUG
Plate 3	D11	L-008746-00	J-008746-05	POLL	27343	NM_013274	3814610	CCAUCGGCCUGAAGC
Plate 3	D11	L-008746-00	J-008746-06	POLL	27343	NM_013274	3814610	GAAGCUGGACCAUAU
Plate 3	D11	L-008746-00	J-008746-07	POLL	27343	NM_013274	3814610	GAACGUAUGCCCAGG
Plate 3	D11	L-008746-00	J-008746-08	POLL	27343	NM_013274	3814610	GAGAAUGGUCAGCAA

Plate 3	E02	L-029875-00	J-029875-05	GTF2H3	2967	NM_001516	2837664	GAAUUGAAUCUUCUG
Plate 3	E02	L-029875-00	J-029875-06	GTF2H3	2967	NM_001516	2837664	GACAUAAAGGGUCAA
Plate 3	E02	L-029875-00	J-029875-07	GTF2H3	2967	NM_001516	2837664	AGAAUGAACAAGGAA
Plate 3	E02	L-029875-00	J-029875-08	GTF2H3	2967	NM_001516	2837664	UCAAGGAUAUUGGUG
Plate 3	E03	L-016420-01	J-016420-09	EME1	1E+05	NM_152463	2274896	GAAUUUGCUCGCAGA
Plate 3	E03	L-016420-01	J-016420-10	EME1	1E+05	NM_152463	2274896	GUGCAGUUGUGAAUG
Plate 3	E03	L-016420-01	J-016420-11	EME1	1E+05	NM_152463	2274896	CCGCAUUGGACCAGA
Plate 3	E03	L-016420-01	J-016420-12	EME1	1E+05	NM_152463	2274896	GCUAAGCAGUGAAAG
Plate 3	E04	L-015180-01	J-015180-09	POLQ	10721	NM_199420	7688181	CAACAACCCUUAUCG
Plate 3	E04	L-015180-01	J-015180-10	POLQ	10721	NM_199420	7688181	CGACUAAGAUAGAUC
Plate 3	E04	L-015180-01	J-015180-11	POLQ	10721	NM_199420	7688181	ACACAGUAGGCGAGA
Plate 3	E04	L-015180-01	J-015180-12	POLQ	10721	NM_199420	7688181	CCUUAAGACUGUAGG
Plate 3	E05	L-010534-00	J-010534-05	RAD51C	5889	NM_002876	1740289	GUUCAGCACUAGAUG
Plate 3	E05	L-010534-00	J-010534-06	RAD51C	5889	NM_002876	1740289	GUGAAACCCUCCGAG
Plate 3	E05	L-010534-00	J-010534-07	RAD51C	5889	NM_002876	1740289	UUUGAAAUGCAGCGG
Plate 3	E05	L-010534-00	J-010534-08	RAD51C	5889	NM_002876	1740289	GCAGAAGCCUUAGAA
Plate 3	E06	L-011337-00	J-011337-05	MSH5	4439	NM_172166	2663866	GGCACGAGCAGCUGU
Plate 3	E06	L-011337-00	J-011337-06	MSH5	4439	NM_172166	2663866	GCCAGACAUUAGUGG
Plate 3	E06	L-011337-00	J-011337-07	MSH5	4439	NM_172166	2663866	GCAACGAUCUUGUCU
Plate 3	E06	L-011337-00	J-011337-08	MSH5	4439	NM_172166	2663866	GAGAAUAUGACUCGA
Plate 3	E07	L-004289-00	J-004289-05	DEPC-1	2E+05	NM_139178	2104027	CAUUAUUGCUUCACU
Plate 3	E07	L-004289-00	J-004289-06	DEPC-1	2E+05	NM_139178	2104027	CACGAGUGAUUGACA
Plate 3	E07	L-004289-00	J-004289-07	DEPC-1	2E+05	NM_139178	2104027	GAACCUGACCUUUCG
Plate 3	E07	L-004289-00	J-004289-08	DEPC-1	2E+05	NM_139178	2104027	GAAAGAAGCUGACUG
Plate 3	E08	L-004254-00	J-004254-09	LIG4	3981	NM_206937	4625505	GCACAAAGAUGGAGA
Plate 3	E08	L-004254-00	J-004254-10	LIG4	3981	NM_206937	4625505	GGGAGUGUCUCAUGU
Plate 3	E08	L-004254-00	J-004254-11	LIG4	3981	NM_206937	4625505	GGUAUGAGAUUCUUA
Plate 3	E08	L-004254-00	J-004254-12	LIG4	3981	NM_206937	4625505	GAAGAGGGAAUUAUG
Plate 3	E09	L-003201-00	J-003201-11	ATM	472	NM_138292	7348666	GCAAAGCCCUAGUAA
Plate 3	E09	L-003201-00	J-003201-12	ATM	472	NM_138292	7348666	GGUGUGAUCUUCAGU
Plate 3	E09	L-003201-00	J-003201-13	ATM	472	NM_138292	7348666	GAGAGGAGACAGCUU
Plate 3	E09	L-003201-00	J-003201-14	ATM	472	NM_138292	7348666	GAUGGGAGGCCUAG
Plate 3	E10	L-006833-00	J-006833-05	SMC1L1	8243	NM_006306	3058113	GGACAGCUCUAUUUG
Plate 3	E10	L-006833-00	J-006833-06	SMC1L1	8243	NM_006306	3058113	GCUCGUAACUUCCUC
Plate 3	E10	L-006833-00	J-006833-07	SMC1L1	8243	NM_006306	3058113	GUACAAGGGUCGACA
Plate 3	E10	L-006833-00	J-006833-08	SMC1L1	8243	NM_006306	3058113	GAACUGGCCUCAAAG
Plate 3	E11	L-003241-00	J-003241-09	CDK7	1022	NM_001799	1695065	CAUACAAGGCUUAUU
Plate 3	E11	L-003241-00	J-003241-10	CDK7	1022	NM_001799	1695065	AAACUGAUCUAGAGG
Plate 3	E11	L-003241-00	J-003241-11	CDK7	1022	NM_001799	1695065	CAACAUUGGAUCCUA
Plate 3	E11	L-003241-00	J-003241-12	CDK7	1022	NM_001799	1695065	GAUGACUCUUCAAGG
Plate 3	F02	L-019283-00	J-019283-07	FANCA	2175	NM_0010181	6687966	GGGCCAUGCUUUCUG
Plate 3	F02	L-019283-00	J-019283-08	FANCA	2175	NM_0010181	6687966	GCAGGUCACGGUUGA
Plate 3	F02	L-019283-00	J-019283-09	FANCA	2175	NM_0010181	6687966	GUAGAAGGUCCACUG
Plate 3	F02	L-019283-00	J-019283-10	FANCA	2175	NM_0010181	6687966	GUUAGAGUUUGCUCA
Plate 3	F03	L-021420-00	J-021420-05	KIAA0625	23064	NM_015046	3762015	GCACGUCAGUCAUGC
Plate 3	F03	L-021420-00	J-021420-06	KIAA0625	23064	NM_015046	3762015	GCAAUAAGCUCAUCC
Plate 3	F03	L-021420-00	J-021420-07	KIAA0625	23064	NM_015046	3762015	GCUCAACUCUCCAAA
Plate 3	F03	L-021420-00	J-021420-08	KIAA0625	23064	NM_015046	3762015	UAGCACAGGUUGUUA
Plate 3	F04	L-022320-01	J-022320-09	FLJ10719	55215	NM_018193	8283043	ACAGAGUGGUGACGA
Plate 3	F04	L-022320-01	J-022320-10	FLJ10719	55215	NM_018193	8283043	GCAGAAAGAAAUAGC
Plate 3	F04	L-022320-01	J-022320-11	FLJ10719	55215	NM_018193	8283043	GAUACUUGUCCUUCG
Plate 3	F04	L-022320-01	J-022320-12	FLJ10719	55215	NM_018193	8283043	ACGAAGACCUAGAUG
Plate 3	F05	L-008823-00	J-008823-05	UBE2V2	7336	NM_003350	1202566	GUUAAAGUUCCUCGU
Plate 3	F05	L-008823-00	J-008823-06	UBE2V2	7336	NM_003350	1202566	CAAGAGCUAAGACGU
Plate 3	F05	L-008823-00	J-008823-07	UBE2V2	7336	NM_003350	1202566	CACCAAGGACAAAUU
Plate 3	F05	L-008823-00	J-008823-08	UBE2V2	7336	NM_003350	1202566	GAGCAUACCAGUGUU
Plate 3	F06	L-012838-01	J-012838-09	SMUG1	23583	NM_014311	7657596	GCAACUACGUGACUC
Plate 3	F06	L-012838-01	J-012838-10	SMUG1	23583	NM_014311	7657596	UCUACAAUCCCGUGG
Plate 3	F06	L-012838-01	J-012838-11	SMUG1	23583	NM_014311	7657596	ACUUCUAAGGUCACG
Plate 3	F06	L-012838-01	J-012838-12	SMUG1	23583	NM_014311	7657596	AGAAGUGAGUGGUGC
Plate 3	F07	L-006832-00	J-006832-06	RAD21	5885	NM_006265	5453993	GCUCAGCCUUUGUGG
Plate 3	F07	L-006832-00	J-006832-07	RAD21	5885	NM_006265	5453993	GGGAGUAGUUCGAAU
Plate 3	F07	L-006832-00	J-006832-08	RAD21	5885	NM_006265	5453993	GACCAAGGUUCCAUA
Plate 3	F07	L-006832-00	J-006832-09	RAD21	5885	NM_006265	5453993	GCAUUGGAGCCUAUU
Plate 3	F08	L-011373-00	J-011373-05	RAD51L1	5890	NM_133510	4625503	GAGCUGUGGUGUACA
Plate 3	F08	L-011373-00	J-011373-06	RAD51L1	5890	NM_133510	4625503	GUAUUUGGCUGAGGA
Plate 3	F08	L-011373-00	J-011373-07	RAD51L1	5890	NM_133510	4625503	CCACCAACAUGGGAG
Plate 3	F08	L-011373-00	J-011373-08	RAD51L1	5890	NM_133510	4625503	CCAGUUAUCUUGACG
Plate 3	F09	L-011795-00	J-011795-05	UNG	7374	NM_080911	1971875	UUAUCAAGCUAAUGG
Plate 3	F09	L-011795-00	J-011795-06	UNG	7374	NM_080911	1971875	GAACUCGAAUGGCCU
Plate 3	F09	L-011795-00	J-011795-07	UNG	7374	NM_080911	1971875	GAAGCGGCACCAUGU
Plate 3	F09	L-011795-00	J-011795-08	UNG	7374	NM_080911	1971875	UAUAGAGGGUUCUUU
Plate 3	F10	L-003255-00	J-003255-10	CHEK1	1111	NM_001274	2012741	CAAGAUGUGUGGUAC
Plate 3	F10	L-003255-00	J-003255-11	CHEK1	1111	NM_001274	2012741	GAGAAGGCAAUAUCC
Plate 3	F10	L-003255-00	J-003255-12	CHEK1	1111	NM_001274	2012741	CCACAUGUCCUGAUC
Plate 3	F10	L-003255-00	J-003255-13	CHEK1	1111	NM_001274	2012741	GAAGUUGGGCUAUCA
Plate 3	F11	L-180657-00	J-180657-01	ATRIP	84126	NM_032166	1839034	GCUCCAGACCAGUGA
Plate 3	F11	L-180657-00	J-180657-02	ATRIP	84126	NM_032166	1839034	UGGUGAAAUUAGCCG
Plate 3	F11	L-180657-00	J-180657-03	ATRIP	84126	NM_032166	1839034	GAAUCUGGUUGCCCG
Plate 3	F11	L-180657-00	J-180657-04	ATRIP	84126	NM_032166	1839034	UCACUACAUCAGACG

Plate 3	G02	L-010258-00	J-010258-05	DUT	1854	NM_0010252	7090644	GCUCAUUUGCGAACG
Plate 3	G02	L-010258-00	J-010258-06	DUT	1854	NM_0010252	7090644	UGUAGGAGCUGGUG
Plate 3	G02	L-010258-00	J-010258-07	DUT	1854	NM_0010252	7090644	UAGAGGAAAUGUUGG
Plate 3	G02	L-010258-00	J-010258-08	DUT	1854	NM_0010252	7090644	UGCCUAUGAUUACAC
Plate 3	G03	L-006783-00	J-006783-07	PNKP	11284	NM_007254	3154341	GUGAAACAGCUGGGA
Plate 3	G03	L-006783-00	J-006783-08	PNKP	11284	NM_007254	3154341	CCGGAUAUGUCCACG
Plate 3	G03	L-006783-00	J-006783-09	PNKP	11284	NM_007254	3154341	GACCGGAAGUGCUCC
Plate 3	G03	L-006783-00	J-006783-10	PNKP	11284	NM_007254	3154341	GGAAACGGGUCGCCA
Plate 3	G04	L-007287-00	J-007287-06	BLM	641	NM_000057	4557364	CUAAAUCUGUGGAGG
Plate 3	G04	L-007287-00	J-007287-07	BLM	641	NM_000057	4557364	GAUCAAUGCUGCACU
Plate 3	G04	L-007287-00	J-007287-08	BLM	641	NM_000057	4557364	GGAUGACUCAGAAUG
Plate 3	G04	L-007287-00	J-007287-09	BLM	641	NM_000057	4557364	GCAACUAGAACGUCA
Plate 3	G05	L-013730-01	J-013730-09	APEX2	27301	NM_014481	1837550	GAGCCAUGUGUGAUG
Plate 3	G05	L-013730-01	J-013730-10	APEX2	27301	NM_014481	1837550	CAACAAUCAAACCCG
Plate 3	G05	L-013730-01	J-013730-11	APEX2	27301	NM_014481	1837550	GGACGAGCUGGAUGC
Plate 3	G05	L-013730-01	J-013730-12	APEX2	27301	NM_014481	1837550	GAGAAGGAGUUACGG
Plate 3	G06	L-003462-00	J-003462-05	BRCA2	675	NM_000059	4502450	GAAACGGACUUGCUA
Plate 3	G06	L-003462-00	J-003462-06	BRCA2	675	NM_000059	4502450	GGUAUCAGAUGCUUC
Plate 3	G06	L-003462-00	J-003462-07	BRCA2	675	NM_000059	4502450	GAAGAAUGCAGGUUU
Plate 3	G06	L-003462-00	J-003462-08	BRCA2	675	NM_000059	4502450	UAAGGAACGUCAAGA
Plate 3	G07	L-005084-00	J-005084-08	G22P1	2547	NM_001469	5109384	AUAAAGCUCUAUCGG
Plate 3	G07	L-005084-00	J-005084-09	G22P1	2547	NM_001469	5109384	CAGGGUGGGAGUCAU
Plate 3	G07	L-005084-00	J-005084-10	G22P1	2547	NM_001469	5109384	UUAGUGAUGUCCAAU
Plate 3	G07	L-005084-00	J-005084-11	G22P1	2547	NM_001469	5109384	GAUCCAGGUUUGAUG
Plate 3	G08	L-004801-00	J-004801-09	CLK2	1196	NM_001291	4771713	GCUACAGACGCAACG
Plate 3	G08	L-004801-00	J-004801-10	CLK2	1196	NM_001291	4771713	GGAGAUGCCUACUAU
Plate 3	G08	L-004801-00	J-004801-11	CLK2	1196	NM_001291	4771713	AAGCAUAAGCGACGA
Plate 3	G08	L-004801-00	J-004801-12	CLK2	1196	NM_001291	4771713	CAGACUAUCGGCAUU
Plate 3	G09	L-012649-00	J-012649-05	POLG	5428	NM_002693	4505936	GGUAUCGGCUGUCG
Plate 3	G09	L-012649-00	J-012649-06	POLG	5428	NM_002693	4505936	AGUGGGACCUGCAAG
Plate 3	G09	L-012649-00	J-012649-07	POLG	5428	NM_002693	4505936	GCUUACUAAUGCAGU
Plate 3	G09	L-012649-00	J-012649-08	POLG	5428	NM_002693	4505936	UCAGUGCAGUCGAUA
Plate 3	G10	L-010210-00	J-010210-06	BRE	9577	NM_199191	4035376	GAGGAUAACUGACUU
Plate 3	G10	L-010210-00	J-010210-07	BRE	9577	NM_199191	4035376	CGUGGAAUAUGAUGC
Plate 3	G10	L-010210-00	J-010210-08	BRE	9577	NM_199191	4035376	GCAACAAUAUCACCA
Plate 3	G10	L-010210-00	J-010210-09	BRE	9577	NM_199191	4035376	UGAUUACGUUCCUCA
Plate 3	G11	L-010491-00	J-010491-05	XRCC5	7520	NM_021141	1240865	GCAUGGAUGUGAUUC
Plate 3	G11	L-010491-00	J-010491-06	XRCC5	7520	NM_021141	1240865	CGAGUAACCAGCUCA
Plate 3	G11	L-010491-00	J-010491-07	XRCC5	7520	NM_021141	1240865	GAGCAGCGCUUUAAC
Plate 3	G11	L-010491-00	J-010491-08	XRCC5	7520	NM_021141	1240865	AAACUUCCGUGUUCU
Plate 3	H02	L-020432-00	J-020432-05	HSU24186	29935	NM_013347	9558730	GAUGAGAGUCACCGC
Plate 3	H02	L-020432-00	J-020432-06	HSU24186	29935	NM_013347	9558730	GAUAAAGCCCGUCGU
Plate 3	H02	L-020432-00	J-020432-07	HSU24186	29935	NM_013347	9558730	GAGUAUAUGUCAAAG
Plate 3	H02	L-020432-00	J-020432-08	HSU24186	29935	NM_013347	9558730	GACCCUGUGUUCAAG
Plate 3	H03	L-012067-00	J-012067-05	XRCC3	7517	NM_005432	1240864	AAACUGAAAUCGGUA
Plate 3	H03	L-012067-00	J-012067-06	XRCC3	7517	NM_005432	1240864	UGUUGGAGUGUGUG
Plate 3	H03	L-012067-00	J-012067-07	XRCC3	7517	NM_005432	1240864	GGACCUGAAUCCCAG
Plate 3	H03	L-012067-00	J-012067-08	XRCC3	7517	NM_005432	1240864	GGACCAGACUUGAAG
Plate 3	H04	L-015737-00	J-015737-05	NPM1	4869	NM_0010377	8364186	GUAGAAGACAUUAAA
Plate 3	H04	L-015737-00	J-015737-06	NPM1	4869	NM_0010377	8364186	AAUGCAAGCAAGUAU
Plate 3	H04	L-015737-00	J-015737-07	NPM1	4869	NM_0010377	8364186	ACAAGAAUCCUUCAA
Plate 3	H04	L-015737-00	J-015737-08	NPM1	4869	NM_0010377	8364186	UAAAGGCCGACAAAG
Plate 3	H05	L-020222-01	J-020222-10	ASF1A	25842	NM_014034	1154302	CGAUCAAGUUUUAGA
Plate 3	H05	L-020222-01	J-020222-11	ASF1A	25842	NM_014034	1154302	CAUUAGACCAGGUUG
Plate 3	H05	L-020222-01	J-020222-12	ASF1A	25842	NM_014034	1154302	AGCCAUAUGAUGCAG
Plate 3	H05	L-020222-02	J-020222-17	ASF1A	25842	NM_014034	1154302	GGCAUAUGUUUGUAU
Plate 3	H06	L-011682-00	J-011682-08	H2AFX	3014	NM_002105	5263033	GGGACGAAGCACUUG
Plate 3	H06	L-011682-00	J-011682-09	H2AFX	3014	NM_002105	5263033	CGACUAGAACCUUAG
Plate 3	H06	L-011682-00	J-011682-10	H2AFX	3014	NM_002105	5263033	GGAAAGAGCUGAGCC
Plate 3	H06	L-011682-00	J-011682-11	H2AFX	3014	NM_002105	5263033	GAACUGGAAUUCUGC
Plate 3	H07	L-014224-01	J-014224-13	FLJ22833	64859	NM_0010317	7253472	GGAGAUAGGACGCGU
Plate 3	H07	L-014224-01	J-014224-14	FLJ22833	64859	NM_0010317	7253472	CGUGCAAAGUAGCAG
Plate 3	H07	L-014224-01	J-014224-15	FLJ22833	64859	NM_0010317	7253472	UCGGUUGACCAGAGG
Plate 3	H07	L-014224-01	J-014224-16	FLJ22833	64859	NM_0010317	7253472	UGAGAUCGGAGGUCU
Plate 3	H08	L-003920-00	J-003920-06	UBE2N	7334	NM_003348	3757713	AACCAGGUCUUUAGA
Plate 3	H08	L-003920-00	J-003920-07	UBE2N	7334	NM_003348	3757713	UGACUGACAUGUAGG
Plate 3	H08	L-003920-00	J-003920-08	UBE2N	7334	NM_003348	3757713	AGUAUCAAGUCCUCA
Plate 3	H08	L-003920-00	J-003920-09	UBE2N	7334	NM_003348	3757713	GAUGAUCAUUGGUGU
Plate 3	H09	L-019946-00	J-019946-05	ERCC4	2072	NM_005236	4885216	CCAAACAGCUUUAUG
Plate 3	H09	L-019946-00	J-019946-06	ERCC4	2072	NM_005236	4885216	GCACCUCGAUGUUUA
Plate 3	H09	L-019946-00	J-019946-07	ERCC4	2072	NM_005236	4885216	CGGAAGAAAUUAAGC
Plate 3	H09	L-019946-00	J-019946-08	ERCC4	2072	NM_005236	4885216	UGACAAGGGUACUAC
Plate 3	H10	L-006311-00	J-006311-05	ERCC1	2067	NM_001983	4254417	CGACGUAAUUCCCGA
Plate 3	H10	L-006311-00	J-006311-06	ERCC1	2067	NM_001983	4254417	GGCGGUACCUGGAGA
Plate 3	H10	L-006311-00	J-006311-07	ERCC1	2067	NM_001983	4254417	GGAAGAAAUUUGUGA
Plate 3	H10	L-006311-00	J-006311-08	ERCC1	2067	NM_001983	4254417	GCAAUCCCGUACUGA
Plate 3	H11	L-010379-00	J-010379-06	RRM2	6241	NM_001034	4557844	GGAGUGAUGUCAAGU
Plate 3	H11	L-010379-00	J-010379-07	RRM2	6241	NM_001034	4557844	GCGAUGGCAUAGUAA
Plate 3	H11	L-010379-00	J-010379-08	RRM2	6241	NM_001034	4557844	CCACGGAGCCGAAAA
Plate 3	H11	L-010379-00	J-010379-09	RRM2	6241	NM_001034	4557844	GAAUUGCACUCUAAU

Table A.4. Tables listing siRNA sequences from DDR library from Dharmacon

A.2.3 – Custom Screen Plates.

TMOSLR Custom Plate								
Order Numbers 449324-449326								
Plate	Well	Pool Catalog Number	Duplex Catalog Number		GENE ID	Gene Accession	GI Number	Sequence
Plate 1	A02	L-021207-01	J-021207-09	TELO2	9894	NM_016111	7705345	UGGCCAGAUUCCUGCGCGA
Plate 1	A02	L-021207-01	J-021207-10	TELO2	9894	NM_016111	7705345	UGGAGUCCCUGAAGCGGUA
Plate 1	A02	L-021207-01	J-021207-11	TELO2	9894	NM_016111	7705345	CCCUGAAAUUCCAGUACGA
Plate 1	A02	L-021207-01	J-021207-12	TELO2	9894	NM_016111	7705345	UGAUGUGCCUGGCUGUUAA
Plate 1	A03	L-008977-00	J-008977-05	RUVBL1	8607	NM_003707	4506752	AUAAGGUGGUGAACAAGUA
Plate 1	A03	L-008977-00	J-008977-06	RUVBL1	8607	NM_003707	4506752	GGGAAGGACAGCAUUGAGA
Plate 1	A03	L-008977-00	J-008977-07	RUVBL1	8607	NM_003707	4506752	CAGGAUAAGUACAUGAAGU
Plate 1	A03	L-008977-00	J-008977-08	RUVBL1	8607	NM_003707	4506752	CUCAGGAGCUGGGUAGUAA
Plate 1	A04	L-020420-01	J-020420-09	PPP6R1	22870	NM_014931	55749688	UCAAUUGGCUCAACGAGGA
Plate 1	A04	L-020420-01	J-020420-10	PPP6R1	22870	NM_014931	55749688	CAGUGUGGCCUGCGAGAUU
Plate 1	A04	L-020420-01	J-020420-11	PPP6R1	22870	NM_014931	55749688	CCUCACGCCUCCUCCGAUA
Plate 1	A04	L-020420-01	J-020420-12	PPP6R1	22870	NM_014931	55749688	GGGAGGAGAACGACCGUGU
Plate 1	A05	L-011494-00	J-011494-05	COPS3	8533	NM_003653	23238221	GCACAAGUGUAUUCAACCA
Plate 1	A05	L-011494-00	J-011494-06	COPS3	8533	NM_003653	23238221	CAAUGCAUACCACGAGUUA
Plate 1	A05	L-011494-00	J-011494-07	COPS3	8533	NM_003653	23238221	CAAACCAGCUGACCUCAAU
Plate 1	A05	L-011494-00	J-011494-08	COPS3	8533	NM_003653	23238221	GAAUUGGCAUCCUUAAGCA
Plate 1	A06	L-019488-00	J-019488-05	TIMELESS	8914	NM_003920	52851463	UCAAUCGUCUGCUUAGUGA
Plate 1	A06	L-019488-00	J-019488-06	TIMELESS	8914	NM_003920	52851463	CAGGGUAGCUUAGUCCUUU
Plate 1	A06	L-019488-00	J-019488-07	TIMELESS	8914	NM_003920	52851463	GAGGGAGACACUUACCAUA
Plate 1	A06	L-019488-00	J-019488-08	TIMELESS	8914	NM_003920	52851463	CUACUGCUGGUCAGAAAUA
Plate 1	A07	L-004176-01	J-004176-09	INO80	54617	NM_017553	38708320	GGAAUUGAGUUUCGAUAGA
Plate 1	A07	L-004176-01	J-004176-10	INO80	54617	NM_017553	38708320	GGAGUUAUUUGAACGGCAA
Plate 1	A07	L-004176-01	J-004176-11	INO80	54617	NM_017553	38708320	GAAUCAACUUUCUCGCUUA
Plate 1	A07	L-004176-01	J-004176-12	INO80	54617	NM_017553	38708320	GAGGAAACCAACCGAGUGA
Plate 1	A08	L-007244-00	J-007244-09	PARP4	143	NM_006437	11496990	GUACAAUGGUGUCGACUAC
Plate 1	A08	L-007244-00	J-007244-10	PARP4	143	NM_006437	11496990	CGUCACGUCUUAAGGAUUU
Plate 1	A08	L-007244-00	J-007244-11	PARP4	143	NM_006437	11496990	GGAUUAGCCUCAACGAUGU
Plate 1	A08	L-007244-00	J-007244-12	PARP4	143	NM_006437	11496990	GCAACUGAACCACUAUUUA
Plate 1	A09	L-004420-00	J-004420-05	DAXX	1616	NM_001350	53828721	CAGCCAAGCUCUAUGUCUA
Plate 1	A09	L-004420-00	J-004420-06	DAXX	1616	NM_001350	53828721	GAGGUUAACAGGCGCAUUG
Plate 1	A09	L-004420-00	J-004420-07	DAXX	1616	NM_001350	53828721	GCAAAACAAAGGACGCAUA
Plate 1	A09	L-004420-00	J-004420-08	DAXX	1616	NM_001350	53828721	GGAGUUGGAUCUCUCAGAA
Plate 1	A10	L-020873-01	J-020873-09	COPS7A	50813	NM_016319	7705329	GGACAUACGCUGACUACUU
Plate 1	A10	L-020873-01	J-020873-10	COPS7A	50813	NM_016319	7705329	CAUUACAUGUCAUUGAGUA
Plate 1	A10	L-020873-01	J-020873-11	COPS7A	50813	NM_016319	7705329	GGUCCAAGUCGAAUUGAAA
Plate 1	A10	L-020873-01	J-020873-12	COPS7A	50813	NM_016319	7705329	GAAUAAGCUUCGACACCUC
Plate 1	A11	L-005248-01	J-005248-09	UBA2	10054	NM_005499	50592990	GUGCAAAGAGGUCACGUAU
Plate 1	A11	L-005248-01	J-005248-10	UBA2	10054	NM_005499	50592990	GGACAAACUAUGGCGGAAA
Plate 1	A11	L-005248-01	J-005248-11	UBA2	10054	NM_005499	50592990	CAUAACCAGUCAUGAGAUA
Plate 1	A11	L-005248-01	J-005248-12	UBA2	10054	NM_005499	50592990	GCUAGAACUGUUAGACACA
Plate 1	B02	L-021219-00	J-021219-05	TERF2IP	54386	NM_018975	52627148	GAUGAGAGCCCUCCUGAUU
Plate 1	B02	L-021219-00	J-021219-06	TERF2IP	54386	NM_018975	52627148	GGAAAGCGAUGGAGAAGAG
Plate 1	B02	L-021219-00	J-021219-07	TERF2IP	54386	NM_018975	52627148	GGUGGGAGCUGCCAUUAAG
Plate 1	B02	L-021219-00	J-021219-08	TERF2IP	54386	NM_018975	52627148	GGAAGCCACCCGGGAGUUU
Plate 1	B03	L-017750-00	J-017750-05	PPP4R2	151987	NM_174907	28372530	GCGACUAUGUGAAUUGUUA
Plate 1	B03	L-017750-00	J-017750-06	PPP4R2	151987	NM_174907	28372530	ACAAAUGGGUUGCCUGAGA
Plate 1	B03	L-017750-00	J-017750-07	PPP4R2	151987	NM_174907	28372530	AAACGAAGGCCCUGUAAGU
Plate 1	B03	L-017750-00	J-017750-08	PPP4R2	151987	NM_174907	28372530	UGACUGCCGUGAAACAGAA
Plate 1	B04	L-013386-00	J-013386-05	GAR1	54433	NM_032993	77812668	GAGAGGACAUUAAGUGAAA
Plate 1	B04	L-013386-00	J-013386-06	GAR1	54433	NM_032993	77812668	UCCAGAACGUGUAGUCUUA
Plate 1	B04	L-013386-00	J-013386-07	GAR1	54433	NM_032993	77812668	CCGCGGAGGCUUUAACAAA
Plate 1	B04	L-013386-00	J-013386-08	GAR1	54433	NM_032993	77812668	GAAGAUGACAUAGUUUGUA
Plate 1	B05	L-020566-02	J-020566-17	NSMCE4A	54780	NM_017615	8923008	AAUGAAGUGUCCCGAGCAA
Plate 1	B05	L-020566-02	J-020566-18	NSMCE4A	54780	NM_017615	8923008	GUGAAGUCCAAAACGGAAA
Plate 1	B05	L-020566-02	J-020566-19	NSMCE4A	54780	NM_017615	8923008	ACACAGAGCCGUCGGAUUC
Plate 1	B05	L-020566-02	J-020566-20	NSMCE4A	54780	NM_017615	8923008	GUGCCAAAGCCACGAGUUG
Plate 1	B06	L-013319-02	J-013319-18	NHP2	55651	NM_001034833	77812673	AGGAGUACCAGGAGGCUUA
Plate 1	B06	L-013319-02	J-013319-19	NHP2	55651	NM_001034833	77812673	GCGGUGAAGCAGAAGCAGA
Plate 1	B06	L-013319-02	J-013319-20	NHP2	55651	NM_001034833	77812673	AAAUAAAGGCAGAUCCCGA
Plate 1	B06	L-013319-02	J-013319-21	NHP2	55651	NM_001034833	77812673	CCUGUGUGAUAAUGGUCAA
Plate 1	B07	L-020553-00	J-020553-05	ASF1B	55723	NM_018154	67782340	GCACUCCUAUCAAGGGCUU
Plate 1	B07	L-020553-00	J-020553-06	ASF1B	55723	NM_018154	67782340	GACAGGAGUUCAUCCGAGU
Plate 1	B07	L-020553-00	J-020553-07	ASF1B	55723	NM_018154	67782340	CGGACGACCUGGAGUGGAA
Plate 1	B07	L-020553-00	J-020553-08	ASF1B	55723	NM_018154	67782340	GCAGGGAGACACAUGUUUG
Plate 1	B08	L-004205-00	J-004205-05	POT1	25913	NM_015450	13123773	GUAGAAGCCUUACGUGUUU
Plate 1	B08	L-004205-00	J-004205-06	POT1	25913	NM_015450	13123773	GAUAAAACAUCGUGGAUUC
Plate 1	B08	L-004205-00	J-004205-07	POT1	25913	NM_015450	13123773	GCAUAUCCGUGGUUGGAAU
Plate 1	B08	L-004205-00	J-004205-08	POT1	25913	NM_015450	13123773	UAACUUGCCUGCUCUUUAG
Plate 1	B09	L-006837-00	J-006837-05	SMC4	10051	NM_001002799	50658066	GUUAAACGCUUACACAAUA
Plate 1	B09	L-006837-00	J-006837-06	SMC4	10051	NM_001002799	50658066	GAAGUUAUGGAUAGCCUUA
Plate 1	B09	L-006837-00	J-006837-07	SMC4	10051	NM_001002799	50658066	GCAAGCAUCCAGCGUUUAA
Plate 1	B09	L-006837-00	J-006837-08	SMC4	10051	NM_001002799	50658066	GCACUGGACUACAUUGUUG
Plate 1	B10	L-010362-00	J-010362-05	PDS5B	23047	NM_015928	7705287	GAAAUAUGCUUUACAGUCA
Plate 1	B10	L-010362-00	J-010362-06	PDS5B	23047	NM_015928	7705287	UGAUAAAGAUGUUCGCUUA
Plate 1	B10	L-010362-00	J-010362-07	PDS5B	23047	NM_015928	7705287	GCAUAGUGAUGGAGACUUG
Plate 1	B10	L-010362-00	J-010362-08	PDS5B	23047	NM_015928	7705287	GGUCAAUGAUCACUUACUU
Plate 1	B11	L-006941-00	J-006941-05	BAZ1A	11177	NM_182648	32967604	CAAGUUAGAUUGCCAGUUA
Plate 1	B11	L-006941-00	J-006941-06	BAZ1A	11177	NM_182648	32967604	GAACUAAGGCUGAGAGAUU
Plate 1	B11	L-006941-00	J-006941-07	BAZ1A	11177	NM_182648	32967604	GCCAUAGCCUGUACCAAUA
Plate 1	B11	L-006941-00	J-006941-08	BAZ1A	11177	NM_182648	32967604	GAAUGCGCGUUGCAAGAUA

Plate 1	C02	L-009645-00	J-009645-05	CHRAC1	54108	NM_017444	24432041	CCACGGAGCUCUUUGUUCA
Plate 1	C02	L-009645-00	J-009645-06	CHRAC1	54108	NM_017444	24432041	ACACGGCAGUGGAAAGGAA
Plate 1	C02	L-009645-00	J-009645-07	CHRAC1	54108	NM_017444	24432041	GGACGUGGUCGUGGGUAAA
Plate 1	C02	L-009645-00	J-009645-08	CHRAC1	54108	NM_017444	24432041	GACUUACAGUGAUUUAGCA
Plate 1	C03	L-008460-01	J-008460-09	POLE3	54107	NM_017443	31543422	GAGGGAUUCUGAACGACUA
Plate 1	C03	L-008460-01	J-008460-10	POLE3	54107	NM_017443	31543422	CUUGAAAUGAGACGUGCUA
Plate 1	C03	L-008460-01	J-008460-11	POLE3	54107	NM_017443	31543422	CAUAUAGGCGGGAGCAGAA
Plate 1	C03	L-008460-01	J-008460-12	POLE3	54107	NM_017443	31543422	UGGAAUGGUAUUAGUCAAA
Plate 1	C04	L-009850-02	J-009850-18	POLE4	56655	NM_019896	38455393	GAGUGAAGGCCUUGGUGAA
Plate 1	C04	L-009850-02	J-009850-19	POLE4	56655	NM_019896	38455393	GAGGAGAGACUUGGAUAAU
Plate 1	C04	L-009850-02	J-009850-20	POLE4	56655	NM_019896	38455393	ACGUGACGCUAGCGGGACA
Plate 1	C04	L-009850-02	J-009850-21	POLE4	56655	NM_019896	38455393	CUUCACCUAUGCCGGGAUA
Plate 1	C05	L-020297-00	J-020297-05	BRD7	29117	NM_013263	41350211	GUGCCAAGAUUAUCCGUAU
Plate 1	C05	L-020297-00	J-020297-06	BRD7	29117	NM_013263	41350211	GCACGUAUGGAGUUCGAAA
Plate 1	C05	L-020297-00	J-020297-07	BRD7	29117	NM_013263	41350211	GUACUAAUGCCAUGAUUUA
Plate 1	C05	L-020297-00	J-020297-08	BRD7	29117	NM_013263	41350211	GCAAGUAACUCCAGGUGAU
Plate 1	C06	L-013332-02	J-013332-17	NOP10	55505	NM_018648	77812675	UAACCAAACUCUUCGGACU
Plate 1	C06	L-013332-02	J-013332-18	NOP10	55505	NM_018648	77812675	CAACGAGCAGGGAGAUCGA
Plate 1	C06	L-013332-02	J-013332-19	NOP10	55505	NM_018648	77812675	CAUAAAGGGAACACAUUUG
Plate 1	C06	L-013332-02	J-013332-20	NOP10	55505	NM_018648	77812675	GAAGAAAUUUGACCCGAUG
Plate 1	C07	L-004898-00	J-004898-05	UBE2T	29089	NM_014176	7661807	CCUGCGAGCUCAAAUAUUA
Plate 1	C07	L-004898-00	J-004898-06	UBE2T	29089	NM_014176	7661807	GAAGGCCAGUCAGCUAGUA
Plate 1	C07	L-004898-00	J-004898-07	UBE2T	29089	NM_014176	7661807	GGAAGGAUUUGUCUGGAUG
Plate 1	C07	L-004898-00	J-004898-08	UBE2T	29089	NM_014176	7661807	GUACACAACUCAACACAGA
Plate 1	C08	L-014013-01	J-014013-09	POLD4	57804	NM_021173	379056363	CCUAUGAGGCACCACGUAA
Plate 1	C08	L-014013-01	J-014013-10	POLD4	57804	NM_021173	47271453	GGUGUCGGGCCAAGCAUAU
Plate 1	C08	L-014013-01	J-014013-11	POLD4	57804	NM_021173	379056363	AGUCAGACAUGGACAGUUG
Plate 1	C08	L-014013-01	J-014013-12	POLD4	57804	NM_021173	47271453	GGCAGGUGCUGAAGACCCA
Plate 1	C09	L-005288-00	J-005288-05	CLSPN	63967	NM_022111	21735568	GCAGAUGGGUUCUUAAAUG
Plate 1	C09	L-005288-00	J-005288-06	CLSPN	63967	NM_022111	21735568	GAGUAGAUGUUUCCAUUAA
Plate 1	C09	L-005288-00	J-005288-07	CLSPN	63967	NM_022111	21735568	GCAGAUAGUCCUUCAGAUA
Plate 1	C09	L-005288-00	J-005288-08	CLSPN	63967	NM_022111	21735568	GAAGACAGGCUCACUGCUA
Plate 1	C10	L-014207-02	J-014207-17	COPS7B	64708	NM_022730	12232384	GGACAUACCCAGAUUACAU
Plate 1	C10	L-014207-02	J-014207-18	COPS7B	64708	NM_022730	12232384	CUGCAUGAAUGGUGUGAUG
Plate 1	C10	L-014207-02	J-014207-19	COPS7B	64708	NM_022730	12232384	CGUCAAGAUGCGCUGCUUU
Plate 1	C10	L-014207-02	J-014207-20	COPS7B	64708	NM_022730	12232384	CGUGCAGGAGCUUGCGGAA
Plate 1	C11	L-018395-01	J-018395-09	ACTR5	79913	NM_024855	31542679	CCACUGUAUUCACGGCAAA
Plate 1	C11	L-018395-01	J-018395-10	ACTR5	79913	NM_024855	31542679	GCUACAUCGCUGAGGAUUA
Plate 1	C11	L-018395-01	J-018395-11	ACTR5	79913	NM_024855	31542679	CUCGAUGUGCAGUGGGCUA
Plate 1	C11	L-018395-01	J-018395-12	ACTR5	79913	NM_024855	31542679	GCGUCUGGACCGACUGCUA
Plate 1	D02	L-016441-01	J-016441-09	ACTR8	93973	NM_022899	39812114	GGUGAUACGGAGAACGGAA
Plate 1	D02	L-016441-01	J-016441-10	ACTR8	93973	NM_022899	39812114	AAUAUGGUCUCAUGCGAUA
Plate 1	D02	L-016441-01	J-016441-11	ACTR8	93973	NM_022899	39812114	GAUAGUAUGUGACGAGGGA
Plate 1	D02	L-016441-01	J-016441-12	ACTR8	93973	NM_022899	39812114	CCACCAUCCUUCAGGCGAA
Plate 1	D03	L-016208-02	J-016208-17	OBFC1	79991	NM_024928	194394164	GUAUAUAUCCGUAGAGAGA
Plate 1	D03	L-016208-02	J-016208-18	OBFC1	79991	NM_024928	194394164	GCACAAUGGAGCACUACUA
Plate 1	D03	L-016208-02	J-016208-19	OBFC1	79991	NM_024928	194394164	CAUACAGAGAAGAGCGAGA
Plate 1	D03	L-016208-02	J-016208-20	OBFC1	79991	NM_024928	194394164	GGACACGAUCCGAGUCAGA
Plate 1	D04	L-014564-01	J-014564-13	PIF1	80119	NM_025049	82546871	CAUAUCUGCUAAAGCGAAU
Plate 1	D04	L-014564-01	J-014564-14	PIF1	80119	NM_025049	82546871	GGGAAUAUGAGGACUCGGA
Plate 1	D04	L-014564-01	J-014564-15	PIF1	80119	NM_025049	82546871	GAAGACAGGUGCUCCGGAA
Plate 1	D04	L-014564-01	J-014564-16	PIF1	80119	NM_025049	82546871	GUACACAGAUUUGAGGCUA
Plate 1	D05	L-013801-00	J-013801-05	SMARCAD1	56916	NM_020159	14149729	CCACACAUGUUUAGUAGUA
Plate 1	D05	L-013801-00	J-013801-06	SMARCAD1	56916	NM_020159	14149729	GAGGAUGGCUAUAAAGGUA
Plate 1	D05	L-013801-00	J-013801-07	SMARCAD1	56916	NM_020159	14149729	GGCCAAUCAUCCUUUAUUA
Plate 1	D05	L-013801-00	J-013801-08	SMARCAD1	56916	NM_020159	14149729	GCACGUAGAAAUGAUGAUA
Plate 1	D06	L-009848-01	J-009848-09	INO80B	83444	NM_031288	323276648	GGCUGGAUGAAGACAGUAA
Plate 1	D06	L-009848-01	J-009848-10	INO80B	83444	NM_031288	323276648	AUAAUGAAGAGGAACCUAU
Plate 1	D06	L-009848-01	J-009848-11	INO80B	83444	NM_031288	13775201	UAAAUUACAUCCGGUGCAA
Plate 1	D06	L-009848-01	J-009848-12	INO80B	83444	NM_031288	323276648	GGACCUAUCAGGAGGGUUA
Plate 1	D07	L-020843-00	J-020843-09	TIPIN	54962	NM_017858	8923484	GAGAGGACUUCCAGCCUUA
Plate 1	D07	L-020843-00	J-020843-10	TIPIN	54962	NM_017858	8923484	GGACAAUCCAUGUAAUGAU
Plate 1	D07	L-020843-00	J-020843-11	TIPIN	54962	NM_017858	8923484	UGAAUUAGAUCCCUUUCUG
Plate 1	D07	L-020843-00	J-020843-12	TIPIN	54962	NM_017858	8923484	CGACUUGAUCUCCCUAUUU
Plate 1	D08	L-021146-02	J-021146-11	WRAP53	55135	NM_001143992	221136865	GCAGAAGAAGCAAACGGGA
Plate 1	D08	L-021146-02	J-021146-12	WRAP53	55135	NM_001143992	221136865	CUGAUAACAUCUUGCGAAU
Plate 1	D08	L-021146-02	J-021146-13	WRAP53	55135	NM_001143992	221136865	AGAAGAAGCGAACGGGCCA
Plate 1	D08	L-021146-02	J-021146-14	WRAP53	55135	NM_001143992	221136865	UUUGGAGACUCAACCGUUA
Plate 1	D09	L-021037-02	J-021037-17	COPS4	51138	NM_016129	38373689	CAAUAGUCCACGAAAGUGA
Plate 1	D09	L-021037-02	J-021037-18	COPS4	51138	NM_016129	38373689	CAGUCCAGGCAGAGGCUUA
Plate 1	D09	L-021037-02	J-021037-19	COPS4	51138	NM_016129	38373689	AAUGAUAACCGAAGGACGU
Plate 1	D09	L-021037-02	J-021037-20	COPS4	51138	NM_016129	38373689	CAACGUGGGAUAAGCAGAU
Plate 1	D10	L-019951-00	J-019951-05	TINF2	26277	NM_012461	6912715	AGGAAGAACAUGCGAUAUA
Plate 1	D10	L-019951-00	J-019951-06	TINF2	26277	NM_012461	6912715	CAACCCAGGUCAUAUCUAA
Plate 1	D10	L-019951-00	J-019951-07	TINF2	26277	NM_012461	6912715	GGAAGUAUAAGGGUCCAUA
Plate 1	D10	L-019951-00	J-019951-08	TINF2	26277	NM_012461	6912715	GUACUGGAGUUUCUGCGAU
Plate 1	D11	L-020341-00	J-020341-05	MYBBP1A	10514	NM_014520	7657350	UCGCAGACCUCCUGUUGAA
Plate 1	D11	L-020341-00	J-020341-06	MYBBP1A	10514	NM_014520	7657350	CGACCGCUAUGGCCUAUUG
Plate 1	D11	L-020341-00	J-020341-07	MYBBP1A	10514	NM_014520	7657350	CGACUUGAAUAUAAUACUC
Plate 1	D11	L-020341-00	J-020341-08	MYBBP1A	10514	NM_014520	7657350	CCCCAGAGAUGGACGAUUA

Plate	E02	L-032694-01	J-032694-05	HAUS7	55559	NM_207106	66346718	CUGUGGAGGUGUUCGG
Plate	E02	L-032694-01	J-032694-06	HAUS7	55559	NM_207106	66346718	AGAUCCAAGAAAUGACG
Plate	E02	L-032694-01	J-032694-07	HAUS7	55559	NM_207106	66346718	ACGACUACUCAGAGGAC
Plate	E02	L-032694-01	J-032694-08	HAUS7	55559	NM_207106	66346718	UGAAGAAGCAGCAAGGC
Plate	E03	L-032280-00	J-032280-05	TREX2	11219	NM_080701	63079717	CCGGAAGGCUGGCUUU
Plate	E03	L-032280-00	J-032280-06	TREX2	11219	NM_080701	63079717	CGACGAGUCUGGUGCC
Plate	E03	L-032280-00	J-032280-07	TREX2	11219	NM_080701	63079717	ACAAUGGCUUUGAUUAU
Plate	E03	L-032280-00	J-032280-08	TREX2	11219	NM_080701	63079717	CCAUGUACUUGCCGCCU
Plate	E04	L-006835-00	J-006835-05	NCAPG	64151	NM_022346	50658080	GGAGGCUGCUGUCGAU
Plate	E04	L-006835-00	J-006835-06	NCAPG	64151	NM_022346	50658080	GCAGUGAGAUUUAGAGU
Plate	E04	L-006835-00	J-006835-07	NCAPG	64151	NM_022346	50658080	GCAAAUUGAUGAUGUCA
Plate	E04	L-006835-00	J-006835-08	NCAPG	64151	NM_022346	50658080	AUUCAUAGGUCAACAAU
Plate	E05	L-012377-00	J-012377-05	TEP1	7011	NM_007110	21536370	GAACUGAAGAGCUACCU
Plate	E05	L-012377-00	J-012377-06	TEP1	7011	NM_007110	21536370	GCAUGCGGGUUGCCAG
Plate	E05	L-012377-00	J-012377-07	TEP1	7011	NM_007110	21536370	GAUGGAUGGUCCCUGA
Plate	E05	L-012377-00	J-012377-08	TEP1	7011	NM_007110	21536370	GAGAAUGGACCACAGGU
Plate	E06	L-003873-00	J-003873-09	BARD1	580	NM_000465	4557348	UGGUUUAGCCCUCGAA
Plate	E06	L-003873-00	J-003873-10	BARD1	580	NM_000465	4557348	GAGCACAUCUUCUGUAG
Plate	E06	L-003873-00	J-003873-11	BARD1	580	NM_000465	4557348	CGACAUACCUUCUGUUG
Plate	E06	L-003873-00	J-003873-12	BARD1	580	NM_000465	4557348	UCAGAUAUGUUGUGAGU
Plate	E07	L-015831-02	J-015831-18	COPS8	10920	NM_006710	40805828	GAAAUGAGUUGUAUGGU
Plate	E07	L-015831-02	J-015831-19	COPS8	10920	NM_006710	40805828	GCAUAUUAGAACAAGGA
Plate	E07	L-015831-02	J-015831-20	COPS8	10920	NM_006710	40805828	GAGACGGUCCAGCCAAU
Plate	E07	L-015831-02	J-015831-21	COPS8	10920	NM_006710	40805828	CAAGCUGAUUCCACCAC
Plate	E08	L-011237-00	J-011237-05	CDC5L	988	NM_001253	16357499	CGAGACAAGUUAAACAU
Plate	E08	L-011237-00	J-011237-06	CDC5L	988	NM_001253	16357499	GAGAGGAGUUGAUUAUA
Plate	E08	L-011237-00	J-011237-07	CDC5L	988	NM_001253	16357499	CGAGGAAUCUGGCAUAA
Plate	E08	L-011237-00	J-011237-08	CDC5L	988	NM_001253	16357499	GCUCUCAAGUGAAGCUU
Plate	E09	L-017227-02	J-017227-17	NDNL2	56160	NM_138704	29826297	GCAUUUAAUUUUCGGAG
Plate	E09	L-017227-02	J-017227-18	NDNL2	56160	NM_138704	29826297	ACUUUGUGCGACAGCG
Plate	E09	L-017227-02	J-017227-19	NDNL2	56160	NM_138704	29826297	UCCAGUACGUCUUCGG
Plate	E09	L-017227-02	J-017227-20	NDNL2	56160	NM_138704	29826297	GCUGUAAACGCUUCAAU
Plate	E10	L-018070-00	J-018070-05	NSMCE2	286053	NM_173685	27734760	GCUGUUCAAUCUACAAU
Plate	E10	L-018070-00	J-018070-06	NSMCE2	286053	NM_173685	27734760	GCAACUAAACCAUUAUG
Plate	E10	L-018070-00	J-018070-07	NSMCE2	286053	NM_173685	27734760	GCACUUAGAAGGGCAAU
Plate	E10	L-018070-00	J-018070-08	NSMCE2	286053	NM_173685	27734760	CAACUGGUUUCAUCUCC
Plate	E11	L-017244-00	J-017244-05	SMARCD1	6602	NM_139071	21264347	GGCAAUAUAUUAAGACA
Plate	E11	L-017244-00	J-017244-06	SMARCD1	6602	NM_139071	21264347	UAAGUCAGAUGCCGAGG
Plate	E11	L-017244-00	J-017244-07	SMARCD1	6602	NM_139071	21264347	UUAAUCAUGUCAUCAGU
Plate	E11	L-017244-00	J-017244-08	SMARCD1	6602	NM_139071	21264347	GACAAUGACUGAUGUGG
Plate	F02	L-018557-01	J-018557-09	MCRS1	10445	NM_00101230	59799165	GGCAUGAGCUCUCCGG
Plate	F02	L-018557-01	J-018557-10	MCRS1	10445	NM_00101230	59799165	GAGGAAGAAGUUCGAUG
Plate	F02	L-018557-01	J-018557-11	MCRS1	10445	NM_00101230	59799165	CUGGAAGAUAUCCCGGA
Plate	F02	L-018557-01	J-018557-12	MCRS1	10445	NM_00101230	59799165	AGCUCAAGGACAUGCGA
Plate	F03	L-015684-01	J-015684-09	RMI2	116028	NM_152308	24308244	UCAGAGAUGUUGAGACG
Plate	F03	L-015684-01	J-015684-10	RMI2	116028	NM_152308	24308244	ACUCAAACAUUUAGACG
Plate	F03	L-015684-01	J-015684-11	RMI2	116028	NM_152308	24308244	AUAACCAGUUUGCGAGU
Plate	F03	L-015684-01	J-015684-12	RMI2	116028	NM_152308	24308244	GCAGGGUAGUGAUGGC
Plate	F04	L-018972-00	J-018972-05	PINX1	54984	NM_017884	31982866	UGACGCAGGUAGAACGU
Plate	F04	L-018972-00	J-018972-06	PINX1	54984	NM_017884	14874755	AGCCACAGAUCAUAUUA
Plate	F04	L-018972-00	J-018972-07	PINX1	54984	NM_017884	14874755	UGGCCGAACUGAACACU
Plate	F04	L-018972-00	J-018972-08	PINX1	54984	NM_017884	14874755	GGUCUAAAGGAAAGGGU
Plate	F05	L-017522-00	J-017522-05	SMARCE1	6605	NM_003079	45827732	AAACGAAUACGAAGCAG
Plate	F05	L-017522-00	J-017522-06	SMARCE1	6605	NM_003079	45827732	GAAAGGAGAACCGUACA
Plate	F05	L-017522-00	J-017522-07	SMARCE1	6605	NM_003079	45827732	CCGCGUACCUUGCUUAC
Plate	F05	L-017522-00	J-017522-08	SMARCE1	6605	NM_003079	45827732	CAAGAUUAUUGGUGGCA
Plate	F06	L-019553-00	J-019553-05	CUL5	8065	NM_003478	67514034	GACACGACGUCUUAUAU
Plate	F06	L-019553-00	J-019553-06	CUL5	8065	NM_003478	67514034	GCAAAUAGAGUGGCUAA
Plate	F06	L-019553-00	J-019553-07	CUL5	8065	NM_003478	67514034	UAAACAAGCUUGCUAGA
Plate	F06	L-019553-00	J-019553-08	CUL5	8065	NM_003478	67514034	CGUCUAAUCUGUUAAAG
Plate	F07	L-010813-00	J-010813-05	SMARCC1	6599	NM_003074	21237801	GAGCAGACCAAUCACAU
Plate	F07	L-010813-00	J-010813-06	SMARCC1	6599	NM_003074	21237801	GUACUGACAUUUACUCC
Plate	F07	L-010813-00	J-010813-07	SMARCC1	6599	NM_003074	21237801	GAACAUUUACGGAUGAG
Plate	F07	L-010813-00	J-010813-08	SMARCC1	6599	NM_003074	21237801	CAACACCUGUACCCAAU
Plate	F08	L-005814-00	J-005814-07	COPS5	10987	NM_006837	38027922	UAGAAACGCAUGACCGA
Plate	F08	L-005814-00	J-005814-08	COPS5	10987	NM_006837	38027922	GGACUAAGGAUCACCAU
Plate	F08	L-005814-00	J-005814-09	COPS5	10987	NM_006837	38027922	GCAAUCGGGUGGUAUC
Plate	F08	L-005814-00	J-005814-10	COPS5	10987	NM_006837	38027922	CUUGAGCUGUUGUGGA
Plate	F09	L-003208-00	J-003208-10	CCNB3	85417	NM_033670	16306524	GUCUCAAGGCUGUGUA
Plate	F09	L-003208-00	J-003208-11	CCNB3	85417	NM_033670	16306524	GCGCAGAUAUGCUAGG
Plate	F09	L-003208-00	J-003208-12	CCNB3	85417	NM_033670	16306524	UGAACAAACUGCUGACU
Plate	F09	L-003208-00	J-003208-13	CCNB3	85417	NM_033670	16306524	CAACUCACCUCGUGUGG
Plate	F10	L-010638-01	J-010638-09	STAG1	10274	NM_005862	62243695	GAAUAGAGAUGUUUCGA
Plate	F10	L-010638-01	J-010638-10	STAG1	10274	NM_005862	62243695	UCAAGAAAUCGGCGAGA
Plate	F10	L-010638-01	J-010638-11	STAG1	10274	NM_005862	62243695	GAUUAGAGCCAUUUGUA
Plate	F10	L-010638-01	J-010638-12	STAG1	10274	NM_005862	62243695	GAAUGUUGGUGAAUGU
Plate	F11	L-007157-00	J-007157-05	NSMCE1	197370	NM_145080	39725702	GAACUGGAUUUGUUUAG
Plate	F11	L-007157-00	J-007157-06	NSMCE1	197370	NM_145080	39725702	GGAACUGAUUAUUGACU
Plate	F11	L-007157-00	J-007157-07	NSMCE1	197370	NM_145080	39725702	GGAGUCUGGUGUCUUG
Plate	F11	L-007157-00	J-007157-08	NSMCE1	197370	NM_145080	39725702	GAUGACCCAUGGCGUG

Plate 1	G02	L-019912-00	J-019912-05	PPP4R1	9989	NM_005134	4826933	GCCCGGAGUUUGCUCGAUA
Plate 1	G02	L-019912-00	J-019912-06	PPP4R1	9989	NM_005134	4826933	CAGGAUAGGUGUUCUUAAA
Plate 1	G02	L-019912-00	J-019912-07	PPP4R1	9989	NM_005134	4826933	GGAGAUAUUUGCAGUGUAG
Plate 1	G02	L-019912-00	J-019912-08	PPP4R1	9989	NM_005134	4826933	GAUCAGGAAUUGUAUAACU
Plate 1	G03	L-008312-00	J-008312-05	SMARCC2	6601	NM_139067	21237807	UCACUAAACUGCCGAUCAA
Plate 1	G03	L-008312-00	J-008312-06	SMARCC2	6601	NM_139067	21237807	GAGAAGCACUGGAGUAUCA
Plate 1	G03	L-008312-00	J-008312-07	SMARCC2	6601	NM_139067	21237807	GCUACUAUCCUGACAGUUA
Plate 1	G03	L-008312-00	J-008312-08	SMARCC2	6601	NM_139067	21237807	UAAGAAAGGUCCCUCAACA
Plate 1	G04	L-016462-01	J-016462-09	WDR48	57599	NM_020839	21314694	CUUAAAGGGCACACGGAUA
Plate 1	G04	L-016462-01	J-016462-10	WDR48	57599	NM_020839	21314694	CGUCAGAAGUCCACGUGAA
Plate 1	G04	L-016462-01	J-016462-11	WDR48	57599	NM_020839	21314694	ACACAUAAGGAUUACGUAA
Plate 1	G04	L-016462-01	J-016462-12	WDR48	57599	NM_020839	21314694	AAACAGAGAUGGCACGCAA
Plate 1	G05	L-017519-00	J-017519-05	HUS1B	135458	NM_148959	82659116	GGAUGACCCUGAGUAUAGA
Plate 1	G05	L-017519-00	J-017519-06	HUS1B	135458	NM_148959	82659116	GCAAAUACAUCCUACGACG
Plate 1	G05	L-017519-00	J-017519-07	HUS1B	135458	NM_148959	82659116	CAAAGGCUGUCUAGAGCUG
Plate 1	G05	L-017519-00	J-017519-08	HUS1B	135458	NM_148959	82659116	CAUGGAAGGUGUCUCGGAA
Plate 1	G06	L-013970-01	J-013970-09	ARID1B	57492	NM_175863	40068461	UGAUCAACAUGGCGGACAA
Plate 1	G06	L-013970-01	J-013970-10	ARID1B	57492	NM_175863	40068461	CCGAAUUACAAACGCCAUA
Plate 1	G06	L-013970-01	J-013970-11	ARID1B	57492	NM_175863	40068461	UCUCAAAGCAGACGGCAAA
Plate 1	G06	L-013970-01	J-013970-12	ARID1B	57492	NM_175863	40068461	ACGAGCAUCCAGAGAGAAA
Plate 1	G07	L-015461-01	J-015461-09	SMC1B	27127	NM_148674	71565159	AGGAAGAGGCAGAACGUUA
Plate 1	G07	L-015461-01	J-015461-10	SMC1B	27127	NM_148674	71565159	UCAAUAAAGGACAGCGAAA
Plate 1	G07	L-015461-01	J-015461-11	SMC1B	27127	NM_148674	71565159	UAGAGAAGUUAGAGGAGUA
Plate 1	G07	L-015461-01	J-015461-12	SMC1B	27127	NM_148674	71565159	GAGCAUGUGAAUAGGGAUU
Plate 1	G08	L-018625-01	J-018625-09	NFATC2IP	84901	NM_032815	46447822	GGAUACAGGCCACGAUAAA
Plate 1	G08	L-018625-01	J-018625-10	NFATC2IP	84901	NM_032815	46447822	GGGAUUUACACCACGCCUA
Plate 1	G08	L-018625-01	J-018625-11	NFATC2IP	84901	NM_032815	46447822	ACGUAGUGUCUGUGGACUU
Plate 1	G08	L-018625-01	J-018625-12	NFATC2IP	84901	NM_032815	46447822	GACAUUUGCUUGAGGCUUA
Plate 1	G09	L-003994-01	J-003994-09	INO80E	283899	NM_173618	27734726	CAUCAUCAGAUAACAGCGA
Plate 1	G09	L-003994-01	J-003994-10	INO80E	283899	NM_173618	27734726	CGGCAGAUGUUCAGCGAUG
Plate 1	G09	L-003994-01	J-003994-11	INO80E	283899	NM_173618	27734726	CCUUGGAUGGAGACGAUGA
Plate 1	G09	L-003994-01	J-003994-12	INO80E	283899	NM_173618	27734726	GCGCAAAGGAAAUUACUGA
Plate 1	G10	L-030080-00	J-030080-05	ANKRD52	283373	XM_370696	51471077	GGAACGAGCUGACAUCACA
Plate 1	G10	L-030080-00	J-030080-06	ANKRD52	283373	XM_370696	51471077	CAACGAGGCCGACUGUAAA
Plate 1	G10	L-030080-00	J-030080-07	ANKRD52	283373	XM_370696	51471077	GGAAUGGUCUAGCUUCUGU
Plate 1	G10	L-030080-00	J-030080-08	ANKRD52	283373	XM_370696	51471077	GAAGUGCGUUCCCUACUCU
Plate 1	G11	L-015710-01	J-015710-09	ANKRD44	91526	NM_153697	24233529	UCGCAAAUUUAUCGGUAAU
Plate 1	G11	L-015710-01	J-015710-10	ANKRD44	91526	NM_153697	24233529	CCACAGGGGCCAACGUUAA
Plate 1	G11	L-015710-01	J-015710-11	ANKRD44	91526	NM_153697	24233529	GCACUAUGCAGCUGCGAAU
Plate 1	G11	L-015710-01	J-015710-12	ANKRD44	91526	NM_153697	24233529	CUAUGGAAAUACAGCGCUU
Plate 1	H02	L-011007-00	J-011007-08	CDKN2A	1029	NM_058195	47132605	GAUCAUCAGUCACCGAAGG
Plate 1	H02	L-011007-00	J-011007-09	CDKN2A	1029	NM_058195	47132605	AAACACCGCUUCUGCCUUU
Plate 1	H02	L-011007-00	J-011007-10	CDKN2A	1029	NM_058195	47132605	UAACGUAGAUAUAUGCCUU
Plate 1	H02	L-011007-00	J-011007-11	CDKN2A	1029	NM_058195	47132605	CAGAACCAAAGCUCAAAUA
Plate 1	H03	L-021351-00	J-021351-05	STAG2	10735	NM_006603	31563530	GAAAUUUACUUGCAGCAUU
Plate 1	H03	L-021351-00	J-021351-06	STAG2	10735	NM_006603	31563530	GUAGAUGAUUGGAUAGAAU
Plate 1	H03	L-021351-00	J-021351-07	STAG2	10735	NM_006603	31563530	GGGAUUUAUUUGCUUGUAA
Plate 1	H03	L-021351-00	J-021351-08	STAG2	10735	NM_006603	31563530	CCACUGAUGUCUUACCGAA
Plate 1	H04	L-027334-00	J-027334-05	CORT	1325	NM_001302	56121821	GGAGAUUGGGCUUAAAAUA
Plate 1	H04	L-027334-00	J-027334-06	CORT	1325	NM_001302	56121821	CCAGUCAGCCCACAAGAUG
Plate 1	H04	L-027334-00	J-027334-07	CORT	1325	NM_001302	56121821	GACCUUCUCCUCCUGCAAA
Plate 1	H04	L-027334-00	J-027334-08	CORT	1325	NM_001302	56121821	GCCGAGACAGCGAGCAUAU
Plate 1	H05	L-034901-02	J-034901-17	EID3	493861	NM_001008394	56605997	CAAUAUUAGAGCCGAUGAA
Plate 1	H05	L-034901-02	J-034901-18	EID3	493861	NM_001008394	56605997	UGAAUUGGAUGGAAGGCGA
Plate 1	H05	L-034901-02	J-034901-19	EID3	493861	NM_001008394	56605997	UUGCAAACCUACUUUCGAA
Plate 1	H05	L-034901-02	J-034901-20	EID3	493861	NM_001008394	56605997	CGAACAACUCCUUAACCGA
Plate 1	H06	L-014895-00	J-014895-05	SLX4	84464	NM_032444	63252862	UCAAACGGCACUCAGAUAA
Plate 1	H06	L-014895-00	J-014895-06	SLX4	84464	NM_032444	63252862	GCGGAGACUUUGUUGAAAU
Plate 1	H06	L-014895-00	J-014895-07	SLX4	84464	NM_032444	63252862	CAAGUGAGCCCGAGGAACA
Plate 1	H06	L-014895-00	J-014895-08	SLX4	84464	NM_032444	63252862	UCAGAGCCGUCCCAAAUAA
Plate 1	H07	L-027056-00	J-027056-05	AMN1	196394	NM_207337	46559738	GAUCUACGGAGCUGCGAUA
Plate 1	H07	L-027056-00	J-027056-06	AMN1	196394	NM_207337	46559738	CGAUUUAGGUGGCUGCUUA
Plate 1	H07	L-027056-00	J-027056-07	AMN1	196394	NM_207337	46559738	GGUGUGAUUGCACUUGUUA
Plate 1	H07	L-027056-00	J-027056-08	AMN1	196394	NM_207337	46559738	CAUGGACUGUUUAUUGAUG
Plate 1	H08	L-014117-01	J-014117-09	SMC5	23137	NM_015110	24850455	CGAAAUAAUUGAUAAGCGA
Plate 1	H08	L-014117-01	J-014117-10	SMC5	23137	NM_015110	24850455	GAAAGAAUUGAACGGGUAA
Plate 1	H08	L-014117-01	J-014117-11	SMC5	23137	NM_015110	24850455	GAAACUUGUUACCGAAUUA
Plate 1	H08	L-014117-01	J-014117-12	SMC5	23137	NM_015110	24850455	GAACAGGGAAGUCGAGCAU
Plate 1	H09	L-018283-01	J-018283-09	NCAPG2	54892	NM_017760	116812585	ACGGAAGGUUUCUGACGUA
Plate 1	H09	L-018283-01	J-018283-10	NCAPG2	54892	NM_017760	40255236	CCUCAGUAGAUAAGGCGUA
Plate 1	H09	L-018283-01	J-018283-11	NCAPG2	54892	NM_017760	116812585	CUUCAUGUUCCACGGGAUA
Plate 1	H09	L-018283-01	J-018283-12	NCAPG2	54892	NM_017760	116812585	GGCCAAACUUUACACGAUU
Plate 1	H10	L-187549-00	J-187549-01	TEN1	100134934	NM_001113324	164519030	AUGAUUCAGUCCAGAGUAA
Plate 1	H10	L-187549-00	J-187549-02	TEN1	100134934	NM_001113324	164519030	GGGAGCACGCUGAGAACAU
Plate 1	H10	L-187549-00	J-187549-03	TEN1	100134934	NM_001113324	164519030	GGGAGCAGAGACUGUACAA
Plate 1	H10	L-187549-00	J-187549-04	TEN1	100134934	NM_001113324	164519030	GGUUAGUGCAGGCCAAGUU
Plate 1	H11	L-017845-01	J-017845-09	SMG6	23293	NM_017575	30425541	CCAGUGAUACAGCGAAUUA
Plate 1	H11	L-017845-01	J-017845-10	SMG6	23293	NM_017575	30425541	CAGAUUGGAUGCUCGGCUA
Plate 1	H11	L-017845-01	J-017845-11	SMG6	23293	NM_017575	30425541	GCAGCAAGCCAUUACGCAA
Plate 1	H11	L-017845-01	J-017845-12	SMG6	23293	NM_017575	30425541	UGGAGAAAACCUCGGAUAA

Plate 2	A02	L-008692-01	J-008692-09	PBRM1	55193	NM_181042	93102368	GUUAGGAGUUGUCGGAAUA
Plate 2	A02	L-008692-01	J-008692-10	PBRM1	55193	NM_181042	93102368	AGCUAAAUUUGCCGAGUUA
Plate 2	A02	L-008692-01	J-008692-11	PBRM1	55193	NM_181042	93102368	AUAUAGAUCUCCUCGCAAA
Plate 2	A02	L-008692-01	J-008692-12	PBRM1	55193	NM_181042	93102368	UGACAUGUAUUCUCGGAAA
Plate 2	A03	L-017017-00	J-017017-05	COPS6	10980	NM_006833	38027945	CGAAAUAUCGAGGUGAUGA
Plate 2	A03	L-017017-00	J-017017-06	COPS6	10980	NM_006833	38027945	UUUCUGAAGUUGAACCCUA
Plate 2	A03	L-017017-00	J-017017-07	COPS6	10980	NM_006833	38027945	CCACGUAGCCCGAAUGACA
Plate 2	A03	L-017017-00	J-017017-08	COPS6	10980	NM_006833	38027945	CAGACAAGUUCAAGACAGA
Plate 2	A04	L-012795-00	J-012795-05	PAXIP1	22976	NM_007349	40804749	UGUUUGCAAUUGCGGAUUA
Plate 2	A04	L-012795-00	J-012795-06	PAXIP1	22976	NM_007349	40804749	CAACUGGUUUAAAGUAUGA
Plate 2	A04	L-012795-00	J-012795-07	PAXIP1	22976	NM_007349	40804749	AGGCAUAGAUGUUCACAAU
Plate 2	A04	L-012795-00	J-012795-08	PAXIP1	22976	NM_007349	40804749	CAAAUAUACGGGUUAUCUA
Plate 2	A05	L-016177-01	J-016177-09	RAD9B	144715	NM_152442	41393615	GCACGAGUUUGCAUGUUUA
Plate 2	A05	L-016177-01	J-016177-10	RAD9B	144715	NM_152442	169234616	AGGAAGUGUUAACUGGCAA
Plate 2	A05	L-016177-01	J-016177-11	RAD9B	144715	NM_152442	169234616	CACAUUAGCUGAUGAACAA
Plate 2	A05	L-016177-01	J-016177-12	RAD9B	144715	NM_152442	169234616	GGCAAGAGCAAGUGACAGU
Plate 2	A06	L-019327-01	J-019327-09	INO80C	125476	NM_194281	42822883	UGAGGAAGGCCACGAGCAU
Plate 2	A06	L-019327-01	J-019327-10	INO80C	125476	NM_194281	42822883	GAAACAAAUCCUCGCUUCU
Plate 2	A06	L-019327-01	J-019327-11	INO80C	125476	NM_194281	42822883	CAGAGCAAACUGCGGUUCA
Plate 2	A06	L-019327-01	J-019327-12	INO80C	125476	NM_194281	42822883	GCGCAGUAGCUGGCAAGAA
Plate 2	A07	L-015648-00	J-015648-05	NFRKB	4798	NM_006165	23346419	CAUCAUGACUCGAGUAAAU
Plate 2	A07	L-015648-00	J-015648-06	NFRKB	4798	NM_006165	23346419	GGCAGGAAGUGUUAAGUGA
Plate 2	A07	L-015648-00	J-015648-07	NFRKB	4798	NM_006165	23346419	CAGGAGCGUUACAGGUAUA
Plate 2	A07	L-015648-00	J-015648-08	NFRKB	4798	NM_006165	23346419	GCUUAAGGACUCCCAGUUU
Plate 2	A08	L-013007-00	J-013007-05	PPP4R4	57718	NM_020958	17402883	CGACAGAAUCCCACUGAGA
Plate 2	A08	L-013007-00	J-013007-06	PPP4R4	57718	NM_020958	17402883	AUAGAAAGAUUGACAGUCG
Plate 2	A08	L-013007-00	J-013007-07	PPP4R4	57718	NM_020958	17402883	GCUCAGUGCUGGUCAAGAU
Plate 2	A08	L-013007-00	J-013007-08	PPP4R4	57718	NM_020958	17402883	GCGAUGGAUUUCAGUCAGA
Plate 2	A09	L-016186-01	J-016186-09	NCAPH2	29781	NM_014551	34303963	GGACUAACGUGGAUCUCAA
Plate 2	A09	L-016186-01	J-016186-10	NCAPH2	29781	NM_014551	34303963	AGGCAGCGUUGUUGAUCCA
Plate 2	A09	L-016186-01	J-016186-11	NCAPH2	29781	NM_014551	34303963	UGUACAGCCGUCAGGGUGA
Plate 2	A09	L-016186-01	J-016186-12	NCAPH2	29781	NM_014551	34303963	CGGAAGGAUUUCAGGAUGA
Plate 2	A10	L-032350-02	J-032350-19	SUMO4	387082	NM_001002255	50400080	CGAAAAGCCCACAGAAGAA
Plate 2	A10	L-032350-02	J-032350-20	SUMO4	387082	NM_001002255	50400080	GCAACCAAUCAGUGGAACA
Plate 2	A10	L-032350-02	J-032350-21	SUMO4	387082	NM_001002255	50400080	AGACCAAGAUUACUGCAUU
Plate 2	A10	L-032350-02	J-032350-22	SUMO4	387082	NM_001002255	50400080	GAAGUAACUGGUAUGUGUA
Plate 2	A11	L-026945-01	J-026945-09	ARID2	196528	NM_152641	56549667	CUAUACAUGCUCACGGAAA
Plate 2	A11	L-026945-01	J-026945-10	ARID2	196528	NM_152641	56549667	GCAAUUAGGCCUUGACACA
Plate 2	A11	L-026945-01	J-026945-11	ARID2	196528	NM_152641	56549667	CCAAAUAAAGUAGGAGUUA
Plate 2	A11	L-026945-01	J-026945-12	ARID2	196528	NM_152641	56549667	GCUGAAAUCAUGUGGGUAU
Plate 2	B02	L-027983-01	J-027983-09	RIF1	55183	NM_018151	56676334	CCUCAAAUGAAAUGCGAAA
Plate 2	B02	L-027983-01	J-027983-10	RIF1	55183	NM_018151	56676334	UCACGUAGCCCUAAAUUUA
Plate 2	B02	L-027983-01	J-027983-11	RIF1	55183	NM_018151	56676334	GAAUCAAAUCUAAGGACUA
Plate 2	B02	L-027983-01	J-027983-12	RIF1	55183	NM_018151	56676334	GCAAGUUCCUGAUGAUUUA
Plate 2	B03	L-027284-00	J-027284-05	SMEK2	57223	NM_020463	39930396	CCAUCUAUAUUGCGUAGUA
Plate 2	B03	L-027284-00	J-027284-06	SMEK2	57223	NM_020463	39930396	GCGGAUAAUUGGACUUAAA
Plate 2	B03	L-027284-00	J-027284-07	SMEK2	57223	NM_020463	39930396	CCACAUGUGAACUCAAUAA
Plate 2	B03	L-027284-00	J-027284-08	SMEK2	57223	NM_020463	39930396	UGAAACUAGUCAUCUGAUU
Plate 2	B04	L-031625-00	J-031625-05	UBE2NL	389898	NM_001012989	61175264	GGUCAUUGCUGGGGAAUCA
Plate 2	B04	L-031625-00	J-031625-06	UBE2NL	389898	NM_001012989	61175264	AAACGUGAACUAUUACUUG
Plate 2	B04	L-031625-00	J-031625-07	UBE2NL	389898	NM_001012989	61175264	GAUCCAAUCAUUAAGUGUG
Plate 2	B04	L-031625-00	J-031625-08	UBE2NL	389898	NM_001012989	61175264	AAUAUGCUCUCUAUCCAAG
Plate 2	B05	L-014646-01	J-014646-09	PPP6R3	55291	NM_018312	55925644	CCAAAGUAUUAGGCGGUUU
Plate 2	B05	L-014646-01	J-014646-10	PPP6R3	55291	NM_018312	55925644	GAGGAACACGGUAGAUCUA
Plate 2	B05	L-014646-01	J-014646-11	PPP6R3	55291	NM_018312	55925644	CCAUUCAGCUUGUUCAGUA
Plate 2	B05	L-014646-01	J-014646-12	PPP6R3	55291	NM_018312	55925644	GGGGAUUACUGGUAGAUAA
Plate 2	B06	L-020757-01	J-020757-09	INO80D	54891	NM_017759	38488717	CGGGCAGAAUCUCGUCAAA
Plate 2	B06	L-020757-01	J-020757-10	INO80D	54891	NM_017759	38488717	GCUAUUGAAUGGGCGUAUA
Plate 2	B06	L-020757-01	J-020757-11	INO80D	54891	NM_017759	38488717	CUGAUGAGUUGCCGGAUGA
Plate 2	B06	L-020757-01	J-020757-12	INO80D	54891	NM_017759	38488717	CGGCAUACGUUUAGGAAAG
Plate 2	B07	L-014151-01	J-014151-09	CRY2	1408	NM_021117	29789121	GGGACUACAUCAGGCGAUA
Plate 2	B07	L-014151-01	J-014151-10	CRY2	1408	NM_021117	29789121	GGGCAGAGAUAGAGCGAGC
Plate 2	B07	L-014151-01	J-014151-11	CRY2	1408	NM_021117	29789121	UGGAAGUAGUGACGGAGAA
Plate 2	B07	L-014151-01	J-014151-12	CRY2	1408	NM_021117	29789121	GGCUUAACAUUGAACGAAU
Plate 2	B08	L-024139-02	J-024139-21	UVSSA	57654	NM_020894	190358542	GAUAAUCAGUUGACCAAAA
Plate 2	B08	L-024139-02	J-024139-22	UVSSA	57654	NM_020894	190358542	GGCCAGGAGUUUAUAUGUA
Plate 2	B08	L-024139-02	J-024139-23	UVSSA	57654	NM_020894	190358542	GCUCGUGGAUCCAGCGCUU
Plate 2	B08	L-024139-02	J-024139-24	UVSSA	57654	NM_020894	190358542	GGUUCAGCACGGACGGAAU
Plate 2	B09	L-014585-01	J-014585-09	CTC1	80169	NM_025099	50055056	CCUCCUAGAUUUCGUCCAA
Plate 2	B09	L-014585-01	J-014585-10	CTC1	80169	NM_025099	50055056	CGGGACAGGUGUACCGACU
Plate 2	B09	L-014585-01	J-014585-11	CTC1	80169	NM_025099	50055056	UCAGAGGUGUGCAGCGAAA
Plate 2	B09	L-014585-01	J-014585-12	CTC1	80169	NM_025099	50055056	CAGAAAGUCUUGUCCGGUA
Plate 2	B10	L-014071-01	J-014071-09	PDS5A	23244	NM_015200	22094120	GAUAAACGGUGGCGAGUAA
Plate 2	B10	L-014071-01	J-014071-10	PDS5A	23244	NM_015200	22094120	CCAAUAAAGAUGUGCGUCU
Plate 2	B10	L-014071-01	J-014071-11	PDS5A	23244	NM_015200	22094120	GAACAGCAUUGACGACAAA
Plate 2	B10	L-014071-01	J-014071-12	PDS5A	23244	NM_015200	22094120	GAGAGAAAUAGCCCGGAAA
Plate 2	B11	L-015421-00	J-015421-05	CRY1	1407	NM_004075	19923246	CAGCAGCUUUCACGAUAUA
Plate 2	B11	L-015421-00	J-015421-06	CRY1	1407	NM_004075	19923246	GGAGUAGAAGUCAUUGUAA
Plate 2	B11	L-015421-00	J-015421-07	CRY1	1407	NM_004075	19923246	UAUAUGACCUAGACAAGAU
Plate 2	B11	L-015421-00	J-015421-08	CRY1	1407	NM_004075	19923246	CAACUGUUAUGGCGUGAAU

Plate 2	C02	L-003546-00	J-003546-13	TERF2	7014	NM_005652	21536372	GAACAAGCGCAUGACAAUA
Plate 2	C02	L-003546-00	J-003546-14	TERF2	7014	NM_005652	21536372	GCAAGGCAGCUACGGAAUC
Plate 2	C02	L-003546-00	J-003546-15	TERF2	7014	NM_005652	21536372	GACAGUACAACCAAUAUAA
Plate 2	C02	L-003546-00	J-003546-16	TERF2	7014	NM_005652	21536372	CCGAACAGCUGUGAUGAUU
Plate 2	C03	L-012376-00	J-012376-08	TCEB2	6923	NM_207013	46276892	GCCAAGAGCAGAAACACAA
Plate 2	C03	L-012376-00	J-012376-09	TCEB2	6923	NM_207013	46276892	GAACUGAAGCGCAUCGUCG
Plate 2	C03	L-012376-00	J-012376-10	TCEB2	6923	NM_207013	46276892	GGGCAGAUGACACCUUUGA
Plate 2	C03	L-012376-00	J-012376-11	TCEB2	6923	NM_207013	46276892	CAUGUCCACUCCCAGACGA
Plate 2	C04	L-010541-00	J-010541-09	TCEB1	6921	NM_005648	16933562	GGCCAUGAAUUUAUUGUAA
Plate 2	C04	L-010541-00	J-010541-10	TCEB1	6921	NM_005648	16933562	GCUGCGAACUUCUUAGAUU
Plate 2	C04	L-010541-00	J-010541-11	TCEB1	6921	NM_005648	16933562	GUACAAGGUUCGCUACACU
Plate 2	C04	L-010541-00	J-010541-12	TCEB1	6921	NM_005648	16933562	CAUGUGCUAUCGAAAGUAU
Plate 2	C05	L-026692-01	J-026692-09	POLD3	10714	NM_006591	38492355	ACGAAAACGCGUACUAAAA
Plate 2	C05	L-026692-01	J-026692-10	POLD3	10714	NM_006591	38492355	GGCAUUAUGUCUAGGACUA
Plate 2	C05	L-026692-01	J-026692-11	POLD3	10714	NM_006591	38492355	CAAUUAGUGGUUAGGGAAA
Plate 2	C05	L-026692-01	J-026692-12	POLD3	10714	NM_006591	38492355	UGUAUAGCAAGCUGAGUAA
Plate 2	C06	L-021198-01	J-021198-09	NCAPD2	9918	NM_014865	41281520	GGUAAGAAAGCUCGGACCA
Plate 2	C06	L-021198-01	J-021198-10	NCAPD2	9918	NM_014865	41281520	GAAAAUUACAUGAUGCGUA
Plate 2	C06	L-021198-01	J-021198-11	NCAPD2	9918	NM_014865	41281520	AGUCAGUGCUAGUAUGUAA
Plate 2	C06	L-021198-01	J-021198-12	NCAPD2	9918	NM_014865	41281520	GAGCAUAGUGGGAGAGAUU
Plate 2	C07	L-012853-01	J-012853-09	NCAPH	23397	NM_015341	81295814	CUUUAGGCCUCGACGCAAA
Plate 2	C07	L-012853-01	J-012853-10	NCAPH	23397	NM_015341	81295814	GGGCAGAUCCCUCGUGAAU
Plate 2	C07	L-012853-01	J-012853-11	NCAPH	23397	NM_015341	81295814	UGACAGCGCUCUCCGGAAA
Plate 2	C07	L-012853-01	J-012853-12	NCAPH	23397	NM_015341	81295814	GCAAAAGGGCAGCCGGCAA
Plate 2	C08	L-007167-00	J-007167-05	SHPRH	257218	NM_173082	27436872	GCACAAAUCAGUCGUGUUA
Plate 2	C08	L-007167-00	J-007167-06	SHPRH	257218	NM_173082	27436872	AAAGAAAUCUCGUAUGUCU
Plate 2	C08	L-007167-00	J-007167-07	SHPRH	257218	NM_173082	27436872	GCCAGAAGCUAGUAAGAGA
Plate 2	C08	L-007167-00	J-007167-08	SHPRH	257218	NM_173082	27436872	GAAAUCACAUUAUCAAGGU
Plate 2	C09	L-004984-01	J-004984-09	MVP	9961	NM_005115	19913411	CCAUCGAAACGGCGGAUCA
Plate 2	C09	L-004984-01	J-004984-10	MVP	9961	NM_005115	19913411	GGAAGGAAGUGGAGGUCGU
Plate 2	C09	L-004984-01	J-004984-11	MVP	9961	NM_005115	19913411	CCACAACUACUGCGUGAUU
Plate 2	C09	L-004984-01	J-004984-12	MVP	9961	NM_005115	19913411	CAGGAUGUCAAGACCGGAA
Plate 2	C10	L-006448-00	J-006448-06	HLTF	6596	NM_139048	21071053	CCAGAUGACUUUCUAACUA
Plate 2	C10	L-006448-00	J-006448-07	HLTF	6596	NM_139048	21071053	GAUAGAGAAUGGUGGCAUA
Plate 2	C10	L-006448-00	J-006448-08	HLTF	6596	NM_139048	21071053	GCAGGAUCUUCUAAGGUUA
Plate 2	C10	L-006448-00	J-006448-09	HLTF	6596	NM_139048	21071053	GGAUUUGUGUUUACUCGUU
Plate 2	C11	L-007770-02	J-007770-21	HES1	3280	NM_005524	8400709	ACGAAGAGCAAGAAUAAAU
Plate 2	C11	L-007770-02	J-007770-22	HES1	3280	NM_005524	8400709	AGGCUGGAGAGGCGGCUAA
Plate 2	C11	L-007770-02	J-007770-23	HES1	3280	NM_005524	8400709	UCAACACGACACCGGAUAA
Plate 2	C11	L-007770-02	J-007770-24	HES1	3280	NM_005524	8400709	ACUGCAUGACCCAGAUCAA
Plate 2	D02	L-005143-00	J-005143-07	TCEB3	6924	NM_003198	4507388	GUAAAUAGCUUGCGAAAAC
Plate 2	D02	L-005143-00	J-005143-08	TCEB3	6924	NM_003198	4507388	AGAUGUACGUCGACCACUA
Plate 2	D02	L-005143-00	J-005143-09	TCEB3	6924	NM_003198	4507388	GAAAGGUGCCUGAUGUGUU
Plate 2	D02	L-005143-00	J-005143-10	TCEB3	6924	NM_003198	4507388	GACCAGGAGCCCAUUGUUU
Plate 2	D03	L-012610-00	J-012610-05	CUL4A	8451	NM_003589	57165422	GCACAGAUCCUUCCGUUUA
Plate 2	D03	L-012610-00	J-012610-06	CUL4A	8451	NM_003589	57165422	GAACAGCGAUCGUAAUCAA
Plate 2	D03	L-012610-00	J-012610-07	CUL4A	8451	NM_003589	57165422	GCAUGUGGAUUCAAAGUAA
Plate 2	D03	L-012610-00	J-012610-08	CUL4A	8451	NM_003589	57165422	GCGAGUACAUCAAGACUUU
Plate 2	D04	L-010224-00	J-010224-06	CUL3	8452	NM_003590	45827792	GAAGGAAUGUUUAGGGAUA
Plate 2	D04	L-010224-00	J-010224-07	CUL3	8452	NM_003590	45827792	GAGAUCAAGUUGUACGUUA
Plate 2	D04	L-010224-00	J-010224-08	CUL3	8452	NM_003590	45827792	GAAAGUAGACGACGACAGA
Plate 2	D04	L-010224-00	J-010224-09	CUL3	8452	NM_003590	45827792	GCACAUGAAGACUAUAGUA
Plate 2	D05	L-005279-00	J-005279-05	TOP3A	7156	NM_004618	52487034	UCGCCGACCUGCUGUCAAA
Plate 2	D05	L-005279-00	J-005279-06	TOP3A	7156	NM_004618	52487034	CCACACGGCUUGCCUAGUU
Plate 2	D05	L-005279-00	J-005279-07	TOP3A	7156	NM_004618	52487034	CAAAGAUGGUAUCGUAGAA
Plate 2	D05	L-005279-00	J-005279-08	TOP3A	7156	NM_004618	52487034	GAAACUAUCUGGAUGUGUA
Plate 2	D06	L-012272-00	J-012272-05	GPS1	2873	NM_004127	47078239	CCUUUAACGUGGACAUGUA
Plate 2	D06	L-012272-00	J-012272-06	GPS1	2873	NM_004127	47078239	GAAUGCACCUGACGUCAAC
Plate 2	D06	L-012272-00	J-012272-07	GPS1	2873	NM_004127	47078239	GAAUUGGUCUCAUGUGCUC
Plate 2	D06	L-012272-00	J-012272-08	GPS1	2873	NM_004127	47078239	UCACCAAGCUCAAGUGUGC
Plate 2	D07	L-010536-00	J-010536-05	SMARCB1	6598	NM_001007468	55956800	GUGACGAUCUGGAUUUGAA
Plate 2	D07	L-010536-00	J-010536-06	SMARCB1	6598	NM_001007468	55956800	GAAACUACCUCCGUAUGUU
Plate 2	D07	L-010536-00	J-010536-07	SMARCB1	6598	NM_001007468	55956800	GAUGACGCCUGAGAUGUUU
Plate 2	D07	L-010536-00	J-010536-08	SMARCB1	6598	NM_001007468	55956800	GGCAGAAGCCCGUGAAGUU
Plate 2	D08	L-017139-01	J-017139-09	C17orf70	80233	NM_025161	52851424	GCGGUUGACCAGCGGAACA
Plate 2	D08	L-017139-01	J-017139-10	C17orf70	80233	NM_025161	52851424	CCAUCAAGGUGUCGGCGGA
Plate 2	D08	L-017139-01	J-017139-11	C17orf70	80233	NM_025161	52851424	GAGAGGUGGCCAUGACCGA
Plate 2	D08	L-017139-01	J-017139-12	C17orf70	80233	NM_025161	52851424	GUGCAGUACCUCCGCCAGA
Plate 2	D09	L-004240-00	J-004240-07	TOP2B	7155	NM_001068	19913407	GAAGUUGUCUGUUGAGAGA
Plate 2	D09	L-004240-00	J-004240-08	TOP2B	7155	NM_001068	19913407	CGAAAGACCUAAAUACACA
Plate 2	D09	L-004240-00	J-004240-09	TOP2B	7155	NM_001068	19913407	GAUCAUAUGGGAUGUCUGA
Plate 2	D09	L-004240-00	J-004240-10	TOP2B	7155	NM_001068	19913407	GGUGUAUGAUGAAGAUGUA
Plate 2	D10	L-003279-00	J-003279-11	MDM2	4193	NM_006879	46488908	GCCAGUAUAUUAUGACUAA
Plate 2	D10	L-003279-00	J-003279-12	MDM2	4193	NM_006879	46488908	GAACAAGAGACCCUGGUUA
Plate 2	D10	L-003279-00	J-003279-13	MDM2	4193	NM_006879	46488908	GAAUUUAGACAACCUGAAA
Plate 2	D10	L-003279-00	J-003279-14	MDM2	4193	NM_006879	46488908	GAUGAGAAGCAACAACAUA
Plate 2	D11	L-003204-00	J-003204-09	CCNA1	8900	NM_003914	16306528	GAUAUAUCCUCCUGAAGUA
Plate 2	D11	L-003204-00	J-003204-10	CCNA1	8900	NM_003914	16306528	GGACUGAGAACCUGGCUAA
Plate 2	D11	L-003204-00	J-003204-11	CCNA1	8900	NM_003914	16306528	CAUAAAGCGUACCUUGAUA
Plate 2	D11	L-003204-00	J-003204-12	CCNA1	8900	NM_003914	16306528	UCCCGAUGCUUGUCAGAUA

Plate 2	E02	L-006557-00	J-006557-07	RNF4	6047	NM_002938	34305289	GCUAAUACUUGCCCAACUU
Plate 2	E02	L-006557-00	J-006557-08	RNF4	6047	NM_002938	34305289	GAAUGGACGUCUCAUCGUU
Plate 2	E02	L-006557-00	J-006557-09	RNF4	6047	NM_002938	34305289	GACAGAGACGUAUAUGUGA
Plate 2	E02	L-006557-00	J-006557-10	RNF4	6047	NM_002938	34305289	GCAAUAAAUUCUAGACAAG
Plate 2	E03	L-004910-00	J-004910-05	UBE2I	7329	NM_194260	35493995	GGGAAGGAGGCUUGUUUAA
Plate 2	E03	L-004910-00	J-004910-06	UBE2I	7329	NM_194260	35493995	GAAGUUUGCGCCCUCAUAA
Plate 2	E03	L-004910-00	J-004910-07	UBE2I	7329	NM_194260	35493995	GGCCAGCCAUCACAAUCAA
Plate 2	E03	L-004910-00	J-004910-08	UBE2I	7329	NM_194260	35493995	GAACCACCAUUAUUUCACC
Plate 2	E04	L-016005-00	J-016005-07	SUMO1	7341	NM_001005781	54792064	GUGCAUAUAUGAUACAGUU
Plate 2	E04	L-016005-00	J-016005-08	SUMO1	7341	NM_001005781	54792064	GCACUGAAAGUUACUGAAG
Plate 2	E04	L-016005-00	J-016005-09	SUMO1	7341	NM_001005781	54792064	CAUAAAUACUGGAAAUUGC
Plate 2	E04	L-016005-00	J-016005-10	SUMO1	7341	NM_001005781	54792064	AAUACUCAGUGUUCUGUUU
Plate 2	E05	L-004087-00	J-004087-07	RBX1	9978	NM_014248	22091459	GAAGCGCUUUGAAGUGAAA
Plate 2	E05	L-004087-00	J-004087-08	RBX1	9978	NM_014248	22091459	GGGAUAUUGUGGUUGAUAA
Plate 2	E05	L-004087-00	J-004087-09	RBX1	9978	NM_014248	22091459	GGAACCACAUUAUGGAUCU
Plate 2	E05	L-004087-00	J-004087-10	RBX1	9978	NM_014248	22091459	CAUAGAAUGUCAAGCUAAC
Plate 2	E06	L-013133-01	J-013133-09	POLR2L	5441	NM_021128	45359860	GUGGCAAGAUCGUCGGCAA
Plate 2	E06	L-013133-01	J-013133-10	POLR2L	5441	NM_021128	45359860	UCGAGAAGCUGCUCAAUUA
Plate 2	E06	L-013133-01	J-013133-11	POLR2L	5441	NM_021128	45359860	GGAAGGAACCAUCCAGUAA
Plate 2	E06	L-013133-01	J-013133-12	POLR2L	5441	NM_021128	45359860	CGUAAUGCCUGGCCGCAGU
Plate 2	E07	L-011357-00	J-011357-05	POLR2G	5436	NM_002696	4505946	GGACCCGUGUGGACAAGAA
Plate 2	E07	L-011357-00	J-011357-06	POLR2G	5436	NM_002696	4505946	AGAUGGAGUUUGAUCCUAA
Plate 2	E07	L-011357-00	J-011357-07	POLR2G	5436	NM_002696	4505946	ACGAUGAGAUCCGCUUAAA
Plate 2	E07	L-011357-00	J-011357-08	POLR2G	5436	NM_002696	4505946	GCUCCCUGAUGGACGAUUA
Plate 2	E08	L-004723-01	J-004723-09	POLR2F	5435	NM_021974	14602451	AGGCCAACCAGAAGCGAAU
Plate 2	E08	L-004723-01	J-004723-10	POLR2F	5435	NM_021974	14602451	GCUCAUCAUCACCGACUGA
Plate 2	E08	L-004723-01	J-004723-11	POLR2F	5435	NM_021974	14602451	CAUACAUGACCAAGUACGA
Plate 2	E08	L-004723-01	J-004723-12	POLR2F	5435	NM_021974	14602451	GGCUAGAUGACUUGGAGAA
Plate 2	E09	L-012683-00	J-012683-05	COPS2	9318	NM_004236	4759263	GCAAUGACGAAUUUAGUAA
Plate 2	E09	L-012683-00	J-012683-06	COPS2	9318	NM_004236	4759263	GCAUUAAGCAGUUUCCAAA
Plate 2	E09	L-012683-00	J-012683-07	COPS2	9318	NM_004236	4759263	GGUACACAGUUAUUAGAAA
Plate 2	E09	L-012683-00	J-012683-08	COPS2	9318	NM_004236	4759263	CUAAGGAGUUAAACAUAGA
Plate 2	E10	L-008486-00	J-008486-06	PPP4C	5531	NM_002720	4506026	GCACUGAGAUCUUUGACUA
Plate 2	E10	L-008486-00	J-008486-07	PPP4C	5531	NM_002720	4506026	GACAAUCGACCGAAAGCAA
Plate 2	E10	L-008486-00	J-008486-08	PPP4C	5531	NM_002720	4506026	GCACUUAAGGUUCGCUAUC
Plate 2	E10	L-008486-00	J-008486-09	PPP4C	5531	NM_002720	4506026	GGAGCCGGCUACCUAUUUG
Plate 2	E11	L-011545-01	J-011545-09	PER3	8863	NM_016831	8567387	CGGCAUAAAGUUCGAACGA
Plate 2	E11	L-011545-01	J-011545-10	PER3	8863	NM_016831	8567387	CGGAAGAAUUUAAACACGU
Plate 2	E11	L-011545-01	J-011545-11	PER3	8863	NM_016831	8567387	CCAAAGAGCUGCACGGUAU
Plate 2	E11	L-011545-01	J-011545-12	PER3	8863	NM_016831	8567387	AAGGGAAGCACAAGCGGAA
Plate 2	F02	L-019730-00	J-019730-05	SUMO3	6612	NM_006936	48928057	GCAAGCUGAUGAAGGCCUA
Plate 2	F02	L-019730-00	J-019730-06	SUMO3	6612	NM_006936	48928057	GCAGGGCACAGUUUCUAGA
Plate 2	F02	L-019730-00	J-019730-07	SUMO3	6612	NM_006936	48928057	GUGGUGCAGUUCAAGAUCA
Plate 2	F02	L-019730-00	J-019730-08	SUMO3	6612	NM_006936	48928057	GGGAUGAAUCUGUAACUUA
Plate 2	F03	L-016450-00	J-016450-05	SUMO2	6613	NM_001005849	54792070	GUACGUAGCUGUUACAUGU
Plate 2	F03	L-016450-00	J-016450-06	SUMO2	6613	NM_001005849	54792070	GCGUCUUGUUGUUUAAAUA
Plate 2	F03	L-016450-00	J-016450-07	SUMO2	6613	NM_001005849	54792070	UUGCAUACCUUGUUCAAUU
Plate 2	F03	L-016450-00	J-016450-08	SUMO2	6613	NM_001005849	54792070	GCUCUUAUCUUUAUAUUCC
Plate 2	F04	L-010542-00	J-010542-05	TERF1	7013	NM_003218	189409139	CAAAUUCUCAUAUGCCUUU
Plate 2	F04	L-010542-00	J-010542-06	TERF1	7013	NM_003218	9257244	CAGUAGUAGUCCUUUGAUA
Plate 2	F04	L-010542-00	J-010542-07	TERF1	7013	NM_003218	189409139	AGAGUAACCUAUAAGCAUG
Plate 2	F04	L-010542-00	J-010542-08	TERF1	7013	NM_003218	189409139	UACCAGAGUUAAAGCAUAU
Plate 2	F05	L-011979-01	J-011979-09	POLR2K	5440	NM_005034	62422569	ACUAAAAGAUUGGUCGUUU
Plate 2	F05	L-011979-01	J-011979-10	POLR2K	5440	NM_005034	62422569	GUUGUAUAGCUUUCGAUUU
Plate 2	F05	L-011979-01	J-011979-11	POLR2K	5440	NM_005034	62422569	ACUACUGUACUUAGGAAUA
Plate 2	F05	L-011979-01	J-011979-12	POLR2K	5440	NM_005034	62422569	AUAUAUAUCUGUGGAGAGU
Plate 2	F06	L-012249-01	J-012249-09	POLR2J	5439	NM_006234	62422568	CUAAUAAAGUAUAGCGGGA
Plate 2	F06	L-012249-01	J-012249-10	POLR2J	5439	NM_006234	62422568	GCUUUCGGGUGGCCAUAAA
Plate 2	F06	L-012249-01	J-012249-11	POLR2J	5439	NM_006234	62422568	UGUCCACAGUAGAGUUUAA
Plate 2	F06	L-012249-01	J-012249-12	POLR2J	5439	NM_006234	62422568	GCGGUGACUUCGCAAGCAA
Plate 2	F07	L-012247-01	J-012247-09	POLR2H	5437	NM_006232	14589952	GAAGUUUGACCGAGUGUCU
Plate 2	F07	L-012247-01	J-012247-10	POLR2H	5437	NM_006232	14589952	CUGACCAGUUUGAGUAUGU
Plate 2	F07	L-012247-01	J-012247-11	POLR2H	5437	NM_006232	14589952	GAAACUGACUCGCCUGUGA
Plate 2	F07	L-012247-01	J-012247-12	POLR2H	5437	NM_006232	14589952	CUGCAUUGUGAGAGUGAAU
Plate 2	F08	L-010431-00	J-010431-05	SMARCA4	6597	NM_003072	21071055	GCACACCGCUGCAGAACAA
Plate 2	F08	L-010431-00	J-010431-06	SMARCA4	6597	NM_003072	21071055	CCAAGCCGGUCGUGAGUGA
Plate 2	F08	L-010431-00	J-010431-07	SMARCA4	6597	NM_003072	21071055	GCGACUCACUGACGGAGAA
Plate 2	F08	L-010431-00	J-010431-08	SMARCA4	6597	NM_003072	21071055	GACCAGCACUCCCAAGGUU
Plate 2	F09	L-017253-00	J-017253-05	SMARCA2	6595	NM_139045	48255897	CAAAGCAGAUGAACGCUAU
Plate 2	F09	L-017253-00	J-017253-06	SMARCA2	6595	NM_139045	48255897	GAAAGGAGGUGCUAAGACA
Plate 2	F09	L-017253-00	J-017253-07	SMARCA2	6595	NM_139045	48255897	CCGCAUAGCUCAUAGGAUA
Plate 2	F09	L-017253-00	J-017253-08	SMARCA2	6595	NM_139045	48255897	CAACUUGAACGGAAUCUUA
Plate 2	F10	L-020131-01	J-020131-09	POLD2	5425	NM_006230	5453923	CGUGAUGCCAGGCGAGUUU
Plate 2	F10	L-020131-01	J-020131-10	POLD2	5425	NM_006230	5453923	AAGAUGAACUGCAGCGUAU
Plate 2	F10	L-020131-01	J-020131-11	POLD2	5425	NM_006230	5453923	GGGUUAUCCUCGCUGGCAA
Plate 2	F10	L-020131-01	J-020131-12	POLD2	5425	NM_006230	5453923	GGACAGAACGUGAGUGACA
Plate 2	F11	L-011007-00	J-011007-08	CDKN2A	1029	NM_058195	47132605	GAUCAUCAGUCACCGAAGG
Plate 2	F11	L-011007-00	J-011007-09	CDKN2A	1029	NM_058195	47132605	AAACACCGCUUCUGCCUUU
Plate 2	F11	L-011007-00	J-011007-10	CDKN2A	1029	NM_058195	47132605	UAACGUAGAUAUAUGCCUU
Plate 2	F11	L-011007-00	J-011007-11	CDKN2A	1029	NM_058195	47132605	CAGAACCAAAGCUCAAAUA

Plate 2	G02	L-026539-01	J-026539-09	NCAPD3	23310	NM_015261	76880473	GAUUAACAGUCCUACGUUU
Plate 2	G02	L-026539-01	J-026539-10	NCAPD3	23310	NM_015261	76880473	GAUGAGAAGACCAACGUUA
Plate 2	G02	L-026539-01	J-026539-11	NCAPD3	23310	NM_015261	76880473	CAGGGAAUAUGGACGAAGA
Plate 2	G02	L-026539-01	J-026539-12	NCAPD3	23310	NM_015261	76880473	GGGAAUACGCUAUGUUCAU
Plate 2	G03	L-019086-01	J-019086-09	RFC3	5983	NM_181558	31795537	CAGCAUGCCUUGCGAAGAA
Plate 2	G03	L-019086-01	J-019086-10	RFC3	5983	NM_181558	31795537	GGAAAUAGUGACCGAGUAG
Plate 2	G03	L-019086-01	J-019086-11	RFC3	5983	NM_181558	31795537	CCUUGGGACGGCUGGACUA
Plate 2	G03	L-019086-01	J-019086-12	RFC3	5983	NM_181558	31795537	AGACAGAUUGGGAGGUGUA
Plate 2	G04	L-009773-01	J-009773-09	RFC5	5985	NM_007370	31795541	GCUUCAGAUGACCGAGGAA
Plate 2	G04	L-009773-01	J-009773-10	RFC5	5985	NM_007370	31795541	GGCCGAAACUAUUAUACUU
Plate 2	G04	L-009773-01	J-009773-11	RFC5	5985	NM_007370	31795541	GCGUAGGGCUCUGAACAUU
Plate 2	G04	L-009773-01	J-009773-12	RFC5	5985	NM_007370	31795541	UUGCAGAGGCCUAGAUGCU
Plate 2	G05	L-003471-00	J-003471-09	CDKN1A	1026	NM_000389	17978496	CGACUGUGAUGCGCUAAUG
Plate 2	G05	L-003471-00	J-003471-10	CDKN1A	1026	NM_000389	17978496	CCUAAUCCGCCCACAGGAA
Plate 2	G05	L-003471-00	J-003471-11	CDKN1A	1026	NM_000389	17978496	CGUCAGAACCCAUGCGGCA
Plate 2	G05	L-003471-00	J-003471-12	CDKN1A	1026	NM_000389	17978496	AGACCAGCAUGACAGAUUU
Plate 2	G06	L-012248-01	J-012248-09	POLR2I	5438	NM_006233	47933390	CGCACGAAGUGGACGAACU
Plate 2	G06	L-012248-01	J-012248-10	POLR2I	5438	NM_006233	47933390	CCAGAUUCCAUGCGUGAAA
Plate 2	G06	L-012248-01	J-012248-11	POLR2I	5438	NM_006233	47933390	AAGACAAGGAGAACCGCAU
Plate 2	G06	L-012248-01	J-012248-12	POLR2I	5438	NM_006233	47933390	ACAAGGAGGCUGUGUUCUU
Plate 2	G07	L-009290-00	J-009290-05	RFC1	5981	NM_002913	32528305	GUAAAUAGCUCCCGUAAAG
Plate 2	G07	L-009290-00	J-009290-06	RFC1	5981	NM_002913	32528305	GGAAUUAAUUGGCCUGAUA
Plate 2	G07	L-009290-00	J-009290-07	RFC1	5981	NM_002913	32528305	GUCCAAAGAUCUAAUAAGA
Plate 2	G07	L-009290-00	J-009290-08	RFC1	5981	NM_002913	32528305	CAUAUGCGAUGGUGACCUA
Plate 2	G08	L-019061-00	J-019061-05	RFC2	5982	NM_002914	31563535	CUUGUAAUGCUUCGGAUAA
Plate 2	G08	L-019061-00	J-019061-06	RFC2	5982	NM_002914	31563535	GAACUGCCGUGGGUUGAAA
Plate 2	G08	L-019061-00	J-019061-07	RFC2	5982	NM_002914	31563535	CGGCAAGACCACAAGCAUU
Plate 2	G08	L-019061-00	J-019061-08	RFC2	5982	NM_002914	31563535	GCUGUGCAGUCCUCCGGUA
Plate 2	G09	L-008691-00	J-008691-06	RFC4	5984	NM_181573	31881686	UCAAAGCGCUACUCGAUUA
Plate 2	G09	L-008691-00	J-008691-07	RFC4	5984	NM_181573	31881686	GACCAAGGAUCGAGGAGUA
Plate 2	G09	L-008691-00	J-008691-08	RFC4	5984	NM_181573	31881686	CAGCAGUUAUCUCAGAAUU
Plate 2	G09	L-008691-00	J-008691-09	RFC4	5984	NM_181573	31881686	GAACGUGGAAUACAAGUAG
Plate 2	G10	L-011187-00	J-011187-05	POLR2B	5431	NM_000938	4505940	CCAAUUAUGUUGCGGUCAA
Plate 2	G10	L-011187-00	J-011187-06	POLR2B	5431	NM_000938	4505940	GAAAUGAGGUCCUGUACAA
Plate 2	G10	L-011187-00	J-011187-07	POLR2B	5431	NM_000938	4505940	GGAACGAGAUUGUCAGAUU
Plate 2	G10	L-011187-00	J-011187-08	POLR2B	5431	NM_000938	4505940	GAAGCAUGCUGGAUUGUAA
Plate 2	G11	L-003227-00	J-003227-10	CDC25B	994	NM_212530	47078254	GAGAUUACUCUAAGGCCUU
Plate 2	G11	L-003227-00	J-003227-11	CDC25B	994	NM_212530	47078254	GCAGAUACCCCUAUGAAUA
Plate 2	G11	L-003227-00	J-003227-12	CDC25B	994	NM_212530	47078254	UGGAUAAGUUUGUGAUUGU
Plate 2	G11	L-003227-00	J-003227-13	CDC25B	994	NM_212530	47078254	AGAGUGACUUAAAGGAUGA
Plate 2	H02	L-003226-00	J-003226-10	CDC25A	993	NM_201567	42490759	GGGCAGUGAUUAUGAGCAA
Plate 2	H02	L-003226-00	J-003226-11	CDC25A	993	NM_201567	42490759	UCAGGUUUCUGUCUAGAUU
Plate 2	H02	L-003226-00	J-003226-12	CDC25A	993	NM_201567	42490759	GCAAGCGUGUCAUUGUUGU
Plate 2	H02	L-003226-00	J-003226-13	CDC25A	993	NM_201567	42490759	CAUGACAUCUUUCAGCUCA
Plate 2	H03	L-005050-00	J-005050-05	WEE1	7465	NM_003390	19718775	AAUAGAACAUCUCGACUUA
Plate 2	H03	L-005050-00	J-005050-06	WEE1	7465	NM_003390	19718775	AAUAUGAAGUCCCGGUAUA
Plate 2	H03	L-005050-00	J-005050-07	WEE1	7465	NM_003390	19718775	GAUCAUAUGCUUAUACAGA
Plate 2	H03	L-005050-00	J-005050-08	WEE1	7465	NM_003390	19718775	CGACAGACUCCUCAAGUGA
Plate 2	H04	L-003212-00	J-003212-10	CCND3	896	NM_001760	16950657	GGACCUGGCUGCUGUGAUU
Plate 2	H04	L-003212-00	J-003212-11	CCND3	896	NM_001760	16950657	UGCGGAAGAUGCUGGCUUA
Plate 2	H04	L-003212-00	J-003212-12	CCND3	896	NM_001760	16950657	GAGCUGCUGUGUUGCGAAG
Plate 2	H04	L-003212-00	J-003212-13	CCND3	896	NM_001760	16950657	GAUCGAAGCUGCACUCAGG
Plate 2	H05	L-003211-00	J-003211-10	CCND2	894	NM_001759	16950656	GAUCGCAACUGGAAGUGUG
Plate 2	H05	L-003211-00	J-003211-11	CCND2	894	NM_001759	16950656	UGACUGAGCUGCUGGCUAA
Plate 2	H05	L-003211-00	J-003211-12	CCND2	894	NM_001759	16950656	GCUCAGACCUUCAUUGCUC
Plate 2	H05	L-003211-00	J-003211-13	CCND2	894	NM_001759	16950656	UCUCAAAGCUUGCCAGGAG
Plate 2	H06	L-003236-00	J-003236-11	CDK2	1017	NM_052827	16936529	GAGCUUAACCAUCCUAAUA
Plate 2	H06	L-003236-00	J-003236-12	CDK2	1017	NM_052827	16936529	GAAACAAGUUGACGGGAGA
Plate 2	H06	L-003236-00	J-003236-13	CDK2	1017	NM_052827	16936529	GGAGUUACUUCUAUGCCUG
Plate 2	H06	L-003236-00	J-003236-14	CDK2	1017	NM_052827	16936529	GGGCCUAGCUUUCUGCCAU
Plate 2	H07	L-011186-00	J-011186-06	POLR2A	5430	NM_000937	14589948	UAAUAGAGGUCAUCGAGAA
Plate 2	H07	L-011186-00	J-011186-07	POLR2A	5430	NM_000937	14589948	CAGGUGAACCGCAUUCUUA
Plate 2	H07	L-011186-00	J-011186-08	POLR2A	5430	NM_000937	14589948	GGGAUGAGAUGAACUUGCA
Plate 2	H07	L-011186-00	J-011186-09	POLR2A	5430	NM_000937	14589948	CAACUAUAGUCCCACAUCA
Plate 2	H08	L-003213-00	J-003213-10	CCNE1	898	NM_057182	17318560	GUACUGAGCUGGGCAAAUA
Plate 2	H08	L-003213-00	J-003213-11	CCNE1	898	NM_057182	17318560	UGUCCUGGCUGAAUGUAUA
Plate 2	H08	L-003213-00	J-003213-12	CCNE1	898	NM_057182	17318560	GGACAAUAAUGCAGUCUGU
Plate 2	H08	L-003213-00	J-003213-13	CCNE1	898	NM_057182	17318560	GGAGGUGUGUGAAGUCUAU
Plate 2	H09	L-003209-00	J-003209-09	CCNC	892	NM_001013399	61676092	GAUUGUUGCUUGAUAGUGU
Plate 2	H09	L-003209-00	J-003209-10	CCNC	892	NM_001013399	61676092	ACAUGUAGCCUGUGUUGUA
Plate 2	H09	L-003209-00	J-003209-11	CCNC	892	NM_001013399	61676092	GGAUAGUGAAUGAUACCUA
Plate 2	H09	L-003209-00	J-003209-12	CCNC	892	NM_001013399	61676092	GAAGUCAGAACUCUAGCUA
Plate 2	H10	L-003210-00	J-003210-15	CCND1	595	NM_053056	77628152	ACAACUUCCUGUCCUACUA
Plate 2	H10	L-003210-00	J-003210-16	CCND1	595	NM_053056	77628152	GUUCGUGGCCUCUAAGAUG
Plate 2	H10	L-003210-00	J-003210-17	CCND1	595	NM_053056	77628152	GCAUGUAGUCACUUUAUAA
Plate 2	H10	L-003210-00	J-003210-18	CCND1	595	NM_053056	77628152	GCGUGUAGCUAUGGAAGUU
Plate 2	H11	L-004270-00	J-004270-05	RRM1	6240	NM_001033	21071083	UAUGAGGGCUCUCCAGUUA
Plate 2	H11	L-004270-00	J-004270-06	RRM1	6240	NM_001033	21071083	UGAGAGAGGUGCUUUCAUU
Plate 2	H11	L-004270-00	J-004270-07	RRM1	6240	NM_001033	21071083	UGGAAGACCUCUAUAACUA
Plate 2	H11	L-004270-00	J-004270-08	RRM1	6240	NM_001033	21071083	CUACUAAGCACCCUGACUA

Plate 3	A02	L-004509-00	J-004509-05	UBA1	7317	NM_153280	23510339	GCGUGGAGAUCGCUAAGAA
Plate 3	A02	L-004509-00	J-004509-06	UBA1	7317	NM_153280	23510339	CCUUAUACCUUUAGCAUCU
Plate 3	A02	L-004509-00	J-004509-07	UBA1	7317	NM_153280	23510339	CCACAUAUCCGGGUGACAA
Plate 3	A02	L-004509-00	J-004509-08	UBA1	7317	NM_153280	23510339	GAAGUCAAAUCUGAAUCGA
Plate 3	A03	L-003205-00	J-003205-10	CCNA2	890	NM_001237	16950653	GGAAAUGGAGGUUAAAUGU
Plate 3	A03	L-003205-00	J-003205-11	CCNA2	890	NM_001237	16950653	UAGCAGAGUUUGUGUACAU
Plate 3	A03	L-003205-00	J-003205-12	CCNA2	890	NM_001237	16950653	AUGAGGAUAUUCACACAUA
Plate 3	A03	L-003205-00	J-003205-13	CCNA2	890	NM_001237	16950653	UGAUAGAUGCUGACCCAUA
Plate 3	A04	L-004739-01	J-004739-09	POLR2E	5434	NM_002695	14589950	CGAUAUAAGCUCCGAGAGA
Plate 3	A04	L-004739-01	J-004739-10	POLR2E	5434	NM_002695	14589950	CAUCACGGAGCACGAGCUA
Plate 3	A04	L-004739-01	J-004739-11	POLR2E	5434	NM_002695	14589950	CCUGUGGAUUUGUGCGAGA
Plate 3	A04	L-004739-01	J-004739-12	POLR2E	5434	NM_002695	14589950	GAGGAGACGUACCGGCUCU
Plate 3	A05	L-009620-01	J-009620-09	POLR2C	5432	NM_032940	89276761	CAGCCUACCGUGCGGAUCA
Plate 3	A05	L-009620-01	J-009620-10	POLR2C	5432	NM_032940	89276761	UCAAUUAAGCCACGAGAUC
Plate 3	A05	L-009620-01	J-009620-11	POLR2C	5432	NM_032940	89276761	GGAGCUCACUGACGAGAAU
Plate 3	A05	L-009620-01	J-009620-12	POLR2C	5432	NM_032940	89276761	CCUAUGACCCCAACGGCAA
Plate 3	A06	L-003206-00	J-003206-09	CCNB1	891	NM_031966	34304372	CAACAUUACCUGUCAUAUA
Plate 3	A06	L-003206-00	J-003206-10	CCNB1	891	NM_031966	34304372	UGCACUAGUUCAAGAUUUA
Plate 3	A06	L-003206-00	J-003206-11	CCNB1	891	NM_031966	34304372	GAAUGUAGUCAUGGUAAAU
Plate 3	A06	L-003206-00	J-003206-12	CCNB1	891	NM_031966	34304372	CUAAUUGACUGGCUAGUAC
Plate 3	A07	L-003238-00	J-003238-12	CDK4	1019	NM_000075	16936531	CAAGGUAACCCUGGUGUUU
Plate 3	A07	L-003238-00	J-003238-13	CDK4	1019	NM_000075	16936531	GAGCUCUGCAGCACUCUUA
Plate 3	A07	L-003238-00	J-003238-14	CDK4	1019	NM_000075	16936531	CAGCACAGUUCGUGAGGUG
Plate 3	A07	L-003238-00	J-003238-15	CDK4	1019	NM_000075	16936531	GCACUUACACCCGUGGUUG
Plate 3	A08	L-005278-00	J-005278-05	TOP1	7150	NM_003286	19913404	GAAAAUGGCUUCUCUAGUC
Plate 3	A08	L-005278-00	J-005278-06	TOP1	7150	NM_003286	19913404	GAUUUCCGAUUGAAUGAUU
Plate 3	A08	L-005278-00	J-005278-07	TOP1	7150	NM_003286	19913404	GCACAUCAAUCUACACCCA
Plate 3	A08	L-005278-00	J-005278-08	TOP1	7150	NM_003286	19913404	CGAAGAAGGUAGUAGAGUC
Plate 3	A09	L-020381-00	J-020381-05	TFPT	29844	NM_013342	7019370	GGAAUUAAAUCGCAGAAAG
Plate 3	A09	L-020381-00	J-020381-06	TFPT	29844	NM_013342	7019370	AGACGGAAGUGGAGUUUGU
Plate 3	A09	L-020381-00	J-020381-07	TFPT	29844	NM_013342	7019370	GACUGACGCAUGCCCAAUA
Plate 3	A09	L-020381-00	J-020381-08	TFPT	29844	NM_013342	7019370	CGGUGCAGAUUAAGGUUGA
Plate 3	A10	L-009702-00	J-009702-05	DNTT	1791	NM_001017520	63054851	GCAGGAAGGUUGAUGCUUU
Plate 3	A10	L-009702-00	J-009702-06	DNTT	1791	NM_001017520	63054851	GGGAUUGGAUUAUAUUGAA
Plate 3	A10	L-009702-00	J-009702-07	DNTT	1791	NM_001017520	63054851	GUCAAAGAGUGGACAGUGA
Plate 3	A10	L-009702-00	J-009702-08	DNTT	1791	NM_001017520	63054851	CGGAAGAUGAUUCUGGAUA
Plate 3	A11	L-005282-00	J-005282-07	TOP3B	8940	NM_003935	34335290	UCACCAGGUUUCAGACUAA
Plate 3	A11	L-005282-00	J-005282-08	TOP3B	8940	NM_003935	34335290	GUGCACGGCUACUAUAAGA
Plate 3	A11	L-005282-00	J-005282-09	TOP3B	8940	NM_003935	34335290	CGAGUACACUGGGACCUUU
Plate 3	A11	L-005282-00	J-005282-10	TOP3B	8940	NM_003935	34335290	CGUGGCGGCUCUAUGAGUA
Plate 3	B02	L-006836-01	J-006836-09	SMC2	10592	NM_006444	5453590	GCAGAGGCUCAGCGAGUUA
Plate 3	B02	L-006836-01	J-006836-10	SMC2	10592	NM_006444	5453590	GGUUCGGGCUUCUAAUUUA
Plate 3	B02	L-006836-01	J-006836-11	SMC2	10592	NM_006444	5453590	CAGCAAAGCUCAUAUCACA
Plate 3	B02	L-006836-01	J-006836-12	SMC2	10592	NM_006444	5453590	CCCAAGACACUGUAAUUAA
Plate 3	B03	L-004740-00	J-004740-05	TNKS	8658	NM_003747	4507612	CUACAACAGAGUUCGAAUA
Plate 3	B03	L-004740-00	J-004740-06	TNKS	8658	NM_003747	4507612	GCAUGGAGCUUGUGUUAAU
Plate 3	B03	L-004740-00	J-004740-07	TNKS	8658	NM_003747	4507612	CGAAAGAGCCCAUAAUGAU
Plate 3	B03	L-004740-00	J-004740-08	TNKS	8658	NM_003747	4507612	GAGAGUACACCUAUACGUA
Plate 3	B04	L-003207-00	J-003207-09	CCNB2	9133	NM_004701	10938017	GUGACUACGUUAAGGAUAU
Plate 3	B04	L-003207-00	J-003207-10	CCNB2	9133	NM_004701	10938017	GUACAUGUGCGUUGGCAUU
Plate 3	B04	L-003207-00	J-003207-11	CCNB2	9133	NM_004701	10938017	CAAGUCCACUCCAAGUUUA
Plate 3	B04	L-003207-00	J-003207-12	CCNB2	9133	NM_004701	10938017	UAACGAAGAUUGGGAGAAC
Plate 3	B05	L-012708-00	J-012708-05	BCAS2	10286	NM_005872	49472833	GCAGAUACCGACCUACUAA
Plate 3	B05	L-012708-00	J-012708-06	BCAS2	10286	NM_005872	49472833	GCAUCAAGCAGUUAGAAUU
Plate 3	B05	L-012708-00	J-012708-07	BCAS2	10286	NM_005872	49472833	UGGAUGCGCUGCCGUAUUU
Plate 3	B05	L-012708-00	J-012708-08	BCAS2	10286	NM_005872	49472833	GAGAUUGAACGGACUAUUG
Plate 3	B06	L-021331-01	J-021331-09	PPP6R2	9701	NM_014678	55749632	CCGAACAGGUGAUUACGUU
Plate 3	B06	L-021331-01	J-021331-10	PPP6R2	9701	NM_014678	55749632	UGUCAGCAGCAGCGUACUA
Plate 3	B06	L-021331-01	J-021331-11	PPP6R2	9701	NM_014678	55749632	CAGUGACAAAGGACGGGAA
Plate 3	B06	L-021331-01	J-021331-12	PPP6R2	9701	NM_014678	55749632	CAAUAAAAGCCGUGACGUU
Plate 3	B07	L-013639-00	J-013639-05	DKC1	1736	NM_001363	15011921	CAAGGUGACUGGUUGUUUA
Plate 3	B07	L-013639-00	J-013639-06	DKC1	1736	NM_001363	15011921	GCAGGUAGUUGCCGAAGCA
Plate 3	B07	L-013639-00	J-013639-07	DKC1	1736	NM_001363	15011921	UCUCAUAAACGGCUGGUUA
Plate 3	B07	L-013639-00	J-013639-08	DKC1	1736	NM_001363	15011921	GGACAGGUUUCAUUAAUCU
Plate 3	B08	L-011478-00	J-011478-05	SMARCA5	8467	NM_003601	21071057	GGAAUGGUAUACUCGGAUA
Plate 3	B08	L-011478-00	J-011478-06	SMARCA5	8467	NM_003601	21071057	GGGCAAAUAGAUUCGAGUA
Plate 3	B08	L-011478-00	J-011478-07	SMARCA5	8467	NM_003601	21071057	GGAUUUACCAAUUGGAAUA
Plate 3	B08	L-011478-00	J-011478-08	SMARCA5	8467	NM_003601	21071057	GUUCUUUCCUCCACGUUUA
Plate 3	B09	L-019593-00	J-019593-05	PLRG1	5356	NM_002669	77404429	AUUAACACAUUGACGGUAA
Plate 3	B09	L-019593-00	J-019593-06	PLRG1	5356	NM_002669	77404429	CAGUGAAUCAGGAAUAUUU
Plate 3	B09	L-019593-00	J-019593-07	PLRG1	5356	NM_002669	77404429	UCUGAAAGUCGAUUACUAA
Plate 3	B09	L-019593-00	J-019593-08	PLRG1	5356	NM_002669	77404429	CAUCUUGGCUGGGUUCGAU
Plate 3	B10	L-011943-00	J-011943-05	POLR2D	5433	NM_004805	14589949	GUAUUAAUCUCCAAACAUC
Plate 3	B10	L-011943-00	J-011943-06	POLR2D	5433	NM_004805	14589949	GAGAGACCAUUGCCAGUGU
Plate 3	B10	L-011943-00	J-011943-07	POLR2D	5433	NM_004805	14589949	AGUUUGAGUUGGCCUGUUU
Plate 3	B10	L-011943-00	J-011943-08	POLR2D	5433	NM_004805	14589949	GAAUUAAACCGCUGUUAGU
Plate 3	B11	L-008266-00	J-008266-06	UBD	10537	NM_006398	222352095	GAACAUGUCCGGUCUAAGA
Plate 3	B11	L-008266-00	J-008266-07	UBD	10537	NM_006398	222352095	GCAAUGAUCGAGACUAAGA
Plate 3	B11	L-008266-00	J-008266-08	UBD	10537	NM_006398	50355987	CCUCUCAUCUUACGGCAUU
Plate 3	B11	L-008266-00	J-008266-09	UBD	10537	NM_006398	222352095	GAUCUUAAAGCCACGGAGA

Plate 3	C02	L-006536-00	J-006536-06	MDM4	4194	NM_002393	4505138	CGUCAGAGCUUCUCCGUAA
Plate 3	C02	L-006536-00	J-006536-07	MDM4	4194	NM_002393	323510635	CCACGAGACGGGAACAUUA
Plate 3	C02	L-006536-00	J-006536-08	MDM4	4194	NM_002393	323510635	AAGCAUGGGAGAACAGUUA
Plate 3	C02	L-006536-00	J-006536-09	MDM4	4194	NM_002393	323510635	CCUAAAGAUGCGUAUAUAA
Plate 3	C03	L-023451-00	J-023451-05	ANKRD28	23243	NM_015199	68131556	UCAGAAUGCUUACGGCUAU
Plate 3	C03	L-023451-00	J-023451-06	ANKRD28	23243	NM_015199	68131556	GGAAGGACAGCGUUGCAUA
Plate 3	C03	L-023451-00	J-023451-07	ANKRD28	23243	NM_015199	68131556	GUAGUGAAAUUGCUUGUGU
Plate 3	C03	L-023451-00	J-023451-08	ANKRD28	23243	NM_015199	68131556	GUAAUCGACUGUGAGGAUA
Plate 3	C04	L-012977-00	J-012977-05	PER2	8864	NM_003894	12707560	GAAUGGAUACGCGGAAUUU
Plate 3	C04	L-012977-00	J-012977-06	PER2	8864	NM_003894	12707560	CUUCAGCGAUGCCAAGUUU
Plate 3	C04	L-012977-00	J-012977-07	PER2	8864	NM_003894	12707560	GCAGUGGAGCAGAUUCUUU
Plate 3	C04	L-012977-00	J-012977-08	PER2	8864	NM_003894	12707560	CGACCAGUCUUCGAAAGUG
Plate 3	C05	L-003547-00	J-003547-06	TERT	7015	NM_198254	38201699	GAACGGGCCUGGAACCAUA
Plate 3	C05	L-003547-00	J-003547-07	TERT	7015	NM_198254	38201699	CGCCUGAGCUGUACUUUGU
Plate 3	C05	L-003547-00	J-003547-08	TERT	7015	NM_198254	38201699	GGUAUGCCGUGGUCCAGAA
Plate 3	C05	L-003547-00	J-003547-09	TERT	7015	NM_198254	38201699	GCGACGACGUGCUGGUUCA
Plate 3	C06	L-017263-00	J-017263-05	ARID1A	8289	NM_018450	21264568	GAAUAGGGCCUGAGGGAAA
Plate 3	C06	L-017263-00	J-017263-06	ARID1A	8289	NM_018450	21264568	AGAUGUGGGUGGACCGUUA
Plate 3	C06	L-017263-00	J-017263-07	ARID1A	8289	NM_018450	21264568	GCAACGACAUGAUUCCUAU
Plate 3	C06	L-017263-00	J-017263-08	ARID1A	8289	NM_018450	21264568	GGACCUCUAUCGCCUCUAU
Plate 3	C07	L-009935-00	J-009935-06	PPP6C	5537	NM_002721	20127429	CUAAAUGGCCUGAUCGUAU
Plate 3	C07	L-009935-00	J-009935-07	PPP6C	5537	NM_002721	20127429	CGCUAGACCUGGACAAGUA
Plate 3	C07	L-009935-00	J-009935-08	PPP6C	5537	NM_002721	20127429	GUUUGGAGACCUUCACUUA
Plate 3	C07	L-009935-00	J-009935-09	PPP6C	5537	NM_002721	20127429	CGAACGGAAUCAGGAAAUU
Plate 3	C08	L-016829-01	J-016829-09	STRA13	201254	NM_144998	71559138	CCUUUCCAGCCAUGCGAUA
Plate 3	C08	L-016829-01	J-016829-10	STRA13	201254	NM_144998	71559138	CAUCAAAGCUGGCGUGUGA
Plate 3	C08	L-016829-01	J-016829-11	STRA13	201254	NM_144998	71559138	ACGUGGACCAGCUGGAGAA
Plate 3	C08	L-016829-01	J-016829-12	STRA13	201254	NM_144998	71559138	GGAAGGACCUGAAGGAUUU
Plate 3	C09	L-021627-01	J-021627-09	HFM1	164045	NM_001017975	130484566	UCACAGAAAUUCCGGCAAA
Plate 3	C09	L-021627-01	J-021627-10	HFM1	164045	NM_001017975	130484566	GCACAUCAGUAUUCCGGAA
Plate 3	C09	L-021627-01	J-021627-11	HFM1	164045	NM_001017975	130484566	GAUAGCAUGACUAGGAAAU
Plate 3	C09	L-021627-01	J-021627-12	HFM1	164045	NM_001017975	63025209	AGCAAUAGUAAGCAGAAAU
Plate 3	C10	L-004164-00	J-004164-09	PIAS3	10401	NM_006099	31543399	GAGCCGACAUCCAAGGUUU
Plate 3	C10	L-004164-00	J-004164-10	PIAS3	10401	NM_006099	31543399	UAAGAAGAAGGUCGAAGUU
Plate 3	C10	L-004164-00	J-004164-11	PIAS3	10401	NM_006099	31543399	GGAAGCGCACUUUACCUUU
Plate 3	C10	L-004164-00	J-004164-12	PIAS3	10401	NM_006099	31543399	GACAGAGAGUCAGCACUAU
Plate 3	C11	L-020943-02	J-020943-17	PARPBP	55010	NM_017915	90819238	AGUAAAUACAACCGUGAUA
Plate 3	C11	L-020943-02	J-020943-18	PARPBP	55010	NM_017915	90819238	GAAUAGAUUGUACGGCAAA
Plate 3	C11	L-020943-02	J-020943-19	PARPBP	55010	NM_017915	90819238	CGAGAGAAACAAAUGUCUA
Plate 3	C11	L-020943-02	J-020943-20	PARPBP	55010	NM_017915	90819238	CAACAAUUGGAACGAGUUU
Plate 3	D02	L-013665-00	J-013665-05	TONSL	4796	NM_013432	34304357	CAAGGAAGGCUGUGCUCUA
Plate 3	D02	L-013665-00	J-013665-06	TONSL	4796	NM_013432	34304357	GUCAGAACCUCCAGCAUGU
Plate 3	D02	L-013665-00	J-013665-07	TONSL	4796	NM_013432	34304357	GACAACCGCAGGCCCAGUA
Plate 3	D02	L-013665-00	J-013665-08	TONSL	4796	NM_013432	34304357	GGACCCGCCUCUAUCUCAA
Plate 3	D03	L-017404-00	J-017404-05	FBXO18	84893	NM_178150	30795118	CCUCAACGCUGGUCAAGUA
Plate 3	D03	L-017404-00	J-017404-06	FBXO18	84893	NM_178150	30795118	AGGGAAGGGUGGAUUCAUA
Plate 3	D03	L-017404-00	J-017404-07	FBXO18	84893	NM_178150	30795118	GUGCCUAUUUGGUGUAAGA
Plate 3	D03	L-017404-00	J-017404-08	FBXO18	84893	NM_178150	30795118	AAACAAAACCUCGUCAUUA
Plate 3	D04	L-006445-00	J-006445-05	PIAS4	51588	NM_015897	24850132	GAAUUAGUCCCACAGAACA
Plate 3	D04	L-006445-00	J-006445-06	PIAS4	51588	NM_015897	24850132	GUACUUAAACGGACUGGGA
Plate 3	D04	L-006445-00	J-006445-07	PIAS4	51588	NM_015897	24850132	CAAGACAGGUGGAGUUGAU
Plate 3	D04	L-006445-00	J-006445-08	PIAS4	51588	NM_015897	24850132	GGAACUACGGCAAGAGCUA
Plate 3	D05	L-015697-01	J-015697-09	SFR1	119392	NM_001002759	50593525	AUACAAAUAGUUCCCGAAA
Plate 3	D05	L-015697-01	J-015697-10	SFR1	119392	NM_001002759	50593525	AAACAAAGAUUAAACGCUG
Plate 3	D05	L-015697-01	J-015697-11	SFR1	119392	NM_001002759	50593525	ACUAUGGGUUAGAUGAUAA
Plate 3	D05	L-015697-01	J-015697-12	SFR1	119392	NM_001002759	50593525	CUGAUAGUCUAGCAGGUAA
Plate 3	D06	L-027225-02	J-027225-19	MMS22L	253714	NM_198468	115583682	AAUCCUACCUUGAGUAUAA
Plate 3	D06	L-027225-02	J-027225-20	MMS22L	253714	NM_198468	115583682	GGAAUACCUUGGUGAAGUA
Plate 3	D06	L-027225-02	J-027225-21	MMS22L	253714	NM_198468	115583682	AAGACUUGCUGUUGCGAUA
Plate 3	D06	L-027225-02	J-027225-22	MMS22L	253714	NM_198468	115583682	GCUACUGAAUCAUGCUUUA
Plate 3	D07	L-014591-01	J-014591-09	TTI2	80185	NM_025115	13376690	GCACGACGAGGCAACGUAA
Plate 3	D07	L-014591-01	J-014591-10	TTI2	80185	NM_025115	387942386	CAAGAAACCUGCCGGCUUU
Plate 3	D07	L-014591-01	J-014591-11	TTI2	80185	NM_025115	387942386	GUGAUGAGGUCCUGCGGCU
Plate 3	D07	L-014591-01	J-014591-12	TTI2	80185	NM_025115	387942386	AGACCUCGGUGAUCUAAUA
Plate 3	D08	L-029596-02	J-029596-18	SWI5	375757	NM_001040011	148664191	CUGAAAUGUCGCAGUGAUA
Plate 3	D08	L-029596-02	J-029596-19	SWI5	375757	NM_001040011	148664191	GAACCAAGACUUACCCGAA
Plate 3	D08	L-029596-02	J-029596-20	SWI5	375757	NM_001040011	148664191	AGAGUUGUAUCCAGAGUUU
Plate 3	D08	L-029596-02	J-029596-21	SWI5	375757	NM_001040011	148664191	GUUCGUAUCUGAAGGCUAC
Plate 3	D09	L-184374-00	J-184374-09	ZSWIM7	125150	NM_001042698	111607458	GAUGAAGUUUCGACGAGUA
Plate 3	D09	L-184374-00	J-184374-10	ZSWIM7	125150	NM_001042698	111607458	UCUGAGACGCUUCGGUAAA
Plate 3	D09	L-184374-00	J-184374-11	ZSWIM7	125150	NM_001042698	111607458	GAGAGUUAGUAUCGAGAAC
Plate 3	D09	L-184374-00	J-184374-12	ZSWIM7	125150	NM_001042698	111607458	CAAAGAAGCAAUAAUACGU
Plate 3	D10	L-011683-00	J-011683-06	H2AFZ	3015	NM_002106	53759146	UCUAAAGGAUGCCUGGAUU
Plate 3	D10	L-011683-00	J-011683-07	H2AFZ	3015	NM_002106	53759146	GAUGCAGAAGUUAUAGUAA
Plate 3	D10	L-011683-00	J-011683-08	H2AFZ	3015	NM_002106	53759146	CAACCAAAUUUCUGCAUUC
Plate 3	D10	L-011683-00	J-011683-09	H2AFZ	3015	NM_002106	53759146	CAAUAAAGGUCAUAUCCCA
Plate 3	D11	L-008167-00	J-008167-06	PIAS1	8554	NM_016166	7706636	GAAUAAGGAAUCCGGAUCA
Plate 3	D11	L-008167-00	J-008167-07	PIAS1	8554	NM_016166	7706636	AAACAAGCACGGACGCAAA
Plate 3	D11	L-008167-00	J-008167-08	PIAS1	8554	NM_016166	7706636	GUUAUGAGCCUUAGAGUUU
Plate 3	D11	L-008167-00	J-008167-09	PIAS1	8554	NM_016166	7706636	CGACCCAGCCGACCAAUUA

Plate 3	E02	L-009428-00	J-009428-06	PIAS2	9063	NM_173206	56699459	ACAACUAGCCUUCGGGUAU
Plate 3	E02	L-009428-00	J-009428-07	PIAS2	9063	NM_173206	56699459	UCGAAGAGUUGAGGAAUAU
Plate 3	E02	L-009428-00	J-009428-08	PIAS2	9063	NM_173206	56699459	UCAUCAAGCCCACGAGUUU
Plate 3	E02	L-009428-00	J-009428-09	PIAS2	9063	NM_173206	56699459	UGAGGGCGCUGCAUUUAUU
Plate 3	E03	L-014188-00	J-014188-05	TTI1	9675	NM_014657	24307960	GAACACACCUGCCAAGUUA
Plate 3	E03	L-014188-00	J-014188-06	TTI1	9675	NM_014657	24307960	AGGAUUUGCUGUAUCUUUA
Plate 3	E03	L-014188-00	J-014188-07	TTI1	9675	NM_014657	24307960	GUGAAUGGGAUCUCUUUAA
Plate 3	E03	L-014188-00	J-014188-08	TTI1	9675	NM_014657	24307960	GCACUGACCAGGCUUAUCA
Plate 3	E04	L-014237-01	J-014237-09	ACD	65057	NM_022914	12597658	GAUGAGAGUAAACGGGCCA
Plate 3	E04	L-014237-01	J-014237-10	ACD	65057	NM_022914	12597658	CCACAUGUCAUCCGAGGAA
Plate 3	E04	L-014237-01	J-014237-11	ACD	65057	NM_022914	12597658	UCAAGGAGUUUGUAGGGUU
Plate 3	E04	L-014237-01	J-014237-12	ACD	65057	NM_022914	12597658	ACGUCACGCAGGACAGAUA
Plate 3	E05	L-008243-00	J-008243-05	ACTL6A	86	NM_177989	30089996	GAACGGAGGUUUAGCUCAU
Plate 3	E05	L-008243-00	J-008243-06	ACTL6A	86	NM_177989	30089996	CCUACUACAUAGAUACUAA
Plate 3	E05	L-008243-00	J-008243-07	ACTL6A	86	NM_177989	30089996	GUAAAGGGGUUAUCAGGAA
Plate 3	E05	L-008243-00	J-008243-08	ACTL6A	86	NM_177989	30089996	UGGGAUAGUUUCCAAGCUA
Plate 3	E06	L-013382-00	J-013382-05	UBB	7314	NM_018955	22538474	GCUGUUAAUUCUUCAGUCA
Plate 3	E06	L-013382-00	J-013382-06	UBB	7314	NM_018955	22538474	GUAUGCAGAUCUUCGUGAA
Plate 3	E06	L-013382-00	J-013382-07	UBB	7314	NM_018955	22538474	UCGAAAAUGUGAAGGCCAA
Plate 3	E06	L-013382-00	J-013382-08	UBB	7314	NM_018955	22538474	CACCUGGUCCUGCGUCUGA
Plate 3	E07	L-019408-00	J-019408-05	UBC	7316	NM_021009	67191207	GUAAGACCAUCACUCUCGA
Plate 3	E07	L-019408-00	J-019408-06	UBC	7316	NM_021009	67191207	GUGAAGACCCUGACUGGUA
Plate 3	E07	L-019408-00	J-019408-07	UBC	7316	NM_021009	67191207	AAGCAAAGAUCCAGGACAA
Plate 3	E07	L-019408-00	J-019408-08	UBC	7316	NM_021009	67191207	GUGAAGACUCUGACUGGUA

Table A. 5. siRNA sequences of Custom library plates from Dharmacon.

A.3 – Screen Data.

A.3.1 – Raw data from first screen.

Screen 1 – Plate 1.

Name / Desc	All	Mean GFP	Mean RFP	R01	Ratio Green/Red	Numerical Ra	Ratio/Scram	Average scra
A1	100	46.4	43.7	100	46.4:43.7	1.0617849	0.96934613	1.09536198
A2	100	41.4	49.6	100	41.4:49.6	0.83467742	0.76201058	
A3	100	42.3	47.8	100	42.3:47.8	0.88493724	0.80789479	
A4	100	43	46.1	100	43:46.1	0.93275488	0.85154944	
A5	100	42.7	48.1	100	7.11666666666666	0.88773389	0.81044796	
A6	100	44.4	45.8	100	44.4:45.8	0.96943231	0.88503374	
A7	100	41.9	45.4	100	41.9:45.4	0.92290749	0.84255936	
A8	100	46	44.5	100	23:22.25	1.03370787	0.94371348	
A9	100	43.7	47.5	100	43.7:47.5	0.92	0.839905	
A10	100	48.2	42.5	100	8.03333333333333	1.13411765	1.03538161	
A11	100	41.9	47.8	100	41.9:47.8	0.87656904	0.80025512	
A12	100	46.2	42.6	100	23.1:21.3	1.08450704	0.99009009	
B1	100	48	40.9	100	6:5.1125	1.17359413	1.07142128	
B2	100	42.7	50.7	100	21.35:25.35	0.84220907	0.76888653	
B3	100	42.8	48.3	100	7.13333333333333	0.88612836	0.80898222	
B4	100	46	44.9	100	23:22.45	1.02449889	0.93530623	
B5	100	40.3	50.5	100	4.03:5.05	0.7980198	0.72854437	
B6	100	45.1	44.2	100	45.1:44.2	1.02036199	0.93152949	
B7	100	45.6	44.7	100	45.6:44.7	1.02013423	0.93132156	
B8	100	43	47.6	100	43:47.6	0.90336134	0.8247149	
B9	100	40.4	49	100	40.4:49	0.8244898	0.75270989	
B10	100	47	42.8	100	47:42.8	1.09813084	1.0025278	
B11	100	60.1	28.8	100	15.025:7.2	2.08680556	1.90512871	
B12	100	46.7	42.9	100	23.35:21.45	1.08857809	0.99380671	
C1	100	20.7	42.9	100	10.35:21.45	0.48251748	0.44050961	
C2	100	57.1	31.5	100	57.1:31.5	1.81269841	1.65488527	
C3	100	45	45.3	100	1:1.006666666666	0.99337748	0.90689425	
C4	100	44.2	47.9	100	44.2:47.9	0.92275574	0.84242082	
C5	100	45.1	43	100	45.1:43	1.04883721	0.95752566	
C6	100	45.1	46.4	100	45.1:46.4	0.97198276	0.88736215	
C7	100	43.2	47.7	100	43.2:47.7	0.90566038	0.82681378	
C8	100	46.5	42.4	100	23.25:21.2	1.09669811	1.00121981	
C9	100	39.4	49.8	100	39.4:49.8	0.79116466	0.72228603	
C10	100	45.4	45.3	100	1.00888888888888	1.00220751	0.91495553	
C11	100	48.1	41.8	100	48.1:41.8	1.1507177	1.05053646	
C12	100	43.8	46.4	100	43.8:46.4	0.94396552	0.86178408	
D1	100	46.3	42.6	100	23.15:21.3	1.08685446	0.99223314	
D2	100	44.3	46.6	100	22.15:23.3	0.95064378	0.86788093	
D3	100	43.6	45.7	100	43.6:45.7	0.95404814	0.87098891	
D4	100	47.2	42.8	100	47.2:42.8	1.10280374	1.00679388	
D5	100	46.6	45.4	100	46.6:45.4	1.02643172	0.93707079	
D6	100	44.7	45.3	100	44.7:45.3	0.98675497	0.90084829	
D7	100	49	39.5	100	49:39.5	1.24050633	1.13250811	
D8	100	46.1	45	100	46.1:45	1.02444444	0.93525653	
D9	100	44.8	45.9	100	44.8:45.9	0.97603486	0.89106147	
D10	100	42.3	47.1	100	42.3:47.1	0.89808917	0.81990172	
D11	100	45.5	45.5	100	1.01111111111111	1	0.91294021	
D12	100	50.5	39.1	100	50.5:39.1	1.2915601	1.17911715	
E1	100	43.5	46.3	100	43.5:46.3	0.93952484	0.85773001	
E2	100	47.1	43.9	100	47.1:43.9	1.07289294	0.97948711	
E3	100	43.3	46.2	100	43.3:46.2	0.93722944	0.85563444	
E4	100	47.9	41	100	47.9:41	1.16829268	1.06658137	
E5	100	49.4	43.3	100	49.4:43.3	1.1408776	1.04155304	
E6	100	41.1	48.5	100	41.1:48.5	0.84742268	0.77364624	
E7	100	47	45	100	47:45	1.04444444	0.95351533	
E8	100	45.3	46	100	45.3:46	0.98478261	0.89904764	
E9	100	43.6	44.9	100	43.6:44.9	0.97104677	0.88650764	
E10	100	49.1	43.6	100	49.1:43.6	1.12614679	1.02810469	
E11	100	41.3	49.9	100	41.3:49.9	0.82765531	0.75559982	
E12	100	22.1	39.7	100	22.1:39.7	0.55667506	0.50821105	
F1	100	50.8	37.6	100	50.8:37.6	1.35106383	1.2334405	
F2	100	39.8	48.2	100	13.2666666666666	0.82572614	0.7538386	
F3	100	44.2	44.4	100	1.00454545454545	0.9954955	0.90882787	
F4	100	46.7	41.8	100	46.7:41.8	1.11722488	1.01995952	
F5	100	44.1	45.8	100	44.1:45.8	0.9628821	0.87905379	
F6	100	44.6	44.6	100	1.01363636363636	1	0.91294021	
F7	100	42.5	47.6	100	42.5:47.6	0.89285714	0.81512519	
F8	100	44	48	100	11:12	0.91666667	0.83686186	
F9	100	49.5	41.1	100	49.5:41.1	1.20437956	1.09952653	
F10	100	42.3	47.5	100	42.3:47.5	0.89052632	0.81299728	
F11	100	47.3	42.5	100	47.3:42.5	1.11294118	1.01604875	
F12	100	46.2	41.9	100	46.2:41.9	1.1026253	1.00663097	
G1	100	50.7	36.4	100	25.35:18.2	1.39285714	1.2715953	
G2	100	46.2	43.8	100	46.2:43.8	1.05479452	0.96296433	
G3	100	51.1	39.4	100	17.0333333333333	1.29695431	1.18404175	
G4	100	48.3	43	100	48.3:43	1.12325581	1.0254654	
G5	100	46	42.6	100	23:21.3	1.07981221	0.98580399	
G6	100	42	47.6	100	42:47.6	0.88235294	0.80553548	
G7	100	42.5	47	100	42.5:47	0.90425532	0.82553104	
G8	100	42	47.6	100	42:47.6	0.88235294	0.80553548	
G9	100	46.4	48.8	100	23.2:24.4	0.95081967	0.86804151	
G10	100	45.1	43.7	100	45.1:43.7	1.03203661	0.94218772	
G11	100	46.9	42.9	100	23.45:21.45	1.09324009	0.99806284	
G12	100	46.7	42	100	23.35:21	1.11190476	1.01510257	
H1	100	47.6	40	100	47.6:40	1.19	1.08639885	
H2	100	39.2	51	100	13.0666666666666	0.76862745	0.70171091	
H3	100	43.8	46.5	100	43.8:46.5	0.94193548	0.85993078	
H4	100	45.7	44.7	100	45.7:44.7	1.02237136	0.93336393	
H5	100	43.7	45.2	100	43.7:45.2	0.96681416	0.88264352	
H6	100	42.8	46	100	21.4:23	0.93043478	0.84943133	
H7	100	45	44.2	100	45:44.2	1.01809955	0.92946402	
H8	100	42.5	48.5	100	7.08333333333333	0.87628866	0.79999916	
H9	100	45.7	45.9	100	1.01555555555555	0.9956427	0.90896226	
H10	100	47.4	40.7	100	47.4:40.7	1.16461916	1.06322767	
H11	100	50	41.9	100	50:41.9	1.19331742	1.08942746	
H12	100	47.8	40.2	100	47.8:40.2	1.18905473	1.08553587	

Table A.6. Percentages from screen 1 plate 1

Screen 1 – Plate 2.

Name / Desc	All	Mean GFP	Mean RFP	R01	Ratio Green/	Numerical Ra	Ratio/Scraml	Average scra
A1	100	48	41.1	100	48:41.1	1.16788321	1.04544673	1.11711403
A2	100	48.6	40.5	100	6.075:5.0625	1.2	1.07419651	
A3	100	40.5	47.3	100	40.5:47.3	0.85623679	0.76647214	
A4	100	47	43.6	100	47:43.6	1.07798165	0.96497011	
A5	100	44.4	43	100	44.4:43	1.03255814	0.92430863	
A6	100	44.4	46.2	100	22.2:23.1	0.96103896	0.86028725	
A7	100	42.3	44.6	100	21.15:22.3	0.94843049	0.84900061	
A8	100	44.7	45.5	100	44.7:45.5	0.98241758	0.87942462	
A9	100	46	45.8	100	46:45.8	1.00436681	0.89907277	
A10	100	43.6	43.6	100	1.013953488	1	0.89516376	
A11	100	44.3	42.6	100	22.15:21.3	1.0399061	0.93088626	
A12	100	44.3	43.7	100	44.3:43.7	1.01372998	0.90745434	
B1	100	47.7	40.9	100	47.7:40.9	1.16625917	1.04399294	
B2	100	43.8	47.3	100	43.8:47.3	0.92600423	0.82892543	
B3	100	46.3	41.6	100	46.3:41.6	1.11298077	0.99630005	
B4	100	46.3	44.7	100	23.15:22.35	1.03579418	0.92720542	
B5	100	49.3	39.5	100	49.3:39.5	1.24810127	1.11725502	
B6	100	41.8	46.8	100	41.8:46.8	0.89316239	0.79952661	
B7	100	42.3	46.7	100	21.15:23.35	0.90578158	0.81082285	
B8	100	43.7	44.9	100	43.7:44.9	0.97327394	0.87123956	
B9	100	40.4	48.5	100	5.05:6.0625	0.83298969	0.74566218	
B10	100	37.6	49.8	100	37.6:49.8	0.75502008	0.67586661	
B11	100	38.1	51.4	100	38.1:51.4	0.74124514	0.66353578	
B12	100	45.6	42.1	100	15.2:14.0333	1.08313539	0.96958355	
C1	100	23.1	43	100	23.1:43	0.5372093	0.4808903	
C2	100	42.2	49.3	100	6.028571428	0.85598377	0.76624565	
C3	100	45.4	45.3	100	1.008888888	1.00220751	0.89713984	
C4	100	43.8	45.3	100	43.8:45.3	0.96688742	0.86552258	
C5	100	45.7	42.8	100	15.23333333	1.06775701	0.95581738	
C6	100	44.5	47.5	100	44.5:47.5	0.93684211	0.8386271	
C7	100	40.4	48.1	100	5.05:6.0125	0.83991684	0.75186312	
C8	100	43.9	47.7	100	43.9:47.7	0.92033543	0.82385092	
C9	100	43	46.8	100	43:46.8	0.91880342	0.82247952	
C10	100	48.8	41.8	100	48.8:41.8	1.16746411	1.04507157	
C11	100	44.4	46.1	100	22.2:23.05	0.96312364	0.86215338	
C12	100	46.4	38.6	100	23.2:19.3	1.20207254	1.07605177	
D1	100	41.8	45.6	100	41.8:45.6	0.91666667	0.82056678	
D2	100	42.6	43.2	100	42.6:43.2	0.98611111	0.88273093	
D3	100	43.8	41.2	100	43.8:41.2	1.0631068	0.95165468	
D4	100	41.8	47.5	100	41.8:47.5	0.88	0.78774411	
D5	100	44.4	44.1	100	1.009090909	1.00680272	0.90125331	
D6	100	35.4	56.3	100	5.057142857	0.62877442	0.56285608	
D7	100	41.8	44.7	100	41.8:44.7	0.93512304	0.83708826	
D8	100	40.2	48	100	5.025:6	0.8375	0.74969965	
D9	100	44.2	44.3	100	1.004545454	0.99774266	0.89314308	
D10	100	37.7	53.7	100	37.7:53.7	0.70204842	0.6284483	
D11	100	46.8	43.6	100	46.8:43.6	1.0733945	0.96086385	
D12	100	45.4	41.8	100	45.4:41.8	1.0861244	0.9722592	
E1	100	44.8	39.6	100	44.8:39.6	1.13131313	1.01271052	
E2	100	40.7	46.5	100	20.35:23.25	0.87526882	0.78350893	
E3	100	43.7	46.5	100	43.7:46.5	0.93978495	0.84126143	
E4	100	45.6	45.4	100	1.013333333	1.00440529	0.89910721	
E5	100	40.8	47.6	100	40.8:47.6	0.85714286	0.76728322	
E6	100	42.8	49	100	6.114285714	0.87346939	0.78189814	
E7	100	40.4	47.9	100	40.4:47.9	0.8434238	0.75500242	
E8	100	41.8	44.9	100	41.8:44.9	0.93095768	0.83335958	
E9	100	41.7	47.7	100	41.7:47.7	0.87421384	0.78256455	
E10	100	40.9	46.7	100	20.45:23.35	0.875803	0.78398711	
E11	100	45	45.7	100	1:1.0155555	0.98468271	0.88145228	
E12	100	22.7	38	100	11.35:19	0.59736842	0.53474256	
F1	100	43.6	44	100	43.6:44	0.99090909	0.88702591	
F2	100	42.4	44.9	100	21.2:22.45	0.94432071	0.84532168	
F3	100	44.2	46.2	100	22.1:23.1	0.95670996	0.85641208	
F4	100	40.2	48.7	100	5.025:6.0875	0.82546201	0.73892368	
F5	100	45	43.7	100	45:43.7	1.02974828	0.92179335	
F6	100	41.4	48	100	41.4:48	0.8625	0.77207874	
F7	100	41.7	47.6	100	41.7:47.6	0.87605042	0.78420859	
F8	100	41.8	48	100	41.8:48	0.87083333	0.77953844	
F9	100	41.7	45.7	100	41.7:45.7	0.91247265	0.81681245	
F10	100	41.2	49.2	100	41.2:49.2	0.83739837	0.74960868	
F11	100	42.7	46.9	100	21.35:23.45	0.91044776	0.81499984	
F12	100	42.7	43.6	100	42.7:43.6	0.9793578	0.87668561	
G1	100	44.5	42.3	100	22.25:21.15	1.05200946	0.94172074	
G2	100	45.4	43	100	45.4:43	1.05581395	0.94512639	
G3	100	37.9	48.7	100	37.9:48.7	0.77823409	0.69664695	
G4	100	43.2	48.7	100	43.2:48.7	0.88706366	0.79406724	
G5	100	48.4	40.6	100	6.05:5.075	1.19211823	1.06714103	
G6	100	41.4	47.9	100	41.4:47.9	0.86430063	0.7736906	
G7	100	38.5	52.6	100	19.25:26.3	0.73193916	0.65520541	
G8	100	41.1	49	100	41.1:49	0.83877551	0.75084144	
G9	100	39.8	47.8	100	39.8:47.8	0.83263598	0.74534556	
G10	100	40.8	46.7	100	20.4:23.35	0.87366167	0.78207027	
G11	100	41.3	47.6	100	41.3:47.6	0.86764706	0.7766862	
G12	100	46.2	41.5	100	46.2:41.5	1.11325301	0.99654375	
H1	100	43.7	40.4	100	43.7:40.4	1.08168317	0.96828357	
H2	100	42.7	43.7	100	42.7:43.7	0.9771167	0.87467946	
H3	100	44.7	42.5	100	22.35:21.25	1.05176471	0.94150165	
H4	100	44.1	45.5	100	44.1:45.5	0.96923077	0.86762026	
H5	100	41.9	46.6	100	41.9:46.6	0.89914163	0.804879	
H6	100	43.8	43.6	100	1.018604651	1.00458716	0.89927002	
H7	100	32.8	53.4	100	32.8:53.4	0.61423221	0.54983841	
H8	100	42.8	48.2	100	7.133333333	0.8879668	0.7948757	
H9	100	41.9	46.2	100	41.9:46.2	0.90692641	0.81184765	
H10	100	44.2	40.2	100	11.05:10.05	1.09950249	0.98423478	
H11	100	34.5	53.3	100	34.5:53.3	0.64727955	0.5794212	
H12	100	51.6	38.1	100	51.6:38.1	1.35433071	1.21234777	

Table A.7. Percentages from screen 1 plate 2

Screen 1 – Plate 3.

Name / Desc	All	Mean GFP	Mean RFP	R01	Ratio Green/	Numerical Ra	Ratio/Scram	Average scra
A1	100	39.9	44.9	100	39.9:44.9	0.88864143	0.96867637	0.917377
A2	100	40.7	44.2	100	10.175:11.05	0.92081448	1.00374707	
A3	100	45	39.2	100	15:13.06666	1.14795918	1.25134943	
A4	100	38.6	47.1	100	38.6:47.1	0.81953291	0.89334364	
A5	100	37.8	50.8	100	37.8:50.8	0.74409449	0.8111109	
A6	100	42	44	100	21:22	0.95454545	1.04051601	
A7	100	43.1	44.9	100	43.1:44.9	0.95991091	1.0463647	
A8	100	41.2	43.6	100	41.2:43.6	0.94495413	1.03006085	
A9	100	41.2	44	100	41.2:44	0.93636364	1.02069666	
A10	100	45	43	100	45:43	1.04651163	1.14076506	
A11	100	37.8	42.5	100	37.8:42.5	0.88941176	0.96951609	
A12	100	42.7	41.3	100	42.7:41.3	1.03389831	1.12701573	
B1	100	40.8	44.1	100	10.2:11.025	0.92517007	1.00849495	
B2	100	44.3	44.2	100	1.006818181	1.00226244	1.0925306	
B3	100	38.3	50.9	100	19.15:25.45	0.7524558	0.82022527	
B4	100	42.8	46.8	100	21.4:23.4	0.91452991	0.99689649	
B5	100	40.2	50.6	100	4.02:5.06	0.7944664	0.86601954	
B6	100	41.6	47.3	100	41.6:47.3	0.8794926	0.95870357	
B7	100	37.6	50.8	100	37.6:50.8	0.74015748	0.80681931	
B8	100	43.5	44.8	100	43.5:44.8	0.97098214	1.05843306	
B9	100	41.7	46.3	100	41.7:46.3	0.90064795	0.98176426	
B10	100	40	46.4	100	20:23.2	0.86206897	0.93971068	
B11	100	43.7	42.2	100	43.7:42.2	1.03554502	1.12881076	
B12	100	42	44.9	100	21:22.45	0.93541203	1.01965934	
C1	100	21.7	45.1	100	7.233333333	0.48115299	0.52448774	
C2	100	42.2	47	100	42.2:47	0.89787234	0.97873867	
C3	100	47.1	43.7	100	47.1:43.7	1.0778032	1.17487489	
C4	100	43	45.8	100	43:45.8	0.93886463	1.0234229	
C5	100	43.3	45.2	100	43.3:45.2	0.9579646	1.0442431	
C6	100	43.3	46.5	100	43.3:46.5	0.9311828	1.01504921	
C7	100	43.3	48	100	43.3:48	0.90208333	0.98332892	
C8	100	39.3	50.3	100	39.3:50.3	0.78131213	0.85168053	
C9	100	42.1	46.8	100	21.05:23.4	0.89957265	0.98059211	
C10	100	43.3	46.8	100	43.3:46.8	0.92521368	1.00854248	
C11	100	41.7	47.7	100	41.7:47.7	0.87421384	0.95294937	
C12	100	40.4	42.3	100	20.2:21.15	0.95508274	1.04110169	
D1	100	43.4	40.5	100	43.4:40.5	1.07160494	1.16811838	
D2	100	45.6	47	100	45.6:47	0.97021277	1.05759439	
D3	100	44.6	45.6	100	44.6:45.6	0.97807018	1.06615947	
D4	100	44.6	44.7	100	1.013636363	0.99776286	1.08762577	
D5	100	44.2	44.6	100	1.004545454	0.99103139	1.08028803	
D6	100	46	42.7	100	23:21.35	1.07728337	1.17430824	
D7	100	40.7	47.5	100	40.7:47.5	0.85684211	0.93401307	
D8	100	44.1	45.1	100	44.1:45.1	0.97782705	1.06589445	
D9	100	43.6	43.8	100	1.013953488	0.99543379	1.08508693	
D10	100	44.4	44.4	100	1.009090909	1	1.09006439	
D11	100	46.6	39.5	100	46.6:39.5	1.17974684	1.28600002	
D12	100	39	42.9	100	13:14.3	0.90909091	0.99096763	
E1	100	41.2	44	100	41.2:44	0.93636364	1.02069666	
E2	100	42.2	44.5	100	21.1:22.25	0.94831461	1.03372398	
E3	100	43.8	44.4	100	43.8:44.4	0.98648649	1.07533379	
E4	100	40.1	48.1	100	5.0125:6.012	0.83367983	0.9087647	
E5	100	41	46.5	100	41:46.5	0.88172043	0.96113204	
E6	100	43.8	46.7	100	43.8:46.7	0.9379015	1.02237303	
E7	100	41	48.1	100	41:48.1	0.85239085	0.92916092	
E8	100	43.9	44.9	100	43.9:44.9	0.97772829	1.06578679	
E9	100	41.2	44.8	100	41.2:44.8	0.91964286	1.00246993	
E10	100	45.5	43.1	100	45.5:43.1	1.05568445	1.15076403	
E11	100	42.1	47.1	100	42.1:47.1	0.89384289	0.9743463	
E12	100	17	44	100	17:44	0.38636364	0.42116124	
F1	100	39.1	44.4	100	39.1:44.4	0.88063063	0.95994409	
F2	100	42.2	47.2	100	42.2:47.2	0.8940678	0.97459147	
F3	100	41.6	45.5	100	41.6:45.5	0.91428571	0.9966303	
F4	100	44	45.5	100	44:45.5	0.96703297	1.0541282	
F5	100	42.5	47.3	100	42.5:47.3	0.89852008	0.97944475	
F6	100	41	48.8	100	41:48.8	0.84016393	0.91583279	
F7	100	40.7	47.6	100	40.7:47.6	0.85504202	0.93205086	
F8	100	40.6	50.4	100	4.06:5.04	0.80555556	0.87810743	
F9	100	42.7	44.2	100	21.35:22.1	0.96606335	1.05307126	
F10	100	44.3	43.5	100	44.3:43.5	1.0183908	1.11011155	
F11	100	45.7	42.7	100	15.23333333	1.07025761	1.16664971	
F12	100	42.1	42.2	100	1.002380952	0.99763033	1.0874813	
G1	100	39.5	43.4	100	39.5:43.4	0.91013825	0.9921093	
G2	100	41.7	48.4	100	41.7:48.4	0.86157025	0.93916705	
G3	100	40.4	47.7	100	40.4:47.7	0.84696017	0.92324112	
G4	100	39.6	50.1	100	39.6:50.1	0.79041916	0.86160778	
G5	100	39.8	52.6	100	3.061538461	0.75665399	0.82480157	
G6	100	40.7	49.7	100	40.7:49.7	0.81891348	0.89266842	
G7	100	44.5	46.1	100	22.25:23.05	0.96529284	1.05223135	
G8	100	45.7	46.5	100	45.7:46.5	0.9827957	1.07131059	
G9	100	37.4	52.2	100	37.4:52.2	0.7164751	0.78100399	
G10	100	46.6	43.3	100	46.6:43.3	1.07621247	1.17314089	
G11	100	42.6	46.3	100	21.3:23.15	0.92008639	1.00295341	
G12	100	41.8	43.7	100	41.8:43.7	0.95652174	1.04267029	
H1	100	44.5	39.6	100	44.5:39.6	1.12373737	1.2249461	
H2	100	44	42.4	100	22:21.2	1.03773585	1.1311989	
H3	100	40.9	47.8	100	40.9:47.8	0.85564854	0.932712	
H4	100	41.8	46.3	100	41.8:46.3	0.90280778	0.98411861	
H5	100	42.9	47.9	100	42.9:47.9	0.89561587	0.97627896	
H6	100	42.3	46.9	100	21.15:23.45	0.90191898	0.98314976	
H7	100	40.9	46.9	100	20.45:23.45	0.87206823	0.95061052	
H8	100	41	47.3	100	41:47.3	0.86680761	0.94487611	
H9	100	39.9	46.1	100	39.9:46.1	0.86550976	0.94346137	
H10	100	41.7	44.5	100	41.7:44.5	0.93707865	1.02147607	
H11	100	38.3	48	100	19.15:24	0.79791667	0.86978055	
H12	100	43.6	40.8	100	43.6:40.8	1.06862745	1.16487273	

Table A.8. Percentages from screen 1 plate 3

Screen 1 – Plate 4

Name / Desc	All	Mean GFP	Mean RFP	R01	Ratio Green/	Numerical Ra	Ratio/Scraml	Average scra
A1	100	44.7	44.8	100	1.01590909(	0.99776786	0.95914911	1.04026355
A2	100	43	46.3	100	43:46.3	0.9287257	0.89277924	
A3	100	42.7	47.5	100	42.7:47.5	0.89894737	0.86415348	
A4	100	45.2	45.5	100	1.004444444	0.99340659	0.95495665	
A5	100	44	48.7	100	11:12.175	0.90349076	0.86852102	
A6	100	43.5	47.5	100	43.5:47.5	0.91578947	0.88034371	
A7	100	39.6	49.5	100	39.6:49.5	0.8	0.76903589	
A8	100	42.7	45	100	14.23333333	0.94888889	0.91216201	
A9	100	44.5	44.3	100	1.011363636	1.00451467	0.96563479	
A10	100	46.7	43.9	100	46.7:43.9	1.06378132	1.02260751	
A11	100	43.9	45.8	100	43.9:45.8	0.95851528	0.92141581	
A12	100	44.7	45.1	100	44.7:45.1	0.99113082	0.95276896	
B1	100	45.3	42.3	100	15.1:14.1	1.07092199	1.0294718	
B2	100	47.8	43.9	100	47.8:43.9	1.08883827	1.04669463	
B3	100	47.3	45	100	47.3:45	1.05111111	1.01042771	
B4	100	42.6	48.7	100	7.1:8.116666	0.87474333	0.84088626	
B5	100	42.7	47.9	100	42.7:47.9	0.8914405	0.85693717	
B6	100	41.2	50.7	100	41.2:50.7	0.81262327	0.78117057	
B7	100	44.4	48.5	100	11.1:12.125	0.91546392	0.88003076	
B8	100	43.2	48.4	100	43.2:48.4	0.89256198	0.85801524	
B9	100	45.7	44.9	100	45.7:44.9	1.01781737	0.97842261	
B10	100	46.8	42.9	100	23.4:21.45	1.09090909	1.0486853	
B11	100	48.1	42.5	100	8.016666666	1.13176471	1.08795959	
B12	100	45.6	42.4	100	15.2:14.1333	1.0754717	1.03384541	
C1	100	26	41.4	100	26:41.4	0.62801932	0.60371175	
C2	100	45.8	46.8	100	45.8:46.8	0.97863248	0.94075437	
C3	100	45.8	46.4	100	45.8:46.4	0.98706897	0.94886432	
C4	100	43.5	50.1	100	43.5:50.1	0.86826347	0.83465721	
C5	100	43.9	46.4	100	43.9:46.4	0.94612069	0.90950095	
C6	100	41.1	50.1	100	41.1:50.1	0.82035928	0.78860716	
C7	100	40.4	49.5	100	40.4:49.5	0.81616162	0.78457196	
C8	100	41.1	51.1	100	41.1:51.1	0.80430528	0.77317453	
C9	100	41.8	45.5	100	41.8:45.5	0.91868132	0.88312363	
C10	100	47.3	43	100	47.3:43	1.1	1.05742434	
C11	100	45.1	44.6	100	45.1:44.6	1.01121076	0.97207171	
C12	100	44.5	42.6	100	22.25:21.3	1.04460094	1.00416951	
D1	100	50.2	35.5	100	10.04:7.1	1.41408451	1.35935217	
D2	100	43.6	46.9	100	43.6:46.9	0.92963753	0.89365577	
D3	100	44.2	44.8	100	1.004545454	0.98660714	0.94842037	
D4	100	45	44.8	100	45:44.8	1.00446429	0.96558635	
D5	100	46.3	44.9	100	23.15:22.45	1.0311804	0.99126842	
D6	100	38.6	52	100	19.3:26	0.74230769	0.71357657	
D7	100	41	48.6	100	41:48.6	0.8436214	0.81096891	
D8	100	46.1	44	100	23.05:22	1.04772727	1.00717484	
D9	100	46.6	44.4	100	23.3:22.2	1.04954955	1.00892658	
D10	100	40.2	50.7	100	4.02:5.07	0.79289941	0.76221012	
D11	100	42.4	46.4	100	21.2:23.2	0.9137931	0.87842461	
D12	100	43.3	45	100	43.3:45	0.96222222	0.92497927	
E1	100	47.5	42.2	100	47.5:42.2	1.12559242	1.0820262	
E2	100	42	49.9	100	6:7.1285714	0.84168337	0.80910589	
E3	100	41.6	49.4	100	41.6:49.4	0.84210526	0.80951146	
E4	100	44.9	48.7	100	11.225:12.17	0.92197125	0.88628622	
E5	100	43.2	47.3	100	43.2:47.3	0.91331924	0.87796909	
E6	100	42	50.1	100	21:25.05	0.83832335	0.80587593	
E7	100	38.5	48.6	100	19.25:24.3	0.79218107	0.76151959	
E8	100	45.2	46.8	100	45.2:46.8	0.96581197	0.92843008	
E9	100	37.8	51.4	100	37.8:51.4	0.73540856	0.70694447	
E10	100	47	40	100	47:40	1.175	1.12952146	
E11	100	47.3	43.3	100	47.3:43.3	1.09237875	1.05009808	
E12	100	23.5	39.7	100	23.5:39.7	0.59193955	0.56902844	
F1	100	44.6	44.3	100	1.013636363	1.00677201	0.96780476	
F2	100	45.3	43.4	100	45.3:43.4	1.0437788	1.00337919	
F3	100	39.7	49.6	100	39.7:49.6	0.80040323	0.76942351	
F4	100	42.8	43.4	100	42.8:43.4	0.98617512	0.94800507	
F5	100	39.8	48.3	100	13.26666666	0.82401656	0.79212288	
F6	100	37.6	53.6	100	37.6:53.6	0.70149254	0.67434117	
F7	100	43.3	45.8	100	43.3:45.8	0.94541485	0.90882243	
F8	100	39.5	47.9	100	39.5:47.9	0.82463466	0.79271705	
F9	100	42.3	46.1	100	21.15:23.05	0.9175705	0.8820558	
F10	100	45.1	46.2	100	45.1:46.2	0.97619048	0.93840688	
F11	100	41.2	51.1	100	41.2:51.1	0.80626223	0.77505574	
F12	100	45.5	45.7	100	1.011111111	0.99562363	0.95708788	
G1	100	44.8	46.7	100	22.4:23.35	0.95931478	0.92218436	
G2	100	43.7	44.7	100	43.7:44.7	0.97762864	0.93978938	
G3	100	44.4	46.2	100	22.2:23.1	0.96103896	0.92384181	
G4	100	42.9	43	100	42.9:43	0.99767442	0.95905929	
G5	100	41.4	49	100	41.4:49	0.84489796	0.81219606	
G6	100	44.4	47.8	100	44.4:47.8	0.92887029	0.89291824	
G7	100	46.1	40.6	100	23.05:20.3	1.13546798	1.09151953	
G8	100	43	48.6	100	43:48.6	0.88477366	0.85052837	
G9	100	47.5	43.5	100	47.5:43.5	1.09195402	1.04968979	
G10	100	40.5	49	100	40.5:49	0.82653061	0.79453963	
G11	100	46.5	44	100	23.25:22	1.05681818	1.01591388	
G12	100	42.6	44.3	100	21.3:22.15	0.96162528	0.92440544	
H1	100	41.8	44.8	100	41.8:44.8	0.93303571	0.89692243	
H2	100	45.1	44.4	100	45.1:44.4	1.01576577	0.97645041	
H3	100	44.9	41.8	100	44.9:41.8	1.07416268	1.03258706	
H4	100	45	45.9	100	1:1.02	0.98039216	0.94244594	
H5	100	48.1	41.4	100	48.1:41.4	1.16183575	1.11686673	
H6	100	43.7	46.4	100	43.7:46.4	0.94181034	0.90535744	
H7	100	47.1	45.1	100	47.1:45.1	1.0443459	1.00392434	
H8	100	43.4	46.8	100	43.4:46.8	0.92735043	0.8914572	
H9	100	45.6	45.3	100	1.013333333	1.00662252	0.96766105	
H10	100	44	47.3	100	44:47.3	0.93023256	0.89422777	
H11	100	41.8	47.9	100	41.8:47.9	0.87265136	0.83887526	
H12	100	46.9	40.8	100	23.45:20.4	1.1495098	1.10501786	

Table A.9. Percentages from screen 1 plate 4

Screen 1 – Plate 5.

Name / Desc	All	Mean GFP	Mean RFP	R01	Ratio Green/	Numerical Ra	Ratio/Scram	Average scra
A1	100	47.8	41.1	100	47.8:41.1	1.16301703	1.04739478	1.11039033
A2	100	48.4	40.5	100	6.05:5.0625	1.19506173	1.07625372	
A3	100	40.4	47.3	100	40.4:47.3	0.85412262	0.76920935	
A4	100	46.8	43.6	100	46.8:43.6	1.0733945	0.96668214	
A5	100	44.2	43	100	44.2:43	1.02790698	0.92571679	
A6	100	44.3	46.2	100	22.15:23.1	0.95887446	0.8635472	
A7	100	42.2	44.6	100	21.1:22.3	0.94618834	0.85212228	
A8	100	44.6	45.5	100	44.6:45.5	0.98021978	0.88277046	
A9	100	45.8	45.8	100	1.017777777	1	0.90058421	
A10	100	43.3	43.6	100	1.006976744	0.99311927	0.89438753	
A11	100	44.1	42.6	100	22.05:21.3	1.03521127	0.93229492	
A12	100	44.1	43.7	100	44.1:43.7	1.00915332	0.90882755	
B1	100	47.6	40.9	100	47.6:40.9	1.16381418	1.04811268	
B2	100	43.7	47.3	100	43.7:47.3	0.92389006	0.8320408	
B3	100	46.1	41.6	100	46.1:41.6	1.10817308	0.99800318	
B4	100	46.2	44.7	100	23.1:22.35	1.03355705	0.93080516	
B5	100	49.1	39.5	100	49.1:39.5	1.24303797	1.11946037	
B6	100	41.7	46.8	100	41.7:46.8	0.89102564	0.80244362	
B7	100	42.1	46.7	100	21.05:23.35	0.90149893	0.8118757	
B8	100	43.4	44.9	100	43.4:44.9	0.96659243	0.87049788	
B9	100	40.2	48.5	100	5.025:6.0625	0.82886598	0.74646361	
B10	100	37.4	49.8	100	37.4:49.8	0.75100402	0.67634236	
B11	100	38	51.4	100	38:51.4	0.73929961	0.66580156	
B12	100	45.4	42.1	100	15.13333333	1.0783848	0.97117632	
C1	100	22.8	43	100	22.8:43	0.53023256	0.47751907	
C2	100	42	49.3	100	6:7.0428571	0.85192698	0.76723199	
C3	100	45.3	45.3	100	1.006666666	1	0.90058421	
C4	100	43.6	45.3	100	43.6:45.3	0.96247241	0.86678745	
C5	100	45.4	42.8	100	15.13333333	1.06074766	0.9552926	
C6	100	44.3	47.5	100	44.3:47.5	0.93263158	0.83991328	
C7	100	40.1	48.1	100	5.0125:6.012	0.83367983	0.7507989	
C8	100	43.8	47.7	100	43.8:47.7	0.91823899	0.82695154	
C9	100	42.7	46.8	100	21.35:23.4	0.91239316	0.82168688	
C10	100	48.6	41.8	100	48.6:41.8	1.16267943	1.04709073	
C11	100	44.3	46.1	100	22.15:23.05	0.96095445	0.8654204	
C12	100	46.1	38.6	100	23.05:19.3	1.19430052	1.07556819	
D1	100	41.6	45.6	100	41.6:45.6	0.9122807	0.8215856	
D2	100	42.3	43.2	100	42.3:43.2	0.97916667	0.88182204	
D3	100	43.5	41.2	100	43.5:41.2	1.05582524	0.95085954	
D4	100	41.5	47.5	100	41.5:47.5	0.87368421	0.78682621	
D5	100	44.2	44.1	100	1.004545454	1.00226757	0.90262635	
D6	100	35.2	56.3	100	5.028571428	0.62522202	0.56306508	
D7	100	41.6	44.7	100	41.6:44.7	0.93064877	0.83812759	
D8	100	39.9	48	100	13.3:16	0.83125	0.74861063	
D9	100	44.1	44.3	100	1.002272727	0.99548533	0.89651837	
D10	100	37.6	53.7	100	37.6:53.7	0.70018622	0.63057665	
D11	100	46.8	43.6	100	46.8:43.6	1.0733945	0.96668214	
D12	100	45.1	41.8	100	45.1:41.8	1.07894737	0.97168297	
E1	100	44.4	39.6	100	44.4:39.6	1.12121212	1.00974593	
E2	100	40.6	46.5	100	20.3:23.25	0.87311828	0.78631654	
E3	100	43.6	46.5	100	43.6:46.5	0.93763441	0.84441874	
E4	100	45.5	45.4	100	1.011111111	1.00220264	0.90256788	
E5	100	40.3	47.6	100	40.3:47.6	0.84663866	0.76246941	
E6	100	42.6	49	100	6.085714285	0.86938776	0.78295689	
E7	100	40.2	47.9	100	40.2:47.9	0.83924843	0.75581389	
E8	100	41.7	44.9	100	41.7:44.9	0.92873051	0.83640004	
E9	100	41.5	47.7	100	41.5:47.7	0.87002096	0.78352714	
E10	100	40.7	46.7	100	20.35:23.35	0.87152034	0.78487746	
E11	100	44.8	45.7	100	44.8:45.7	0.98030635	0.88284842	
E12	100	22.4	38	100	11.2:19	0.58947368	0.53087069	
F1	100	43.4	44	100	43.4:44	0.98636364	0.88830352	
F2	100	42.2	44.9	100	21.1:22.45	0.93986637	0.84642881	
F3	100	44	46.2	100	22:23.1	0.95238095	0.85769925	
F4	100	40.1	48.7	100	5.0125:6.087	0.82340862	0.74154881	
F5	100	45	43.7	100	45:43.7	1.02974828	0.92737505	
F6	100	41.3	48	100	41.3:48	0.86041667	0.77487767	
F7	100	41.5	47.6	100	41.5:47.6	0.87184874	0.78517321	
F8	100	41.7	48	100	41.7:48	0.86875	0.78238253	
F9	100	41.6	45.7	100	41.6:45.7	0.91028446	0.81978782	
F10	100	41.1	49.2	100	41.1:49.2	0.83536585	0.7523173	
F11	100	42.5	46.9	100	21.25:23.45	0.90618337	0.81609444	
F12	100	42.6	43.6	100	42.6:43.6	0.97706422	0.87992861	
G1	100	44.4	42.3	100	22.2:21.15	1.04964539	0.94529407	
G2	100	45.3	43	100	45.3:43	1.05348837	0.948755	
G3	100	37.7	48.7	100	37.7:48.7	0.77412731	0.69716683	
G4	100	43.2	48.7	100	43.2:48.7	0.88706366	0.79887552	
G5	100	48.3	40.6	100	6.0375:5.075	1.18965517	1.07138467	
G6	100	41.1	47.9	100	41.1:47.9	0.85803758	0.7727351	
G7	100	38.3	52.6	100	19.15:26.3	0.72813688	0.65574858	
G8	100	41	49	100	41:49	0.83673469	0.75355005	
G9	100	39.7	47.8	100	39.7:47.8	0.83054393	0.74797475	
G10	100	40.5	46.7	100	20.25:23.35	0.86723769	0.78102057	
G11	100	41.3	47.6	100	41.3:47.6	0.86764706	0.78138924	
G12	100	46	41.5	100	46:41.5	1.10843373	0.99823792	
H1	100	43.5	40.4	100	43.5:40.4	1.07673267	0.96968845	
H2	100	42.4	43.7	100	42.4:43.7	0.97025172	0.87379338	
H3	100	44.6	42.5	100	22.3:21.25	1.04941176	0.94508367	
H4	100	43.8	45.5	100	43.8:45.5	0.96263736	0.86693601	
H5	100	41.5	46.6	100	41.5:46.6	0.89055794	0.80202242	
H6	100	43.8	43.6	100	1.018604651	1.00458716	0.90471533	
H7	100	32.7	53.4	100	32.7:53.4	0.61235955	0.55148134	
H8	100	42.7	48.2	100	7.116666666	0.88589212	0.79782045	
H9	100	41.7	46.2	100	41.7:46.2	0.9025974	0.81286497	
H10	100	43.9	40.2	100	43.9:40.2	1.0920398	0.9834738	
H11	100	34.2	53.3	100	34.2:53.3	0.64165103	0.57786079	
H12	100	51.4	38.1	100	51.4:38.1	1.34908136	1.21496138	

Table A.10. Percentages from screen 1 plate 5

Screen 1 – Plate 6.

Name / Desc	All	Mean GFP	Mean RFP	R01	Ratio Green/	Numerical Ra	Ratio/Scraml	Average scra
A1	100	39.9	44.9	100	39.9:44.9	0.88864143	0.96867637	0.917377
A2	100	40.7	44.2	100	10.175:11.05	0.92081448	1.00374707	
A3	100	45	39.2	100	15:13.06666	1.14795918	1.25134943	
A4	100	38.6	47.1	100	38.6:47.1	0.81953291	0.89334364	
A5	100	37.8	50.8	100	37.8:50.8	0.74409449	0.8111109	
A6	100	42	44	100	21:22	0.95454545	1.04051601	
A7	100	43.1	44.9	100	43.1:44.9	0.95991091	1.0463647	
A8	100	41.2	43.6	100	41.2:43.6	0.94495413	1.03006085	
A9	100	41.2	44	100	41.2:44	0.93636364	1.02069666	
A10	100	45	43	100	45:43	1.04651163	1.14076506	
A11	100	37.8	42.5	100	37.8:42.5	0.88941176	0.96951609	
A12	100	42.7	41.3	100	42.7:41.3	1.03389831	1.12701573	
B1	100	40.8	44.1	100	10.2:11.025	0.92517007	1.00849495	
B2	100	44.3	44.2	100	1.006818181	1.00226244	1.0925306	
B3	100	38.3	50.9	100	19.15:25.45	0.7524558	0.82022527	
B4	100	42.8	46.8	100	21.4:23.4	0.91452991	0.99689649	
B5	100	40.2	50.6	100	4.02:5.06	0.7944664	0.86601954	
B6	100	41.6	47.3	100	41.6:47.3	0.8794926	0.95870357	
B7	100	37.6	50.8	100	37.6:50.8	0.74015748	0.80681931	
B8	100	43.5	44.8	100	43.5:44.8	0.97098214	1.05843306	
B9	100	41.7	46.3	100	41.7:46.3	0.90064795	0.98176426	
B10	100	40	46.4	100	20:23.2	0.86206897	0.93971068	
B11	100	43.7	42.2	100	43.7:42.2	1.03554502	1.12881076	
B12	100	42	44.9	100	21:22.45	0.93541203	1.01965934	
C1	100	21.7	45.1	100	7.233333333	0.48115299	0.52448774	
C2	100	42.2	47	100	42.2:47	0.89787234	0.97873867	
C3	100	47.1	43.7	100	47.1:43.7	1.0778032	1.17487489	
C4	100	43	45.8	100	43:45.8	0.93886463	1.0234229	
C5	100	43.3	45.2	100	43.3:45.2	0.9579646	1.0442431	
C6	100	43.3	46.5	100	43.3:46.5	0.9311828	1.01504921	
C7	100	43.3	48	100	43.3:48	0.90208333	0.98332892	
C8	100	39.3	50.3	100	39.3:50.3	0.78131213	0.85168053	
C9	100	42.1	46.8	100	21.05:23.4	0.89957265	0.98059211	
C10	100	43.3	46.8	100	43.3:46.8	0.92521368	1.00854248	
C11	100	41.7	47.7	100	41.7:47.7	0.87421384	0.95294937	
C12	100	40.4	42.3	100	20.2:21.15	0.95508274	1.04110169	
D1	100	43.4	40.5	100	43.4:40.5	1.07160494	1.16811838	
D2	100	45.6	47	100	45.6:47	0.97021277	1.05759439	
D3	100	44.6	45.6	100	44.6:45.6	0.97807018	1.06615947	
D4	100	44.6	44.7	100	1.013636363	0.99776286	1.08762577	
D5	100	44.2	44.6	100	1.004545454	0.99103139	1.08028803	
D6	100	46	42.7	100	23:21.35	1.07728337	1.17430824	
D7	100	40.7	47.5	100	40.7:47.5	0.85684211	0.93401307	
D8	100	44.1	45.1	100	44.1:45.1	0.97782705	1.06589445	
D9	100	43.6	43.8	100	1.013953488	0.99543379	1.08508693	
D10	100	44.4	44.4	100	1.009090909	1	1.09006439	
D11	100	46.6	39.5	100	46.6:39.5	1.17974684	1.28600002	
D12	100	39	42.9	100	13:14.3	0.90909091	0.99096763	
E1	100	41.2	44	100	41.2:44	0.93636364	1.02069666	
E2	100	42.2	44.5	100	21.1:22.25	0.94831461	1.03372398	
E3	100	43.8	44.4	100	43.8:44.4	0.98648649	1.07533379	
E4	100	40.1	48.1	100	5.0125:6.012	0.83367983	0.9087647	
E5	100	41	46.5	100	41:46.5	0.88172043	0.96113204	
E6	100	43.8	46.7	100	43.8:46.7	0.9379015	1.02237303	
E7	100	41	48.1	100	41:48.1	0.85239085	0.92916092	
E8	100	43.9	44.9	100	43.9:44.9	0.97772829	1.06578679	
E9	100	41.2	44.8	100	41.2:44.8	0.91964286	1.00246993	
E10	100	45.5	43.1	100	45.5:43.1	1.05568445	1.15076403	
E11	100	42.1	47.1	100	42.1:47.1	0.89384289	0.9743463	
E12	100	17	44	100	17:44	0.38636364	0.42116124	
F1	100	39.1	44.4	100	39.1:44.4	0.88063063	0.95994409	
F2	100	42.2	47.2	100	42.2:47.2	0.8940678	0.97459147	
F3	100	41.6	45.5	100	41.6:45.5	0.91428571	0.9966303	
F4	100	44	45.5	100	44:45.5	0.96703297	1.0541282	
F5	100	42.5	47.3	100	42.5:47.3	0.89852008	0.97944475	
F6	100	41	48.8	100	41:48.8	0.84016393	0.91583279	
F7	100	40.7	47.6	100	40.7:47.6	0.85504202	0.93205086	
F8	100	40.6	50.4	100	4.06:5.04	0.80555556	0.87810743	
F9	100	42.7	44.2	100	21.35:22.1	0.96606335	1.05307126	
F10	100	44.3	43.5	100	44.3:43.5	1.0183908	1.11011155	
F11	100	45.7	42.7	100	15.23333333	1.07025761	1.16664971	
F12	100	42.1	42.2	100	1.002380952	0.99763033	1.0874813	
G1	100	39.5	43.4	100	39.5:43.4	0.91013825	0.9921093	
G2	100	41.7	48.4	100	41.7:48.4	0.86157025	0.93916705	
G3	100	40.4	47.7	100	40.4:47.7	0.84696017	0.92324112	
G4	100	39.6	50.1	100	39.6:50.1	0.79041916	0.86160778	
G5	100	39.8	52.6	100	3.061538461	0.75665399	0.82480157	
G6	100	40.7	49.7	100	40.7:49.7	0.81891348	0.89266842	
G7	100	44.5	46.1	100	22.25:23.05	0.96529284	1.05223135	
G8	100	45.7	46.5	100	45.7:46.5	0.9827957	1.07131059	
G9	100	37.4	52.2	100	37.4:52.2	0.7164751	0.78100399	
G10	100	46.6	43.3	100	46.6:43.3	1.07621247	1.17314089	
G11	100	42.6	46.3	100	21.3:23.15	0.92008639	1.00295341	
G12	100	41.8	43.7	100	41.8:43.7	0.95652174	1.04267029	
H1	100	44.5	39.6	100	44.5:39.6	1.12373737	1.2249461	
H2	100	44	42.4	100	22:21.2	1.03773585	1.1311989	
H3	100	40.9	47.8	100	40.9:47.8	0.85564854	0.932712	
H4	100	41.8	46.3	100	41.8:46.3	0.90280778	0.98411861	
H5	100	42.9	47.9	100	42.9:47.9	0.89561587	0.97627896	
H6	100	42.3	46.9	100	21.15:23.45	0.90191898	0.98314976	
H7	100	40.9	46.9	100	20.45:23.45	0.87206823	0.95061052	
H8	100	41	47.3	100	41:47.3	0.86680761	0.94487611	
H9	100	39.9	46.1	100	39.9:46.1	0.86550976	0.94346137	
H10	100	41.7	44.5	100	41.7:44.5	0.93707865	1.02147607	
H11	100	38.3	48	100	19.15:24	0.79791667	0.86978055	
H12	100	43.6	40.8	100	43.6:40.8	1.06862745	1.16487273	

Table A.11. Percentages from screen 1 plate 6

A.3.2 – Raw data from second screen

Screen 2 – Plate 1.

Name / Desc	All	Mean GFP	Mean RFP	R01	Ratio Green/Red	Numerical Ra	Ratio/Scraml	Average scra
A1	100	44.2	49.8	100	44.2:49.8	0.8875502	0.99132611	0.89531608
A2	100	40.9	49.6	100	40.9:49.6	0.82459677	0.92101192	
A3	100	40	54.2	100	20:27.1	0.73800738	0.82429815	
A4	100	37.8	58.1	100	37.8:58.1	0.65060241	0.72667344	
A5	100	37.5	54.2	100	37.5:54.2	0.69188192	0.77277951	
A6	100	35.7	58.1	100	35.7:58.1	0.61445783	0.68630269	
A7	100	41.1	49.4	100	41.1:49.4	0.83198381	0.92926267	
A8	100	44.8	51.9	100	44.8:51.9	0.86319846	0.96412706	
A9	100	46.2	48.3	100	23.1:24.15	0.95652174	1.06836207	
A10	100	48	45.6	100	16:15.2	1.05263158	1.17570946	
A11	100	40.1	53.1	100	40.1:53.1	0.75517891	0.84347744	
A12	100	36.8	51.4	100	12.2666666666666	0.71595331	0.79966542	
B1	100	42.7	51.6	100	14.2333333333333	0.82751938	0.92427624	
B2	100	43.6	46.8	100	43.6:46.8	0.93162393	1.04055312	
B3	100	39	54	100	13:18	0.72222222	0.80666732	
B4	100	39	52.1	100	3:4.00769230769	0.74856046	0.83608513	
B5	100	42.1	47.5	100	42.1:47.5	0.88631579	0.98994736	
B6	100	41.2	53.7	100	41.2:53.7	0.76722533	0.85693237	
B7	100	44.3	51.1	100	44.3:51.1	0.86692759	0.96829222	
B8	100	39	56.3	100	39:56.3	0.69271758	0.77371289	
B9	100	49.9	45.4	100	49.9:45.4	1.09911894	1.22763231	
B10	100	38.6	56.5	100	19.3:28.25	0.68318584	0.76306665	
B11	100	41.5	53.8	100	41.5:53.8	0.77137546	0.86156776	
B12	100	47.3	48.5	100	47.3:48.5	0.97525773	1.08928875	
C1	100	1.7	59.6	100	1.7:59.6	0.02852349	0.03185857	
C2	100	45.9	46.6	100	45.9:46.6	0.98497854	1.10014616	
C3	100	28.3	58.7	100	14.15:29.35	0.48211244	0.53848294	
C4	100	44.6	49.7	100	44.6:49.7	0.89738431	1.00231006	
C5	100	50.2	38	100	25.1:19	1.32105263	1.47551537	
C6	100	40	54.4	100	20:27.2	0.73529412	0.82126764	
C7	100	46.3	50.1	100	23.15:25.05	0.9241517	1.0322072	
C8	100	39	54.7	100	13:18.233333333	0.71297989	0.79634434	
C9	100	38.9	54.5	100	19.45:27.25	0.71376147	0.7972173	
C10	100	43.1	52.3	100	43.1:52.3	0.82409178	0.92044787	
C11	100	43.5	53.5	100	43.5:53.5	0.81308411	0.90815315	
C12	100	38.8	56	100	19.4:28	0.69285714	0.77386876	
D1	100	34.6	57.7	100	34.6:57.7	0.59965338	0.66976724	
D2	100	38.2	56.5	100	19.1:28.25	0.67610619	0.75515923	
D3	100	41.6	51.2	100	41.6:51.2	0.8125	0.90750074	
D4	100	41.3	53.3	100	41.3:53.3	0.77485929	0.86545892	
D5	100	42.3	50	100	21.15:25	0.846	0.94491769	
D6	100	45.8	47.8	100	45.8:47.8	0.958159	1.07019077	
D7	100	38.2	53.6	100	38.2:53.6	0.71268657	0.79601672	
D8	100	43.7	48.2	100	43.7:48.2	0.906639	1.01264685	
D9	100	48.7	43.7	100	48.7:43.7	1.11441648	1.24471849	
D10	100	36.9	56.4	100	9.225:14.1	0.65425532	0.73075346	
D11	100	37	56.8	100	37:56.8	0.65140845	0.72757372	
D12	100	42.8	51.4	100	14.2666666666666	0.83268482	0.93004565	
E1	100	44.2	49.9	100	44.2:49.9	0.88577154	0.98933948	
E2	100	40.8	52	100	10.2:13	0.78461538	0.87635574	
E3	100	36.2	57.7	100	12.0666666666666	0.62738302	0.70073914	
E4	100	38.5	50.9	100	19.25:25.45	0.75638507	0.84482463	
E5	100	52.8	28.5	100	13.2:7.125	1.85263158	2.06924865	
E6	100	43.8	48.4	100	43.8:48.4	0.90495868	1.01077005	
E7	100	39.7	51.5	100	13.2333333333333	0.77087379	0.86100742	
E8	100	41.9	48.6	100	41.9:48.6	0.86213992	0.96294475	
E9	100	43.8	47.8	100	43.8:47.8	0.91631799	1.02345754	
E10	100	48.2	43.7	100	48.2:43.7	1.10297483	1.23193904	
E11	100	38.4	58	100	19.2:29	0.66206897	0.73948071	
E12	100	1.1	57.9	100	1.1:57.9	0.01899827	0.02121963	
F1	100	38.8	48.9	100	19.4:24.45	0.79345603	0.88623008	
F2	100	37.8	57.4	100	37.8:57.4	0.65853659	0.73553531	
F3	100	43.8	50.6	100	43.8:50.6	0.86561265	0.96682353	
F4	100	39.3	49.4	100	39.3:49.4	0.79554656	0.88856503	
F5	100	40.9	50.3	100	4.09:5.03	0.81312127	0.90819465	
F6	100	35.5	53.4	100	35.5:53.4	0.66479401	0.74252437	
F7	100	44.8	49.8	100	44.8:49.8	0.89959839	1.00478302	
F8	100	40.7	52.8	100	10.175:13.2	0.77083333	0.86096224	
F9	100	39.9	52.1	100	3.0692307692307	0.76583493	0.85537941	
F10	100	39	52.7	100	3:4.05384615384	0.74003795	0.82656614	
F11	100	47.4	46.5	100	47.4:46.5	1.01935484	1.13854187	
F12	100	41.4	52.8	100	41.4:52.8	0.78409091	0.87576994	
G1	100	36.9	52.5	100	9.225:13.125	0.70285714	0.785038	
G2	100	42	49.7	100	6:7.1	0.84507042	0.94387943	
G3	100	42.2	51.1	100	14.0666666666666	0.8258317	0.92239124	
G4	100	36.4	56.1	100	9.1:14.025	0.64884135	0.72470647	
G5	100	42.8	46.9	100	21.4:23.45	0.91257996	1.01928244	
G6	100	44.2	47.1	100	44.2:47.1	0.93842887	1.04815372	
G7	100	40.9	54.1	100	20.45:27.05	0.75600739	0.84440279	
G8	100	43	51.1	100	43:51.1	0.84148728	0.93987733	
G9	100	42.5	54.5	100	7.0833333333333	0.77981651	0.87099577	
G10	100	41.1	51.6	100	41.1:51.6	0.79651163	0.88964294	
G11	100	39.1	53.6	100	39.1:53.6	0.72947761	0.81477104	
G12	100	41	46.7	100	41:46.7	0.87794433	0.98059708	
H1	100	42.2	45.6	100	14.0666666666666	0.9254386	1.03364457	
H2	100	41.6	50.9	100	41.6:50.9	0.8172888	0.91284947	
H3	100	38.5	55.5	100	38.5:55.5	0.69369369	0.77480313	
H4	100	40.4	53.4	100	40.4:53.4	0.75655431	0.84501365	
H5	100	39.5	53.1	100	39.5:53.1	0.74387947	0.83085683	
H6	100	38.7	53.2	100	38.7:53.2	0.72744361	0.81249922	
H7	100	42.6	51.8	100	14.2:17.2666666666	0.82239382	0.91855139	
H8	100	44.5	47.6	100	44.5:47.6	0.93487395	1.04418314	
H9	100	41.4	49.7	100	41.4:49.7	0.83299799	0.93039543	
H10	100	49.1	43.3	100	49.1:43.3	1.13394919	1.26653505	
H11	100	41.3	51.9	100	41.3:51.9	0.79576108	0.88880464	
H12	100	38	51.9	100	38:51.9	0.73217726	0.81778635	

Table A.12. Percentages from screen 2 plate 1

Screen 2 – Plate 2.

Name / Desc	All	Mean GFP	Mean RFP	R01	Ratio Green/	Numerical Ra	Ratio/Scram	Average scra
A1	100	42.4	47.2	100	42.4:47.2	0.89830508	0.97671339	0.9197223
A2	100	47.7	44.8	100	47.7:44.8	1.06473214	1.15766699	
A3	100	38.4	55.5	100	38.4:55.5	0.69189189	0.75228348	
A4	100	35	54.3	100	35:54.3	0.64456722	0.70082809	
A5	100	41.6	53	100	41.6:53	0.78490566	0.85341593	
A6	100	45.2	47.9	100	45.2:47.9	0.94363257	1.02599727	
A7	100	40.2	53.4	100	40.2:53.4	0.75280899	0.81851771	
A8	100	32.9	58.3	100	16.45:29.15	0.56432247	0.6135792	
A9	100	40.8	53.1	100	40.8:53.1	0.76836158	0.83542781	
A10	100	36.2	57.4	100	12.06666666	0.63066202	0.68570918	
A11	100	43.5	50.1	100	43.5:50.1	0.86826347	0.94404961	
A12	100	40.6	36.5	100	10.15:9.125	1.11232877	1.20941807	
B1	100	38.4	54.1	100	19.2:27.05	0.70979667	0.77175108	
B2	100	42.1	50.8	100	21.05:25.4	0.82874016	0.90107651	
B3	100	39	52.9	100	3:4.0692307	0.73724008	0.80158987	
B4	100	45.6	47.4	100	45.6:47.4	0.96202532	1.04599543	
B5	100	42.9	52.2	100	21.45:26.1	0.82183908	0.89357307	
B6	100	42.5	47.3	100	42.5:47.3	0.89852008	0.97694716	
B7	100	42	51.4	100	14:17.13333	0.81712062	0.88844277	
B8	100	41.7	49	100	41.7:49	0.85102041	0.92530149	
B9	100	38.8	52	100	19.4:26	0.74615385	0.81128168	
B10	100	25.5	65.5	100	5.1:13.1	0.38931298	0.42329405	
B11	100	38.3	55.2	100	38.3:55.2	0.69384058	0.75440226	
B12	100	47.1	46.2	100	47.1:46.2	1.01948052	1.10846559	
C1	100	0.7	57.6	100	0.012280701	0.01215278	0.01321353	
C2	100	42.9	50.3	100	21.45:25.15	0.8528827	0.92732633	
C3	100	33.3	58.2	100	33.3:58.2	0.57216495	0.62210621	
C4	100	37.1	48	100	37.1:48	0.77291667	0.84038048	
C5	100	41.9	52.3	100	41.9:52.3	0.80114723	0.87107514	
C6	100	47.9	41.1	100	47.9:41.1	1.16545012	1.26717611	
C7	100	37	55	100	37:55	0.67272727	0.73144608	
C8	100	44.6	49.4	100	44.6:49.4	0.90283401	0.98163762	
C9	100	40.5	53.3	100	40.5:53.3	0.75984991	0.82617319	
C10	100	42	51.3	100	14:17.1	0.81871345	0.89017462	
C11	100	40.8	50.8	100	4.08:5.08	0.80314961	0.87325229	
C12	100	40.1	53	100	40.1:53	0.75660377	0.82264372	
D1	100	39.2	51.3	100	13.06666666	0.76413255	0.83082965	
D2	100	44.7	47.9	100	44.7:47.9	0.93319415	1.01464774	
D3	100	37	50.3	100	37:50.3	0.73558648	0.79979194	
D4	100	39.8	51	100	13.26666666	0.78039216	0.84850847	
D5	100	40.7	51.2	100	40.7:51.2	0.79492188	0.86430641	
D6	100	41.8	46.7	100	41.8:46.7	0.89507495	0.97320131	
D7	100	40.2	50.3	100	4.02:5.03	0.79920477	0.86896314	
D8	100	44.5	44.8	100	1.011363636	0.99330357	1.08000379	
D9	100	37.6	54.7	100	37.6:54.7	0.68738574	0.74738401	
D10	100	45.5	47.8	100	45.5:47.8	0.95188285	1.03496767	
D11	100	38.7	47	100	38.7:47	0.82340426	0.89527486	
D12	100	43.6	49.8	100	43.6:49.8	0.87550201	0.95191995	
E1	100	44.9	50.7	100	22.45:25.35	0.88560158	0.96290106	
E2	100	38.9	53.3	100	38.9:53.3	0.72983114	0.79353425	
E3	100	40.5	48.9	100	5.0625:6.112	0.82822086	0.90051188	
E4	100	34.5	56.2	100	17.25:28.1	0.613879	0.66746126	
E5	100	40.7	49.6	100	40.7:49.6	0.82056452	0.89218726	
E6	100	40.4	49.9	100	40.4:49.9	0.80961924	0.88028663	
E7	100	41.4	51.2	100	41.4:51.2	0.80859375	0.87917163	
E8	100	40.8	46.5	100	20.4:23.25	0.87741935	0.95400466	
E9	100	45.7	46.6	100	45.7:46.6	0.9806867	1.06628566	
E10	100	41.9	47.8	100	41.9:47.8	0.87656904	0.95308012	
E11	100	44.6	47.8	100	44.6:47.8	0.93305439	1.01449578	
E12	100	2.8	55.5	100	2.8:55.5	0.05045045	0.054854	
F1	100	37.5	45.6	100	37.5:45.6	0.82236842	0.89414862	
F2	100	36.9	52.9	100	9.225:13.225	0.69754253	0.75842734	
F3	100	38.7	51.7	100	38.7:51.7	0.74854932	0.81388624	
F4	100	41.2	48.4	100	41.2:48.4	0.85123967	0.92553988	
F5	100	38	52.8	100	19:26.4	0.71969697	0.78251552	
F6	100	38.3	54.3	100	19.15:27.15	0.7053407	0.76690616	
F7	100	41.3	48.6	100	41.3:48.6	0.84979424	0.92396829	
F8	100	44.4	47	100	44.4:47	0.94468085	1.02713705	
F9	100	44.3	45.8	100	44.3:45.8	0.96724891	1.05167496	
F10	100	45	48.5	100	15:16.16666	0.92783505	1.00882087	
F11	100	42.6	49.1	100	6.085714285	0.86761711	0.94334682	
F12	100	45.5	44.7	100	45.5:44.7	1.01789709	1.10674395	
G1	100	36.4	47.8	100	36.4:47.8	0.76150628	0.82797414	
G2	100	40.3	47.8	100	40.3:47.8	0.84309623	0.91668565	
G3	100	36.1	58.9	100	18.05:29.45	0.61290323	0.66640031	
G4	100	38.5	52.9	100	19.25:26.45	0.72778828	0.79131308	
G5	100	39.5	55.9	100	39.5:55.9	0.70661896	0.768296	
G6	100	39.7	50.5	100	39.7:50.5	0.78613861	0.8547565	
G7	100	37.3	55.7	100	37.3:55.7	0.66965889	0.72810987	
G8	100	39.4	50.3	100	39.4:50.3	0.7833002	0.85167034	
G9	100	40	47.7	100	40:47.7	0.83857442	0.91176916	
G10	100	38.7	51.7	100	38.7:51.7	0.74854932	0.81388624	
G11	100	43.3	48	100	43.3:48	0.90208333	0.98082142	
G12	100	41.3	48.1	100	41.3:48.1	0.85862786	0.93357295	
H1	100	37.9	46.2	100	37.9:46.2	0.82034632	0.89195002	
H2	100	35	52.1	100	35:52.1	0.67178503	0.7304216	
H3	100	43.7	42.5	100	43.7:42.5	1.02823529	1.11798452	
H4	100	32.5	56.4	100	4.0625:7.05	0.57624113	0.62653818	
H5	100	36.5	50.5	100	18.25:25.25	0.72277228	0.78585925	
H6	100	39.7	50	100	39.7:50	0.794	0.86330407	
H7	100	39.1	51.4	100	13.03333333	0.76070039	0.82709791	
H8	100	39.2	54.9	100	13.06666666	0.7140255	0.77634902	
H9	100	40	53.6	100	40:53.6	0.74626866	0.81140651	
H10	100	39.4	52.4	100	3.030769230	0.7519084	0.81753851	
H11	100	43.8	49.7	100	43.8:49.7	0.88128773	0.95821068	
H12	100	39.2	49.2	100	39.2:49.2	0.79674797	0.86629189	

Table A.13. Percentages from screen 2 plate 2

Screen 2 – Plate 3.

Name / Desc	All	Mean GFP	Mean RFP	R01	Ratio Green/	Numerical Ra	Ratio/Scraml	Average scra
A1	100	43.5	48.6	100	43.5:48.6	0.89506173	0.94921328	0.94295113
A2	100	38.8	50.6	100	19.4:25.3	0.76679842	0.81318999	
A3	100	41.5	50.4	100	41.5:50.4	0.8234127	0.87322946	
A4	100	39.1	52.7	100	3.007692307	0.74193548	0.78682284	
A5	100	43.7	49.4	100	43.7:49.4	0.88461538	0.93813493	
A6	100	37.5	51.8	100	37.5:51.8	0.72393822	0.76773674	
A7	100	28.8	64.6	100	7.2:16.15	0.44582043	0.47279273	
A8	100	35.8	54.6	100	35.8:54.6	0.65567766	0.69534638	
A9	100	30.2	53	100	30.2:53	0.56981132	0.60428511	
A10	100	39.9	52.7	100	3.069230769	0.75711575	0.80292152	
A11	100	40.8	53.5	100	40.8:53.5	0.76261682	0.80875541	
A12	100	37.6	46.7	100	37.6:46.7	0.80513919	0.85385039	
B1	100	37.6	50.7	100	37.6:50.7	0.74161736	0.78648547	
B2	100	39.1	51.6	100	13.03333333	0.75775194	0.8035962	
B3	100	44	46.7	100	22:23.35	0.94218415	0.99918663	
B4	100	40.4	47.8	100	40.4:47.8	0.84518828	0.89632247	
B5	100	40	51	100	40:51	0.78431373	0.83176498	
B6	100	42.3	52.7	100	21.15:26.35	0.80265655	0.85121755	
B7	100	36.4	55.2	100	36.4:55.2	0.65942029	0.69931545	
B8	100	40.9	50.9	100	4.09:5.09	0.80353635	0.85215058	
B9	100	42	47.5	100	42:47.5	0.88421053	0.93770557	
B10	100	39.2	51.9	100	13.06666666	0.75529865	0.80099449	
B11	100	42.4	48.4	100	7.066666666	0.87603306	0.92903337	
B12	100	44.8	45.7	100	44.8:45.7	0.98030635	1.03961522	
C1	100	2.7	57.2	100	2.7:57.2	0.0472028	0.05005858	
C2	100	38	49.2	100	38:49.2	0.77235772	0.81908564	
C3	100	36.8	52.5	100	9.2:13.125	0.70095238	0.74336025	
C4	100	33.6	53.5	100	33.6:53.5	0.62803738	0.66603387	
C5	100	43.1	43	100	1.002325581	1.00232558	1.06296663	
C6	100	39.3	52.6	100	3.023076923	0.74714829	0.79235102	
C7	100	34	52.9	100	17:26.45	0.64272212	0.68160703	
C8	100	40.5	45.9	100	8.1:9.18	0.88235294	0.9357356	
C9	100	41.5	48.7	100	41.5:48.7	0.85215606	0.9037118	
C10	100	37.9	51.7	100	37.9:51.7	0.73307544	0.77742676	
C11	100	38.5	51.2	100	38.5:51.2	0.75195313	0.79744655	
C12	100	37.1	52.9	100	37.1:52.9	0.70132325	0.74375355	
D1	100	39.3	49.6	100	39.3:49.6	0.79233871	0.84027548	
D2	100	42.5	47.9	100	42.5:47.9	0.88726514	0.94094499	
D3	100	37.8	49.8	100	37.8:49.8	0.75903614	0.8049581	
D4	100	37.2	47.7	100	37.2:47.7	0.77987421	0.82705688	
D5	100	38.8	47	100	38.8:47	0.82553191	0.87547689	
D6	100	38.7	49.3	100	38.7:49.3	0.78498986	0.83248202	
D7	100	38.1	47.8	100	38.1:47.8	0.79707113	0.84529421	
D8	100	39.1	45.6	100	13.03333333	0.85745614	0.90933254	
D9	100	35.2	50.1	100	7.04:10.02	0.70259481	0.74510204	
D10	100	39.6	50.1	100	39.6:50.1	0.79041916	0.8382398	
D11	100	40.8	51.4	100	40.8:51.4	0.79377432	0.84179794	
D12	100	45.7	46.4	100	45.7:46.4	0.98491379	1.04450142	
E1	100	44.3	48.6	100	11.075:12.15	0.91152263	0.96667007	
E2	100	40.6	47.7	100	40.6:47.7	0.85115304	0.9026481	
E3	100	38.5	46.9	100	19.25:23.45	0.82089552	0.87055999	
E4	100	36.7	48	100	3.058333333	0.76458333	0.81084089	
E5	100	39.4	47.3	100	39.4:47.3	0.83298097	0.88337661	
E6	100	36.9	46.4	100	18.45:23.2	0.79525862	0.84337205	
E7	100	36.2	48.6	100	3.016666666	0.74485597	0.78992002	
E8	100	15.3	70.7	100	3.06:14.14	0.21640736	0.22950008	
E9	100	38.5	48.7	100	19.25:24.35	0.79055441	0.83838323	
E10	100	37.9	49.7	100	37.9:49.7	0.76257545	0.80871154	
E11	100	38.1	49	100	38.1:49	0.77755102	0.82459313	
E12	100	3.7	55.7	100	3.7:55.7	0.06642729	0.07044616	
F1	100	36.4	43	100	36.4:43	0.84651163	0.89772588	
F2	100	39	47.5	100	39:47.5	0.82105263	0.8707266	
F3	100	43.1	46.7	100	43.1:46.7	0.92291221	0.97874872	
F4	100	39.5	46.3	100	39.5:46.3	0.85313175	0.90474652	
F5	100	40.4	45.5	100	8.08:9.1	0.88791209	0.94163108	
F6	100	38.7	48.6	100	19.35:24.3	0.7962963	0.8444725	
F7	100	39.3	49.2	100	39.3:49.2	0.79878049	0.84710699	
F8	100	37.8	49.8	100	37.8:49.8	0.75903614	0.8049581	
F9	100	40.3	43.3	100	40.3:43.3	0.93071594	0.98702458	
F10	100	36.9	46.5	100	18.45:23.25	0.79354839	0.84155834	
F11	100	41	45.6	100	41:45.6	0.89912281	0.95352005	
F12	100	43.4	48	100	43.4:48	0.90416667	0.95886907	
G1	100	35	46.3	100	35:46.3	0.75593952	0.80167413	
G2	100	38.9	47.1	100	38.9:47.1	0.82590234	0.87586972	
G3	100	40.3	46.9	100	20.15:23.45	0.85927505	0.9112615	
G4	100	40	46.2	100	20:23.1	0.86580087	0.91818212	
G5	100	39.9	47.4	100	39.9:47.4	0.84177215	0.89269966	
G6	100	34.2	52.6	100	17.1:26.3	0.65019011	0.68952684	
G7	100	43	46.4	100	43:46.4	0.92672414	0.98279127	
G8	100	36	51.8	100	12:17.26666	0.69498069	0.73702727	
G9	100	40.8	49.6	100	40.8:49.6	0.82258065	0.87234706	
G10	100	41.3	49	100	41.3:49	0.84285714	0.8938503	
G11	100	38.3	49.9	100	38.3:49.9	0.76753507	0.81397121	
G12	100	39.2	45.8	100	13.06666666	0.8558952	0.90767716	
H1	100	39.1	42.9	100	13.03333333	0.91142191	0.96656326	
H2	100	41.1	49	100	41.1:49	0.83877551	0.88952172	
H3	100	38.2	51	100	38.2:51	0.74901961	0.79433556	
H4	100	40.6	49	100	40.6:49	0.82857143	0.87870029	
H5	100	33.8	56.3	100	33.8:56.3	0.60035524	0.63667694	
H6	100	40.3	50	100	4.03:5	0.806	0.85476328	
H7	100	39.3	52.2	100	3.023076923	0.75287356	0.79842268	
H8	100	43.1	48	100	43.1:48	0.89791667	0.95224094	
H9	100	40.7	52.4	100	10.175:13.1	0.77671756	0.82370924	
H10	100	38.8	53.2	100	38.8:53.2	0.72932331	0.77344762	
H11	100	27.6	59.5	100	27.6:59.5	0.46386555	0.49192957	
H12	100	42.4	42.5	100	1.009523809	0.99764706	1.05800506	

Table A.14. Percentages from screen 2 plate 3

Screen 2 – Plate 4.

Name / Desc	All	Mean GFP	Mean RFP	R01	Ratio Green/	Numerical Ra	Ratio/Scram	Average scra
A1	100	42.1	48.8	100	7.016666666	0.86270492	0.96695981	0.89218281
A2	100	38.1	52	100	19.05:26	0.73269231	0.82123563	
A3	100	34.5	55.8	100	34.5:55.8	0.61827957	0.69299651	
A4	100	33.5	56.9	100	33.5:56.9	0.5887522	0.65990085	
A5	100	36.6	53.5	100	36.6:53.5	0.68411215	0.76678472	
A6	100	39.5	48.9	100	13.16666666	0.80777096	0.90538727	
A7	100	41	49.1	100	41:49.1	0.83503055	0.93594109	
A8	100	42.5	49.3	100	6.071428571	0.86206897	0.966247	
A9	100	39.9	50.1	100	39.9:50.1	0.79640719	0.89265023	
A10	100	38.6	53	100	38.6:53	0.72830189	0.81631464	
A11	100	41.9	50	100	41.9:50	0.838	0.93926939	
A12	100	37.5	49.9	100	37.5:49.9	0.75150301	0.84231953	
B1	100	38	51.6	100	38:51.6	0.73643411	0.82542961	
B2	100	40.5	47	100	40.5:47	0.86170213	0.96583583	
B3	100	37.3	51.5	100	37.3:51.5	0.72427184	0.81179758	
B4	100	36.7	49.4	100	36.7:49.4	0.74291498	0.83269367	
B5	100	18	70.3	100	9:35.15	0.25604552	0.28698773	
B6	100	45.1	45.2	100	1.002222222	0.99778761	1.11836677	
B7	100	41.4	48.9	100	41.4:48.9	0.84662577	0.94893755	
B8	100	37.3	53.7	100	37.3:53.7	0.69459963	0.77853958	
B9	100	42	47.9	100	42:47.9	0.87682672	0.98278818	
B10	100	37.5	55.2	100	37.5:55.2	0.67934783	0.76144465	
B11	100	42.8	46	100	21.4:23	0.93043478	1.04287459	
B12	100	46.9	46.3	100	1.019565217	1.01295896	1.13537153	
C1	100	2.1	57.5	100	2.1:57.5	0.03652174	0.04093526	
C2	100	40.2	50.4	100	4.02:5.04	0.79761905	0.89400854	
C3	100	34.8	54.5	100	17.4:27.25	0.63853211	0.7156965	
C4	100	25.4	61	100	25.4:61	0.41639344	0.46671314	
C5	100	37.8	52.8	100	37.8:52.8	0.71590909	0.80242422	
C6	100	34.2	53.1	100	34.2:53.1	0.6440678	0.72190115	
C7	100	35.6	52	100	35.6:52	0.68461538	0.76734877	
C8	100	37.8	53.8	100	37.8:53.8	0.70260223	0.78750927	
C9	100	39.1	47.4	100	39.1:47.4	0.82489451	0.92458015	
C10	100	36.7	52.4	100	9.175:13.1	0.70038168	0.78502037	
C11	100	37.3	51.6	100	37.3:51.6	0.72286822	0.81022433	
C12	100	40.4	50.6	100	4.04:5.06	0.79841897	0.89490513	
D1	100	38.7	52.8	100	19.35:26.4	0.73295455	0.82152955	
D2	100	41	47	100	41:47	0.87234043	0.97775973	
D3	100	41.4	49.5	100	41.4:49.5	0.83636364	0.93743527	
D4	100	41.7	46.1	100	41.7:46.1	0.90455531	1.01386768	
D5	100	40.8	47	100	40.8:47	0.86808511	0.97299017	
D6	100	40	47.3	100	40:47.3	0.84566596	0.94786175	
D7	100	37.6	50.4	100	37.6:50.4	0.74603175	0.83618709	
D8	100	36.8	49.2	100	36.8:49.2	0.74796748	0.83835675	
D9	100	45.6	48.7	100	15.2:16.233	0.93634497	1.049499	
D10	100	37.7	51.9	100	37.7:51.9	0.72639692	0.81417946	
D11	100	37.3	50.4	100	37.3:50.4	0.74007937	0.82951538	
D12	100	44	48.5	100	11:12.125	0.90721649	1.01685045	
E1	100	41.1	52.3	100	41.1:52.3	0.78585086	0.8808182	
E2	100	38.7	50.7	100	19.35:25.35	0.76331361	0.85555741	
E3	100	37.8	47.1	100	37.8:47.1	0.80254777	0.89953288	
E4	100	36.6	51.2	100	12.2:17.066	0.71484375	0.80123013	
E5	100	38.2	47.7	100	38.2:47.7	0.80083857	0.89761713	
E6	100	36.9	53.4	100	36.9:53.4	0.69101124	0.77451754	
E7	100	39.5	48.4	100	13.16666666	0.8161157	0.91474045	
E8	100	37.6	47.9	100	37.6:47.9	0.78496868	0.87982942	
E9	100	32.1	55	100	32.1:55	0.58363636	0.65416679	
E10	100	40.5	47.5	100	40.5:47.5	0.85263158	0.95566914	
E11	100	40.1	51.4	100	40.1:51.4	0.78015564	0.87443474	
E12	100	3.1	55.1	100	3.1:55.1	0.05626134	0.06306033	
F1	100	35	47.1	100	35:47.1	0.74309979	0.83290081	
F2	100	42.2	48.3	100	7.033333333	0.873706	0.97929034	
F3	100	38.4	51.8	100	38.4:51.8	0.74131274	0.83089781	
F4	100	37	52	100	37:52	0.71153846	0.79752541	
F5	100	39.9	47.9	100	39.9:47.9	0.83298539	0.93364877	
F6	100	47.3	37.7	100	47.3:37.7	1.25464191	1.40626102	
F7	100	36.8	52	100	9.2:13	0.70769231	0.79321446	
F8	100	42.4	48.7	100	7.066666666	0.87063655	0.97584995	
F9	100	37.1	53.1	100	37.1:53.1	0.69868173	0.78311499	
F10	100	39.5	50.2	100	39.5:50.2	0.78685259	0.88194099	
F11	100	37.5	52.1	100	37.5:52.1	0.71976967	0.80675134	
F12	100	34.6	57.1	100	34.6:57.1	0.60595447	0.67918196	
G1	100	36.6	44.5	100	9.15:11.125	0.82247191	0.92186478	
G2	100	20.2	68.9	100	5.05:17.225	0.29317852	0.32860812	
G3	100	38.8	51.3	100	38.8:51.3	0.75633528	0.84773577	
G4	100	39.8	48.2	100	13.26666666	0.82572614	0.92551227	
G5	100	38.7	52.1	100	19.35:26.05	0.7428023	0.83256738	
G6	100	38.3	51.1	100	38.3:51.1	0.74951076	0.84008653	
G7	100	36.7	55.6	100	36.7:55.6	0.66007194	0.73983934	
G8	100	42.3	47.7	100	42.3:47.7	0.88679245	0.99395824	
G9	100	41.1	49.6	100	41.1:49.6	0.82862903	0.92876597	
G10	100	37.7	51.2	100	37.7:51.2	0.73632813	0.82531082	
G11	100	38.8	50.5	100	19.4:25.25	0.76831683	0.86116525	
G12	100	38.5	47.9	100	38.5:47.9	0.80375783	0.90088917	
H1	100	40.5	40.6	100	1.0125:1.015	0.99753695	1.11808582	
H2	100	36.5	53.6	100	36.5:53.6	0.68097015	0.76326302	
H3	100	38.3	51.7	100	38.3:51.7	0.74081238	0.83033698	
H4	100	40.4	50.8	100	4.04:5.08	0.79527559	0.89138188	
H5	100	38.5	54.2	100	19.25:27.1	0.7103321	0.79617327	
H6	100	40.8	50.9	100	4.08:5.09	0.80157171	0.89843886	
H7	100	39.8	52.7	100	3.061538461	0.75521822	0.84648371	
H8	100	41.6	50.1	100	41.6:50.1	0.83033932	0.93068294	
H9	100	37.7	55.8	100	37.7:55.8	0.67562724	0.75727444	
H10	100	38.8	52.4	100	19.4:26.2	0.74045802	0.82993979	
H11	100	39.8	50.1	100	39.8:50.1	0.79441118	0.89041301	
H12	100	39.1	48.8	100	13.03333333	0.80122951	0.89805531	

Table A.15. Percentages from screen 2 plate 4

Screen 2 – Plate 5.

Name / Desc	All	Mean GFP	Mean RFP	R01	Ratio Green/	Numerical Ra	Ratio/Scram	Average scra
A1	100	42.6	53.6	100	42.6:53.6	0.79477612	0.87991321	0.90324376
A2	100	42	49	100	6:7	0.85714286	0.94896073	
A3	100	35.7	56.1	100	5.1:8.014285	0.63636364	0.70453145	
A4	100	40.5	51.4	100	40.5:51.4	0.78793774	0.8723423	
A5	100	40.3	51.3	100	40.3:51.3	0.78557505	0.86972652	
A6	100	45.3	49.6	100	45.3:49.6	0.91330645	1.01114061	
A7	100	40.5	52.3	100	10.125:13.07	0.77437859	0.85733068	
A8	100	41.1	50.3	100	41.1:50.3	0.81709742	0.90462558	
A9	100	40.3	53.2	100	40.3:53.2	0.7575188	0.83866485	
A10	100	37.7	55.7	100	37.7:55.7	0.67684022	0.74934391	
A11	100	40.6	52.2	100	10.15:13.05	0.77777778	0.86109399	
A12	100	42.3	44.9	100	21.15:22.45	0.94209354	1.0430114	
B1	100	43.4	47.4	100	43.4:47.4	0.91561181	1.01369293	
B2	100	44.5	47.6	100	44.5:47.6	0.93487395	1.03501844	
B3	100	43.9	49.9	100	43.9:49.9	0.87975952	0.97400011	
B4	100	41.1	49.4	100	41.1:49.4	0.83198381	0.92110662	
B5	100	46.6	45.7	100	46.6:45.7	1.01969365	1.1289241	
B6	100	42.7	49.6	100	6.1:7.085714	0.8608871	0.95310605	
B7	100	40.8	52.8	100	10.2:13.2	0.77272727	0.85550247	
B8	100	45.1	48.1	100	15.03333333	0.93762994	1.03806965	
B9	100	45.2	48.9	100	15.06666666	0.92433538	1.02335097	
B10	100	44.9	49.1	100	44.9:49.1	0.91446029	1.01241805	
B11	100	41.1	51.1	100	41.1:51.1	0.80430528	0.89046315	
B12	100	49.2	46	100	49.2:46	1.06956522	1.18413795	
C1	100	1.7	62.5	100	1.7:62.5	0.0272	0.03011369	
C2	100	37.4	56.2	100	37.4:56.2	0.66548043	0.73676726	
C3	100	40.5	49.4	100	40.5:49.4	0.81983806	0.90765981	
C4	100	45.8	43.3	100	45.8:43.3	1.05773672	1.17104238	
C5	100	39.7	48.8	100	13.23333333	0.81352459	0.90067004	
C6	100	40.7	48.7	100	5.0875:6.087	0.83572895	0.92525295	
C7	100	41.6	50.2	100	41.6:50.2	0.82868526	0.91745473	
C8	100	44	49.7	100	44:49.7	0.88531187	0.98014723	
C9	100	43.9	50.5	100	43.9:50.5	0.86930693	0.96242783	
C10	100	39.2	53.8	100	39.2:53.8	0.72862454	0.80667541	
C11	100	42.6	50.5	100	21.3:25.25	0.84356436	0.93392769	
C12	100	38.3	54.7	100	19.15:27.35	0.70018282	0.77518699	
D1	100	38.9	55.8	100	38.9:55.8	0.69713262	0.77181005	
D2	100	45	46.9	100	45:46.9	0.95948827	1.06226947	
D3	100	46.1	49	100	46.1:49	0.94081633	1.04159737	
D4	100	44.8	43	100	44.8:43	1.04186047	1.15346544	
D5	100	40.9	49.1	100	40.9:49.1	0.83299389	0.9222249	
D6	100	40.6	48.2	100	5.075:6.025	0.84232365	0.93255408	
D7	100	41.7	48.1	100	41.7:48.1	0.86694387	0.95981163	
D8	100	46	45.7	100	46:45.7	1.00656455	1.1143886	
D9	100	38.1	52.3	100	19.05:26.15	0.72848948	0.8065259	
D10	100	44.3	48.7	100	11.075:12.17	0.90965092	1.0070935	
D11	100	40.5	52.5	100	10.125:13.12	0.77142857	0.85406466	
D12	100	44.7	48.7	100	11.175:12.17	0.91786448	1.0161869	
E1	100	43.2	52	100	43.2:52	0.83076923	0.91976194	
E2	100	40.1	53.3	100	40.1:53.3	0.75234522	0.83293707	
E3	100	41.9	49.5	100	41.9:49.5	0.84646465	0.93713866	
E4	100	43.6	47.6	100	43.6:47.6	0.91596639	1.01408548	
E5	100	38.2	50.9	100	19.1:25.45	0.75049116	0.83088441	
E6	100	43	47.9	100	43:47.9	0.89770355	0.99386632	
E7	100	45.1	44.7	100	45.1:44.7	1.00894855	1.11702797	
E8	100	39.8	49.4	100	39.8:49.4	0.80566802	0.89197186	
E9	100	38.4	51.2	100	38.4:51.2	0.75	0.83034064	
E10	100	42.7	49.3	100	6.1:7.042857	0.86612576	0.95890589	
E11	100	44.7	49.1	100	44.7:49.1	0.91038697	1.00790839	
E12	100	2.2	60.6	100	1.1:30.3	0.03630363	0.04019251	
F1	100	43.7	44	100	43.7:44	0.99318182	1.0995723	
F2	100	39.2	55.3	100	39.2:55.3	0.70886076	0.78479453	
F3	100	43.3	50.8	100	43.3:50.8	0.8523622	0.94366797	
F4	100	41.6	46.7	100	41.6:46.7	0.89079229	0.98621472	
F5	100	41.5	49.2	100	41.5:49.2	0.84349593	0.93385194	
F6	100	46.9	41.8	100	46.9:41.8	1.12200957	1.24220019	
F7	100	45.7	45.9	100	1.015555555	0.9956427	1.10229679	
F8	100	42.9	47.6	100	42.9:47.6	0.9012605	0.9978043	
F9	100	48.5	44.3	100	12.125:11.07	1.09480813	1.2120849	
F10	100	40.1	47.2	100	40.1:47.2	0.84957627	0.9405836	
F11	100	45.1	49.8	100	45.1:49.8	0.90562249	1.00263354	
F12	100	64.9	24.3	100	8.1125:3.037	2.67078189	2.95687832	
G1	100	38.1	47	100	38.1:47	0.8106383	0.89747456	
G2	100	43.7	50	100	43.7:50	0.874	0.96762362	
G3	100	43.7	51.5	100	43.7:51.5	0.84854369	0.93944041	
G4	100	39.8	50.3	100	39.8:50.3	0.79125249	0.87601212	
G5	100	44.1	46.7	100	22.05:23.35	0.94432548	1.04548243	
G6	100	38.6	52.6	100	19.3:26.3	0.7338403	0.8124499	
G7	100	40.2	53.3	100	40.2:53.3	0.75422139	0.83501422	
G8	100	45.3	47.2	100	45.3:47.2	0.95974576	1.06255454	
G9	100	38.3	55	100	38.3:55	0.69636364	0.7709587	
G10	100	39.1	51.8	100	13.03333333	0.75482625	0.83568388	
G11	100	40.5	52.1	100	10.125:13.02	0.77735125	0.86062177	
G12	100	42.5	47.8	100	42.5:47.8	0.88912134	0.98436477	
H1	100	40.3	45.6	100	8.06:9.12	0.88377193	0.97844233	
H2	100	42.4	51.3	100	14.13333333	0.82651072	0.91504725	
H3	100	43.7	50.4	100	43.7:50.4	0.86706349	0.95994407	
H4	100	41.4	49.6	100	41.4:49.6	0.83467742	0.92408877	
H5	100	41.2	52.1	100	41.2:52.1	0.79078695	0.87549672	
H6	100	36	56.7	100	9:14.175	0.63492063	0.70293387	
H7	100	37.1	56.6	100	37.1:56.6	0.65547703	0.72569229	
H8	100	42.9	50.7	100	21.45:25.35	0.84615385	0.93679456	
H9	100	40.5	53.8	100	40.5:53.8	0.7527881	0.83342741	
H10	100	39.7	53.5	100	39.7:53.5	0.74205607	0.82154575	
H11	100	38.1	55.1	100	38.1:55.1	0.69147005	0.76554091	
H12	100	43.6	46.7	100	43.6:46.7	0.93361884	1.03362889	

Table A.16. Percentages from screen 2 plate 5

Screen 2 – Plate 6.

Name / Desc	All	Mean GFP	Mean RFP	R01	Ratio Green/	Numerical Ra	Ratio/Scram	Average scra
A1	100	43.6	49.7	100	43.6:49.7	0.87726358	1.20457532	0.72827624
A2	100	47.3	36.7	100	47.3:36.7	1.28882834	1.76969709	
A3	100	44.3	42.6	100	22.15:21.3	1.0399061	1.42790064	
A4	100	38.1	45.1	100	38.1:45.1	0.84478936	1.15998479	
A5	100	40.4	48.1	100	5.05:6.0125	0.83991684	1.15329431	
A6	100	41.7	47.1	100	41.7:47.1	0.88535032	1.21567926	
A7	100	42.9	48.7	100	7.15:8.11666	0.88090349	1.2095733	
A8	100	41.2	47.8	100	41.2:47.8	0.86192469	1.1835134	
A9	100	34.7	56.7	100	17.35:28.35	0.61199295	0.84033079	
A10	100	39.5	54	100	13.16666666	0.73148148	1.00440114	
A11	100	37.5	54.6	100	37.5:54.6	0.68681319	0.94306686	
A12	100	42.3	40.4	100	21.15:20.2	1.0470297	1.43768209	
B1	100	38.8	51.5	100	38.8:51.5	0.75339806	1.03449491	
B2	100	32.1	56.2	100	4.0125:7.025	0.57117438	0.78428259	
B3	100	38.7	47.4	100	38.7:47.4	0.8164557	1.12107969	
B4	100	38.6	50.2	100	19.3:25.1	0.7689243	1.05581408	
B5	100	38.7	50.8	100	19.35:25.4	0.76181102	1.04604679	
B6	100	39.9	45.1	100	13.3:15.0333	0.88470067	1.21478722	
B7	100	39.3	48.6	100	13.1:16.2	0.80864198	1.11035062	
B8	100	41.1	46.1	100	41.1:46.1	0.89154013	1.22417852	
B9	100	44.2	44.9	100	1.004545454	0.9844098	1.35169836	
B10	100	38.5	49.5	100	38.5:49.5	0.77777778	1.06797083	
B11	100	41.7	49.4	100	41.7:49.4	0.84412955	1.15907881	
B12	100	22.5	69.4	100	22.5:69.4	0.32420749	0.44517104	
C1	100	1.6	63.4	100	1.6:63.4	0.02523659	0.0346525	
C2	100	36.8	50.5	100	18.4:25.25	0.72871287	1.00059954	
C3	100	40.5	47.6	100	40.5:47.6	0.85084034	1.16829342	
C4	100	39.1	46.8	100	39.1:46.8	0.83547009	1.14718845	
C5	100	39.5	47.9	100	39.5:47.9	0.82463466	1.13231026	
C6	100	38.1	46	100	19.05:23	0.82826087	1.13728943	
C7	100	40.2	43.8	100	40.2:43.8	0.91780822	1.26024738	
C8	100	46	40	100	23:20	1.15	1.57907116	
C9	100	39.5	47	100	39.5:47	0.84042553	1.1539928	
C10	100	36.3	51.1	100	12.1:17.0333	0.71037182	0.97541535	
C11	100	43.5	48.6	100	43.5:48.6	0.89506173	1.22901405	
C12	100	36.9	53.5	100	36.9:53.5	0.68971963	0.94705771	
D1	100	43.9	44.6	100	43.9:44.6	0.98430493	1.35155437	
D2	100	41.3	45.9	100	41.3:45.9	0.89978214	1.23549567	
D3	100	39.3	49.8	100	39.3:49.8	0.78915663	1.08359519	
D4	100	41.9	44.7	100	41.9:44.7	0.93736018	1.28709428	
D5	100	40.5	44.7	100	10.125:11.17	0.90604027	1.24408874	
D6	100	44	41.2	100	44:41.2	1.06796117	1.46642319	
D7	100	37.4	45.9	100	37.4:45.9	0.81481481	1.11882658	
D8	100	34.3	48.2	100	17.15:24.1	0.71161826	0.97712684	
D9	100	38	51.1	100	38:51.1	0.74363992	1.02109596	
D10	100	45.5	45.5	100	1.011111111	1	1.37310535	
D11	100	44	48.8	100	11:12.2	0.90163934	1.23804581	
D12	100	46.3	45.8	100	46.3:45.8	1.01091703	1.38809559	
E1	100	39.1	55.8	100	39.1:55.8	0.70071685	0.96215805	
E2	100	43.8	45.8	100	43.8:45.8	0.95633188	1.31314442	
E3	100	41.8	44.8	100	41.8:44.8	0.93303571	1.28115633	
E4	100	42.2	45.5	100	14.06666666	0.92747253	1.27351749	
E5	100	42.2	41.8	100	42.2:41.8	1.00956938	1.38624512	
E6	100	41.2	44.8	100	41.2:44.8	0.91964286	1.26276653	
E7	100	37.2	49.1	100	37.2:49.1	0.75763747	1.04031607	
E8	100	39	43.3	100	39:43.3	0.90069284	1.23674616	
E9	100	39.8	46.2	100	39.8:46.2	0.86147186	1.18289162	
E10	100	36.1	48.5	100	3.008333333	0.7443299	1.02204337	
E11	100	38.4	48.3	100	19.2:24.15	0.79503106	1.0916614	
E12	100	3.3	60	100	1.1:20	0.055	0.07552079	
F1	100	38.2	46.2	100	19.1:23.1	0.82683983	1.13533819	
F2	100	43.4	45.9	100	43.4:45.9	0.94553377	1.29831748	
F3	100	40.9	45.5	100	8.18:9.1	0.8989011	1.23428591	
F4	100	39.8	50.2	100	39.8:50.2	0.79282869	1.08863731	
F5	100	39	43.3	100	39:43.3	0.90069284	1.23674616	
F6	100	42.2	46.4	100	21.1:23.2	0.90948276	1.24881564	
F7	100	40.5	45.3	100	8.1:9.06	0.89403974	1.22761075	
F8	100	36.7	44.7	100	9.175:11.175	0.82102908	1.12735943	
F9	100	41.9	48.8	100	41.9:48.8	0.85860656	1.17895726	
F10	100	40.6	49.1	100	40.6:49.1	0.82688391	1.13539872	
F11	100	39.7	50.1	100	39.7:50.1	0.79241517	1.08806951	
F12	100	43.4	46.6	100	43.4:46.6	0.93133047	1.27881486	
G1	100	37.5	45.5	100	37.5:45.5	0.82417582	1.13168024	
G2	100	39.9	48.7	100	13.3:16.2333	0.81930185	1.12498775	
G3	100	42.9	44.8	100	21.45:22.4	0.95758929	1.31487097	
G4	100	41.4	47.1	100	41.4:47.1	0.87898089	1.20693337	
G5	100	39.8	42	100	13.26666666	0.94761905	1.30118079	
G6	100	42.2	45.9	100	14.06666666	0.91938998	1.2624193	
G7	100	41.8	47.2	100	41.8:47.2	0.88559322	1.21601279	
G8	100	37.9	50.4	100	37.9:50.4	0.75198413	1.03255343	
G9	100	43.8	49.2	100	43.8:49.2	0.8902439	1.22239867	
G10	100	40	50.5	100	4:5.05	0.79207921	1.0876082	
G11	100	44.9	46.5	100	22.45:23.25	0.9655914	1.32585872	
G12	100	41.8	46.3	100	41.8:46.3	0.90280778	1.23965019	
H1	100	38	42.4	100	19:21.2	0.89622642	1.23061329	
H2	100	41.4	50.6	100	41.4:50.6	0.81818182	1.12344983	
H3	100	37.9	51.2	100	37.9:51.2	0.74023438	1.01641978	
H4	100	36.4	55.9	100	36.4:55.9	0.65116279	0.89411511	
H5	100	39.8	40.8	100	39.8:40.8	0.9754902	1.33945081	
H6	100	44.8	49.3	100	44.8:49.3	0.90872211	1.24777119	
H7	100	35.6	58.7	100	35.6:58.7	0.60647359	0.83275214	
H8	100	38.7	52.9	100	19.35:26.45	0.731569	1.00452131	
H9	100	43.7	43.2	100	1.016279069	1.01157407	1.38899778	
H10	100	44.2	49.2	100	44.2:49.2	0.89837398	1.23356213	
H11	0	0	0	0	#DIV/0!	#DIV/0!	#DIV/0!	
H12	100	38.5	51.5	100	38.5:51.5	0.74757282	1.02649623	

Table A.17. Percentages from screen 2 plate 6

A.3.3 – Raw data from third screen.

Screen 3 – Plate 1.

Name / Desc	All	Mean GFP	Mean RFP	R01	Ratio Green/Red	Numerical Ra	Ratio/Scram	Average scra
A1	100	46.5	47.5	100	46.5:47.5	0.97894737	1.07964148	0.90673375
A2	100	38	58.2	100	19:29.1	0.65292096	0.72008014	
A3	100	43.3	47.6	100	43.3:47.6	0.90966387	1.00323151	
A4	100	34.3	61.8	100	34.3:61.8	0.55501618	0.61210491	
A5	100	38.7	56.7	100	19.35:28.35	0.68253968	0.75274543	
A6	100	36.8	54.8	100	2.0444444444444	0.67153285	0.74060643	
A7	100	44.8	47.5	100	44.8:47.5	0.94315789	1.04017072	
A8	100	35.1	61	100	35.1:61	0.57540984	0.63459625	
A9	100	43.3	52	100	43.3:52	0.83269231	0.91834269	
A10	100	44.9	47.4	100	44.9:47.4	0.94725738	1.04469188	
A11	100	35.4	60.1	100	7.08:12.02	0.5890183	0.64960448	
A12	100	45	47.9	100	45:47.9	0.9394572	1.03608938	
B1	100	38.6	54.2	100	19.3:27.1	0.71217712	0.78543136	
B2	100	37.6	56.4	100	37.6:56.4	0.66666667	0.73523972	
B3	100	39.2	57.4	100	13.066666666666	0.68292683	0.7531724	
B4	100	40.2	54.5	100	20.1:27.25	0.73761468	0.81348541	
B5	100	33.8	58.1	100	33.8:58.1	0.58175559	0.64159473	
B6	100	32.9	62.4	100	16.45:31.2	0.52724359	0.58147564	
B7	100	33.9	60.3	100	11.3:20.1	0.56218905	0.62001558	
B8	100	35.6	60.8	100	7.12:12.16	0.58552632	0.64575331	
B9	100	35.7	57.9	100	35.7:57.9	0.61658031	0.6800015	
B10	100	39.4	54.1	100	13.133333333333	0.72828096	0.80319163	
B11	100	36.9	55.8	100	36.9:55.8	0.66129032	0.72931037	
B12	100	43.8	52.4	100	43.8:52.4	0.83587786	0.92185591	
C1	100	3.4	70.6	100	3.4:70.6	0.04815864	0.05311222	
C2	100	38.7	56.5	100	19.35:28.25	0.68495575	0.75541001	
C3	100	40.4	55.1	100	8.08:11.02	0.73321234	0.80863025	
C4	100	39.4	56.3	100	39.4:56.3	0.69982238	0.77180582	
C5	100	47.6	48.6	100	47.6:48.6	0.97942387	1.080167	
C6	100	40.5	54.2	100	20.25:27.1	0.74723247	0.82409249	
C7	100	42.8	52.6	100	21.4:26.3	0.81368821	0.89738384	
C8	100	39.4	54.1	100	13.133333333333	0.72828096	0.80319163	
C9	100	33.9	64	100	33.9:64	0.5296875	0.58417093	
C10	100	35.4	60.3	100	7.08:12.06	0.58706468	0.6474499	
C11	100	38.4	57.1	100	2.0210526315789	0.67250438	0.7416779	
C12	100	41.8	51	100	41.8:51	0.81960784	0.90391236	
D1	100	44.4	51.5	100	44.4:51.5	0.86213592	0.95081486	
D2	100	34.7	58	100	17.35:29	0.59827586	0.65981427	
D3	100	40.8	52	100	10.2:13	0.78461538	0.86532059	
D4	100	41	52.5	100	41:52.5	0.78095238	0.86128081	
D5	100	41.7	50.4	100	41.7:50.4	0.82738095	0.91248501	
D6	100	39.3	54.4	100	13.1:18.133333333	0.72242647	0.79673495	
D7	100	43.2	50.2	100	43.2:50.2	0.86055777	0.94907438	
D8	100	41.9	53.3	100	41.9:53.3	0.78611632	0.86697592	
D9	100	42.2	53.5	100	42.2:53.5	0.78878505	0.86991915	
D10	100	45.1	46.8	100	45.1:46.8	0.96367521	1.06279844	
D11	100	38.4	56.1	100	19.2:28.05	0.68449198	0.75489854	
D12	100	46.9	47.6	100	46.9:47.6	0.98529412	1.08664106	
E1	100	44.4	53.7	100	44.4:53.7	0.82681564	0.91186155	
E2	100	41.9	53.8	100	41.9:53.8	0.77881041	0.85891852	
E3	100	35.8	58.3	100	35.8:58.3	0.61406518	0.67722767	
E4	100	39.7	54.5	100	13.233333333333	0.72844037	0.80336744	
E5	100	42	52.2	100	21:26.1	0.8045977	0.88735828	
E6	100	43.6	51.3	100	43.6:51.3	0.84990253	0.93732315	
E7	100	43	51.7	100	43:51.7	0.83172147	0.91727199	
E8	100	38	57.1	100	2:3.00526315789	0.66549912	0.73395208	
E9	100	41.9	53.4	100	41.9:53.4	0.78464419	0.86535237	
E10	100	36	57.7	100	12:19.233333333	0.62391681	0.68809263	
E11	100	39.6	55.3	100	39.6:55.3	0.71609403	0.78975116	
E12	100	4.4	63.6	100	4.4:63.6	0.06918239	0.07629846	
F1	100	44.8	47.2	100	44.8:47.2	0.94915254	1.04678197	
F2	100	37.4	57.9	100	37.4:57.9	0.64594128	0.71238253	
F3	100	41.8	54.2	100	41.8:54.2	0.77121771	0.85054484	
F4	100	37.3	58.1	100	37.3:58.1	0.64199656	0.70803205	
F5	100	43.7	48.2	100	43.7:48.2	0.906639	0.99989551	
F6	100	43.6	53	100	43.6:53	0.82264151	0.90725807	
F7	100	39.8	56.8	100	39.8:56.8	0.70070423	0.77277837	
F8	100	43.9	51.4	100	43.9:51.4	0.8540856	0.94193649	
F9	100	36.7	59	100	36.7:59	0.6220339	0.68601604	
F10	100	42.3	51.6	100	14.1:17.2	0.81976744	0.90408838	
F11	100	37.4	58.2	100	37.4:58.2	0.64261168	0.70871045	
F12	100	48.7	45.5	100	16.233333333333	1.07032967	1.18042333	
G1	100	53.5	38	100	53.5:38	1.40789474	1.5527102	
G2	100	38.6	55.2	100	38.6:55.2	0.69927536	0.77120253	
G3	100	42.3	54.4	100	7.05:9.0666666666	0.77757353	0.85755442	
G4	100	37.1	59.6	100	37.1:59.6	0.62248322	0.68651158	
G5	100	40.4	54.1	100	20.2:27.05	0.74676525	0.82357721	
G6	100	39.6	54.5	100	13.2:18.166666666	0.7266055	0.80134384	
G7	100	41.1	54.3	100	41.1:54.3	0.75690608	0.83476112	
G8	100	37.7	56.1	100	37.7:56.1	0.67201426	0.74113736	
G9	100	37.1	60.4	100	37.1:60.4	0.61423841	0.67741872	
G10	100	44.9	49.3	100	44.9:49.3	0.91075051	1.00442992	
G11	100	47.7	46.9	100	47.7:46.9	1.01705757	1.12167168	
G12	100	39.3	53.5	100	39.3:53.5	0.73457944	0.81013797	
H1	100	42.1	47.4	100	42.1:47.4	0.88818565	0.97954406	
H2	100	36.6	58.5	100	18.3:29.25	0.62564103	0.6899942	
H3	100	39.4	56.4	100	39.4:56.4	0.69858156	0.77043737	
H4	100	32.7	61.4	100	32.7:61.4	0.53257329	0.58735355	
H5	100	47.3	48.4	100	47.3:48.4	0.97727273	1.07779459	
H6	100	37.9	55.3	100	37.9:55.3	0.68535262	0.7558477	
H7	100	41.6	50.8	100	41.6:50.8	0.81889764	0.9031291	
H8	100	41.1	53	100	41.1:53	0.7754717	0.85523639	
H9	100	42.6	49	100	6.0857142857142	0.86938776	0.95881261	
H10	100	36.5	58.8	100	18.25:29.4	0.6207483	0.68459821	
H11	100	46.6	49.9	100	46.6:49.9	0.93386774	1.02992498	
H12	100	42.3	52.8	100	21.15:26.4	0.80113636	0.88354091	

Table A.18. Percentages from screen 3 plate 1

Screen 3 – Plate 2.

Name / Desc	All	Mean GFP	Mean RFP	R01	Ratio Green/	Numerical Ra	Ratio/Scraml	Average scra
A1	100	49.2	47.7	100	49.2:47.7	1.03144654	1.05800744	0.97489536
A2	100	47.7	49.3	100	47.7:49.3	0.96754564	0.99246102	
A3	100	48.1	48.8	100	1.002083333	0.98565574	1.01103747	
A4	100	42.4	53.9	100	42.4:53.9	0.78664193	0.80689884	
A5	100	50	48.6	100	25:24.3	1.02880658	1.0552995	
A6	100	44.7	52.3	100	11.175:13.07	0.85468451	0.87669359	
A7	100	43.7	53.2	100	43.7:53.2	0.82142857	0.84258128	
A8	100	40.5	55	100	8.1:11	0.73636364	0.75532582	
A9	100	44.9	52.7	100	11.225:13.17	0.85199241	0.87393217	
A10	100	40.8	56.2	100	5.1:7.025	0.72597865	0.74467341	
A11	100	47.4	50	100	47.4:50	0.948	0.97241206	
A12	100	40.5	52.3	100	10.125:13.07	0.77437859	0.7943197	
B1	100	43.7	52.2	100	43.7:52.2	0.83716475	0.85872268	
B2	100	48.8	48.4	100	1.016666666	1.00826446	1.0342284	
B3	100	46	51.1	100	46:51.1	0.90019569	0.92337674	
B4	100	43.5	54.4	100	43.5:54.4	0.79963235	0.82022378	
B5	100	45.2	52.8	100	45.2:52.8	0.85606061	0.87810512	
B6	100	46.3	50.5	100	23.15:25.25	0.91683168	0.94044112	
B7	100	39.1	57.7	100	13.03333333	0.67764298	0.69509304	
B8	100	42.6	53.3	100	42.6:53.3	0.79924953	0.8198311	
B9	100	44	52.1	100	11:13.025	0.84452975	0.86627734	
B10	100	44.1	50.7	100	22.05:25.35	0.86982249	0.89222139	
B11	100	43	53.1	100	43:53.1	0.80979284	0.83064591	
B12	100	48.5	48.6	100	1.010416666	0.99794239	1.02364052	
C1	100	2.7	61.9	100	2.7:61.9	0.04361874	0.04474197	
C2	100	42.3	53.3	100	42.3:53.3	0.79362101	0.81405764	
C3	100	43.2	51.7	100	43.2:51.7	0.83558994	0.85710732	
C4	100	46.9	48.8	100	23.45:24.4	0.96106557	0.98581409	
C5	100	44	52.4	100	11:13.1	0.83969466	0.86131773	
C6	100	45.3	51.8	100	15.1:17.2666	0.87451737	0.89703717	
C7	100	42.9	52.6	100	21.45:26.3	0.81558935	0.83659169	
C8	100	43.1	53.1	100	43.1:53.1	0.81167608	0.83257765	
C9	100	41	55.8	100	41:55.8	0.73476703	0.7536881	
C10	100	45.2	51.3	100	15.06666666	0.88109162	0.90378071	
C11	100	48.4	47.9	100	48.4:47.9	1.01043841	1.03645833	
C12	100	45.9	51.4	100	15.3:17.1333	0.89299611	0.91599176	
D1	100	46.5	52.2	100	23.25:26.1	0.8908046	0.91374381	
D2	100	43.7	51.7	100	43.7:51.7	0.84526112	0.86702754	
D3	100	43.3	52.4	100	43.3:52.4	0.82633588	0.84761495	
D4	100	43.3	54.1	100	43.3:54.1	0.80036969	0.8209801	
D5	100	41.3	53.7	100	41.3:53.7	0.76908752	0.78889239	
D6	100	46.3	49.4	100	46.3:49.4	0.93724696	0.96138212	
D7	100	44.1	52	100	11.025:13	0.84807692	0.86991585	
D8	100	45.5	51	100	15.16666666	0.89215686	0.9151309	
D9	100	48.8	47.6	100	48.8:47.6	1.02521008	1.05161039	
D10	100	40	56.2	100	5:7.025	0.71174377	0.73007197	
D11	100	46.3	51.4	100	46.3:51.4	0.90077821	0.92397426	
D12	100	44.7	53.8	100	44.7:53.8	0.83085502	0.85225046	
E1	100	50.2	48.3	100	25.1:24.15	1.03933747	1.06610158	
E2	100	41.1	56	100	41.1:56	0.73392857	0.75282805	
E3	100	45.3	51.6	100	15.1:17.2	0.87790698	0.90051406	
E4	100	40.3	56.5	100	5.0375:7.062	0.71327434	0.73164195	
E5	100	46.6	48.6	100	23.3:24.3	0.95884774	0.98353914	
E6	100	45.7	49.7	100	45.7:49.7	0.9195171	0.9431957	
E7	100	41.9	53.4	100	41.9:53.4	0.78464419	0.80484966	
E8	100	43.2	52.1	100	43.2:52.1	0.82917466	0.85052684	
E9	100	41.1	53.5	100	41.1:53.5	0.7682243	0.78800693	
E10	100	40.7	55.9	100	8.14:11.18	0.72808587	0.74683489	
E11	100	44.8	51.2	100	44.8:51.2	0.875	0.89753223	
E12	100	7.2	54.5	100	7.2:54.5	0.13211009	0.13551207	
F1	100	45.3	49.6	100	45.3:49.6	0.91330645	0.93682511	
F2	100	40.8	56.5	100	5.1:7.0625	0.72212389	0.74071939	
F3	100	45.9	50.4	100	9.18:10.08	0.91071429	0.9341662	
F4	100	42.8	53.7	100	42.8:53.7	0.79702048	0.81754465	
F5	100	44.1	52.4	100	11.025:13.1	0.84160305	0.86327527	
F6	100	49.3	46.9	100	49.3:46.9	1.05117271	1.07824158	
F7	100	50.3	45.6	100	10.06:9.12	1.10307018	1.13147547	
F8	100	45.4	50.3	100	9.08:10.06	0.90258449	0.92582705	
F9	100	41.7	54.2	100	41.7:54.2	0.76937269	0.7891849	
F10	100	43.2	53.7	100	43.2:53.7	0.80446927	0.82518526	
F11	100	44.2	53.5	100	44.2:53.5	0.82616822	0.84744298	
F12	100	46.8	51.6	100	46.8:51.6	0.90697674	0.93033241	
G1	100	48.3	47.7	100	48.3:47.7	1.01257862	1.03865365	
G2	100	48	48.3	100	1:1.00625	0.99378882	1.01937999	
G3	100	43.8	54.7	100	43.8:54.7	0.80073126	0.82135099	
G4	100	43	55	100	43:55	0.78181818	0.80195087	
G5	100	44	52.2	100	11:13.05	0.84291188	0.8646178	
G6	100	42.1	54.3	100	7.016666666	0.77532228	0.7952877	
G7	100	38.9	57.9	100	2.047368421	0.67184801	0.68914885	
G8	100	44.3	53	100	44.3:53	0.83584906	0.8573731	
G9	100	38.7	58.4	100	19.35:29.2	0.66267123	0.67973576	
G10	100	40.6	56.3	100	5.075:7.0375	0.72113677	0.73970684	
G11	100	43.6	53.2	100	43.6:53.2	0.81954887	0.84065317	
G12	100	44.1	50.1	100	22.05:25.05	0.88023952	0.90290667	
H1	100	44.3	49.7	100	44.3:49.7	0.89134809	0.9143013	
H2	100	41.8	56	100	41.8:56	0.74642857	0.76564994	
H3	100	49.7	47.1	100	49.7:47.1	1.0552017	1.08237432	
H4	100	48.5	49	100	48.5:49	0.98979592	1.01528427	
H5	100	44.8	51	100	44.8:51	0.87843137	0.90105196	
H6	100	43.3	53.7	100	43.3:53.7	0.80633147	0.82709541	
H7	100	48.1	48	100	1.002083333	1.00208333	1.0278881	
H8	100	41.2	56	100	41.2:56	0.73571429	0.75465975	
H9	100	42.4	55.4	100	42.4:55.4	0.76534296	0.7850514	
H10	100	43.5	53.9	100	43.5:53.9	0.80705009	0.82783253	
H11	100	39.3	57.6	100	13.1:19.2	0.68229167	0.69986144	
H12	100	44.4	48.9	100	11.1:12.225	0.90797546	0.93135684	

Table A.19. Percentages from screen 3 plate 2

Screen 3 – Plate 3.

Name / Desc	All	Mean GFP	Mean RFP	R01	Ratio Green/	Numerical Ra	Ratio/Scram	Average scra
A1	100	51	44.7	100	51:44.7	1.1409396	1.19326096	0.95615263
A2	100	43.5	54.1	100	43.5:54.1	0.80406654	0.84093953	
A3	100	40.8	56	100	5.1:7	0.72857143	0.76198235	
A4	100	43.5	53.4	100	43.5:53.4	0.81460674	0.85196309	
A5	100	49.4	47.6	100	49.4:47.6	1.03781513	1.08540739	
A6	100	45.9	50.6	100	9.18:10.12	0.90711462	0.94871321	
A7	100	38.1	59.4	100	38.1:59.4	0.64141414	0.6708282	
A8	100	41.8	53.8	100	41.8:53.8	0.77695167	0.81258123	
A9	100	39.1	56.4	100	39.1:56.4	0.69326241	0.72505413	
A10	100	42.4	54.9	100	7.066666666	0.7723133	0.80773014	
A11	100	39.7	57.7	100	13.23333333	0.68804159	0.7195939	
A12	100	41.4	50.2	100	41.4:50.2	0.8247012	0.86252045	
B1	100	45.6	50.7	100	9.12:10.14	0.89940828	0.94065347	
B2	100	49.2	48.3	100	49.2:48.3	1.01863354	1.06534617	
B3	100	45.1	52.9	100	45.1:52.9	0.85255198	0.89164843	
B4	100	47.2	49.3	100	47.2:49.3	0.95740365	1.00130839	
B5	100	40.4	56.7	100	5.05:7.0875	0.71252205	0.74519698	
B6	100	40.5	56.8	100	5.0625:7.1	0.71302817	0.74572631	
B7	100	45	52.8	100	45:52.8	0.85227273	0.89135636	
B8	100	44.1	54.2	100	22.05:27.1	0.81365314	0.85096575	
B9	100	45.4	53	100	45.4:53	0.85660377	0.89588602	
B10	100	43.5	53.5	100	43.5:53.5	0.81308411	0.85037063	
B11	100	43.7	53.6	100	43.7:53.6	0.81529851	0.85268657	
B12	100	45.7	51.1	100	15.23333333	0.89432485	0.93533692	
C1	100	10.4	53.6	100	10.4:53.6	0.19402985	0.2029277	
C2	100	42.9	55.4	100	42.9:55.4	0.77436823	0.80987931	
C3	100	45.8	51.2	100	15.26666666	0.89453125	0.93555278	
C4	100	42.9	54.2	100	7.15:9.03333	0.79151292	0.82781022	
C5	100	48.1	48.6	100	1.002083333	0.98971193	1.03509828	
C6	100	42.8	54.2	100	7.133333333	0.7896679	0.82588059	
C7	100	35.4	62.2	100	35.4:62.2	0.56913183	0.59523116	
C8	100	42.7	52.6	100	21.35:26.3	0.81178707	0.84901411	
C9	100	43.1	53.6	100	43.1:53.6	0.80410448	0.84097921	
C10	100	43.3	53.6	100	43.3:53.6	0.80783582	0.84488166	
C11	100	49.6	47.4	100	49.6:47.4	1.0464135	1.09440007	
C12	100	44.8	51.3	100	44.8:51.3	0.87329435	0.913342	
D1	100	48.4	48.7	100	1.008333333	0.99383984	1.03941547	
D2	100	48.2	48	100	1.004166666	1.00416667	1.05021588	
D3	100	40.5	57	100	40.5:57	0.71052632	0.74310973	
D4	100	40.7	55.5	100	8.14:11.1	0.73333333	0.76696263	
D5	100	48.5	47.5	100	48.5:47.5	1.02105263	1.0678762	
D6	100	43	54.3	100	43:54.3	0.79189687	0.82821178	
D7	100	43.4	53.5	100	43.4:53.5	0.81121495	0.84841576	
D8	100	40.9	55.7	100	8.18:11.14	0.73429084	0.76796405	
D9	100	46.9	50.8	100	23.45:25.4	0.92322835	0.96556587	
D10	100	48.5	47.9	100	48.5:47.9	1.0125261	1.05895865	
D11	100	46.3	50.7	100	23.15:25.35	0.91321499	0.95509332	
D12	100	41.4	54.3	100	41.4:54.3	0.76243094	0.7973946	
E1	100	49.6	48.3	100	49.6:48.3	1.02691511	1.07400752	
E2	100	47.2	49.8	100	47.2:49.8	0.94779116	0.9912551	
E3	100	41.9	55.3	100	41.9:55.3	0.75768535	0.79243139	
E4	100	45.5	51.5	100	15.16666666	0.88349515	0.92401058	
E5	100	46.6	49.3	100	46.6:49.3	0.94523327	0.9885799	
E6	100	46	49.7	100	46:49.7	0.92555332	0.96799747	
E7	100	43.9	51.3	100	43.9:51.3	0.85575049	0.89499361	
E8	100	47.1	49.2	100	47.1:49.2	0.95731707	1.00121785	
E9	100	48	49.1	100	48:49.1	0.97759674	1.0224275	
E10	100	42.8	53.2	100	42.8:53.2	0.80451128	0.84140466	
E11	100	43.5	53.6	100	43.5:53.6	0.81156716	0.84878412	
E12	100	9	55	100	9:55	0.16363636	0.17114042	
F1	100	46.3	49.2	100	46.3:49.2	0.94105691	0.98421202	
F2	100	44.2	52.5	100	11.05:13.125	0.84190476	0.88051294	
F3	100	47.1	50.5	100	47.1:50.5	0.93267327	0.97544392	
F4	100	46.9	49.4	100	46.9:49.4	0.94939271	0.99293009	
F5	100	49.5	47.3	100	49.5:47.3	1.04651163	1.0945027	
F6	100	46.6	50.7	100	23.3:25.35	0.91913215	0.96128183	
F7	100	45.7	50.8	100	9.14:10.16	0.8996063	0.94086056	
F8	100	45.9	49.8	100	45.9:49.8	0.92168675	0.96395358	
F9	100	42.7	54	100	7.116666666	0.79074074	0.82700263	
F10	100	46.3	49.2	100	46.3:49.2	0.94105691	0.98421202	
F11	100	40.4	56.7	100	5.05:7.0875	0.71252205	0.74519698	
F12	100	40.7	56.7	100	5.0875:7.087	0.71781305	0.75073062	
G1	100	45.9	49.9	100	45.9:49.9	0.91983968	0.96202181	
G2	100	42	56	100	3:4	0.75	0.7843936	
G3	100	39.4	58.8	100	39.4:58.8	0.67006803	0.7007961	
G4	100	40.8	57.1	100	40.8:57.1	0.7145359	0.74730318	
G5	100	45.6	51.8	100	15.2:17.2666	0.88030888	0.9206782	
G6	100	20.4	76.2	100	5.1:19.05	0.26771654	0.27999352	
G7	100	45.2	51.3	100	15.06666666	0.88109162	0.92149683	
G8	100	44.6	51.6	100	44.6:51.6	0.86434109	0.90397815	
G9	100	48.5	48.1	100	1.010416666	1.00831601	1.0545555	
G10	100	48	48.7	100	1:1.0145833	0.98562628	1.03082526	
G11	100	42.8	54	100	7.133333333	0.79259259	0.82893941	
G12	100	42.8	51.8	100	14.26666666	0.82625483	0.86414533	
H1	100	47.8	46.2	100	47.8:46.2	1.03463203	1.08207833	
H2	100	47.1	50.8	100	47.1:50.8	0.92716535	0.96968343	
H3	100	46	51.9	100	46:51.9	0.88631985	0.92696482	
H4	100	45.4	50.7	100	9.08:10.14	0.89546351	0.9365278	
H5	100	46	51.5	100	46:51.5	0.89320388	0.93416455	
H6	100	47.7	49.2	100	47.7:49.2	0.9695122	1.01397221	
H7	100	41.8	54.4	100	41.8:54.4	0.76838235	0.80361893	
H8	100	47.8	49.8	100	47.8:49.8	0.95983936	1.0038558	
H9	100	47.4	48.6	100	47.4:48.6	0.97530864	1.02003448	
H10	100	40.5	56.3	100	5.0625:7.037	0.71936057	0.7523491	
H11	100	37.1	59.5	100	37.1:59.5	0.62352941	0.65212331	
H12	100	39.9	52.8	100	3.069230769	0.75568182	0.79033598	

Table A.20. Percentages from screen 3 plate 3

Screen 3 – Plate 4.

Name / Desc	All	Mean GFP	Mean RFP	R01	Ratio Green/	Numerical Ra	Ratio/Scraml	Average scra
A1	100	45.5	52.1	100	45.5:52.1	0.87332054	0.94362724	0.92549314
A2	100	53.2	43.4	100	53.2:43.4	1.22580645	1.32449004	
A3	100	39.5	58.3	100	39.5:58.3	0.67753002	0.73207459	
A4	100	52.5	43.3	100	52.5:43.3	1.21247113	1.31008116	
A5	100	45.1	50.6	100	9.02:10.12	0.89130435	0.96305883	
A6	100	45.8	50.2	100	9.16:10.04	0.9123506	0.98579941	
A7	100	49.7	46.7	100	49.7:46.7	1.06423983	1.14991649	
A8	100	44.7	52.1	100	11.175:13.02	0.85796545	0.92703599	
A9	100	44.4	52.2	100	11.1:13.05	0.85057471	0.91905026	
A10	100	43.9	51.9	100	43.9:51.9	0.84585742	0.9139532	
A11	100	47.1	50	100	47.1:50	0.942	1.01783574	
A12	100	42	50.9	100	21:25.45	0.82514735	0.89157586	
B1	100	45	52.7	100	45:52.7	0.85388994	0.92263238	
B2	100	47.8	50.6	100	47.8:50.6	0.94466403	1.02071424	
B3	100	47.6	49.4	100	47.6:49.4	0.96356275	1.0411344	
B4	100	46.9	51	100	46.9:51	0.91960784	0.9936409	
B5	100	46.5	50.2	100	23.25:25.1	0.92629482	1.00086621	
B6	100	45.2	51.4	100	15.06666666	0.87937743	0.95017174	
B7	100	47.5	49.1	100	47.5:49.1	0.96741344	1.04529509	
B8	100	48.7	48.3	100	1.014583333	1.00828157	1.08945331	
B9	100	44.2	52	100	11.05:13	0.85	0.91842928	
B10	100	42.3	54.7	100	7.05:9.11666	0.77330896	0.83556422	
B11	100	41.9	55.5	100	41.9:55.5	0.75495495	0.81573263	
B12	100	44.3	52.7	100	11.075:13.17	0.84060721	0.90828032	
C1	100	7.9	62.4	100	7.9:62.4	0.12660256	0.13679471	
C2	100	50.8	47.1	100	50.8:47.1	1.07855626	1.16538547	
C3	100	47.6	50.6	100	47.6:50.6	0.94071146	1.01644347	
C4	100	47	51.1	100	47:51.1	0.91976517	0.99381089	
C5	100	47.2	50.8	100	47.2:50.8	0.92913386	1.00393381	
C6	100	48.4	47	100	48.4:47	1.02978723	1.11269029	
C7	100	49.3	47.5	100	49.3:47.5	1.03789474	1.12145049	
C8	100	41.5	56	100	41.5:56	0.74107143	0.80073141	
C9	100	43.8	53.9	100	43.8:53.9	0.81261596	0.87803563	
C10	100	47	48.6	100	47:48.6	0.96707819	1.04493285	
C11	100	41.1	56.3	100	41.1:56.3	0.73001776	0.78878787	
C12	100	42.3	53.2	100	42.3:53.2	0.79511278	0.85912336	
D1	100	49.5	49	100	1.010204081	1.01020408	1.09153059	
D2	100	47.4	50.4	100	47.4:50.4	0.94047619	1.01618926	
D3		44.8	53.1	100	44.8:53.1	0.84369115	0.91161253	
D4	100	47	49.8	100	47:49.8	0.9437751	1.01975375	
D5	100	51.4	45.6	100	17.13333333	1.12719298	1.21793769	
D6	100	44.8	51.8	100	44.8:51.8	0.86486486	0.93449084	
D7	100	45.5	50.9	100	9.1:10.18	0.89390963	0.96587385	
D8	100	45.4	51.6	100	15.13333333	0.87984496	0.95067691	
D9	100	47.9	49.7	100	47.9:49.7	0.9637827	1.04137205	
D10	100	41.3	54.4	100	41.3:54.4	0.75919118	0.82030989	
D11	100	43.8	53.7	100	43.8:53.7	0.81564246	0.88130578	
D12	100	47.3	50.1	100	47.3:50.1	0.94411178	1.02011753	
E1	100	49.9	47.8	100	49.9:47.8	1.04393305	1.12797492	
E2	100	41.5	57	100	41.5:57	0.72807018	0.78668349	
E3	100	49.3	48.3	100	49.3:48.3	1.02070393	1.10287574	
E4	100	50.5	46.7	100	25.25:23.35	1.08137045	1.16842621	
E5	100	48.6	46.6	100	24.3:23.3	1.04291845	1.12687864	
E6	100	49.2	47	100	49.2:47	1.04680851	1.13108186	
E7	100	49.4	49.4	100	1.008163265	1	1.08050503	
E8	100	45.3	52.5	100	45.3:52.5	0.86285714	0.93232148	
E9	100	46.5	51.3	100	46.5:51.3	0.90643275	0.97940515	
E10	100	44.5	51.1	100	44.5:51.1	0.87084149	0.94094861	
E11	100	41.4	55.1	100	41.4:55.1	0.75136116	0.81184952	
E12	100	6.5	59.6	100	6.5:59.6	0.1090604	0.11784031	
F1	100	48.4	47.9	100	48.4:47.9	1.01043841	1.09178379	
F2	100	46	52.6	100	23:26.3	0.87452471	0.94492836	
F3	100	47.5	50.2	100	47.5:50.2	0.94621514	1.02239022	
F4	100	45.6	51.6	100	15.2:17.2	0.88372093	0.95486491	
F5	100	50	48	100	25:24	1.04166667	1.12552608	
F6	100	48.9	47	100	48.9:47	1.04042553	1.12418502	
F7	100	46.5	50.3	100	23.25:25.15	0.92445328	0.99887642	
F8	100	43.9	54.3	100	43.9:54.3	0.80847145	0.87355748	
F9	100	42.8	55.8	100	42.8:55.8	0.76702509	0.82877447	
F10	100	46.7	48.4	100	23.35:24.2	0.96487603	1.04255341	
F11	100	44.4	53.2	100	44.4:53.2	0.83458647	0.90177488	
F12	100	43.8	54.5	100	43.8:54.5	0.80366972	0.86836918	
G1	100	43.8	51.6	100	43.8:51.6	0.84883721	0.91717288	
G2	100	41.8	56.2	100	41.8:56.2	0.74377224	0.80364965	
G3	100	47.8	49.3	100	47.8:49.3	0.96957404	1.04762963	
G4	100	44.9	53.1	100	44.9:53.1	0.84557439	0.91364738	
G5	100	43.9	54.3	100	43.9:54.3	0.80847145	0.87355748	
G6	100	49	48.9	100	49:48.9	1.00204499	1.08271465	
G7	100	46.8	50.8	100	23.4:25.4	0.92125984	0.9954259	
G8	100	46.6	51.7	100	46.6:51.7	0.90135397	0.9739175	
G9	100	44	54.3	100	22:27.15	0.81031308	0.87554736	
G10	100	45.4	51.6	100	15.13333333	0.87984496	0.95067691	
G11	100	38.5	59.3	100	38.5:59.3	0.64924115	0.70150833	
G12	100	47.3	46.8	100	47.3:46.8	1.01068376	1.09204889	
H1	100	41.7	53.2	100	41.7:53.2	0.78383459	0.84693721	
H2	100	49.1	49.1	100	1.002040816	1	1.08050503	
H3	100	42.7	55.3	100	42.7:55.3	0.7721519	0.83431401	
H4	100	41	58	100	41:58	0.70689655	0.76380528	
H5	100	44	52.3	100	11:13.075	0.84130019	0.90902909	
H6	100	49.4	48.8	100	49.4:48.8	1.01229508	1.09378993	
H7	100	48.6	48	100	1.0125:1	1.0125	1.09401134	
H8	100	50.1	47.2	100	50.1:47.2	1.06144068	1.14689199	
H9	100	44.9	51.6	100	44.9:51.6	0.87015504	0.9402069	
H10	100	41.9	56.1	100	41.9:56.1	0.74688057	0.80700821	
H11	100	43.3	55.3	100	43.3:55.3	0.78300181	0.84603739	
H12	100	47.3	46.1	100	47.3:46.1	1.02603037	1.10863098	

Table A.21. Percentages from screen 3 plate 4

Screen 3 – Plate 5.

Name / Desc	All	Mean GFP	Mean RFP	R01	Ratio Green/	Numerical Ra	Ratio/Scraml	Average scra
A1	100	42.3	53.5	100	42.3:53.5	0.79065421	0.9705336	0.81465928
A2	100	49.9	48.7	100	49.9:48.7	1.02464066	1.25775362	
A3	100	40.1	58.6	100	20.05:29.3	0.68430034	0.83998348	
A4	100	50.4	47.1	100	50.4:47.1	1.07006369	1.31351071	
A5	100	44	53.6	100	44:53.6	0.82089552	1.00765503	
A6	100	46.2	52.6	100	23.1:26.3	0.878327	1.07815257	
A7	100	49.2	48.4	100	49.2:48.4	1.01652893	1.24779641	
A8	100	42	56.2	100	3:4.0142857	0.74733096	0.91735401	
A9	100	39.7	56.7	100	39.7:56.7	0.70017637	0.85947142	
A10	100	43.1	54.2	100	43.1:54.2	0.79520295	0.97611722	
A11	100	37.9	60.6	100	37.9:60.6	0.62541254	0.7676983	
A12	100	41.2	53	100	41.2:53	0.77735849	0.95421302	
B1	100	45	53	100	45:53	0.8490566	1.04222296	
B2	100	44.8	52.4	100	11.2:13.1	0.85496183	1.04947167	
B3	100	43.3	53.5	100	43.3:53.5	0.80934579	0.99347766	
B4	100	43.7	54.8	100	43.7:54.8	0.79744526	0.97886966	
B5	100	40.6	57.5	100	40.6:57.5	0.70608696	0.86672671	
B6	100	45.4	52.8	100	45.4:52.8	0.85984848	1.05547007	
B7	100	51.1	46.2	100	51.1:46.2	1.10606061	1.35769718	
B8	100	48.3	49.8	100	48.3:49.8	0.96987952	1.19053393	
B9	100	44.2	53.4	100	44.2:53.4	0.82771536	1.01602642	
B10	100	50.7	46.9	100	25.35:23.45	1.08102345	1.3269639	
B11	100	46.3	51.5	100	46.3:51.5	0.89902913	1.10356458	
B12	100	47.4	50.4	100	47.4:50.4	0.94047619	1.15444114	
C1	100	6.8	51.2	100	2.266666666	0.1328125	0.16302828	
C2	100	46	51.2	100	46:51.2	0.8984375	1.10283835	
C3	100	47.2	50.1	100	47.2:50.1	0.94211577	1.15645374	
C4	100	44.6	52.8	100	11.15:13.2	0.84469697	1.03687147	
C5	100	41.7	55.8	100	41.7:55.8	0.74731183	0.91733053	
C6	100	51.2	46.8	100	51.2:46.8	1.09401709	1.34291368	
C7	100	45.6	52.5	100	45.6:52.5	0.86857143	1.06617754	
C8	100	46	52.4	100	23:26.2	0.8778626	1.07758251	
C9	100	49.8	47.1	100	49.8:47.1	1.05732484	1.29787368	
C10	100	43.3	52.6	100	43.3:52.6	0.82319392	1.01047633	
C11	100	38.1	58.3	100	19.05:29.15	0.6535163	0.80219585	
C12	100	45.1	52	100	45.1:52	0.86730769	1.0646263	
D1	100	44.7	53.7	100	44.7:53.7	0.83240223	1.0217796	
D2	100	44	53.7	100	44:53.7	0.81936685	1.00577858	
D3	100	49.7	47.6	100	49.7:47.6	1.04411765	1.28166176	
D4	100	46.8	49.2	100	46.8:49.2	0.95121951	1.16762865	
D5	100	42.7	54.4	100	7.116666666	0.78492647	0.96350277	
D6	100	44.7	52.3	100	11.175:13.07	0.85468451	1.04913125	
D7	100	44.4	53.8	100	44.4:53.8	0.82527881	1.01303555	
D8	100	43.8	54.8	100	43.8:54.8	0.79927007	0.98110964	
D9	100	46.2	51.6	100	46.2:51.6	0.89534884	1.099047	
D10	100	48	49.6	100	48:49.6	0.96774194	1.18791004	
D11	100	46.8	51.1	100	46.8:51.1	0.91585127	1.12421388	
D12	100	43	54.5	100	43:54.5	0.78899083	0.96849179	
E1	100	41.8	56.6	100	41.8:56.6	0.7385159	0.90653347	
E2	100	44.9	51.9	100	44.9:51.9	0.86512524	1.06194732	
E3	100	48	50.8	100	24:25.4	0.94488189	1.15984917	
E4	100	44.9	53.1	100	44.9:53.1	0.84557439	1.03794851	
E5	100	45	52.5	100	45:52.5	0.85714286	1.05214889	
E6	100	49.8	47.7	100	49.8:47.7	1.04402516	1.28154823	
E7	100	48.2	48.9	100	1.004166666	0.98568507	1.20993536	
E8	100	44.2	53.8	100	44.2:53.8	0.82156134	1.00847232	
E9	100	45.1	51.4	100	15.03333333	0.87743191	1.07705384	
E10	100	49	49.2	100	1:1.0040816	0.99593496	1.22251717	
E11	100	42.6	56.2	100	3.042857142	0.75800712	0.93045907	
E12	100	4.4	55.8	100	4.4:55.8	0.07885305	0.09679267	
F1	100	46.1	49.2	100	46.1:49.2	0.93699187	1.15016411	
F2	100	40.3	57.2	100	40.3:57.2	0.70454545	0.8648345	
F3	100	50.6	47.9	100	50.6:47.9	1.05636743	1.29669846	
F4	100	44.3	53.3	100	44.3:53.3	0.83114447	1.02023568	
F5	100	36.8	61	100	36.8:61	0.60327869	0.74052884	
F6	100	46.4	50.8	100	23.2:25.4	0.91338583	1.12118753	
F7	100	47.3	49.5	100	47.3:49.5	0.95555556	1.17295117	
F8	100	43.6	53.9	100	43.6:53.9	0.80890538	0.99293705	
F9	100	40.2	57.6	100	40.2:57.6	0.69791667	0.85669762	
F10	100	54	40.4	100	27:20.2	1.33663366	1.64072723	
F11	100	41.1	56.2	100	41.1:56.2	0.73131673	0.89769643	
F12	100	47.8	50.8	100	47.8:50.8	0.94094488	1.15501646	
G1	100	43.8	52.4	100	43.8:52.4	0.83587786	1.02604596	
G2	100	44.6	53.7	100	44.6:53.7	0.83054004	1.01949374	
G3	100	48.7	47.6	100	48.7:47.6	1.02310924	1.2558738	
G4	100	44.1	54.2	100	22.05:27.1	0.81365314	0.99876495	
G5	100	50.5	47.5	100	50.5:47.5	1.06315789	1.3050338	
G6	100	43.6	51	100	43.6:51	0.85490196	1.04939817	
G7	100	38.7	57.9	100	2.036842105	0.66839378	0.82045807	
G8	100	41.4	55.3	100	41.4:55.3	0.74864376	0.91896549	
G9	100	44.6	53.3	100	44.6:53.3	0.83677298	1.02714473	
G10	100	43.6	53.8	100	43.6:53.8	0.81040892	0.99478265	
G11	100	43.6	53.2	100	43.6:53.2	0.81954887	1.00600201	
G12	100	48.2	47.4	100	48.2:47.4	1.01687764	1.24822446	
H1	100	46.3	48.7	100	23.15:24.35	0.95071869	1.16701388	
H2	100	43.7	54.1	100	43.7:54.1	0.8077634	0.99153526	
H3	100	45	51.3	100	15:17.1	0.87719298	1.07676056	
H4	100	43.1	55.1	100	43.1:55.1	0.78221416	0.96017338	
H5	100	41	56.8	100	41:56.8	0.72183099	0.88605261	
H6	100	42.3	55.5	100	42.3:55.5	0.76216216	0.93555942	
H7	100	41.5	55.8	100	41.5:55.8	0.7437276	0.91293086	
H8	100	39.4	58.1	100	39.4:58.1	0.67814114	0.83242302	
H9	100	39.5	59.5	100	39.5:59.5	0.66386555	0.81489963	
H10	100	45.7	51.4	100	15.23333333	0.88910506	1.09138272	
H11	100	48.8	49.4	100	48.8:49.4	0.98785425	1.21259804	
H12	100	45.3	49.8	100	45.3:49.8	0.90963855	1.11658773	

Table A.22. Percentages from screen 3 plate 5

Screen 3 – Plate 6.

Name / Desc	All	Mean GFP	Mean RFP	R01	Ratio Green/	Numerical Ra	Ratio/Scraml	Average scra
A1	100	43.7	54.1	100	43.7:54.1	0.8077634	1.00554196	0.80331148
A2	100	46.2	52.3	100	23.1:26.15	0.8833652	1.09965465	
A3	100	42.3	56.7	100	3.021428571	0.74603175	0.92869549	
A4	100	45.2	53.8	100	45.2:53.8	0.8401487	1.04585671	
A5	100	47.2	51.6	100	47.2:51.6	0.91472868	1.13869739	
A6	100	38.1	57.5	100	2.005263157	0.6626087	0.82484654	
A7	100	34.1	61.9	100	34.1:61.9	0.55088853	0.68577201	
A8	100	39.1	58.8	100	39.1:58.8	0.66496599	0.82778101	
A9	100	44	54.3	100	22:27.15	0.81031308	1.00871592	
A10	100	43.2	54.5	100	43.2:54.5	0.79266055	0.98674122	
A11	100	37.8	60.1	100	37.8:60.1	0.62895175	0.78294879	
A12	100	50.6	45.9	100	10.12:9.18	1.10239651	1.37231515	
B1	100	42.9	55.4	100	42.9:55.4	0.77436823	0.96397008	
B2	100	40.7	56.8	100	5.0875:7.1	0.7165493	0.89199434	
B3	100	40.6	56.5	100	5.075:7.0625	0.71858407	0.89452733	
B4	100	43.2	54.3	100	43.2:54.3	0.79558011	0.99037563	
B5	100	43.4	54.2	100	43.4:54.2	0.80073801	0.99679642	
B6	100	43.2	54.6	100	43.2:54.6	0.79120879	0.984934	
B7	100	44.6	53.6	100	44.6:53.6	0.83208955	1.0358243	
B8	100	40	57.5	100	40:57.5	0.69565217	0.86598062	
B9	100	44.9	51.9	100	44.9:51.9	0.86512524	1.07694869	
B10	100	42.8	54.7	100	7.133333333	0.78244973	0.97403031	
B11	100	49.9	48.7	100	49.9:48.7	1.02464066	1.275521	
B12	100	40.8	54.4	100	20.4:27.2	0.75	0.93363536	
C1	100	7.3	60.1	100	7.3:60.1	0.12146423	0.1512044	
C2	100	39.8	57.5	100	13.26666666	0.69217391	0.86165072	
C3	100	51.7	43.5	100	51.7:43.5	1.18850575	1.47950799	
C4	100	47.2	50.9	100	47.2:50.9	0.92730845	1.15435727	
C5	100	49.3	48.2	100	49.3:48.2	1.02282158	1.27325652	
C6	100	48.2	50.2	100	24.1:25.1	0.96015936	1.19525164	
C7	100	44.2	53.7	100	44.2:53.7	0.82309125	1.02462279	
C8	100	48.2	49.1	100	48.2:49.1	0.98167006	1.22202917	
C9	100	46	51.6	100	46:51.6	0.89147287	1.10974745	
C10	100	45.4	51.9	100	15.13333333	0.87475915	1.08894143	
C11	100	39.3	58.2	100	39.3:58.2	0.67525773	0.84059266	
C12	100	41.7	55.8	100	41.7:55.8	0.74731183	0.93028899	
D1	100	50.3	47.7	100	50.3:47.7	1.05450734	1.31270045	
D2	100	44.2	53.3	100	44.2:53.3	0.82926829	1.03231227	
D3	100	48.7	49.7	100	48.7:49.7	0.97987928	1.21979992	
D4	100	43.6	52.5	100	43.6:52.5	0.83047619	1.03381591	
D5	100	46.6	51.5	100	46.6:51.5	0.90485437	1.12640538	
D6	100	44.9	51.5	100	44.9:51.5	0.87184466	1.08531334	
D7	100	47.1	50.8	100	47.1:50.8	0.92716535	1.15417914	
D8	100	42.8	54.9	100	7.133333333	0.77959927	0.97048193	
D9	100	41.9	55.2	100	41.9:55.2	0.75905797	0.94491115	
D10	100	42.1	54.5	100	7.016666666	0.77247706	0.96161587	
D11	100	40.9	56.6	100	5.1125:7.075	0.72261484	0.89954502	
D12	100	40.7	55.2	100	8.14:11.04	0.73731884	0.91784925	
E1	100	46	50.1	100	23:25.05	0.91816367	1.14297343	
E2	100	40.5	56.9	100	5.0625:7.112	0.71177504	0.88605113	
E3	100	49.2	49.6	100	1.004081632	0.99193548	1.23480805	
E4	100	50.3	48	100	25.15:24	1.04791667	1.30449607	
E5	100	51.1	47.4	100	51.1:47.4	1.07805907	1.34201876	
E6	100	47.9	49.7	100	47.9:49.7	0.9637827	1.19976214	
E7	100	48.8	48.5	100	1.016666666	1.00618557	1.25254723	
E8	100	46	51.9	100	46:51.9	0.88631985	1.10333273	
E9	100	42.3	54.8	100	7.05:9.13333	0.77189781	0.96089478	
E10	100	44.4	52.8	100	11.1:13.2	0.84090909	1.04680328	
E11	100	46.6	50.3	100	23.3:25.15	0.92644135	1.15327787	
E12	100	3.5	65.2	100	3.5:65.2	0.05368098	0.06682462	
F1	100	44.8	51.5	100	44.8:51.5	0.86990291	1.08289616	
F2	100	41.5	56.1	100	41.5:56.1	0.73975045	0.92087623	
F3	100	52.8	44.9	100	13.2:11.225	1.17594655	1.4638737	
F4	100	47.9	49.5	100	47.9:49.5	0.96767677	1.20460966	
F5	100	42.7	53.8	100	42.7:53.8	0.7936803	0.98801065	
F6	100	45.5	52.2	100	45.5:52.2	0.87164751	1.08506791	
F7	100	45.8	51.8	100	15.26666666	0.88416988	1.10065636	
F8	100	43.7	53.3	100	43.7:53.3	0.81988743	1.02063453	
F9	100	47.8	49.8	100	47.8:49.8	0.95983936	1.19485328	
F10	100	46.4	49.5	100	46.4:49.5	0.93737374	1.16688702	
F11	100	49.6	48.7	100	49.6:48.7	1.01848049	1.26785253	
F12	100	31.7	66.3	100	31.7:66.3	0.47812971	0.59519841	
G1	100	44.9	50	100	22.45:25	0.898	1.11787274	
G2	100	42.3	56	100	3.021428571	0.75535714	0.94030418	
G3	100	51.6	45.5	100	17.2:15.1666	1.13406593	1.41173874	
G4	100	44.1	53.2	100	44.1:53.2	0.82894737	1.03191276	
G5	100	44.9	52.2	100	11.225:13.05	0.86015326	1.07075933	
G6	100	52.6	45.3	100	52.6:45.3	1.1611479	1.44545165	
G7	100	44.6	53.6	100	44.6:53.6	0.83208955	1.0358243	
G8	100	54.3	44	100	27.15:22	1.23409091	1.53625454	
G9	100	50.2	48.4	100	25.1:24.2	1.03719008	1.29114311	
G10	100	51.4	47	100	51.4:47	1.09361702	1.36138603	
G11	100	45	51.9	100	15:17.3	0.86705202	1.07934723	
G12	100	39.2	55	100	39.2:55	0.71272727	0.88723651	
H1	100	40.6	52.9	100	10.15:13.225	0.76748582	0.95540253	
H2	100	45.1	53	100	45.1:53	0.8509434	1.05929446	
H3	100	30.5	68	100	15.25:34	0.44852941	0.55835056	
H4	100	42.9	55	100	42.9:55	0.78	0.97098077	
H5	100	46.5	51.1	100	46.5:51.1	0.90998043	1.13278654	
H6	100	35.6	62.3	100	35.6:62.3	0.57142857	0.71134123	
H7	100	37	62.1	100	37:62.1	0.5958132	0.74169637	
H8	100	36.9	60.6	100	3.075:5.05	0.60891089	0.75800098	
H9	100	47.6	51.1	100	47.6:51.1	0.93150685	1.15958364	
H10	100	51.6	46.8	100	51.6:46.8	1.1025641	1.37252377	
H11	100	46.5	51	100	46.5:51	0.91176471	1.13500769	
H12	100	47.9	45.3	100	47.9:45.3	1.05739514	1.31629532	

Table A.23. Percentages from screen 3 plate 6

A.3.4 – Combined Screen Z-Score Data.

Gene	Screen1	Screen2	Screen3	Average
BRCA2	-0.1373	-1.2347	-3.9691	-1.7803
DCLRE1C	-1.7078	-2.7163	-0.2414	-1.5552
FLJ12610	-1.8575	-1.0200	-1.4778	-1.4518
RRM2	-0.3031	-2.3343	-1.7033	-1.4469
VCP	-1.3715	-0.6354	-2.1170	-1.3747
PPP4R1	0.2041	-3.2432	-0.7807	-1.2733
POLR2A	-2.6089	-1.0334	-0.1153	-1.2525
RBBP8	-1.5573	-1.3634	-0.6729	-1.1979
USP1	-2.4065	0.2605	-1.4126	-1.1862
MAD2L2	-1.1430	-0.9786	-1.3364	-1.1527
NSMCE4A	-0.3961	-3.4748	0.4201	-1.1503
RUVBL2	-0.4352	-1.0280	-1.9469	-1.1367
FANCB	-1.7971	-0.8737	-0.6163	-1.0957
IHPK3	-0.6295	-0.7662	-1.7421	-1.0459
RAD52	-0.4056	-1.1723	-1.5504	-1.0428
BTG2	0.9761	-2.4408	-1.5894	-1.0180
HEL308	-1.5206	0.0081	-1.4727	-0.9951
UVRAG	-0.2332	-1.6573	-1.0749	-0.9885
RFC1	-1.8535	-0.4250	-0.6784	-0.9856
DNA2L	-1.1302	-0.9567	-0.8653	-0.9841
APTX	-0.8067	-0.3780	-1.7186	-0.9678
APEX1	-0.0342	-2.0752	-0.7504	-0.9533
PMS1	-0.3168	-0.8694	-1.6565	-0.9476
PCNA	0.5195	-1.2788	-2.0497	-0.9363
RUVBL1	-0.3438	-1.2154	-1.2165	-0.9252
COPS6	-1.0316	-1.1512	-0.5595	-0.9141
MEN1	-1.1573	-1.0014	-0.5801	-0.9129
DLG7	-1.2045	0.0021	-1.5352	-0.9125
CHAF1A	-0.8457	-0.7515	-1.0790	-0.8921
POLK	-0.9280	-0.6559	-1.0901	-0.8914
NEIL3	-0.0906	-1.3575	-1.2191	-0.8891
POLE	-1.3262	0.4372	-1.7674	-0.8855
POLE4	-0.5575	-2.4746	0.3771	-0.8850
EXO1	-0.9385	-0.5426	-1.1700	-0.8837
NDNL2	-1.4827	-1.4315	0.2894	-0.8749
FANCC	-0.1926	-1.2526	-1.1645	-0.8699
PRKCG	-0.7329	-0.7714	-1.0906	-0.8650
XPA	-2.0513	0.6877	-1.2287	-0.8641
HTATIP	-0.1192	-1.2559	-1.1398	-0.8383
RPA3	-2.6208	-0.4691	0.5846	-0.8351
POLN	-0.4803	-0.8513	-1.1639	-0.8318
POLD4	-1.0029	-0.6894	-0.7985	-0.8303
TTRAP	-0.7435	-0.5828	-1.0880	-0.8048
RAD50	-1.0838	0.0535	-1.2895	-0.7733
XRCC2	-0.8516	-0.6682	-0.7910	-0.7703
UNG2	0.1575	-0.3694	-2.0976	-0.7698
TINF2	-1.0823	-0.5410	-0.6793	-0.7675
FRAP1	-0.7302	-0.1277	-1.4417	-0.7665
UBE2B	0.1442	-0.3031	-2.1334	-0.7641
C7ORF11	-0.2676	-1.0071	-1.0121	-0.7623

Gene	Screen1	Screen2	Screen3	Average
LIG4	1.1168	-3.7947	0.4222	-0.7519
MRE11A	-0.6457	-0.4742	-1.0849	-0.7350
DDB1	-0.7592	-1.1802	-0.2467	-0.7287
TNP1	0.7902	-1.7091	-1.2592	-0.7260
SPO11	-0.7228	-0.5564	-0.8939	-0.7244
KUB3	-0.1049	-1.6099	-0.4552	-0.7233
MJD	-1.2022	-0.5571	-0.3994	-0.7196
NEIL1	-0.9992	-0.3152	-0.8316	-0.7153
RAD51L3	-0.3744	-0.7601	-0.9829	-0.7058
BRIP1	0.0096	-1.0230	-1.0775	-0.6970
XAB2	-0.3157	-0.2248	-1.5493	-0.6966
RNF8	-1.1345	-0.1793	-0.7734	-0.6957
YBX1	-0.4505	-0.5503	-1.0717	-0.6909
TDP1	-2.5265	0.3440	0.1797	-0.6676
XRCC4	-1.1647	-0.3324	-0.4536	-0.6502
HAUS7	-0.7426	-0.3107	-0.8840	-0.6458
GIYD1	-0.8974	-0.3500	-0.6752	-0.6408
CNOT7	-0.3303	-0.4431	-1.1366	-0.6367
MSH6	-1.2510	0.0787	-0.6961	-0.6228
CCNC	-0.7154	-0.4339	-0.7122	-0.6205
MMS19L	-0.9246	0.2320	-1.1266	-0.6064
MSH4	-0.7685	0.1585	-1.1613	-0.5904
NSMCE1	-0.9893	-0.5823	-0.1832	-0.5849
REV1L	0.8247	-1.0389	-1.4939	-0.5694
GPS1	-2.5250	0.1178	0.7140	-0.5644
CETN2	-1.0531	0.0887	-0.7173	-0.5606
ERCC6	-0.7732	-0.6986	-0.1876	-0.5532
ALKBH2	0.0242	0.0504	-1.7317	-0.5524
MSH3	-0.6236	-0.3728	-0.5913	-0.5292
SUMO3	-0.4722	-0.7045	-0.4082	-0.5283
CCNB3	-0.2142	-0.7139	-0.6277	-0.5186
POLS	0.3865	-1.1718	-0.7609	-0.5154
RRM1	-2.4178	-0.8117	1.7093	-0.5067
DCLRE1A	-0.4536	-0.5169	-0.5437	-0.5047
HUS1B	-0.7202	-0.4387	-0.3550	-0.5046
RAD18	-1.0340	0.7188	-1.1972	-0.5041
TRIM28	-1.0515	-0.8854	0.4820	-0.4850
BLM	-0.3623	0.0378	-1.1238	-0.4828
RAD51	0.4194	-0.5712	-1.2925	-0.4814
MDC1	0.1427	0.3166	-1.8988	-0.4798
RAD54B	-0.3187	-1.5852	0.5079	-0.4654
RFC4	-1.1855	-0.7815	0.5801	-0.4623
TOP2A	-0.7144	-0.4721	-0.1692	-0.4519
TEN1	-0.1260	-0.4533	-0.7602	-0.4465
RAD54L	-0.1757	-0.5015	-0.6562	-0.4445
PNKP	0.0842	-0.0007	-1.4069	-0.4412
RAD52B	-0.1324	-0.6932	-0.4865	-0.4374
CCNE1	-0.8244	0.1414	-0.6055	-0.4295
TCEA1	0.2325	0.2935	-1.8100	-0.4280
PMS2L5	-1.1736	0.5422	-0.6496	-0.4270

Gene	Screen1	Screen2	Screen3	Average
CCND2	-0.7939	-0.1998	-0.2790	-0.4242
INO80B	-1.4346	0.2029	0.0160	-0.4052
ANKRD52	-0.8481	-0.4790	0.1145	-0.4042
MUTYH	-0.0751	-0.2620	-0.8705	-0.4026
RENT1	0.8099	-1.3654	-0.6336	-0.3964
CDK2	-0.0500	-1.1601	0.0225	-0.3959
SMG6	-0.5270	-0.1168	-0.5226	-0.3888
POLH	-0.5399	-0.2361	-0.3772	-0.3844
PARP2	-0.6990	0.5197	-0.9687	-0.3827
ABL1	-0.9775	0.3864	-0.5554	-0.3822
ARID2	0.1498	-0.2799	-0.9996	-0.3766
CDKN2D	0.3411	-0.3349	-1.1334	-0.3757
FLJ22833	0.2825	-0.6287	-0.7809	-0.3757
C11ORF13	0.0096	-0.9398	-0.1499	-0.3600
MPG	0.8580	-1.2023	-0.7263	-0.3569
ERCC1	0.7958	-0.7677	-1.0930	-0.3550
FANCE	0.0737	-0.7172	-0.4177	-0.3537
ASF1A	0.4684	-1.5288	0.0140	-0.3488
HRMT1L6	-0.9397	-0.1731	0.0690	-0.3480
SMC6L1	-0.6999	0.1778	-0.5140	-0.3454
XPC	-0.0911	0.2869	-1.2051	-0.3364
MYBBP1A	-0.2405	-0.4556	-0.3079	-0.3347
HES1	-0.3347	0.1254	-0.7895	-0.3329
ACTR5	0.4379	-0.5630	-0.8712	-0.3321
LIG1	-0.0895	-0.2676	-0.6379	-0.3317
POLR2B	-0.9461	-0.4213	0.3831	-0.3281
TERF2	-1.0460	-0.9718	1.0410	-0.3256
TDG	-0.5013	0.5060	-0.9746	-0.3233
GTF2H5	0.1716	-0.4191	-0.7208	-0.3228
TREX1	0.6585	-0.8254	-0.7835	-0.3168
RPA2	-0.9349	0.8620	-0.8759	-0.3163
TIPIN	-0.7291	-0.4185	0.2070	-0.3135
MIZF	-0.3999	-0.5426	0.0140	-0.3095
COPS3	-0.3122	-0.8047	0.1899	-0.3090
RMI2	-1.0301	-0.4480	0.5511	-0.3090
ANKRD44	0.7555	-0.2795	-1.4026	-0.3089
POLR2K	0.1141	0.1250	-1.1650	-0.3086
NCAPH2	-0.0799	-0.4047	-0.4408	-0.3085
SIRT1	-1.1512	1.7599	-1.5335	-0.3083
EME2	-1.0108	-0.8041	0.8912	-0.3079
CORT	0.2233	-0.1114	-1.0233	-0.3038
MGC32020	0.2035	-0.6144	-0.4962	-0.3024
RAD23B	-0.2925	0.0774	-0.6822	-0.2991
DUT	0.1996	-0.1977	-0.8979	-0.2987
CSNK1E	-0.6644	-1.0053	0.7972	-0.2908
TREX2	-0.0909	-0.4227	-0.3528	-0.2888
COPS5	-0.8613	0.3587	-0.3550	-0.2859
CRY1	-1.7807	-0.1165	1.0454	-0.2839
MLH1	-0.6358	0.3909	-0.6046	-0.2832
NOP10	-0.8911	-1.0545	1.1009	-0.2816

Gene	Screen1	Screen2	Screen3	Average
ERCC3	0.2900	-0.6211	-0.5130	-0.2813
POLR2I	-1.0061	-0.5506	0.7156	-0.2804
UBE2A	-1.0456	-0.1069	0.3146	-0.2793
TP53	-0.5669	0.2371	-0.4953	-0.2750
BAZ1B	-0.4342	0.1355	-0.5045	-0.2677
CSNK1D	-0.7685	0.7611	-0.7947	-0.2674
POLE2	-0.7514	-0.4847	0.4345	-0.2672
APEX2	-0.6289	-0.1040	-0.0681	-0.2670
RBX1	-1.0805	-0.4480	0.7323	-0.2654
MNAT1	-0.6868	0.7807	-0.8688	-0.2583
ATF2	0.6491	-0.6402	-0.7835	-0.2582
CDC25B	-0.9434	-0.2825	0.4514	-0.2582
DEPC-1	0.1271	-0.6760	-0.2245	-0.2578
POLA	0.4862	-0.5137	-0.7428	-0.2567
SHFM1	-0.5097	-0.0606	-0.1909	-0.2537
POLI	-0.5415	-0.2806	0.0613	-0.2536
SUMO4	-0.1248	-0.9018	0.2694	-0.2524
BRCA1	-0.2943	-0.0217	-0.4052	-0.2404
ERCC2	0.1622	-0.3678	-0.5081	-0.2379
SETMAR	0.7848	-0.1270	-1.3629	-0.2350
RAD51L1	-0.2428	-0.5923	0.1953	-0.2132
DNMT1	0.5260	-0.5223	-0.6335	-0.2099
POLQ	-0.0207	-0.5596	-0.0479	-0.2094
POLD1	1.1195	-0.5923	-1.1493	-0.2074
RFC5	-0.8167	-0.1969	0.4073	-0.2021
GAR1	-0.5124	-0.4380	0.3761	-0.1914
POLB	0.7021	-0.7455	-0.5296	-0.1910
UBE2T	-0.9203	-0.8016	1.1543	-0.1892
DMC1	0.7493	-0.6625	-0.6453	-0.1862
RNF4	-0.9077	-0.4366	0.7920	-0.1841
GTF2H1	-0.8086	0.7390	-0.4666	-0.1787
CDK7	0.4544	-0.4830	-0.5059	-0.1782
XRCC3	0.1528	-0.6514	-0.0299	-0.1762
XRCC5	0.6616	-0.5422	-0.6267	-0.1691
COPS2	-0.9279	-0.4511	0.8840	-0.1650
CLSPN	-0.2064	0.0734	-0.3278	-0.1536
RAD17	1.3612	-0.3117	-1.4969	-0.1491
EYA1	0.6674	-0.5465	-0.5536	-0.1443
PDS5B	0.9929	-0.8345	-0.5864	-0.1426
ADPRTL3	0.3719	0.1808	-0.9783	-0.1418
FLJ21816	-0.6621	0.4886	-0.2449	-0.1395
POLG	-0.9462	-0.2173	0.7470	-0.1388
TRIP13	-0.9995	0.5530	0.0332	-0.1378
NCAPG2	0.4060	-0.8577	0.0508	-0.1336
TP73	-0.3339	-0.3952	0.3284	-0.1336
PRPF19	-0.8120	0.3648	0.0522	-0.1317
CDKN2A	-0.6920	0.5078	-0.2081	-0.1308
RFC2	-1.1451	0.8412	-0.0786	-0.1275
TP53BP1	-0.9568	0.6441	-0.0368	-0.1165
GADD45G	-1.1730	0.9383	-0.1019	-0.1122

Gene	Screen1	Screen2	Screen3	Average
PPP4R4	-0.2090	-0.0377	-0.0884	-0.1117
OGG1	0.3202	-0.2244	-0.4296	-0.1113
EYA3	-0.1338	-0.9127	0.7291	-0.1058
BARD1	-0.7660	-0.7617	1.2129	-0.1049
NCAPH	-1.1650	0.0337	0.8177	-0.1045
TOP3B	0.4194	0.1763	-0.9067	-0.1037
POLE3	0.2698	-1.0891	0.5149	-0.1014
TERF1	-1.2320	0.4164	0.5380	-0.0925
SMARCC1	-0.0203	-0.6577	0.4080	-0.0900
PINX1	0.2636	-0.6337	0.1400	-0.0767
KIAA1596	-0.0202	0.3085	-0.4952	-0.0690
MGMT	1.2750	-0.4693	-1.0041	-0.0661
POLR2F	-0.5449	-0.1081	0.4664	-0.0622
BRD7	-0.0153	-0.6064	0.4388	-0.0610
GTF2H4	1.0063	-0.0180	-1.1580	-0.0566
STAG2	0.8763	-0.4511	-0.5940	-0.0563
POT1	-0.3883	-0.7393	0.9595	-0.0561
COPS8	-1.0873	0.0186	0.9050	-0.0546
SMUG1	0.0305	-0.3724	0.1791	-0.0543
RAD21	0.1480	-0.3578	0.0547	-0.0517
RPA1	-0.6143	0.6723	-0.2100	-0.0507
CSPG6	0.4916	-0.1950	-0.4442	-0.0492
ALKBH	0.4996	-0.0427	-0.5534	-0.0322
SMARCA4	-0.9362	0.4809	0.3718	-0.0278
FANCA	0.4562	-0.2263	-0.3127	-0.0276
CCND3	-0.3237	0.0706	0.1723	-0.0269
RECQL5	1.1266	-0.7963	-0.4095	-0.0264
POLG2	-0.3719	0.6378	-0.3360	-0.0233
TYMS	0.3035	-0.2804	-0.0889	-0.0219
CTC1	-1.1964	0.6230	0.5124	-0.0203
CDC5L	0.1218	-0.1757	0.0027	-0.0170
NUDT1	0.6134	-0.6111	-0.0517	-0.0164
CHEK2	-0.5990	-0.0574	0.6232	-0.0111
FANCL	1.1226	-0.3705	-0.7824	-0.0101
DCLRE1B	-0.2093	0.5746	-0.3948	-0.0098
HMGB2	-0.0780	0.8837	-0.8228	-0.0057
XRCC1	0.1293	0.0398	-0.1750	-0.0020
POLM	0.6895	-0.2556	-0.4298	0.0013
CLK2	1.1568	-0.9703	-0.1698	0.0055
HUS1	-0.1819	0.6236	-0.4050	0.0122
MDM2	-2.0359	0.5326	1.5589	0.0185
FLJ40869	-0.3583	-0.2123	0.6368	0.0221
SMARCD1	1.0032	-0.2057	-0.7308	0.0222
TIMELESS	-0.2266	-0.0334	0.3284	0.0228
TADA3L	1.1176	-0.0115	-0.9980	0.0360
CDC25A	-0.2740	0.0203	0.3633	0.0365
EME1	1.1860	-0.2272	-0.8490	0.0366
MGC2731	-0.2185	0.5738	-0.2091	0.0487
PRKDC	-0.2359	-0.0178	0.4142	0.0535
COPS7A	0.8040	-0.5291	-0.1091	0.0553

Gene	Screen1	Screen2	Screen3	Average
POLD3	0.3164	-0.0597	-0.0885	0.0561
MBD4	0.1129	0.7491	-0.6798	0.0607
TOP3A	-0.0651	0.0603	0.1926	0.0626
INO80D	-0.7909	0.2321	0.7526	0.0646
DAXX	0.3913	-0.1043	-0.0781	0.0696
RAD23A	0.3567	-0.0897	-0.0481	0.0730
GTF2H2	-0.2099	-0.4482	0.8885	0.0768
SMARCB1	-0.5324	0.2694	0.4942	0.0771
TREX2	-0.7397	-0.0660	1.0412	0.0785
CIB1	0.9337	-0.7994	0.1025	0.0789
CKN1	1.0635	-0.3297	-0.4926	0.0804
C17orf70	-1.1808	1.1297	0.2998	0.0829
ERCC5	-0.0192	0.1057	0.1640	0.0835
REV3L	0.1844	0.1866	-0.1180	0.0843
FEN1	-0.5003	0.0994	0.6594	0.0862
RTEL1	-0.5195	0.8735	-0.0824	0.0906
NFATC2IP	-0.4425	0.4595	0.2560	0.0910
TNKS	-0.6621	1.1669	-0.2274	0.0925
ERCC4	0.2307	-0.4880	0.5368	0.0932
PARP4	0.0039	0.3053	-0.0294	0.0933
OBFC1	0.2666	0.1449	-0.1233	0.0961
MSH2	1.6599	-0.6036	-0.7558	0.1002
WDR48	0.3437	0.0786	-0.1110	0.1038
NHP2	-0.9450	1.1518	0.1114	0.1061
PER3	-0.2084	0.5371	-0.0086	0.1067
TOP2B	-0.1094	-0.5836	1.0179	0.1083
RAD9B	0.1021	-0.2319	0.4614	0.1106
IGHMBP2	0.1712	0.5635	-0.3951	0.1132
MLH3	-0.7281	0.1488	0.9348	0.1185
SMC2	1.3105	-0.7074	-0.2428	0.1201
C2ORF13	-0.9230	0.0700	1.2153	0.1208
NPM1	0.5252	-0.1819	0.0284	0.1239
ARID1B	-0.1355	-0.3968	0.9184	0.1287
WRAP53	0.6922	-0.4064	0.1145	0.1334
INO80	-1.0329	0.1366	1.3276	0.1438
PARP1	0.5081	0.1464	-0.2191	0.1452
SMARCE1	-0.8656	0.1239	1.1791	0.1458
SMARCC2	0.0885	-0.3543	0.7048	0.1464
SOD1	0.5374	0.6004	-0.6594	0.1595
UBE2NL	0.1390	0.0541	0.2862	0.1597
CXORF53	0.0919	-0.3226	0.7515	0.1736
ATRX	1.2566	-0.9254	0.2052	0.1788
FANCG	0.2214	-0.1210	0.4418	0.1807
RAD51C	0.3587	-0.1559	0.3453	0.1827
CDKN2A	0.4696	-0.8243	0.9050	0.1834
SMARCA2	-0.6652	1.6733	-0.4577	0.1835
MDM4	0.4862	0.4964	-0.4275	0.1850
RECQL	0.1396	0.1817	0.2468	0.1894
RFC3	-1.5535	0.1561	1.9727	0.1918
SMC1L1	1.7324	-0.5714	-0.5508	0.2034

Gene	Screen1	Screen2	Screen3	Average
NCAPG	-0.1835	-0.6131	1.4403	0.2146
MSH5	0.8023	-0.3785	0.2200	0.2146
NTHL1	0.2994	-0.6341	0.9896	0.2183
SHPRH	-0.6133	0.3826	0.8872	0.2188
PER1	0.7565	1.2641	-1.3587	0.2206
ASF1B	-0.2288	0.2089	0.6906	0.2236
RRM2B	0.9667	-0.1181	-0.1710	0.2259
H2AFX	0.5182	-0.3151	0.4999	0.2343
STAG1	0.1941	-0.1639	0.6739	0.2347
EID3	1.4868	-0.6412	-0.1391	0.2355
SMC1B	1.3032	-0.9547	0.3870	0.2452
UBA2	0.0710	0.1551	0.5234	0.2498
ACTR8	-0.1301	0.3693	0.5134	0.2509
INO80E	1.0002	0.0967	-0.3429	0.2513
SMC4	0.4839	0.3973	-0.0818	0.2665
ATM	0.6581	-0.4063	0.5514	0.2677
CCNH	0.2427	0.0295	0.5328	0.2683
UNG	1.0247	0.4209	-0.6385	0.2690
BCAS2	-0.3303	0.7493	0.3953	0.2714
PPP4R2	0.7158	-0.5542	0.6653	0.2756
RIF1	-0.5765	0.6880	0.7160	0.2758
PARG	1.9029	-0.4391	-0.6311	0.2776
TFPT	0.7902	-0.3955	0.4679	0.2875
TEP1	-0.2438	-0.0767	1.1873	0.2890
SLX4	-0.0454	-0.0721	0.9859	0.2895
HLTF	0.9814	-0.5828	0.4786	0.2924
UBE2N	0.2409	0.2273	0.4383	0.3022
ATRIP	1.8475	0.2344	-1.1366	0.3151
KIAA1018	0.6178	-0.0839	0.4228	0.3189
DKC1	-0.7592	1.1072	0.6329	0.3270
CCND1	0.5205	-0.5000	0.9712	0.3306
RAD9A	1.9070	-0.9351	0.0224	0.3315
COPS7B	1.0562	-0.7033	0.6884	0.3471
UBE2I	-0.4868	0.1433	1.3881	0.3482
GADD45A	1.6001	-0.6421	0.1047	0.3543
RNF168	1.4896	-0.0992	-0.3274	0.3544
TCEB3	-0.2159	0.8396	0.4500	0.3579
INO80C	-0.3482	0.5551	0.8907	0.3658
NCAPD3	0.2690	0.3129	0.5335	0.3718
PPP4C	-0.9181	0.2644	1.7696	0.3720
MCRS1	0.6647	0.3778	0.0795	0.3740
CDK4	0.9761	1.6594	-1.4984	0.3790
RPS27L	0.8438	1.7838	-1.4843	0.3811
SUMO1	-0.0656	0.5715	0.6459	0.3839
MGC4189	1.5734	0.0982	-0.4821	0.3965
NFRKB	-0.4310	-0.3009	1.9236	0.3972
GTF2H3	0.8845	-0.0487	0.3616	0.3991
RECQL4	2.4610	-0.2124	-1.0344	0.4048
PPP6R1	0.3139	-1.3996	2.3028	0.4057
LIG3	-0.5288	1.9799	-0.2121	0.4130

Gene	Screen1	Screen2	Screen3	Average
ATR	0.6262	-0.5377	1.1556	0.4147
CCNA1	0.3989	-0.3190	1.1711	0.4170
KIAA0625	0.6158	0.3748	0.2653	0.4187
PDS5A	-1.7044	0.5622	2.4056	0.4211
TCEB2	-0.0799	-0.0208	1.3674	0.4222
SMC5	-0.1461	0.1073	1.3092	0.4235
AMN1	0.6687	-0.3612	0.9872	0.4316
BAZ1A	1.2774	0.7317	-0.7071	0.4340
PMS2	-0.1489	1.8549	-0.3772	0.4429
POLR2D	0.2035	0.8714	0.2567	0.4438
SMEK2	0.6258	0.3484	0.3751	0.4498
G22P1	1.0186	0.3973	-0.0632	0.4509
FLJ10719	1.0323	-0.0370	0.3718	0.4557
CHEK1	1.4379	-0.3886	0.3187	0.4560
WEE1	0.2424	0.2702	0.8822	0.4649
PIF1	0.3909	0.5703	0.5351	0.4988
PARPBP	0.2994	1.7676	-0.5558	0.5037
RAD1	1.3105	-0.5999	0.8127	0.5078
CHRAC1	0.2111	-0.0967	1.4218	0.5120
CRY2	-0.7226	-0.3110	2.5927	0.5197
MUS81	1.0983	1.9764	-1.5056	0.5230
NEIL2	1.9734	0.0612	-0.4525	0.5274
POLR2H	-0.9160	1.0624	1.4679	0.5381
UBE2V2	0.4913	0.1683	0.9902	0.5499
POLR2L	-0.9320	0.4590	2.1291	0.5520
UBE2V1	1.2927	-0.4071	0.7738	0.5531
HSU24186	1.5907	-0.1217	0.2302	0.5664
POLR2G	-1.1287	1.1444	1.6930	0.5696
SWI5	1.1176	0.3658	0.2351	0.5728
TOP1	0.8580	1.5143	-0.6338	0.5795
TELO2	-0.1365	-0.5017	2.3905	0.5841
RAP80	1.2881	-0.1257	0.5970	0.5865
TCEB1	-0.3248	1.4449	0.6393	0.5865
CCNB2	0.6178	0.8037	0.3562	0.5926
TERF2IP	0.9785	0.3030	0.5409	0.6075
FANCF	1.2218	-0.1999	0.8281	0.6167
MVP	-0.6515	0.2840	2.2285	0.6203
POLR2C	-0.7281	1.3462	1.2593	0.6258
CUL3	-0.9040	1.3471	1.4355	0.6262
NSMCE2	1.5785	0.2464	0.0553	0.6267
DDB2	1.0575	0.1645	0.7206	0.6475
POLR2E	-0.1324	1.3834	0.6940	0.6483
ZSWIM7	1.2566	0.6105	0.0794	0.6488
CCNB1	0.9337	1.6933	-0.6516	0.6585
UVSSA	-0.2979	0.7050	1.5749	0.6607
POLR2J	-0.9906	1.8409	1.1527	0.6677
SUMO2	-0.3906	0.1796	2.2213	0.6701
PIAS3	0.7021	0.3563	0.9564	0.6716
NCAPD2	-0.5194	0.0771	2.5027	0.6868
COPS4	0.7049	0.7686	0.6667	0.7134

Gene	Screen1	Screen2	Screen3	Average
CUL5	-1.7189	2.7539	1.1709	0.7353
HMGB1	0.2165	1.1497	0.9164	0.7608
PPP6R3	1.5056	1.2106	-0.3966	0.7732
PPP6R2	0.3411	1.6884	0.3231	0.7842
BRE	1.8945	-0.0976	0.6025	0.7998
SMARCA5	1.0635	1.7406	-0.4012	0.8010
NBS1	0.9607	0.8435	0.6285	0.8109
POLL	2.7120	-0.3873	0.1414	0.8220
PAXIP1	0.3989	-0.2173	2.3237	0.8351
DNTT	1.6599	0.5176	0.3341	0.8372
SMARCAD1	0.5770	0.3428	1.7418	0.8872
TTI2	0.1622	1.1544	1.3536	0.8900
UBC	0.1271	0.7175	1.9525	0.9323
PIAS2	0.8845	2.2357	-0.2790	0.9471
FLJ13614	1.1777	1.3705	0.3689	0.9724
HFM1	0.4996	1.3501	1.0830	0.9776
PPP6C	0.5195	1.9414	0.5647	1.0085
GCN5L2	0.8965	1.4709	0.6869	1.0181
CUL4A	0.2843	0.7246	2.1298	1.0462
POLD2	-1.1540	0.1624	4.3160	1.1081
PBRM1	1.1926	0.2091	1.9842	1.1286
TONSL	1.0575	1.8036	0.6116	1.1575
PER2	0.8099	1.3122	1.3546	1.1589
ARID1A	0.7493	1.2571	1.6036	1.2033
FBXO18	1.1195	0.9583	1.7531	1.2770
PLRG1	0.5081	2.4503	0.8833	1.2806
PIAS4	1.2750	2.0908	0.6207	1.3288
H2AFZ	1.2927	2.5694	0.1811	1.3477
CDKN1A	1.1574	0.7462	2.2721	1.3919
SFR1	1.2218	1.8514	1.1845	1.4192
ACD	-0.0207	2.0152	2.2688	1.4211
TERT	0.9607	1.2294	2.0786	1.4229
PIAS1	2.7120	1.8178	-0.1968	1.4443
TOPBP1	0.3325	3.1393	0.9029	1.4583
UBB	0.8023	1.9554	1.6311	1.4629
UBD	1.5734	1.3784	2.0924	1.6814
STRA13	-0.4342	3.7156	1.7667	1.6827
TTI1	1.1860	2.0577	1.8445	1.6961
CCNA2	2.4610	2.8744	-0.0193	1.7720
DDX11	5.3843	1.0504	-1.0744	1.7868
ACTL6A	0.3587	2.6425	2.4973	1.8328
WRN	7.1971	-0.2773	-1.2333	1.8955
MMS22L	1.9029	3.0887	0.9343	1.9753
UBA1	0.6674	4.7764	1.0216	2.1551
ANKRD28	1.9070	1.4296	3.3344	2.2237
FANCD2	0.9412	6.4434	-0.2710	2.3712

Table A.24. Combination of average Z-scores

A.3.5 – Counts from all three screens

DDR Screen						
Plate 1	Average gfp cells counted	Average rfp cells counted	Average total cells counted	Total gfp cells counted	Total rfp cells counted	Total total cells counted
Scramble	1210.666667	1210.666667	2633.333333	3632	3632	7900
RAD50	1376	1746.666667	3402.333333	4128	5240	10207
POLE2	1214.666667	1497	2938.666667	3644	4491	8816
RUVBL2	728	1000.666667	1853.333333	2184	3002	5560
PRKCG	1328.333333	1745.666667	3352.333333	3985	5237	10057
FANCC	1059.666667	1347.333333	2625	3179	4042	7875
FEN1	1354	1532.333333	3236	4062	4597	9708
TCEA1	1107.333333	1240.666667	2500.333333	3322	3722	7501
RTEL1	1400.333333	1508.666667	3111.333333	4201	4526	9334
GCN5L2	1417	1328	2967.666667	4251	3984	8903
APTX	1274.333333	1617.666667	3148	3823	4853	9444
X	1647.666667	1910.333333	3984	4943	5731	11952
T. Reagent	1471.333333	1570.333333	3330	4414	4711	9990
RAD18	1577.333333	1918	3786	4732	5754	11358
TTRAP	1392.333333	1815.666667	3444	4177	5447	10332
GTF2H5	1879	2261	4504.333333	5637	6783	13513
POLE	1866	2338.666667	4653.333333	5598	7016	13960
UBE2B	1607	1987.333333	3879	4821	5962	11637
MDC1	1857	2177.333333	4333	5571	6532	12999
IHPK3	1422	1903.333333	3556.333333	4266	5710	10669
SIRT1	1524	1790	3586.666667	4572	5370	10760
TREX1	1478.666667	1784.666667	3520.333333	4436	5354	10561
WRN	2206.333333	1794.333333	4369	6619	5383	13107
Scramble	1523.333333	1491.666667	3261	4570	4475	9783
siGFP	297.3333333	1019.333333	2063	892	3058	6189
DDX11	2084.333333	1750	4203.333333	6253	5250	12610
APEX1	1822.333333	2815.666667	5180	5467	8447	15540
TDG	2169.333333	2531.333333	5010.333333	6508	7594	15031
TOPBP1	3043	2624.333333	6302	9129	7873	18906
RAD54L	1853.666667	2256	4402	5561	6768	13206
RPA1	1468.333333	1659.666667	3336.666667	4405	4979	10010
ATF2	1999	2364.333333	4753.666667	5997	7093	14261
VCP	1588	2236.666667	4138.333333	4764	6710	12415
ALKBH2	1935	2341.666667	4572	5805	7025	13716
GTF2H4	1639.666667	1814.666667	3694.666667	4919	5444	11084
T. Reagent	1587.666667	1960.333333	3834.333333	4763	5881	11503
SMC3	817	844.6666667	1839	2451	2534	5517
PMS1	1227.333333	1648.333333	3098.333333	3682	4945	9295
BRCA1	2215	2580.333333	5246.666667	6645	7741	15740
POLM	2154.333333	2417.333333	4950	6463	7252	14850
REV3L	2745.333333	3094.666667	6339.666667	8236	9284	19019
HMGB2	2118	2374	4865.333333	6354	7122	14596
GADD45A	2436.666667	2681	5620	7310	8043	16860
IGHMBP2	2219.333333	2414.333333	5018.666667	6658	7243	15056
PMS2	2390.666667	2426.666667	5214	7172	7280	15642
CSNK1E	1911.666667	2285.333333	4591	5735	6856	13773
BRIP1	1610.333333	2026.666667	3921	4831	6080	11763
Scramble	1618	1505.333333	3409.666667	4854	4516	10229
Scramble	872	956.3333333	1990.666667	2616	2869	5972
CSPG6	1641.333333	1868.666667	3784	4924	5606	11352
RAD52	1710.333333	2306.666667	4364	5131	6920	13092
FANCL	2163.666667	2512	5173	6491	7536	15519
FANCD2	3413.333333	2678.333333	6946	10240	8035	20838
TRIP13	1816.333333	2083.333333	4240.666667	5449	6250	12722
TYMS	2396	2778	5595.666667	7188	8334	16787
XPC	2373.333333	2802.333333	5638	7120	8407	16914
HUS1	2184	2426.333333	5047.333333	6552	7279	15142
RPS27L	2174.333333	2252.333333	4777	6523	6757	14331
DNA2L	1236.666667	1653	3087.333333	3710	4959	9262
siGFP	346	1057.666667	2283	1038	3173	6849
X	1791	1817.666667	4059.333333	5373	5453	12178
MAD2L2	1351.666667	1880	3506	4055	5640	10518
KIAA1596	1482.666667	1670	3413.333333	4448	5010	10240
SETMAR	2073.666667	2464	5032.333333	6221	7392	15097
PRKDC	2250	2557.666667	5288	6750	7673	15864
C11ORF13	2037.333333	2523	5017	6112	7569	15051
PARP2	1985.333333	2372.333333	4654.666667	5956	7117	13964
POLI	1880.666667	2237.333333	4404	5642	6712	13212
RAD17	2058.333333	2456	4879.666667	6175	7368	14639
TOP2A	1891.666667	2341	4612	5675	7023	13836
PER1	2046	2180.666667	4559.333333	6138	6542	13678
SMC3	1420.666667	1457	3148.333333	4262	4371	9445
X	1522.333333	1544	3434.666667	4567	4632	10304
ADPRTL3	1385	1583.333333	3241.333333	4155	4750	9724
NEIL2	1864.333333	1894	4050.333333	5593	5682	12151
REV1L	1381.666667	1648.666667	3266	4145	4946	9798
SOD1	1900.666667	2045.666667	4372.666667	5702	6137	13118
CSNK1D	1891	2202.333333	4480	5673	6607	13440
MSH3	1637.333333	2012.666667	3933.333333	4912	6038	11800
MSH4	1828.666667	2249.333333	4408.333333	5486	6748	13225
XAB2	1023.333333	1291.333333	2399.333333	3070	3874	7198
FANCG	1745.666667	1939	4020.333333	5237	5817	12061
ATR	1954	2123	4431.666667	5862	6369	13295
X	2144.333333	2335.333333	5040.333333	6433	7006	15121
X	1642.333333	1678	3764.333333	4927	5034	11293
HEL308	836.3333333	1088.666667	2087.333333	2509	3266	6262
RAD51L3	1081.333333	1387	2658	3244	4161	7974
UNG2	1168.666667	1439.666667	2821	3506	4319	8463
GTF2H2	1508.666667	1788.666667	3594.333333	4526	5366	10783
YBX1	1606	2041	4008.666667	4818	6123	12026
XRCC1	1549.333333	1752.666667	3579.333333	4648	5258	10738
GTF2H1	1632.666667	1865.666667	3791	4898	5597	11373
ERCC5	1639.666667	1820.333333	3787	4919	5461	11361
MUS81	1404.666667	1359.333333	3026.666667	4214	4078	9080
RAP80	1510.333333	1576.666667	3314.333333	4531	4730	9943
X	1773.666667	2001.666667	4193.666667	5321	6005	12581

Plate 2	Average gfp cells counted	Average rfp cells counted	Average total cells counted	Total gfp cells counted	Total rfp cells counted	Total total cells counted
Scramble	1490.333333	1452	3320.333333	4471	4356	9961
FLJ13614	1572	1604	3411	4716	4812	10233
TRIM28	1609	1710.666667	3535.333333	4827	5132	10606
POLS	1461	1874.666667	3650	4383	5624	10950
CXORF53	1703.333333	1752.333333	3705.666667	5110	5257	11117
POLG2	1815.666667	1849	3914.666667	5447	5547	11744
DCLRE1A	1565.666667	1876	3683.333333	4697	5628	11050
UVRAG	1387.666667	1691.333333	3359.666667	4163	5074	10079
TREX2	1557	1703.666667	3530.333333	4671	5111	10591
HTATIP	1681.666667	1954	3922.333333	5045	5862	11767
RECQL	1770.666667	1860.333333	3927.333333	5312	5581	11782
X	2533	2580.666667	6025.666667	7599	7742	18077
T. Reagent	1684	2042.333333	4064.666667	5052	6127	12194
CHEK2	2149.333333	2338.666667	4858.666667	6448	7016	14576
NUDT1	1941	2299.333333	4504	5823	6898	13512
MBD4	1586.333333	1769.333333	3546.333333	4759	5308	10639
RNF168	2222.666667	2406.666667	4934	6668	7220	14802
PRPF19	1471.333333	1590	3299	4414	4770	9897
FRAP1	2148	2623.333333	5136.666667	6444	7870	15410
RAD23B	2579.666667	2858	5868.666667	7739	8574	17606
MJD	2097.666667	2402.333333	4860	6293	7207	14580
DCLRE1C	2772.333333	3810.333333	7190	8317	11431	21570
FANCB	2001.333333	2511	4841.333333	6004	7533	14524
Scramble	1768	1817.666667	3927.666667	5304	5453	11783
siGFP	421	1085.666667	2195.666667	1263	3257	6587
CETN2	2039.333333	2280.333333	4633.666667	6118	6841	13901
KUB3	2588.666667	3021.333333	6058.333333	7766	9064	18175
TP73	2468.333333	2608	5632.333333	7405	7824	16897
OGG1	2578.333333	2963.333333	5966.666667	7735	8890	17900
LIG3	2725.333333	2699	5849	8176	8097	17547
MEN1	2558.333333	2696.666667	5659	7675	8090	16977
MLH1	3091.333333	3406	6927	9274	10218	20781
MRE11A	2587.333333	3004	5951.666667	7762	9012	17855
RRM2B	3053.666667	3490.666667	7026	9161	10472	21078
FLJ40869	2523.333333	2879.333333	5858	7570	8638	17574
T. Reagent	2096.666667	2256	4706.666667	6290	6768	14120
SMC3	1549.333333	1585.333333	3513.333333	4648	4756	10540
DCLRE1B	2721	2996.666667	6138.666667	8163	8990	18416
ERCC3	2507.666667	2903.666667	5910.666667	7523	8711	17732
GIYD1	2255.666667	2671.666667	5305	6767	8015	15915
MUTYH	2717.666667	3188.666667	6402	8153	9566	19206
TDP1	2670.333333	2653	5789.333333	8011	7959	17368
POLH	2851	3187.666667	6538.666667	8553	9563	19616
GADD45G	3196.666667	3194.333333	6964.666667	9590	9583	20894
EYA3	2859.333333	3171	6468	8578	9513	19404
XPA	3175	3876.333333	7541	9525	11629	22623
RAD23A	2787.333333	3023	6397.666667	8362	9069	19193
Scramble	1714	1720	3743.333333	5142	5160	11230
Scramble	1355.666667	1474.666667	3131	4067	4424	9393
POLK	2442.333333	2910	5721.666667	7327	8730	17165
SHFM1	2075	2417.333333	4855.666667	6225	7252	14567
NEIL3	2603.666667	3196.666667	6232.666667	7811	9590	18698
UBE2A	2809.666667	2953.666667	6234	8429	8861	18702
HRMT1L6	2713.333333	3071	6249.333333	8140	9213	18748
RNF8	2706.666667	3092.666667	6282.333333	8120	9278	18847
TP53	3237.333333	3318.333333	7196.666667	9712	9955	21590
RPA2	2620.666667	2972	6086.666667	7862	8916	18260
MMS19L	3179.666667	3690	7468.333333	9539	11070	22405
MGC2731	2738.666667	2995	6157	8216	8985	18471
siGFP	559	1212.333333	2494.666667	1677	3637	7484
X	2522.333333	2750	5936	7567	8250	17808
POLN	2707	3075	6271.333333	8121	9225	18814
MIZF	2657	2991.333333	6078.333333	7971	8974	18235
MSH6	2535.333333	2847	5821.333333	7606	8541	17464
FANCE	2718	2881	6085.333333	8154	8643	18256
EME2	2654	2859.333333	5943	7962	8578	17829
C2ORF13	2855.333333	2896.333333	6192	8566	8689	18576
TP53BP1	2893.666667	2991.666667	6354.333333	8681	8975	19063
MNAT1	2862.333333	3256.333333	6612.666667	8587	9769	19838
PMS2L5	3016.666667	3310.333333	6836.666667	9050	9931	20510
SMC6L1	2607	2792.333333	5768	7821	8377	17304
SMC3	1709	1664	3713	5127	4992	11139
X	2382.333333	2619.333333	5563.666667	7147	7858	16691
CCNH	2315	2403.333333	5161.666667	6945	7210	15485
RBBP8	1922.666667	2240.666667	4426.666667	5768	6722	13280
XRCC2	2351	2817	5566.333333	7053	8451	16699
RECQL5	2459.666667	2742.333333	5582.333333	7379	8227	16747
NEIL1	2393	2715	5575.666667	7179	8145	16727
FLJ12610	2206	2797	5407.666667	6618	8391	16223
XRCC4	2765.333333	3144.333333	6414.666667	8296	9433	19244
DLG7	2079	2462.333333	4965	6237	7387	14895
EXO1	2488.666667	2992.666667	5921	7466	8978	17763
ABL1	2376	2581.333333	5360.333333	7128	7744	16081
X	3255.666667	2670	6741	9767	8010	20223
X	2398	2597.333333	5693.333333	7194	7792	17080
C7ORF11	1739	1986.666667	4130.666667	5217	5960	12392
HMGB1	1770.333333	1817	3936.333333	5311	5451	11809
RAD54B	1627	1944	3906.666667	4881	5832	11720
ERCC6	1612	1863	3837	4836	5589	11511
LIG1	1720	1993.666667	4067	5160	5981	12201
RPA3	1973	2127.333333	4444	5919	6382	13332
CHAF1A	1223.333333	1459.666667	2882.333333	3670	4379	8647
SPO11	2014	2399.333333	4734.666667	6042	7198	14204
DNMT1	2356.333333	2664.666667	5512.333333	7069	7994	16537
USP1	1814	2003.666667	4179	5442	6011	12537
X	2440.333333	2526	5495.666667	7321	7578	16487

Plate 3	Average gfp cells counted	Average rfp cells counted	Average total cells counted	Total gfp cells counted	Total rfp cells counted	Total total cells counted
Scramble	1360	1493.666667	3234.333333	4080	4481	9703
EYA1	1547	1572	3572.333333	4641	4716	10717
RECQL4	1487	1264.333333	3148.666667	4461	3793	9446
RAD52B	1439.333333	1681.333333	3528.666667	4318	5044	10586
MLH3	1387.333333	1560	3238.333333	4162	4680	9715
CIB1	1528.333333	1599	3558.666667	4585	4797	10676
BTG2	1368.333333	1503.666667	3167.333333	4105	4511	9502
MPG	1496.666667	1651.333333	3579.333333	4490	4954	10738
TNP1	1454.666667	1611	3568.333333	4364	4833	10705
MSH2	1652	1633.333333	3619.333333	4956	4900	10858
RAD51	1339	1451	3225	4017	4353	9675
X	2120.333333	2200	5094	6361	6600	15282
T. Reagent	1778.333333	1915.333333	4243	5335	5746	12729
RAD1	1975	1840.333333	4209	5925	5521	12627
FLJ21816	1553.666667	1698.666667	3590	4661	5096	10770
KIAA1018	2036.333333	2078.333333	4587.333333	6109	6235	13762
CNOT7	1717	1918	3957	5151	5754	11871
CDKN2D	1807	1840.666667	3976	5421	5522	11928
DDB1	1619	1968	3935.666667	4857	5904	11807
CKN1	2075.333333	2120.333333	4624.333333	6226	6361	13873
PARP1	2218.666667	2216.666667	4931	6656	6650	14793
MGC32020	1797	1974.333333	4219	5391	5923	12657
MGC4189	2133.666667	2126.333333	4767.666667	6401	6379	14303
Scramble	1825	1853.666667	4137.333333	5475	5561	12412
siGFP	564	1587.333333	3331.333333	1692	4762	9994
POLA	1712	1815.333333	3953	5136	5446	11859
RAD9A	1928	1983	4301.666667	5784	5949	12905
RENT1	2049.333333	2375.666667	4970	6148	7127	14910
NBS1	2157.666667	1976	4646.666667	6473	5928	13940
DMC1	2127.666667	2294	4838	6383	6882	14514
PCNA	1961.666667	2274	4700	5885	6822	14100
BAZ1B	2040.333333	2170	4736.333333	6121	6510	14209
ALKBH	2077.333333	2136.333333	4648.666667	6232	6409	13946
POLB	2106.666667	2293.333333	4848.333333	6320	6880	14545
NTHL1	2016	2250.333333	4736	6048	6751	14208
T. Reagent	1864	2194.666667	4672.666667	5592	6584	14018
SMC3	1582.666667	1598	3693	4748	4794	11079
DDB2	1983.333333	1800.333333	4088.666667	5950	5401	12266
POLD1	1962.333333	1854.666667	4227.333333	5887	5564	12682
MGMT	2193	2263.333333	5063	6579	6790	15189
FANCF	1970.666667	1937.333333	4441.333333	5912	5812	13324
PARG	2213.666667	2170.333333	4927.333333	6641	6511	14782
ERCC2	2249	2300	5157.333333	6747	6900	15472
TADA3L	2469.666667	2394.666667	5551	7409	7184	16653
ATRX	2382	2617.333333	5744.666667	7146	7852	17234
UBE2V1	2406	2411.333333	5336.666667	7218	7234	16010
POLL	2271.666667	2240.333333	5001.333333	6815	6721	15004
Scramble	1909	2006.666667	4506.333333	5727	6020	13519
Scramble	1301.666667	1363.333333	3012.666667	3905	4090	9038
GTF2H3	2165.333333	2131.666667	4853.666667	6496	6395	14561
EME1	1839.666667	1822.333333	4167	5519	5467	12501
POLQ	2035.666667	2229.666667	4880.333333	6107	6689	14641
RAD51C	2041.666667	2130.666667	4706	6125	6392	14118
MSH5	2204	2347.666667	5197.333333	6612	7043	15592
DEPC-1	2053	2316.333333	5015.666667	6159	6949	15047
LIG4	1883	3573.666667	6228.666667	5649	10721	18686
ATM	2317	2341.666667	5338.666667	6951	7025	16016
SMC1L1	2583.666667	2657	5912	7751	7971	17736
CDK7	2287.666667	2651.333333	5578.333333	6863	7954	16735
siGFP	408	1619.666667	3367	1224	4859	10101
X	2191.666667	2339.333333	5451.333333	6575	7018	16354
FANCA	1727	1965.666667	4160.666667	5181	5897	12482
KIAA0625	1983.666667	2004	4450	5951	6012	13350
FLJ10719	2292.333333	2266.666667	5129.333333	6877	6800	15388
UBE2V2	1969.333333	3032.666667	5615.333333	5908	9098	16846
SMUG1	2166	2334.333333	5043.333333	6498	7003	15130
RAD21	1959.666667	2216.333333	4678.666667	5879	6649	14036
RAD51L1	1992	2217	4690.666667	5976	6651	14072
UNG	2260.333333	2197.333333	5146.333333	6781	6592	15439
CHEK1	2400.333333	2510.333333	5690	7201	7531	17070
ATRIP	2555.666667	2467.333333	5677	7667	7402	17031
SMC3	1690.333333	1791	3988.333333	5071	5373	11965
X	2181.666667	2496.333333	5629.666667	6545	7489	16889
DUT	1470	1494	3316.666667	4410	4482	9950
PNKP	1653.666667	1675.333333	3750	4961	5026	11250
BLM	1938.666667	2012.666667	4445	5816	6038	13335
APEX2	1515.333333	1680.666667	3563	4546	5042	10689
BRCA2	1644.333333	1989.333333	4077.333333	4933	5968	12232
G22P1	1871.333333	1840	4095.333333	5614	5520	12286
CLK2	1698	1852.666667	3918	5094	5558	11754
POLG	1938	2376.333333	4752.666667	5814	7129	14258
BRE	2215	2211	4875.666667	6645	6633	14627
XRCC5	1890	2044.333333	4399.333333	5670	6133	13198
X	2226	2296.333333	5242.666667	6678	6889	15728
X	2055.333333	1861	4651	6166	5583	13953
HSU24186	1532	1504.333333	3409.666667	4596	4513	10229
XRCC3	1381.666667	1527.333333	3240.666667	4145	4582	9722
NPM1	1563.333333	1716.333333	3667	4690	5149	11001
ASF1A	1160	1330	2730	3480	3990	8190
H2AFX	1714.333333	1858.333333	3950.666667	5143	5575	11852
FLJ22833	1719.666667	1931	4033	5159	5793	12099
UBE2N	1803.666667	1894	4100	5411	5682	12300
ERCC4	1773.666667	2033.666667	4241.666667	5321	6101	12725
ERCC1	1600.666667	1869.333333	3904.666667	4802	5608	11714
RRM2	965.3333333	1326	2620	2896	3978	7860
X	1991.666667	1919	4574	5975	5757	13722

Custom Screen						
Plate 4	Average gfp cells counted	Average rfp cells counted	Average total cells counted	Total gfp cells counted	Total rfp cells counted	Total total cells counted
Scramble	1181.666667	1275.333333	2679.333333	3545	3826	8038
TELO2	1335.666667	1472.333333	3059	4007	4417	9177
RUVBL1	1048	1514.333333	2766.666667	3144	4543	8300
PPP6R1	1360	1608.666667	3221.666667	4080	4826	9665
COPS3	1225.333333	1515.333333	2961.666667	3676	4546	8885
TIMELESS	1408.333333	1624	3318	4225	4872	9954
INO80	1531	1685.666667	3490	4593	5057	10470
PARP4	1741	1945.666667	4025	5223	5837	12075
DAXX	1882	2099.333333	4339.666667	5646	6298	13019
COPS7A	1735.666667	1961	3981.666667	5207	5883	11945
UBA2	2045	2227.666667	4568.666667	6135	6683	13706
X	2092.666667	2492.666667	5073.666667	6278	7478	15221
T. Reagent	1436	1670.333333	3388.333333	4308	5011	10165
TERF2IP	1829.666667	1954	4115.333333	5489	5862	12346
PPP4R2	1876	2112.666667	4289	5628	6338	12867
GAR1	1758.333333	2098	4213.666667	5275	6294	12641
NSMCE4A	1944.333333	3699.666667	6188.333333	5833	11099	18565
NHP2	2000	2238.333333	4520.333333	6000	6715	13561
ASF1B	2153	2355.333333	4817	6459	7066	14451
POT1	2012	2297	4600.666667	6036	6891	13802
SMC4	2317.333333	2552.666667	5274.666667	6952	7658	15824
PDS5B	2052.333333	2541	4882	6157	7623	14646
BAZ1A	2197	2407.666667	4975.666667	6591	7223	14927
Scramble	1317.333333	1333	2891	3952	3999	8673
siGFP	315	822.6666667	1698.666667	945	2468	5096
CHRAC1	1943.666667	2092.666667	4305	5831	6278	12915
POLE3	2237.666667	2694.666667	5261.666667	6713	8084	15785
POLE4	2189.333333	3301	5965.666667	6568	9903	17897
BRD7	2177	2506.666667	4995.666667	6531	7520	14987
NOP10	2529	2987	6007.333333	7587	8961	18022
UBE2T	2299.666667	2654	5364.333333	6899	7962	16093
POLD4	2045	2759.666667	5086.333333	6135	8279	15259
CLSPN	2344	2802.333333	5631.666667	7032	8407	16895
COPS7B	2533.333333	2878.666667	5851	7600	8636	17553
ACTR5	2095.333333	2711.666667	5165	6286	8135	15495
T. Reagent	2026.666667	2364.666667	4785	6080	7094	14355
SMC3	981.6666667	904.3333333	2107	2945	2713	6321
ACTR8	1958	2146.666667	4438.333333	5874	6440	13315
OBFC1	1917.333333	2213.666667	4386	5752	6641	13158
PIF1	2453.666667	2592	5472.333333	7361	7776	16417
SMARCAD1	2183.666667	2171.333333	4722	6551	6514	14166
INO80B	2149.333333	2576.666667	5116.666667	6448	7730	15350
TIPIN	2546.333333	3070.333333	6125	7639	9211	18375
WRAP53	2360.333333	2700	5544	7081	8100	16632
COPS4	2783.333333	2843.666667	5934.666667	8350	8531	17804
TINF2	2562.333333	3376.333333	6397.666667	7687	10129	19193
MYBBP1A	2359	2882.333333	5679.333333	7077	8647	17038
Scramble	1318.333333	1403.333333	2963.333333	3955	4210	8890
Scramble	1002	1066	2241.333333	3006	3198	6724
HAUS7	1775	2343.666667	4368.666667	5325	7031	13106
TREX2	2189.333333	2453	5108.666667	6568	7359	15326
NCAPG	2122	2341	4798.333333	6366	7023	14395
TEP1	2399	2596.666667	5504	7197	7790	16512
BARD1	2290	2590.666667	5222	6870	7772	15666
COPS8	2003.666667	2265	4640	6011	6795	13920
CDC5L	2398.333333	2788.333333	5621	7195	8365	16863
NDNL2	2392.333333	3216.333333	6108	7177	9649	18324
NSMCE2	2847.666667	3045	6478	8543	9135	19434
SMARCD1	2476.666667	2952	5799	7430	8856	17397
siGFP	353.3333333	1093	2314	1060	3279	6942
X	2068.666667	2361.666667	5070	6206	7085	15210
MCRS1	2173	2377	4884.333333	6519	7131	14653
RMI2	2098.666667	2458.666667	4866.333333	6296	7376	14599
PINX1	1863.333333	2221.333333	4409	5590	6664	13227
SMARCE1	2366.666667	2584	5376.333333	7100	7752	16129
CUL5	2491.666667	2400.666667	5388.333333	7475	7202	16165
SMARCC1	1897.333333	2212	4451.666667	5692	6636	13355
COPS5	2002.666667	2407	4705	6008	7221	14115
CCNB3	1875.666667	2418.333333	4613.333333	5627	7255	13840
STAG1	2604.666667	2897	5958	7814	8691	17874
NSMCE1	2339	2955	5651.666667	7017	8865	16955
SMC3	1422.333333	1768.666667	3413.333333	4267	5306	10240
X	1933.666667	2252.666667	4789.666667	5801	6758	14369
PPP4R1	1794.666667	3640.666667	5933.666667	5384	10922	17801
SMARCC2	1650	1840.333333	3724	4950	5521	11172
WDR48	1789.333333	2070	4174.666667	5368	6210	12524
HUS1B	1656.333333	2096.333333	4003.333333	4969	6289	12010
ARID1B	1855.666667	2074.333333	4201.666667	5567	6223	12605
SMC1B	1780	2052	4122.666667	5340	6156	12368
NFATC2IP	2289	2565.333333	5177.666667	6867	7696	15533
INO80E	2243	2516.333333	5088.666667	6729	7549	15266
ANKRD52	2273.333333	2761	5431.666667	6820	8283	16295
ANKRD44	2263.333333	2946.666667	5575.333333	6790	8840	16726
X	2620.333333	2848	6125	7861	8544	18375
X	1890.666667	2056	4596	5672	6168	13788
CDKN2A	1731	2043	4129.666667	5193	6129	12389
STAG2	1475.333333	1678.333333	3514	4426	5035	10542
CORT	1173.333333	1456	2810	3520	4368	8430
EID3	1364	1632.333333	3207.333333	4092	4897	9622
SLX4	1682	1873.666667	3827.666667	5046	5621	11483
AMN1	1385.333333	1521	3097.666667	4156	4563	9293
SMC5	1775	1934.666667	4011.666667	5325	5804	12035
NCAPG2	1675.666667	2057	3993.666667	5027	6171	11981
TEN1	1414.333333	1826.666667	3464.333333	4243	5480	10393
SMG6	1777	2207.333333	4276.333333	5331	6622	12829
X	2315.333333	2401	5239	6946	7203	15717

Plate 5	Average gfp cells counted	Average rfp cells counted	Average total cells counted	Total gfp cells counted	Total rfp cells counted	Total total cells counted
Scramble	1149.666667	1260	2583	3449	3780	7749
PBRM1	1434.333333	1413.666667	3110.666667	4303	4241	9332
COPS6	1059	1525.666667	2762.333333	3177	4577	8287
PAXIP1	1429.666667	1508.333333	3180.333333	4289	4525	9541
RAD9B	1218.333333	1394.666667	2845.333333	3655	4184	8536
INO80C	1242.666667	1345	2756.666667	3728	4035	8270
NFRKB	1305	1411	2980	3915	4233	8940
PPP4R4	1318.333333	1527.333333	3075.666667	3955	4582	9227
NCAPH2	1186	1472	2832	3558	4416	8496
SUMO4	1486.333333	1781.666667	3575	4459	5345	10725
ARID2	1569.333333	1968	3826.333333	4708	5904	11479
X	1805	1988.333333	4245.333333	5415	5965	12736
T. Reagent	1678	1682.666667	3685	5034	5048	11055
RIF1	1619	1801.666667	3647.666667	4857	5405	10943
SMEK2	1698.333333	1896.666667	3840.666667	5095	5690	11522
UBE2NL	2044	2273	4668.333333	6132	6819	14005
PPP6R3	2573.666667	2470.666667	5511	7721	7412	16533
INO80D	1733.666667	1996.333333	4009.333333	5201	5989	12028
CRY2	2273.666667	2456	5103.666667	6821	7368	15311
UVSSA	1730.333333	1809.333333	3759.333333	5191	5428	11278
CTC1	1702.666667	1970	3899.333333	5108	5910	11698
PDS5A	1825.666667	1993.666667	4105.666667	5477	5981	12317
CRY1	1997	2454.666667	4783	5991	7364	14349
Scramble	1731.333333	1705.333333	3695	5194	5116	11085
siGFP	341	892.6666667	1906	1023	2678	5718
TERF2	1783.666667	2249.666667	4267.333333	5351	6749	12802
TCEB2	2324	2559.333333	5285	6972	7678	15855
TCEB1	2409	2529.333333	5374	7227	7588	16122
POLD3	2425	2796	5747.333333	7275	8388	17242
NCAPD2	2786.666667	2955.666667	6193.666667	8360	8867	18581
NCAPH	2069	2455	4883	6207	7365	14649
SHPRH	2134	2391.666667	4794.666667	6402	7175	14384
MVP	1915.333333	2031	4178.666667	5746	6093	12536
HLTF	2117	2428.666667	4886	6351	7286	14658
HES1	1851	2319.666667	4459.333333	5553	6959	13378
T. Reagent	1869.333333	2166.666667	4411.333333	5608	6500	13234
SMC3	1098.333333	1306	2657.333333	3295	3918	7972
TCEB3	1871	2057.333333	4263.333333	5613	6172	12790
CUL4A	2617	2591.333333	5683.666667	7851	7774	17051
CUL3	2135.666667	2196	4763	6407	6588	14289
TOP3A	2420	2750	5677.666667	7260	8250	17033
GPS1	1911	2350.666667	4618.666667	5733	7052	13856
SMARCB1	2157.333333	2481.666667	5077.666667	6472	7445	15233
C17orf70	1932	2146.333333	4394	5796	6439	13182
TOP2B	2143.333333	2522	5079.666667	6430	7566	15239
MDM2	1926	2198.666667	4386.666667	5778	6596	13160
CCNA1	1893.333333	2101	4270.666667	5680	6303	12812
Scramble	1384.333333	1536.666667	3138.333333	4153	4610	9415
Scramble	1265.666667	1426.333333	2932.333333	3797	4279	8797
RNF4	1615.666667	1955	3828	4847	5865	11484
UBE2I	2075	2305.666667	4694.666667	6225	6917	14084
SUMO1	2253.333333	2447	5060	6760	7341	15180
RBX1	1624	2022.666667	4004.333333	4872	6068	12013
POLR2L	1998.333333	2128.333333	4428.333333	5995	6385	13285
POLR2G	2435.666667	2554.333333	5482	7307	7663	16446
POLR2F	1809.333333	2154.333333	4376	5428	6463	13128
COPS2	2014	2475.666667	4913.666667	6042	7427	14741
PPP4C	2210.666667	2434.666667	5026	6632	7304	15078
PER3	1943	2220.666667	4408	5829	6662	13224
siGFP	309	808.6666667	1839	927	2426	5517
X	2039	2088.333333	4605.333333	6117	6265	13816
SUMO3	2128.333333	2670	5210.333333	6385	8010	15631
SUMO2	2276	2382.666667	4943.333333	6828	7148	14830
TERF1	1739	2027	4106.333333	5217	6081	12319
POLR2K	1877	2277.666667	4526	5631	6833	13578
POLR2J	2013	2039.666667	4430	6039	6119	13290
POLR2H	2188.333333	2301	4859	6565	6903	14577
SMARCA4	2094.666667	2420.666667	4903.666667	6284	7262	14711
SMARCA2	1880.666667	2121	4320	5642	6363	12960
POLD2	2288.333333	2332.333333	5113	6865	6997	15339
CDKN2A	1874	2222	4363.666667	5622	6666	13091
SMC3	2131.333333	1304.333333	3846.333333	6394	3913	11539
X	2202	2489	5315.666667	6606	7467	15947
NCAPD3	1878.333333	2077	4229.333333	5635	6231	12688
RFC3	1996.666667	2265.666667	4605	5990	6797	13815
RFC5	1790.666667	2182.333333	4289	5372	6547	12867
CDKN1A	2236.666667	2156.333333	4771.333333	6710	6469	14314
POLR2I	1953.666667	2411.333333	4760	5861	7234	14280
RFC1	1673	2330.666667	4254.333333	5019	6992	12763
RFC2	2061.333333	2427	4856	6184	7281	14568
RFC4	1351.333333	1764	3323	4054	5292	9969
POLR2B	1836	2286.333333	4494.666667	5508	6859	13484
CDC25B	1752.666667	2158.333333	4189.666667	5258	6475	12569
X	2399.333333	2442	5336.333333	7198	7326	16009
X	2214.333333	2311.333333	5177	6643	6934	15531
CDC25A	1602	1835.666667	3754.666667	4806	5507	11264
WEE1	1245.333333	1325.666667	2808	3736	3977	8424
CCND3	1280.666667	1528	3028.666667	3842	4584	9086
CCND2	1757.666667	2148.666667	4253.666667	5273	6446	12761
CDK2	1062.333333	1400	2653.666667	3187	4200	7961
POLR2A	675.3333333	1013.333333	1818.333333	2026	3040	5455
CCNE1	1117.333333	1369.333333	2655	3352	4108	7965
CCNC	1191	1506.666667	2917.666667	3573	4520	8753
CCND1	1405.333333	1630	3306.333333	4216	4890	9919
RRM1	768.3333333	1023.666667	1924	2305	3071	5772
X	1824.333333	1814.333333	3974.333333	5473	5443	11923

Plate 6	Average gfp cells counted	Average rfp cells counted	Average total cells counted	Total gfp cells counted	Total rfp cells counted	Total total cells counted
Scramble	1311	1541.333333	3086.333333	3933	4624	9259
UBA1	1730	1633	3903	5190	4899	11709
CCNA2	1461.333333	1520	3328.333333	4384	4560	9985
POLR2E	1316.666667	1582	3308	3950	4746	9924
POLR2C	1353.333333	1663.333333	3302.333333	4060	4990	9907
CCNB1	1141.666667	1470.666667	2895	3425	4412	8685
CDK4	1014.666667	1313	2516.333333	3044	3939	7549
TOP1	1212	1435.666667	2907.666667	3636	4307	8723
TFPT	1561.666667	2151.333333	4085.333333	4685	6454	12256
DNTT	1434.666667	1652.333333	3398.666667	4304	4957	10196
TOP3B	1537	1954	3809.666667	4611	5862	11429
X	1853.666667	1766.333333	4169.666667	5561	5299	12509
T. Reagent	1741.333333	2133.666667	4275	5224	6401	12825
SMC2	1959	2732	5212.666667	5877	8196	15638
TNKS	1736.333333	2086.333333	4260.666667	5209	6259	12782
CCNB2	1551	1948.666667	3840.666667	4653	5846	11522
BCAS2	1703.666667	2078.666667	4103	5111	6236	12309
PPP6R2	1631	1947	4007	4893	5841	12021
DKC1	1565	1823	3693	4695	5469	11079
SMARCA5	2053.333333	2501.666667	5048	6160	7505	15144
PLRG1	2304.666667	2530.666667	5422.333333	6914	7592	16267
POLR2D	1992.666667	2391	4771.333333	5978	7173	14314
UBD	1907	1978.666667	4247	5721	5936	12741
Scramble	1901	2773.666667	5130	5703	8321	15390
siGFP	304.3333333	1162.666667	2217.333333	913	3488	6652
MDM4	1801	2353.666667	4590.666667	5403	7061	13772
ANKRD28	2354.333333	2388.666667	5257.333333	7063	7166	15772
PER2	1889.666667	2175	4509	5669	6525	13527
TERT	2065	2257.666667	4708.333333	6195	6773	14125
ARID1A	2120.666667	2344	5063	6362	7032	15189
PPP6C	2204.333333	2468	5208	6613	7404	15624
STRA13	2446	2359	5404.666667	7338	7077	16214
HFM1	2410.333333	2672.666667	5685	7231	8018	17055
PIAS3	2174	2656.666667	5306.666667	6522	7970	15920
PARPBP	2074.333333	2420.666667	4840	6223	7262	14520
T. Reagent	1743	2233.333333	4439.333333	5229	6700	13318
SMC3	1824.666667	1974	4294	5474	5922	12882
TONSL	2280.666667	2562.666667	5363.666667	6842	7688	16091
FBXO18	1905	2262.333333	4552	5715	6787	13656
PIAS4	1898.666667	2042	4360.666667	5696	6126	13082
SFR1	1973.666667	2222.333333	4687	5921	6667	14061
MMS22L	2117.333333	2171.666667	4792.666667	6352	6515	14378
TTI2	2377.333333	2656	5692	7132	7968	17076
SWI5	2160.333333	2689.666667	5603.333333	6481	8069	16810
ZSWIM7	2383	2895.333333	5765	7149	8686	17295
H2AFZ	2305	2531.666667	5248.666667	6915	7595	15746
PIAS1	1882	2179.666667	4383	5646	6539	13149
Scramble	1870	2114.333333	4402	5610	6343	13206
Scramble	1454	1643.333333	3368.666667	4362	4930	10106
PIAS2	1864.333333	2161.333333	4389	5593	6484	13167
TTI1	1886.333333	2064.666667	4367.666667	5659	6194	13103
ACD	1635.666667	1751.333333	3705	4907	5254	11115
ACTL6A	1870.666667	1788.333333	4127	5612	5365	12381
UBB	1482	1675.666667	3580.333333	4446	5027	10741
UBC	1627	2078.666667	4157.666667	4881	6236	12473

Table A.3.5 - Tables showing how many cells were screened throughout the screen for each individual siRNA.

Rank	Gene	Z-Score		Gene	Z-Score
1	FANCD2	2.371226157	26	PBRM1	1.128625207
2	ANKRD28	2.223687837	27	POLD2	1.108143778
3	UBA1	2.155136078	28	CUL4A	1.046200294
4	MMS22L	1.975310599	29	GCN5L2	1.018129746
5	WRN	1.895486236	30	PPP6C	1.008524759
6	ACTL6A	1.832822746	31	HFM1	0.977579347
7	DDX11	1.786757943	32	FLJ13614	0.972381862
8	CCNA2	1.772018176	33	PIAS2	0.947098759
9	TTI1	1.696055909	34	UBC	0.932338568
10	STRA13	1.682697484	35	TTI2	0.890048567
11	UBD	1.681362053	36	SMARCAD1	0.88717796
12	UBB	1.462931525	37	DNTT	0.837208313
13	TOPBP1	1.458268776	38	PAXIP1	0.835078719
14	PIAS1	1.444346487	39	POLL	0.822046726
15	TERT	1.422905864	40	NBS1	0.810919402
16	ACD	1.421108355	41	SMARCA5	0.80099811
17	SFR1	1.419249869	42	BRE	0.799785496
18	CDKN1A	1.391872776	43	PPP6R2	0.78418333
19	H2AFZ	1.347733201	44	PPP6R3	0.773177971
20	PIAS4	1.328828247	45	HMGB1	0.760837595
21	PLRG1	1.280585814	46	CUL5	0.735335985
22	FBXO18	1.276967996	47	COPS4	0.713391486
23	ARID1A	1.203333067	48	NCAPD2	0.686794871
24	PER2	1.158918357	49	PIAS3	0.671583663
25	TONSL	1.157544822	50	SUMO2	0.670106114

Table A.3.6. Top synthetic viable hits. This suggests a synthetic viable interaction between NSMCE4a shRNA and the siRNA target listed above.

Gene	Z-Score	Gene	Z-Score	Gene	Z-Score	Gene	Z-Score
CDKN2A	-0.130770893	SMARCA4	-0.027837235	POLD3	0.056056307	IGHMBP2	0.113194574
RFC2	-0.127476448	FANCA	-0.027610979	MBD4	0.06072921	MLH3	0.118519823
TP53BP1	-0.116495888	CCND3	-0.026904166	TOP3A	0.062576681	SMC2	0.120124491
GADD45G	-0.112188201	RECQL5	-0.026400627	INO80D	0.064603052	C2ORF13	0.120777511
PPP4R4	-0.111677087	POLG2	-0.023345603	DAXX	0.069643075	NPM1	0.12387029
OGG1	-0.111255741	TYMS	-0.021928002	RAD23A	0.072984937	ARID1B	0.128714931
EYA3	-0.105832585	CTC1	-0.020320305	GTF2H2	0.076798087	WRAP53	0.133423246
BARD1	-0.104931808	CDC5L	-0.017042716	SMARCB1	0.077084592	INO80	0.143776608
NCAPH	-0.104504697	NUDT1	-0.01644549	TREX2	0.078503947	PARP1	0.145155216
TOP3B	-0.103687066	CHEK2	-0.011077175	CIB1	0.078946672	SMARCE1	0.145770753
POLE3	-0.101436234	FANCL	-0.010102563	CKN1	0.080414599	SMARCC2	0.146368258
TERF1	-0.092532716	DCLRE1B	-0.009822113	C17orf70	0.08287303	SOD1	0.15948017
SMARCC1	-0.089982804	HMGB2	-0.005704655	ERCC5	0.08351333	UBE2NL	0.159733289
PINX1	-0.076695659	XRCC1	-0.001964441	REV3L	0.084301229	CXORF53	0.173598552
KIAA1596	-0.068972231	POLM	0.001343793	FEN1	0.086189995	ATRX	0.178787779
MGMT	-0.066131346	CLK2	0.005548086	RTEL1	0.090553021	FANCG	0.180729563
POLR2F	-0.062190661	HUS1	0.012239773	NFATC2IP	0.090978356	RAD51C	0.182681801
BRD7	-0.060996106	MDM2	0.01853754	TNKS	0.092488979	CDKN2A	0.18342756
GTF2H4	-0.05657404	FLJ40869	0.022070058	ERCC4	0.093168569	SMARCA2	0.183469574
STAG2	-0.056255183	SMARCD1	0.022236805	PARP4	0.093251935	MDM4	0.185035054
POT1	-0.05605787	TIMELESS	0.022789444	OBFC1	0.096056379	RECQL	0.189382217
COPS8	-0.05457413	TADA3L	0.036047614	MSH2	0.100152422	RFC3	0.191772039
SMUG1	-0.054271682	CDC25A	0.036532818	WDR48	0.1037588	SMC1L1	0.203381473
RAD21	-0.05166911	EME1	0.036575537	NHP2	0.106084697	NCAPG	0.214578234
RPA1	-0.05066241	MGC2731	0.048719284	PER3	0.106697657	MSH5	0.214578491
CSPG6	-0.049174483	PRKDC	0.053491101	TOP2B	0.10830065	NTHL1	0.218290794
ALKBH	-0.03216964	COPS7A	0.055267724	RAD9B	0.110557997	SHPRH	0.218821704

Table A.3.7. Results from the middle of the screen These indicate no preferential growth advantage or disadvantage on NSMCE4a or Non-silencing cells.

RNRval1	0	12	14		0	12	14
Non-silencing	65.334	85.822	87.839	Non Silencing	59.536	82.261	85.475
	58.159	82.928	85.913	NSMCE4 861 old	58.705	79.469	83.253
	58.447	76.514	82.179				
	56.202	83.778	85.969				
NSMCE4a 861 old	59.137	79.025	85.097				
	60.219	78.439	80.787				
	57.694	79.763	85.749				
	57.772	80.648	81.380				
RNRval2	0	12	14		0	12	14
Non-silencing	61.259	82.458	86.397	Non Silencing	66.101	84.856	86.846
	67.442	86.521	87.030	NSMCE4 861 old	59.001	80.947	82.937
	64.711	84.837	86.964				
	70.991	85.607	86.990				
NSMCE4a 861 old	55.320	79.995	80.565				
	60.513	79.049	83.595				
	58.554	80.638	82.587				
	61.618	84.105	85				
RNRval3	0	12	14		0	12	14
Non-silencing	63.695	82.267	88.556	Non Silencing	63.529	84.715	88.783
	63.168	84.314	88.638	NSMCE4 861 old	62.012	83.039	83.113
	61.559	85.987	87.067				
	65.694	86.290	90.871				
NSMCE4a 861 old	56.553	83.581	82.867				
	64.4534	84.004	85.559				
	64.335	81.645	81.228				
	62.706	82.925	82.798				
average		0	12	14			
	Non-silencing shRNA	63.055	83.944	87.035			
	NSMCE4a shRNA	50.364	75.287	79.605			
stdev		0	12	14			
	Non Silencing	3.308	1.459	1.662			
	NSMCE4a shRNA	2.106	1.826	2.765			
ttest		0.004918113	0.002519956	0.058546629			

Table A.3.8 – RNR Validation

	high TxRE	18	16	14	12	10	8	6	5	4	3	2	0
861	A	1062	809	424	178	63	16	30	3	28	41	64	1565
	B	452	1011	495	259	25	32	18	41	39	13	23	1390
	C	328	542	283	161	12	19	7	12	11	18	20	1159
	D	77	399	229	150	17	4	9	7	10	7	10	677
NS	E	402	777	602	252	57	93	33	27	43	34	33	577
	F	241	468	507	319	72	58	20	32	21	85	23	393
	G	218	344	314	319	22	21	18	18	63	25	65	822
	H	166	332	168	403	30	12	8	17	3	2	14	487
		0.292	0.272	0.138	0.048	0.014	0.003	0.005	0.0006	0.007	0.008	0.011	0.277
		0.155	0.289	0.122	0.049	0.004	0.006	0.003	0.0087	0.009	0.003	0.004	0.288
		0.191	0.225	0.111	0.054	0.005	0.008	0.001	0.0026	0.004	0.006	0.006	0.294
		0.069	0.158	0.091	0.048	0.005	0.001	0.001	0.001	0.003	0.004	0.003	0.243
		0.236	0.284	0.213	0.089	0.018	0.021	0.005	0.007	0.011	0.010	0.0188	0.304
		0.263	0.280	0.253	0.128	0.026	0.018	0.007	0.009	0.004	0.018	0.011	0.386
		0.310	0.396	0.254	0.179	0.015	0.014	0.010	0.007	0.021	0.010	0.018	0.275
		0.235	0.340	0.194	0.192	0.019	0.010	0.007	0.010	0.002	0.002	0.006	0.298
	hours		stdev										
	0	14	0	14									
Non-silencing shRNA	31.610	22.894	0.316106738	0.228942172									
NSMCE4a shRNA	27.593	11.570	0.22988623	0.19660137									

Table A.3.8.1 – RNR Validation with high EdU incorporation.

A.4.1 – Western Blot Quantification.

A

	Scramble			SMC6 siRNA				
	24	48	72	96	24	48	72	96
SMC6	0	34.99	170.24	61.58	0	0	0	0
SMC5	99.61	63.19	671.07	502.38	240.60	44.52	47.56	45.54
Tubublin	100	100	100	100	100	100	100	100

B

	Scramble			NSE4 siRNA				
	24	48	72	96	24	48	72	96
SMC6	50.6	45.85	161.97	241.70	0	0	0	0
SMC5	52.0	213.44	234.24	150.11	355.87	210.74	24.64	21.26
Tubulin	100	100	100	100	100	100	100	100

C

	NS	GAPDH	EG5	C1	C2	C3
SMC6	60.73	456.27	39.06	28.16	167.30	122.76
SMC5	121.08	693.54	120.14	24.80	146.80	21.09
Ponceau	100	100	100	100	100	100

D

	NS RFP	NS GFP	C1	C2
SMC6	47.13	89.55	10.27	36.29
SMC5	92.17	129.56	67.03	24.74
Tubulin	100	100	100	100

Table A.4.1 – Quantification of western blotting. A. Quantification of initial siRNA testing using SMC6 and scramble siRNA in osteosarcoma cells. B. As in A however cells were exposed to NSMCE4a siRNA. C. Creation of cells with shRNA, quantification of SMC5/6 levels after incorporation of plasmid expressing shRNA. D. Quantification of SMC5/6 levels after incorporation of plasmid expressing shRNA expressing either non-silencing shRNA with NLS GFP and RFP and two constructs targeting NSMCE4a and NLS GFP.

A

	NS	C1
Smc6	53.05	34.43
Smc5	135.22	51.63
Tubulin	100	100

B

	WT1	NSMCE3-L264F	Artemis	BRCA2 deficient	WT1	NSMCE3-L264F	Artemis	BRCA2 deficient
	Scramble	Scramble	Scramble	Scramble	NSMCE4a	NSMCE4a	NSMCE4a	NSMCE4a
SMC6	67.51	13.12	85.41	0.00	26.07	89.30	320.34	0.00
SMC5	70.93	0.00	137.45	31.70	0.00	0.00	0.00	0.00
Ponceau	100	100	100	100	100	100	100	100

	BRCA2 def	
	Scramble	NSMCE4a
SMC6	89.05	54.01
Ponceau	100	100

C

	WT1	NSMCE3-L264F	TDP1	XLF	WT1	NSMCE3-L264F	TDP1	XLF
Scramble siRNA	-	+	+	+	+	-	-	-
NSMCE4a siRNA	+	-	-	-	-	+	+	+
SMC6	72.43	186.71	249.88	531.03	313.38	303.95	332.42	183.20
Ponceau	100	100	100	100	100	100	100	100

D

	Scramble siRNA		BRCA1 siRNA	
	Non-Silencing	NSMCE4a C1	Non-Silencing	NSMCE4a C1
BRCA1	83.07	42.07	69.05	35.68
Ponceau	100	100	100	100

Table A.4.2 – Quantification of western blotting. A. Quantification of SMC5/6 levels in cells as in Table A.4.1.D after screen had been carried out. B. Quantification of SMC5/6 levels in patient fibroblasts after incorporation of NSMCE4a siRNA. Right hand panel shows quantification of SMC6 reduction in BRCA2 deficient cells. C. As in B however with different cell lines. D. Quantification of BRCA1 knockdown in screen cells after BRCA1 siRNA treatment.

A

	WT1	NSMCE3-L264F	WT2
SMC6	77.66	33.71	320.90
SMC5	107.28	41.65	200.91
Tubulin	100	100	100

Table A.4.3 – A. Quantification of western blotting of SMC5/6 levels using cells isolated from two sets of wild-type patients and NSMCE3-L264F patient cells.

References.

Ahmad, A.S., Ormiston-Smith, N. & Sasieni, P.D. (2015) Trends in the lifetime risk of developing cancer in Great Britain: comparison of risk for those born from 1930 to 1960. *British Journal of Cancer*. [Online] 112 (5), 943–947. Available from: doi:10.1038/bjc.2014.606.

Ahnesorg, P., Smith, P. & Jackson, S.P. (2006a) XLF Interacts with the XRCC4-DNA Ligase IV Complex to Promote DNA Nonhomologous End-Joining. *Cell*. [Online] 124 (2), 301–313. Available from: doi:10.1016/j.cell.2005.12.031.

Ahnesorg, P., Smith, P. & Jackson, S.P. (2006b) XLF Interacts with the XRCC4-DNA Ligase IV Complex to Promote DNA Nonhomologous End-Joining. *Cell*. [Online] 124 (2), 301–313. Available from: doi:10.1016/j.cell.2005.12.031.

Alt, A., Dang, H.Q., Wells, O.S., Polo, L.M., et al. (2016) Specialised interfaces of Smc5/6 control hinge stability and DNA-association. *Nature communications*. 1–38.

Aly, A. & Ganesan, S. (2011) BRCA1, PARP, and 53BP1: conditional synthetic lethality and synthetic viability. *Journal of Molecular Cell Biology*. [Online] 3 (1), 66–74. Available from: doi:10.1093/jmcb/mjq055.

Ampatzidou, E., Irmisch, A., O'Connell, M.J. & Murray, J.M. (2006) Smc5/6 Is Required for Repair at Collapsed Replication Forks. *Molecular and Cellular Biology*. [Online] 26 (24), 9387–9401. Available from: doi:10.1128/MCB.01335-06.

Andrews, E.A., Palecek, J., Sergeant, J., Taylor, E., et al. (2005) Nse2, a component of the Smc5-6 complex, is a SUMO ligase required for the response to DNA damage. *Molecular and Cellular Biology*. [Online] 25 (1), 185–196. Available from: doi:10.1128/MCB.25.1.185-196.2005.

Argunhan, B. (2016) *Interplay Between Dbf4-Dependent Cdc7 Kinase and Polo-Like Kinase Unshackles Mitotic Recombination Mechanisms by Promoting Synaptonemal Complex Disassembly*. 1–236.

Álvarez-Quilón, A., Serrano-Benítez, A., Lieberman, J.A., Quintero, C., et al. (2014) ATM specifically mediates repair of double-strand breaks with blocked DNA ends. *Nature communications*. [Online] 53347. Available from: doi:10.1038/ncomms4347.

Bagasra, O. & Prilliman, K.R. (2004) RNA interference: the molecular immune system. *Journal of molecular histology*.

Ball, H.L., Myers, J.S. & Cortez, D. (2005) ATRIP binding to replication protein

A-single-stranded DNA promotes ATR-ATRIP localization but is dispensable for Chk1 phosphorylation. *Molecular Biology of the Cell*. [Online] 16 (5), 2372–2381. Available from: doi:10.1091/mbc.E04-11-1006.

Barber, T.D., McManus, K., Yuen, K.W.Y., Reis, M., et al. (2008) Chromatid cohesion defects may underlie chromosome instability in human colorectal cancers. *Proceedings of the National Academy of Sciences of the United States of America*. [Online] 105 (9), 3443–3448. Available from: doi:10.1073/pnas.0712384105.

Barbour, L. & Xiao, W. (2006) Synthetic lethal screen. *Yeast Protocol*.

Barker, P.A. & Salehi, A. (2002) The MAGE proteins: Emerging roles in cell cycle progression, apoptosis, and neurogenetic disease. *Journal of Neuroscience Research*. [Online] 67 (6), 705–712. Available from: doi:10.1002/jnr.10160.

Barlow, J.H., Faryabi, R.B., Callén, E., Wong, N., et al. (2013) Identification of Early Replicating Fragile Sites that Contribute to Genome Instability. *Cell*. [Online] 152 (3), 620–632. Available from: doi:10.1016/j.cell.2013.01.006.

Bartek, J., Lukas, C. & Lukas, J. (2004) Checking on DNA damage in S phase. *Nature reviews. Molecular cell biology*. [Online] 5 (10), 792–804. Available from: doi:10.1038/nrm1493.

Bartkova, J., Horejsí, Z., Koed, K., Krämer, A., et al. (2005) DNA damage response as a candidate anti-cancer barrier in early human tumorigenesis. *Nature*. [Online] 434 (7035), 864–870. Available from: doi:10.1038/nature03482.

Bavner, A. (2005) EID3 is a novel EID family member and an inhibitor of CBP-dependent co-activation. *Nucleic Acids Research*. [Online] 33 (11), 3561–3569. Available from: doi:10.1093/nar/gki667.

BÃ¼rkle, A. & Virág, L. (2013) Poly(ADP-ribose): PARadigms and PARadoxes. *Molecular Aspects of Medicine*. [Online] 34 (6), 1046–1065. Available from: doi:10.1016/j.mam.2012.12.010.

Bermudez, V.P., Farina, A. & Higashi, T.L. (2012) *In vitro loading of human cohesin on DNA by the human Scc2-Scc4 loader complex*. In: [Online]. 2012 Available from: doi:10.1073/pnas.1206840109/-/DCSupplemental.

Bermudez, V.P., Farina, A., Higashi, T.L., Du, F., et al. (2012) In vitro loading of human cohesin on DNA by the human Scc2-Scc4 loader complex. *Proceedings of the National Academy of Sciences of the United States of America*. [Online] 109 (24), 9366–9371. Available from: doi:10.2307/41602669?ref=search-gateway:3dbd8b1174595159ce39e600cdcbc86b.

Bernstein, C., R, A., Nfonsam, V. & Bernstei, H. (2013) DNA Damage, DNA

Repair and Cancer. In: *New Research Directions in DNA Repair*. [Online]. InTech. pp. 1–55. Available from: doi:10.5772/53919.

Betts Lindroos, H., Ström, L., Itoh, T., Katou, Y., et al. (2006) Chromosomal Association of the Smc5/6 Complex Reveals that It Functions in Differently Regulated Pathways. *Molecular Cell*. [Online] 22 (6), 755–767. Available from: doi:10.1016/j.molcel.2006.05.014.

Beucher, A., (null), (null), Birraux, J., et al. (2009) ATM and Artemis promote homologous recombination of radiation-induced DNA double-strand breaks in G2. *The EMBO journal*. [Online] 28 (21), 3413–3427. Available from: doi:10.1038/emboj.2009.276.

Bienko, M., Green, C.M., Sabbioneda, S., Crosetto, N., et al. (2010) Regulation of translesion synthesis DNA polymerase eta by monoubiquitination. *Molecular Cell*. [Online] 37 (3), 396–407. Available from: doi:10.1016/j.molcel.2009.12.039.

Boersma, V., Moatti, N., Segura-Bayona, S., Peuscher, M.H., et al. (2015) MAD2L2 controls DNA repair at telomeres and DNA breaks by inhibiting 5′ end resection. *Nature*. [Online] 521 (7553), 537–540. Available from: doi:10.1038/nature14216.

Bougen-Zhukov, N., Loh, S.Y., Lee, H.K. & Loo, L.-H. (2016) Large-scale image-based screening and profiling of cellular phenotypes. *Cytometry*. [Online] 1–11. Available from: doi:10.1002/cyto.a.22909.

Boutros, M., Heigwer, F. & Laufer, C. (2015) Microscopy-Based High-Content Screening. *Cell*. [Online] 163 (6), 1314–1325. Available from: doi:10.1016/j.cell.2015.11.007.

Branzei, D., Sollier, J., Liberi, G., Zhao, X., et al. (2006) Ubc9- and Mms21-Mediated Sumoylation Counteracts Recombinogenic Events at Damaged Replication Forks. *Cell*. [Online] 127 (3), 509–522. Available from: doi:10.1016/j.cell.2006.08.050.

Bridges, C.B. (1922) The Origin of Variations in Sexual and Sex-Limited Characters. *The American Naturalist*. [Online] 56 (642), 51–63. Available from: doi:10.2307/2556299?ref=no-x-route:d4d689223f23d64ad9cfa2bb70fc271f.

Brooker, A.S. & Berkowitz, K.M. (2014) The Roles of Cohesins in Mitosis, Meiosis, and Human Health and Disease. In: *Cell Cycle Synchronization*. Methods in Molecular Biology. [Online]. New York, NY, Springer New York. pp. 229–266. Available from: doi:10.1007/978-1-4939-0888-2_11.

Brooks, S.C., Adhikary, S., Rubinson, E.H. & Eichman, B.F. (2013) Recent advances in the structural mechanisms of DNA glycosylases. *Biochimica et Biophysica Acta (BBA) - Proteins and Proteomics*. [Online] 1834 (1), 247–271. Available from: doi:10.1016/j.bbapap.2012.10.005.

Brouwer, A.K., Schimmel, J., Wiegant, J.C.A.G., Vertegaal, A.C.O., et al. (2009) Telomeric DNA mediates de novo PML body formation. *Molecular Biology of the Cell*. [Online] 20 (22), 4804–4815. Available from: doi:10.1091/mbc.E09-04-0309.

Bryant, H.E., Schultz, N., Thomas, H.D., Parker, K.M., et al. (2005) Specific killing of BRCA2-deficient tumours with inhibitors of poly(ADP-ribose) polymerase. *Nature*. [Online] 434 (7035), 913–917. Available from: doi:10.1038/nature03443.

Burrows, A.E. & Elledge, S.J. (2008) How ATR turns on: TopBP1 goes on ATRIP with ATR. *Genes & Development*. [Online] 22 (11), 1416–1421. Available from: doi:10.1101/gad.1685108.

Bush, J.R. & Wevrick, R. (2008) The Prader–Willi syndrome protein necdin interacts with the E1A-like inhibitor of differentiation EID-1 and promotes myoblast differentiation. *Differentiation*. [Online] 76 (9), 994–1005. Available from: doi:10.1111/j.1432-0436.2008.00281.x.

Bustard, D.E., Ball, L.G. & Cobb, J.A. (2016) Non-Smc element 5 (Nse5) of the Smc5/6 complex interacts with SUMO pathway components. *Biology open*. [Online] 5 (6), 777–785. Available from: doi:10.1242/bio.018440.

Bustard, D.E., Menolfi, D., Jeppsson, K., Ball, L.G., et al. (2012) During Replication Stress, Non-Smc Element 5 (Nse5) Is Required for Smc5/6 Protein Complex Functionality at Stalled Forks. *Journal of Biological Chemistry*. [Online] 287 (14), 11374–11383. Available from: doi:10.1074/jbc.M111.336263.

Calcerrada, P., Peluffo, G. & Radi, R. (2011) Nitric oxide-derived oxidants with a focus on peroxynitrite: molecular targets, cellular responses and therapeutic implications. *Current pharmaceutical design*. 17 (35), 3905–3932.

Caldecott, K.W. (2014) DNA single-strand break repair. *Experimental Cell Research*. [Online] 1–7. Available from: doi:10.1016/j.yexcr.2014.08.027.

Caldecott, K.W., Abrahams, B.S. & Geschwind, D.H. (2008) Single-strand break repair and genetic disease. *Nature Reviews Genetics*. [Online] 9 (8), 619–631. Available from: doi:10.1038/nrg2380.

Carthew, R.W. & Sontheimer, E.J. (2009) Origins and Mechanisms of miRNAs and siRNAs. *Cell*. [Online] 136 (4), 642–655. Available from: doi:10.1016/j.cell.2009.01.035.

Cesare, A.J. & Reddel, R.R. (2010) Alternative lengthening of telomeres: models, mechanisms and implications. *Nature Publishing Group*. [Online] 11 (5), 319–330. Available from: doi:10.1038/nrg2763.

Chance, B., Sies, H. & Boveris, A. (1979) Hydroperoxide metabolism in

mammalian organs. *Physiological reviews*.

Chen, Y.-H., Choi, K., Szakal, B., Arenz, J., et al. (2009) Interplay between the Smc5/6 complex and the Mph1 helicase in recombinational repair. *Proceedings of the National Academy of Sciences of the United States of America*. [Online] 106 (50), 21252–21257. Available from: doi:10.1073/pnas.0908258106.

Chen, Y.H., Szakal, B. & Castellucci, F. (2013) DNA damage checkpoint and recombinational repair differentially affect the replication stress tolerance of smc6 mutants. *… biology of the cell*.

Chendrimada, T.P., Gregory, R.I., Kumaraswamy, E., Norman, J., et al. (2005) TRBP recruits the Dicer complex to Ago2 for microRNA processing and gene silencing. *Nature*. [Online] 436 (7051), 740–744. Available from: doi:10.1038/nature03868.

Chun, J., Buechelmaier, E.S. & Powell, S.N. (2012) Rad51 Paralog Complexes BCDX2 and CX3 Act at Different Stages in the BRCA1-BRCA2-Dependent Homologous Recombination Pathway. *Molecular and Cellular Biology*. [Online] 33 (2), 387–395. Available from: doi:10.1128/MCB.00465-12.

Conrad, C. & Gerlich, D.W. (2010) Automated microscopy for high-content RNAi screening. *The Journal of cell biology*. [Online] 188 (4), 453–461. Available from: doi:10.1083/jcb.200910105.

Copsey, A., Tang, S., Jordan, P.W., Blitzblau, H.G., et al. (2013) Smc5/6 Coordinates Formation and Resolution of Joint Molecules with Chromosome Morphology to Ensure Meiotic Divisions Michael Lichten (ed.). *PLoS Genetics*. [Online] 9 (12), e1004071. Available from: doi:10.1371/journal.pgen.1004071.

Costanzo, M., Baryshnikova, A., Bellay, J., Kim, Y., et al. (2010) The Genetic Landscape of a Cell. *Science*. [Online] 327 (5964), 425–431. Available from: doi:10.1126/science.1180823.

de Lange, T. (2005) Shelterin: the protein complex that shapes and safeguards human telomeres. *Genes & Development*. [Online] 19 (18), 2100–2110. Available from: doi:10.1101/gad.1346005.

Deb, S., Xu, H., Tuynman, J., George, J., et al. (2014) RAD21 cohesin overexpression is a prognostic and predictive marker exacerbating poor prognosis in KRAS mutant colorectal carcinomas. *British Journal of Cancer*. [Online] 110 (6), 1606–1613. Available from: doi:10.1038/bjc.2014.31.

Dianov, G.L. & Hübscher, U. (2013) Mammalian base excision repair: the forgotten archangel. *Nucleic Acids Research*. [Online] 41 (6), 3483–3490. Available from: doi:10.1093/nar/gkt076.

Dijk, M., Typas, D., Mullenders, L. & Pines, A. (2014) Insight in the multilevel regulation of NER. *Experimental Cell Research*. [Online] 329 (1), 1–8. Available from: doi:10.1016/j.yexcr.2014.08.010.

Dixon, S.J., Costanzo, M., Baryshnikova, A., Andrews, B., et al. (2009) Systematic Mapping of Genetic Interaction Networks. *Annual review of genetics*. [Online] 43 (1), 601–625. Available from: doi:10.1146/annurev.genet.39.073003.114751.

Dobzhansky, T. (1946) Genetics of Natural Populations. Xiii. Recombination and Variability in Populations of Drosophila Pseudoobscura. *Genetics*. [Online] 31 (3), 269–290. Available from: doi:10.2307/2406962?ref=search-gateway:a1f96e3cca83712ff45d2ab2fec017cc.

Doyle, J.M., Gao, J., Wang, J., Yang, M., et al. (2010) MAGE-RING Protein Complexes Comprise a Family of E3 Ubiquitin Ligases. *Molecular Cell*. [Online] 39 (6), 963–974. Available from: doi:10.1016/j.molcel.2010.08.029.

Draskovic, I., Arnoult, N., Steiner, V., Bacchetti, S., et al. (2009) Probing PML body function in ALT cells reveals spatiotemporal requirements for telomere recombination. *Proceedings of the National Academy of Sciences of the United States of America*. [Online] 106 (37), 15726–15731. Available from: doi:10.1073/pnas.0907689106.

Dupré, A., Boyer-Chatenet, L., Sattler, R.M., Modi, A.P., et al. (2008) A forward chemical genetic screen reveals an inhibitor of the Mre11–Rad50–Nbs1 complex. *Nature Chemical Biology*. [Online] 4 (2), 119–125. Available from: doi:10.1038/nchembio.63.

Duro, E., Lundin, C., Ask, K., Sanchez-Pulido, L., et al. (2010) Identification of the MMS22L-TONSL Complex that Promotes Homologous Recombination. *Molecular Cell*. [Online] 40 (4), 632–644. Available from: doi:10.1016/j.molcel.2010.10.023.

Echeverri, C.J. & Perrimon, N. (2006) High-throughput RNAi screening in cultured cells: a user's guide. *Nature Reviews Genetics*. [Online] 7 (5), 373–384. Available from: doi:10.1038/nrg1836.

Farmer, H., McCabe, N., Lord, C.J., Tutt, A.N.J., et al. (2005) Targeting the DNA repair defect in BRCA mutant cells as a therapeutic strategy. *Nature*. [Online] 434 (7035), 917–921. Available from: doi:10.1038/nature03445.

Fece de la Cruz, F., Gapp, B.V. & Nijman, S.M.B. (2015) Synthetic Lethal Vulnerabilities of Cancer. *Annual Review of Pharmacology and Toxicology*. [Online] 55 (1), 513–531. Available from: doi:10.1146/annurev-pharmtox-010814-124511.

Fernandez-Capetillo, O., Lee, A., Nussenzweig, M. & Nussenzweig, A. (2004) H2AX: the histone guardian of the genome. *DNA Repair*. [Online] 3 (8-9), 959–967. Available from: doi:10.1016/j.dnarep.2004.03.024.

Fernius, J., Nerusheva, O.O., Galander, S., de Lima Alves, F., et al. (2013) Cohesin-Dependent Association of Scc2/4 with the Centromere Initiates Pericentromeric Cohesion Establishment. *Current biology : CB*. [Online] 23 (7), 599–606. Available from: doi:10.1016/j.cub.2013.02.022.

Fire, A., Xu, S., Montgomery, M.K., Kostas, S.A., et al. (1998) Potent and specific genetic interference by double-stranded RNA in Caenorhabditis elegans. *Nature*. [Online] 391 (6669), 806–811. Available from: doi:10.1038/35888.

Fischer, D.F., De Vos, R.A.I., Van Dijk, R., De Vrij, F.M.S., et al. (2003) Disease-specific accumulation of mutant ubiquitin as a marker for proteasomal dysfunction in the brain. *FASEB journal : official publication of the Federation of American Societies for Experimental Biology*. [Online] 17 (14), 2014–2024. Available from: doi:10.1096/fj.03-0205com.

Floyd, R.A., West, M. & Hensley, K. (2001) Oxidative biochemical markers; clues to understanding aging in long-lived species. *Experimental gerontology*. 36 (4-6), 619–640.

Forsburg, S.L. (2001) The art and design of genetic screens: yeast. *Nature Reviews Genetics*. [Online] 2 (9), 659–668. Available from: doi:10.1038/35088500.

Fousteri, M.I. & Lehmann, A.R. (2000) A novel SMC protein complex in Schizosaccharomyces pombe contains the Rad18 DNA repair protein. *The EMBO journal*. [Online] 19 (7), 1691–1702. Available from: doi:10.1093/emboj/19.7.1691.

Fox, M.H. (2004) Methods for synchronizing mammalian cells. *Methods in molecular biology (Clifton, N.J.)*. 24111–16.

Fragkos, M., Ganier, O., Coulombe, P. & Méchali, M. (2015) DNA replication origin activation in space and time. *Nature Publishing Group*. [Online] 16 (6), 360–374. Available from: doi:10.1038/nrm4002.

Gallego-Paez, L.M., Tanaka, H., Bando, M., Takahashi, M., et al. (2014) Smc5/6-mediated regulation of replication progression contributes to chromosome assembly during mitosis in human cells. *Molecular Biology of the Cell*. [Online] 25 (2), 302–317. Available from: doi:10.1091/mbc.E13-01-0020.

Gard, S., Light, W., Xiong, B., Bose, T., et al. (2009) Cohesinopathy mutations disrupt the subnuclear organization of chromatin. *The Journal of cell biology*. [Online] 187 (4), 455–462. Available from: doi:10.1083/jcb.200906075.

Garvey, C.M., Spiller, E., Lindsay, D., Chiang, C.-T., et al. (2016) A high-content image-based method for quantitatively studying context- dependent cell population dynamics. *Nature Publishing Group*. [Online] 61–12. Available

from: doi:10.1038/srep29752.

Genschel, J., Bazemore, L.R. & Modrich, P. (2002) Human Exonuclease I Is Required for 5′ and 3′ Mismatch Repair. *The Journal of biological chemistry*. [Online] 277 (15), 13302–13311. Available from: doi:10.1074/jbc.M111854200.

Ghospurkar, P.L., Wilson, T.M., Severson, A.L. & Klein, S.J. (2015) The DNA damage response and checkpoint adaptation in Saccharomyces cerevisiae: distinct roles for the replication protein A2 (Rfa2) N-terminus. *….* [Online] Available from: doi:10.1534/genetics.114.173211/-/DC1.

Giaever, G. & Nislow, C. (2014) The Yeast Deletion Collection: A Decade of Functional Genomics. *Genetics*. [Online] 197 (2), 451–465. Available from: doi:10.1534/genetics.114.161620.

Goellner, G.M., Tester, D. & Thibodeau, S. (1997) Different mechanisms underlie DNA instability in Huntington disease and colorectal cancer. *American journal of ….*

Gomez, R., Jordan, P.W., Viera, A., Alsheimer, M., et al. (2013) Dynamic localization of SMC5/6 complex proteins during mammalian meiosis and mitosis suggests functions in distinct chromosome processes. *Journal of cell science*. [Online] 126 (18), 4239–4252. Available from: doi:10.1242/jcs.130195.

Gong, D. & Ferrell, J.E. (2010) The roles of cyclin A2, B1, and B2 in early and late mitotic events. *Molecular Biology of the Cell*. [Online] 21 (18), 3149–3161. Available from: doi:10.1091/mbc.E10-05-0393.

Goodarzi, A.A., Yu, Y., Riballo, E., Douglas, P., et al. (2006) DNA-PK autophosphorylation facilitates Artemis endonuclease activity. *The EMBO journal*. [Online] 25 (16), 3880–3889. Available from: doi:10.1038/sj.emboj.7601255.

Green, L.C., Kalitsis, P., Chang, T.M., Cipetic, M., et al. (2012) Contrasting roles of condensin I and condensin II in mitotic chromosome formation. *Journal of cell science*. [Online] 125 (Pt 6), 1591–1604. Available from: doi:10.1242/jcs.097790.

Groen, E.J.N. & Gillingwater, T.H. (2015) UBA1: At the Crossroads of Ubiquitin Homeostasis and Neurodegeneration. *Trends in Molecular Medicine*. [Online] 21 (10), 622–632. Available from: doi:10.1016/j.molmed.2015.08.003.

Gupta, R.C. & Lutz, W.K. (1999) Background DNA damage for endogenous and unavoidable exogenous carcinogens: a basis for spontaneous cancer incidence? *Mutation Research/Fundamental and Molecular Mechanisms of Mutagenesis*. 424 (1-2), 1–8.

Haber, J.E., Ira, G., Malkova, A. & Sugawara, N. (2004) Repairing a double-strand chromosome break by homologous recombination: revisiting Robin Holliday's model. *Philosophical transactions of the Royal Society of London. Series B, Biological sciences*. [Online] 359 (1441), 79–86. Available from: doi:10.1098/rstb.2003.1367.

Haering, C.H., Löwe, J., Hochwagen, A. & Nasmyth, K. (2002) Molecular architecture of SMC proteins and the yeast cohesin complex. *Molecular Cell*.

Hamilton, A., Voinnet, O., Chappell, L. & Baulcombe, D. (2002) Two classes of short interfering RNA in RNA silencing. *The EMBO journal*. 21 (17), 4671–4679.

Hanada, K., Budzowska, M., Davies, S.L., van Drunen, E., et al. (2007) The structure-specific endonuclease Mus81 contributes to replication restart by generating double-strand DNA breaks. *Nature structural & molecular biology*. [Online] 14 (11), 1096–1104. Available from: doi:10.1038/nsmb1313.

Harada, Y.N., Shiomi, N., Koike, M., Ikawa, M., et al. (1999) Postnatal growth failure, short life span, and early onset of cellular senescence and subsequent immortalization in mice lacking the xeroderma pigmentosum group G gene. *Molecular and Cellular Biology*. 19 (3), 2366–2372.

Heideker, J., Prudden, J., Perry, J.J.P., Tainer, J.A., et al. (2011) SUMO-Targeted Ubiquitin Ligase, Rad60, and Nse2 SUMO Ligase Suppress Spontaneous Top1–Mediated DNA Damage and Genome Instability Wolf-Dietrich Heyer (ed.). *PLoS Genetics*. [Online] 7 (3), e1001320–12. Available from: doi:10.1371/journal.pgen.1001320.

Helt, C.E., Cliby, W.A., Keng, P.C., Bambara, R.A., et al. (2005) Ataxia Telangiectasia Mutated (ATM) and ATM and Rad3-related Protein Exhibit Selective Target Specificities in Response to Different Forms of DNA Damage. *The Journal of biological chemistry*. [Online] 280 (2), 1186–1192. Available from: doi:10.1074/jbc.M410873200.

Henson, J.D., Neumann, A.A. & Yeager, T.R. (2002) Alternative lengthening of telomeres in mammalian cells. *Oncogene*. [Online] Available from: doi:10.1038/sj/onc.

Heyer, W.-D. (2015) Regulation of Recombination and Genomic Maintenance. *Cold Spring Harbor perspectives in biology*. [Online] 7 (8), a016501–a016524. Available from: doi:10.1101/cshperspect.a016501.

Hill, V.K., Kim, J.-S. & Waldman, T. (2016) Cohesin Mutations in Human Cancer. *BBA - Reviews on Cancer*. [Online] 1–34. Available from: doi:10.1016/j.bbcan.2016.05.002.

Hirano, T. (2006) At the heart of the chromosome: SMC proteins in action.

Nature reviews. Molecular cell biology. [Online] 7 (5), 311–322. Available from: doi:10.1038/nrm1909.

Hirano, T. (2015) Chromosome Dynamics during Mitosis. *Cold Spring Harbor perspectives in biology*. [Online] a015792. Available from: doi:10.1101/cshperspect.a015792.

Hirano, T. (2005) Condensins: organizing and segregating the genome. *Current biology : CB*. [Online] 15 (7), R265–R275. Available from: doi:10.1016/j.cub.2005.03.037.

Hirano, T. (2012) Condensins: universal organizers of chromosomes with diverse functions. *Genes & Development*. [Online] 26 (15), 1659–1678. Available from: doi:10.1101/gad.194746.112.

Holliday, R. & Ho, T. (1998a) Evidence for gene silencing by endogenous DNA methylation. *Proceedings of the National Academy of Sciences*. 95 (15), 8727–8732.

Holliday, R. & Ho, T. (1998b) Gene silencing and endogenous DNA methylation in mammalian cells. *Mutation Research/Fundamental and Molecular Mechanisms of Mutagenesis*. 400 (1-2), 361–368.

Hopkins, S.R., McGregor, G.A., Murray, J.M., Downs, J.A., et al. (2016) Novel synthetic lethality screening method identifies TIP60-dependent radiation sensitivity in the absence of BAF180. *DNA Repair*. [Online] 4647–54. Available from: doi:10.1016/j.dnarep.2016.05.030.

Hwang, J.-Y., Smith, S., Ceschia, A., Torres-Rosell, J., et al. (2008) Smc5–Smc6 complex suppresses gross chromosomal rearrangements mediated by break-induced replications. *DNA Repair*. [Online] 7 (9), 1426–1436. Available from: doi:10.1016/j.dnarep.2008.05.006.

Irmisch, A., Ampatzidou, E., Mizuno, K., O'Connell, M.J., et al. (2009) Smc5/6 maintains stalled replication forks in a recombination-competent conformation. *The EMBO journal*. [Online] 28 (2), 144–155. Available from: doi:10.1038/emboj.2008.273.

Ivashkevich, A., Redon, C.E., Nakamura, A.J., Martin, R.F., et al. (2012) Use of the γ-H2AX assay to monitor DNA damage and repair in translational cancer research. *Cancer Letters*. [Online] 327 (1-2), 123–133. Available from: doi:10.1016/j.canlet.2011.12.025.

Iyama, T. & Wilson, D.M., III (2013) DNA repair mechanisms in dividing and non-dividing cells. *DNA Repair*. [Online] 12 (8), 620–636. Available from: doi:10.1016/j.dnarep.2013.04.015.

Jackson, A.L. & Loeb, L.A. (2001) The contribution of endogenous sources of DNA damage to the multiple mutations in cancer. *Mutation Research/Fundamental and Molecular Mechanisms of Mutagenesis*. 477 (1-

2), 7–21.

Jackson, A.L., Chen, R. & Loeb, L.A. (1998) Induction of microsatellite instability by oxidative DNA damage. *Proceedings of the National Academy of Sciences*. 95 (21), 12468–12473.

Jacobs, A.L. & Schär, P. (2011) DNA glycosylases: in DNA repair and beyond. *Chromosoma*. [Online] 121 (1), 1–20. Available from: doi:10.1007/s00412-011-0347-4.

Jacome, A., Gutierrez-Martinez, P., Schiavoni, F., Tenaglia, E., et al. (2015) NSMCE2 suppresses cancer and aging in mice independently of its SUMO ligase activity. *The EMBO journal*. [Online] 34 (21), 2604–2619. Available from: doi:10.15252/embj.201591829.

Jazayeri, A., Falck, J., Lukas, C., Bartek, J., et al. (2006) ATM- and cell cycle-dependent regulation of ATR in response to DNA double-strand breaks. *Nature Cell Biology*. [Online] 8 (1), 37–45. Available from: doi:10.1038/ncb1337.

Jeggo, P.A. & Downs, J.A. (2014) Roles of chromatin remodellers in DNA double strand break repair. *Experimental Cell Research*. [Online] 329 (1), 69–77. Available from: doi:10.1016/j.yexcr.2014.09.023.

Jiang, N., Benard, C.Y., Kebir, H., Shoubridge, E.A., et al. (2003) Human CLK2 Links Cell Cycle Progression, Apoptosis, and Telomere Length Regulation. *The Journal of biological chemistry*. [Online] 278 (24), 21678–21684. Available from: doi:10.1074/jbc.M300286200.

Kacsinta, A.D. & Dowdy, S.F. (2015) Current views on inducing synthetic lethal RNAi responses in the treatment of cancer. *Expert Opinion on Biological Therapy*. [Online] 16 (2), 161–172. Available from: doi:10.1517/14712598.2016.1110141.

Kais, Z., Rondinelli, B., Holmes, A., O'Leary, C., et al. (2016) FANCD2 Maintains Fork Stability in BRCA1/2- Deficient Tumors and Promotes Alternative End- Joining DNA Repair. *CellReports*. [Online] 15 (11), 2488–2499. Available from: doi:10.1016/j.celrep.2016.05.031.

Kass, E.M. & Jasin, M. (2010) Collaboration and competition between DNA double-strand break repair pathways. *FEBS Letters*. [Online] 584 (17), 3703–3708. Available from: doi:10.1016/j.febslet.2010.07.057.

Kawasaki, Y. & Sugino, A. (2001) Yeast replicative DNA polymerases and their role at the replication fork. *Molecules and cells*.

Kikuchi, S., Borek, D.M., Otwinowski, Z., Tomchick, D.R., et al. (2016) Crystal structure of the cohesin loader Scc2 and insight into cohesinopathy. *Proceedings of the National Academy of Sciences*. [Online] 201611333–201611336. Available from: doi:10.1073/pnas.1611333113.

Kim, H. & D'Andrea, A.D. (2012) Regulation of DNA cross-link repair by the Fanconi anemia/BRCA pathway. *Genes & Development*. [Online] 26 (13), 1393–1408. Available from: doi:10.1101/gad.195248.112.

Kim, H.J., Kim, A., Miyata, K. & Kataoka, K. (2016) Recent progress in development of siRNA delivery vehicles for cancer therapy. *Advanced Drug Delivery Reviews*. [Online] 1041–17. Available from: doi:10.1016/j.addr.2016.06.011.

Kliszczak, M., Stephan, A.K., Flanagan, A.-M. & Morrison, C.G. (2012) SUMO ligase activity of vertebrate Mms21/Nse2 is required for efficient DNA repair but not for Smc5/6 complex stability. *DNA Repair*. [Online] 11 (10), 799–810. Available from: doi:10.1016/j.dnarep.2012.06.010.

Kohler, R.E. (1994) *Lords of the fly: Drosophila genetics and the experimental life*.

Krejci, L., Altmannova, V., Spirek, M. & Zhao, X. (2012) Homologous recombination and its regulation. *Nucleic Acids Research*. [Online] 40 (13), 5795–5818. Available from: doi:10.1093/nar/gks270.

Krishnakumar, R. & Kraus, W.L. (2010) The PARP Side of the Nucleus: Molecular Actions, Physiological Outcomes, and Clinical Targets. *Molecular Cell*. [Online] 39 (1), 8–24. Available from: doi:10.1016/j.molcel.2010.06.017.

Kunkel, T.A. (2003) Considering the cancer consequences of altered DNA polymerase function. *Cancer cell*. 3 (2), 105–110.

Kunkel, T.A. & Erie, D.A. (2005) DNA mismatch repair. *Annual Review of Biochemistry*. [Online] 74681–710. Available from: doi:10.1146/annurev.biochem.74.082803.133243.

Kuroda, S., Urata, Y. & Fujiwara, T. (2012) Ataxia-telangiectasia mutated and the Mre11-Rad50-NBS1 complex: promising targets for radiosensitization. *Acta medica Okayama*. 66 (2), 83–92.

Lange, S.S., Takata, K.-I. & Wood, R.D. (2011) DNA polymerases and cancer. *Nature Reviews Cancer*. [Online] 11 (2), 1–15. Available from: doi:10.1038/nrc2998.

Lawrence, C.W., Borden, A., Banerjee, S.K. & LeClerc, J.E. (1990) Mutation frequency and spectrum resulting from a single abasic site in a single-stranded vector. *Nucleic Acids Research*. 18 (8), 2153–2157.

Lee, J.M., Niles, J.C., Wishnok, J.S. & Tannenbaum, S.R. (2002) Peroxynitrite Reacts with 8-Nitropurines to Yield 8-Oxopurines. *Chemical Research in Toxicology*. [Online] 15 (1), 7–14. Available from: doi:10.1021/tx010093d.

Lees-Miller, S. (2003) Repair of DNA double strand breaks by non-homologous end joining. *Biochimie*. [Online] 85 (11), 1161–1173. Available from:

doi:10.1016/j.biochi.2003.10.011.

Lehmann, A.R., Walicka, M., Griffiths, D.J., Murray, J.M., et al. (1995) The rad18 gene of Schizosaccharomyces pombe defines a new subgroup of the SMC superfamily involved in DNA repair. *Molecular and Cellular Biology*. 15 (12), 7067–7080.

Lessel, D., Vaz, B., Halder, S., Lockhart, P.J., et al. (2014) Mutations in SPRTN cause early onset hepatocellular carcinoma, genomic instability and progeroid features. *Nature Genetics*. [Online] 46 (11), 1239–1244. Available from: doi:10.1038/ng.3103.

Lieber, M.R., Gu, J., Lu, H., Shimazaki, N., et al. (2009) Nonhomologous DNA End Joining (NHEJ) and Chromosomal Translocations in Humans. In: *Genome Stability and Human Diseases*. Subcellular Biochemistry. [Online]. Dordrecht, Springer Netherlands. pp. 279–296. Available from: doi:10.1007/978-90-481-3471-7_14.

Lilienthal, I., Kanno, T. & SjÃ gren, C. (2013) Inhibition of the Smc5/6 Complex during Meiosis Perturbs Joint Molecule Formation and Resolution without Significantly Changing Crossover or Non-crossover Levels Nancy M Hollingsworth (ed.). *PLoS Genetics*. [Online] 9 (11), e1003898–18. Available from: doi:10.1371/journal.pgen.1003898.

Lindahl, T. (1993) Instability and decay of the primary structure of DNA. *Nature*.

Lindahl, T. (1999) Quality Control by DNA Repair. *Science*. [Online] 286 (5446), 1897–1905. Available from: doi:10.1126/science.286.5446.1897.

Lindahl, T. & Karlström, O. (1973) Heat-induced depyrimidination of deoxyribonucleic acid in neutral solution. *Biochemistry*. 12 (25), 5151–5154.

Link, P.A., Baer, M.R., James, S.R., Jones, D.A., et al. (2008) p53-Inducible Ribonucleotide Reductase (p53R2/RRM2B) Is a DNA Hypomethylation-Independent Decitabine Gene Target That Correlates with Clinical Response in Myelodysplastic Syndrome/Acute Myelogenous Leukemia. *Cancer Research*. [Online] 68 (22), 9358–9366. Available from: doi:10.1158/0008-5472.CAN-08-1860.

Liu, J., Doty, T., Gibson, B. & Heyer, W.-D. (2010) Human BRCA2 protein promotes RAD51 filament formation on RPA-covered single-stranded DNA. *Nature Publishing Group*. [Online] 17 (10), 1260–1262. Available from: doi:10.1038/nsmb.1904.

Liu, L.F., Desai, S.D., Li, T.K., Mao, Y., et al. (2000) Mechanism of action of camptothecin. *Annals of the New York Academy of Sciences*. 9221–10.

Liu, P., Long, L., Xiong, K., Yu, B., et al. (2014) Heritable/conditional genome editing in C. elegans using a CRISPR-Cas9 feeding system. *Nature Publishing Group*. [Online] 24 (7), 886–889. Available from:

doi:10.1038/cr.2014.73.

Loeb, L.A. & Monnat, R.J. (2008) DNA polymerases and human disease. *Nature Reviews Genetics*. [Online] 9 (8), 594–604. Available from: doi:10.1038/nrg2345.

Lok, B.H. & Powell, S.N. (2012) Molecular Pathways: Understanding the Role of Rad52 in Homologous Recombination for Therapeutic Advancement. *Clinical Cancer Research*. [Online] 18 (23), 6400–6406. Available from: doi:10.1158/1078-0432.CCR-11-3150.

Lord, C.J., Tutt, A.N.J. & Ashworth, A. (2015) Synthetic Lethality and Cancer Therapy: Lessons Learned from the Development of PARP Inhibitors. *Annual Review of Medicine*. [Online] 66 (1), 455–470. Available from: doi:10.1146/annurev-med-050913-022545.

Löbrich, M., Shibata, A., Beucher, A., Fisher, A., et al. (2014) γH2AX foci analysis for monitoring DNA double-strand break repair: Strengths, limitations and optimization. *Cell Cycle*. [Online] 9 (4), 662–669. Available from: doi:10.4161/cc.9.4.10764.

Lundholt, B.K. (2003) A Simple Technique for Reducing Edge Effect in Cell-Based Assays. *Journal of Biomolecular Screening*. [Online] 8 (5), 566–570. Available from: doi:10.1177/1087057103256465.

Lundin, C. (2005) Methyl methanesulfonate (MMS) produces heat-labile DNA damage but no detectable in vivo DNA double-strand breaks. *Nucleic Acids Research*. [Online] 33 (12), 3799–3811. Available from: doi:10.1093/nar/gki681.

Luo, J., Emanuele, M.J., Li, D., Creighton, C.J., et al. (2009) A Genome-wide RNAi Screen Identifies Multiple Synthetic Lethal Interactions with the Ras Oncogene. *Cell*. [Online] 137 (5), 835–848. Available from: doi:10.1016/j.cell.2009.05.006.

Macheret, M. & Halazonetis, T.D. (2015) DNA replication stress as a hallmark of cancer. *Annual review of pathology*. [Online] 10425–448. Available from: doi:10.1146/annurev-pathol-012414-040424.

MacRae, I.J., Zhou, K., Li, F., Repic, A., et al. (2006) Structural Basis for Double-Stranded RNA Processing by Dicer. *Science*. [Online] 311 (5758), 195–198. Available from: doi:10.2307/3843253?ref=search-gateway:72486f61c561bce5ba0a587ce19e665b.

Maier, P., Hartmann, L., Wenz, F. & Herskind, C. (2016) Cellular Pathways in Response to Ionizing Radiation and Their Targetability for Tumor Radiosensitization. *International Journal of Molecular Sciences*. [Online] 17 (1), 102–132. Available from: doi:10.3390/ijms17010102.

Marechal, A. & Zou, L. (2013) DNA Damage Sensing by the ATM and ATR

Kinases. *Cold Spring Harbor perspectives in biology*. [Online] 5 (9), a012716–a012716. Available from: doi:10.1101/cshperspect.a012716.

Marnett, L.J., Riggins, J.N. & West, J.D. (2003) Endogenous generation of reactive oxidants and electrophiles and their reactions with DNA and protein. *Journal of Clinical Investigation*. [Online] 111 (5), 583–593. Available from: doi:10.1172/JCI18022.

Marteijn, J.A., Lans, H., Vermeulen, W. & Hoeijmakers, J.H.J. (2014) Understanding nucleotide excision repair and its roles in cancer and ageing. *Nature Publishing Group*. [Online] 15 (7), 465–481. Available from: doi:10.1038/nrm3822.

Mattoscio, D. & Chiocca, S. (2015) SUMO pathway components as possible cancer biomarkers. *Future Oncology*. [Online] 11 (11), 1599–1610. Available from: doi:10.2217/fon.15.41.

McDonald, W.H. (2003) Novel Essential DNA Repair Proteins Nse1 and Nse2 Are Subunits of the Fission Yeast Smc5-Smc6 Complex. *Journal of Biological Chemistry*. [Online] 278 (46), 45460–45467. Available from: doi:10.1074/jbc.M308828200.

Melby, T.E., Ciampaglio, C.N., Briscoe, G. & Erickson, H.P. (1998) The symmetrical structure of structural maintenance of chromosomes (SMC) and MukB proteins: long, antiparallel coiled coils, folded at a flexible hinge. *The Journal of cell biology*. 142 (6), 1595–1604.

Menolfi, D., Delamarre, A., Lengronne, A., Pasero, P., et al. (2015) Essential Roles of the Smc5/6 Complex in Replication through Natural Pausing Sites and Endogenous DNA Damage Tolerance. *Molecular Cell*. [Online] 60 (6), 835–846. Available from: doi:10.1016/j.molcel.2015.10.023.

Michael, S., Auld, D., Klumpp, C., Jadhav, A., et al. (2008) A Robotic Platform for Quantitative High-Throughput Screening. *ASSAY and Drug Development Technologies*. [Online] 6 (5), 637–657. Available from: doi:10.1089/adt.2008.150.

Migliore, L., Coppede, F., Fenech, M. & Thomas, P. (2010) Association of micronucleus frequency with neurodegenerative diseases. *Mutagenesis*. [Online] 26 (1), 85–92. Available from: doi:10.1093/mutage/geq067.

Mizuguchi, T., Mizuguchi, T., Fudenberg, G., Fudenberg, G., et al. (2014) Cohesin-dependent globules and heterochromatin shape 3D genome architecture in S. pombe. *Nature*. [Online] 516 (7531), 432–435. Available from: doi:10.1038/nature13833.

Modrich, P. (1994) Mismatch repair, genetic stability, and cancer. *Science*. 266 (5193), 1959–1960.

Moffat, J. & Sabatini, D.M. (2006) Building mammalian signalling pathways with

RNAi screens. *Nature reviews. Molecular cell biology*. [Online] 7 (3), 177–187. Available from: doi:10.1038/nrm1860.

Mohr, S.E., Smith, J.A., Shamu, C.E., Neumüller, R.A., et al. (2014) RNAi screening comes of age: improved techniques and complementary approaches. *Nature Publishing Group*. [Online] 15 (9), 591–600. Available from: doi:10.1038/nrm3860.

Moshous, D., Callebaut, I., de Chasseval, R., Corneo, B., et al. (2001) Artemis, a novel DNA double-strand break repair/V(D)J recombination protein, is mutated in human severe combined immune deficiency. *Cell*. 105 (2), 177–186.

Murray, J.M. & Carr, A.M. (2008) Smc5/6: a link between DNA repair and unidirectional replication? *Nature reviews. Molecular cell biology*. [Online] 9 (2), 177–182. Available from: doi:10.1038/nrm2309.

Nasheuer, H.P., Smith, R. & Bauerschmidt, C. (2002) Initiation of eukaryotic DNA replication: regulation and mechanisms. *Progress in nucleic acid …*.

Nasim, A. & Smith, B.P. (1975) Genetic control of radiation sensitivity in Schizosaccharomyces pombe. *Genetics*. 79 (4), 573–582.

Nasmyth, K. & Haering, C.H. (2009) Cohesin: its roles and mechanisms. *Annual review of genetics*. [Online] 43 (1), 525–558. Available from: doi:10.1146/annurev-genet-102108-134233.

Ocampo-Hafalla, M.T. & Uhlmann, F. (2011) Cohesin loading and sliding. *Journal of cell science*. [Online] 124 (Pt 5), 685–691. Available from: doi:10.1242/jcs.073866.

Ogi, T., Limsirichaikul, S., Overmeer, R.M., Volker, M., et al. (2010) Three DNA Polymerases, Recruited by Different Mechanisms, Carry Out NER Repair Synthesis in Human Cells. *Molecular Cell*. [Online] 37 (5), 714–727. Available from: doi:10.1016/j.molcel.2010.02.009.

Oh, C., Park, S., Lee, E.K. & Yoo, Y.J. (2013) Downregulation of ubiquitin level via knockdown of polyubiquitin gene Ubb as potential cancer therapeutic intervention. *Scientific Reports*. [Online] 31–9. Available from: doi:10.1038/srep02623.

Otoshi, E., Yagi, T., Mori, T., Matsunaga, T., et al. (2000) Respective roles of cyclobutane pyrimidine dimers,(6–4) photoproducts, and minor photoproducts in ultraviolet mutagenesis of repair-deficient xeroderma …. *Cancer Research*.

O'Driscoll, M. & Jeggo, P.A. (2006) The role of double-strand break repair — insights from human genetics. *Nature Reviews Genetics*. [Online] 7 (1), 45–54. Available from: doi:10.1038/nrg1746.

O'Neil, N.J., van Pel, D.M. & Hieter, P. (2013) Synthetic lethality and cancer: cohesin and PARP at the replication fork. *Trends in Genetics*. [Online] 29 (5), 290–297. Available from: doi:10.1016/j.tig.2012.12.004.

Palecek, J., Vidot, S., Feng, M., Doherty, A.J., et al. (2006) The Smc5-Smc6 DNA repair complex. bridging of the Smc5-Smc6 heads by the KLEISIN, Nse4, and non-Kleisin subunits. *The Journal of biological chemistry*. [Online] 281 (48), 36952–36959. Available from: doi:10.1074/jbc.M608004200.

Panier, S. & Boulton, S.J. (2013) Double-strand break repair: 53BP1 comes into focus. *Nature Publishing Group*. [Online] 15 (1), 7–18. Available from: doi:10.1038/nrm3719.

Payne, F., Colnaghi, R., Rocha, N., Seth, A., et al. (2014) Hypomorphism in human NSMCE2 linked to primordial dwarfism and insulin resistance. *Journal of Clinical Investigation*. [Online] 124 (9), 4028–4038. Available from: doi:10.1172/JCI73264.

Paz, M.M., Zhang, X., Lu, J. & Holmgren, A. (2012) A New Mechanism of Action for the Anticancer Drug Mitomycin C: Mechanism-Based Inhibition of Thioredoxin Reductase. *Chemical Research in Toxicology*. [Online] 25 (7), 1502–1511. Available from: doi:10.1021/tx3002065.

Pebernard, S., McDonald, W.H., Pavlova, Y., Yates, J.R., et al. (2004) Nse1, Nse2, and a novel subunit of the Smc5-Smc6 complex, Nse3, play a crucial role in meiosis. *Molecular Biology of the Cell*. [Online] 15 (11), 4866–4876. Available from: doi:10.1091/mbc.E04-05-0436.

Pebernard, S., Perry, J.J.P., Tainer, J.A. & Boddy, M.N. (2008) Nse1 RING-like domain supports functions of the Smc5-Smc6 holocomplex in genome stability. *Molecular Biology of the Cell*. [Online] 19 (10), 4099–4109. Available from: doi:10.1091/mbc.E08-02-0226.

Pebernard, S., Schaffer, L., Campbell, D., Head, S.R., et al. (2008) Localization of Smc5/6 to centromeres and telomeres requires heterochromatin and SUMO, respectively. *The EMBO journal*. [Online] 27 (22), 3011–3023. Available from: doi:10.1038/emboj.2008.220.

Pebernard, S., Wohlschlegel, J., McDonald, W.H., Yates, J.R., et al. (2006) The Nse5-Nse6 dimer mediates DNA repair roles of the Smc5-Smc6 complex. *Molecular and Cellular Biology*. [Online] 26 (5), 1617–1630. Available from: doi:10.1128/MCB.26.5.1617-1630.2006.

Perrimon, N. & Mathey-Prevot, B. (2006) Applications of High-Throughput RNA Interference Screens to Problems in Cell and Developmental Biology. *Genetics*. [Online] 175 (1), 7–16. Available from: doi:10.1534/genetics.106.069963.

Petermann, E., Orta, M.L., Issaeva, N., Schultz, N., et al. (2010a) Hydroxyurea-

Stalled Replication Forks Become Progressively Inactivated and Require Two Different RAD51-Mediated Pathways for Restart and Repair. *Molecular Cell*. [Online] 37 (4), 492–502. Available from: doi:10.1016/j.molcel.2010.01.021.

Petermann, E., Orta, M.L., Issaeva, N., Schultz, N., et al. (2010b) Hydroxyurea-Stalled Replication Forks Become Progressively Inactivated and Require Two Different RAD51-Mediated Pathways for Restart and Repair. *Molecular Cell*. [Online] 37 (4), 492–502. Available from: doi:10.1016/j.molcel.2010.01.021.

Petronczki, M., Siomos, M.F. & Nasmyth, K. (2003) Un menage a quatre: the molecular biology of chromosome segregation in meiosis. *Cell*.

Piazza, I., Haering, C.H. & Rutkowska, A. (2013) Condensin: crafting the chromosome landscape. *Chromosoma*. [Online] 122 (3), 175–190. Available from: doi:10.1007/s00412-013-0405-1.

Potts, P.R. (2009) The Yin and Yang of the MMS21–SMC5/6 SUMO ligase complex in homologous recombination. *DNA Repair*. [Online] 8 (4), 499–506. Available from: doi:10.1016/j.dnarep.2009.01.009.

Potts, P.R. & Yu, H. (2007) The SMC5/6 complex maintains telomere length in ALT cancer cells through SUMOylation of telomere-binding proteins. *Nature structural & molecular biology*. [Online] 14 (7), 581–590. Available from: doi:10.1038/nsmb1259.

Potts, P.R., Porteus, M.H. & Yu, H. (2006a) Human SMC5/6 complex promotes sister chromatid homologous recombination by recruiting the SMC1/3 cohesin complex to double-strand breaks. *The EMBO journal*.

Potts, P.R., Porteus, M.H. & Yu, H. (2006b) Human SMC5/6 complex promotes sister chromatid homologous recombination by recruiting the SMC1/3 cohesin complex to double-strand breaks. *The EMBO journal*. [Online] 25 (14), 3377–3388. Available from: doi:10.1038/sj.emboj.7601218.

Rajendra, E., Garaycoechea, J.I., Patel, K.J. & Passmore, L.A. (2014) Abundance of the Fanconi anaemia core complex is regulated by the RuvBL1 and RuvBL2 AAA+ ATPases. *Nucleic Acids Research*. [Online] 42 (22), 13736–13748. Available from: doi:10.1093/nar/gku1230.

Rajkumar, S.V. & Kyle, R.A. (2005) Multiple myeloma: diagnosis and treatment. *Mayo Clinic Proceedings*.

Ramlee, M., Wang, J., Toh, W. & Li, S. (2016) Transcription Regulation of the Human Telomerase Reverse Transcriptase (hTERT) Gene. *Genes*. [Online] 7 (8), 50–43. Available from: doi:10.3390/genes7080050.

Rapin, I., Lindenbaum, Y., Dickson, D.W. & Kraemer, K.H. (2000) Cockayne syndrome and xeroderma pigmentosum DNA repair disorders with

overlaps and paradoxes. *Neurology*.

Räschle, M., Smeenk, G., Hansen, R.K., Temu, T., et al. (2015) DNA repair. Proteomics reveals dynamic assembly of repair complexes during bypass of DNA cross-links. *Science*. [Online] 348 (6234), 1253671–1253671. Available from: doi:10.1126/science.1253671.

Riballo, E., Woodbine, L., Stiff, T., Walker, S.A., et al. (2008) XLF-Cernunnos promotes DNA ligase IV-XRCC4 re-adenylation following ligation. *Nucleic Acids Research*. [Online] 37 (2), 482–492. Available from: doi:10.1093/nar/gkn957.

Richards, J.D., Johnson, K.A., Liu, H., McRobbie, A.-M., et al. (2008) Structure of the DNA repair helicase hel308 reveals DNA binding and autoinhibitory domains. *The Journal of biological chemistry*. [Online] 283 (8), 5118–5126. Available from: doi:10.1074/jbc.M707548200.

Rivera-Calzada, A., Spagnolo, L., Pearl, L.H. & Llorca, O. (2006) Structural model of full-length human Ku70–Ku80 heterodimer and its recognition of DNA and DNA-PKcs. *EMBO reports*. [Online] 8 (1), 56–62. Available from: doi:10.1038/sj.embor.7400847.

Roy, R., Chun, J. & Powell, S.N. (2012) BRCA1 and BRCA2: different roles in a common pathway of genome protection. *Nature Reviews Cancer*. [Online] 12 (1), 68–78. Available from: doi:10.1038/nrc3181.

Rydberg, B. & Lindahl, T. (1982) Nonenzymatic methylation of DNA by the intracellular methyl group donor S-adenosyl-L-methionine is a potentially mutagenic reaction. *The EMBO journal*. 1 (2), 211–216.

Sale, J.E. (2013) Translesion DNA Synthesis and Mutagenesis in Eukaryotes. *Cold Spring Harbor perspectives in biology*. [Online] 5 (3), a012708–a012708. Available from: doi:10.1101/cshperspect.a012708.

Sale, J.E., Lehmann, A.R. & Woodgate, R. (2012) Y-family DNA polymerases and their role in tolerance of cellular DNA damage. *Nature Publishing Group*. [Online] 13 (3), 141–152. Available from: doi:10.1038/nrm3289.

San Filippo, J., Sung, P. & Klein, H. (2008) Mechanism of Eukaryotic Homologous Recombination. *Annual Review of Biochemistry*. [Online] 77 (1), 229–257. Available from: doi:10.1146/annurev.biochem.77.061306.125255.

Santivasi, W.L. & Xia, F. (2014) Ionizing Radiation-Induced DNA Damage, Response, and Repair. *Antioxidants & Redox Signaling*. [Online] 21 (2), 251–259. Available from: doi:10.1089/ars.2013.5668.

Schellenberg, M.J., Tumbale, P.P. & Williams, R.S. (2015) Molecular underpinnings of Aprataxin RNA/DNA deadenylase function and dysfunction in neurological disease. *Progress in Biophysics and Molecular*

Biology. [Online] 117 (2-3), 157–165. Available from: doi:10.1016/j.pbiomolbio.2015.01.007.

Schlacher, K., Christ, N., Siaud, N., Egashira, A., et al. (2011) Double-Strand Break Repair-Independent Role for BRCA2 in Blocking Stalled Replication Fork Degradation by MRE11. *Cell*. [Online] 145 (4), 529–542. Available from: doi:10.1016/j.cell.2011.03.041.

Sergeant, J., Taylor, E., Palecek, J., Fousteri, M., et al. (2005) Composition and architecture of the Schizosaccharomyces pombe Rad18 (Smc5-6) complex. *Molecular and Cellular Biology*. [Online] 25 (1), 172–184. Available from: doi:10.1128/MCB.25.1.172-184.2005.

Shaheen, M., Allen, C., Nickoloff, J.A. & Hromas, R. (2011) Synthetic lethality: exploiting the addiction of cancer to DNA repair. *Blood*. [Online] 117 (23), 6074–6082. Available from: doi:10.1182/blood-2011-01-313734.

Sharma, S. & Rao, A. (2009) RNAi screening: tips and techniques. *Nature Immunology*. [Online] 10 (8), 799–804. Available from: doi:10.1038/ni0809-799.

Sheedy, D.M. (2005) Brc1-Mediated DNA Repair and Damage Tolerance. *Genetics*. [Online] 171 (2), 457–468. Available from: doi:10.1534/genetics.105.044966.

Shibata, A., Conrad, S., Birraux, J., Geuting, V., et al. (2011) Factors determining DNA double-strand break repair pathway choice in G2 phase. *The EMBO journal*. [Online] 30 (6), 1079–1092. Available from: doi:10.1038/emboj.2011.27.

Stark, J.M., Pierce, A.J., Oh, J., Pastink, A., et al. (2004) Genetic Steps of Mammalian Homologous Repair with Distinct Mutagenic Consequences. *Molecular and Cellular Biology*. [Online] 24 (21), 9305–9316. Available from: doi:10.1128/MCB.24.21.9305-9316.2004.

Stephan, A.K., Kliszczak, M. & Morrison, C.G. (2011) The Nse2/Mms21 SUMO ligase of the Smc5/6 complex in the maintenance of genome stability. *FEBS Letters*. [Online] 585 (18), 2907–2913. Available from: doi:10.1016/j.febslet.2011.04.067.

Stephan, A.K., Kliszczak, M., Dodson, H., Cooley, C., et al. (2011) Roles of vertebrate Smc5 in sister chromatid cohesion and homologous recombinational repair. *Molecular and Cellular Biology*. [Online] 31 (7), 1369–1381. Available from: doi:10.1128/MCB.00786-10.

Sugiyama, T. & Kantake, N. (2009) Dynamic Regulatory Interactions of Rad51, Rad52, and Replication Protein-A in Recombination Intermediates. *Journal of Molecular Biology*. [Online] 390 (1), 45–55. Available from: doi:10.1016/j.jmb.2009.05.009.

Sun, Y., Kucej, M., Fan, H.-Y., Yu, H., et al. (2009) Separase Is Recruited to Mitotic Chromosomes to Dissolve Sister Chromatid Cohesion in a DNA-Dependent Manner. *Cell*. [Online] 137 (1), 123–132. Available from: doi:10.1016/j.cell.2009.01.040.

Sutani, T., Sakata, T., Nakato, R., Masuda, K., et al. (2015) Condensin targets and reduces unwound DNA structures associated with transcription in mitotic chromosome condensation. *Nature communications*. [Online] 67815. Available from: doi:10.1038/ncomms8815.

Tafel, A.A., Wu, L. & McHugh, P.J. (2011) Human HEL308 Localizes to Damaged Replication Forks and Unwinds Lagging Strand Structures. *The Journal of biological chemistry*. [Online] 286 (18), 15832–15840. Available from: doi:10.1074/jbc.M111.228189.

Tapia-Alveal, C. & O'Connell, M.J. (2011a) Nse1-dependent recruitment of Smc5/6 to lesion-containing loci contributes to the repair defects of mutant complexes. *Molecular Biology of the Cell*. [Online] 22 (23), 4669–4682. Available from: doi:10.1091/mbc.E11-03-0272.

Tapia-Alveal, C. & O'Connell, M.J. (2011b) Nse1-dependent recruitment of Smc5/6 to lesion-containing loci contributes to the repair defects of mutant complexes. *Molecular Biology of the Cell*. [Online] 22 (23), 4669–4682. Available from: doi:10.1091/mbc.E11-03-0272.

Tapia-Alveal, C., Lin, S.-J. & O'Connell, M.J. (2014) Functional interplay between cohesin and Smc5/6 complexes. *Chromosoma*. [Online] 123 (5), 437–445. Available from: doi:10.1007/s00412-014-0474-9.

Tapia-Alveal, C., Lin, S.J., Yeoh, A., Jabado, O.J., et al. (2014) H2A.Z-Dependent Regulation of Cohesin Dynamics on Chromosome Arms. *Molecular and Cellular Biology*. [Online] 34 (11), 2092–2104. Available from: doi:10.1128/MCB.00193-14.

Tariq, M. (2009) *Oxidative Stress and Neurodegenerative Diseases: A Review of Upstream and Downstream Antioxidant Therapeutic Options*. 1–10.

Tarsounas, M., Davies, D. & West, S.C. (2003) BRCA2-dependent and independent formation of RAD51 nuclear foci. *Oncogene*. [Online] 22 (8), 1115–1123. Available from: doi:10.1038/sj.onc.1206263.

Taylor, E.M., Copsey, A.C., Hudson, J.J.R., Vidot, S., et al. (2008a) Identification of the Proteins, Including MAGEG1, That Make Up the Human SMC5-6 Protein Complex. *Molecular and Cellular Biology*. [Online] 28 (4), 1197–1206. Available from: doi:10.1128/MCB.00767-07.

Taylor, E.M., Copsey, A.C., Hudson, J.J.R., Vidot, S., et al. (2008b) Identification of the Proteins, Including MAGEG1, That Make Up the Human SMC5-6 Protein Complex. *Molecular and Cellular Biology*. [Online] 28 (4), 1197–1206. Available from: doi:10.1128/MCB.00767-07.

Taylor, E.M., Moghraby, J.S., Lees, J.H., Smit, B., et al. (2001) Characterization of a novel human SMC heterodimer homologous to the Schizosaccharomyces pombe Rad18/Spr18 complex. *Molecular Biology of the Cell*. 12 (6), 1583–1594.

Tudek, B., Bioteux, S. & Laval, J. (1992) Biological properties of imidazole ring-opened N7-methylguanine in M13mp18 phage DNA. *Nucleic Acids Research*.

Turner, N.C., Lord, C.J., Iorns, E., Brough, R., et al. (2008) A synthetic lethal siRNA screen identifying genes mediating sensitivity to a PARP inhibitor. *The EMBO journal*. [Online] 27 (9), 1368–1377. Available from: doi:10.1038/emboj.2008.61.

Uhlmann, F. (2016) SMC complexes: from DNA to chromosomes. *Nature reviews. Molecular cell biology*. [Online] 17 (7), 399–412. Available from: doi:10.1038/nrm.2016.30.

van den Boom, J., Wolf, M., Weimann, L., Schulze, N., et al. (2016) VCP/p97 Extracts Sterically Trapped Ku70/80 Rings from DNA in Double-Strand Break Repair. *Molecular Cell*. [Online] 64 (1), 189–198. Available from: doi:10.1016/j.molcel.2016.08.037.

van der Crabben, S.N., Hennus, M.P., McGregor, G.A., Ritter, D.I., et al. (2016) Destabilized SMC5/6 complex leads to chromosome breakage syndrome with severe lung disease. *Journal of Clinical Investigation*. [Online] 1–12. Available from: doi:10.1172/JCI82890.

Verkade, H.M., Bugg, S.J., Lindsay, H.D., Carr, A.M., et al. (1999) Rad18 is required for DNA repair and checkpoint responses in fission yeast. *Molecular Biology of the Cell*. 10 (9), 2905–2918.

Verver, D.E., Hwang, G.H., Jordan, P.W. & Hamer, G. (2015) Resolving complex chromosome structures during meiosis: versatile deployment of Smc5/6. *Chromosoma*. [Online] 1–13. Available from: doi:10.1007/s00412-015-0518-9.

Vral, A., Thierens, H. & De Ridder, L. (1996) Micronucleus induction by 60Co gamma-rays and fast neutrons in ataxia telangiectasia lymphocytes. *International Journal of Radiation Biology*. [Online] 70 (2), 171–176. Available from: doi:10.1080/095530096145166.

Walker, J.R., Corpina, R.A. & Goldberg, J. (2001) Structure of the Ku heterodimer bound to DNA and its implications for double-strand break repair. *Nature*.

Wang, J., Lu, Z., Wientjes, M.G. & Au, J.L.S. (2010) Delivery of siRNA therapeutics: barriers and carriers. *The AAPS journal*. [Online] 12 (4), 492–503. Available from: doi:10.1208/s12248-010-9210-4.

Wang, J., Su, F., Smilenov, L.B., Zhou, L., et al. (2011) Mechanisms of increased risk of tumorigenesis in Atm and Brca1 double heterozygosity. *Radiation oncology (London, England)*. [Online] 6 (1), 96. Available from: doi:10.1186/1748-717X-6-96.

Wang, W.-Y., Pan, L., Su, S.C., Quinn, E.J., et al. (2013) Interaction of FUS and HDAC1 regulates DNA damage response and repair in neurons. *Nature Publishing Group*. [Online] 16 (10), 1383–1391. Available from: doi:10.1038/nn.3514.

Wanrooij, P.H. & Burgers, P.M. (2015) Yet another job for Dna2: Checkpoint activation. *DNA Repair*. [Online] 1–7. Available from: doi:10.1016/j.dnarep.2015.04.009.

Watson, A.T., Garcia, V., Bone, N., Carr, A.M., et al. (2008) Gene tagging and gene replacement using recombinase-mediated cassette exchange in Schizosaccharomyces pombe. *Gene*. [Online] 407 (1-2), 63–74. Available from: doi:10.1016/j.gene.2007.09.024.

Wojcik, E.J., Buckley, R.S., Richard, J., Liu, L., et al. (2013) Kinesin-5: Cross-bridging mechanism to targeted clinical therapy. *Gene*. [Online] 531 (2), 133–149. Available from: doi:10.1016/j.gene.2013.08.004.

Woodman, I.L. & Bolt, E.L. (2011) Winged helix domains with unknown function in Hel308 and related helicases. *Biochemical Society transactions*. [Online] 39 (1), 140–144. Available from: doi:10.1042/BST0390140.

Wu, N. & Yu, H. (2012) The Smc complexes in DNA damage response. *Cell & Bioscience*. [Online] 2 (1), 5. Available from: doi:10.1186/2045-3701-2-5.

Wu, N., Kong, X., Ji, Z., Zeng, W., et al. (2012) Scc1 sumoylation by Mms21 promotes sister chromatid recombination through counteracting Wapl. *Genes & Development*. [Online] 26 (13), 1473–1485. Available from: doi:10.1101/gad.193615.112.

Xaver, M., Huang, L., Chen, D. & Klein, F. (2013) Smc5/6-Mms21 Prevents and Eliminates Inappropriate Recombination Intermediates in Meiosis Michael Lichten (ed.). *PLoS Genetics*. [Online] 9 (12), e1004067. Available from: doi:10.1371/journal.pgen.1004067.

Xu, B., Lu, S. & Gerton, J.L. (2014) Roberts syndrome: A deficit in acetylated cohesin leads to nucleolar dysfunction. *Rare diseases (Austin, Tex.)*. [Online] 2 (1), e27743. Available from: doi:10.4161/rdis.27743.

Xu, B., Sowa, N., Cardenas, M.E. & Gerton, J.L. (2015) l-leucine partially rescues translational and developmental defects associated with zebrafish models of Cornelia de Lange syndrome. *Human molecular genetics*. [Online] 24 (6), 1540–1555. Available from: doi:10.1093/hmg/ddu565.

Xu, H., Balakrishnan, K., Malaterre, J., Beasley, M., et al. (2010) Rad21-

Cohesin Haploinsufficiency Impedes DNA Repair and Enhances Gastrointestinal Radiosensitivity in Mice Kerstin Borgmann (ed.). *PLoS ONE*. [Online] 5 (8), e12112–e12115. Available from: doi:10.1371/journal.pone.0012112.

Ye, R., Chen, Z., Lian, B., Rowley, M.J., et al. (2015) A Dicer-Independent Route for Biogenesis of siRNAs that Direct DNA Methylation in Arabidopsis. *Molecular Cell*. [Online] 61 (2), 1–15. Available from: doi:10.1016/j.molcel.2015.11.015.

Yokoyama, Y., Zhu, H., Zhang, R. & Noma, K.-I. (2015) A novel role for the condensin II complex in cellular senescence. *Cell Cycle*. [Online] 0–00. Available from: doi:10.1080/15384101.2015.1049778.

Yong-Gonzales, V., Hang, L.E., Castellucci, F., Branzei, D., et al. (2012) The Smc5-Smc6 Complex Regulates Recombination at Centromeric Regions and Affects Kinetochore Protein Sumoylation during Normal Growth Anja-Katrin Bielinsky (ed.). *PLoS ONE*. [Online] 7 (12), e51540. Available from: doi:10.1371/journal.pone.0051540.

Youds, J.L. & Boulton, S.J. (2011) The choice in meiosis - defining the factors that influence crossover or non-crossover formation. *Journal of cell science*. [Online] 124 (Pt 4), 501–513. Available from: doi:10.1242/jcs.074427.

Zabrady, K., Adamus, M., Vondrova, L., Liao, C., et al. (2016) Chromatin association of the SMC5/6 complex is dependent on binding of its NSE3 subunit to DNA. *Nucleic Acids Research*. [Online] 44 (3), 1064–1079. Available from: doi:10.1093/nar/gkv1021.

Zabrady, K., Adamus, M., Vondrova, L., Liao, C., et al. (2015) Chromatin association of the SMC5/6 complex is dependent on binding of its NSE3 subunit to DNA. *Nucleic Acids Research*. [Online] gkv1021–16. Available from: doi:10.1093/nar/gkv1021.

Zhang, X.D. (2011) *Optimal high-throughput screening: practical experimental design and data analysis for genome-scale RNAi research*.

Zhao, X. & Blobel, G. (2005) A SUMO ligase is part of a nuclear multiprotein complex that affects DNA repair and chromosomal organization. *Proceedings of the National Academy of Sciences of the United States of America*. [Online] 102 (13), 4777–4782. Available from: doi:10.1073/pnas.0500537102.